CHARACTERISATION OF IMMUNE RESPONSES TO MYCOBACTERIAL INFECTIONS IN A MURINE MODEL OF TYPE 2 DIABETES

Thesis submitted by
Md Abdul Alim (DVM, MSc)
James Cook University
in April 2018

for the degree of Doctor of Philosophy
in the College of Public Health, Medical and Veterinary Sciences,
James Cook University, Australia

This thesis is dedicated to my beloved parents……

STATEMENT OF ACCESS

I, the undersigned, author of this work, understand that James Cook University will make this thesis available for use within the University Library and, via the Australian Digital Theses network, for use elsewhere.

I understand that, as an unpublished work, a thesis has significant protection under the Copyright Act and I do not wish to place any further restriction on access to this work.

Md Abdul Alim
April 2018

STATEMENT OF SOURCES DECLARATION

I declare that this thesis is my own work and has not been submitted in any form for another degree or diploma at any university or other institution of tertiary education. Information derived from the published or unpublished work of others has been acknowledged in the text and a list of references is given.

Md Abdul Alim
April 2018

ELECTRONIC COPY

I, the undersigned, the author of this work, declare that the electronic copy of this thesis provided to the James Cook University Library is an accurate copy of the print thesis submitted, within the limits of the technology available.

Md Abdul Alim
April 2018

DECLARATION OF ETHICS AND BIOSAFETY APPROVALS

The research presented and reported in this thesis was conducted within the guidelines for research ethics outlined in the NHMRC/AVCC Statement and Guidelines on Research Practice (1997), the James Cook University Policy on Experimentation Ethics. Standard Practices and Guidelines (2001), and the James Cook University Statement and Guidelines on Research Practice (2001). *Mycobacterium tuberculosis* (H37Rv) ATCC strain was imported (permit number # 0000281462) from BEI resources of United States of America (USA) under licence by Professor Natkunam Ketheesan with prior approval from the Department of Agriculture and Water Resources, Australian Government. The proposed research methodology received clearance from the James Cook University Experimentation Ethics Review (Approval #A2016) and Biosafety Committee (approvals # JCUIBC-160601-007, JCUIBC-160601-011 and MI14-08).

Md Abdul Alim
April 2018

STATEMENT OF CONTRIBUTION OF OTHERS

Supervision and intellectual support: Supervision of my thesis research project, along with intellectual support for designing the project proposal, data analysis, manuscript preparation and editing of my thesis was provided by my supervisors Associate Professor Brenda Govan, Catherine Rush and Professor Natkunam Ketheesan.

Financial support: The research project was supported by internal grants provided by James Cook University to the supervisors. Minor financial supports (~9000 AUD) for this research project was also achieved by myself from Graduate Research School of the same institute. I also received the highly prestigious Endeavour Postgraduate Scholarship (Grant ID: PGPhD_DCD-3871_2014) funded by the Australian Government for the tuition fees and living allowances. Travel grants were also awarded by the committees of 'Australasian Society for Immunology Conference 2015' and 'The 10th International conference on the Pathogenesis of Mycobacterial infections 2017' to attend conferences in Canberra, Australia and Stockholm, Sweden, respectively.

Technical support: Chris Wright, Laboratory Manager, Australian Institute of Tropical Health and Medicine (AITHM) helped in establishing and maintaining the PC3 laboratory. He also helped in obtaining all the relevant biosafety approvals related to *Mycobacterium tuberculosis* work. Scott Blyth (Senior Technical Officer) and Serrin Rowarth (Manager, Small Animal Operations) assisted by providing mice for the experiments and looking after them throughout the study period. Most of the laboratory work was undertaken with the assistance from Suchandan Sikder, PhD candidate AITHM, Dr Jodie Morris, Senior Research Associate, Infectious Diseases and Immunopathogenesis Research Group and my supervisors. In addition, I was also assisted with some laboratory work by Dr Andreas Kupz, NH&MRC CJ Martin Research Fellow, Harindra Sathkumara, PhD student, AITHM and Tahnee Bridson, 4th year medical student of James Cook University. All the works related to histopathology and imaging were assisted by Laurie Reilly, Senior laboratory technician, Biomedicine Department of JCU.

Statistical analysis support: Data analysis support and instruction were provided by Associate Professor Leigh Owens, College of Public Health, Medical & Veterinary Sciences and Dr Rabiul Beg, College of Business, Law & Governance of James Cook university.

ACKNOWLEDGEMENTS

This dissertation is the result of effort, support and guidance of many people for whom I will remain grateful forever. I am especially grateful to have the opportunity to conduct this research under an inspirational group of supervisors: Associate Professor Brenda Govan, Catherine Rush and Professor Natkunam Ketheesan. This research would not have been possible without their close supervision, encouragement and mentorship. Also, thanks from my heart for their continuous care and love to me and my family here in Australia since commencing my PhD.

Other than my supervisors, I have had enormous support in learning relevant techniques from Dr Jodie Morris, Senior Research Associate, Infectious Disease and Immunopathogenesis Research Group (IDIRG) of James Cook University (JCU). I would like to thank Dr Andreas Kupz, NH&MRC CJ Martin Research Fellow, JCU for sharing his working experiences in PC3 and also helping me in some of my experiments. Also, thanks to my fellow colleagues Suchandan Sikder, Tahnee Bridson, Harindra Sathkumara who made time to help me in my lab experiments. Special thanks to Associate Professor Leigh Owens, College of Public Health, Medical and Veterinary Sciences (CPHMVS) and Dr Rabiul Beg, College of Business, Law and Governance (CBLG) for their advice and guidance in the statistical analysis of my data.

I am very grateful for the friendly, supportive work environment provided by the staff and fellow PhD students of CPHMVS. A special thanks to Scott Blyth and Serrin Rowarth for providing me the laboratory mice and their support in looking after them throughout my study period. I would like to mention Chris Wright (laboratory manager) for his tremendous work to set up the PC3 laboratory and helping me in getting all appropriate approvals. Without these it wouldn't have been possible to complete the *Mycobacterium tuberculosis* related work of this project. I would like to especially mention all the laboratory technicians (Grace Stanton, Katy Christi, Sandra Pollard, Helen Long, Karen Reeks, Louise Costanzo and others) who never felt bored when I asked for their help. Special thanks to Laurie Reilly for his teaching and sharing of knowledge regarding histopathology. Also, thanks to the administrative staff (Sherie Everingham, Shane Walker) for their support in processing all the PhD paperwork very smoothly which made this journey much easier.

Special thanks to Jeff Warner and Kerrianne Watt, former and current Associate Dean, Research Education, CPHMVS, respectively for taking care and troubleshooting the problems of all HDR students, including me. I am also grateful to them for their mental support to overcome the situation when one of my supervisors resigned from JCU.

I would like to acknowledge all the financial bodies for their support to enable me to continue my study. Firstly, Australian Government, for offering me the Endeavour Postgraduate research scholarship (PhD) to study at JCU. Secondly, Graduate Research School of this university for providing me the supplementary research grants and partial support of the travel costs for attending a conference. Finally, the organising committees of 'The 10th International conference on the Pathogenesis of Mycobacterial infections 2017, Stockholm, Sweden', and 'Australasian Society for Immunology Conference 2015, Canberra, Australia' for financial support to attend the conferences.

I would like to thank Drs Rabiul Beg, Rafiuddin Ahmed, CBLG and Associate Professor Jeff Warner, CPHMVS of JCU, who acted as local guardians and taking care of my health and wellbeing throughout this period. Also acknowledging the generous supports from the 'Townsville Bangladeshi Community'.

I would like to acknowledge all the academic staff of Department of Pathology and Parasitology, Chittagong Veterinary and Animal Sciences University (CVASU), Bangladesh who inspired and supported me to complete this journey. Many thanks to Professor Dr Md Ahasanul Hoque from CVASU for all his encouragement and guidelines during scholarship application process to study at JCU.

Finally, I would like to thank my family members particularly my elder brothers (M A Mannan, M A Hossain and M Morshed) for their continuous support and encouragement since my childhood to reach this stage. Special thanks to my beloved wife "Rizia Sathi" for all her sacrifices and constant support. Without her mental support, it would have been very tough to complete this dissertation.

PUBLICATIONS

Publications resulting from this thesis:

ALIM, M. A., SIKDER, S., BRIDSON, T. L., RUSH, C. M., GOVAN, B. L. & KETHEESAN, N. 2017. Anti-mycobacterial function of macrophages is impaired in a diet-induced model of type 2 diabetes. *Tuberculosis (Edinb),* 102**,** 47-54.

ALIM, M. A., KUPZ, A., SIKDER, S., SATHKUMARA, H.D., RUSH, C. M., GOVAN, B. L. & KETHEESAN, N. (2018). Increased tuberculosis susceptibility in a diet-induced murine model of type 2 diabetes. Manuscript in preparation for submission to *Infection and Immunity*.

ALIM, M. A., SIKDER, S., KUPZ, A., SATHKUMARA, H.D., RUSH, C. M., GOVAN, B. L. & KETHEESAN, N. (2018). Increased susceptibility to *Mycobacterium bovis* (BCG strain) infection in Type 2 diabetes mice is associated cytokine dysregulation. Manuscript in preparation for submission to *Tuberculosis*.

Additional publications:

SIKDER, S., WILLIAMS, N. L., SORENSON, A. E., **ALIM, M. A.,** VIDGEN, M. E., MORELAND, N. J., RUSH, C. M., SIMPSON, R. S., GOVAN, B. L., NORTON, R. E., CUNNINGHAM, M. W., MCMILLAN, D. J., SRIPRAKASH, K. S. & KETHEESAN, N. 2017. Group G streptococcus induces an autoimmune IL-17A/IFN-gamma mediated carditis in the Lewis rat model of Rheumatic Heart Disease. *J Infect Dis*. 2017 Dec 9. doi: 10.1093/infdis/jix637.

HALEAGRAHARA, N., MIRANDA-HERNANDEZ, S., **ALIM, M. A.,** HAYES, L., BIRD, G. & KETHEESAN, N. 2017. Therapeutic effect of quercetin in collagen-induced arthritis. *Biomed Pharmacother,* 90**,** 38-46.

MORRIS, J. L., BRIDSON, T. L., **ALIM, M. A.,** RUSH, C. M., RUDD, D. M., GOVAN, B. L. & KETHEESAN, N. 2016. Development of a diet-induced murine model of diabetes featuring cardinal metabolic and pathophysiological abnormalities of type 2 diabetes. *Biol Open,* 5**,** 1149-62.

Conference presented:

Alim et al. (2017). Oral presentation on "**Increased mycobacterial susceptibility in a murine model of type 2 diabetes"** at "The 10th International conference on the Pathogenesis of Mycobacterial infections" held in Stockholm, Sweden, 23-25 August 2017.

Alim et al. (2016). Poster presentation on "**Type 2 diabetes increases tuberculosis susceptibility** " at "Australasian Tropical Health Conference" held in Brisbane, Australia, 22-23 September 2016.

Alim et al. (2015). Poster presentation on "**Impact of type 2 diabetes on macrophage functions in mycobacterial infection**" at "Australasian Society for Immunology Conference" held in Canberra, Australia, 29 November to 03 December 2015.

ABSTRACT

Tuberculosis (TB) caused by *Mycobacterium tuberculosis* remains one of the major global health threats. The disease is responsible for significant morbidity and mortality, with an estimated one third of the world's population having latent TB infections (LTBI). Reactivation of LTBI occurs in immunocompromised individuals. Diabetes mellitus (DM) is a condition that impairs host defence, leading to higher morbidity and mortality in individuals with TB. The global burden of DM is unprecedented with 425 million people living with diabetes in 2017 and 4 million diabetes-associated deaths. Type 2 diabetes (T2D) comprises more than 90% of the global diabetes incidence and is attributed to genetic, environment and life style factors. Obesity, caused mostly by a combination of sedentary life style and consumption of an energy-dense diet rich in refined carbohydrate and fat, is considered a leading cause of the global increase of T2D. The resurgent interest in TB-T2D co-morbidity is due to the slow reduction in global TB incidence and the rapid escalation of T2D particularly in TB endemic areas. Epidemiological studies have found a strong correlation of T2D with increased TB susceptibility, reactivation of LTBI and treatment failure, however the underlying mechanisms for this are unclear. Non-tuberculous mycobacterial (NTM) infections are also increasing in individuals with diabetes in comparison to the general population. Among the NTM species, *Mycobacterium fortuitum* is a leading cause of skin and soft tissue infections and capable of causing severe pulmonary infections. There is no data available on T2D-*M. fortuitum* co-morbid conditions.

A few studies have investigated the reason for increased TB susceptibility in diabetics although the findings are often contradictory. Animal model studies designed to investigate immune dysregulation in diabetes/mycobacterium co-morbidity have typically used streptozotocin induced type 1 diabetic murine models rather than models of T2D. Hence, characterisation of a T2D murine model that incorporates the Western diet and accurately models the clinical features of human T2D is highly desirable. Such a model is also required to investigate the immunological dysfunction in host-mycobacterial co-morbid infections and thus allow the development of therapeutic and preventative strategies.

The first Aim of this study was to characterise a diet-induced diabetic mouse model of T2D for subsequent mycobacterial infection studies. Male C57BL/6 mice were used for all experiments with groups receiving either an energy-dense diet (EDD) for a period of 30 weeks to induce diabetes or a standard rodent diet (SRD) for the same time period. The metabolic and biochemical parameters including body weight, fasting blood glucose (FBG) level, glucose

tolerance test (GTT), glycated haemoglobin (HbA1c) level, urine albumin, creatinine and albumin creatinine ratio (ACR) were assessed after 25 and 30 weeks. Visceral adipose tissue, liver, pancreas and kidney from mice were analysed using a variety of histological stains and image analysis techniques. Body weight gain was increased in EDD fed mice compared to SRD fed control animals. After both 25 and 30 weeks, EDD fed mice had a significantly higher FBG levels, glucose intolerance and HbA1c levels compared to controls. Analysis of urine biochemical parameters demonstrated higher microalbumin, lower creatinine and higher ACR in EDD fed mice compared to controls. Histological examination of visceral adipose tissue, liver and pancreas revealed adipocyte hypertrophy, hepatic steatosis and a compensatory pancreatic islet hyperplasia, respectively in mice fed the EDD compared to controls. Mesangial matrix thickening within the glomeruli, thickening of the Bowman's capsules and glomerular size were increased in the kidneys of EDD fed mice compared to controls. These results suggested that feeding an EDD for 30 weeks can induce a T2D phenotype in mice. The metabolic, biochemical and histological findings demonstrated a chronic hyperglycaemic state due to insulin resistance. The urine biochemical parameters together with histological observations also confirmed renal damage which is one of the common complications of diabetes in humans.

The second Aim of this research was to investigate macrophage phagocytic function *in vitro*. In initial experiments, peritoneal exudate macrophages (PEM), resident peritoneal macrophages (RPM) and alveolar macrophages (AM) isolated from diabetic and control mice were assessed for the respective abilities to phagocytose mycolic acid coated beads and induce cytokines. Subsequently, the phagocytic uptake, bacterial killing capacity and cytokine secretion of these macrophages was assessed by co-culture with *M. fortuitum*, *M. bovis* (BCG) and *M. tuberculosis* (H37Rv). Results demonstrated that uptake of the mycolic acid coated beads was reduced significantly in PEM, RPM and AM from diabetic mice compared to controls. There were no significant differences in the production of cytokines from these cells following co-culture with the beads. However, there was a significant reduction in mycobacterial uptake and killing in both RPM and AM from the diabetic mice compared to controls. Furthermore, there was a reduction in TNF-α, MCP-1, IL-6 and IL-1β production by both RPM and AM from diabetic mice compared to controls during co-culture. These findings indicated that the uptake, killing and cytokine production were impaired in macrophages from diabetic mice compared to controls.

The final Aim of this study was to investigate the susceptibility of diabetic and control mice to *M. fortuitum*, *M. bovis* (BCG) and *M. tuberculosis* (H37Rv) infections by evaluating animal

survival, organ bacterial loads, tissue pathology and organ cytokine levels during the course of high- or low-dose intravenous infections. Diabetic mice showed higher mortality compared to controls following challenge with a high-dose of all mycobacteria. Following low-dose challenge with all mycobacteria species, the bacillary burden was higher in spleen, liver and lungs of diabetic mice compared to controls at 14 and 30/35 days post infection. Estimation of the number and size of inflammatory granuloma-like lesions in the liver, revealed increased inflammation, with higher loads of acid-fast bacilli in diabetic mice compared to controls. Furthermore, the total area of inflammation observed in the lungs of diabetic mice was significantly higher than controls. Assessment of tissue cytokines demonstrated an overall lower production of TNF-α, MCP-1, IL-6 and IL-1β in the liver and lungs of diabetic mice compared to controls although an opposite trend was observed in the spleen. The overall production of IL-12, IL-2 and IFN-γ was reduced in the spleen, liver and lungs of diabetic mice compared to controls.

In summary, this thesis describes the influence of an EDD on the induction of diabetes in a mouse model and the increased susceptibility of these diabetic animals to mycobacterial infection. It was found that the EDD has the potential to induce overt clinical features of T2D in mice that closely mirror the pathology observed in human T2D patients. Investigation of antimycobacterial immune responses (*in vitro* and *in vivo*) showed that the uptake, killing and cytokine production (TNF-α, MCP-1, IL-6 and IL-1β) by macrophages was impaired in T2D. A higher bacterial load and high numbers of inflammatory lesions were observed in the organs of diabetic mice which is also indicative of impairment of macrophage phagocytic function. Decreased production of pro-inflammatory cytokines including IL-12, IL-2 and IFN-γ in diabetic mice indicated that T helper 1 cells mediated responses in mycobacterial infections maybe delayed or impaired. This immune defect in diabetics may ultimately lead to delayed or defective granuloma formation. Our results also suggest the possibility of a breakdown of the granuloma due to the persistent hyperglycaemia that occurs in diabetes. The current study has demonstrated that antimycobacterial immunity was dysregulated in T2D mice which is one of the key reasons for increased mycobacterial susceptibility. Moreover, the diet-induced murine model of T2D that we have developed can be used for future in depth studies of host-mycobacterial susceptibility. The model can also be used to investigate other infections that are exacerbated by diabetes.

TABLE OF CONTENTS

LIST OF FIGURES

LIST OF TABLES

LIST OF ABBREVIATIONS

GENERAL

AAM	alternatively activated macrophages
ACR	albumin creatinine ratio
ADA	American Diabetes Association
AIDS	acquired immune deficiency syndrome
AL	alveolar leucocytes
AM	alveolar macrophages
ANOVA	analysis of variance
APC	allophycocyanin
APC	antigen presenting cells
ARC	animal resource centre
ATCC	American Type Culture Collection
AUC	area under the curve
BALF	broncho-alveolar lavage fluid
BCG	Bacillus Calmette-Guérin
BEI	biological exposure index
BSA	bovine serum albumin
CB	control bead
CBA	cytometric bead array
CCL	chemokine ligand
CD	cluster of differentiation
CFP	culture filtrate protein
CFU	colony forming unit
CI	confidence interval
CO_2	carbon dioxide
CR	complement receptor
DC	dendritic cells
DC-SIGN	dendritic cell specific intracellular adhesion molecule grabbing nonintegrin
DID	diet induced diabetic
DM	diabetes mellitus
DN	diabetic nephropathy
DPI	days post-infection
e.g.	for an example
EDD	energy-dense diet
EDTA	ethylenediaaminetraacetic acid
ESAT-6	early secretory antigenic target-6
ESRD	end-stage renal disease
etc.	et cetera
FA	fatty acid

FB	fresh bead
FBG	fasting blood glucose
FFA	free fatty acid
FITC	fluorescein isothiocyanate
G	Gauge
GDM	gestational diabetes mellitus
GM-CSF	granulocyte macrophage colony-stimulating factor
GSH	glutathione
GTT	glucose tolerance test
H&E	haematoxylin and eosin
Hb	haemoglobin
HBC	high burden country
HDL	high density lipoprotein
HFD	high-fat diet
HFHC	high-fat high-carbohydrate
HF-HG	high-fat high-glycaemic
HG	high glycaemic
HI-FBS	heat inactivated fetal bovine serum
HIV	human immunodeficiency virus
HOMA-IR	homeostasis model assessment insulin resistance
i.e.	that is to say or in other words
ICR	Institute of Cancer Research
IDF	International Diabetes Federation
IFG	impaired fasting glucose
IFN	interferon
IGRA	Interferon-gamma release assay
IGT	impaired glucose tolerance
IL	interleukin
iNOS	inducible nitric oxide synthase
IV	intravenous
IVC	individually ventilated cage
LAM	lipoarabinomannan
LDL	low density lipoprotein
LM	lipomannan
LN	lymph node
LPS	lipopolysaccharide
LTBI	latent tuberculosis infection
M1	classically activated macrophages
M2	alternatively activated macrophages
MACB	mycolic acid coated bead
ManLAM	mannose-capped lipoarabinomannan
MARCO	macrophage receptors with collagenous structure

MCP	monocyte chemoattractant protein
Mft	*Mycobacterium fortuitum*
MHC	major histocompatibility complex
MIC	minimum inhibitory concentration
MOI	multiplicity of infection
MR	mannose receptor
Mtb	*Mycobacterium tuberculosis*
NA	nicotinamide
NADPH	nicotinamide adenine dinucleotide phosphate
NBF	neutral buffered formalin
NCD	non-communicable diseases
NHMRC	national health and medical research council
NK	natural killer
NLR	nucleotide-binding oligomerisation domain like receptors
NOD	nucleotide-binding oligomerisation domain
NTM	non-tuberculous mycobacteria
OADC	oleic acid-dextrose-catalase
OCT	optimum cutting temperature
OD	optical density
OGTT	oral glucose tolerance test
PAMP	pathogen associated molecular pattern
PAS	periodic acid schiff
PBMC	peripheral blood mononuclear cells
PBS	phosphate buffer saline
PC2	physical containment 2
PC3	physical containment 3
PEC	peritoneal exudate cells
PEM	peritoneal exudate macrophages
PFA	paraformaldehyde
pH	potential of hydrogen
PI	post-infection
PI3P	phosphatidylinositol 3-phosphate
PIM	phosphatidyl-myo-inositol mannosides
POC	point of care
PPD	purified protein derivative
PRR	pattern recognition receptors
PTB	pulmonary tuberculosis
RBC	red blood cells
RD	regions of difference
ROI	region of interest
ROS	reactive oxygen species
RPC	resident peritoneal cells

RPEC	resident peritoneal exudate cells
RPM	rotation or revolution per minute
RPM	resident peritoneal macrophages
RT	room temperature
SAB	standard azide buffer
SABU	Small animal and breeding unit
SEM	standard error of the mean
Sp-A	surfactant protein-A
SPSS	statistical package for the social sciences
SRD	standard rodent diet
SSCM	single strength culture media
STZ	streptozotocin
T1D	type 1 diabetes
T2D	type 2 diabetes
TAG	triglycerides
TB	tuberculosis
Tc	cytotoxic T cells
TDM	trehalose 6,6′ dimycolate
TDMCB	trehalose 6, 6′-dimycolate coated beads
T_{eff}	effector T cells
Th	helper T cells
TLR	toll like receptor
T_M	memory T cells
TNF	tumor necrosis factor
Treg	regulatory T cells
USD	United States dollar
VAT	visceral adipose tissue
WHO	World Health Organisation
ZN	Ziehl Neelsen

UNITS OF TIME

hr	hour
min	minute

UNITS OF MEASURMENTS

µg	microgram
µL	microlitre
µm	micrometre

^{0}C	degrees Celsius
g	gram
IU	international unit
L	litre
M	molar
mg	milligram
mL	millilitre
mM	millimolar
nm	nanometre
pg	picogram
U	unit
xg	relative centrifugal force

SYMBOLS

%	percentage
<	less than
>	greater than
±	plus/minus
≤	less than or equal to
≥	greater than or equal to
®	registered trademark
μ	micro
n	number
α	alpha
β	beta
γ	gamma
™	trade mark

CHAPTER 1
GENERAL INTRODUCTION

The global burden of non-communicable diseases (NCD) has increased dramatically in recent decades and is now the leading cause of death globally killing more individuals than all other causes combined. With the exception of human immunodeficiency virus (HIV) disease, mortality from communicable diseases has decreased in recent years (Boutayeb, 2006, Capizzi et al., 2015, Jakovljevic and Milovanovic, 2015). The implications of the growing NCD burden on infectious disease risk are immense, with Tuberculosis (TB) at the forefront of this growing epidemic. Tuberculosis is a deadly communicable disease caused by the acid-fast bacteria; *Mycobacterium tuberculosis*. It typically affects the lungs but can disseminate to other parts of the body. The organism spreads via air droplets released during coughing, sneezing or via other respiratory fluids from individuals with active disease (Frieden et al., 2003). It is the number one leading cause of death from an infectious disease after HIV infection and remains a major cause of global mortality (WHO., 2017). While *M. tuberculosis* is responsible for the majority of mycobacterial infections, there are more than 150 non-tuberculous mycobacterial (NTM) species that are capable of causing a wide spectrum of diseases (Orme and Ordway, 2014). The NTM species are widely distributed in the environment able to cause diseases affecting a variety of tissues including lungs, lymph nodes, skin, soft and skeletal tissues. Some of these species can also cause respiratory disease (De Groote and Huitt, 2006, Jackson et al., 2007, Hoefsloot et al., 2013). The rapid escalation of immune suppressing NCD has contributed to the growing risk of TB and NTM infections. Diabetes is one of the NCD conditions considered a major risk factor for increased TB and NTM susceptibility (Jeon and Murray, 2008, Martinez and Kornfeld, 2014, Bridson et al., 2016).

Diabetes mellitus (DM), in particular, type 2 diabetes (T2D) is a multifactorial metabolic disease. It is characterised by a hyperglycaemic state due to insulin resistance in peripheral tissues or inadequate secretion of insulin from the pancreatic β-cells (Weyer et al., 1999, ADA., 2010). The key factors that contribute to the development of T2D include dietary factors, sedentary lifestyle, obesity, smoking, generous consumption of alcohol, older age, stress, ethnicity, prior history of glucose intolerance (genetic) and gestational diabetes (Hu et al., 2001, Smyth and Heron, 2006, Sobngwi et al., 2008). Obesity is considered one of the foremost risk factors for developing T2D (Walley et al., 2006). The principal cause behind the rapid rise in

global obesity is the nutritional shift towards an energy-dense diet (EDD) with excess consumption of refined carbohydrate and increased fat (Popkin and Nielsen, 2003, Morris et al., 2016). The high glycaemic index diet associated with persistent hyperglycaemia results in the deposition of advanced glycation end products in tissues and cells, leading to oxidative stress, chronic inflammation, immune defects and microvascular (e.g. retinopathy, nephropathy and neuropathy) and macrovascular complications (e.g. atherosclerosis, cardiovascular diseases) (Shah and Hux, 2003, Leutholtz and Ripoll, 2011). The disease also increases susceptibility to infections resulting in a higher morbidity and mortality in diabetic individuals (Martinez and Kornfeld, 2014, Hodgson et al., 2015).

The global burden of TB and T2D is alarming. An estimated one-third of the world's population is infected with *Mtb*. New infections occur in about 1% of the population each year (WHO., 2015). In 2016, there were an estimated 10.4 million people with active TB (including 10% TB-HIV patients). TB killed an estimated 1.3 million people (without TB-HIV related mortality) of those afflicted in 2016. Furthermore, there are 2 billion latent TB infections with 5-10% reactivating every year (WHO., 2017). In contrast, the global burden of T2D has increased markedly over the past 50 years. In 2017, approximately 425 million people were living with the disease compared to around 30 million in 1985 (Smyth and Heron, 2006, IDF., 2017). The disease is predicted to afflict 629 million people by 2045 (IDF., 2017). The association between these two diseases has co-existed for many thousands of years (Kapur et al., 2013). The resurgent interest in this co-morbidity is due to the sluggish reduction of global TB incidence (2.2% reduction annually) (WHO., 2013a) along with the worldwide rapid escalation of T2D in TB affected people (Hodgson et al., 2015, Workneh et al., 2017). Several epidemiological studies have shown that T2D is one of the strongest risk factors for TB susceptibility or its reactivation. Particularly, in low-income countries, malnutrition and diabetes are key factors impeding the reduction of the global TB burden. T2D confers a three-eight times higher susceptibility for developing active TB in comparison to non-diabetics (Restrepo et al., 2007, Jeon and Murray, 2008). There is also growing evidence of an increased prevalence of NTM infections in immunocompromised HIV and diabetic patients (Tortoli et al., 1995, Piersimoni et al., 1997, Gholizadeh et al., 1998, Uslan et al., 2006, Orme and Ordway, 2014, Bridson et al., 2016, Xu et al., 2016). A recent retrospective review of 20 years Townsville (Australia) hospital data showed that NTM infections in diabetic patients were three times over-represented in comparison to the general population (Bridson et al., 2016). According to the available epidemiological data relating to NTM, 16.7% of patients with soft tissue infection with *M.*

fortuitum had co-morbid diabetes (Uslan et al., 2006). Despite the high TB burden and rising incidence of NTM infections such as *M. fortuitum*, the underlying mechanisms for the increased susceptibility of T2D patients is still not clear. In order to develop strategies to prevent TB and other NTM infections in individuals affected by T2D, research is required to explore the reasons for increased mycobacterial susceptibility in these individuals.

Previous studies have demonstrated increased mortality in TB-DM comorbid patients (Oursler et al., 2002, Lindoso et al., 2008, Dooley et al., 2009, Wang et al., 2009). Patients with TB-DM co-morbid infections have increased bacterial burden in sputum and bacterial clearance requires a significantly longer treatment period than in non-diabetic TB patients (Restrepo et al., 2008b, Dooley et al., 2009, Wang et al., 2009). The few studies that investigated cellular immunity in TB-DM co-morbid infections have shown depressed cellular immunity (Goonetilleke et al., 2003, Niazi and Kalra, 2012). Fewer T lymphocytes with reduced production of IFN-γ, TNF-α, IL-1β and IL-6 were also seen among people with concomitant diabetes and TB compared to non-diabetic individuals (Tsukaguchi et al., 1997, Geerlings and Hoepelman, 1999, Stalenhoef et al., 2008). However, conflicting reports have suggested that there is either no difference (Zhang et al., 2012), or even higher production (Legesse et al., 2013) of T helper 1 (Th1) cells specific IFN-γ in diabetic compared to non-diabetic TB patients. Kumar and colleagues (2013) reported that there was the heightened production of type 1 (IFN-γ, IL-2, TNF-α), type 2 (IL-5), type 17 (IL-17A) and other pro-inflammatory cytokines (IL-1 β, IL-6, IL-18) in chronic TB-DM patients. The few studies that have evaluated phagocytic functions in peripheral blood mononuclear cells (PBMCs), observed reduced phagocytosis and killing (Hill et al., 1983, Glass et al., 1987, Chang and Shaio, 1995, Geerlings and Hoepelman, 1999, Restrepo et al., 2008a, Lecube et al., 2011, Tan et al., 2012). To our knowledge, there have been no studies assessing cellular immunity in T2D-*M. fortuitum* infections.

Several previous studies have used streptozotocin (STZ)/STZ+NA (Nicotinamide)-induced type 1 diabetes (T1D) animal models to explore the mechanisms underlying the increased TB susceptibility seen in diabetics (Saiki et al., 1980, Sugawara et al., 2004, Yamashiro et al., 2005, Martens et al., 2007, Vallerskog et al., 2010, Podell et al., 2014, Cheekatla et al., 2016). Saiki and colleagues (1980) first reported increased mortality in STZ-induced T1D mice following *M. tuberculosis* infection and proposed that functional alterations in macrophages was one explanation for increased mortality. Martens and colleagues (2007) reported *M. tuberculosis* defence was impaired in chronic diabetic mice (16 weeks post-infection) after an aerosol

infection in T1D mice. Others reported reduced production of IL-12, IFN-γ as well as impaired development of Th1 cells responses as a reason of impaired host resistance against *M. tuberculosis* infection in diabetic mice (Yamashiro et al., 2005, Vallerskog et al., 2010). A recent study observed increased levels of IFN-γ, TNF-α, IL-1β, IL-6 and MCP-1 (monocyte chemoattractant protein-1) in the lungs of STZ+NA-induced diabetic mice 6 months after aerosol infection with *M. tuberculosis,* although the opposite trend was found earlier in infection (Cheekatla et al., 2016). The previous animal model studies provided no information as to the impact of diabetes on the phagocytic functions of macrophages particularly the alveolar macrophages (AM). AM are amongst the first immune cells to interact with bacteria in infected host (Cooper, 2009). However, several previous studies in STZ/STZ+NA-induced diabetic animal models mentioned above evaluated antimycobacterial immunity in chronic *M. tuberculosis* infection. These studies observed a higher bacterial burden, increased inflammatory lesions and heightened production/expression of various pro-inflammatory cytokines in diabetics than controls. Although these studies provided substantial information on the effect of hyperglycaemia on chronic TB susceptibility, there is lack of information of how T2D impairs antimycobacterial immunity during early mycobacterial infections.

The first section of this thesis describes the development and characterisation of a diet-induced diabetic (DID) murine model of T2D. Hodgson and colleagues (2013a) first described the suitability of a 10 weeks energy-dense diet (EDD, 23% fat, 19% protein, 50.5% dextrose, 7.5% fibre) for the induction of diabetes in mice. In the current study, we extended these findings to discover the biochemical, metabolic, pathological consequences of this diet and propose that this model accurately mimics many of the overt biochemical and clinical features of T2D. In the subsequent chapters of this thesis, this murine diabetes model is used to investigate antimycobacterial immunity *in vitro* and in *vivo* during *M. fortuitum*, *M. bovis* (Bacillus Calmette–Guérin; BCG) and *M. tuberculosis* (H37Rv) infections.

The broad Aims investigated in this thesis are:

1. To investigate whether an energy-dense diet can induce T2D in mice (Chapter 4)
2. To determine the phagocytic function of macrophages from T2D mice infected with *M. fortuitum*, *M. bovis* (BCG) and *M. tuberculosis* (H37Rv) *in vitro* (Chapter 5)
3. To evaluate whether antimycobacterial immunity is dysregulated in T2D mice infected with *M. fortuitum*, *M. bovis* (BCG) and *M. tuberculosis* (H37Rv) *in vivo* (Chapter 6, 7 and 8)

CHAPTER 2
LITERATURE REVIEW

2.1 Overview of mycobacterial infections

2.1.1 Tuberculosis: The disease

Tuberculosis (TB) is an often fatal infectious disease caused by various strains of mycobacteria, usually *Mycobacterium tuberculosis* (*Mtb*) (Kumar, 2007). The disease most commonly affects the lungs (about 90% of cases) and is known as pulmonary TB (PTB). In 15-20% of cases of active PTB, the organism may spread to other parts of the body and is known as extrapulmonary TB. This is more common in immunosuppressed individuals (e.g. HIV patients) and children (Golden and Vikram, 2005, Lawn and Zumla, 2011). The symptoms of active TB include chronic cough (lasting more than 2 weeks), haemoptysis, fever, night sweats, weight loss. Most infections with *Mtb* do not produce any clinical signs and are termed latent TB infection (LTBI). Diagnosis can be made based on clinical history, radiological findings and microbial assays (McFadden, 1982). Latent infection can be confirmed by immunological tests, including the tuberculin skin test (TST) and interferon-γ release assay (IGRA) (Al-Orainey, 2009). The therapeutic regimen comprises the use of several antibiotics for 3 to 6 months or longer. The only recommended vaccine for TB protection is the *Mycobacterium bovis* Bacillus Calmette–Guérin (BCG) vaccine (Andersen and Kaufmann, 2014).

2.1.1.1 The bacterium

Mycobacterium tuberculosis (*Mtb*) is in the family Mycobacteriaceae and was discovered by Robert Koch in 1882. The bacterium measures around 1-4 μm long and 0.3-0.6 μm in diameter (Ducati et al., 2006). It does not have a flagellum or a capsule (Figure 2.1 A). *Mtb* can be grown on simple media composed of inorganic salts, asparagine and glycerol. It is an obligate aerobe and strictly mesophilic showing little or no growth below 30^0C or higher than 39^0C. The bacterium is a very slow grower and cell division takes 12 to 20 hours. Culturing the bacterium requires a prolonged period of 2 to 6 weeks. Several different colony morphologies may be seen on solid media, including smooth or rough and opaque or transparent colonies (Figure 2.1 B). In liquid media, the cells clump and float to the surface unless a detergent is added (McFadden, 1982, Kassim, 2004).

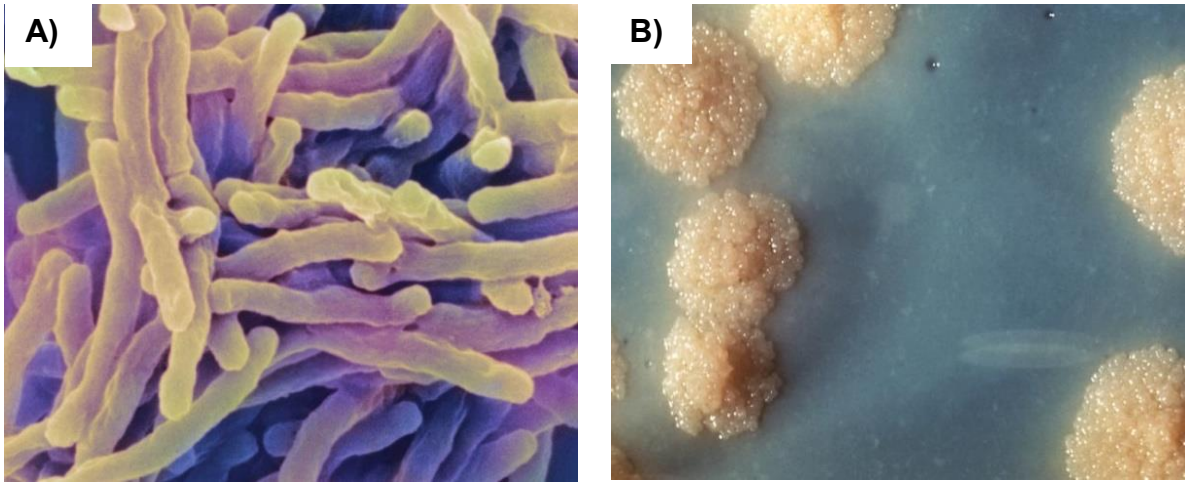

Figure 2.1 Morphology of *Mycobacterium tuberculosis*

Figure illustrates the morphology of *Mycobacterium tuberculosis* under the electron microscope (A) and an example of colony morphology (e.g. rough) on solid media (B) (Kubica, 1976, Jabado and Gros, 2005).

M. tuberculosis is a member of the *M. tuberculosis* complex. This group also comprises *M. bovis, M. canetti, M. africanum, M. microti and M. pinnipedii* as well as *M. caprae* which is considered a variant of *M. bovis*. *M. tuberculosis* was believed to have evolved from *M. bovis* during the domestication of cattle (Stead et al., 1995). Genomic data of *M. bovis* (BCG) and *M. tuberculosis* has shown that *M. bovis* (BCG) has 99.95% homogeneity with *M. tuberculosis* species with several DNA deletions known as the regions of difference (RD) (Brosch et al., 2002). Furthermore, a whole genome study has also suggested that member of the *M. tuberculosis* complex originated from *M. canetti,* also referred to as *M. prototuberculosis* (Gutierrez et al., 2005).

2.1.1.2 Cell wall of *Mycobacterium tuberculosis*

The cell wall of *Mtb* uniquely consists of a thick layer of mycolic acids (Figure 2.2). This waxy layer is found at the external portion of the cell wall and is linked with arabinogalactan, which is further lined with a peptidoglycan layer. Additionally, the cell wall also possesses several lipoglycans comprising lipoarabinomannan (LAM), lipomannan (LM) and phosphatidyl-myo-inositol mannosides (PIM). All these structures are attached non-covalently to the plasma membrane (Briken et al., 2004, Ducati et al., 2006). Lipoarabinomannan consists of a phosphatidyl-myo-inositol anchor, D-mannan polymer (attached to the inositol ring), D-arabinose chains and capping motifs at the end of the arabinose residues (Vergne et al., 2003).

This lipoglycans acts as a virulence factor and inhibits of macrophage functions, particularly phagosomal maturation. It also interferes with cell signalling and alters cytokine responses from pro- to anti-inflammatory (Nigou et al., 2001, Briken et al., 2004, Pathak et al., 2005, Vergne et al., 2005a). In addition, all slow growing pathogenic mycobacteria including *Mtb* also possess a heterogenous lipoglycan structure termed 'mannose-capped LAM (ManLAM) in their cell wall. Rapidly growing mycobacteria contain non-capped AraLAM or phospho-myo-inositol-capped LAM (PILAM) which can initiate immunostimulatory effects (Dao et al., 2004). Phosphatidyl-myo-inositol mannosides are divided into two groups depending on the mannose content that determine immunogenic effects. These structures may also be present on the cell surface as mannoglycoproteins which are secreted during growth (Villeneuve et al., 2005, Torrelles et al., 2009).

.

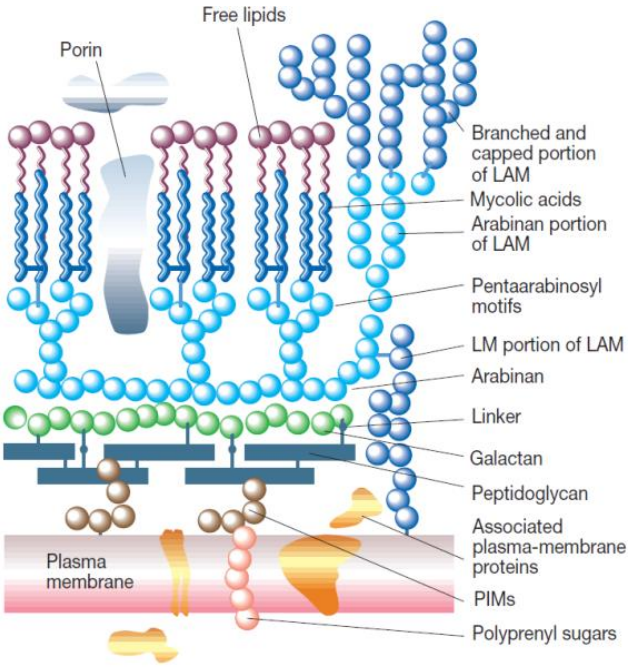

Figure 2.2 Schematic representation of the cell wall of *Mycobacterium tuberculosis* (Park and Bendelac, 2000)

2.1.1.3 Transmission and outcomes of *Mycobacterium tuberculosis* infection

Tuberculosis is transmitted by the inhalation of droplet nuclei (1-5 µm in diameter) containing a small number of organisms (as few as 10 bacilli). These droplet nuclei are released by a person with active TB during coughing, sneezing, singing or talking. A cough can release 3000 droplet nuclei, whereas a sneezing can generate as many as 40,000 droplet nuclei (Frieden et al., 2003, Nicas et al., 2005). These minute droplet nuclei can remain suspended in the air for several minutes to an hour allowing spread to other persons (Frieden et al., 2003, Ahmed and Hasnain,

2011). The spread of *Mtb* from an individual within a community depends on several factors such as the number of droplet nuclei inhaled, extent of exposure to the infected patients, crowding, weather conditions and the immune status of the individual (Frieden et al., 2003, Ahmed and Hasnain, 2011). A person with active but untreated TB reportedly may infect 10-15 (or more) other people per year (WHO., 2013a). Fortunately, the infected person with nonresistant active TB cannot be a source of infection within 2 weeks following the commencement of an effective treatment (Ahmed and Hasnain, 2011).

Transmission of *Mtb* leads to one of three possible consequences for an individual. Firstly, bacteria can be eliminated with no disease state. Secondly, bacteria continuously multiply and the disease progresses actively with clinical manifestations of active TB (Madigan, 2002). The third and final possibility is the dormant state of the TB or latent tuberculosis infection (LTBI), where viable bacilli are present in the host but do not cause active disease (Flynn and Chan, 2001b, Ahmad, 2011). The latent infection might be the result of an effective immune response of the host with granuloma formation or use of an effective chemotherapeutic regimen. Moreover, primary infection by *Mtb* has been reported to be eradicated in only 10% people upon treatment, with the remaining 90% unable to completely clear the bacteria resulting in LTBI (Richard, 2011). Annually, 5-10% of LTBI can be reactivated, particularly in immunosuppressed individuals to cause active disease (Flynn and Chan, 2001b).

2.1.1.4 Immunopathogenesis of tuberculosis

2.1.1.5 Innate immunity and host defence

The innate immune response plays an important role in the protection against *Mtb* infections. This response provides the first line of defence against the invading pathogens and is successful in clearing the infection if it is activated properly. The response initially clears the bacilli by receptor mediated phagocytosis and triggers the adaptive immune responses for effective control of the infection. However, the cells of the innate immune system are also a prerequisite for mycobacterial pathogenesis as the bacterium has the ability to manipulate macrophage functions, enabling survival and replication in the host cells.

2.1.1.5.1 Entry of the organism

Mtb infections start with the inhalation of aerosol droplet nuclei containing tubercle bacilli from an infected individual (Sakamoto, 2012). The inhaled bacilli travel to the lungs' alveoli, where

the primary encounter is initiated by alveolar macrophages (AM) (Dheda et al., 2010). Following the initial encounter, cells such as dendritic cells and monocyte-derived macrophages also participate in the phagocytic process (Henderson et al., 1997, Thurnher et al., 1997). These initial host-pathogen interactions lead to activation of adaptive immune responses and determine whether the infection will become localised (within a granuloma) or continue to spread (Lawn and Zumla, 2011, Natarajan et al., 2011).

2.1.1.5.2 Immune recognition of *Mycobacterium tuberculosis*

The interactions between mycobacterial components and host cells are important for mounting effective immune responses. The process of recognition of *Mtb* by the host cells plays a central role in initiation and coordination of the innate immune system (Akira et al., 2006). These interactions not only activate innate immune mechanisms, but also assist in the development of antigen specific adaptive immunity. After the entry of *Mtb*, the recognition of the bacilli begins via pattern recognition receptors (PRRs) of alveolar macrophages (AM). These PRRs recognise the pathogen associated molecular patterns (PAMP) such as outer coat mannosylated lipoarabinomannan (ManLAM), trehalose dimycolate and N-glycolymuramyl dipeptide. The *Mtb* components are also recognised by the other host receptors comprising Toll like receptors (TLRs), nucleotide-binding oligomerisation domain (NOD) like receptors (NLRs) and C-type lectins (Ahmad, 2011). C-type lectins include mannose receptors (CD207), dendritic cell specific intracellular adhesion molecule grabbing nonintegrin (DC-SIGN) and Dectin (Jo, 2008, Harding and Boom, 2010).

Toll like receptors (TLRs) are important molecules for initiating effective innate immune responses during *Mtb* infections (Jo, 2008, Harding and Boom, 2010). They are essential for microbial recognition by macrophages and dendritic cells (Belvin and Anderson, 1996, Medzhitov et al., 1997, Visintin et al., 2001). To date, 10 human TLRs have been identified, of these, TLR2, TLR4, TLR9 and possibly TLR8 are involved in recognising *Mtb*. The dimer of TLR2 in combination with either TLR1 or TLR6 can recognise the mycobacterial cell wall's glycolipids including LAM, LM, 19 kDa and 38 kDa glycoprotein, phosphatidylinositol mannoside (PIM) and triacylated (TLR2/TLR1) or diacylated (TLR2/TLR6) lipoproteins (Jones et al., 2001, Means et al., 2001, Thoma-Uszynski et al., 2001). The interaction of *Mtb* components with TLRs eventually activates nuclear transcription factors kappa B (NF-kB) which stimulates the cells to produce pro-inflammatory cytokines, chemokines and nitric oxide through MyD88 dependent (myeloid differentiation primary response protein 88) or

independent pathways (Garcia-Perez et al., 2003, Yamamoto et al., 2003, Jo, 2008). For example, TLR2 activates macrophages to produce TNF-α (Underhill et al., 1999, Bafica et al., 2005) and IL-12 (Pompei et al., 2007). Furthermore, activation of TLR2 and TLR6 can also stimulate macrophages to secrete IL-1β (Kleinnijenhuis et al., 2009). An *in vitro* study demonstrated that TLR2 activation can directly lead to the killing of intracellular *Mtb* in AM (Thoma-Uszynski et al., 2001). However, excessive TLR induced pro-inflammatory cytokine responses are harmful for the host and can be mitigated by tyrosine kinases termed Tyro3/As/Mer (TAM). TAM provides a negative feedback to TLRs to suppress pro-inflammatory cytokine production (Hernandez-Pando et al., 2000). Further, the 19 kDa lipoprotein of *Mtb* is also a potential agonist of TLR2 which can modulate innate immunity by interfering with antigen presenting cell function (Noss et al., 2001). Interestingly, mycobacterial infection and pro-inflammatory cytokine release increases surface expression of TLR2 (Wang et al., 2000). Studies have shown binding of TLR2 by the mycobacterial lipoproteins (19-kDa) may inhibit antigen processing by macrophages and expression of Major Histocompatibility Complex (MHC) II (Fulton et al., 2004, Pai et al., 2004b). Consequently, infected macrophages fail to present *Mtb* antigens to T cells (CD4+ or CD8+ T cells) resulting in an opportunity for the organism to survive (Noss et al., 2001, Jo, 2008).

C-type lectins of PRRs are involved in the recognition of polysaccharide structures of *Mtb*. The mannose receptor (MR; CD206) is highly expressed on AM (Gordon, 2003). It interacts with ManLAM of the cell wall component of *Mtb*. Endocytosis of *Mtb* bacilli by the macrophage via the stimulation of the MR leads to the production of anti-inflammatory cytokines (IL-4 and IL-13) which interfere with phagosome-lysosome fusion (Hernandez-Pando et al., 2000, Nigou et al., 2001, Hmama et al., 2004, Kang et al., 2005). Further, ManLAM can also inhibit MR dependent IL-12 production which is essential for T cells priming. These inhibited macrophage responses result in failure to control the infection. As a result, the organism is able to survive in the macrophage (Nigou et al., 2001, Kang et al., 2005).

Dendritic cell specific intracellular adhesion molecule grabbing nonintegrin (DC-SIGN) is another membrane bound PRR which plays an important role in *Mtb*-dendritic cells interactions. It is predominantly expressed on dendritic cells and influences cell migration and T cell interactions (Geijtenbeek et al., 2000a, Geijtenbeek et al., 2000b). After interaction with *Mtb* components, DC-SIGN initiates an anti-inflammatory immune response stimulating the secretion of IL-10 following the maturation of infected dendritic cells (Geijtenbeek et al., 2003).

Dectin-1 is another PRR which is mainly expressed on macrophages, dendritic cells, neutrophils and a subset of T cells suggesting that it may also play a significant role in *Mtb* recognition (Dinadayala et al., 2004). Moreover, dectin-1 has been observed to stimulate bone marrow-derived macrophages of mice to produce TNF-α and IL-6 in a dectin-1-independent or dectin-1-dependent manner, respectively (Yadav and Schorey, 2006). It has also been shown to trigger IL-12 production (Rothfuchs et al., 2007).

Another group of intracellular PRRs are the NOD like receptors (NLRs), which bind bacterial cell wall muramyl-dipeptides and initiate the secretion of TNF-α, IL-1β, IL-6 and bactericidal IL-37 (Brooks et al., 2011, Juarez et al., 2012). Other receptors such as complement receptors, scavenger receptors, surfactant protein A receptors (Sp-A) and cholesterol receptors are also required for optimal *Mtb* recognition resulting in effective phagocytosis of the bacteria (El-Etr and Cirillo, 2001).

2.1.1.5.3 Role of innate immune cells

Apart from macrophages and dendritic cells, neutrophils and natural killer (NK) cells have also participated in the immune defence against *Mtb* infections (Natarajan et al., 2011).

2.1.1.5.3.1 Macrophage: receptor mediated phagocytosis

Macrophages play numerous important roles during host-*Mtb* interactions. These cells are primarily involved in phagocytosis and killing of the mycobacteria. They also initiate adaptive T cell mediated immunity to protect against *Mtb* infections (Kleinnijenhuis, 2011). Phagocytosis of *Mtb* bacilli involves different receptors such as complement receptors (CR), mannose receptors (MR), scavenger receptors and Fcγ receptors (FcγR) (Schlesinger et al., 1990, Roecklein et al., 1992, Hirsch et al., 1994). Receptor mediated phagocytosis of bacilli occurs either by opsonisation (CR with antibodies) or by a non-opsonisation mechanism. This determines the subsequent events in cells as well as the ultimate fate of infections in the host (Pieters, 2008). Macrophage-*Mtb* interactions during phagocytosis involve several receptors (Ernst, 1998) some of which are presented here.

2.1.1.5.3.1.1 Complement receptors

In general, the complement system is activated by antibody complexes or microbes. These complement proteins have roles in opsonising the invading pathogens, chemotaxis, clumping of antigens and lysis of microbial cells. There are several receptors present on the cell surface

of macrophages including CR1 (binds with C3b and C4b), CR3 and CR4 (binds with C3bi and glucan) which facilitate the recognition of complement-opsonised and occasionally un-opsonised pathogens (Ernst, 1998). Macrophage-*Mtb* interactions activate the alternative pathway of the complement system and initiate opsonisation with subsequent C3b and C3bi mediated uptake. *Mtb* can recruit opsonically active C3b without triggering the complement cascade or non-opsonically by binding with C3bi or β-glucan binding domain of CR3 (Schlesinger, 1993, Hirsch et al., 1994, Cywes et al., 1996, Cywes et al., 1997). An i*n vitro* study has shown that CR3 mediates approximately 80% of complement-opsonised *Mtb* phagocytosis (Schlesinger et al., 1990). In contrast, non-opsonic phagocytosis occurs during primary infection in the lungs as complement factors are mostly absent in the alveolar space (Schluger, 2001).

2.1.1.5.3.1.2 Mannose receptors

Fully differentiated macrophages carry the mannose receptor (MR) for phagocytosis of *Mtb*. The MR binds with glycosylated molecules with terminal mannose, fucose or N-acetylglucosamine motifs of *Mtb* which initiate uptake of bacilli either by phagocytosis or pinocytosis. One study showed that the MR alone was not sufficient for phagocytosis, suggesting that other receptors are also required for effective phagocytosis (Le Cabec et al., 2005). Furthermore, signalling events for ligation of MR with the bacilli are poorly characterised, but phagocytosis is mediated by reactive oxygen species (ROS) production upon ligation. This MR ligation can be downregulated by a high level of IFN-γ. Therefore, this receptor is believed to function effectively immediately after the infection, before the onset of T helper 1 (Th1) cells mediated adaptive immune responses (Ernst, 1998, van Crevel et al., 2002)**.** However, this receptor mediated phagocytosis is essential particularly for virulent *Mtb* strains because the bacilli carry mannose-capped ManLAM on their surface to interact with MR (Schlesinger, 1993, Kang and Schlesinger, 1998, Kang et al., 2005).

2.1.1.5.3.1.3 Fcγ receptors

Fcγ receptor mediated phagocytosis particularly occurs during the humoral immune responses. This receptor on the macrophages binds with IgG-opsonised *Mtb* leading to a higher level of phagolysosomal fusion in macrophages (Armstrong and Hart, 1975) and rapid (10-12 minutes) acidification (pH 5) of the phagosome to provide for effective killing of bacilli (Divangahi et al., 2008). Furthermore, FcγR-mediated phagocytosis can also lead to reactive oxygen species (ROS) production and initiate pro-inflammatory responses, suggesting that this pathway is

beneficial for the host in mounting effective macrophage responses against *Mtb* (Caron and Hall, 1998, de Valliere et al., 2005).

2.1.1.5.3.1.4 Additional receptors

In addition to these three major receptors (described above), other receptors or proteins are also present on the macrophage surface for interaction with the *Mtb*. Surfactant proteins in the lungs can coat the bacilli and facilitate either recognition by the surfactant protein receptors on the macrophage (Pasula et al., 1997) or alteration of the uptake mechanism (Gaynor et al., 1995) and thus interfere with MR activity (Berrington and Hawn, 2007). Scavenger receptors on macrophages can bind to sulpholipids and CD14 with LAM of *Mtb* leading to recognition of bacilli for phagocytosis (Ernst, 1998, Berrington and Hawn, 2007).

2.1.1.5.3.1.5 Cytokine and chemokine response of macrophages

Macrophage-*Mtb* interactions result in the secretion of various cytokines and chemokines (Table 2.1). Macrophage polarisation determines the outcomes of the host responses and subsequent elimination of *Mtb* (Benoit et al., 2008). The classically activated macrophage (M1) stimulated by the microbial products or IFN-γ leads to the production of pro-inflammatory cytokines (e.g. TNF-*α*, IL- 1β, IL-12, IL-15, IL-23, IFN-γ) (Doherty et al., 1996, Wang et al., 1999, Verreck et al., 2004, Verreck et al., 2006). In contrast, the non-classically activated macrophage (M2) lacks antimicrobial activity and fails to produce IL-12. The later subsets have a poor antigen presenting capability and also suppress cellular immunity by producing anti-inflammatory cytokines (e.g. IL-10, IL-6, IL-4, TGF-β) (VanHeyningen et al., 1997, Guyot-Revol et al., 2006, Verreck et al., 2006). In addition to the cytokine response, chemokines comprising MCP-1 (monocyte chemoattractant protein-1), MCP-3, MCP-5, RANTES (regulated on activation, normal T cells expressed and secreted) and IFN-γ induced protein 10 kDa from macrophages are crucial for protection against *Mtb* infections (Flynn and Chan, 2001a, Raja, 2004). The specific role of major pro- and anti-inflammatory cytokines and chemokines produced by macrophages (also by other cells) in *Mtb* infection are presented in Table 2.1.

2.1.1.5.3.2 Neutrophils

Neutrophils are one of the first cells to arrive at the site of infection after the initial attack of *Mtb* by AM (Korbel et al., 2008). They can kill the *Mtb* pathogens using a wide range of antimicrobial molecules present in the granules including defensins, lactoferrin, cathelicidin

and lysozyme. These substances are transferred into the phagosome upon fusion (Faurschou and Borregaard, 2003, Martineau et al., 2007, Korbel et al., 2008) allowing the cells to efficiently kill the bacilli in the phagosome using an assembly of NADPH (nicotinamide adenine dinucleotide phosphate) oxidase. This process leads to the production of superoxide and ROS (Faurschou and Borregaard, 2003). Neutrophils subsequently activate macrophages through the release of granule protein (Tan et al., 2006) and heat shock protein 72 (Hsp72). The Hsp72 from apoptotic neutrophils is able to activate macrophages, even though the protein has an inflammation resolving role (Persson et al., 2008). Several studies have documented contradictory evidence suggesting that neutrophils have either protective or tissue-damaging effects during *Mtb* infections (Martineau et al., 2007, Korbel et al., 2008, Persson et al., 2008).

2.1.1.5.3.3 Natural Killer cells

Natural killer cells are granular lymphocytes that have cytotoxic functions. These cells carry out their functions through granules containing perforin and granzyme or granulysin (Korbel et al., 2008) and activate macrophages through IFN-γ secretion during *Mtb* infections (Junqueira-Kipnis et al., 2003, Ducati et al., 2006). These cells can directly lyse the *Mtb* infected macrophages and restrict *Mtb* growth by mounting pro-inflammatory responses (Korbel et al., 2008). One study reported that NK cells can kill regulatory T cells (Treg) that can dampen the immune responses to *Mtb* infections (Roy et al., 2008). However, the exact role of NK cells in TB defence is still imprecise. Prior study has shown that NK cells defects in TB patients were found to be effective (Raja, 2004).

Table 2.1 Cytokine and chemokine production in *Mycobacterium tuberculosis* infection

Pro-inflammatory cytokines		
Cytokines	**Source/Cells**	**Functions**
TNF-α	Monocytes, macrophages, dendritic cells (Valone et al., 1988), CD4+ T cells (Silva Miranda et al., 2012)	-Pro-inflammatory responses -Activation of macrophagess and neutrophil (Orme and Cooper, 1999, Tsenova et al., 1999, Gan et al., 2005) -Organises granuloma formation (Kindler et al., 1989, Flynn et al., 1995, Senaldi et al., 1996) -Containment of latent infections in granuloma (Mohan et al., 2001) -Lack of TNF-α increases susceptibility to infection resulting higher organ bacterial load (Benoit et al., 2008)
IL-1β	Monocytes, macrophages and dendritic cells (Roach et al., 1993, Dahl et al., 1996)	-Granuloma formation (Fantuzzi and Dinarello, 1996, Juffermans et al., 2000) -Stimulates macrophages to produce TNF-α, IL-6 (Toossi et al., 1990) and IFN-γ (Juffermans et al., 2000)
IL-12	Macrophages, dendritic cells (Bermudez et al., 1992, Ladel et al., 1997b)	-Differentiation of Th1 cells for IFN-γ production (Sieling et al., 1994, Cooper et al., 1995, Trinchieri, 1995, O'Neill and Greene, 1998) -Increases proliferation of cytotoxic T (Tc) cells and NK cells (Bertagnolli et al., 1992)
IL-18	Peripheral blood mononuclear cells (Vankayalapati et al., 2000)	-Induces IFN-γ, synergise with IL-12 (O'Neill and Greene, 1998, Sugawara et al., 1999)
IL-15 (IL-2)	Monocytes, macrophages, CD4 T cells (Jullien et al., 1997)	-Stimulates T cells and NK cells proliferation and activation (Doherty et al., 1996, Kennedy and Park, 1996)
IFN-γ	CD4+ T cells (Th1), CD8+ T cells, NKT cells (Martinez et al., 2009), alveolar macrophages (Wang et al., 1999), NK cells in response to IL-12 and IL-18 (Iho et al., 1999)	-Initiates antigen specific cellular immunity (Andersen, 1997) -Activate macrophages and increases expression of MHC class II molecules (Fulton et al., 2004, Herbst et al., 2011) -Induction of reactive oxygen species and nitric oxide synthase for bacterial killing (Martinez et al., 2009)
IL-17	Lymphocytes γ/δ, CD4+ T cells (Th17) (Ouyang et al., 2008)	-Involved in the recruitment of leucocytes and initial granuloma formation (Ouyang et al., 2008) -Stimulates neutrophils to produce IL-6, IL-8 and granulocyte-macrophage colony-stimulating factor (GM-CSF) (Fossiez et al., 1996) - Acts synergistically with TNF-α (Ruddy et al., 2004) and produces IL-17A, IL-17F, IL-21 and IL-22 (Diveu et al., 2008, Dong, 2008)
Anti-inflammatory cytokines		
IL-10	Macrophages (Shaw et al., 2000), Treg cells, alternatively activated	-Anti-inflammatory responses -Suppresses Th1 cells responses (Hirsch et al., 1999a)

	macrophage (AAM), reactive T cells (Barnes et al., 1993, Boussiotis et al., 2000)	-Downregulation of IFN-γ, TNF-α and IL-12 production (Gong et al., 1996, Fulton et al., 1998, Hirsch et al., 1999a)
TGF-β	Monocytes, dendritic cells (Toossi et al., 1995), Treg cells, AAM (Guyot-Revol et al., 2006)	-Anti-inflammatory responses -Suppresses T cells to produce IFN-γ (Hirsch et al., 1999a) -In macrophages, it antagonises antigen presentation, pro-inflammatory cytokine production and cellular activation (Toossi and Ellner, 1998) -Involved with tissue damage and fibrosis (Hernandez-Pando et al., 2004) -Acts synergistically with IL-10 to suppress IFN-γ production (Othieno et al., 1999)
IL-6	Macrophages (VanHeyningen et al., 1997)	-Pro and anti-inflammatory responses (VanHeyningen et al., 1997) -Inhibits the production of TNF-α and IL-1β (Schindler et al., 1990, Denis and Gregg, 1991, Bermudez et al., 1992) -Suppresses T cells proliferation and IL-2 production (VanHeyningen et al., 1997)
IL-4	AAM (Verreck et al., 2006)	-Suppresses of IFN-γ production by downregulation of Th1 cells responses (Powrie and Coffman, 1993, Lucey et al., 1996, Biedermann et al., 2001) -Inhibits macrophage activation (Appelberg et al., 1992, de Waal Malefyt et al., 1993) -Overexpression of it involves with tissue damage/cavitation (Lukacs et al., 1997, van Crevel et al., 2000)
Chemokines		
IL-8 (CXCL8)	AM, epithelia cells of the lungs (Zhang et al., 1995, Juffermans et al., 1999)	-Recruits neutrophils (Zhang et al., 1995, Juffermans et al., 1999)
(MCP-1) /CCL2	Monocytes, macrophages (Kasahara et al., 1994)	- Recruits macrophages and other immune cells (Peters et al., 2001) -Required for granuloma formation (Lu et al., 1998) -Suppressed Th1 type cytokine production (Boring et al., 1997)
RANTES /CCL5	Wide variety of cells and macrophages (Chensue et al., 1999)	-Recruits macrophages and other immune cells - Associated with granuloma formation (Floto et al., 2006)
CXCL9, CXCL10 (IP-10) CXCL11	Bronchial epithelial cells (Silva Miranda et al., 2012)	-Recruits immune cells (Silva Miranda et al., 2012)
CCL19/CCL21	Stromal cells of lymph node (Silva Miranda et al., 2012)	-Recruitment and priming of IFN-γ producing T cells -Migration of DC from lung to draining LN (Silva Miranda et al., 2012)

2.1.1.6 Adaptive immunity and host defence

2.1.1.6.1 Initiation of adaptive immunity

Initiation of adaptive immunity largely depends on innate immune responses. The innate immune cells, particularly macrophages and dendritic cells play central roles in initiating adaptive immune responses. The initiation of adaptive and in particular, cell mediated immunity in *Mtb* infections is underpinned by three processes: antigen presentation, costimulation and cytokine production by the immune cells (van Crevel et al., 2002).

2.1.1.6.1.1 Antigen presentation

Antigen presentation plays an important role in activating subsequent adaptive immune responses. Presentation of exogenous *Mtb* pathogens is achieved following uptake by the antigen presenting cells (APC), particularly macrophages and dendritic cells. The *Mtb* antigens are processed in phagolysosomal compartments of the APC before being presented to T cells (Figure 2.3) (van Crevel et al., 2002). During this process of antigen presentation, *Mtb* antigens, in conjunction with MHC class II molecules, are presented to the antigen specific CD4+ T cells, leading to activation of cellular and/or humoral immune responses. MHC class I molecules are able to present mycobacterial antigens to antigen specific CD8+ T cells. The role of MHC class I mediated antigen presentation has been documented both in murine models (Peters et al., 1991, Sousa et al., 2000) and TB patients (Cho et al., 2000, Geluk et al., 2000). This pathway of presentation is important to kill the infected cells by Tc cells (Peters et al., 1991, Weerdenburg et al., 2010). In addition, nonpolymorphic MHC class I molecules such as type I CD1 (-a,-b and -c) molecules can present *Mtb* lipoproteins to CD1-restricted T cells. This pathway of presentation is usually activated before the development of antigen specificity (Lewinsohn et al., 1998). Moreover, the expression of antigen presentation in *Mtb* infections can also be regulated by the cytokines (Figure 2.3). During host-*Mtb* interactions, expression of antigen presenting molecules in macrophages is enhanced by pro-inflammatory cytokines, whereas their expression is inhibited by anti-inflammatory cytokines (Pancholi et al., 1993, Gercken et al., 1994).

2.1.1.6.1.2 Costimulation

Costimulatory signals are essential for T cell stimulation during antigen presentation. The most well described costimulatory signals for T cell stimulation are B-7.1 (CD80) and B-7.2 (CD86). These molecules are expressed primarily on macrophages and dendritic cells which bind to

CD28 and CTLA-4 (cytotoxic T lymphocyte antigen 4) on T cells. Studies have shown that during Mtb infection B-7.1 (CD80) expression on monocytes is decreased (Saha et al., 1994) whereas dendritic cells show higher expression of B7.1, CD40 and intracellular adhesion molecule-1 (ICAM-1) (Henderson et al., 1997). Furthermore, lack of costimulatory signals during presentation of *Mtb* antigens increased T cell apoptosis followed by T cells hyporesponsiveness (Hirsch et al., 1999b, Hirsch et al., 2001)**.**

2.1.1.6.1.3 Cytokine production

Several cytokines produced by activated macrophages and dendritic cells are crucial for T cells stimulation (van Crevel et al., 2002) (details in Table 2.1 and Figure 2.3). Macrophages and dendritic cells produce type 1 cytokines (IL-12, IL-18 and IL-23) for T cell stimulation (Oppmann et al., 2000). Studies documented that functional mutation of gene encoding for IL-12p40 (Frucht and Holland, 1996, Altare et al., 1998b), IL-12Rβ1 (de Jong et al., 1998, Othieno et al., 1999), IFN-γ receptor 1 (Jouanguy et al., 1996, Holland et al., 1998) and IFN-γ receptor 2 (Dorman and Holland, 1998) in chronic or recurrent TB patients suggesting the failure of IFN-γ receptors signalling in macrophages and dendritic cells. Further, IL-1 and TNF-α have important T cell stimulatory properties (Dinarello, 1996, Tsenova et al., 1999). Decreased production of such pro-inflammatory cytokines delayed T cell stimulation followed by poor T cell mediated immunity. Anti-inflammatory cytokines like IL-10, TGF-β have antagonistic roles in T cell stimulation during antigen presentation (Table 2.1) (Hirsch et al., 1997, Boussiotis et al., 2000).

2.1.1.6.2 Role of T cells

A wide range of immune cells of the adaptive immune system is involved in mounting effective cell mediated immune responses against *Mtb* infections. These cells comprise CD4+ T cells, CD8+ T cells, Treg cells, CD1 restricted T cells and γδ T cells.

The CD4+ T cells are thought to play a major role in *Mtb* protection following infection (Figure 2.3). These cells can produce a stronger IFN-*γ* response than other T cells to mount effective immunity against *Mtb* infections (Schaible et al., 2003, Ngai et al., 2007). The functional role of CD4+ T cells is diverse. One of the significant functions of these cells is the production of cytokines such as IFN-γ, IL-2 and TNF-α. Among the cytokines, IFN-γ plays the central role in controlling *Mtb* infections. Defects in IFN-γ or IFN-γ receptor gene in humans and animals were reported to be the cause of increased susceptibility to *Mtb* infections (Flynn et al., 1993,

Chan and Flynn, 2004, Cooper, 2009). IFN-γ synergises the function of TNF-α to kill *Mtb* through the activation of macrophages and increasing expression of inducible nitric oxide synthase (iNOS) (Scanga et al., 2001, Chan and Flynn, 2004, Cooper, 2009). This crucial cytokine also enhances antigen presentation, recruitment of more CD4+ T cells or cytotoxic CD8+ T cells for killing the bacilli as well as preventing exhaustion of memory T cells (Chan and Flynn, 2004, Russell et al., 2009). Furthermore, it increases gene expression in macrophages for MHC class II molecule expression as well as the production of antimicrobial components (Scanga et al., 2001, Chan and Flynn, 2004, Cooper, 2009). TNF-α (also produced from macrophages and dendritic cells) also has a protective role in TB defence (Bean et al., 1999, Keane, 2005). Studies in mouse models documented that TNF-α or TNF-α receptor deficiency increased *Mtb* infections (Keane, 2005). It also initiates cell migration for granuloma formation as well as its maintenance. In addition, depletion of TNF-α results in overgrowth of *Mtb* (Flynn et al., 1993, Chan and Flynn, 2004). Secondary functions of CD4+ T cells are confinement of bacilli within the granuloma, apoptosis of infected macrophages, induction of macrophages and dendritic cells to produce cytokines (IL-10, IL-12, IL-15) and activation of macrophages through CD40 ligand binding (Flynn et al., 1993, Cella et al., 1996, Oddo et al., 1998, Chan and Flynn, 2004). CD4+ T cells also regulate the function of cytotoxic CD8+ T cells. Studies have documented that inhibition of CD4+ T cells in apoptosis of macrophages affects the activation of CD8+ T cells (Serbina et al., 2001, Cooper, 2009). In contrast, depletion of CD4+ T cells leads to reactivation of latent infections followed by extensive tissue pathology and mortality in mice even though there are higher IFN-γ levels due to CD8+ T cells responses (Scanga et al., 2001). Delayed dissemination of CD8+ T cells from the draining lymph nodes to other organs occurs due to lack of CD4+ T cells, causing impairment of immune protection (Wang et al., 2004). These cells also control the intracellular growth of *Mtb* by a nitric oxide dependent mechanism (Cowley and Elkins, 2003, Cooper, 2009).

CD8+ T cells take part in *Mtb* protection by secreting IFN-γ (Figure 2.3). These cells can directly kill the *Mtb* through a perforin and granulysin-mediated pathway and facilitate the control of both acute and chronic infections (Grotzke and Lewinsohn, 2005, Cooper, 2009). CD8+ T cells kill the infected macrophages directly or by induction of apoptosis via Fas ligand (Woodworth et al., 2008, Dheda et al., 2010). CD8+ T cells also have a protective role in the control of LTBI. Depletion of CD8+ T cells has been reported to initiate the reactivation of latent infections (van Pinxteren et al., 2000) and defective function of CD8+ T cells is also documented in chronic TB patients (Brighenti and Andersson, 2010).

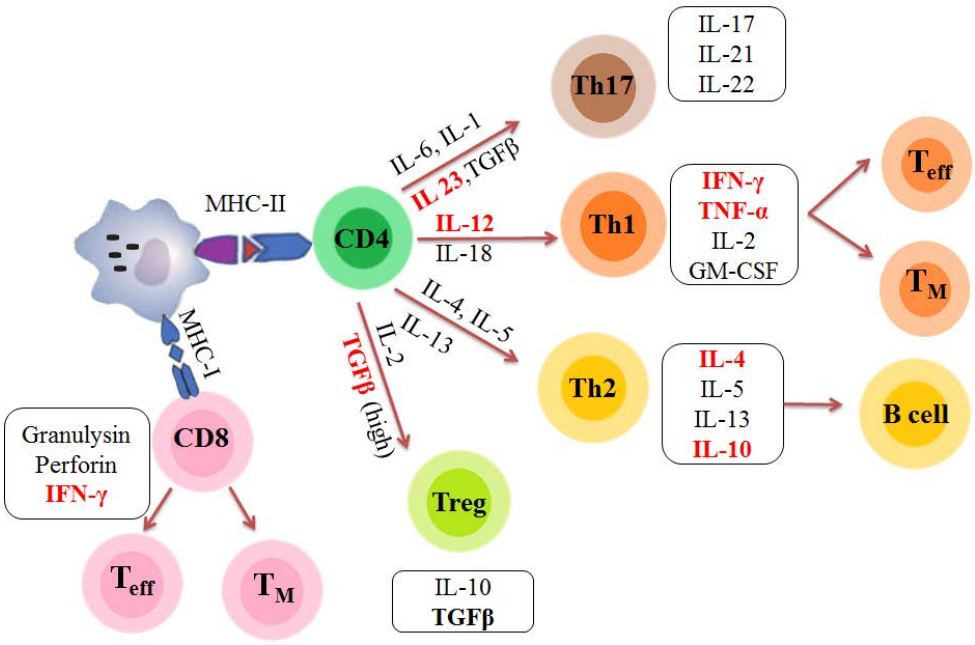

Figure 2.3 Antigen presenting cell and T cell interactions, and the cytokine networks required for mounting an adaptive immune responses during *Mycobacterium tuberculosis* infections

Figure illustrates the antigen presentation by antigen presenting cells (APC) to T cell for mounting adaptive immune responses in *M. tuberculosis* infection. The infected APC (macrophages and dendritic cells) secrete various cytokines including IL-12 and TNF-α to present antigen to T cell populations; CD4+ T cells (MHC class II), CD8+ T cells (MHC class I). Immediately after antigen presentation, CD4+Th1 cells proliferate to produce effector T cells (T_{eff}) and memory T cells (T_M) responses. These cells then produce multiple cytokines such as IFN-γ and TNF-α for further activation of macrophages for effective killing of the bacilli through the secretion antimycobacterial compounds (e.g. ROS and iNOS). In addition, CD8+ cytotoxic T cells can kill the bacilli through granulysin and perforin-mediated pathways. Another major subset of CD4+ T cells is CD4+ Th2 cells and CD4+CD25+FoxP3+ Treg cells which dampen down the Th1 cells through the secretion of anti-inflammatory cytokines (e.g. IL-4, IL-10, TGF-β). Interestingly, Th2 cells also secrete B cells stimulating factors (e.g. IL-4, IL-5, IL-10, IL-13) for antibody production. Th 17 cells, a distinct subset of CD4+Th cell which produced in the presence of IL-23 are able to modulate the inflammatory responses and recall memory responses through the production of IL-17. The Th17 cell population can recruit neutrophils and monocytes and IFN-γ-producing CD4+ T cells and stimulate chemokine responses. Figure adapted and modified from Dheda et al., (2010).

Treg cells have an influence in TB defence as these cells modulate Th1, Th2 and Th17 cells. Natural Treg subsets (CD4+CD25+FoxP3+) can produce either TGF-β and IL-10 to downregulate CD4+ T cells (Figure 2.3) (Kursar et al., 2007, Kaufmann and Parida, 2008, Dorhoi and Kaufmann, 2009, Rahman et al., 2009, Sharma et al., 2009) leading to suppression of immunity and clinical manifestation of TB. Furthermore, CD4+ Treg cells subsets and CD8+

Treg cells can alter cytokine production and inhibition of T cells proliferation (Scott-Browne et al., 2007), resulting in immune suppression and bacillary dissemination (Rahman et al., 2009, Sharma et al., 2009). It was observed that a high percentage of Treg cells ($CD4^+$ $CD25^{high}CD39^+$) were found in patients with active TB. Attenuation of these Treg cells has a positive impact on *Mtb* vaccine efficacy (Bayry et al., 2008, Jaron et al., 2008). However, unconventional T cells such as CD1 restricted T cells, γδ T cells also have a protective role in TB defence (Kaufmann, 2004, Barral and Brenner, 2007, Beetz et al., 2008).

2.1.1.6.3 Role of B cells

The role of B lymphocytes and the humoral immune response for protection against TB is not clear. A study using a mouse model found that B cells were required for optimal protection against *Mtb* infections (Maglione and Chan, 2009). It was also observed that low-dose aerosol infection with *Mtb* in B cell deficient mice showed no difference in susceptibility to infection (Johnson et al., 1997, Bosio et al., 2000, Taylor et al., 2005), however high-dose intravenous challenge increased the susceptibility as well as severity of lesion formation (Vordermeier et al., 1996). Another study reported that granulomas comprise a large population of B cells, particularly B220+ cells, suggesting that these cells have a protective role in TB defence (Kahnert et al., 2007). It has been suggested that the antibody response that occurs during *Mtb* infections can modulate cell mediated immunity through cytokine signalling, triggering the complement system and also promoting antibody-dependent cellular cytotoxicity (de Valliere et al., 2005, Abebe and Bjune, 2009, Maglione and Chan, 2009).

2.1.1.7 Granuloma formation

The granuloma is a hallmark of *Mtb* infections (Silva Miranda et al., 2012). It prevents bacterial dissemination as well as reactivation of bacilli (Ehlers, 2009). Formation of the granuloma results from effective innate and adaptive immune responses (discussed above) (Saunders and Cooper, 2000, Saunders and Britton, 2007, Korbel et al., 2008). Furthermore, the cellular aggregation for the formation of the granuloma occurrs in response to different cytokines and chemokines resulting from both innate and adaptive immune cells (Table 2.1). The balance between pro- and anti-inflammatory cytokines is crucial for the establishment of an effective granuloma in *Mtb* infection.

Macrophages are one of the principal cells found in the granuloma (Jo et al., 2007, Cooper et al., 2011). The granuloma is mainly composed of centrally infected macrophages surrounded

by epithelioid cells, foamy macrophages, multinucleated giant cells of Langhans type with peripherally by T lymphocytes (CD4+, CD8+ T cells) (Gonzalez-Juarrero and Orme, 2001, Puissegur et al., 2004). A mature granuloma is compact, highly stratified, becomes vascularised and develops a fibrotic capsule around it (Russell, 2007).

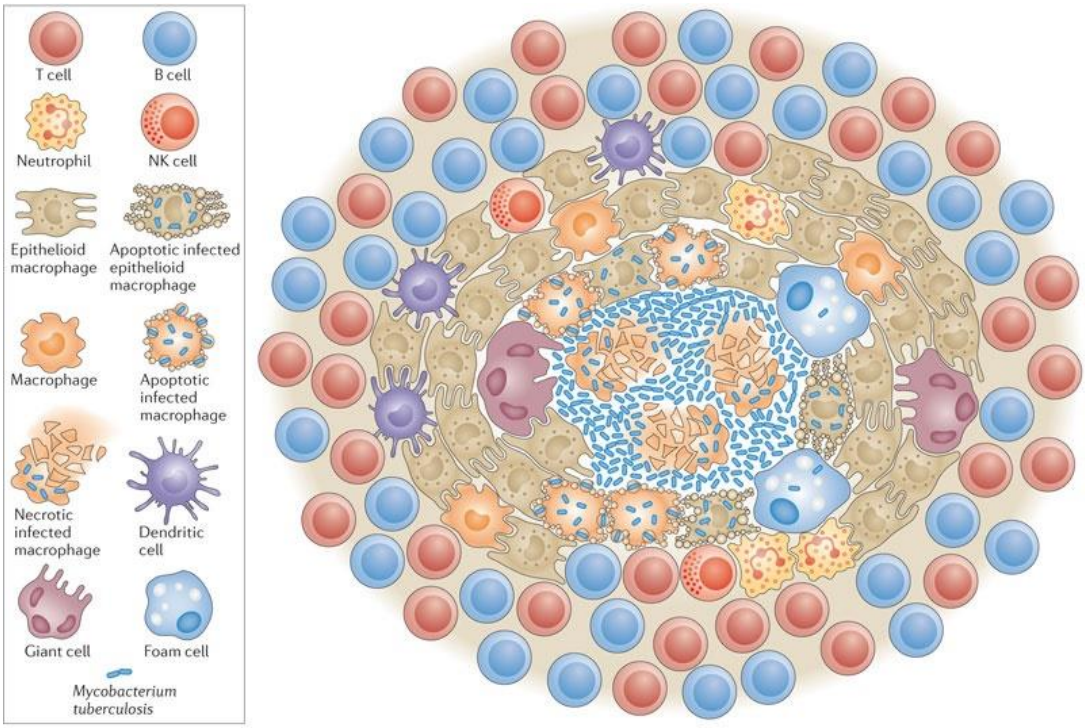

Figure 2.4 Schematic diagram of tuberculosis granuloma (Ramakrishnan, 2012)

In the granuloma, there is no or little multiplication of confined bacteria (Ducati et al., 2006). The environment is considered hypoxic which is important for *Mtb* metabolism and antimycobacterial therapy (Adams, 1989, Aly et al., 2006). Prior studies demonstrated that *Mtb* bacilli adapted to the hypoxic environment of the granuloma by producing a thickened cell wall and also altering the transcription of various proteins (Cunningham and Spreadbury, 1998, Rosenkrands et al., 2002). It provides a microenvironment in which the bacilli can survive for a longer period of time as latent TB infection (LTBI) (Adams, 1976, Sandor et al., 2003). It was also assumed that secondary granuloma formation or reactivation of LTBI can result due to drainage of non-replicating bacilli into the airways to the upper lobes of the lungs (Saunders and Britton, 2007, Cardona, 2009, Cardona, 2010).

Reactivation of LTBI occurs most commonly in the lungs (80% of the cases), whereas in 20% of cases, it reactivates at other tissue sites (e.g. pleural space, lymph nodes, bone, kidney, etc.)

(Frieden et al., 2003). It is assumed that reactivation of TB from LTBI occurs due to immune compromised status (e.g diabetes, HIV infection) of the hosts (Martens et al., 2007, Hodgson et al., 2015). Previous research has shown that in immunocompetent individuals with TB infection, granulomas are small, compact and characterised by the presence of a signfiicant number of IFN-γ producing CD4 T cells. In contrast, in immunodeficient individuals, the TB granuloma is larger in size, rich in activated macrophages and with few surrounding lymphocytes. These granulomas are unable to effectively control and confine the infection (Ulrichs et al., 2005).

2.1.1.8 Vaccines against tuberculosis

2.1.1.8.1 Current vaccine for tuberculosis protection

Bacillus Calmette-Guérin (BCG) is currently the only recommended vaccine against TB (Andersen and Kaufmann, 2014). The vaccine was developed by Albert Calmette and Camille Guérin following 230 *in vitro* passages of a *Mycobacterium bovis* strain over a 13 year period (Calmette, 1927, Calmette and Plotz, 1929). Subsequent comparative genome analyses have shown that the *M. bovis* BCG vaccine strain lacks several gene segments cluster into regions of difference (RD). The RD1 encodes the important virulence factors and T cell antigens early secretary antigenic target-6 (ESAT-6) and culture filtrate protein-10 (CFP10) (Behr et al., 1999). Clinical use of the vaccine began in 1930. Vaccination through the Expanded Program on Immunisation, commenced in the early 1970s and has been successful in preventing infant mortality (Hatherill, 2011, WHO., 2013a) because the vaccine can prevent extra-pulmonary TB (miliary TB or TB meningitis) in children (Andersen and Kaufmann, 2014)

The most controversial aspect of the BCG vaccine is the level of protection. The efficacy of the vaccination is influenced by geography, genetics and the nutritional status of the host, concurrent bacterial infections and condition of the laboratory where the vaccine was produced including genetic differences in the strain, media used for growth etc., (Sutherland and Springett, 1987, Janaszek, 1991, Fine, 1995, Venkataswamy et al., 2012). Studies have shown that vaccination efficacy (based on the occurrence of TB in vaccinated group) is 60-80% in UK populations (Sutherland and Springett, 1987) and as low as 0% in south Indian populations (Indian Council of Medical Research., 2013). A systematic study documented that this vaccine reduces the overall risk of getting TB by approximately 50% (Colditz et al., 1994). Another systemic review has demonstrated that BCG vaccine reduces the infection by 19-27% and

reduce the progression of the active disease by 71% (Roy et al., 2014). The duration of protection offered by the vaccine is also controversial. A study of a native American population reported that protection (based on the reactivity of tuberculin skin test) remained for 50-60 years (Fine, 1995, Aronson et al., 2004). Whereas another study showed that the level of protection waned to 59% after 15 years and to nearly zero after 20 years (Styblo and Meijer, 1976).

2.1.1.8.2 Future vaccines for tuberculosis

To overcome the limitation of the current BCG vaccine and to face the global challenge of increasing TB incidence, several vaccines have been developed that are now under clinical assessment (Table 2.2). These vaccines have been developed based on three immunisation strategies: (i) prime; (ii) prime boost; and (iii) immunotherapeutic (Frick, 2013). These vaccines either boost the current BCG or replace BCG (Montagnani et al., 2014). Several preexposure vaccines have been designed for infants which could be used to boost the level of protection afforded by the current BCG vaccine (Kaufmann, 2012). Postexposure vaccines are formulated to be administered to adolescents and adults with LTBI. These vaccines are again designed to boost BCG or replace BCG given at infancy. The third strategy of future vaccines are for therapeutic purposes to reduce the chemotherapy requirements of active TB patients, drug-resistant TB patients (Frick, 2013, Prabowo et al., 2013) as well as HIV patients suffering from miliary TB (von Reyn et al., 2010).

Table 2.2 Overview of tuberculosis vaccines currently under clinical trial

Vaccine name	Target indication	Antigen name or Rv number	Delivery system	Descriptive notes	Phase	Reference
MTBVAC	Preventive	N/A	Live *Mtb*	Attenuated Mtb with PhoP and FadD26 gene deletions	I	Arbues et al. (2013)
VPM	Preventive	N/A	Live rBCG strain expressing isteriolysin, urease deleted	Improved antigenicity due to perforation of phagosome membrane	IIa	Grode et al. (2013) Grode et al. (2005)
Ad5 Ag85A	Preventive	Ag85A	Adenovirus 5 vector	Replication-deficient viral delivery system	I	Smaill et al. (2013)
Ad35/ MVA85A	Preventive	Ag85A, Ag85B TB10.4	Adenovirus 35 and modified vaccinia Ankara vector	Prime boost combination of two viral delivery systems	I	Abel et al. (2010) Radosevic et al. (2007)
H4/IC31	Preventive	Ag85B TB10.4	IC31	Formulation of cationic peptide and a synthetic TLR-9 agonist	II	Dietrich et al. (2005), Aagaard et al. (2009), Billeskov et al. (2012)
MVA85A	Preventive	Ag85A	Modified vaccinia Ankara	Replication-deficient viral delivery system	IIb	Tameris et al. (2013) Beveridge et al. (2007), Verreck et al. (2009), White et al. (2013)

M72	Preventive / Postexposure	Rv1196 Rv0125	AS01E	Liposomes incorporating the TLR-4 agonist monophosphoryl lipid A	IIa	Leroux-Roels et al. (2013) Reed et al. (2009)
ID93	Preventive/ /Postexposure /Therapeutic	Rv2608 Rv3619 Rv3620 Rv1813	GLA-SE	Synthetic TLR-4 agonist in oil-inwater emulsion	I	Coler et al. (2013) Bertholet et al. (2010)
H1/H56/IC31	Preventive /Postexposure /Therapeutic	Ag85B ESAT-6 Rv2660c	IC31	Formulation of cationic peptide and a synthetic TLR-9 agonist	II	van Dissel et al. (2010), Aagaard et al. (2011) Weinrich Olsen et al. (2001)
RUTI	Therapeutic	N/A	Whole fragmented *Mtb*	-	I	Cardona (2006)
Mycobacterium vaccae	Therapeutic	N/A	Whole killed *Mtb*	-	III	Yang et al. (2010) von Reyn et al. (2010) de Bruyn and Garner (2003)
Mycobacterium indicus pranii	Therapeutic	N/A	Whole killed *Mtb*	-	III	Gupta et al. (2012)

N/A; Not applicable, Adapted and modified from (Andersen and Kaufmann, 2014)

2.1.1.9 Diagnosis of tuberculosis

2.1.1.9.1 Active tuberculosis

The presumptive diagnosis of active tuberculosis is based on a variety of clinical features. Productive, persistent cough (lasting more than two weeks), haemoptysis and chest pain are also considered. Other common manifestations include low grade fever, night sweats, chills, inappetence, fatigue and shortness of breath. (Frieden et al., 2003, Kumar, 2007). Further, medical history including history of previous exposure to an infected individual provides important diagnostic clues. Disease in these patients is usually confirmed with chest X-ray, microscopy of sputum smear and culture of *Mtb*. In many developing countries, diagnostic algorithms and point scoring systems are often used to get a better diagnostic yield (Hesseling et al., 2002). Biomarkers in the peripheral blood such as anaemia and pancytopenia may also be seen in TB patients with bone marrow involvement (Cameron, 1974). Inflammatory markers such as acute phase protein, C-reactive protein (CRP) also considered in the diagnosis of active TB (Breen et al., 2008).

2.1.1.9.1.1 Microscopy

Early TB diagnosis is crucial for its control. The most common method of TB diagnosis, particularly in the poorest parts of the world where disease burden is high, is microscopy (Zumla et al., 2013). Microscopy of a sputum sample is usually performed either by light microscopy with Ziehl-Neelsen/Kinyoun stain or fluorescent microscopy with a stain such as auramine-O. Sputum smear microscopy is considered an easy, cheap and rapid test for diagnosis of TB in a limited resource setting (CDC, 2000). Fluorescent microscopy is more sensitive than conventional microscopy, but requires an expensive fluorescent microscope. In 2009, WHO endorsed low-cost fluorescent LED (light emitting diodes) technology to overcome the use of expensive traditional fluorescence microscopes (Mizuno et al., 2009, WHO., 2009). However, the sensitivity of this diagnostic assay is influenced by the number of samples and sampling time. Ulukanligil and colleagues (2000) documented that early morning samples contained more bacilli and repeated sampling increased the sensitivity. The sensitivity of Ziehl-Neelsen and fluorescence microscopy was reported to be 61% and 83%, respectively, when a single sample was considered, whereas sensitivity increased to 80% and 92%, respectively, when three or more sample was submitted.

2.1.1.9.1.2 Culture

Culture is considered as the gold-standard for the diagnosis of TB (Zumla et al., 2013). The sensitivity of culture is higher than traditional microscopy, as it can detect as few as 10 bacilli per millilitre of respiratory samples (Yeager et al., 1967). Culturing should be performed in both solid (e.g. egg based Lowenstein-Jensen medium or agar based Middlebrook 7H10/7H11) and liquid media (Middlebrook 7H9, 7H12 or Kirshners) because the former allows the examination of colony morphology for identification and the later enables more rapid diagnosis of TB (Frieden et al., 2003).

A recent advance in culturing is the use of automated liquid culture systems such as MB/BacT system (bioMerieux, France) and the MGIT 960 (Becton Dickinson, New Jersey, USA). Both culture systems increase the sensitivity and reduce detection time and have a 10% greater yield than solid media (Palomino et al., 2008, Muyoyeta et al., 2009, Parrish et al., 2009). The MB/BacT system uses a modified Middlebrook 7H9 broth with a pH indicator for detecting pH changes in the presence of CO_2. The MGIT 960 culture system utilises the same broth and detects the release of a fluorophore that is produced after utilisation of oxygen by the bacilli. The MGIT 960 method has been reported to be better over solid culture because it can recover more organisms from extra-pulmonary samples (Hillemann et al., 2007). However in 2007, WHO endorsed the automated liquid culture system as the gold standard for TB diagnosis, although the higher cost and contamination issues limit the use of this method in many low and middle income countries (Zumla et al., 2013).

2.1.1.9.1.3 Imaging

Imaging is an important tool for diagnosing active PTB. Radiographic lesions indicate infiltration or consolidations and/or cavities or tree-in-bud sign (airway obstruction) in the upper lobes of the lungs. This can be with or without the involvement of mediastinal or hilar lymphadenopathy, although lesions may be found anywhere in the lungs (Rossi et al., 2005). A multivariate analysis has also documented that lesions are mostly restricted to the upper lobes upon chest X-ray and they were positively associated with culture proven TB (Wisnivesky et al., 2000). Furthermore, tiny nodules throughout the lungs are also common in disseminated forms of the disease (miliary TB). Moreover, chest radiographs cannot detect all cases of PTB. Pepper et al. (2008) reported that 9% of patients with culture-confirmed PTB had a normal chest X-ray. In this regard, a computed tomography (CT) scan can assist the diagnosis of both pulmonary and extra-pulmonary TB.

2.1.1.9.1.4 Nucleic acid amplification test

Several molecular tools have been introduced over the last two decades for the rapid diagnosis of TB. Popular molecular tools based on nucleic acid amplification are Qiagen Artus TB PCR (Crawley, UK), Roche COBAS TaqMan *Mtb* assays (Indianapolis, USA) and strand displacement amplification (SDA) assay (Becton Dickinson, New Jersey, USA). These techniques use various molecular targets to amplify *Mtb* DNA. For example, Qiagen Artus TB PCR and Roche COBAS TaqMan *Mtb* assay use the 16S rDNA gene, whereas the insertion sequence; IS*6110* is the target for the SDA assay. Higher sensitivity (93%) and specificity (92%) were documented in SDA based assays (McHugh et al., 2004). The insertion sequence IS*6110* is an excellent target for diagnosis of TB as most of the *Mtb* bacilli possess multiple copies of it. However, the specificity of this assay may reduce due to cross reactivity with many other non-tuberculous mycobacterial species, as many of these possess a similar insertion sequence (McHugh et al., 1997). Recently, a new molecular diagnostic test was introduced, Cepheid GeneXpert (Xpert® MTB/RIF) which can identify concurrently *Mtb* specific DNA and the rifampicin resistance mutation. The sensitivity of this assay reportedly was similar to the SDA assay and higher than the Roche Assay (Boehme et al., 2010).

2.1.1.9.2 Drug resistant tuberculosis

The diagnosis of drug resistant tuberculosis remains a challenge. The current standard for detecting first-line drug-susceptibility/resistance is an automated liquid culture system. In 2008, WHO recommended the molecular technique, line probe assays (LPAs) for the rapid detection (within 24 hours) of drug resistance in smear-positive specimens or cultured samples (Ling et al., 2008, WHO., 2010, O'Grady et al., 2011). The WHO also endorsed the use of Xpert MTB/RIF and at the same time also recommended other standard drug-susceptibility tests to confirm rifampicin and other drug resistance (WHO., 2011a). Other molecular assays such as the automated nucleic acid amplification test, loop-mediated isothermal amplification and oligonucleotide microarray are used for drug screening. Microscopic observation direct susceptibility (MODS) assay, light-emitting diode microscopy, multi drug and extremely drug resistant (MDR-XDR)-TB colour test, colorimetric assays and phage amplification are also used as non-molecular assays (Wilson, 2013) for drug susceptibility testing. Unfortunately, most of these methods are not currently available in many TB endemic countries, as the tests require technical expertise and have higher associated costs. An estimated 10% of potential MDR-TB are currently diagnosed globally and only half of such patients receive proper treatment (WHO., 2011b, Zignol et al., 2012).

2.1.1.9.3 Latent tuberculosis

Latent tuberculosis infection (LTBI) is a subclinical form of *Mtb* infection and therefore shows no clinical features or radiological findings (Al-Orainey, 2009). The recommended test for the diagnosis of LTBI is the Mantoux tuberculin skin test (TST). The test is based on a delayed-type hypersensitivity (DTH) response following intradermal injection with purified protein derivative (PPD). The test is interpreted based on the development of a cutaneous induration at the site of injection after 48-72 hours. A positive test suggests previous exposure to *Mtb* or other related mycobacterial species or BCG vaccination (Comstock, 1975, Huebner et al., 1993, Wang et al., 2002). The test result may be affected by the dose of PPD, the reader, repetition of the dose, as well as the immune status of the individual (Magnus and Edwards, 1955, Chaparas et al., 1985, Markowitz et al., 1993, Stuart et al., 2000). A study has shown that a low-dose of PPD may give false negative reactions, whereas a high-dose may show false positive reactions (Stuart et al., 2000). Further, it was observed that cutaneous indurations can reach greater than 10 mm after 12 weeks of BCG vaccination in the first year of infancy (Lifschitz, 1965) and test reactivity may last up to 5 years (Horwitz and Bunch-Christensen, 1972). In some instances, the TST reactivity may continue for up to 15 years post vaccination (Wang et al., 2002). Furthermore, the test also gives false positive reactions in immune suppressed patients (e.g. HIV patients) with impaired T cell responses (Markowitz et al., 1993). Repeated skin tests particularly in health workers, also give strong skin reactions (Magnus and Edwards, 1955). The test cannot differentiate between exposure or infection with *Mtb* and other mycobacterial infections (Frieden et al., 2003). The poor sensitivity and specificity of the test limit its use in immunosuppressed patients as well as diagnosis of LTBI (Markowitz et al., 1993), but it has been used widely because there was no better alternative (Al-Orainey, 2009).

Recently, a more sensitive and specific test, interferon-gamma (IFN-γ) release assay (IGRA), has been developed to diagnose LTBI. The test detects IFN-γ release through stimulation of T cells with two *Mtb* antigens; ESAT-6 and CFP-10 (Brock et al., 2001, Pai et al., 2004a, Whalen, 2005). The IGRA has excellent specificity as the antigens used in this assay are absent in the BCG vaccine (Mahairas et al., 1996, Behr et al., 1999, Pai et al., 2004a). The two commercially available diagnostic IGRAs are the whole blood ELISA based "QuantiFERON (QFN)-TB Gold assay" (Cellestis Ltd., Carnegie, Australia) and Enzyme linked immunospot (ELISPOT) technology based "T-SPOT®TB" using peripheral blood mononuclear cells (PMBC) (Oxford Immunotec, Oxford, UK) (Anonymous, 2014, OIL, 2014). Improvements have been made these original tests and a newer version of QFN-TB Gold assay is the QuantiFERON-TB-Gold-In-Tube that uses TB7.7 peptide along with ESAT-6 and CFP-10 peptides (Cole et al., 1998). The

latest version of T-SPOT-TB also uses specific peptides of ESAT-6 and CFP-10 rather than using whole antigens. Studies have shown that IGRA is more specific and sensitive for the diagnosis of LTBI than the TST (Lalvani et al., 2001, Pathan et al., 2001, Chapman et al., 2002, Menzies et al., 2007). Pai and co-workers (2008) documented that they cannot differentiate latent and active *Mtb* infections in immunosuppressed individuals. To date, IGRA is considered the most effective diagnostic tool for the diagnosis of LTBI but extensive research is required to further improve the test, particularly in immune compromised individuals.

2.1.2 Non-tuberculous mycobacteria: Classification

Non-tuberculous mycobacteria (NTM) or atypical mycobacteria comprises all mycobacterial species other than *M. tuberculosis, M. bovis* and *M. leprae* (Jarzembowski and Young, 2008). According to the Runyon classification, NTM were classified based on pigmentation and growth rates into four groups (Table 2.3). These microbes share many common properties, such as acid-fastness and the ability to cause pulmonary and extrapulmonary granulomatous disorders (Jarzembowski and Young, 2008).

Table 2.3 Runyon classification of non-tuberculosis mycobacteria

Runyon class	Growth	Description	Pigment production	Species
I	Slow	Photochomogens	Yellow-orange (with light)	*Mycobacterium kansaii*, M. marinum**
II		Scotochromogens	Yellow-orange (with or without light)	*M. scrofulaceum*, M. gordonae*, M. szulgai*
III		Nonchromogens	None	*M. avium-intracellulare*, M. xenopi, M. terrae*
IV	Rapid	Rapid growers	None	*M. fortuitum* M. peregrinum, M abscessus*, M cheonae**

*clinically important species

2.1.2.1 Clinical importance of *Mycobacterium fortuitum*

While *M. tuberculosis* mainly contributes to the majority of mycobacterial infections, there are more than 150 non-tuberculous mycobacterial (NTM) species, which are capable of causing a wide spectrum of infections (Orme and Ordway, 2014). Among the species of rapidly growing mycobacteria, *M. fortuitum* is one of the most clinically important pathogenic species. They are widely distributed in the environment and are able to cause a range of diseases affecting a variety of tissues including lungs, lymph nodes, skin, soft and skeletal tissues. The bacteria can

cause severe pulmonary infections in addition to osteomyelitis and peritonitis, (Wallace, 1989, Lessing and Walker, 1993, Sangwan et al., 2013). According to the available epidemiological data on NTM, 16.7% of the patients with soft tissue infections due to *M. fortuitum,* had comorbid diabetes (Uslan et al., 2006). Furthermore, *M. fortuitum* (43.1%) was the leading cause of oedematous lesions in diabetic patients reported in Australian population (O'Brien et al., 2014). The rapid escalation of immune suppressing co-morbidities has contributed not only to an increased incidence of TB, but also NTM infections (e.g. *M. fortuitum* infection).

2.1.2.2 Virulence factors of non-tuberculous mycobacteria

Host immune response to *M. tuberculosis* and non-tuberculous mycobacterial (NTM) infection varies in many aspects. In both *Mtb* and NTM, the most recognised virulence factor is the hydrophobic cell wall, which has various immune-modifying capabilities depending on its composition and ability to interact with host cells. The glycopeptidiolipids (GPL) of the cell wall are mainly produced by NTM but absent in *M. tuberculosis*. The GPL extract of *M. avium* complex reduced the production of IFN-γ and TNF-α (Pourshafie et al., 1999), which are crucial for NTM infections. Non-specific GPL (nsGPL) of *M. avium* stimulated macrophages to secrete immunosuppressive chemical as prostaglandin E_2 resulting in higher intracellular survival (Barrow et al., 1993), whereas the absence of the same structure in *M. abscessus* enhanced intracellular survival (Sweet and Schorey, 2006). Moreover, phagocytosis, inhibition of phagosome-lysosome fusion and cytokine production in macrophages also influenced by serotype specific GPL (ssGPL) (Takegaki, 2000). Such as, ssGPL from serovar 2 of *M. avium* enabled macrophages invasion, reduced TNF-α production and increased intracellular survival, whereas serovar 8 can survive in macrophages regardless of marked pro-inflammatory responses (Cebula et al., 2012). In addition to GPL, lipoglycans as lipoarabinomannans (LAM) considered another important virulent factor in mycobacterial pathogenesis. The structural domain of LAM has similarity and dissimilarity with *Mtb*. ManLAM; a structural domain of LAM present in *M. avium* which is similar to *Mtb*. *M. fortuitum* and *M. smegmatis* possesses phosphatidylinositol-LAM (PILAM) (Chatterjee and Khoo, 1998). Research has shown that Purified PILAM from NTM enhances the secretion of IL-12, TNF-α and IL-8 in macrophages (Maeda et al., 2003). Whereas purified AraLAM (arabinose-capped LAM) from *M. smegmatis* able to trigger an acute inflammatory response (increase TNF-α, IL-6 and IL-1β production) with numerus neutrophil influx for the clearance of the bacteria. The authors also showed that TLR2 is the signaling receptor for purified AraLAM and lack of it delayed the bacterial clearance from the lungs (Wieland et al., 2004). Furthermore, the interaction between *Mtb* and host dendritic cells (DCs) is thought to be critical for mounting protective antimycobacterial

immune responses. Prior research demonstrated that Dendritic Cell Specific Intracellular Adhesion Molecule (DC-SIGN) strongly bind to ManLAM of *Mtb*, whereas ManLAM of *M. avium* bind poorly with same pattern recognition receptor indicating that host recognition of NTM infection is different to *Mtb* (Maeda et al., 2003). It is obvious that multiple factors are necessary for the pathogenesis of NTM infections, which differs based on species specific mycobacterial virulence factors, host susceptibility factors, route of infection etc. Further investigations using the purified NTM-derived cell wall components along with species itself are crucial in understanding the underlying immune responses in host-pathogen interaction.

2.1.2.3 Immune responses to *Mycobacterium fortuitum*

Few studies have investigated the *in vitro* performance of macrophages during *M. fortuitum* infections (Parti et al., 2005, Helguera-Repetto et al., 2014). Unlike *Mtb* infection, *M. fortuitum* (and other many fast-growing mycobacteria) behave differently in terms of growth within the macrophages (Orme and Ordway, 2014). An *in vitro* study of macrophages infected with slow growing (*M. tuberculosis* and *M. celatum*) and fast growing mycobacteria (*M. fortuitum* and *M. abscessus*) reported a lower number of infected cells with a higher survival and proliferation of fast growers within the infected macrophages, compared to slow growers (Helguera-Repetto et al., 2014). A similar observation was also documented by Parti and colleagues (2005) using *M. fortuitum* infected macrophages. A previous study demonstrated that virulent *M. fortuitum* survive within the macrophages by restricting the IFN-γ driven nitric oxide (NO) production and by limiting the phagosome fusion with lysosomes (Da Silva et al., 2002). Higher survival of the mycobacteria is not associated with fatal infections, as the *M. fortuitum* infected macrophages produce more antimycobacterial compounds (reactive oxygen species; ROS) and induce rapid apoptosis of the infected cell (Helguera-Repetto et al., 2014). Prior studies have also reported that the inability of less virulent *M. fortuitum* failed to cause disease despite their higher survival in macrophages due to the rapid induction of host cell apoptosis, as this leads to direct killing of intracellular mycobacteria (Molloy et al., 1994, Keane et al., 2002, Bohsali et al., 2010). Cytokine production during *in vitro* culture of mycobacteria was also found to assist with controlling survival of the *M. fortuitum*. A higher production of TNF-α and IL-1β was observed in *M. fortuitum* infected macrophages compared to *Mtb* infected macrophages following culture (Helguera-Repetto et al., 2014). The difference in the production of TNF-α was explained by the variations in the lipoarabinomannan (LAM) structure on the cell wall (Chatterjee et al., 1992a, Singh and Goyal, 2013). Less pathogenic mycobacteria (e.g. *M. fortuitum*) possess extensive arabinose side-chains on LAM which is a potential inducer of cytokines. Whereas pathogenic mycobacteria such as *Mtb*, comprise the short mannan chain

which extensively masks the arabinose side chain (Chatterjee et al., 1991, Chatterjee et al., 1992a). Another possible mechanism for greater TNF-α induction by the less pathogenic bacteria is the differences in phagolysosome fusion. Phagolysosome fusion is a pre-requisite to enhance the production of cytokines. Phosphatidylinositol 3-phosphate (PI3P) is a membrane trafficking regulatory lipid which is important for the phagosomal acquisition of lysosomal contents (Vergne et al., 2005b). Virulent mycobacteria secrete an acid phosphatase known as SapM which is required to hydrolyse PI3P, resulting in inhibition of the phagolysosomal fusion. Less or non-pathogenic mycobacteria do not produce SapM, thus no inhibition of phagosome with endosome occurs, resulting in more cytokine production (Saleh and Belisle, 2000).

There are few studies investigating the pathogenesis of *M. fortuitum* infection in animal models (Saito and Tasaka, 1969, Da Silva et al., 2002, Parti et al., 2005, Silva et al., 2010). *M. fortuitum* caused disseminated infection when mice were infected intravenously (Parti et al., 2005, Silva et al., 2010). Parti and co-workers (2005) observed a 1000-fold higher bacillary burden in the kidneys of *M. fortuitum* infected mice compared to the bacillary load in the spleen and lungs at 10 days post-infection (dpi). The authors also demonstrated that after 45 and 60 dpi, the bacillary load in spleen and lungs was minimal although a trend of higher bacterial load was maintained in the kidney at the same timepoint. The bacillary burden in the liver was high immediately following infection, although it dropped dramatically after 10 dpi. Silva and co-workers (2010) observed a similar pattern of bacterial burden in the spleen and liver of *M. fortuitum* infected mice. Similar to *Mtb* infections, a granulomatous response in *M. fortuitum* infection is crucial for controlling and confining the infection (Parti et al., 2005, Silva et al., 2010). Granuloma formation is driven by the Th1 cells mediated responses as seen in *Mtb* infection (Flynn et al., 2011). During *M. fortuitum* infection, macrophages and CD4+ T cells are the main components of the granuloma. It was observed that granuloma formation is accelerated by the antigen specific CD4+T cells and is largely dependent on TNF-α and IFN-γ (Appelberg et al., 1994a). Parti and co-workers (2005) reported a higher production of IFN-γ production from the CD4+ T cells compared to CD8+ T cells following infection with *M. fortuitum*. A higher production of IFN-γ by the previous reports confirmed that a Th1 cell response is essential in the control of *M. fortuitum* infection.

2.2 Overview of diabetes

2.2.1 Diabetes

Diabetes mellitus (DM) or diabetes is a group of metabolic diseases. They are characterised by high blood sugar either because the pancreas becomes unable to secrete sufficient insulin (insulin deficiency) or the peripheral cells do not respond to insulin (insulin resistance). This hyperglycaemic condition in diabetic patients produces classical symptoms of polyuria (frequent urination), polydipsia (increased thirst) and polyphagia (increased hunger) (WHO., 2006, Cooke and Plotnick, 2008, Gardner and Shoback, 2011).

The disease is considered one of the oldest human diseases. It was first documented in Egyptian manuscripts about 3000 years ago (Leutholtz and Ripoll, 2011). In 1936, type 1 diabetes (T1D) (insulin dependent) and type 2 diabetes (T2D) (non-insulin dependent) appeared as two distinct types of diabetes (Himsworth, 1936) but T2D was first stated as a component of metabolic syndrome in 1988 (Patlak, 2002). T2D is the most common form of DM (Weyer et al., 1999) accounting for about 90% of cases (ADA., 2010).

2.2.2 Types of diabetes

There are three main types of DM; T1D, T2D and gestational diabetes. Type 1 diabetes or insulin-dependent diabetes mellitus (IDDM) results from insulin deficiency due to pancreatic defects. It is mainly mediated by the loss of insulin-producing β (beta) cells of the islets of Langerhans (Rother, 2007). The cause of β-cell defects can either be idiopathic or the result of T cell mediated autoimmune responses, which are characterised by the presence of auto-antibodies in the pancreas (e.g. islet cell antibodies, anti-glutamic acid decarboxylase antibodies, or protein tyrosine phosphatase-like protein IA-2 antibodies) (Zimmet et al., 2004). Most affected people have good health with normal sensitivity and responsiveness to insulin during the time of onset. Later, the affected individual becomes absolutely insulin deficient and requires additional administration of insulin to prevent severe consequences like ketoacidosis, coma or death (Rabinovitch and Suarez-Pinzon, 1998, Zimmet et al., 2004, WHO., 2006). The risk of developing T1D is mainly influenced by genetics and environmental factors. Genetic factors include human leucocyte antigen markers (e.g. HLA-A, HL-B, HLA-DPβ1) of the host (Barnett et al., 1981, Akerblom et al., 2002). Whereas environmental factors include bacterial or viral infections, or nutritional factors that trigger the autoimmune process (McNally et al., 2006). This type of diabetes mostly affects children but is also found in adults; therefore, it was

traditionally called "juvenile diabetes". There are no effective preventive measures against T1D (WHO., 2016a).

Type 2 diabetes or noninsulin-dependent diabetes mellitus (NIDDM) results from insulin resistance by the peripheral tissue or inadequate secretion of insulin from the pancreas (Weyer et al., 1999, ADA., 2010). The risk factors for developing T2D are many, including older age, dietary intake, sedentary lifestyle, obesity, ethnicity, prior history of glucose intolerance (genetic) or gestational diabetes and other environmental factors as found in T1D (Zimmet et al., 2004, Sobngwi et al., 2008). This type of diabetes is common in adults; therefore, it is also occasionally termed as "adult-onset diabetes". At the early stages of T2D, the defective responsiveness of the body tissues is believed to involve impairment of cell-associated insulin receptors to respond to insulin (i.e. insulin resistance) (Kumar, 2007). In individuals with T2D, there is no auto-immune degeneration of the pancreatic β-cell as is seen T1D patients (Zimmet et al., 2004). However more recently it has become clear that auto-reactive B and T cells may be activated following excessive inflammation of adipose tissue (Winer et al., 2011). The resulting hyperglycaemia due to relative insulin deficiency can be reversed by dietary interventions and medications for improving insulin sensitivity or limiting glucose production by the liver. Sometimes relative insulin deficiency may convert to absolute insulin deficiency requiring external supplementation of insulin (Gardner and Shoback, 2011).

The third form of diabetes is gestational diabetes mellitus (GDM). This form usually occurs around the 24^{th} week of pregnancy, due to transient resistance to insulin. The condition arises because action of insulin is inhibited, probably by hormones produced by the placenta. Women who have the GDM are at a high risk of developing the condition in subsequent pregnancies. GDM may also lead to the development of T2D in later life (Vijan, 2010). Babies born to mothers with GDM also have a higher lifetime risk of developing T2D (WHO., 2016b). Other forms of DM include congenital diabetes, cystic fibrosis-related diabetes, steroid diabetes and several forms of monogenic diabetes.

2.2.3 Criteria for classification and diagnosis of diabetes

The classical symptoms of diabetes include polyuria (frequent urination), polydipsia (increased thirst) and polyphagia (increased hunger) (Cooke and Plotnick, 2008). Several other signs may be seen during the onset of diabetes such as weight loss, blurry vision and headache, weakness and delayed healing, but these are not specific to the disease. Symptoms usually develop rapidly

in T1D (within weeks or months) whereas manifestations of T2D occur slowly and remain asymptomatic (Zimmet et al., 2004).

The World Health Organisation (WHO) and American Diabetic Association (ADA) has provided the updated diagnostic criteria (Table 2.4) for diabetes (ADA., 2010, WHO., 2016a). The disease should be diagnosed when clinical symptoms are present along with diagnostic criteria listed in Table 2.4.

Table 2.4 Diagnostic criteria of diabetes mellitus and intermediate hyperglycaemia

Conditions	WHO		ADA	
	Fasting glucose	2 hours glucose *	Fasting glucose	2 hours glucose *
	mmol/L	mmol/L	mmol/L	mmol/L
Impaired fasting glycaemia (IFG)	6.1-6.9	<7.8	5.6-6.9	-
Impaired glucose tolerance (IGT)	<7.0	≥7.8 & <11.1	-	≥7.8 & <11.1
Diabetes	≥7.0	≥11.1	≥7.0	≥11.1

* Following a 75 g oral glucose challenge, WHO; World Health Organisation, and ADA; American Diabetic Association

2.2.4 Risk factors for type 2 diabetes

The numbers of individuals with T2D is rapidly increasing worldwide. The risk factors for developing T2D are likely to be a combination of lifestyle and genetic factors (Ripsin et al., 2009). Important lifestyle factors that contribute to the development of T2D include diets, lack of physical activity, a sedentary lifestyle, smoking and generous consumption of alcohol, stress, urbanisation and possibly others (Hu et al., 2001, Smyth and Heron, 2006).

2.2.4.1 Dietary factors

Excess caloric intake is a major driving force of increasing obesity and T2D epidemics globally. This nutritional shift typically involves increased consumption of animal fat, a high fat diet (HFD) and more frequent intake of fast foods. Furthermore, consumption of sugar or sweetened beverages (SSB) in large amounts or eating large amounts of white rice is associated with an increased risk of developing T2D (Malik et al., 2010, Hu et al., 2012). A metanalysis showed that that 26% of individuals have the chance of developing T2D who were with SSB intake (most often 1-2 servings/day) (Hu, 2013). A high glycaemic diet can increase insulin demand and may lead to pancreatic β-cell exhaustion resulting in T2D (Hu and Willett, 2002). A HFD, particularly saturated fats and trans fatty acids, has been reported to increase the risk of diabetes

while polyunsaturated and monounsaturated fats decrease the risk (Riserus et al., 2009). The mechanism by which obesity induces insulin resistance is poorly understood. In contrast, dietary fibres, both soluble and insoluble, may improve T2D (Akinmokun et al., 1992). Whole-grain intake (2 servings/day) has been observed to lower the risk (21%) of developing diabetes (de Munter et al., 2007). However, low vitamin D intake enhances the chance of developing T2D (Pittas et al., 2006, Knekt et al., 2008). The possible mechanism is that vitamin D deficiency may lead to β-cell dysfunction and contribute to insulin resistance and excessive inflammation.

Obesity is one of the major risk factors for developing T2D (Walley et al., 2006). The WHO has recognised that the prevalence of obesity is increasing at an alarming rate, putting the populations of most countries at risk of developing many diseases including diabetes (WHO., 2008). Of those diagnosed with T2D, 80% were overweight (Smyth and Heron, 2006). Excess body fat among patients of Chinese and Japanese descent contributes 30% of cases of T2D whereas the rate is 60-80% in those of European and African descent and 100% in Pima Indians and Pacific Islanders. The reasons for the rapid rise in global obesity include increased consumption of diets with a high glycaemic index, the changing structures and compositions of diets (Popkin and Nielsen, 2003) and physical inactivity (Bell et al., 2002). Childhood obesity rates between the 1960s and 2000s has also contributed to the sharp global rise of DM in children and adolescents (Barlow, 2007). Obesity ultimately makes the individual insulin resistant (Ding and Malik, 2008).

2.2.4.2 Smoking

Cigarette smoking is an important independent risk factor for T2D. A meta-analysis reported that smokers had a 45% greater chance of developing T2D compared to non-smokers (Willi et al., 2007) and the risk is influenced by the duration of smoking and number of cigarettes smoked. The relationship between cigarette smoking and diabetes can also be illustrated by possible biological mechanisms including: (i) although smokers tend to be physically leaner they have increased risk of central adiposity or abdominal fat deposition (Barrett-Connor and Khaw, 1989, Shimokata et al., 1989) and (ii) smoking has anti-oestrogenic effects in women and decreases plasma testosterone level in men (Meikle et al., 1988). These factors may promote abdominal fat deposition and enhance the likelihood of insulin resistance. Furthermore, nicotine exposure during the prenatal or neonatal period can cause β-cell dysfunction and increase β-cell apoptosis (Bruin et al., 2008).

2.2.4.3 Physical inactivity

Physical activity reduces the risk of developing diabetes whereas sedentary behaviour increases the risk. An epidemiological study reported that individuals who spend 2 hours/day watching television had a 14% increased chance of developing diabetes (Hu et al., 2003). In contrast, the possibility of developing diabetes decreased by 12% if an individual spends 2 hours/day walking or standing working. The authors also documented that hurried walking may reduce the chances of diabetes by 34%. Another study reported that lack of exercise is believed to cause 7% cases of T2D (Lee et al., 2012).

2.2.4.4 Genetic factors

Type 2 diabetes most likely represents a complex interaction among the genetics of the individual and environmental factors. Genome-wide association studies (GWAS) has identified common factors contributing to diabetes susceptibility (McCarthy, 2010). At least 40 different genetic loci have been identified that are associated with T2D (Herder and Roden, 2011). Most of these genes are associated with impairment of β-cell functions. Studies showed that monozygotic twins have a 90-100% chance of developing diabetes in his/her lifetime if one identical twin is affected by the disease. Conversely, the rate of developing T2D in non-identical offspring is 25-50% (Gardner and Shoback, 2011). Many diabetes-associated genes or poylmorphisms identified in Caucasian populations have also been identified in some Asian populations. For example, the risk allele in the TCF7L2 gene is common in European and South Asian populations (20-30%), but rare in East Asians (~2%) (Ng et al., 2001, Wu et al., 2008). The prevalence of T2D also varies markedly between ethnic groups living in the same geographical area (Knowler et al., 1993). African Americans, Native Americans, Pima Indians and Hispanic Americans have a 2 to 6 times higher chance of being affected by the disease compared with Caucasian Americans (Carter et al., 1996, Harris et al., 1998). The prevalence of T2D is also higher in South Asian people (e.g. > 50% in mass population in India), indicating that genetic factors are more important than environmental factors in developing T2D.

2.2.4.5 Medical conditions

Many medications and other health problems can predispose people to diabetes (Feinglos, 2008). Use of medications including glucocorticoids, beta blockers, thiazides, atypical antipsychotics (Izzedine et al., 2005) and statins may contribute to T2D. Health problems associated with developing diabetes include acromegaly, Cushing's syndrome, hyperthyroidism, thyrotoxicosis, chronic pancreatitis, pheochromocytoma, and certain cancers

such as glucagonomas (Feinglos, 2008). Testosterone deficiency can also influence the occurrence of T2D (Saad and Gooren, 2009, Sampson et al., 2011).

2.2.4.6 Other factors

Individuals with blood glucose levels higher than normal but not high enough to be classified as diabetes are said to have impaired glucose tolerance (IGT) or impaired fasting glucose (IFG). The term 'prediabetes' is used to describe this grey area between normal glucose levels and diabetes. In prediabetes, the pancreatic β-cell can no longer produce enough insulin to overcome insulin resistance, causing blood glucose levels to rise above the normal range. Individuals with pre-diabetes often have no signs or symptoms but have a higher risk of developing T2D and other complications (e.g. cardiovascular). Worldwide there are large numbers of people with prediabetes at risk of developing T2D at any point in their life time if proper preventive measures are not taken (Zhang et al., 2010).

2.2.5 Pathophysiology of type 2 diabetes

Under normal physiological conditions, glucose homeostasis in the body is maintained correctly despite wide fluctuations in supply and demand (Figure 2.5). Plasma concentration remains normal through a tightly regulated and dynamic interaction between tissue sensitivity to insulin (especially in the liver) and insulin secretion (DeFronzo, 1988). In T2D, these mechanisms are disturbed (Figure 2.5). In this situation, the body's insulin sensitive cells fail to uptake glucose, resulting in hyperglycaemia. Further, certain cells such as fat and muscle cells are also disrupted if insulin resistance/deficiency exists. In general, insulin suppresses hepatic glucose release to maintain normal plasma glucose levels (Figure 2.5) (Groop et al., 1993). It was reported that 80-85% of the glucose is disposed in muscle and liver and 4-5% is metabolised by adipocytes by insulin dependent manner (Bergman, 2013). If insulin resistance or deficiency exists, pancreatic β-cell attempts to secrete more insulin to overcome the underlying defects of insulin resistance (DeFronzo et al., 1992). Hyperglycaemia and hyperinsulinimia manifest in the subjects of T2D if this compensatory mechanism fails. Furthermore, fat cells also fail to uptake circulating lipids to store them as triglycerides, causing hydrolysis of these triglycerides (Lipolysis) contributing more fatty acids in plasma. These fatty acid concentrations also reduce muscle glucose uptake, increase liver glucose production and aggravate hyperglycaemia and hyperinsulinemia (Boden, 1999) resulting in severe complications like hypertension (Reaven et al., 1996, Ginsberg, 2000) and other vascular abnormalities (Ginsberg, 2000).

T2D involves two primary pathogenic mechanisms: (i) a progressive decline in pancreatic islet cells function (β-cells) resulting in reduced insulin secretion and inadequate suppression of glucagon secretion (Muller et al., 1970, Weyer et al., 1999); and (ii) peripheral insulin resistance by skeletal muscle, liver and adipose tissue which decrease metabolic responses to insulin (DeFronzo, 1988, ADA., 2010). In fact, both insulin resistance and impairment of insulin secretion/β-cell defects are important components in the pathophysiology of T2D.

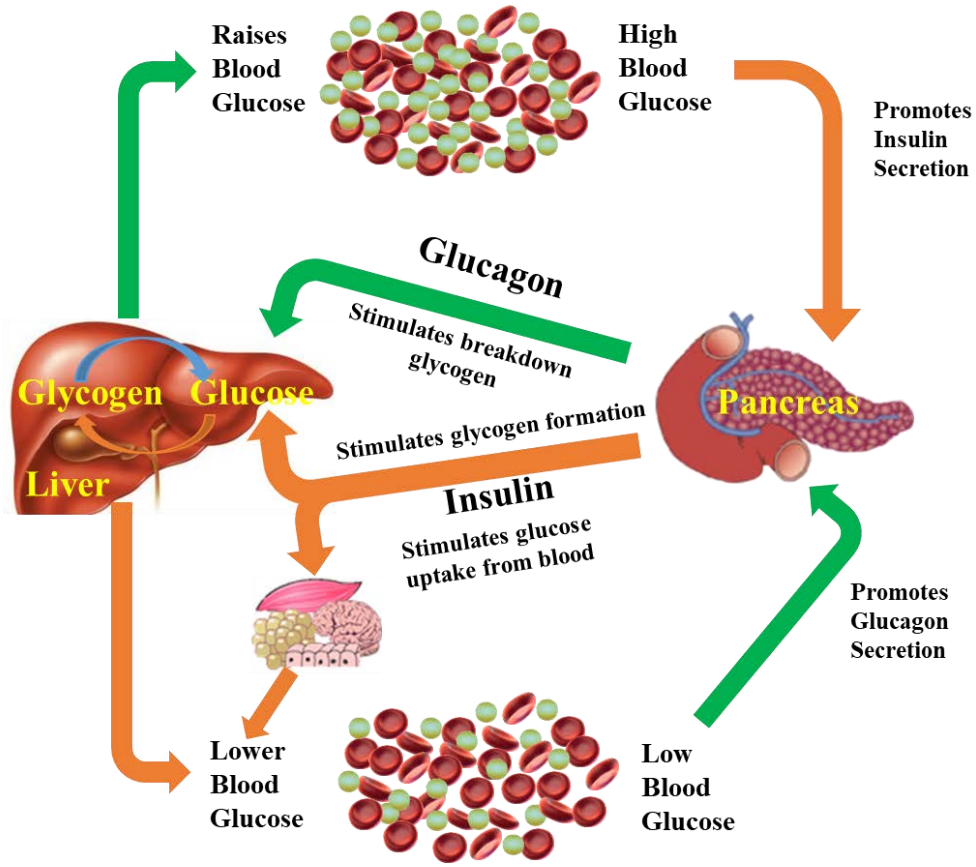

Figure 2.5 Glucose homeostasis and its disruption in individuals with diabetes mellitus

Figure illustrates the mechanism of glucose homeostasis and disruption in diabetes. Glucose homeostasis is mainly maintained by the insulin and glucagon. Insulin is secreted from Pancreatic β-cell and allows glucose to be taken up and used by insulin-dependent tissues (e.g. skeletal muscle, fat). This hormone also stimulates liver cells to convert excess glucose to glycogen (glycogenolysis) to maintain normoglycaemia. In contrast, glucagon is secreted from the alpha cells of Pancreas in response to hypoglycaemia. It increases the blood glucose level by breaking down the liver glycogen into glucose (Glycogenolysis). In case of insulin resistance in diabetes, the function of the insulin is disrupted resulting in hyperglycaemia. Hyperglycaemia further stimulate the Pancreatic β-cell to secrete more insulin. However, due to inadequate suppression of glycogen by insulin, the hyperglaycamic state of diabetic patients further aggravated by glycogenolysis. Figure modified from IDF. (2013).

2.2.5.1 Cellular defects in type 2 diabetes

2.2.5.1.1 Islets of Langerhans dysfunctions

In T2D, the most noticeable alteration in the islets of Langerhans is the deposition of amyloid material in the insulin secretory granules. The amyloid mass is derived from the polymerisation products of β-cell regulatory proteins including the islet amyloid polypeptide (IAPP) or amylin (Westermark et al., 1986, Westermark et al., 1987). High concentrations of amylin may decrease glucose uptake and inhibit endogenous insulin secretion, suggesting that amylin may be directly involved in the pathogenesis of T2D (Hull et al., 2004). Furthermore, it was observed that even a small amyloid particle deposition in the insulin secretory granules shows the ultra-structural signs of cell membrane destruction (Janson et al., 1999). Therefore, it is suggested that in T2D aggregation of amylin could regulate the progressive loss of pancreatic β-cell (Carrera Boada and Martinez-Moreno, 2013). However other studies failed to find a pathological role for amylin with administration of physiologic amounts of amylin showing no acute effect on insulin secretion or insulin actions in humans (Wilding et al., 1994). Hence the precise role of amylin deposits in the pancreas and their contribution to the pathophysiology of T2D remains unclear.

2.2.5.1.2 Loss of β-cells mass and function

Prospective studies have indicated that β-cell functions are impaired and lost progressively during the development of T2D (Gerich, 1998, Xiang et al., 2006). This functional impairment of β-cell is related to the loss of β-cell mass. Autopsy studies of patients with T2D revealed substantial amounts of β-cell mass loss; up to 65% compared with non-diabetic controls (Sakuraba et al., 2002). Studies also demonstrated that β-cell deficit and apoptosis increased with the progression of the disease (Butler et al., 2003, Marchetti et al., 2004). β-cell mass loss may be progressive unless there is concurrently increased β-cell formation. The frequency of pancreatic β-cell apoptosis was reported to increase 10 times in lean compared to 3 times in obese cases of T2D, suggesting that a lower β-cells mass in T2D patients is due to an increase rate of β-cell apoptosis (Butler et al., 2003). Recently, a meta-analysis found a strong relationship between diabetes and telomere length (Wang et al., 2016). This report suggested that islet β-cell undergo apoptosis because the telomere length gradually becomes shorter in diabetes, which in turn worsen the complications of diabetes.

Three possible mechanisms have been proposed to explain the β-cell deficiency of T2D (Scheen and Lefebvre, 1996). Firstly, there may be some genetic β-cell defects , although this prediction

has not been confirmed yet in T2D (Polonsky, 1995). Secondly, insufficient β-cell development is related to in-utero malnutrition which may lead to a partial insulin secretory defect (thrifty phenotype hypothesis) (Hales and Ozanne, 2003). Thirdly, an unfavourable metabolic environment can alter insulin secretion due to glucotoxicity (Yki-Jarvinen, 1992) and lipotoxicity (Unger and Zhou, 2001). Moreover, ectopic deposition of triglycerides in the pancreatic islets can lead to dysfunction of β-cell via a nitric oxide-dependent mechanism which subsequently damages the β-cell by oxidation and induces apoptosis (Unger and Zhou, 2001).

2.2.5.2 Role of adiposity, its distribution and mediators in the development of type 2 diabetes

2.2.5.2.1 Adiposity

Adiposity or obesity is one of the major risk factors in the development of T2D. It decreases the sensitivity of β-cell to glucose (Henry et al., 1985, Carey et al., 1996) by increasing peripheral resistance to insulin-mediated glucose uptake (Henry et al., 1985, DeFronzo and Ferrannini, 1991). The mechanism by which obesity induces insulin resistance is poorly understood. Genetic abnormality in the beta-3-adrenergic receptor is believed to be a possible cause of obesity induced insulin resistance. Further, the c-Jun amino-terminal kinase (JNK) pathway may be an important mediator of insulin resistance as JNK activity is increased in obesity. In animal models, the absence of JNK1 results in decreased adiposity and enhanced insulin sensitivity (Hirosumi et al., 2002).

2.2.5.2.2 Body fat distribution

Body fat distribution seems to be a critical aspect in the pathophysiology of T2D. The intra-abdominal fat deposition is more strongly correlated with insulin resistance than subcutaneous fat (Montague and O'Rahilly, 2000). Several mechanisms have been identified to describe how obesity increases insulin resistance. Excess accumulation of fat in insulin sensitive organs, particularly in skeletal muscle and the pancreatic β-cells, can hamper insulin action and its secretion. Fat from the visceral depots has a significant role in insulin resistance because visceral fat cells are less sensitive to the suppression of lipolysis as well as having direct access to the portal circulation. Increased free fatty acids in the portal circulation may impair metabolism, blocking insulin signalling pathways and increasing gluconeogenesis from the liver (Carey et al., 1996, Lebovitz, 1999).

2.2.5.2.3 Adipose tissue mediators

Adipose tissue is considered to be a storage depot of fat as an energy reserve. Indeed, the role of adipose tissue is diverse and, as an endocrine organ, it is capable of secreting a number of adipose tissue specific chemical mediators such as leptin, adiponectin and resistin. It can also secrete inflammatory cytokines which impair insulin secretion. There may be more than one mechanism by which obesity induces insulin resistance.

Leptin is produced by adipocytes and its secretion is proportional to adipocyte mass. Generally, it has influence on appetite regulation via the central hypothalamic neuroendocrine pathways (Goldstein, 2002). Moreover, it has a more direct role in influencing obesity and insulin resistance. Human and animal model studies have shown that leptin deficiency increases obesity and insulin resistance. Studies in a leptin receptor knock out (LepR KO) mouse model indicated that leptin signalling is associated with improved glucose tolerance in LepR KO group compared to control animals when they were feed a standard diet. On the other hand, rapid weight gain followed by insulin resistance was observed in LepR KO mice fed a HFD and this was due to the functional impairment of β-cell of the pancreas (Morioka et al., 2007, Niswender and Magnuson, 2007).

Adiponectin is an adipocyte-derived collagen like protein (Goldstein, 2002). It reduces the level of blood free fatty acids and improves lipid profiles, reduces inflammation following better glycaemic control in diabetic patients (Mantzoros et al., 2005). Interestingly, adiponectin has also been associated inversely with insulin sensitivity, which increases the risk of developing diabetes (Ferrannini, 1998, Li et al., 2009). The protein is downregulated in obesity (Arita et al., 1999) leading to increased insulin resistance followed by hyperinsulinemia for developing T2D (Kadowaki et al., 2006). However, adiponectin and adiponectin receptors also play an important role in the regulation of diabetes. Two studies have suggested that intake of dietary cereal fibres and food with a lower glycaemic index can improve adiponectin secretion in diabetic patients (Qi et al., 2005) and women (Qi et al., 2006).

Resistin is another adipocyte-specific protein molecule associated with insulin resistance. Administration of resistin decreases insulin mediated glucose uptake by adipocytes (Steppan et al., 2001) and its expression can be reduced by treating patients with thiazolidinediones (glitazones) (Shuldiner et al., 2001).

Studies have reported the role of increased inflammation and obesity in the pathogenesis of diabetes and its complication (Shoelson et al., 2006, Vandanmagsar et al., 2011). Increased

inflammation and diabetic complications are mainly associated with the increased production of reactive oxygen species (ROS) as a result of oxidative stress (Wright et al., 2006). These ROS production increase markers of inflammation reduced nitric oxide availability and chemical modification of lipoproteins leading to macrovascular (e.g. cardiovascular diseases, atherosclerosis) and microvascular (e.g. neuropathy, nephropathy, retinopathy) complications. For an example, in diabetes, advanced glycation end products bind with receptor for AGEs (RAGE) on the surface of endothelial cells triggering the production of ROS, in particular, super oxide anion, by NADPH. Then, these ROS activate nuclear factor kB (NF-kB), results in the transcriptional activation of genes relevant for inflammation leading to atherosclerosis (Wright et al., 2006, Chawla et al., 2016).

However, elevated level of ROS in T2D increase the markers of inflammation, such as C-reactive protein, plasminogen activator inhibitor-1, TNF-α, IL-6, peripheral blood leucocyte counts and cellular adhesion molecules (e.g. intracellular and vascular adhesion molecules) (Pradhan et al., 2001, de Rekeneire et al., 2006, Wright et al., 2006). Among the markers, elevated TNF-α derived is strongly associated with insulin resistance (Hotamisligil et al., 1993, Uysal et al., 1997) by blocking the insulin signalling pathway (Liu et al., 1998). This markers of inflammation further worsen the vascular complication in diabetes (Wright et al., 2006).

2.2.6 Immune defects in diabetes

Immune defects in diabetic patients result in many complications (e.g micro and macrovascular complications) including increased susceptibility to infectious agents (also discussed in section 2.3.5.1). These complications are the result of both defective innate and adaptive immune responses. In T1D, auto-reactive T cells drive the chronic inflammatory changes resulting in dysfunction of pancreatic β-cell (Atkinson and Eisenbarth, 2001). In T2D, insulin resistance is the primary cause which triggers the alteration of immunity particularly innate immune responses (Pedicino et al., 2013). It is suggested that the key factors for immune alteration in diabetes is due to poor control of hyperglycaemia attributed by insulin resistance or insulin deficiency. Systemic low-grade inflammation with higher level of pro-inflammatory proteins such as C-reactive protein, TNF-α and IL-6 in diabetic patients are not only associated with worsening of the insulin resistance (Kroder et al., 1996, Esposito et al., 2002, Freeman et al., 2002, Meigs et al., 2004, Goldberg, 2009) but also enhance vascular damages (Hotamisligil et al., 1993, Uysal et al., 1997, Wright et al., 2006).

Macrophages appear to play the pivotal role in the innate immune dysfunction seen in T2D (Fujiwara and Kobayashi, 2005, Ma et al., 2008). These cells perform many important functions including phagocytosis, antigen processing and presentation and act as a bridge between the innate and adaptive immune systems (Fujiwara and Kobayashi, 2005, Ma et al., 2008). Abnormalities in macrophage phenotype, chemotaxis, phagocytosis and cytokine secretion have been documented in diabetes patients and animal models. Studies in diabetic patients have shown that phagocytic and chemotaxis functions of polymorphonuclear leucocytes were impaired (Mowat and Baum, 1971, Marhoffer et al., 1992, Delamaire et al., 1997). The adherence of these cells was also decreased (Bagdade et al., 1978, Bagdade and Walters, 1980, Andersen et al., 1988) with reduced neutrophil degranulation observed in diabetic patients (Stegenga et al., 2008). An animal model of diabetes has demonstrated a significantly reduced phagocytosis of latex beads by the resident peritoneal macrophages (RPM) with reduced number of F4/80+cells in the peritoneal exudate. These authors also observed macrophages skewed to M2 polarised macrophages with altered phenotype, reduced chemotaxis and adherence capability (Liu et al., 2012). Ma and colleagues (2008) also observed a significantly reduced phagocytic capability of F4/80+ splenic macrophages and peritoneal exudate macrophages (PEM) in streptozotocin (STZ)-induced diabetic mice. In diabetes-co-morbid infections (e.g. tuberculosis, melioidosis), reduced phagocytosis of the bacteria and their killing were also observed in peritoneal or peripheral blood mononuclear cells (PBMCs) (Saiki et al., 1980, Hodgson et al., 2011, Tan et al., 2012). The precise mechanisms underlying this decreased phagocytosis (uptake and killing) by diabetic macrophages remain unclear. Ma and colleagues (2008) suggested the possibility of reduced macrophage numbers due to deficient differentiation of macrophages from bone marrow cells. Defective and lower yields of macrophages (and stem cells) from bone marrow cells have also been observed in diabetes (Nikolic et al., 2004, Fu et al., 2006, Kuki et al., 2006, Rota et al., 2006). Other reasons suggested for impaired phagocytosis in diabetes include reduced association (attachment) between bacteria and monocyte/macrophages, alteration of serum opsonins or complement proteins (C3b) and complement receptors (CR1 and CR3) (Schlesinger et al., 1990, Schlesinger, 1998, Gomez et al., 2013). Recent studies indicated that compromised phagocytosis of mycolic acid coated beads in diabetic macrophages was due to the lower expression of the macrophage receptors with collagenous structure (MARCO), Toll-like receptor 2 (TLR2) and the coreceptor for bacterial LPS (lipopolysaccharide), CD14 (Bowdish et al., 2009, Martinez et al., 2016). Advanced glycation end products accumulation in diabetes has also been shown to alter the expression of macrophage surface receptors (Lachmandas et al., 2015, Martinez et al., 2016). Furthermore, a study has shown that addition of AGEs to the peritoneal macrophages *in vitro*

reduced the phagocytic capability of latex beads, which further confirmed the role of AGEs in phagocytosis (Liu et al., 1999). Another possibility of lower phagocytosis might be due to reduced level of glutathione (GSH). It is noted that in healthy individuals, production of ROS is balanced by an increase in antioxidant activity, primarily mediated by GSH. In diabetes, this balance is impaired with reduced/deficient levels of GSH. A study in a T2D animal model demonstrated that depletion of GSH level increases bacterial (e.g. *Burkholderia pseudomallei*) susceptibility. The authors also showed that bacterial internalisation and killing improved by the addition of GSH in PBMCs culture (Tan et al., 2012). Moreover, cytokine production by the diabetic macrophages may also influence the macrophage functions during phagocytosis. Reduced production of cytokines (TNF-α, IFN-γ, IL-6) from diabetic peritoneal macrophages were observed in diabetic mice (Ma et al., 2008, Sun et al., 2012) and comorbid infections with *Burkholderia pseudomallei* (Hodgson et al., 2011, Hodgson et al., 2013b). Impaired phagocytic activity of macrophages from diabetic mice leads to poor antigen presentation which in turns results in compromised T cell mediated immunity (Ma et al., 2008, Ahmad, 2011).

Other than macrophages, diabetes has impact on the functions of the neutrophil and dendritic cells. Neutrophil is considered one of the earliest cells in phagocytosis. Increased production of inflammatory cytokines (TNF-*α*, IL-6, IL-8, IL-17,) and ROS by unstimulated diabetic neutrophils has been reported in diabetics which further worsen the insulin resistance (Collison et al., 2002, Hatanaka et al., 2006, Talukdar et al., 2012). The function of neutrophils in the host immune response to intracellular bacterial infections is still poorly understood. However, neutrophil responses to infection appear to be suppressed in diabetic hosts (Alba-Loureiro et al., 2006). Prior research demonstrated that impaired activity of glutathione reductase (required for the neutrophil-based ROS production and phagocytosis) contributed to neutrophil dysfunction in diabetic hosts (Yan et al., 2012). Furthermore, ROS production from the diabetic individual stimulates the release of neutrophil extracellular traps; another important bactericidal mechanism. Such defect in neutrophil in diabetics favour the bacteria to hijack neutrophil as a means of refuse and dissemination (Eruslanov et al., 2005). In diabetes-comorbid infection (e.g. melioidosis), defects of neutrophils in terms of impairment of phagocytosis, bacterial killing, neutrophil migration, cytokine production, apoptosis were reported (Chanchamroen et al., 2009, Kewcharoenwong et al., 2013). However, elevated levels of inflammatory cytokines after neutrophil stimulation has also been documented in diabetes (Hatanaka et al., 2006, Morris et al., 2012). It is suggested that excessive neutrophil activation in diabetic individual with intracellular bacterial infection attributed to severe pathology formation in organs (Hodgson et al., 2015).

Dendritic cells (DC) are considered an important link between host innate and adaptive immune responses. Increased expression of activation markers (TNF-α, IL-1β, IL-6, IL-12, IL-23, GM-CSF) from unstimulated DC in diabetics has been documented (Musilli et al., 2011, Bertola et al., 2012, Surendar et al., 2012). In diabetic mice infected with *Mtb*, an initial delay in the recruitment of the immune cells to the lungs were observed in spite of effective trafficking of DC cells to the regional lymph nodes (Martens et al., 2007). It was suggested that DC and macrophages were deficient at the site of infection due to reduced level of chemoattractant factors such as MCP-1/CCL2. In addition, reduced phagocytosis with delayed kinetics of antigen presentation were demonstrated in STZ-induced diabetic mouse model (Williams et al., 2011). Impaired phagocytosis and delayed recruitment of APC to the primary site of infection leads to poor control and impaired T cell activation.

Adaptive immune responses are also altered in diabetes. These alterations are due either to defects in innate cells (described above) or other associated factors (e.g. obesity, diet and smoking) that intensify the conditions of the diabetic patients. Plouffe and colleagues (1978) documented that the cell mediated immunity of diabetes patients was delayed compared to non-diabetic patients. Several studies also documented the role of T cell subset imbalance due to poor glycaemic control (Jagannathan-Bogdan et al., 2011, Zhang et al., 2011, Zeng et al., 2012) In diabetic patients with obesity, there is a shifting in T cell responses. Th1 and Th17 cells increased in comparison to Th2 and Treg cells in diabetes. Consequently, pro-inflammatory cytokines (IL-1β, TNF-α, IL-6) lead to chronic inflammation and worsen insulin resistance (Tiemessen et al., 2007, Olefsky and Glass, 2010, Ouchi et al., 2011). Experimental studies in mice demonstrated that higher levels of IFN-γ affect glucose homeostasis and increase tissue inflammation in T2D (Winer et al., 2009, Zhang et al., 2011). In diabetes-comorbid infection (e.g. tuberculosis) T cells were also impaired (discussed in section 2.3.5.1). It is obvious that functional abnormalities of both innate and adaptive immune cells are believed to increase diabetic related complications and susceptibility to many bacterial infections. How innate and adaptive immune responses in diabetic patients react to an infectious agent need to be addressed.

2.3 Convergence of mycobacterial infection and diabetes: the dual impact

2.3.1 Current global burden of tuberculosis

The current worldwide scenario of TB shows a continuing increase, causing the disease to be one of the leading global health problems resulting in millions of deaths each year. According

to the recent report of World Health Organisation, it is the ninth leading cause of deaths globally and the leading cause from a single infectious agent, ranking above HIV infection (WHO., 2017). The latest estimates revealed 10.4 million new TB cases occurred in 2016 and more than 1.3 million deaths. The incidence of TB is equally high in men, women and children. In 2017, an estimated 6.7 million (range, 4-9.4 million) cases of TB among males were recorded, of which 6.2 million (range, 3.7-8.6 million) were adults and 550 000 (range, 340 000–760 000) were children. There were 3.7 million (range, 2.2-5.2 million) cases of TB in females, of which 3.2 million (range, 1.9-4.5 million) were adults and 490 000 (range, 300 000–680 000) were children (WHO., 2017).

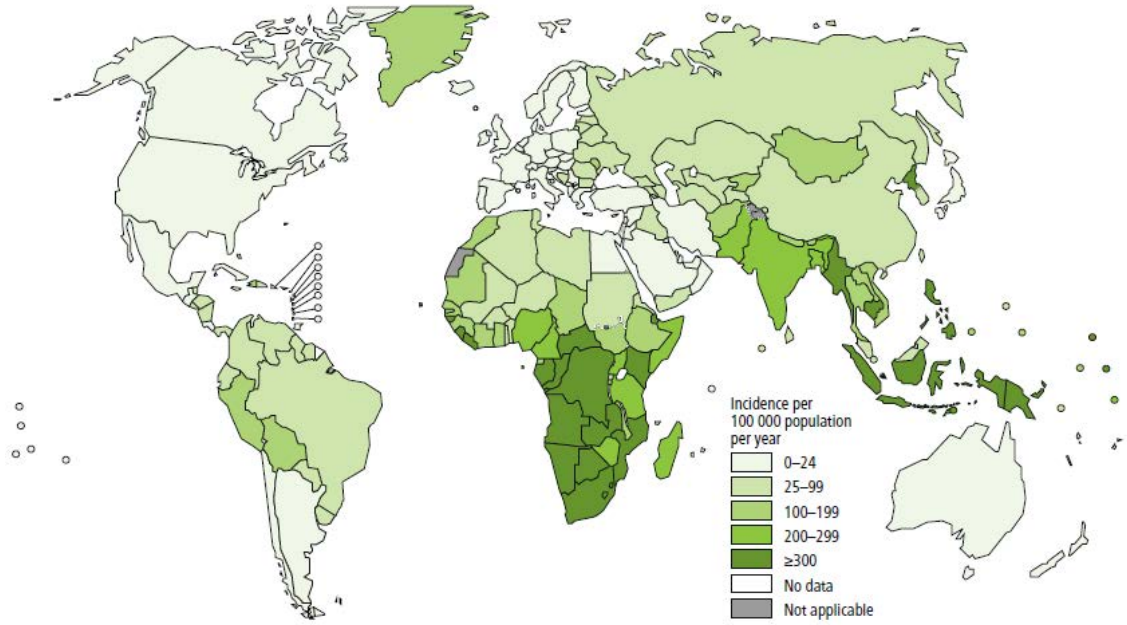

Figure 2.6 Estimated global tuberculosis incidence in 2016 (WHO., 2017)

According to the recent estimate by WHO, most of the TB cases have occurred in South-East Asia Region (45%), African Region (25%) and the Western Pacific Region (17%) (Figure 2.6). Smaller proportions of TB cases have occurred in Eastern Mediterranean Region (7%), European Region (3%) and the Americas (3%). The majority of all estimated cases globally were found in high burden countries (HBCs). Among them, 64% of the total global estimates were contributed by seven high burden countries; India, Indonesia, China, the Philippines, Pakistan, Nigeria, and South Africa. Moreover, in 2016, 85% of TB deaths occurred in African Region and the South-East Asia Region where India itself accounted for 26% of global TB deaths (WHO., 2017).

2.3.2 Current global burden of diabetes

The global burden of diabetes has been estimated regularly over the last two decades (McCarty and Zimmet, 1994, Amos et al., 1997, King et al., 1998, WHO., 2016b, IDF., 2017). Most recently, International Diabetes Federation (IDF) has estimated that approximately 425 million (range, 346.4-545.4 million) people were suffering from diabetes worldwide in 2017. The global prevalence is 8.8% (range, 7.2-11.3%) in the age group 20 to 79 years in the same year. Conversely, the predicted global estimate of diabetic population is 629 million (range, 477.0-808.7 million) contributing to a global prevalence 9.9% in the age group 20 to 79 years by 2045 (IDF., 2017). However, the global prevalence of IGT (impaired glucose tolerance) positive people (352.1 in 2017), those with high blood sugar in pregnancy (21.3 million live births affected in 2017) and additional undiagnosed people (212.4 million) will add significantly to the global occurrence of diabetes. It was also assumed that around 80% of patients will be living in low and middle income countries where developing economies are predominant (WHO., 2016b, IDF., 2017).

The burden of diabetes varies considerably from one geographical area to the other due to environmental and lifestyle risk factors (Olokoba et al., 2012). The regional burden and estimates of diabetes (20-79 age groups) in 2017 and 2045 in the IDF region is presented in Table 2.5.

Table 2.5 Regional estimates of diabetes (20-79 age groups) in 2017 and 2045

	2017		2045	
IDF region	**Prevalence (%)**	**No. of people with diabetes (million)**	**Prevalence (%)**	**No. of people with diabetes (million)**
North America and Caribbean	26.3	17.7	26.9	33.4
Middle East and North Africa	20.4	6.5	22.1	21.5
Western Pacific	20.0	48.1	17.6	96.7
Europe	19.4	28.5	19.8	43.9
South and Central America	19.0	7.9	19.3	20.4
South East Asia	13.5	12.5	13.9	33.0
Africa	5.2	1.6	5.4	4.6
Worldwide	**8.8**	**425**	**9.9**	**629**

(IDF., 2017)

In 2017, the highest prevalence of diabetes was recorded in the North America and Caribbean region (26.3%) where it is expected to rise to 26.9% by 2045. The lowest prevalence of diabetes was recorded in Africa at 5.4%, although the highest proportion of undiagnosed diabetes (69.2%; an estimated 10.7 million) people was also in that region indicating that a lack of diagnostic health care facilities may be the cause of the low numbers (IDF., 2017).

In 2016 China recorded 114.4 million people with diabetes, ranking it first in terms of diabetes sufferers. This number is expected to rise to 119.8 million by 2045 (IDF., 2017). Similarly, in India, the number was 72.9 million and is predicted to grow dramatically to reach 134.3 million by the end of 2045. The other rapidly growing top eight countries with diabetic patients are United States of America (USA), Brazil, Mexico, Indonesia, Russian Federation, Egypt, Germany and Pakistan (IDF., 2017). Moreover, the incidence of diabetes also increases in indigenous populations with over 370 million people in 90 countries reported (>5% of the world's population) (UNDESA, 2009). The Pacific Islanders have the highest rate of diabetes prevalence among the world's indigenous communities. Ten percent of Taiwanese Ami and Atayals (Chen et al., 1997), 30% of Australian Aborigines (Minges et al., 2011) and 40% of North American Sioux (Lee et al., 1995), 2.3% of Pima Indians (Pavkov et al., 2007), 1% of Chilean Aymara (Santos et al., 2001) suffer from diabetes.

2.3.3 The association between diabetes and tuberculosis

The association between DM and TB was documented by reports prior to 1960s (Root, 1934, Oscarsson, 1958) and is known to have existed for at least one thousand years (Kapur and Harries, 2013). In the early 20th century, it was assumed that people died either because of diabetes or TB (Root, 1934, Oscarsson, 1958). Later, following the invention of insulin for diabetes and antibiotics for TB treatment, the potential relationship between these two life threatening diseases was eclipsed. Interest revived due to the sluggish reduction of TB (2.2% reduction annually) through the TB control strategy (WHO, 2011) along with a worldwide rapid escalation of T2D incidence in TB populations (Corris et al., 2012).

Diabetes is indeed positively correlated with TB infection, as documented by multiple studies (Kim et al., 1995, Restrepo, 2007, Jeon and Murray, 2008, Workneh et al., 2017). Surveys carried out before 1960 reported that diabetic patients had a two to four times higher risk of being infected with PTB than other individuals (Banyai, 1931, Root, 1934, Boucot et al., 1952, Oscarsson, 1958). More recently, the association between these two diseases is supported by a growing body of literature (Mugusi et al., 1990, Mori et al., 1992, Kim et al., 1995, Pablos-

Mendez et al., 1997, Restrepo, 2007, Stevenson et al., 2007, Jeon and Murray, 2008, Kapur and Harries, 2013, Workneh et al., 2017) showing that diabetic patients are three to eight times more susceptible to TB compared to the general population (Jeon and Murray, 2008, Corris et al., 2012). Studies using animal models have also demonstrated that poor glycaemic control increases TB susceptibility (Saiki et al., 1980, Yamashiro et al., 2005, Martens et al., 2007, Vallerskog et al., 2010, Podell et al., 2014, Cheekatla et al., 2016). However, the biological basis for the association between both diseases is not completely understood. A compromised immune response in diabetic patients with poor glycaemic control might facilitate either primary progression of TB or reactivation of LTBI resulting in higher morbidity and mortality (Martens et al., 2007, Restrepo et al., 2008a, Vallerskog et al., 2010)

2.3.4 Tuberculosis incidence in diabetic patients

TB incidence in the diabetic population is increasing globally. A recent systematic review documented that the prevalence of diabetes among TB patients ranged from 1.9 to 45% with an overall median global prevalence of 16% (Figure 2.7). In contrast, the prevalence of TB patients with concomitant diabetes was 0.38 to 14%. The review also showed that the highest number of DM-TB co-morbid patients were found in Asia, North America and Oceania (Workneh et al., 2017).

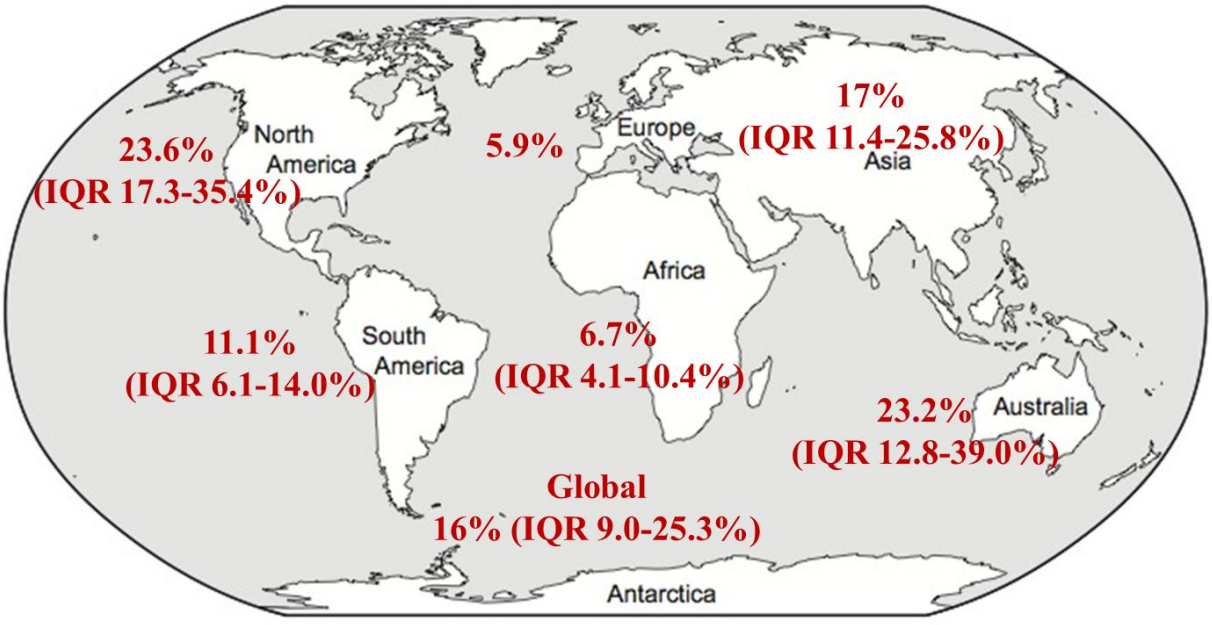

Figure 2.7 Regional prevalence of diabetes among tuberculosis patients (adapted from Workheh et al., 2017)

Studies have been conducted to determine the incidence of TB in diabetic patients in different countries. In India, diabetes combined with PTB was 14.8% in the mass population. The percentage of smear positive TB individuals with diabetes was 20.2% (8.3 to 41.9%) with a higher proportion from urban populations compared to rural (Stevenson et al., 2007). Several other reports have documented figures of 24.5% (Viswanathan et al., 2012), 29% (Balakrishnan et al., 2012) and 44% (Raghuraman et al., 2014) of diabetic patients with TB in the Indian population. TB incidence in diabetic patients in Texas and at the Mexican border was similar to India, at 36 to 39% (Restrepo et al., 2011). Faurholt-Jepsen and colleagues (2011) conducted a study in Mwanza in Tanzania and reported that the rates of diabetes were 16.7% (CI: 14.2–19.4) and 9.4% (CI: 6.6–13.0), in case (n=803) and control populations (n=350), respectively. Another study in Tanzania reported that 9.0% of patients with T2D and 2.7% of patients T1D had developed PTB (Mugusi et al., 1990). Olmos and colleagues (1989) conducted a cohort study considering 1529 diabetic individuals in Chile over 10 years (1959 to 1985) and concluded that the probability of developing TB in T2D was 24% compared to 48% in T1D patients. The authors also noticed that IGT (impaired glucose tolerance) was found in 37.6% (CI: 34.2–41.1%) of TB cases and 21.4% (CI: 17.2-26.1%) of control individuals, suggesting that insulin dependence was an important marker for increased TB susceptibility and its severity. Alisjahbana and others (2006) worked on prospective data from a cohort of TB patients in Indonesia where the prevalence of diabetes was confirmed at 14.8% compared to 3.2% in the general population. A study conducted in Taiwan stated that diabetes accounted for TB incidence was 4.09% and 3.03% in male and female population, respectively (Kuo et al., 2013). The authors also asserted that the relative risk of developing TB in diabetic populations was higher in younger people (from 30 to 70 years). Pablos-Mendez and co-workers (1997) also observed that 25% of Hispanic people aged between 25 and 54 years had a higher risk of being infected with TB attributed by diabetes. Saskatchewan Aboriginal people were also suffering from the epidemics of both T2D and TB. Higher TB incidence was noticed in diabetic women aged 20-59 years than non-diabetic women (Dyck et al., 2007). In Spain, 44% (69) patients were skin test positive among diabetes patients (n=163) indicating a higher burden of LTBI in diabetic patients. Unfortunately, there was no control group and no predictor of the disease was taken into account during this study (Mansilla Bermejo et al., 1995).

2.3.5 Consequences of the associations

2.3.5.1 Diabetes increases tuberculosis susceptibility

Diabetes has severe effects on human health. The major complications include increased occurrence of cardiovascular diseases, nephropathy, retinopathy, impaired wound healing, accelerated atherosclerosis etc. (Shah and Hux, 2003, Leutholtz and Ripoll, 2011). One of the major complications of poorly controlled diabetes is increased susceptibility to infections including TB (Martens et al., 2007, Jeon and Murray, 2008, Hodgson et al., 2015). The possible mechanisms for increased susceptibility to *Mtb* infections are thought to be directly related to hyperglycaemia with insulin resistance or deficiency, which affect both the innate and adaptive immune responses (Dooley and Chaisson, 2009, Tan et al., 2012, Gan, 2013).

The most important effector cells of the innate immune response in TB defence are the tissue macrophages. These cells perform many important functions including phagocytosis, antigen processing and presentation to T cells (CD4+ and CD8+ T cells) to enable an effective immune response to be mounted against TB. Abnormalities in macrophage phenotype, number polarization, chemotaxis, phagocytosis and cytokine responses have been documented in diabetes patients and animal models discussed in section 2.2.6. Such changes to macrophage may increase the susceptibility to *Mtb* infections. Macrophage function was also inhibited in diabetic-TB patients with impairment in the production of ROS, phagocytic and chemotactic functions (Hill et al., 1983, Glass et al., 1987, Abrass, 1991, Chang and Shaio, 1995, Geerlings and Hoepelman, 1999, Restrepo et al., 2008a, Lecube et al., 2011, Tan et al., 2012). Saiki and colleagues (1980) reported that a STZ-induced diabetic mouse model challenged with *Mtb* showed higher susceptibility to infection due to functional impairment of macrophages. Recent studies demonstrated that compromised phagocytosis of mycolic acid coated beads in diabetic macrophages was due to the lower expression of the macrophage receptors with collagenous structure (MARCO), TLR2 and the coreceptor for bacterial LPS (lipopolysaccharide), CD14 (Bowdish et al., 2009, Martinez et al., 2016). However, the success of host defence against TB largely depends on the activation of both $CD4^+$ and $CD8^+$ T cells (Kaufmann, 1991). These activated T cells release IFN-γ which is considered a principal mediator of protective immunity against TB (Wong and Pamer, 2003, Sud et al., 2006). In DM-TB patients, T cell mediated immunity is also adversely affected (Goonetilleke et al., 2003, Niazi and Kalra, 2012). Several studies documented that there were fewer T lymphocytes resulting in reduced production of IFN-γ, TNF-α, IL-1β and IL-6 observed in diabetic patients with TB compared to non-diabetic individuals (Tsukaguchi et al., 1997, Geerlings and Hoepelman, 1999). Furthermore, functional

impairment of T cells in a diabetic mouse model challenged with *Mtb* has also been documented (Saiki et al., 1980, Yamashiro et al., 2005, Martens et al., 2007, Vallerskog et al., 2010). Saiki and colleagues (1980) and Yamashiro and co-workers (200) reported T cell priming was delayed as macrophages failed to produce IL-12, resulting in higher bacterial burden in different organs. Afterwards, two other reports documented that increased TB susceptibility in diabetic mice was associated with reduced production of IL-12 and IFN-γ (Martens et al., 2007, Vallerskog et al., 2010). In fact, the functional abnormalities of both innate and adaptive cells (e.g. macrophage and T cell) in diabetic patients increase susceptibility to *Mtb* infections, as well as being responsible for other diabetic related complications.

2.3.5.2 Diabetes increases non-tuberculous mycobacterial infections

Epidemiological studies indicate a rising incidence of pulmonary and skin and soft tissue infections by NTM infections (De Groote and Huitt, 2006, Jackson et al., 2007, Hoefsloot et al., 2013). However, there is lack of reports relating to DM-NTM infections. Although there is a growing body of evidence of NTM infections in immunocompromised individuals with HIV infection (Tortoli et al., 1995, Piersimoni et al., 1997, Gholizadeh et al., 1998, O'Brien et al., 2014, Orme and Ordway, 2014, Xu et al., 2016), there are few studies reporting a link between diabetes and NTM infections (Uslan et al., 2006, de Mello et al., 2013, Bridson et al., 2016). A recent retrospective review of hospital data covering a 20 year period showed that NTM infections in diabetic patients were three times over-represented in comparison to the general population (Bridson et al., 2016). A study in Brazil showed that 9.8% of diabetes patients had associated pulmonary NTM infections, which was considered one of the leading co-morbid infections in those patients (Falkinham, 1996, de Mello et al., 2013, Orme and Ordway, 2014). Skin and soft tissue infections with NTM are often under-diagnosed; however, recent studies have shown the rates of infection are increasing. Bridson and colleagues (2016) observed 34.1% patients studied had skin and soft tissue infection due to *M. fortuitum* of which 11.4% were in T2D patients. Further, in the same study, 2.3% diabetic patients were infected with *M. ulcerans* (Bridson et al., 2016). Uslan and others (2006) observed 27.6% patients surveyed had skin and soft tissue infections caused by *M. ascessus* or *M. chelonae* and 16.7% by *M. fortuitum* in the same group of patients. A study on an Australian population observed a high rate of patients with oedematous *M. fortuitum* lesions with co-morbid diabetes (O'Brien et al., 2014). There are no studies conducted to date to determine how diabetes increases NTM infections. Therefore, studies are required to investigate the reasons behind increased NTM infections in diabetic patients.

2.3.5.3 Burden of mortality

The burden of mortality due to diabetes and its complications is enormous and rising sharply. In 2017, approximately 4 million (range, 3.2-5.0 million) people aged 20 to 79 years died from diabetes complications, which is equivalent to one death every eight seconds (IDF., 2017). The disease accounted 46.1% deaths due to diabetes itself and 10.7% of global mortality overall for people in this age group. This is higher than the combined number of deaths from any infectious diseases; 1.1, 1.8 and 0.4 million deaths from HIV infection, TB and malaria, respectively (IDF., 2017). On the other hand, TB remains as one of the deadliest diseases in the world and kills nearly 2 million people every year (WHO, 2013a). Alarmingly, between 5-10%, and in some countries more than 50% of diabetic patients suffer from TB, contributing to even more deaths (Dooley and Chaisson, 2009, Workneh et al., 2017). Further, there are 2 billion LTBI globally, where 5-10% reactivate every year due to immune suppressive conditions (Vynnycky and Fine, 2000, Martens et al., 2007, Mack et al., 2009, Dye et al., 2011). Therefore, the global death scenario arising from the association between these two life threatening diseases has revived over the last few years. Although there are no statistics on mortality due to this comorbid situation, several studies have shown that diabetes patients infected with PTB have 6-7% (Oursler et al., 2002, Dooley and Chaisson, 2009), 12.2% (Wang et al., 2009) and 16% (Lindoso et al., 2008) higher chances of death compared to non-diabetic patients. Indeed, the actual prediction of the number of deaths due to diabetes patients infected with TB is challenging because more than one-third of countries globally do not have any data on particular diseases and their mortality rates (Roglic and Unwin, 2010).

2.3.5.4 Economic burden

In addition to burden of mortality due to diabetes and its complications, the disease exerts a serious economic burden on individuals, families and societies. According to IDF, people with diabetes spent USD 232 billion in 2007 which reached to USD 727 billion in 2017 for the age group 20-79 years. This cost was USD 850 billion in 2017 when it was calculated for the expanded age group; 18-99 years (IDF., 2017). Region-wise health expenditure in 2017 clearly makes the difference in healthcare spending on diabetes. The North America and Caribbean region spent the highest among the seven IDF regions with an estimated USD 363 billion, which corresponded to 52% of the total amount spent in 2017. The second highest expenditure on diabetes was the European region (USD 181 billion) followed by Western Pacific region (USD 179 billion), which corresponded to 23% and 17%, respectively of the total global spending. The other regions (South and Central America, Middle East and North Africa, South-East Asia

and African regions) spent significantly less, responsible for only 9% of the total global spending on the diseases. However, the total healthcare expenditure on diabetes is predicted to reach USD 776 billion by 2045 for the age group 20-79 years (IDF., 2017).

TB has devastating economic effects on all ages, but the greatest effects are observed during the most productive years of life (15 to 44 years of age). The social effects of TB particularly on families are significant as it decreases the earning capability of an individual. In addition, failure to treat the infected person leads to a greater risk of infection for other family or community members. The disease reduces the productivity of the afflicted person by an average of 30% (WHO., 2013a). The annual estimated toll of TB infection was USD 1 billion, 2 million deaths and an average loss of 15 years' income per person, adding another 11 billion USD (WHO., 2013b).

Several studies have reported that diabetes leads to the treatment failure of TB (Morsy et al., 2003) and increases the chances of death of afflicted people (Mboussa et al., 2003, Lindoso et al., 2008, Dooley and Chaisson, 2009, Wang et al., 2009). Therefore, the impact would be huge in TB and DM co-morbid infections although no specific statistics on economic burden are available.

2.4 Animal models and their suitability in the investigation of type 2 diabetes-co-morbid infections

There are currently several rodent/murine models in use for diabetes studies, based on either naturally occurring mutations, inbred strains, tissue-specific knockout or transgenic mice. These have been used for studying the pathophysiology of diabetes itself and host-pathogen interactions which occur during co-morbid infection with diabetes. Genetically modified murine models of T2D such as *Lept*$^{db/db}$ and *Lept*$^{ob/ob}$ mice were developed from a spontaneous autosomal recessive mutation in the leptin gene (Zhang et al., 1994, Srinivasan and Ramarao, 2007). Such genetic models fail to incorporate the significant nutritional and polygenic determinants involved in the aetiopathology of the disease in humans. Further, the leptin signalling-deficiency can interfere with the host immune system, as leptin has many physiological and immunological roles, which limits the application of these models for research on T2D and associated diseases (Hodgson et al., 2011). The Kuo Kuondo (KK) mouse model of T2D develops insulin resistance at the age of 16-20 weeks. The problem with this model is that mice die very soon due to the lethal yellow gene (A^y) (Srinivasan and Ramarao, 2007). The Nagoya-Shibata-Yasuda (NSY) mouse model develops diabetes at a very slow rate and insulin resistance appears after 24 weeks of induction. This mouse model does not show

the islet pathology observed in human T2D patients (Ueda et al., 2000). The Zucker diabetic fatty rat (ZDF) and Goto-Katazaki rat model of T2D are also based on genetic defects (Chen et al., 1996, Movassat et al., 1997). The chemically induced mouse model using streptozotocin (STZ)/STZ+Nicotinamide (NA), destroys the pancreatic β-cell to shorten the length of time required for the development of T1D (Gilbert et al., 2011, King and Bowe, 2016). The limitations of those models are that the micro and macrovascular complications associated with clinical T2D require a considerable time to become established and these cannot be achieved in a short-term treatment regime. Moreover, chemically induced models have limited utility due to the toxicity of STZ on the renal and hepatic tissue (Deeds et al., 2011).

The diet-induced diabetic (DID) murine model is considered more akin to the aetiopathology of T2D of human patients (Hodgson et al., 2013a). However, there are considerable discrepancies in the metabolic features reported in the studies using DID models, which are confounded by the differences in dietary composition, fat content, age of the mice, duration of diet intervention, along with gender and inbred strain variability (King and Bowe, 2016). The DID mouse model was first introduced by Surwit and colleagues (1988) in C57BL/6 mice. The authors used an extremely HFD (60% of energy) to induce T2D, which markedly exceeds the typical dietary intake of the human population within any developed nation (34 % of energy) (Ludwig et al., 1999). Subsequently, others worked on the development of a more appropriate dietary model by changing the dietary compositions, however, they failed to fully characterise the model (Srinivasan et al., 2005, Adeyi et al., 2012). Over the past decade, it has become evident that intake of refined carbohydrates is one of the important contributing factors for the development of metabolic dysfunction. An energy-dense diet (EDD) characterised by the higher consumption of processed and red meat, high-fatty foods, sugary drinks and desserts, are positively correlated with the incidence of cardiovascular disease, cancer and T2D (Malik and Hu, 2015; Riccardi et al., 2008; Rizkalla, 2014). Hodgson and colleagues (2013a) investigated the impact of an EDD (23% fat, 19% protein and 50.5% dextrose) on the development of hyperglycaemia and glucose intolerance in male C57BL/6 mice after 10 weeks of the dietary intervention. The authors found a rapid progression of severe hyperglycaemia and glucose intolerance in mice after 10 weeks of dietary intervention. Although the authors used the model for Melioidosis-T2D co-morbid infection studies based on preliminary findings, they didn't fully characterise the model for the chronic clinical signs of T2D and its associated complications. The preliminary findings by Hodgson and co-workers (2013a) suggested that prolonged consumption of an EDD might be useful in developing chronic signs of T2D and its associated complications. Therefore, a fully characterised DID model would be a more

appropriate model of T2D over other genetically or chemically induced models for co-morbid infections studies (e.g. TB, NTM infections, melioidosis, malaria etc.)

2.5 Conclusion

The global burden of mycobacterial infections particularly tuberculosis is enormous. The most alarming aspect is that the association between these and other life-threatening diseases such as T2D, resulting in increasing mortality. The growing literature has provided the proof that T2D is an independent risk factor that increases TB and NTM susceptibility. However, the underlying immune mechanisms have not yet been determined. Studies in animal models have described some aspects of the immune mechanisms occurring in T1D conditions, but rather fewer in T2D. Future research should be directed to clarifying the exact nature of the association between TB and T2D to answers questions such as whether functional impairment of immune cells such as macrophages and T cells in T2D patients leads to increased susceptibility to *Mtb* infections. Furthermore, treatment failure in TB patients with diabetes is becoming another major global health concern. Research should also be directed to justify the use of Metformin as a companion drug to current anti-TB drugs in the treatment of TB-DM comorbid infections. Finally, therapeutic and protective measures should be designed through future research by addressing these burgeoning areas of research, otherwise, the global death toll will continue rising.

CHAPTER 3
GENERAL MATERIALS AND METHODS

3.1 Experimental animals

3.1.1 Animal ethics and biosafety approvals

All animal experiments were conducted according to the National Health and Medical Research Council (NHMRC) guidelines. Institutional ethics approval (#A2016) for the studies was granted by the James Cook University (JCU) Animal Ethics Review Committee. All experimental mice were housed in the Small Animal Breeding Unit (SABU) of JCU (DB86-002) for the induction of diabetes. Mice were moved to a physical containment 2 (PC2) laboratory (DB87-110) for *M. fortuitum* infection studies and a PC3 laboratory (DB87-120) for *M. bovis* (BCG) and *M. tuberculosis* (H37Rv) infection studies. Biosafety approval was granted for all experiments using all three species of mycobacteria (Table 3.1). All experiments and animal manipulations were performed in Class II biological safety cabinets.

Table 3.1 Biosafety approval for type 2 diabetes-mycobacterial infections co-morbidity study

Organism	Risk Assessment number	Biosafety Approval number
M. fortuitum	4339, 4218	JCUIBC-160601-007
M. bovis (BCG)	4892	JCUIBC-160601-011
M. tuberculosis (H37Rv)	4654	MI14-08

3.1.2 Mice and husbandry

Male C57BL/6 mice were used for the induction of diabetes based on previous findings (Hodgson et al., 2013a). Compared to female mice, male mice demonstrated increased susceptibility to obesity and insulin resistance in response to a high-fat diet (Stubbins et al., 2012). For this reason, male mice were used in the current study. Six-week old mice were obtained from two different sources: a) Australian Resource Centre (ARC), Perth, Western Australia (referred to as ARC bred mice) and b) Small Animal Breeding Unit (SABU) at the of College of Public Health, Medical and Veterinary Sciences, James Cook University (referred to as JCU bred mice). All experimental mice were housed in SABU of JCU. Mice at 4 weeks

of age were ear marked (for the identification, Figure 3.1) and housed in standard animal cases (5 mice/cage) in a temperature and light controlled room (18-22^{0}C, 12 hours light/dark cycle and relative humidity 70-75%). Saw dust was used as bedding materials. When the mice were moved to the particular laboratories for infection studies were housed in Tecniplast Green Line IVC (individually ventilated cages) in PC2 and Tecniplast N biocontainment ISOcages in PC3. To get rid of excess dust from the bedding materials, special bedding (Bed-o'Cobs® 1/8″, The Anderson, Ohio, USA) was used in PC3. Animal cages, bedding, water bottles were changed at every seven days interval. Mice were regularly checked for feed and water.

3.1.3 Diets and feeding regime

After two weeks being housed (acclimatisation period), mice were randomly separated into two dietary groups. The control group (Standard Rodent Diet; SRD or non-diabetic group) was provided with 4.5 g (per mouse/day) of SRD (Goldmix Stockfeeds, South Lismore, New South Wales, Australia, Rat and Mouse Nuts: 4.8% fat, 20% protein, 62.8% complex carbohydrates and 12.4% fibre). Experimental groups (Energy-dense diet; EDD or diabetic group) received an *ad libitum* amount of EDD (Specialty Feeds, Glen Forrest, Western Australia, SF03-030: 23% fat, 19% protein, 50.5% refined carbohydrate as dextrose and 7.5% fibre). To control the possible differences in consumption rates due to the palatability of the diets, the control groups were supplied an isometric quantity of feed based on the daily consumption calculated based on previous week (4.5 g/mouse/day or 13.86 kcal/mouse/day). Previous literature states an approximately 3.5 to 3.75 g/mouse/day (equivalent to 13.65 to 14.62 kcal/mouse/day) is the average feed intake for a mouse to reach the maturity (National Research Council Subcommittee on Laboratory Animal Nutrition., 1995). Therefore, the control mice were not given more feed per day beyond the daily requirement. Mice were kept on dietary intervention for a period of 30 weeks.

Moreover, the average daily feed consumption of the mice was measured by subtracting the amount of feed remaining after 24 hours from the initial amount of feed supplied. At least two feed intakes were recorded for each of the cage in a week and then overall average daily feed intake per mouse was calculated. This procedure was repeated at the same time of each week until the end of the diet intervention period. The weekly body weight gain was monitored throughout the period.

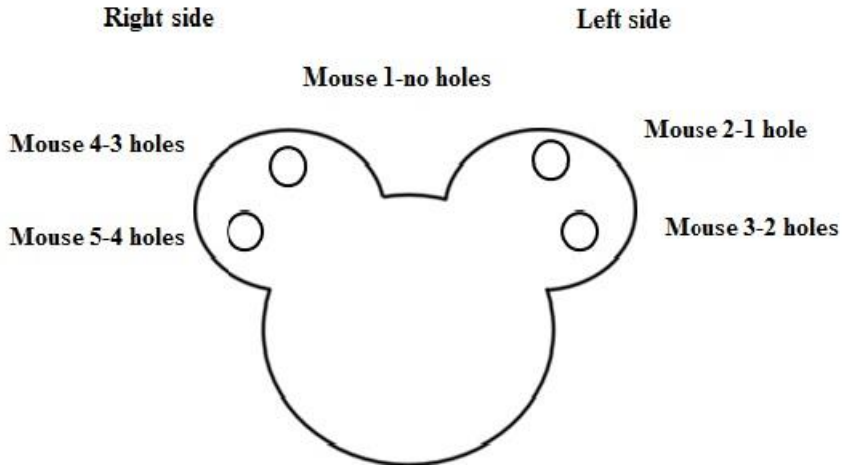

Figure 3.1 Ear marking of mouse for longitudinal tracking

3.2 Assessment of metabolic parameters

3.2.1 Measurement of fasting blood glucose

Feed from cages was removed 6 hours prior to measure the fasting blood glucose (FBG) concentration as per the previous literature (Ayala et al., 2010, Hodgson et al., 2013a). Each mouse was placed in a restraining box with tail exposed. The tip of the tail (<1 mm) was cut using a sterile scalpel blade (Livingstone sterile surgical blades #SBLDCL24). A gentle pressure was applied to get a small drop of blood (~5 µL) which was then placed on the blood glucose test strips of the Accu-Chek® Performa blood glucose meter (Roche, Castle Hill, NSW, Australia).

3.2.2 Glucose tolerance test

Glucose tolerance test (GTT) was performed after the dietary intervention. As per the measurement of FBG concentration (section 3.2.1), it was done on 6 hourly morning fasted (6 am to 12 pm) mice according to the published methods (Ayala et al., 2010, Hodgson et al., 2013a). In short, the glucose solution (2 g/kg lean body weight) was first calculated (70% and 90% of the gross body weight of mice on EDD and SRD, respectively). The baseline FBG level (as '0' minutes) was first measured before injecting the glucose solution. Then, a volume of 100 µL containing the desired amount of glucose was injected intraperitoneally to individual mouse (Appendix 1). The blood glucose level was measured at 15, 30, 60 and 120 minutes post injection from the lateral tail vein. After performing GTT, an appropriate amount of feed was provided and water supply was checked.

Hyperglycaemic threshold was considered as a marker of type 2 diabetes (T2D) if the EDD fed mice demonstrated a raised FBG level with an evidence of glucose intolerance and area under the curve (calculated based on GTT) at levels higher than the upper 99% confidence interval for the mean of age-matched control group fed on a SRD (Hodgson et al., 2013a, Morris et al., 2016). Mice failed to meet the above criteria were not considered for the subsequent studies.

3.3 Mycobacterium spp culture

3.3.1 Mycobacterial isolates

Mycobacterium fortuitum was kindly provided by Dr Jacqueline Picard, College of Public Health, Medical and Veterinary Sciences, Centre for Biosecurity in Tropical Infectious Diseases, JCU. *Mycobacterium bovis* (BCG) was provided by Dr Nick West, School of Chemistry and Molecular Biosciences, The University of Queensland, Australia. *Mycobacterium tuberculosis* (H37Rv) ATCC (American Type Culture Collection) strain was imported (permit number # 0000281462) from BEI resources of United States of America (USA) under licensed by Professor Natkunam Ketheesan with prior approval from the Department of Agriculture and Water Resources, Australian Government.

3.3.2 Preparation of mycobacterial stocks

Mycobacterium fortuitum was grown on 7H11 agar plates (cat. no. M0428, Sigma; Appendix 1) for 10-15 days at 37^0C with 5% CO_2 (Figure 3.2 A). Several single colonies were selected and cultured in 100 mL of 7H9 broth (cat. no. M0178, Sigma; Appendix 1) supplemented with OADC (Oleic Acid–Dextrose-Catalase) medium (cat. no. 212240, BD Biosciences, Australia). The broth was cultured at 37^0C with mild agitation (100 rotation per minute; rpm) for 72-96 hours to bring the bacteria to the logarithmic phase (Optical Density; OD_{600nm} 0.6 to 0.9). The bacteria were pelleted (4000 xg for 10 minutes) and washed twice with phosphate buffer saline (PBS; pH 7.2, Appendix 1). The cell pellet was finally resuspended in 50 mL (half of the originally cultured volume) of storage medium (Appendix 1) and aliquoted into 1 mL screw capped vials for preservation at -80^0C. To determine the concentration (CFU/mL) of this frozen stock, serial 10-fold dilutions were prepared and plated on 7H11 agar plates (10 µL of triplicates/dilution). The colonies were counted after one week of incubation at 37^0C with 5% CO_2. The purity of the culture was checked by plating on 7H11 culture plates (with no added antibiotic or antifungal agents) and blood agar. Gram and Ziehl-Neelsen (ZN) staining (Figure 3.2 B) was also done to confirm the acid-fastness of the bacteria.

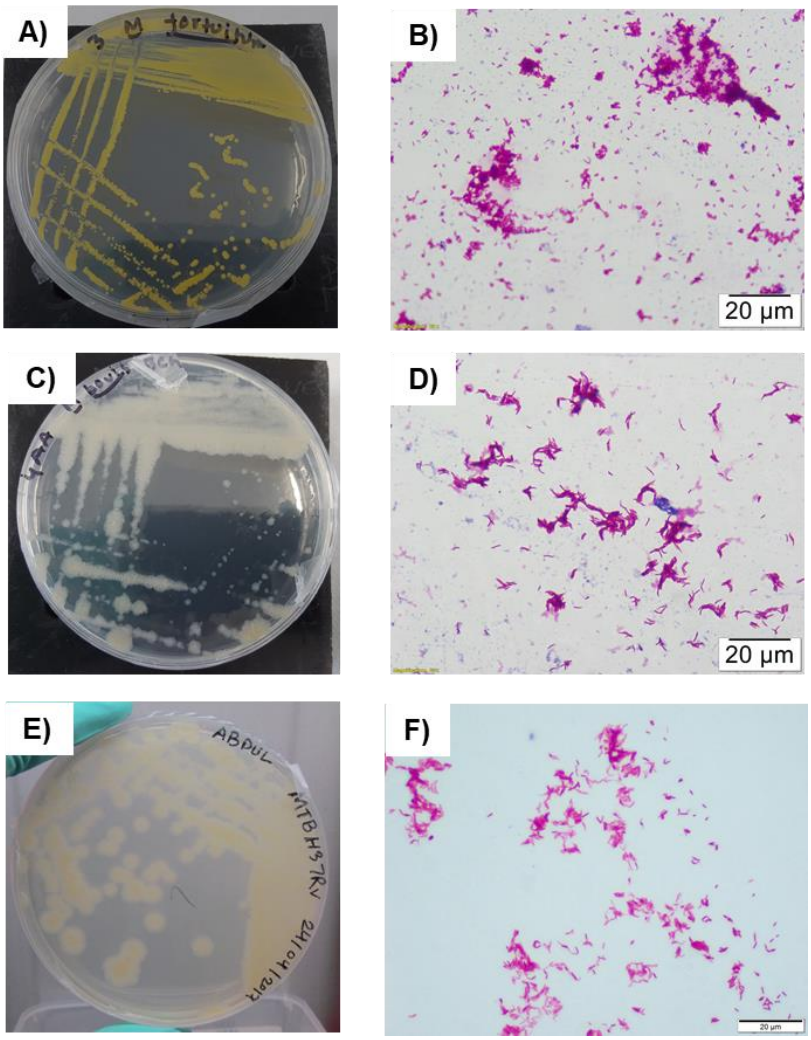

Figure 3.2 Colony morphology and acid-fast staining of the mycobacterial species

Colony morphology (left panel) on 7H11 agar plates and acid-fastness (right panel) of mycobacteria after Ziehl-Neelsen staining. A) & B) *Mycobacterium fortuitum*, C) & D) *M. bovis* (BCG) and E) & F) *Mycobacterium tuberculosis* (H37Rv). Scale bar of the images: B, D & F, 20 µm.

Mycobacterium bovis (BCG) was first grown on the 7H11 agar plates (Figure 3.2 C). A pure single colony was then inoculated into a 50 mL tube having 10 mL of 7H9 broth supplemented with OADC medium. After 1-2 weeks of culture at 37^0C with 120 rpm. The culture was then transferred into a 100 mL of 7H9 broth and further incubated at 37^0C with mild agitation (100 rpm) to bring the culture to the logarithmic phase (OD_{600nm} 0.6 to 0.9). Processing of the bacterial culture, enumeration (after 2-3 weeks of plating) and purity checking were done following the same procedure described for *M. fortuitum*. Acid-fastness of the bacteria was confirmed by using ZN staining (Figure 3.2 D).

Mycobacterium tuberculosis (H37Rv) stock received from BEI resources was cultured on 7H11 agar slant and preserved on cryobeads (Microbank®, PL.170/R, USA). The working stock was

prepared by removing one bead into a 50 mL tube containing 10 mL of 7H9 broth. Further culturing, processing, enumeration and purity checking were done following the same procedure described for *M. bovis* (BCG) and *M. fortuitum* (Figure 3.2 E & F). Previously published protocols were followed for the culturing of the all the mycobacterial species (Larsen et al., 2007, Singh and Reyrat, 2009).

3.4 Amikacin susceptibility testing of *Mycobacterium fortuitum*

To make sure the Amikacin susceptibility of the used *M. fortuitum* strain, a minimum inhibitory concentration (MIC) value was determined by the broth microdilution method (Yang et al., 2003). Briefly, a twofold serial dilution was prepared using amikacin (cat no. A2324-5G, Sigma) in a 96 well plate. The highest and lowest concentration of the antibiotic in the well was 8 µg and 0.25 µg, respectively. After adding the bacteria at a concentration of $1\text{-}10^4$ to $5x10^5$ CFU/well, the plate was incubated at 37^0C with 5% CO_2 for 7 days. The MIC value was interpreted according to the approved guidelines (National Committee for Clinical Laboratory Standards., 2002). The recommended range for amikacin susceptibility for *M. fortuitum* was 1-16 µg/mL. We observed the value of our studied *M. fortuitum* strain was 0.5 µg/mL. However, amikacin susceptibility for *M. bovis* (BCG) and *M. tuberculosis* (H37Rv) was not done as we already know they are susceptibility to Amikacin.

3.5 Histopathological analysis of tissue samples

Tissue samples collected for histopathological examinations were fixed in 10% neutral buffered formalin (NFB) (Appendix 1) for a minimum of 24-48 hours. The preserved tissue samples were processed by a 6 hours cycle using a Shandon Citadel 2000 Tissue Processor (Shandon Southern Products Ltd, United Kingdom). After paraffin embedding, 5 µm sections (at least two sections from each mouse tissue) were cut and stained with the Haematoxylin and Eosin (H&E, Appendix 1), Jones Periodic Acid Schiff's (PAS; Appendix 1) and Ziehl-Neelsen (ZN) stain (Appendix 1) using standard protocols. Cryosections of formalin fixed liver were prepared in optimum cutting temperature (OCT) medium (Tissue Tek, Olympus, Notting Hill, VIC, Australia). Cryosections (5 µm thickness) were then stained with Herxheimer's solution and counterstained with Mayer's Haematoxylin (Appendix 1). Overall, modified Herxheimer's staining of the cryosections of the liver was considered for the quantification of lipid deposition. Haematoxylin and Eosin staining of visceral adipose tissue and pancreas were done to quantify the size of adipocyte and percent islet area over the total pancreatic area, respectively. The PAS staining was performed to quantify the mesangial matrix thickening and thickening of the Bowman's capsule in kidneys. However, H&E staining of the mycobacteria infected liver and

lungs were also done to quantify the inflammatory lesions in those organs. The ZN staining was used to quantify the mycobacterial load in the inflammatory foci/granuloma of the liver.

3.5.1 Assessment of lipid deposition in liver

All stained liver sections were visualised and analysed using a light microscope (BX43 Olympus), connected to CellSens® Image Analysis software. Histological analyses of captured digital images of each tissue were conducted on representative sections. For the determination of the extent of neutral lipid deposition in liver sections, a minimum of 10 images of each liver section of each mouse was taken at the 20x objective (200x magnification). A control slide with desired (red colour as lipid accumulation in the liver, Figure 3.3 A & B) and other lesions were prepared using a threshold-based phase segmentation technique, where lipid, nuclei and other structures were defined as red, deep blue and light blue and yellow, respectively (Figure 3.3 B). The software calculates the intensity of each colour compared to those already defined. The control image was used as a standard image for the calculation of the percentage of each colour intensity in each representative image. Data were expressed as the percentage of red colour (i.e. lipid) on each representative image (Morris et al., 2016). The lipid deposition was determined on liver sections of mice following diet intervention because it has shown that ectopic lipid deposition in liver associated with hepatic insulin resistance in patients with diabetes (Bays et al., 2004, Cusi, 2010).

3.5.2 Assessment of adipocyte size

The mean adipocyte size within visceral adipose tissue (VAT) section from each mouse was assessed by measuring the area of a minimum of 50 adjacent adipocytes per section. At least 5 images (200x magnification) from each VAT section of each mouse were evaluated (Figure 3.3 C & D). Selection bias was minimised by taking 5 continuous images starting from a random point for each section. Microscope fields with incomplete adipocytes or artefacts were not imaged (Morris et al., 2016). The adipocyte size was determined in mice following diet intervention as adiposity and abnormal adipocyte morphology is associated with insulin resistance and complication of diabetes (Black et al., 1998, Herberg, 1998).

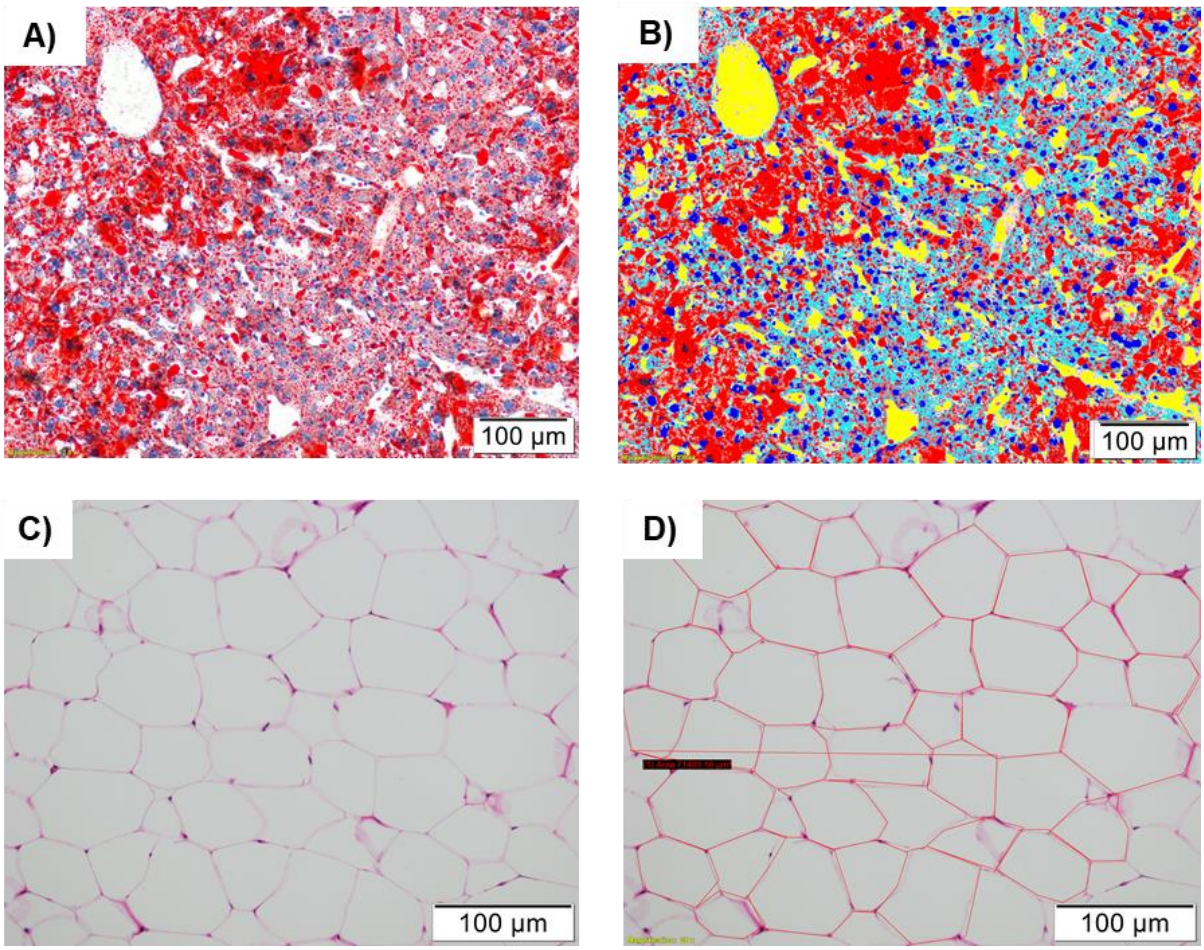

Figure 3.3 Measuring the lipid deposition and size of the adipocyte

The lipid deposition in the liver was quantified based on the phase segmentation technique using the CellSens® Image Analysis software. All the images were taken using a 20x objective. A control image was selected having both desired and other lesions. Then, all the colours on that chosen control image were defined in the software; red as lipid (desired lesion), deep blue as nuclei of the cells and light blue and yellow as cytoplasm and intracellular/empty spaces (B). All the images were then analysed based the control image (B) where, the software provides the percentages of each colour intensity of those already defined. Moreover, the size of each individual adipocyte was determined by taking the photographs at 20x objective (C) and followed by measuring the size of adjacent each individual adipocyte using a polygonal tracing tool of the CellSens® software (D). Scale bar of the images: A-D, 100 µm.

3.5.3 Assessment of pancreatic islet hyperplasia

The total pancreatic area was determined from representative H&E stained sections (40x magnification) from individual mouse (Figure 3.4 A). The area of each islet of Langerhan's measured at 20x objective (200x magnification) (Figure 3.4 B). Data were expressed as the percentage of pancreatic islet area over the total pancreatic area of each mouse (Morris et al., 2016). The pancreatic area over the total pancreatic area was measured because compensatory

hyperplasia represents insulin resistance, which is a characteristic feature of type 2 diabetes (T2D) (Del Prato, 2009, Kahn et al., 2014).

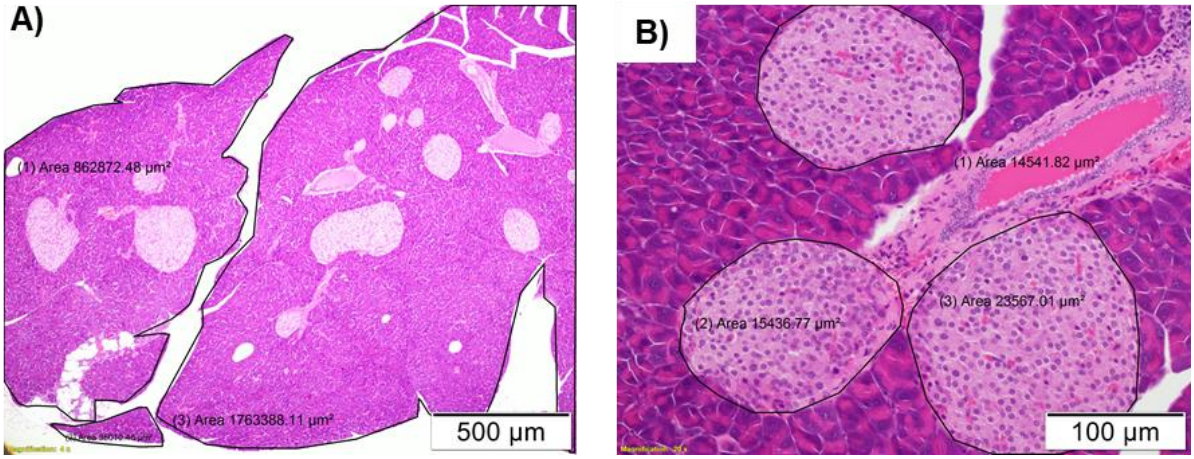

Figure 3.4 Measuring the pancreatic islet hyperplasia

For the quantification of pancreatic islet hyperplasia, the total area of the pancreas was measured using the polygonal tracing tools of the Cellsens® software on images taken at 4x objective (A). Then, the size of each pancreatic islet was measured on the images taken at 20x objective using the same tools (B). Scale bar of the images: A; 500 µm and B; 100 µm.

3.5.4 Assessment of kidney for mesangial thickening and glomerular hypertrophy

Kidney sections were evaluated by the threshold-based phase segmentation technique (described in section 3.5.1) to compare the percentage of the PAS-positive staining within the glomerular capillary tufts, relative to the glomerular area (red colour, Figure 3.5 B). All the photographs of the glomeruli were taken at 20x objective (200x magnification). A control image was prepared and definied based on the colour where red, blue and less pink area represents the deposition of collagen and glycoprotein in the capillary tufts, nuclei of the cells and other structure; respectively on the kidney sections (Figure 3.5 A). The perimeter of each glomerulus was outlined using a polygonal tracing tool of the CellSens® software. The colours of the selected glomerular area were then analysed by the area fraction ROI (region of interest) tool of the software (Figure 3.5 B). All the remaining images were quantified for ROI (colour intensity within the glomerulus only) based on the control image. A minimum of 30 glomeruli per kidney was considered. Glomeruli free of artefacts were selected for measuring. Selection bias was minimised by starting from equivalent points in the outer cortex moving clockwise and selecting the first acceptable glomerulus (Morris et al., 2016). The kidney damages as a measure of microvascular complications in diabetes lead to renal failure (McKenna and

Thompson, 1997). Therefore, kidney damages were measured in terms of mesangial matrix thickening, thickening of the Bowman's capsule and glomerular hypertrophy to ensure that prolong EDD fed mice showed the features of microvascular complications.

.

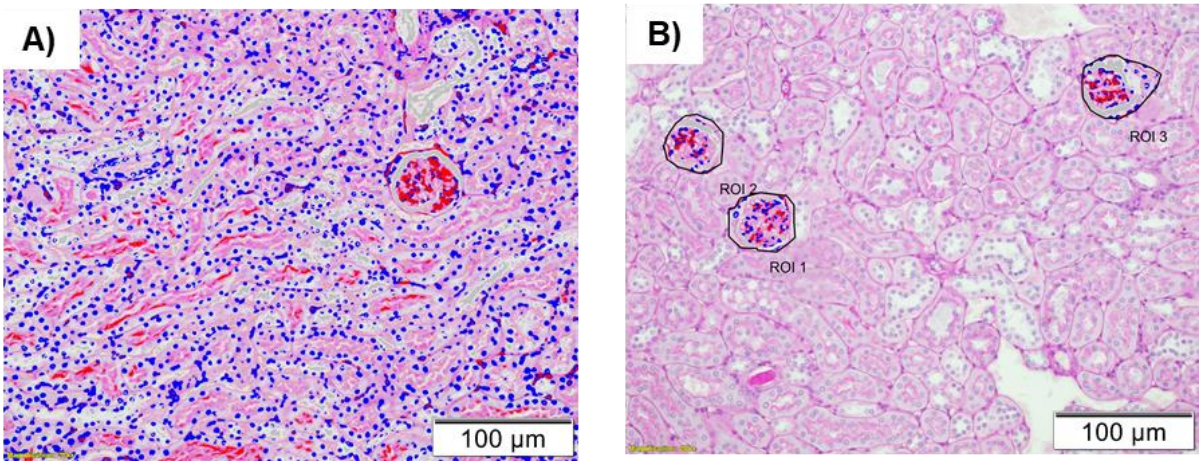

Figure 3.5 Assessment of size of glomerulus and Periodic Acid Schiff's (PAS)-positive stained area in kidney

For the quantification of the PAS-positive stained area within the glomerular capillary tufts, photographs of the glomeruli were taken at 20x objective. A control image was selected comprising both desired (red colour representing the collagen and glycoprotein deposition) and other lesions (other colour such blue for incluei of the cells). Then, all the colours on that chosen image were defined in the software; red as PAS-postive stain, blue as nuclei and rest of the colours (light pink and white) as other structures/empty spaces on the kidney section (A). The colours of the only selected glomerular area were analysed by the area fraction ROI (region of interest) tool of the CellSens® software (B). Scale bar of the images: A-B; 100 µm.

3.5.5 Assessment of organ inflammation

The percentage of the inflamed area over the liver section was quantified on the representative images. A minimum of 10 representative images from each liver section was taken at 20x or 10x objective. The polygonal tracing tool of the CellSens® software was used to measure the total area of the representative tissue and the inflamed area (i.e. size of each inflammatory focus/granuloma) (Figure 3.6 A & B). A minimum number of 50 inflammatory cells (as determined by nuclear staining) was considered to be an area of inflammation on the liver. Previous studies in animal models have demonstrated a diffuse inflammation at the earliest timepoint of infection, whereas the granulomatous response becomes more conspicuous at later timepoints post-infection (pi). This is one of the reasons for choosing 50 inflammatory cells; in the current study, aggregates of cells started to appear from 14 days pi. However, during image capturing, selection bias was minimised by taking 10 continuous images starting from a point

of each liver section. Data were expressed as the percentage of the inflamed area over the total liver area measured on each liver section. The inflammatory foci/granuloma on liver sections were represented as average number of inflammatory foci on each image taken at 200x magnification (Flynn et al., 1998, Chambers et al., 2006, Silva et al., 2010).

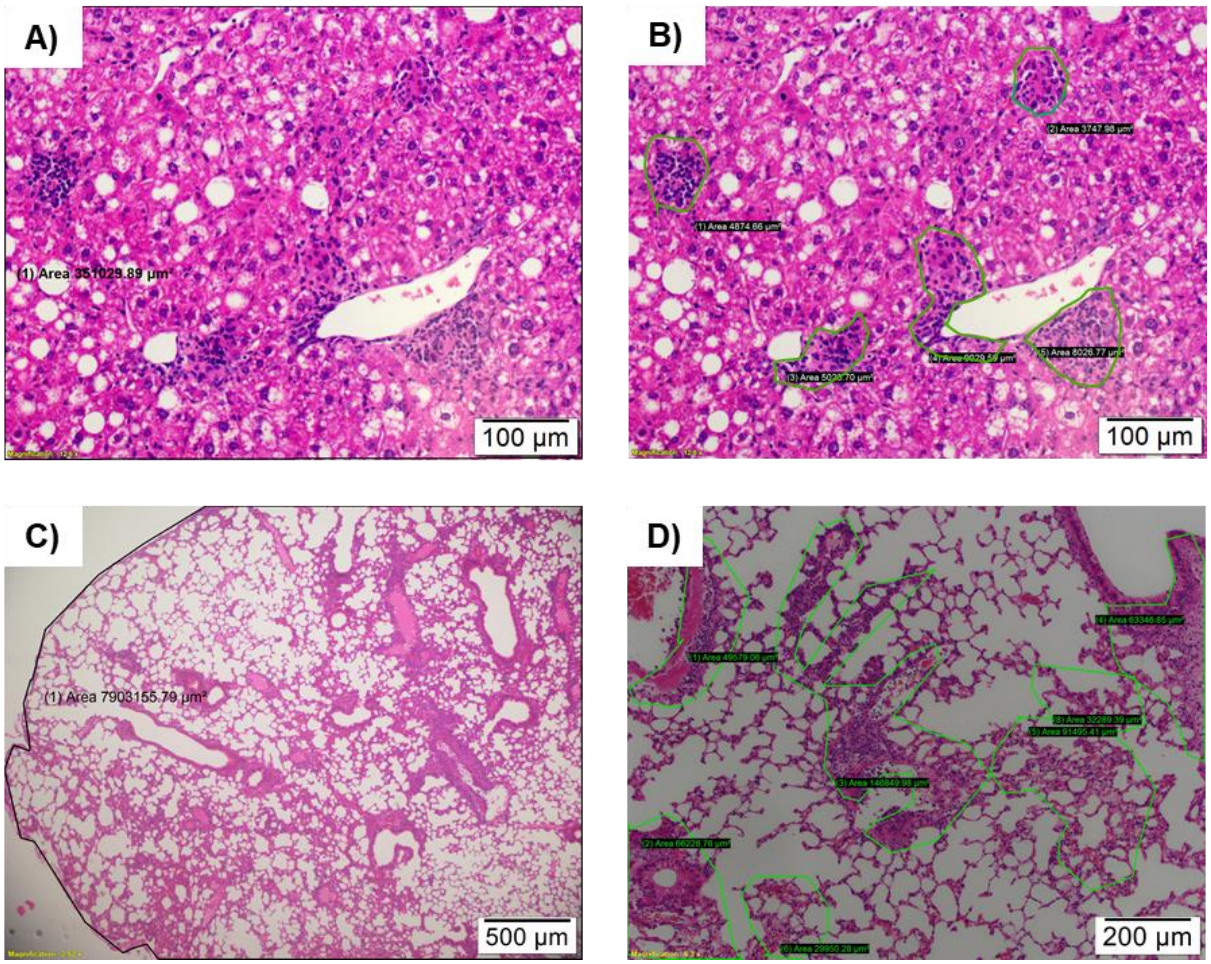

Figure 3.6 Quantification of the inflamed area in liver and lungs

The percentage of the inflamed area over the total area of liver and lungs were quantified on the representative images using the CellSens® software. For the quantification of the inflamed area on the liver section, photographs (starting from a point and then the photo of 10 continuous fields) were taken at 20x or 10x objective followed by the measuring the total area (A) and the inflamed area (B) by a tracing tool of the software. For lungs lesions, the total area of the lungs (area of entire lobes) was measured on the images taken at 4x objective (C) using the same tool of the software. Then, the total inflamed area was computed on images (for the same lungs lobes) taken at 10x objective using the same tracing tool (D). Scale bar of the images: A-B; 100 µm, C; 500 µm and D; 200 µm.

The inflamed area over the total area of the lungs was evaluated on representative images of lung sections. The total area of a representative section (left lobe of lungs from each mouse) was measured by images captured using the 4x objective (Figure 3.6 C). The inflamed area was calculated on the same lung section taking by capturing images using 10x objective (Figure 3.6 D). A minimum number of 50 inflammatory cells in an area on a lung section was considered an inflamed area. Data were expressed as the percentage of the inflamed area over the total lung area measured on each mouse section (Schneider et al., 2010, Kupz et al., 2016).

3.6 Ziehl-Neelsen staining of liver sections for localisation of mycobacteria

A representative liver section from each mouse was deparaffinised. Sections were first stained with Carbol fuschin (Appendix 1) for 5 minutes with mild heat. Decolorisation of the section was done using acetone alcohol (Appendix 1) and followed by staining with 0.5% Methylene blue for 5-10 seconds. Stained sections were dehydrated with a series of graded alcohol solutions before mounting with mounting media (Reynolds et al., 2009).

Stained representative liver sections were imaged using the 100x objective to facilitate the counting of bacteria within inflammatory foci/granulomas. A total of 10 first positive inflammatory foci/granuloma (presence of at least one bacterium) from each liver section were counted for the acid-fast bacilli. Selection bias was minimised by starting from a random point of the liver section and moving back and forth motion until counting the desired number of the positive inflammatory foci/granulomas. Bacilli within the individual cells or dispersed over the liver parenchyma were not counted. Data were expressed as percentage of acid-fast bacilli in each inflammatory focus/granuloma over the total bacilli counted in 10 inflammatory foci/granulomas on each of the liver section (Chambers et al., 2006).

3.7 Flow cytometry

In this investigation, BD FACSCalibur™ flow cytometer (BD Biosciences) was used to determine phagocytosis based on beads labelled with fluorescent dye. Cytokine data during performing bead based multiplex BD cytometric bead array (BD Biosciences) were also acquired by the same flow cytometer. This cytometer comprises one blue laser (488 nm) and a red laser (~635 nm). The blue laser excites FITC (Fluorescein isothiocyanate), PE (Phycoerythrin) and PerCP (peridinin chlorophyll protein) fluorescent dyes, whereas the red laser excites APC (Allophycocyanin) dye. All data were acquired by BD CellQuest™ software (BD Biosciences).

3.8 Cytokine analysis in cell culture and organ homogenates' supernatants

Inflammatory cytokines concentrations in cell culture and organ homogenates' supernatants were determined using the BD Cytometric Bead Array Mouse Inflammation Kit® (cat. no. 552364, TNF-α, MCP-1, IL-6, IFN-γ, IL-10 and IL-12p70), Mouse Th1/Th2/Th17 Cytokine Kit® (cat. no. 60485, IL-2, IL-4, IL-17A) and Mouse IL-1β Flex Set (cat. no. 560232). Manufacturer's instructions were followed to assess the cytokine level. The limit of detection of each cytokine was presented in Table 3.2. The principles of BD Cytometric Bead Array involve capturing of a soluble analyte or set of analytes with beads of known size and fluorescence, making it possible to detect analytes using flow cytometry. When the capture beads and detector reagent are incubated with an unknown sample containing recognised analytes, sandwich complexes (capture bead + analyte + detection reagent) are formed. These complexes can be measured using flow cytometry to identify particles with fluorescence characteristics of both the bead and the detector. Then the flow cytometry data are analysed by the BD FCAP Array ™ software (version 3). The software generates a standard curve based on the known fluorescent intensity of cytokine standard. The fluorescent intensity for each of the sample is compared with the standard curve to generate the concentration of the cytokines. In this investigation, cytokine data were acquired by the BD FACSCalibur™ flow cytometer using BD CellQuest® software and analysed by BD FCAP Array ™ software (version 3.0).

Table 3.2 Limit of detection of cytokines

Name of cytokines	Limit of detection (pg/mL)
TNF (tumor necrosis factor)-α	7.3
MCP (monocyte chemoattractant factor)-1	52.7
IL (interleukin)-6	5.0
IFN (interferon)-γ	2.5
IL-10	17.5
IL-12p70	10.7
IL-2	0.1
IL-4	0.03
IL-17A	0.8
IL-1β	1.9

However, at the last step of the staining, we treated the samples with 3.33% paraformaldehyde (PFA; cat. no. 00-8222-49, Thermofisher Scientific, Australia) for 30 minutes for the killing of all the viable mycobacteria. The mentioned time required for killing of the mycobacteria were determined by performing a separate experiment where mycobacterial cultures (*M. bovis,* BCG

and *M. tuberculosis,* H37Rv) were treated with the 3.33% PFA for 0, 30, 40 and 50 minutes. No growth was observed after 30 minutes of PFA treatment (Appendix 1).

3.9 Animal and animal-derived waste disposal

Mice were monitored daily and moribund/dead animals (if any) were removed from the cages and disposed according to the institutional biosafety guidelines. The mycobacteria infected/uninfected sacrificed mice at the endpoint of the experiment were also disposed following the guidelines. For *M. tuberculosis* (H37Rv) infected wastes were removed from the PC3 lab after an appropriate autoclave cycle and records were maintained strictly.

3.10 Statistical analysis

Statistical analysis was performed using the SPSS version 24.0 and GraphPad Prism 7.03 software. Data were checked for normality using the Shapiro-Wilk's test. Data passed the test of normality if $p \geq 0.05$. The normally distributed data were compared between the groups using the unpaired *t*-test with Welch's correction. The normally distributed data of multiple groups were compared using the ordinary one-way ANOVA with Holm-Sidak's multiple comparisons test. In contrast, the non-normally distributed data were compared between the groups using the non-parametric Mann-Whitney U test. The Kruskal-Wallis test with Dunn's multiple comparisons was performed for non-normally distributed data of multiple groups. However, the two-way ANOVA with Sidak's multiple comparisons test was performed for the data having the repetitive measures (e.g. glucose tolerance test, kinetics of feed and energy intake, body mass). The Kaplan Meier survival curves with log-rank (Mantel-Cox) tests were used to compare diabetic and control mouse survival after mycobacterial infections. All data were presented as mean±SEM (Standard Error of the Mean). The level of significance was indicated as *$p \leq 0.05$, **$p \leq 0.01$, ***$p \leq 0.001$ and ****$p \leq 0.0001$.

CHAPTER 4
CHARACTERISATION OF A DIET-INDUCED MURINE MODEL OF TYPE 2 DIABETES

4.1 Introduction

Diabetes mellitus (DM), in particular, type 2 diabetes (T2D) is a multifactorial metabolic disorder. The key factor that contributes to the development of T2D involves the dynamic interplay between lifestyle factors and genetic predisposition. Obesity is considered one of the key factors for the escalation of global T2D over the last half century (Gerich, 1998, Lewis, 2013, Scheen and Van Gaal, 2014). The consumption of high glycaemia index diet associated with the persistent hyperglycaemia results in the deposition of advanced glycation end products and oxidative stress, chronic inflammation and many immune defects, microvascular (e.g. retinopathy, nephropathy and neuropathy) and macrovascular complications (e.g. atherosclerosis, cardiovascular diseases) (Shah and Hux, 2003, Leutholtz and Ripoll, 2011). Another important complication of T2D includes the increased susceptibility to infections, results in a higher morbidity and mortality of those patients (Bridson et al., 2014, Hodgson et al., 2015). Despite the global health priority of T2D, the pathophysiological mechanisms underlying it are still incomplete. Moreover, the escalating association between T2D with other diseases (e.g. HIV infection, tuberculosis, melioidosis) warranted an appropriate animal model to further understand the mechanisms of host-pathogen interaction and evaluation of potential therapeutic drugs for their treatment.

In addition to clinical studies in human diabetic patients, previous studies using animal models have contributed to our understanding of some aspect of insulin resistance, obesity and diabetes (Surwit et al., 1988, Tomita et al., 1992, Zhang et al., 1994, Black et al., 1998, Suzuki et al., 1999, Sharma et al., 2003, Kawasaki et al., 2005, Cefalu, 2006, Kanetsuna et al., 2007, Brosius et al., 2009, Hodgson et al., 2013a). There are currently several rodent/murine models in use either on naturally occurring mutations, genetically engineered, inbred strains, tissue-specific knockout and transgenic mice. Such genetic models fail to reflect the significant nutritional and polygenic determinants involved in the aetiopathology of the disease in humans (Hodgson et al., 2011). Chemically induced mouse models using streptozotocin (STZ), which destroys the pancreatic β-cell to shorten the length of time required for the development of diabetic symptoms (Gilbert et al., 2011, King and Bowe, 2016). The limitations of those models are that the micro and macrovascular complications associated with clinical T2D require a considerable time to become established and these cannot be achieved in a short-term treatment regime.

Moreover, chemically induced models have limited utility due to the toxicity of STZ on the renal and hepatic tissue (Deeds et al., 2011).

In contrast, the diet-induced diabetic (DID) murine model is considered more akin to the aetiopathology of T2D of human patients. The DID mouse model was first introduced by Surwit and colleagues (1988) in C57BL/6 mice. The authors used an extremely high-fat diet (60% of energy) to induce diabetes, which markedly exceeds the typical dietary intake of the population within any developed nation (34 % of energy) (Ludwig et al., 1999). Subsequently, others worked on the development of a more appropriate DID model by changing the dietary compositions (Srinivasan et al., 2005, Adeyi et al., 2012), but they didn't characterise the model based on the biochemical parameters and vascular complications that occur in human T2D patients. Furthermore, there are considerable discrepancies in the metabolic features reported in the studies using DID models, which are confounded by the differences in dietary composition, fat content, age of the mice, duration of diet intervention, along with gender and inbred strain variability (King and Bowe, 2016).

Considering the global dietary pattern, we have used an energy-dense diet (EDD) (23% fat, 19% protein and 50.5% dextrose) in the development of hyperglycaemia and glucose intolerance in C57BL/6 mice after 10 weeks of dietary intervention (Hodgson et al., 2013a). A rapid progression of hyperglycaemia and glucose intolerance were observed in mice on EDD compared to the controls on standard rodent diet (SRD). The preliminary findings by the Hodgson and co-workers (2013a) suggest that prolonged consumption of EDD can lead to the development of chronic features of T2D and its associated vascular complications. Previous studies on DID mouse models (Surwit et al., 1988, Srinivasan et al., 2005) including our study using EDD (Hodgson et al., 2013a), were only characterised the model for insulin resistance based on fasting blood glucose concentration and glucose tolerance test. The caveats of these studies were the model was not characterised for many biochemical parameters (e.g. HbA1c, lipid profile) and associated pathologies in organs (e.g. pancreas, liver, adipose tissue, kidneys) observed in human T2D patients (Bays et al., 2004, ADA., 2009a, ADA., 2009b, Quan et al., 2013). Research in human diabetic patients has shown that insulin resistance not only develops due to the destruction of pancreatic β-cell but also due to ectopic fat deposition in the body (e.g. hepatic steatosis) (Bays et al., 2004, Cusi, 2010). Furthermore, one of the foremost complications of poorly controlled glycaemia is chronic renal failure (McKenna and Thompson, 1997). The progression to renal failure is commonly screened for by tests for microalbumin, creatinine and albumin creatinine ratio (ACR) and associated pathological

lesions in the kidneys (mesangial expansion and sclerosis) (Mauer et al., 1981, Brito et al., 1998, Katz et al., 2002). Based on the preliminary findings of Hodgson and colleagues (2013a), the current study used the same EDD for a period of 30 weeks to further characterise the model based on different metabolic and biochemical parameters along with histological findings in pancreas, liver, adipose tissue and kidneys. Similar to our previous study (Hodgson et al., 2013a), male C57BL/6 mice was considered for this study as females are shown to be more protective to adipocyte inflammation and insulin resistance due to higher levels of oestrogen (Stubbins et al., 2012). In this current investigation, mice were sourced from the Small Animal Breeding Unit of James Cook University (named as JCU bred mice) and commercially available mice from Animal Resource centre, Perth, Western Australia (named as ARC bred mice) having the same parent stocks. The use of the same mouse strain from two separate sources will also facilitate our understanding of any phenotypic and environmental differences.

Therefore, the specific Aims of the research described in this Chapter are:

1. To determine the effect of prolonged consumption of EDD on body weight, glucose parameters, glucose tolerance and HbA1c level
2. To assess the effects of EDD on the renal function through the analysis of urine (microalbuminuria, creatininuria, albumin creatinine ratio and glycosuria)
3. To investigate the effect of EDD on hepatic, renal, visceral adipose tissue and pancreatic islet pathology by histopathological examination

4.2 Materials and Methods

4.2.1 Animal ethics and biosafety approvals

The animal ethics and relevant biosafety approvals are described in Chapter 3 (section 3.1.1).

4.2.2 Experimental animals and study design

Male C57BL/6 mice were used for this study. Mice originated from two sources; the Small Animal Breeding Unit of James Cook University (referred in this Chapter as JCU bred mice) and the Animal Resource Centre, Perth, Western Australia (referred in this Chapter as ARC bred mice). Mice at 4 weeks of age were randomly housed in cages (5 mice/cage) within a temperature and light controlled environment. Ear marking was done to allow longitudinal analysis of individual mouse across the study period. After 2 weeks of being housed with a regular diet, mice were randomly divided into two dietary groups. One group of mice received an *ad libitum* access to an EDD (Energy-dense diet, JCU bred mice, n=34, ARC bred mice,

n=39) and the control group received SRD (Standard rodent diet, JCU bred mice, n=35, ARC bred mice, n=40) based on the daily requirement (4.5 g/mouse/day). The experimental groups of mice were kept on the EDD for a total period of 30 weeks. The details of animal care and nutritional provisions are described in Chapter 3 (section 3.1.2 and 3.1.3).

4.2.3 Sample collection following diet intervention

4.2.3.1 Blood sample

The whole blood was collected from both JCU and ARC bred mice after 25 and 30 weeks of diet intervention. It was collected from retro-orbital sinus from the 6 hourly fasted mice according to the published standard procedure (Donovan and Brown, 2005). The mouse was manually restrained, neck gently scuffed with ears pulled back to expose the eyes. The sterile capillary tube (Livingstone Microhaematocrit capillary tubes with sodium-heparin 80 IU/mL #CAPTUBH) was then inserted at the medial canthus of the orbit to an appropriate depth (indicated by a red line on each tube). The capillary tube very gently rotated until blood flows through the tube. Immediately after collection of 200-300 µL of blood per mouse, the capillary tube was removed and the excess blood was wiped by a swab moistened with PBS (phosphate buffer saline, pH 7.2). Mice were observed to ensure bleeding had stopped and feed and water provided. The whole blood was preserved at -80^0C until analysis.

4.2.3.2 Urine sample

Urine samples (≥80 µL/mouse) was collected from both JCU and ARC bred mice after 30 weeks of diet intervention. For the collection of urine, mice were individually housed in reusable food storage containers until spontaneous urination occurred (spot collection). If mice did not provide a sample within 20 minutes, a gentle palpation of the lower abdominal area or minor handling was done to induce urination. All urine samples were collected into appropriately labelled sterile microcentrifuge tubes and preserved at -80^0C until analysis.

4.2.3.3 Tissue sample

The JCU bred mice were sacrificed after 30 weeks of diet intervention to collect visceral adipose tissue, liver, pancreas and kidney for histological examinations. The collected tissue samples were kept in 10% neutral buffered formalin (NBF) for a minimum period of 24 hours before they are processed for histological examinations. No tissue samples were collected from ARC bred mice after the diet intervention as another researcher of the same research group used them for her study (Bridson, 2015).

4.2.4 Assessment of metabolic and biochemical parameters following diet intervention

4.2.4.1 Feed intake and body weight

The average daily feed intake and weekly body weight of the JCU bred mice (both EDD and SRD groups) was measured for the duration of the diet intervention (Chapter 3, section 3.1.3). The kinetics of the daily feed and weekly body weight gain of ARC bred mice were not considered for this study as these parameters were determined previously by another researcher of the same research group (Bridson, 2015).

4.2.4.2 Fasting blood glucose and glucose tolerance test

The fasting blood glucose (FBG) concentration and glucose tolerance test (GTT) of both JCU and ARC bred mice were determined after 25 and 30 weeks of diet intervention. The detailed procedure is described in Chapter 3 (section 3.2.1 and 3.2.2).

4.2.4.3 Biochemical analysis of the blood and urine samples

Biochemical analyses of the whole blood and urine samples were performed using the AU480 Chemistry Analyser (Beckman Coulter, Mt Waverly, VIC, Australia) according to the manufacturer's instructions. Measurement of specific parameters using the AU480 Chemistry Analyser requires loading of the appropriate reagents and calibrators. For the measurement of glycosylated haemoglobin (HbA1c) from whole blood and microalbumin, creatinine and glucose from urine samples, all appropriate reagents (Appendix 1) were loaded into the specific location of the analyser. Then, the blood samples were thawed and thoroughly mixed. The whole blood was first lysed by mixing with the haemoglobin denaturant (cat. no. OSR004) in a 1:41 dilution (25 µL blood and 1000 µL haemoglobin denaturant) followed by 5 minutes incubation at room temperature. Five hundred µL of the lysed blood was taken into to Beckman Coulter sample cups (0.5 mL; cat. no. 651412). Afterwards, sample racks were loaded into the rack supply unit of the analyser. For the measurement of urine parameters, urine samples were defrosted thoroughly and briefly centrifuged (350 xg, 5 minutes at room temperature). Eighty µL of the urine sample was taken into each Beckman Coulter sample cup followed by loading of the samples racks to the analyser. The data for whole blood (total haemoglobin; Hb and total glycosylated haemoglobin; HbA1c) and urine (microalbumin, creatinine and glucose) was retrieved form the analyser after end of the run. The percentage of HbA1c was then calculated based on the total Hb and total HbA1c. However, the percent of urine albumin creatinine ratio (ACR) was calculated based on microalbumin and creatinine value.

4.2.5 Histopathological examination of tissue samples

The formalin fixed tissue samples were processed for histological examination. To assess the neutral lipid accumulation, the liver samples were cryosectioned (5 μm thickness) in OCT (optimum cutting temperature) medium and stained with the modified Herxheimer's solution and counter stained with the Mayer's Haematoxylin (Appendix 1). The adipose tissue, pancreas and kidney samples were embedded in paraffin and sectioned at 5 μm thickness. The adipose tissue and pancreas were stained with Haematoxylin and Eosin (H&E) for morphological evaluation and quantification of the tissue specific lesions. The kidney sections were stained with periodic acid-Schiff (PAS) stain for the quantification of lesions in the glomeruli (Chapter 3, section 3.5 and Appendix 1).

Stained sections were visualised on a computer connected to a light microscope (BX43 Olympus). Quantitative analysis of tissue sections was performed on the representative digital images (200x magnification) using the CellSens® Image Analysis software (Olympus). For the determination of the extent of lipid deposition in the liver section from each mouse, a threshold-based phase segmentation technique was used. A minimum of 10 images of each liver section of each mouse was considered for the evaluation (Chapter 3, section 3.5.1). The mean adipocyte size within visceral adipose tissue (VAT) section from each mouse was assessed by measuring the area of a minimum of 50 adjacent adipocytes per image. At least 5 images from each VAT section of each mouse were evaluated (Chapter 3, section 3.5.2). The total pancreatic area of each mouse was measured on H&E stained sections. The total number of pancreatic islet of each section was counted and each islet area were measured. Data were expressed as the percentage of pancreatic islet area over the total pancreatic area of each mouse (Chapter 3, section 3.5.3). Kidney sections were evaluated by the threshold-based phase segmentation technique to compare the percentage of the PAS-positive staining within the glomerular capillary tufts, relative to the glomerular area. The perimeter of each glomerulus was outlined using a polygonal tracing tool of the CellSens® software. (Chapter 3, section 3.5.4).

4.3 Statistical analysis

Statistical analysis was performed using the GraphPad Prism 7.03 software. All glycaemic, biochemical parameters (e.g. FBG level, HbA1c, albumin, creatinine, urine glucose) and histological findings (e.g. lipid deposition in liver, adipocyte size) were checked for normality using the Shapiro-Wilk's test. Data passed the test of normality if $p \geq 0.05$. The normally distributed data (e.g. 30th week feed and energy intake) were compared between the groups (SRD *vs* EDD) using unpaired *t*-test with Welch's correction. The normally distributed data of

multiple groups (e.g. 30th week body weight of SRD *vs* EDD of JCU and ARC bred mice) were compared using the ordinary one-way ANOVA with Holm-Sidak's multiple comparisons test. In contrast, the non-normally distributed data (e.g. lipid deposition in liver) were compared between the groups using the non-parametric Mann-Whitney U test. The Kruskal-Wallis test with Dunn's multiple comparisons test was performed for non-normally distributed data of multiple groups (e.g. 25th week HbA1c data of SRD *vs* EDD of JCU and ARC bred mice). However, the two-way ANOVA with Sidak's multiple comparisons test was performed for the data having the repetitive measures (e.g. glucose tolerance test, kinetics of feed and energy intake, body mass). All the data were presented as mean±SEM. The level of significance was indicated as *p≤0.05, **p≤0.01, ***p≤0.001 and ****p≤0.0001.

4.4 Results

4.4.1 Metabolic parameters following diet intervention

4.4.1.1 Energy-dense diet changes body mass kinetics

Prior to the diet intervention, the commencing body weights of both dietary groups of the JCU bred (EDD, 15.49±0.29 *vs* SRD, 15.03±0.43, g, p= >0.9999) and ARC bred mice (EDD, 19.21±0.22 SRD *vs* 19.78±0.20, g, p= >0.9999) were equivalent. Although the daily feed intake was lower in EDD fed mice, the daily energy intake was significantly higher (1.36 fold) (Figure 4.1 A). Higher energy intake of the EDD fed mice corresponded with a significant increase of body mass in both JCU bred and ARC bred mice (Figure 4.1 B, C, & D). The daily feed and energy intake (Appendix 2) and body weight gain of JCU bred mice showed that body mass gain was significantly higher in EDD group from the first week to the 30th week of diet intervention (Figure 4.1 B). The highest body weight gain was recorded at the 30th week of diet intervention in both JCU bred mice and ARC bred mice (Figure 4.1). After 30 weeks, an overall increase of body mass was 208.11% (EDD) and 79.86% (SRD) in JCU bred mice and 142.79% (EDD) and 41.05% (SRD) in ARC bred mice.

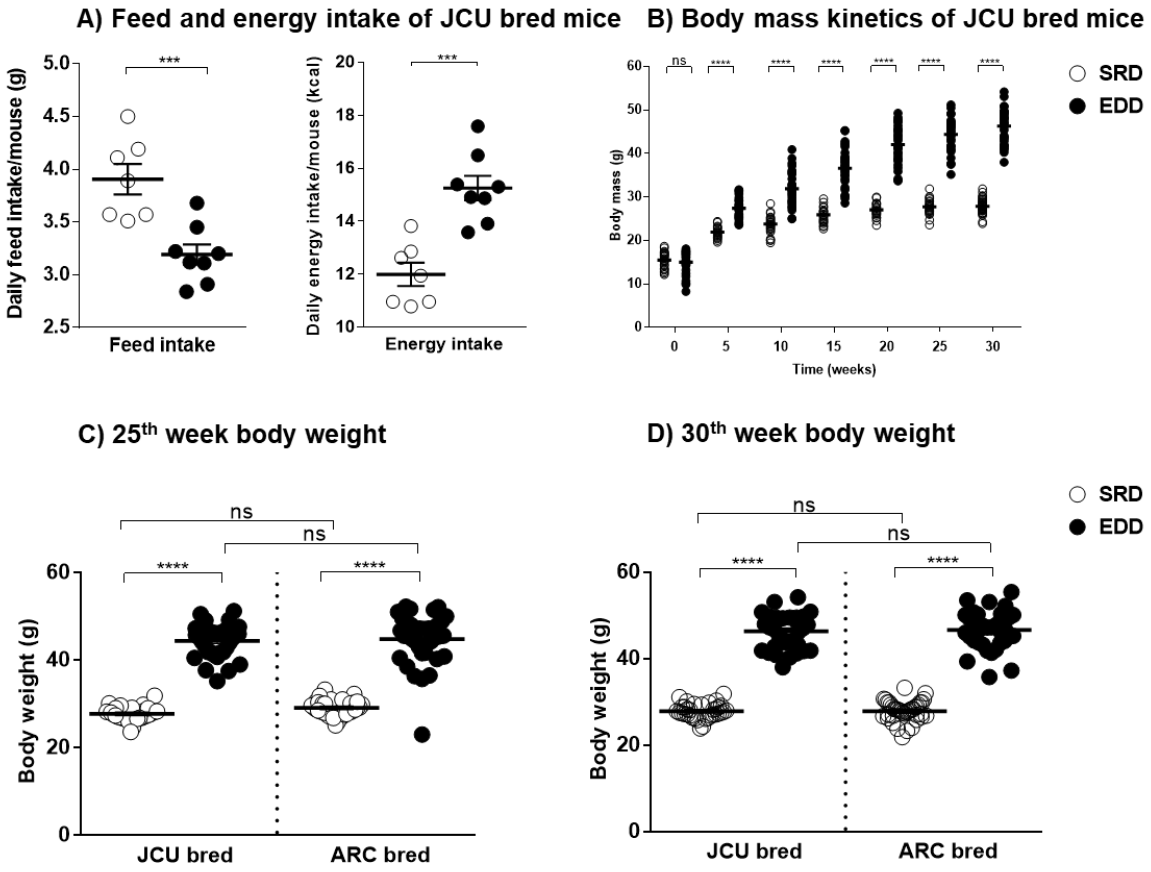

Figure 4.1 Changes in mouse body mass in response to energy-dense diet

Male C57BL/6 JCU (EDD, n=34 *vs* SRD, n=35) and ARC bred mice (EDD, n=39 *vs* SRD, n=40) were fed either an energy-dense diet (EDD) or a standard rodent diet (SRD) for a period of 30 weeks. Daily feed and energy intake and body mass of JCU bred mice were monitored throughout the study period. Feed intake was significantly higher in mice on SRD, whereas energy intake was significantly higher in mice on EDD (A). Changes in the body mass kinetics were also comparable between the two groups following the diet intervention (B). Body mass was significantly higher in mice on EDD of both JCU and ARC bred mice at 25th and 30th week of diet intervention (C & D). Data presented as mean±SEM (Appendix 2). The significant differences were determined using the unpaired *t*-test with Welch's correction (A), two-way ANOVA with Sidak's multiple comparisons tests (B), Kruskal-Wallis test with Dunn's multiple comparisons test (C) and the ordinary one-way ANOVA with Holm-Sidak's multiple comparisons test (D). The level of significance was indicated as **p≤0.01, ***p≤0.001, ****p≤0.0001 and ns=non-significant.

4.4.1.2 Energy-dense diet increased fasting blood glucose and glucose intolerance

Glucose tolerance test (GTT) demonstrated that the blood glucose level was significantly higher in mice fed on EDD compared to controls at both 25th and 30th week of diet intervention (Figure 4.2 A, B, D & E). Immediately after the intraperitoneal glucose challenge, the blood glucose concentration rose significantly in EDD group compared to SRD group. At 30th week of diet intervention, the 2 hours post-glucose challenge blood glucose level of JCU bred (EDD,

10.10±0.24 *vs* SRD, 8.71±0.22, mmol/L) and ARC bred mice (EDD, 11.73±0.42 *vs* SRD, 8.46±0.22, mmol/L) was comparable to the baseline blood glucose level (0 minutes) of JCU bred (EDD, 8.8±0.25 *vs* SRD, 8.5±0.25, mmol/L) and ARC bred mice (EDD, 9.34±0.23, SRD, 8.68±0.23 mmol/L) indicating the higher glucose intolerance in EDD fed mice compared to controls. Overall, compared to the control group on SRD, the baseline fasting blood glucose (FBG) of mice on EDD was higher at both 25th and 30th week of diet intervention and the mice were less efficient in clearing the circulatory blood glucose even after 2 hours post-glucose challenge (Figure 4.2 A, B, D & E). Moreover, the FBG concentration was also assessed from the retro-orbital sites before the collection of whole blood for the determination of HbA1c. Similar to the baseline FBG level (0 minutes) determined from tail vein (Figure 4.2 A, B, D & E), an elevated blood glucose level was recorded in EDD fed mice compared to SRD group at both 25th and 30th week of diet intervention. At week 30, the FBG level (retro-orbital bleeding) was significantly higher in EDD fed mice compared to the control groups in both JCU bred (EDD, 11.07±0.43 *vs* SRD, 8.61±0.27, mmol/L, p=0.0405) and ARC bred mice (EDD, 11.85±0.33 *vs* SRD, 9.33±0.29, mmol/L, p= <0.0001). At the 25th week, a similar trend was observed in both JCU bred (EDD, 10.47±0.35 *vs* SRD, 9.12±0.27, mmol/L, p=0.0002) and ARC bred mice (EDD, 11.32±0.35 *vs* SRD, 8.92±0.24, mmol/L, p= <0.0001).

The area under the curve (AUC) based on GTT (AUC-GTT) was significantly higher in EDD group compared to SRD group at both 25th and 30th week (Figure 4.2 C & F). At 30th week, the AUC-GTT was 1.21 and 1.29 times higher in EDD group compared to controls of JCU and ARC bred mice, respectively (Figure 4.2 F). This finding indicates the higher glucose intolerance by the mice on EDD compared to control group. A similar trend of AUC-GTT was observed in the EDD group compared to SRD group of JCU and ARC bred mice at 25th week (Figure 4.2 C).

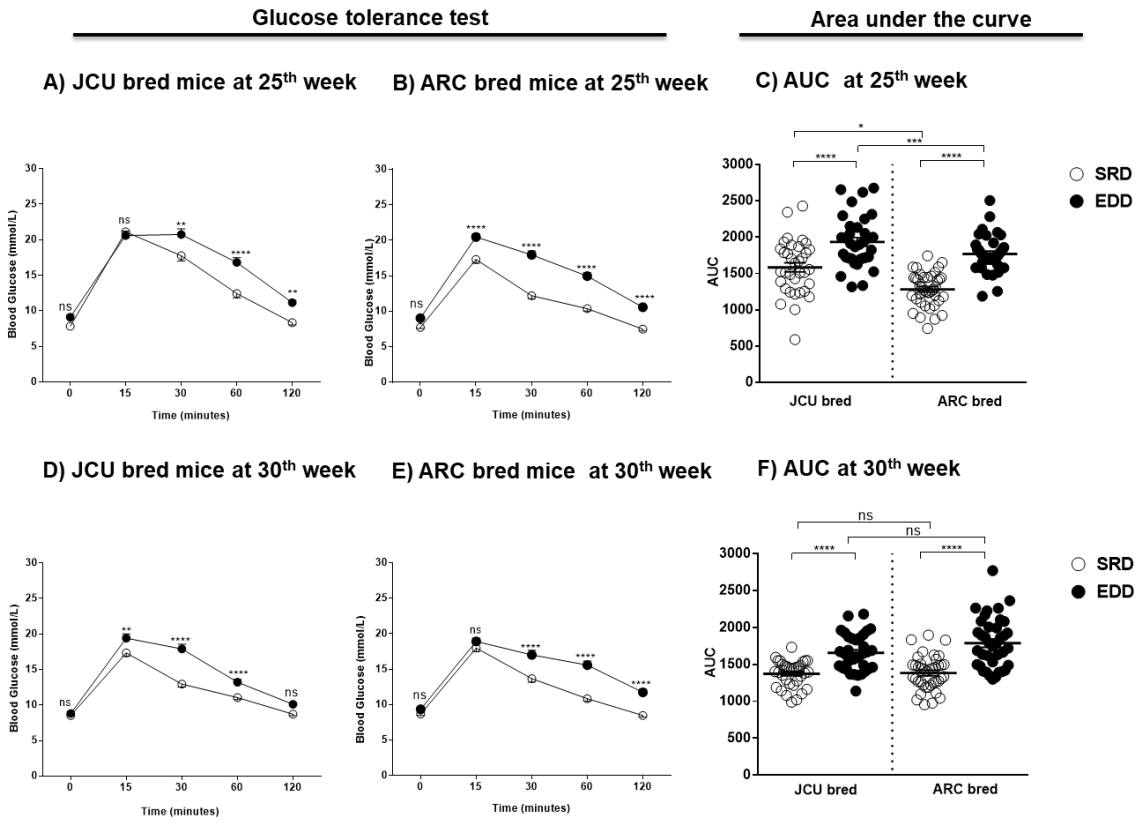

Figure 4.2 Glucose tolerance in mice following diet intervention

The blood glucose level was measured at 0 (baseline), 15, 30, 60 and 120 minutes of post-intraperitoneal glucose challenge after 6 hours fasting of mice. Significantly impaired glucose tolerance was observed in mice (JCU and ARC bred) fed on EDD compared to control mice on SRD after both 25th and 30th week of diet intervention (A, B, D & E). A significantly higher AUC was also observed in mice fed EDD compared to SRD group indicating an impaired glucose intolerance or insulin resistance (C & F). Data presented as mean±SEM; n=34-35 (JCU bred) and 39-40 (ARC bred) mice/group (Appendix 2). The Significant differences were determined using the two-way ANOVA with Sidak's multiple comparisons tests (A, B, D & E) and the ordinary one-way ANOVA with Holm-Sidak's multiple comparisons test (C & F). The level of significance was indicated as * p≤0.05, **p≤0.01. ***p≤0.001. ****p≤0.0001 and ns=non-significant.

4.4.1.3 Energy-dense diet changes glycosylated haemoglobin

Glycosylated haemoglobin (HbA1c) was measured from retro-orbital blood after 6 hours of fasting. At 25 and 30 weeks, an elevated level of HbA1c was recorded in mice fed on EDD compared to the control mice fed on SRD (Figure 4.3 A & B). At 30 weeks on diet, the HbA1c level of JCU bred mice was 2.70±0.05 *vs* 2.34±0.08, % (EDD *vs* SRD, p=0.0115) and ARC bred mice 2.85±0.06 *vs* 2.51±0.08, % (EDD *vs* SRD, p=0.0012) (Figure 4.3 B). A higher level of glycosylated haemoglobin was also measured in EDD fed mice at 25th week at both JCU (p=0.0589) and ARC bred mice (Figure 4.3 A).

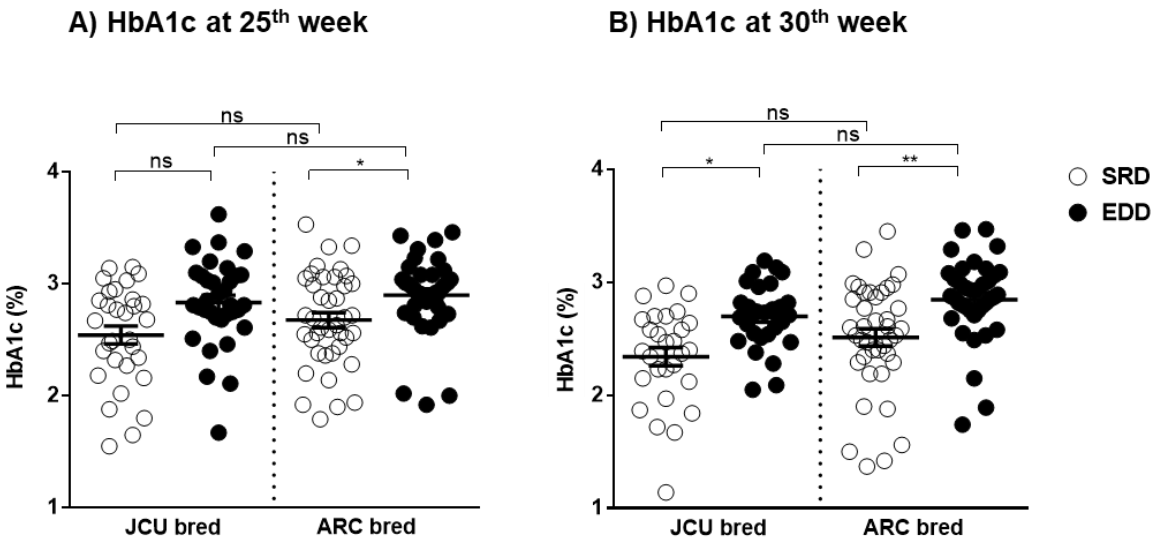

Figure 4.3 Glycosylated haemoglobin (HbA1c) level of mice following diet intervention

The percentage of the HbA1c level was comparable between the dietary groups at both 25th (A) and 30th (B) week of diet intervention. The HbA1c level was higher in mice on EDD compared to controls on SRD. Data presented as mean±SEM; n=31-35 (JCU bred) and 38-40 (ARC bred) mice/group (Appendix 2). The significant differences were determined using the Kruskal-Wallis test with Dunn's multiple comparisons test. The level of significance was indicated as *p≤0.05, **p≤0.01 and ns=non-significant.

4.4.1.4 Energy-dense diet changes renal function

Microalbumin, creatinine and glucose in urine were investigated after 30 weeks of diet intervention. The primary evidence of renal impairment in response to EDD was assessed by microalbuminuria, which was significantly higher in EDD fed mice compared to controls of both JCU and ARC bred mice (Figure 4.4 A). The urine creatinine value also differed significantly between the dietary groups in both JCU and ARC bred mice (Figure 4.4 B). Compared to the control mice on SRD, the lower urinary creatinine value in EDD fed mice indicated that they may be less efficient in clearing the high circulating creatinine due to impairment of renal function (Morris et al., 2016). Furthermore, the urine albumin creatinine ratio (ACR) was significantly higher in mice fed on EDD of JCU and ARC bred mice (Figure 4.4 C) suggesting some kidney damage. However, the EDD groups demonstrated the symptoms of glycosuria as measured by an elevated urine glucose concentration (Figure 4.4 D). Although a slightly higher level of glycosuria was recorded in EDD fed mice of JCU mice at 30th week, the differences were not statistically significant. A larger volume of urine was collected from the EDD fed mice at both 25th and 30th week, which was an indication of polyuria. This evidence

was not further confirmed as the current study did not measure the water intake and urine output during the diet intervention period.

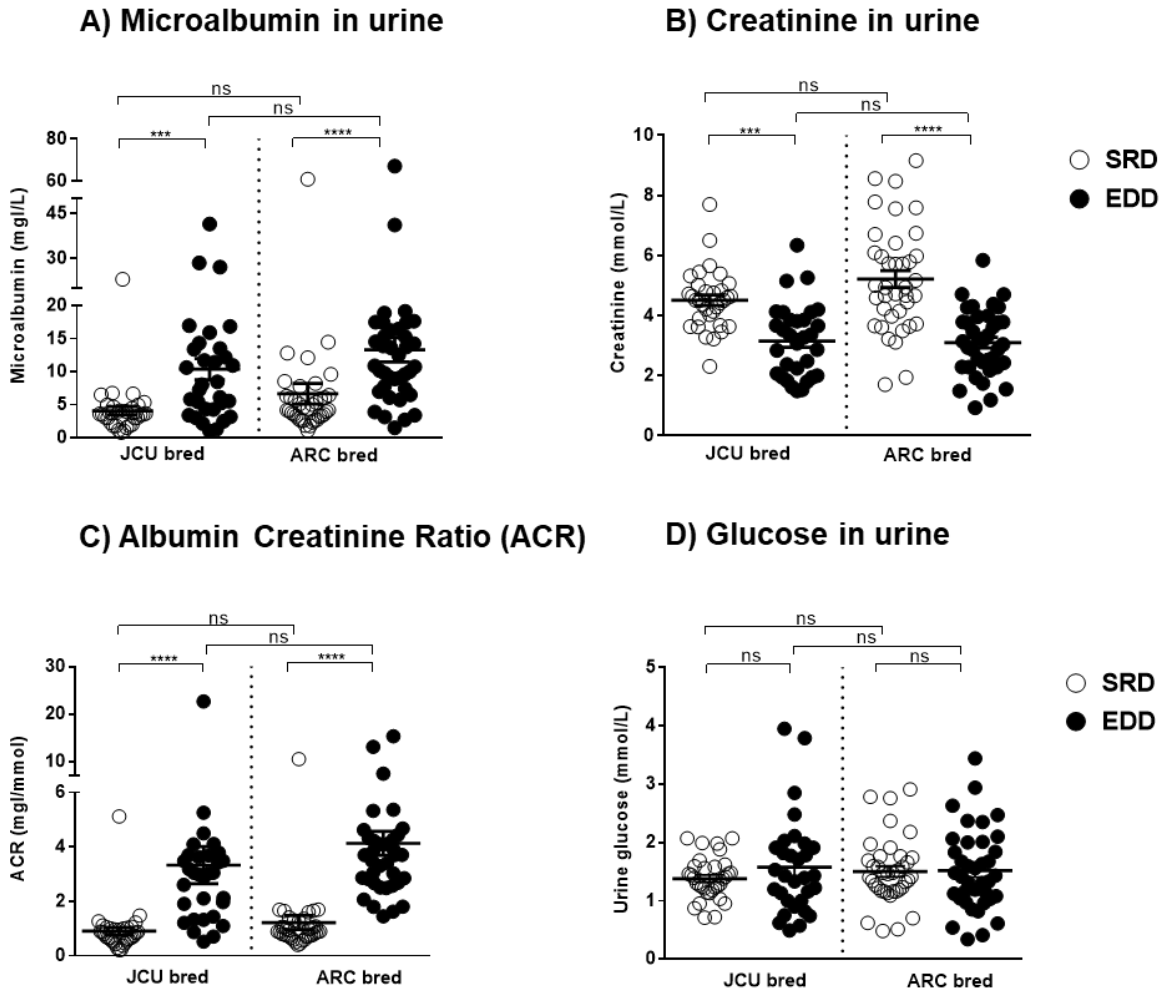

Figure 4.4 Renal profile of mice after 30 weeks of the diet intervention

Microalbumin, creatinine and the albumin creatinine ratio (ACR) were comparable between the dietary groups of both JCU and ARC bred mice. A significantly higher concentration of microalbumin in urine was recorded in EDD fed mice compared to SRD fed mice (A). Whereas the creatinine concentration was significantly lower in the urine of EDD fed mice in comparison to controls (B). The ACR was significantly higher in mice fed on EDD compared to the control mice (C). However, there was no significant difference was observed in the urine glucose concentration of EDD and SRD fed JCU and ARC bred mice (D). Data presented as mean±SEM; n=31-33 (JCU bred) and 38 (ARC bred) mice/group. The significant differences were determined using the Kruskal-Wallis test with Dunn's multiple comparisons test. The level of significance was indicated as ***p≤0.001, ****p≤0.0001 and ns= non-significant.

4.4.2 Histopathological changes in response to energy-dense diet

4.4.2.1 Energy-dense diet results in lipid deposition in liver

The lipid deposition in the liver was comparable in mice fed on EDD and SRD for 30 weeks. The Modified Herxheimer's staining (red colour indicates lipid deposition) of liver sections demonstrated marked lipid deposition in the liver of EDD fed mice compared to control mice on SRD (Figure 4.5 A & B). Quantification of the Herxheimer's stained area on the liver sections also demonstrated a marked hepatic steatosis in EDD fed mice compared to control mice (Figure 4.5 C).

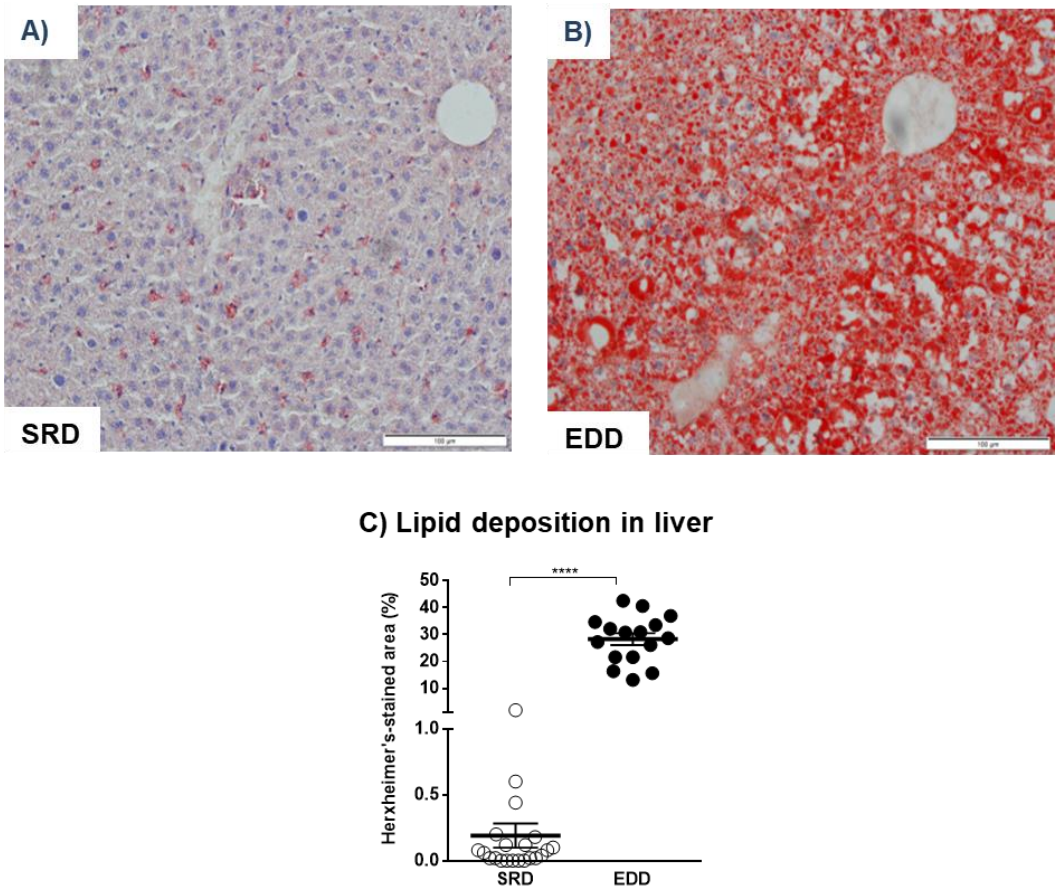

Figure 4.5 Lipid deposition in liver of mice after 30 weeks of the diet intervention

Representative cryosections of liver of JCU bred mice were stained by the Modified Herxheimer's stain and quantified using CellSens® Image Analysis software. The photomicrographs of a representative liver section of mice on SRD (A) and EDD (B) showed the deposition of lipid (red colour) in the liver parenchyma. A significantly higher percentage of Herxheimer's stained area over the total liver area measured in EDD fed mice compared to controls (C). Scale bar of the photomicrographs: 100 µm. Data presented as mean±SEM; n=16-21 mice/group (Appendix 2). The significant differences were determined using the Mann-Whitney U test. The level of significance was indicated as ****p≤0.0001. Images from other animals are given in Appendix 2, Figure A2.1-A2.2.

4.4.2.2 Energy-dense diet results in ectopic fat deposition and abnormal adipocyte morphology

After 30 weeks, a marked fat deposition (gross morphology) was evident as visceral (dotted circle in Figure 4.6) and subcutaneous adiposity (dotted lines in Figure 4.6) in EDD group compared to control group on SRD. Haematoxylin and Eosin staining of the visceral adipose tissue sections demonstrated the abnormal adipocyte morphology of the EDD group compared to SRD group (Figure 4.6 C & D). Measurement of the size of each of adipocyte showed that the mean size of each adipocyte was 3.99 times higher in EDD fed mice compared to control mice on SRD (Figure 4.6 B).

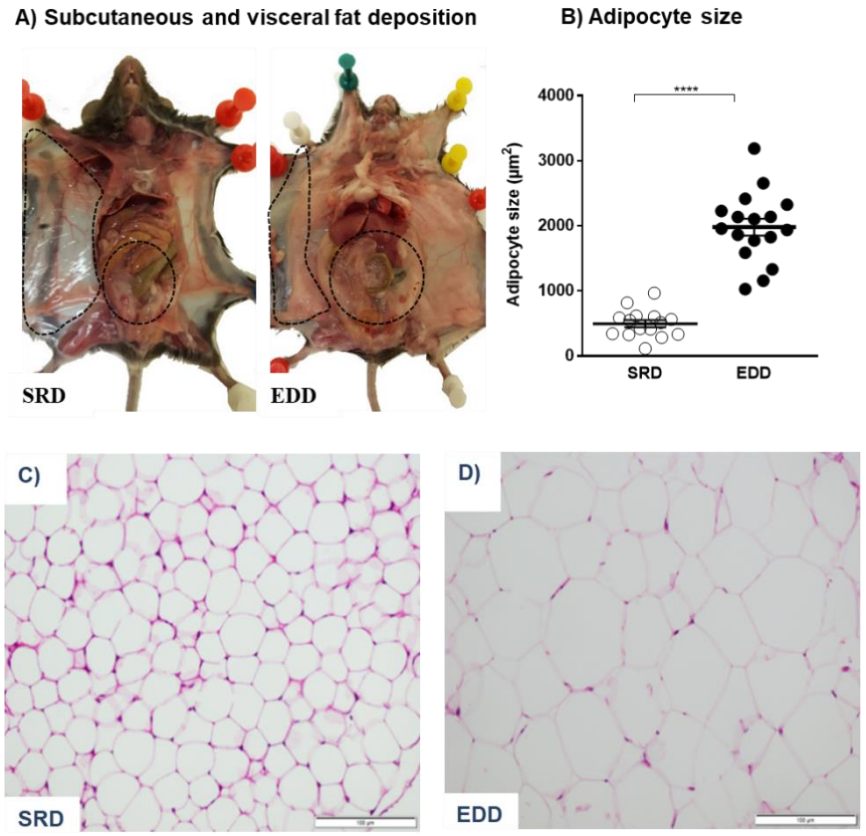

Figure 4.6 Ectopic lipid deposition and abnormal adipocyte morphology in mice after 30 weeks of diet intervention

The photographs demonstrated the gross ectopic subcutaneous (dotted line) and visceral fat deposition (dotted circle) (A) in JCU bred mice after 30 weeks of the diet intervention (A). Quantification of the H&E stained visceral adipose tissue (VAT) sections demonstrated significantly increased size of adipocyte (adipocyte hypertrophy) of mice fed on EDD compared to control mice on SRD (B). The photomicrographs of a representative VAT section of mice on SRD (C) and EDD (D) showed the comparative size of the adipocyte. Scale bar of the photomicrographs: C-D; 100 µm. Data presented as mean±SEM; n=15-17 mice/group (Appendix 2). The significant differences were determined using the unpaired *t*-test with Welch's correction. The level of significance was indicated as ****p≤0.0001. Images from other animals are given in Appendix 2, Figure A2.3-A2.4.

4.4.2.3 Energy-dense diet results in pancreatic islet hyperplasia

Hyperplasia of pancreatic islet, an indication of insulin resistance, was measured after 30 weeks in JCU bred mice (Figure 4.7 A & B. The total pancreatic islet area over the total pancreatic area were 2.35 times higher in EDD fed mice compared to controls on SRD (Figure 4.7 C).

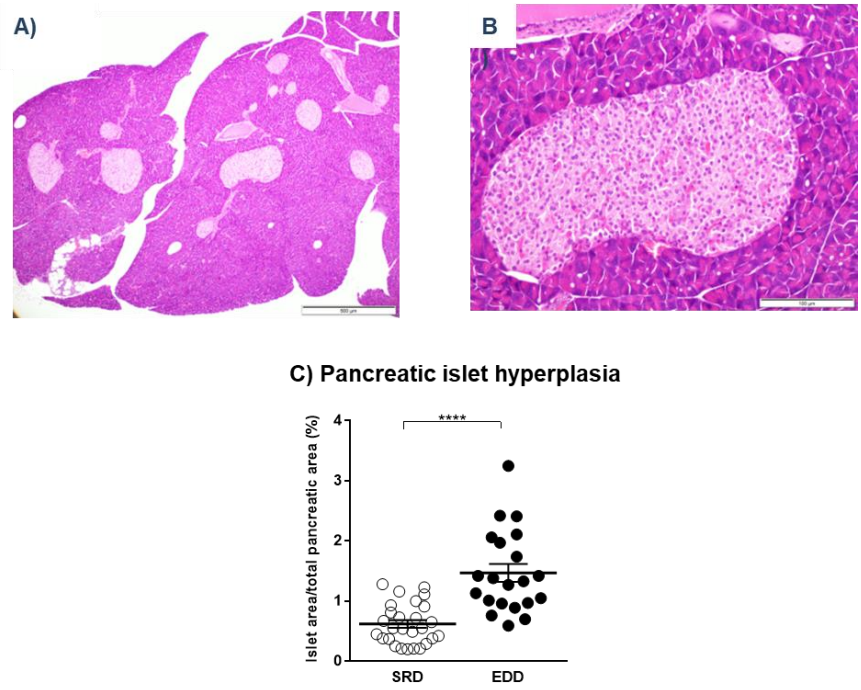

Figure 4.7 Hyperplasia of pancreatic islet in mice after 30 weeks of diet intervention

The H&E stained photomicrographs of representative pancreatic sections of JCU bred mice demonstrated the variable size and islet density on the pancreatic section of a mouse on EDD (A). Compensatory pancreatic islet hyperplasia was evident in the pancreas of mice on EDD (B). Quantification of the percent (%) islet area over the total pancreatic area demonstrated a significantly higher islet area in mice on EDD compared to control mice on SRD (C). Scale bar of the photomicrographs: A; 500 µm and B; 100 µm. Data presented as mean±SEM; n=21-27 mice/group (Appendix 2). The significant differences were determined using the unpaired *t*-test with Welch's correction. The level of significance was indicated as ****p≤0.0001. Images from other animals are given in Appendix 2, Figure A2.7-A2.8.

4.4.2.4 Energy-dense diet results in renal pathology

Renal pathology was assessed by semi-quantitative analysis of the PAS-positive stained area of the glomeruli of kidney section of mice after 30 weeks. Compared to control mice on SRD, EDD fed mice demonstrated a higher glomerular damage as thickening of basement membrane of the Bowman's capsule (Figure 4.8 B, arrow), expansion and thickening of the mesangial matrix (Figure 4.8 B, asterisk) and hypertrophy of glomeruli (Figure 4.8 B & D). The percentage of the PAS-positive stain within the glomerular area was significantly higher in

EDD fed mice compared to controls (Figure 4.8 C). Furthermore, the EDD fed mice demonstrated a 1.60 times higher area of each glomerulus (glomerular hypertrophy) compared to SRD fed mice (Figure 4.8 D). Histopathological findings together with the urine ACR and glycosuria suggested that mice fed on EDD over the period of 30 weeks developed renal impairment and pathologies. These findings are characteristic features of nephropathy associated with clinical T2D in human patients.

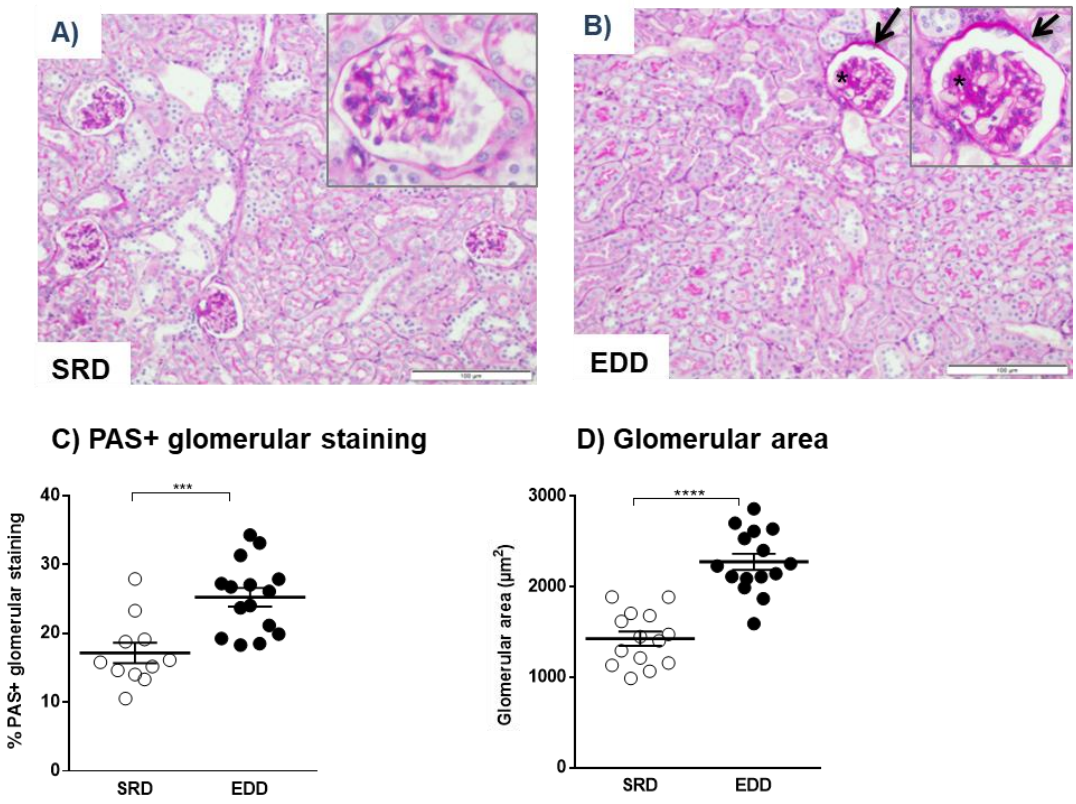

Figure 4.8 Nephropathy in mice after 30 weeks of diet intervention

Representative kidney sections were taken after 30 weeks of diet intervention and stained with the Periodic Acid-Schiff's (PAS) stain. Pronounced nephropathy was observed in mice fed on EDD, which includes the thickening of the Bowman's capsule (B, indicated by arrows) and mesangial matrix thickening (B, asterisk) compared to the control mice on SRD (A). The PAS-positive staining of the kidney sections demonstrated significant mesangial thickening within the glomeruli of kidneys of mice fed on EDD compared to mice on SRD (C). Glomerular size (glomerular hypertrophy) was also significantly higher in mice on EDD compared to SRD (D). Data presented as mean±SEM; n=11-15 mice/group (Appendix 2). The significant differences were determined using the unpaired *t*-test with Welch's correction. The level of significance was indicated as ***$p \leq 0.001$ and ****$p \leq 0.0001$. Images from other animals are given in Appendix 2, Figure A2.5-A2.6.

4.4.3 Energy-dense diet consumption drives progression to type 2 diabetes

The diagnostic criteria for clinical type 2 diabetes (T2D) in human comprises a fasting blood glucose (FBG) level >7 mmol/L (>126 mg/dL), a 2 hours blood glucose level after a 75 g of oral glucose tolerance test (OGTT) showing >11.1 mmol/L (>200 mg/dL) and HbA1c > 6.5% (>48 mmol/L) (WHO., 2006, ADA., 2009b, ADA., 2010, Vijan, 2010, d'Emden et al., 2012). Mice in the present study EDD fed mice were considered as having T2D if they demonstrated a raised FBG level and HbA1c with evidence of glucose intolerance at levels higher the upper 99% confidence interval for the mean of age-matched control group fed on a SRD. The JCU bred and ARC bred mice fed on EDD for a period of 25 and 30 weeks demonstrated the clinical features of T2D (Table 4.1, Appendix 2). After 30 weeks of EDD commencement, 76.47 % of JCU and 76.31 % of ARC bred mice had higher FBG level and this was supported by the data form GTT at the same timepoint. Furthermore, FBG levels (after 2 hours of glucose challenge) demonstrated a higher percentage of mice (76.47, JCU *vs* 97.43, %, ARC bred mice) had developed insulin resistance at 25th week compared to 30th week (67.64, JCU *vs* 84.21, %, ARC bred mice). There was a rising trend of the HbA1c level from 25th week to 30th week in both JCU and ARC bred mice. After 30 weeks, 73.33% of JCU bred and 76.31% of ARC bred mice demonstrated an elevated level of HbA1c (Table 4.1).

Table 4.1 Percentage of mice demonstrating metabolic features of type 2 diabetes following consumption of the energy-dense diet

Parameters	Length of time on EDD			
	25th week		30th week	
	JCU bred mice	ARC bred mice	JCU bred mice	ARC bred mice
*FBG	67.64% (23/34)	78.94% (30/38)	76.47% (26/34)	76.31% (29/38)
*HbA1c	64.70% (22/34)	68.42% (26/38)	73.33% (22/30)	76.31% (29/38)
*GTT (AUC)	64.70% (22/34)	94.43% (37/39)	76.47% (26/34)	78.94% (30/38)
**FBG+glucose challenge	76.47% (26/34)	97.43% (38/39)	67.64% (23/34)	84.21% (32/38)

*6 hours fasting, **6 hours fasting and 2 hours after glucose challenge, FBG; fasting blood glucose, HbA1c; glycosylated haemoglobin, GTT; glucose tolerance test, AUC; area under the curve

Histological evidence after 30 week of diet intervention in JCU bred mice also demonstrated that EDD feeding can induce features indicative of diabetic nephropathy and pancreatic

pathology. Overall, diabetic nephropathy was evident in more than 80% of mice based on elevated urine ACR (83.87%; 26 of 31 mice), glomerular hypertrophy (93.33%; 14 of 15 mice) combined with mesangial thickening (73.33%; 11 of 15 mice). Pancreatic hyperplasia was also evident in 85.71% (18 of 21 mice) of the EDD fed mice.

Our findings on metabolic and pathological changes in organs demonstrated that feeding of JCU or ARC bred mice with EDD for a prolong period (either 25 or 30 weeks) can induce overt clinical features of T2D.

4.5 Discussion

The objectives of the research described in this Chapter were to evaluate whether prolonged consumption of EDD can induce the development of key metabolic, biochemical and pathophysiological features of clinical T2D in male C57BL/6 mice. The key aims (1-3) of the current study were to evaluate the differences in the body weight, systemic glucose concentration and glucose tolerance, glycosylated haemoglobin (HbA1c) concentration, renal and pancreatic pathology in mice during diet intervention. The parameters were measured at two terminal timepoints at the 25th and 30th week of diet intervention and data analysed to determine whether the mice demonstrated the overt clinical features of T2D similar to human patients. We have demonstrated that prolonged EDD feeding induces overt clinical features of T2D in mice.

Obesity is one of the major risk factors for developing T2D (Walley et al., 2006, Eckel et al., 2011). In humans, 80% of the diagnosed cases of diabetes are in overweight individuals (Smyth and Heron, 2006). Obesity-induced diabetes has also been observed in animal models of diabetes (Surwit et al., 1988, Tomita et al., 1992, Lee et al., 1994, Black et al., 1998, Loskutoff et al., 2000, Finegood et al., 2001, Leiter and Reifsnyder, 2004, Kawasaki et al., 2005, Shafrir et al., 2006, Hodgson et al., 2013a). Researchers linked obesity to insulin resistance, abnormal glucose metabolism (glucotoxicity), lipotoxicity and pancreatic dysfunction (Baetens et al., 1978, Kawasaki et al., 2005, Shafrir et al., 2006, Hodgson et al., 2013a). Therefore, in the current study, mice were weighed on a weekly basis throughout the diet intervention period to monitor the weight gain. The body mass gain was significantly higher in EDD fed mice and an increasing trend of body mass gain was observed in the same group from 1 to 30 weeks of the diet intervention period (Figure 4.1 B, C & D). A similar type of trend was observed by Bridson (2015) using the same diet. Control mice fed SRD gained weight very slowly in first few weeks and remained almost steady during the entire diet intervention period (Figure 4.1 B). This

finding was in agreement with other studies (Kawasaki et al., 2005, Bridson, 2015, Envigo research laboratory., 2015, Jackson laboratory., 2015). The overall body mass increase in EDD fed mice was comparable with C57BL/6 (Black et al., 1998) and db/db mice (Kawasaki et al., 2005). In contrast to our results, Han and co-workers (2015) fed mice a high-fat diet (HFD) for a period of 8 weeks and did not see these significant differences in early weight grain. Mice in that study were treated with Cathepsin k inhibitor which prevents body weight gain and insulin resistance. The higher body mass of EDD fed mice of the current study was due to the prolonged diet intervention period. Excessive subcutaneous and visceral fat deposition (Figure 4.6 A) also correlated with higher body mass. Although this study didn't quantify the gross ectopic fat deposition, a study done by Hodgson and colleagues (2013a) found significantly higher amounts of subcutaneous (2.17 fold) and visceral fat deposition (8.88 fold) in EDD fed mice compared to controls after 10 weeks of the diet intervention. Histopathological analysis of visceral adipose tissue demonstrated adipocyte hypertrophy in mice fed an EDD (Figure 4.6 B, C & D). This finding was supported by previous studies, where a high-fat high-glycaemic (HF-HG) index diet was used (Black et al., 1998, Herberg, 1998, Bridson, 2015). The correlation among increased adipose tissue, insulin resistance and hyperglycaemia has been noted in clinical settings. Obesity induced T2D has been shown to have an effect on insulin resistance and glucose intolerance leading to micro- and macro-vascular complications (Arner, 2003, Cefalu, 2006).

Diabetes mellitus includes a variety of metabolic abnormalities. Abnormalities in glucose metabolism are one of the most specific diagnostic criteria of hyperglycaemia often measured as fasting blood glucose (FBG) level and impaired glucose tolerance (post-oral glucose load) (REC, 1997, Sacks et al., 2002, ADA., 2010, Vijan, 2010). Similar to human patients with T2D, animals should also demonstrate the signs of hyperglycaemia to be called diabetic. Other animal model studies classified the animals as diabetic based on the systemic glucose concentration often determined by the POC test using a glucose meter (Hodgson et al., 2013a, Bridson, 2015, Morris et al., 2016). In addition, impaired glucose tolerance, insulin resistance based on glucose tolerance test (GTT)-Area Under the Curve (AUC) and circulatory insulin level are also criteria for advance classification of diabetes in some animal models (Surwit et al., 1988, Cefalu, 2006, Zhang et al., 2008, Ayala et al., 2010). In this study, mice fed an EDD demonstrated a significantly elevated FBG concentration (Figure 4.2). This is similar to previous studies using mouse models where a higher FBG level was observed in the diabetic group (Surwit et al., 1988, Tomita et al., 1992, Suzuki et al., 1999, Leiter and Reifsnyder, 2004, Kawasaki et al., 2005, Hodgson et al., 2013a, Bridson, 2015). Blood glucose concentrations of mice fed an SRD

were also consistent with those reported in prior studies (Surwit et al., 1988, Hodgson et al., 2013a, Bridson, 2015). An impaired blood glucose and the increased GTT-AUC of mice on EDD demonstrated insulin resistance (Figure 4.2 C & F). Hodgson and co-workers (2013a) observed insulin resistance using the same diet for a period of 10 weeks. The current study didn't quantify the plasma insulin level or pancreatic insulin content to further confirm the insulin resistance in EDD fed mice compared to controls.

In addition to FBG level and impaired glucose tolerance, the measurment of the advanced glycation end products particularly HbA1c is another important diagnostic feature of T2D (ADA., 2009b, ADA., 2010). In humans, the HbA1c is a form of haemoglobin that is measured to detect the 3 months average plasma glucose concentration. Therefore, it is considered a precise measure for diagnosing and monitoring the chronic hyperglycaemic status of the patient as it is well correlated with diabetic associated complications (ADA., 2009b). In the clinical setting, a HbA1c level greater than or equal to 6.5% is considered indicative of T2D (ADA., 2009a, ADA., 2009b, ADA., 2010). In the current study, JCU bred and ARC bred mice fed on EDD had an elevated HbA1c level at both the 25th and 30th week (Figure 4.3 A & B). Furthermore, the level of HbA1c was higher at the 25th week compared to the 30th week. The HbA1c level at any timepoint is contributed by all circulating Red Blood Cells (RBCs) from the oldest to the youngest, which might be one of the reasons for variation of HbA1c in the mentioned timepoints (National Glycohemoglobin Standardization Program., 2010). Analyses of blood samples in two different batches in the AU480 analyser might also be a reason of slightly variable results in the timepoints mentioned. If the current study had determined the plasma glucose concentration, an appropriate interpretation could be drawn about the variation of HbA1c level in two different timepoints. However, there are no standard criteria for defining diabetes in a mouse model based on the HbA1c concentration in blood. The range for HbA1c in mice was between 3-4.5% determined by the previous studies (Morris et al., 2016). The AGEs including HbA1c are formed when haemoglobin of RBCs is exposed to systemic glucose. In diabetes, insulin resistance or decreased systemic insulin levels causes more AGEs products to be formed against an increased concentration of systemic plasma glucose (Vistoli et al., 2013). Differences in HbA1c concentration in humans and mice are due to the exposure time of haemoglobin to plasma glucose because human RBCs have three times longer lifespan compared to RBCs of mice (120 *vs* 40 days). A study on HbA1c and plasma glucose levels in a diabetic mouse model also suggested that HbA1c concentration is related to the reduced lifespan of RBCs and reduced HbA1c half-life in mice (14 days in mice *vs* 35 days in humans) (Dan et al., 1997). The current study determined the HbA1c level to be 1-4% in EDD fed mice

at 25 and 30 weeks. This finding was consistent with Bridson (2015), who used the same dietary composition for the induction of diabetes in mice and this observation was also comparable with the findings of Dan and co-workers (1997).

Glycosuria is often used as a tool for the screening of diabetes. The hyperglycaemic condition of diabetic patients results in the classical signs of diabetes such as polyuria (frequent urination), polydipsia (increased thirst) and polyphagia (increased hunger) (WHO., 2006, Cooke and Plotnick, 2008, ADA., 2010). In the present investigation, mice fed an EDD demonstrated a slightly elevated (JCU bred mice) or similar urine glucose concentration (ARC bred mice) compared to controls (Figure 4.4 D). Polyuria and a larger volume of urine might be the determining factors of such glucose urine concentration in EDD fed mice of this experiment. Polyuria in mice fed on EDD was evident, which is supported by the prior studies on animal models (Suzuki et al., 1999, Nagata et al., 2006). In the current study polyuria was not specifically quantified (i.e. by regular monitoring of water intake of output). However, we did observe increased urine volume.

Hepatic insulin resistance is associated with the accumulation of triglycerides (TAG) and free fatty acid (FA) metabolites (fatty acyl-CoA, diacylglycerol, ceramide and glycosphingolipid (Nagale, 2009). In the current study, mice became diabetic in response to the EDD with the demonstration of lipid deposition in different sites of the body including the liver. Histology of liver tissues demonstrated extensive lipid accumulation in EDD fed mice (Figure 4.5), which has been associated with hepatic insulin resistance. Hepatic steatosis in diabetic animal models has also been reported previously (Leiter and Reifsnyder, 2004, Harishankar et al., 2011). The current study did not measure the TAG levels to correlate to hepatic lipid deposition and insulin resistance. Bridson (2015) demonstrated an elevated level of TAG in EDD fed mice at 10, 20, 30 weeks of diet intervention, which supports excess lipid accumulation in different organs of the body. Other researchers have reported previously that excess lipids and their FA metabolites are directed to diabesity leading to impairment of insulin signalling and insulin resistance (Bays et al., 2004, Cusi, 2010).

Diabetic nephropathy (DN) is one of the foremost microvascular complications in diabetic patients. This complication may ultimately lead to renal failure (Gross et al., 2005, Fowler, 2008, Dabla, 2010). The renal impairment or damage is diagnosed by measuring albuminuria as microalbuminuria, macroalbuminuria and the urine albumin creatinine ratio (ACR) (Gross et al., 2005). In the current study, microalbuminuria and ACR and renal histology were assessed to determine if the EDD fed mice show the signs of DN and produce associated pathological

lesions in kidneys. Microalbuminuria (spot collection) and a higher urine ACR were found in EDD fed mice (Figure 4.4 A & C), which indicated kidney damage. A higher trend for microalbuminuria and the ACR was also observed previously in diabetic animal models (Leiter and Reifsnyder, 2004, Zheng et al., 2004, Zhao et al., 2006, Kanetsuna et al., 2007, Mohan et al., 2008). Microalbumin and ACR of control mice were higher in comparison to prior study (Jackson laboratory., 2015). This particular laboratory reared the mice for a period of 10 weeks, whereas in the current study, mice were on diet for a period of 30 weeks. The degree of variation in the results may have been due to genetic background of the mouse strain and environmental factors including diet, duration of diet intervention, housing, dark and light cycle, handling etc., which might explain reasons for overall variations of the above mentioned parameters of the current study (Brosius et al., 2009).

Diabetic albuminuria in humans is associated with the development of characteristic histopathological changes such as glomerulosclerosis. Glomerulosclerosis in diabetic patients is characterised by increased glomerular basement membrane width, diffuse mesangial sclerosis, hyalinosis, microaneurysm, hyaline arteriosclerosis (Mauer et al., 1981), interstitial changes (Brito et al., 1998) and extreme mesangial expansion (Katz et al., 2002). In the current study, histopathological changes of the kidney samples were assessed to observe if mice on prolonged dietary interventions demonstrated the lesions of glomerulosclerosis similar to human patients. Results showed that mice fed on the EDD demonstrated thickening of the basement membrane of Bowmans's capsule, mesangial matrix thickening and hypertrophy of glomeruli compared to control mice on the SRD (Figure 4.8). These findings were consistent with other studies using diabetic animal models (Koya et al., 2000, Cohen et al., 2001, Reifsnyder and Leiter, 2002, Leiter and Reifsnyder, 2004, Danda et al., 2005, Mohan et al., 2008). These observations suggested that prolonged EDD intervention is able to induce some aspects of DN which are similar to human patients. The current study did not assess the plasma creatinine level and other histopathological changes in kidney associated with DN.

At the onset of T2D, the ability of insulin to stimulate glucose uptake is impaired. Subsequently, pancreatic β-cell become over activated to produce more insulin resulting in an elevated insulin level in the circulation. Compensatory hyperplasia of the pancreatic islet occurs because of a compensatory increase in circulatory insulin levels (Del Prato, 2009, Kahn et al., 2014). One of the Aims (3) of the current study was to determine the total pancreatic islet area over the total pancreatic area to understand the over activity of the pancreatic β-cell and insulin resistance. Metabolic parameters such as FBG, impaired glucose tolerance and AUC-GTT

already demonstrated that mice on the EDD for a prolonged period became insulin resistant. Further confirmation of the hyperactivity of pancreatic islet cells and insulin resistance of EDD fed mice was determined by observing pancreatic pathology. Histological examination of the pancreas revealed an increase in the size of pancreatic islet (pancreatic hyperplasia) in EDD fed mice compared to aged-matched control littermates on SRD (Figure 4.7). The increased area of the pancreatic islet was an indication of insulin resistance, which is one of the characteristic features of T2D in humans (Quan et al., 2013). Previous studies in animal models observed a similar type of compensatory hyperplasia of pancreatic islet in diabetic mice (Lavine et al., 1977, Suzuki et al., 1999, Bock et al., 2003, Leiter and Reifsnyder, 2004, Kawasaki et al., 2005, Nagata et al., 2006, Kanetsuna et al., 2007). Pancreatic insulin content, HOMA-IR (Homeostasis Model Assessment-Insulin Resistance) is also an important marker to further confirm the insulin resistance. The current study did not determine the pancreatic insulin content and HOMA-IR. In the same laboratory, Morris and colleagues (2016) demonstrated an elevated total pancreatic insulin and HOMA-IR in EDD fed ARC bred mice compared to control mice on SRD.

In this investigation, both the JCU and ARC bred mice demonstrated the clinical features of T2D at 25 and 30 weeks of diet intervention. Based on the metabolic features (FBG, AUC-GTT, HbA1c and the FBG after 2 hours of glucose challenge), 25 weeks of diet intervention was sufficient for the development of diabetic related features in most of the ARC and JCU bred mice. However after 30 weeks of diet intervention, the maximum number of mice become diabetic based on the same metabolic parameters. Histopathological evidences also demonstrated that the JCU bred mice mimicked several aspects of diabetic related complications including diabetic nephropathy and pancreatic pathology. Overall, at the 30^{th} week of diet intervention, more ARC bred mice (overall 78.94%) showed clinical features of T2D compared to JCU bred mice (overall 73.45 %). Bridson (2015) also found a higher proportion of ARC bred mice (82% based on FBG) showed the features of diabetes in response to the same diet. In the current study, histopathology of ARC mice was not done which was a limitation of the study. In an earlier study, histological evidence of ARC bred mice in response to the EDD feeding also supported the diabetic related complications observed in JCU bred mice (Morris et al., 2016).

In this study, we didn't observe any statistically significant differences in the metabolic parameters (body weight, AUC, HbA1c, microalbumin, creatinine and ACR) between the SRD (control *vs* control) and EDD fed groups (EDD *vs* EDD) of JCU and ARC bred mice. A slight

variation (high or low) in the diabetic parameters in EDD and SRD fed JCU and ARC bred mice might be due to use of separate sources of the mice, genetic background and breeding environment (Bernard et al., 2013). It is important to note that under the same experimental setting, there was variation in feed consumption, body weight gain and metabolic changes in mice fed an EDD. A smaller portion of mice failed to develop hyperglycaemia or an elevated level of HbA1c even after the 30 weeks of diet intervention. This is also the case in the human diabetic population. Not all obese individuals with poor dietary habits develop diabetes or not all the diabetic patients lead an unhealthy lifestyle (Prando et al., 1998). Although obesity and lifestyle factors are important predictors of the development of diabetes, there are many other risk factors that contribute to the progression of this disease (Fletcher et al., 2002).

The work described in this Chapter has demonstrated that EDD feeding to C57BL/6 mice induces overt features of T2D. The polygenic DID murine model described in the present study proposes some advantages over the conventional murine models of T2D such as i) use of a diet containing the moderate level of fat with high glycaemic index reflects the global dietary pattern, ii) unlike other models which use short-term diet intervention, the present study described prolonged diet intervention for progression of pre-diabetes to overt/chronic T2D diabetes and its associated complications similar to human T2D patients. Therefore, this model can be used for future studies of diabetes alone or host-pathogen interaction in diabetes.

CHAPTER 5
EFFECT OF TYPE 2 DIABETES ON MACROPHAGE FUNCTIONS DURING MYCOBACTERIAL INFECTIONS

5.1 Introduction

In mycobacterial infections, some of the first cells to encounter the organism are macrophages, in particular, alveolar macrophages (Tascon et al., 2000, Gonzalez-Juarrero et al., 2001, Dheda et al., 2010). The primary function of the alveolar macrophage is phagocytosis (uptake and killing) of the bacilli (Henderson et al., 1997, Thurnher et al., 1997). If the mycobacteria are not killed during this initial encounter, bacteria survive and proliferate within macrophages (Iona et al., 2012, Helguera-Repetto et al., 2014). Mycolic acid on the cell wall of mycobacteria is a key factor influencing phagocytosis and bacterial killing. Trehalose 6,6′ dimycolate (TDM) is considered the most abundant and toxic mycolic acid which elicits major immunological events (Karakousis et al., 2004). It is crucial for the survival of the bacteria within the macrophages. It prevents phagosome-lysosome fusion, inhibits acidification of the phagolysosome, decreases macrophage expression for pattern recognition receptors (PRR) and costimulatory molecules leading to impaired antigen presentation followed by T cell mediated immune responses (Indrigo et al., 2002, Indrigo et al., 2003, Kan-Sutton et al., 2009). Bowdish and colleagues (2009) demonstrated that the phagocytosis of TDM coated latex beads by macrophages (resident peritoneal and bone marrow-derive) was reduced due to impaired recognition of it by the PRR (e.g. Toll like receptors 2; TLR2) including scavenging receptors (e.g. macrophage receptors with collagenous structure; MARCO). In the literature, the impact of diabetes on the phagocytosis of mycobacteria by macrophages has not been extensively investigated. Previous studies on the impact of diabetes in phagocytosis were evaluated mostly in peripheral blood mononuclear cells (PBMC) infected with various organisms and beads (Geisler et al., 1982, Marhoffer et al., 1992, Delamaire et al., 1997, Geerlings and Hoepelman, 1999, Lecube et al., 2011, Kumar Nathella and Babu, 2017). The role of alveolar macrophages in the primary defence of *M. tuberculosi*s infection, has been poorly investigated in TB-T2D co-morbid infection.

During phagocytosis, macrophages elaborate pro-inflammatory (e.g. TNF-α, MCP-1, IL-1β, IL-12, IFN-γ, IL-6) and anti-inflammatory cytokines (e.g. IL-10, IL-4) (Cooper, 2009, Cooper et al., 2011).These cytokines are key factors that determines the fate of infections. Studies have shown that mice lacking TNF-α promptly succumb to infection with increased bacterial loads in spleen, liver and lungs compared to control mice (Flynn et al., 1995, Benoit et al., 2008).

TNF-α is essential for the activation of macrophages and neutrophils (Orme and Cooper, 1999, Tsenova et al., 1999, Gan et al., 2005) and subsequent lung granuloma formation (Kindler et al., 1989, Flynn et al., 1995, Senaldi et al., 1996). The production of IL-1β is also required for macrophage activation and it enhances the secretion of TNF-α, IL-6, IFN-γ for an effective granuloma formation (Toossi et al., 1990, Juffermans et al., 2000). IL-12 is required for T helper 1 cell differentiation (e.g. CD4+ T cells for IFN-γ production) (Sieling et al., 1994, Cooper et al., 1995, Trinchieri, 1995, O'Neill and Greene, 1998). Secretion of IFN-*γ* from CD4+, CD8+ T cells and Natural Killer (NK) cells not only activates macrophages but also increases MHC (Major Histocompatibility Complex) class II molecule expression on antigen presenting cells. A deficiency of IL-12 and IFN-*γ* is known to increase susceptibility to TB, further demonstrating the importance of these cytokines (Altare et al., 1998a, de Jong et al., 1998, Ottenhoff et al., 2002). In contrast, anti-inflammatory cytokines such as IL-10 and TGF-β secreted by macrophages are responsible for the downregulation of IFN-γ, TNF-α and IL-12, causing adverse TB-related pathology in the host (Redford et al., 2011). It is the intricate interplay of these cytokines that orchestrates effective innate and adaptive immunity in response to TB. Although the production of cytokines by macrophages is well documented in TB research, there is limited informaton on the impact of diabetes on cytokine production by macrophages in mycobacterial infections. Previous research has determined cytokine production using *in vitro* PBMC, but not in alveolar macrophages (Geerlings and Hoepelman, 1999, Lachmandas et al., 2015). Further, *in vivo* studies examined the cytokine production in diabetic patients with or without TB but yielded contradictory results. Some reports have shown an elevated production of pro-inflammatory cytokines in diabetes-TB patients whereas other reported the opposite (Restrepo et al., 2008a, Stalenhoef et al., 2008, Tan et al., 2012, Kumar et al., 2013, Kumar et al., 2014).

Therefore, we investigated the phagocytic function and cytokine production by two different types of macrophages (resident peritoneal and alveolar) from diabetic and control mice. We used both inert mycolic acid coated latex particles and *in vitro* mycobacterial infections to explore the impact of T2D on macrophage function in mycobacterial infections, in particular, *M. tuberculosis* infection.

The specific Aims of the research described in this Chapter are:

1. To determine the uptake capability of alveolar and resident peritoneal macrophages from diabetic and control mice following co-culture with mycolic acid coated beads
2. To investigate the uptake and killing capability of alveolar and resident peritoneal macrophages from diabetic and control mice following infection with of *M. fortuitum, M. bovis* (BCG) and *M. tuberculosis* (H37Rv)
3. To assess pro-inflammatory (TNF-α, MCP-1, IL-1β, IL-12, IFN-γ, IL-6) and anti-inflammatory cytokine (IL-10) production by alveolar and resident peritoneal macrophages from diabetic and control mice following co-culture with *M. fortuitum, M. bovis* (BCG) and *M. tuberculosis* (H37Rv)

5.2 Materials and Methods

5.2.1 Experimental animals

The mice used for the characterisation of diet-induced murine model of T2D described in Chapter 4 were used for the study presented in this Chapter. In addition, other T2D and control mice sets were also used for this study.

5.2.2 Assessment of mycolic acid coated bead phagocytosis

5.2.2.1 Preparation of mycolic acid coated beads

Fluoresbrite® 2 µm Yellow Green Microspheres (411 nm excitation and 485 nm emission, Polysciences, Inc, USA) were coated with two commercially available cell wall extracts of *Mycobacterium tuberculosis* (bovine strain): (i) mycolic acid (cat. no. M4537, Sigma) and (ii) Trehalose 6, 6′ dimycolate, cat. no. T3034, Sigma). Initially, mycolic acid stocks were prepared by dissolving the powder in chloroform: methanol solution (Appendix 1). The amount of mycolic acid required to deposit as a monolayer was calculated as described by Retzinger and colleagues (1981). Lipid coated beads were prepared according to the protocol described by Indrigo and co-workers (2003) with some modifications. Briefly, Fluoresbrite® beads were washed three times with carbonate-bicarbonate buffer (cat. no. C3041, Sigma; Appendix 1) by centrifugation at 3000 xg for 15 minutes at 15^0C. Beads to be coated with either mycolic acids were further washed once in 30% ethanol followed by 1% ethanol (Appendix 1). The required volume of mycolic acids (20 µg/1x10^8 beads) was then added to the beads suspension in carbonate bicarbonate buffer. The beads and mycolic acid mixtures were alternatively vortexed and sonicated (50% of the maximum frequency) at 55^0C for 5 minutes and incubated for 12 hours at 37^0C with constant gentle mixing (120 rpm in an orbital shaker). Following coating,

beads were washed twice with PBS. Mycolic acid coated beads were further washed once in 0.1% F68 buffer (cat. no. P566, Sigma; Appendix 1) followed by RPMI 1640 (Invitrogen, Mulgrave, Australia) before resuspending in RPMI. Lipid coated beads were stored at 4^0C and further sonicated for 2 minutes before adding to cell suspensions for phagocytosis assays. The control beads were prepared exactly the same way where carbonate bicarbonate buffer was added instead of mycolic acids. However, we have also used fresh beads to assess the phagocytosis. They were not treated with anything as described for mycolic acid coated beads and control beads. Finally, the mycolic acid coated beads were assessed using the BD FACSCalibur™ flow cytometer to evaluate the light scattering properties as an indicator of the successful coating. The higher forward scatter (indicates the relative size) of the lipid coated beads in comparison to uncoated beads confirmed the successful coating with mycolic acids (Figure 5.1). The exact amount of mycolic acid coated onto the beads surface was not determined.

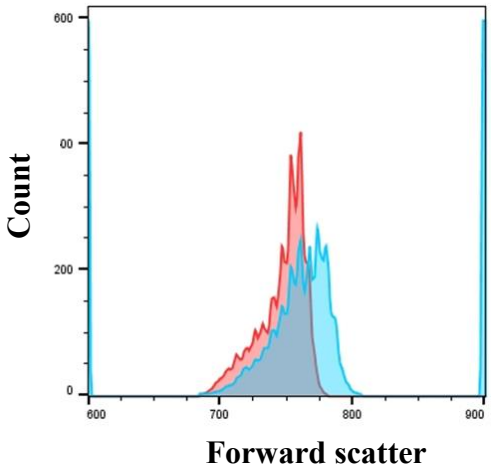

Figure 5.1 Scattering of mycolic acid coated beads and control beads

Figure illustrated the higher forward scattering of the mycolic acid coated beads (blue) compared to the uncoated control beads (light red).

5.2.2.2 Isolation of thioglycollate-elicited and resident peritoneal cells

Thioglycollate-elicited peritoneal and resident peritoneal cells were collected according to the protocol described by Hodgson and co-workers (2011) and Williams and colleagues (2011). Briefly, mouse peritoneal exudate cells (PEC) were elicited for 3 days by injecting mice intraperitoneally with 2 mL of 3% Brewer's thioglycollate medium (Appendix 1). After carbon dioxide (CO_2) asphyxiation, the elicited PEC were collected aseptically from the peritoneal cavity of mice by injecting 10 mL of the cold harvest medium with heparin (5 IU/mL, Appendix

1) followed by aspirating the fluids. Non-elicited resident peritoneal exudate cells (RPEC) were collected from other mice using the same harvesting method as described for PEC. The PEC and RPEC from each mouse within an experimental group were pooled separately and treated with Red Blood Cells (RBC) lysis buffer (cat no. 004300, eBioscience, Australia; Appendix 1). Then the treated cells were washed twice with RPMI 1640 at 500 xg for 10 minutes at 15^0C. Cells were counted using the trypan blue (0.4%) exclusion technique (Appendix 1). Finally, cells were resuspended to a concentration of $1x10^6$ or $1x10^5$ cells/mL in single strength culture medium (SSCM, Appendix 1) for plating into 48 well cell culture plates. However, the average cell (PEC) yield from the thioglycollate-elicited diabetic and non-diabetic mice was $1x10^7$ cells/mouse. Whereas the non-elicited RPEC yield from the non-elicited diabetic and control mice was $5x10^6$ cells/mouse.

5.2.2.3 Isolation of leucocytes from broncho-alveolar lavage fluid

Broncho-alveolar lavage fluid (BALF) from mouse lungs was collected according to the protocol described by Collins and co-workers (2014) with some modifications. In short, a ventral midline incision was made to open the abdominal and thoracic region after CO_2 euthanasia. The vena cava was cut to allow for drainage of the blood from the upper trunk of the body. The ribs and the lower portion of the sternum were removed to make room for the lung inflation during BALF collection. The trachea was exposed carefully after removing skin, glands and muscles and raised using blunt forceps. A 21-gauge blunted butterfly needle (Surflo® winged infusion set, cat. no. SV 21B2K, TERUMO, Japan) or an 18-gauge blunt needle was inserted into the proximal end of the trachea (Figure 5.2). To secure the needle into the trachea, it was tied with a sterile surgical suture (Supramid white, cat. F1184040, Spain). Care was taken not to puncture the trachea. One to two mL of broncho-alveolar buffer (Appendix 1) was gently injected into the lungs and slowly extracted. Subsequently, another 2 mL of same buffer was injected slowly and sucked with back and forth motion (4-5 times) and the procedure was repeated twice. The collected fluid was kept in a 50 mL polypropylene tube with 5 mL of RPMI 1640 on the ice. The collected BALF from both diabetic and control mice was centrifuged at 500 xg for 10 minutes at 15^0C. Five hundred µL of RBC lysis buffer was added to the cell pellet for 2 minutes and then diluted it with RPMI 1640. Finally, the cells were filtered with a sterile 63 µm nylon mesh and washed. The cell pellet was resuspended at a concentration of $1x10^5$ cells/mL with SSCM for plating into 48 well cell culture plates. However, the average alveolar leucocytes (AL) yield from each diabetic and non-diabetic mouse was $1x10^5$ cells.

Figure 5.2 Collection of broncho-alveolar lavage fluid from a mouse

5.2.2.4 Culture of peritoneal cells and alveolar leucocytes

The resuspended peritoneal (PEC), resident peritoneal (RPEC) and alveolar leucocytes (AL) were seeded into 48 well cell culture plates (3-7 replicates per sample). The PEC and RPEC were plated at $1x10^5$ cells/well ($5x10^5$ cells/well in some experiments), whilst AL were seeded at $1x10^5$ cells/well in 500 µL of SSCM (Appendix 1). Plates were incubated for one hour at 37^0C with 5% CO_2 to allow cell adherence. Fluoresbrite® Yellow Green Microspheres (2 µm), trehalose 6,6′ dimycolate coated beads (TDMCB) and whole mycolic acid coated beads (MACB), control beads (CB) including fresh beads (FB; without washing) were added to appropriate wells at two different ratios 1:1 and 1:10 (cell:bead). After 4 hours incubation, cell supernatants were collected for cytokine analysis and stored at -80^0C. Adherent cells were scraped from the base of wells and all cells were transferred into flow cytometry tubes for macrophage surface staining. Replicate wells were stained individually.

5.2.2.5 Staining of macrophage surface markers and flow cytometry

Following 4 hours incubation of peritoneal (PEC) and resident peritoneal exudate cells (RPEC) with mycolic acid coated beads, they were surface stained for macrophage surface markers F4/80 and CD11b (Table 5.1). The harvested PEC and RPEC were washed (2000 rpm for 5 minutes) with standard azide buffer (SAB; Appendix 1) to obtain the cell pellets. The antibody master mix (Fc blocker, CD11b and F4/80 antibodies; Table 5.1) was added to cell pellets and incubated for 20 minutes at 4^0C followed by washing once with SAB. The cell pellets were stained with PE Streptavidin for 10 minutes followed by washing once with SAB. Then, the cell pellets were resuspended in 300 µL of PBS. Similarly, the harvested alveolar leucocytes (AL) were surface stained for CD11c and PE Streptavidin according to the methods described

above. A cell viability dye (7-Amino-Actinomycin D, cat no. 559925, BD Pharmingen™) was added to the cell suspensions (PEC, RPEC and AL) for 10 minutes before acquring the samples by BD FACSCalibur™ flow cytometer. This particular dye will only stain the dead cells with the compromised cell membrane. The flow cytometry data were acquired and analysed using BD CellQuest® Pro software. The gating strategies for acquiring the samples were described in Figure 5.3 and 5.4. However, the F4/80 and CD11b positive cells from PEC and RPEC were considered as peritoneal macrophages (PEM) and resident peritoneal macrophages (RPM), respectively. The CD11c+ cells from AL were considered as alveolar macrophages (AM).

Table 5.1 Antibodies used for surface staining of the macrophages

Antibodies	Catalogue number	Dose/test	Supplier
Anti-mouse CD16/32 Purified, clone: 6F12, isotype: Rat IgG2a, λ	14-0161	0.25 µg	BD Pharmingen™
Purified Rat Anti-Mouse F4/80 biotin, clone: 6F12, isotype: Rat IgG2a, κ,	552958		
Alexa Fluor® 647 Rat Ani-Mouse CD11b, clone: M1/70, isotype: Rat IgG2b, κ,	557686		
Biotin Hamster Anti-Mouse CD11c, clone: HL3, isotype: Hamster IgG1, λ,	55380		

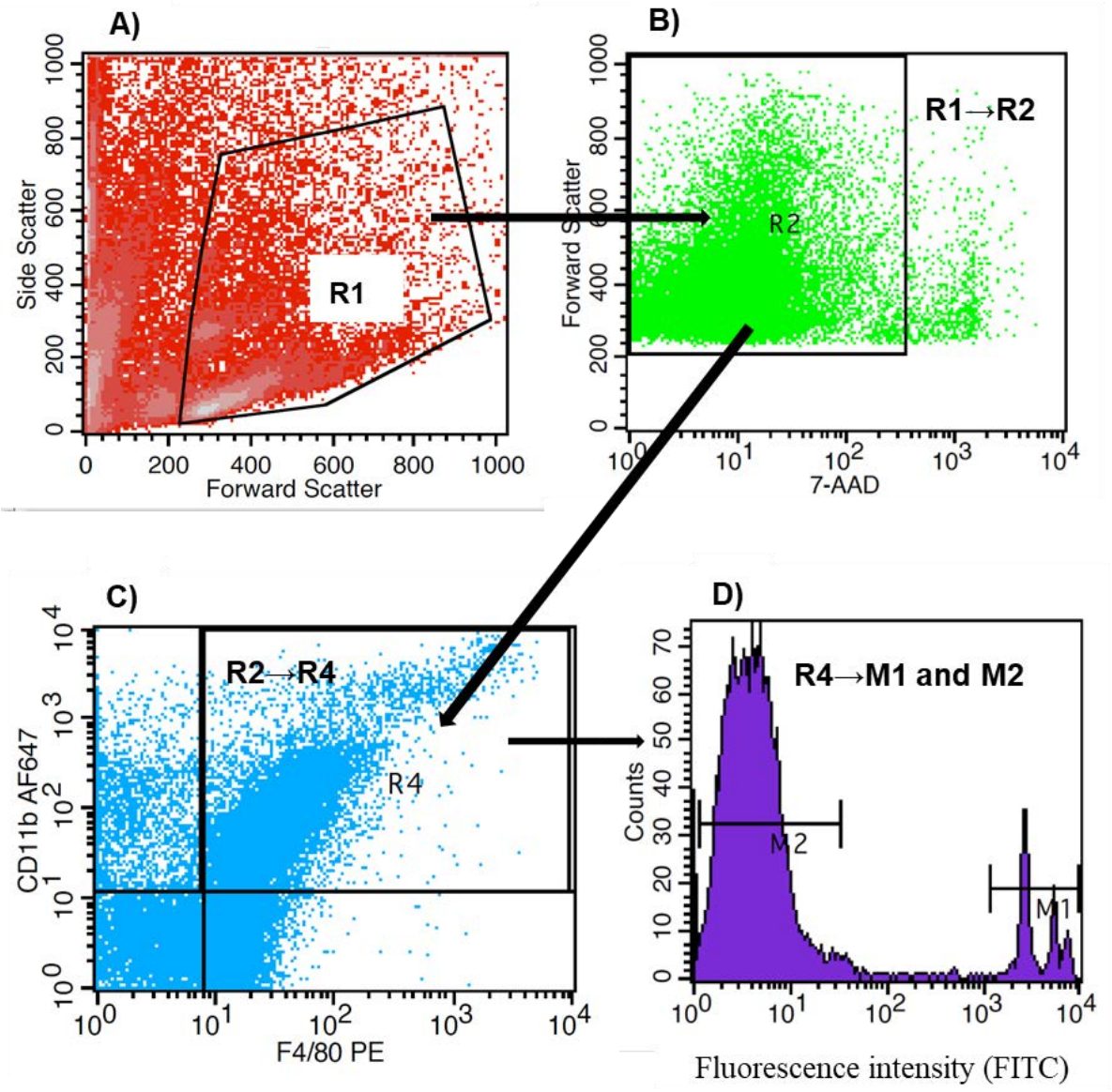

Figure 5.3 Flow cytometry gating strategy for assessing phagocytosis of beads by peritoneal macrophages

The peritoneal (elicited, PEC) and resident peritoneal exudate cells (non-elicited, RPEC) were surface stained for macrophage surface marker F4/80 and CD11b. Phagocytosis of Fluoresbrite beads (FITC) was assessed in both F4/80 and CD11b positive macrophages from PEC and RPEC. Region 1 (R1) indicated either PEC and RPEC (A). A total of 30 thousand events were acquired in R1. Region 2 (R2) indicated live and dead cells (located outside of R2 based on cell viability dye; 7-Amino-Actinomycin; D) (B). Region 4 (R4) indicated the live peritoneal (elicited) or resident (non-elicited) peritoneal exudate macrophages (PEM/RPM; CD11b and F4/80 double positive cells) (C). Counting of the internalised and cell-associated FITC conjugated Fluoresbrite beads; 'M1' (marker 1) indicated PEM or RPM with beads and 'M2' showed the macrophages without beads (D).

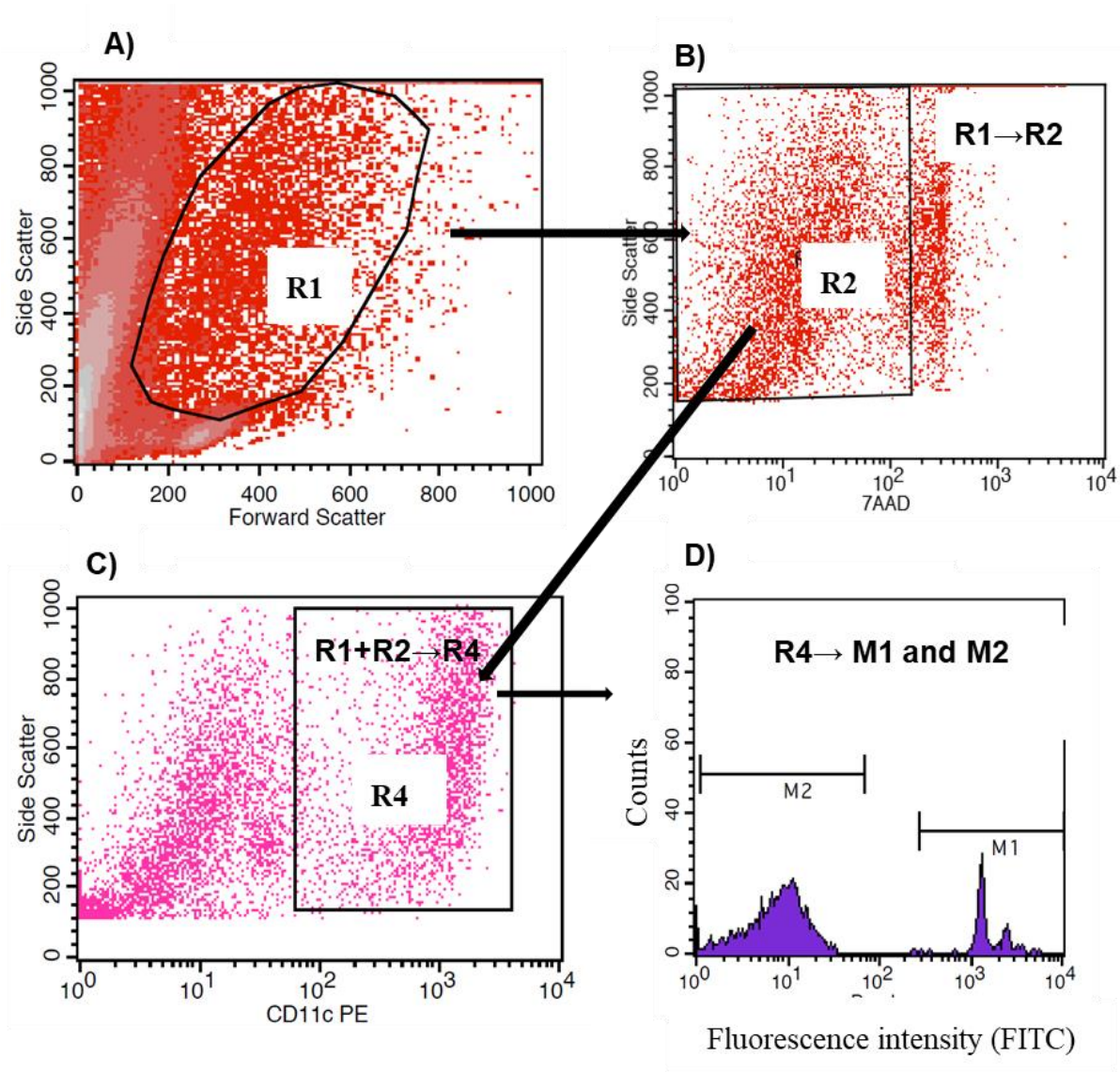

Figure 5.4 Flow cytometry gating strategy for assessing phagocytosis of beads by alveolar macrophages

The alveolar leucocytes (AL) were stained with macrophage surface marker CD11c. Phagocytosis of Fluoresbrite beads (FITC) was assessed in CD11c positive macrophages from AL. Region 1 (R1) indicated AL (A). A total of 30 thousand events were acquired in R1. Region 2 (R2) indicated live cells, whereas dead cells were located outside of R2 (based on cell viability dye; 7-Amino-Actinomycin; D) (B). Region 4 (R4) indicated the live alveolar macrophages (AM; CD11c positive cells) (C). Counting of internalised and cell-associated FITC conjugated Fluoresbrite beads; 'M1' (marker 1) indicated AM with beads and 'M2' showed the macrophages without beads (D).

5.2.3 Assessment of mycobacterial uptake and killing

5.2.3.1 Mycobacterial isolates

The details of bacterial isolates are described in Chapter 3 (section 3.3.1)

5.2.3.2 Preparation of mycobacterial inoculum for *in vitro* uptake and killing assays

The details of mycobacterial culture are described in Chapter 3 (section 3.3.2). Preparation of *M. fortuitum*, *M. bovis* (BCG) and *M. tuberculosis* (H37Rv) inocula for *in vitro* uptake and killing assays were done from the frozen aliquots. The required number of frozen aliquots were thawed, vortexed and passed through a 27-gauge needle a total of 10-15 times. The bacterial suspensions were further sonicated for 10 seconds before adding to the cell culture. The bacterial suspension was further plated on 7H11 agar plates to confirm the number of bacteria in the inocula.

5.2.3.3 Isolation of CD11b+ cells from resident peritoneal exudate cells

CD11b+ cells were separated from the resident peritoneal exudate cells (non-elicited, RPEC) using Anti-CD11b Magnetic Particles-DM (cat. no. 558013, BD Biosciences, Australia) according to the manufacturer's instructions. In short, The RPEC were collected (section 5.2.2.2) and filtered through a sterile 63 μm nylon mesh to remove clumps of cells and/or debris. Mouse FcR blocking reagent (purified rat Anti-Mouse CD16/CD32, cat. no. 553141, BD Biosciences; Australia, 0.25 μg for $1x10^6$ cells) was added and incubated at 4^0C for 15 minutes. Cells were washed with at least an equal volume of 1x BD IMag™ buffer (cat. no. 55236, BD Biosciences, Australia; Appendix 1) and the supernatant was carefully aspirated. The CD11b magnetic particles (50 μL of particles/$1x10^7$ cells) were added and the cell/bead suspension was incubated at 4^0C for 30 minutes. The volume was brought to 2 mL with the 1x BD IMag™ buffer and immediately placed into the BD IMagnet™ for 8 minutes. With the tube on the BD IMagnet™, the supernatant was aspirated (negative fraction) using a glass pasteur pipette. To wash the cells again, tubes were removed from the magnet and an equal amount of 1x BD IMag™ buffer was added and kept in the magnet for another 8 minutes (second wash). To increase the purity of the CD11b positive fraction, the washing step was repeated. After the final wash, the cell pellet (positive fraction) was diluted in a smaller volume (3-5 mL) for counting by trypan blue exclusion technique using a haemocytometer. The cells were resuspended in the desired volume of SSCM to give a concentration of $1x10^5$ cells/well in 1 mL. The purity of the positively selected CD11b+ cells (referred to from now as resident

peritoneal macrophages; RPM) was assessed by flow cytometry after staining with CD11b surface marker (BD FACSCalibur™) and found to be above 85% (Figure 5.5 A & B).

5.2.3.4 Isolation of CD11c+ cells from the broncho-alveolar lavage fluid

CD11c+ cells were positively selected from the broncho-alveolar lavage fluid using the EasySep™ Mouse CD11c positive selection kit (cat. no. 18758, STEMCELL™ technologies) according to the manufacturer's instructions. In brief, following collection (section 5.2.2.3) the BALF was filtered through a sterile 63 μm nylon mesh to remove clumps of cells and/or debris. Mouse FcR blocking antibody (10 μL/1x10^8 cells) and CD11c PE labelling reagent was added to the cell pellet and incubated at room temperature for 15 minutes. The EasySep™ PE Selection Cocktail (100 μL/mL cells) was added and incubated for another 15 minutes. Finally, the magnetic nanoparticles were added to the pellet and incubated for further 10 minutes. The cell pellet was resuspended in 2.5 mL with 1x BD IMag™ buffer (Appendix 1) and kept in EasySep® magnet (cat. no.18000, STEMCELL™ technologies). After 15 minutes of incubation, the supernatant was poured off by inverting the magnet. The tube was removed from the magnet and resuspended in an equal volume of IMag™ buffer and placed in the magnet for 10 minutes (second wash). To increase the purity of the CD11c positive cells, the washing step was repeated. After the final wash, the cell pellet (positive fraction) was diluted in a smaller volume (2-3 mL) and counted by trypan blue exclusion technique using a haemocytometer. The cells were then resuspended in the desired volume of SSCM give a concentration of 1x10^5 cells/well in 1 mL. Moreover, the purity of the CD11c+ cells (referred to from now as alveolar macrophages; AM) were assessed by flow cytometry (BD FACSCalibur™) and found to be around 95% (Figure 5.5 C & D).

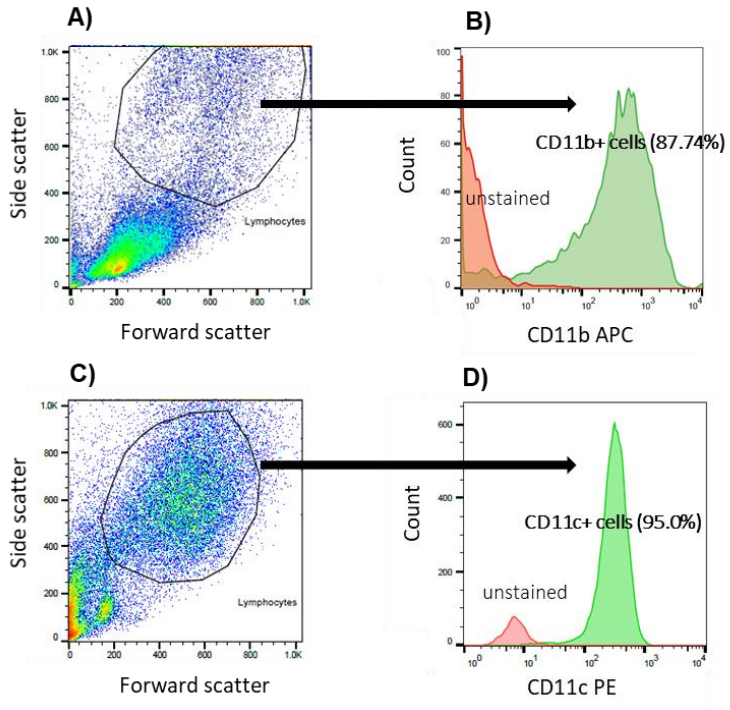

Figure 5.5 Purity checking of CD11b+ and CD11c+ cells

CD11b+ cells were isolated from resident peritoneal exudate cells (RPEC). Figure illustrates the forward and side scatter of RPEC (A). An overlay histogram showed unstained (unpurified RPEC, light red) and CD11b+ cells population (purified; light green) (B). CD11c+ cells were isolated from alveolar leucocytes (AL) from broncho-alveolar lavage fluid. Figure indicates the forward and side scatter of AL (C). An overlay histogram demonstrated unstained (unpurified AL, light red) and CD11c+ cells population (green).

5.2.3.5 Bacteria internalisation and killing assay

The magnetically separated cell suspensions (CD11b+ cells as RPM and CD11c+ cells as AM) were resuspended in SSCM at a concentration of $1x10^5$ cells/well in 1 mL and added to 48 well cell culture plates. Three-five replicates were used for each organism. After 4 hours incubation, internalisation was assessed and killing of the internalised bacteria was measured after 24 hours (48 hours in some experiments) according to previously described protocols (Parti et al., 2005, Williams et al., 2008, Hodgson et al., 2011). Briefly, *M. fortuitum, M. bovis* (BCG) and *M. tuberculosis* (H37Rv) were added to the cells seeded into 48 well plates at MOI 1:10 (cell: bacteria). After 4 hours of co-culture, supernatants were collected for cytokine assays. The wells were washed and treated with Amikacin (200 µg/mL) for a further 2 hours to kill any extracellular bacteria. To determine bacterial uptake, cell culture pellets were washed (3000 rpm for 5 minutes) with PBS and cells were lysed with 0.1% Triton X-100^{TM} (Sigma) for 10 minutes. The cell lysates were further washed with PBS and plated on 7H11 agar plates to determine the viable bacteria (CFU). Duplicate plates were used to determine bacterial killing after 24/48 hours. For these experiments, plates were washed after Amikacin treatment. After

adding the fresh cell culture media, the cells were further incubated at 37^0C for 24/48 hours. Following collection of supernatants, the cells were washed, lysed with Triton X-100™. Finally, the washed cell lysates were plated on 7H11 agar plates to determine the viable bacteria. In some experiments, 4 hours uptake by non-elicited resident peritoneal cells (REPC, without CD11b+ cells separation) were assessed to determine the internalised and cell associated bacteria. The above described procedures were followed except treating the plates with Amikacin. The killing capability of the RPEC was also assessed after 24 hours as described above. Bacterial uptake and survival were calculated based on the following formula.

$$\textbf{4 hours uptake} = \frac{(No.\,of\ internalised\ bacteria\ after\ 4\ hours)}{(No.\,of\ bacteria\ given\ intially)} X100$$

$$\textbf{24 or 48 hours survival} = \frac{(No.\,of\ survived\ bacteria\ after\ 24/48\ hours)}{(No.\,of\ bacteria\ internalised\ after\ 4\ hours)} X100$$

5.2.4 Assessment of cytokines

Culture supernatants following 4, 24 and 48 hours of macrophages: bacterial co-culture were used to determined cytokine production using the BD Cytometric Bead Array Mouse Inflammation Kit® (cat. no. 552364) and Mouse IL-1β Flex Set® (cat. no. 560232, BD Bioscience, Australia). Manufacturer's instructions were followed to measure the cytokine secretion (TNF-α, MCP-1, IL-6, IL-12, IFN-γ, IL-10, IL-1β). Samples were acquired using the BD FACSCalibur™ flow cytometer with BD CellQuest Pro® software. The acquired data were analysed by BD FCAP Array ™ software (version 3.0) (Chapter 3, section 3.8). Cytokine levels that were below the limit of detection (Chapter 3, Table 3.2) are shown as zero ('0').

5.3 Statistical analysis

Statistical analysis was performed using the GraphPad Prism 7.03 and SPSS version 24 software. All the data were checked for normal distribution using the Shapiro-Wilk's test. Data passed the test of normality if the $p \geq 0.05$. Normally distributed data (e.g. mycobacterial uptake and killing) were compared between the groups using the unpaired *t*-test with Welch's correction. The non-normally distributed data were compared between the groups using the Mann-Whitney U test. An ordinary one-way ANOVA with Holm Sidak's multiple comparisons test was performed to compare within the groups if the data sets were normally distributed (e.g. cytokine production by stimulated and unstimulated AM from diabetic and control mice). When all 3 sets of data out of 4 were normally distributed, in those circumstances, one-way ANOVA with Holm Sidak's multiple comparisons test was done assuming all the data sets were normally

distributed. The non-normally distributed data were compared within the groups using the Kruskal-Wallis test with Dunn's multiple comparisons test. All the data were expressed as mean±SEM. The level of significance was indicated as *p≤0.05, **p≤0.01, ***p≤0.001 and ****p≤0.0001.

5.4 Results

5.4.1 Features of the diabetic mice following diet intervention

The effects of energy-dense diet (EDD) intervention on mice were optimised and described in detail in Chapter 4. The same mice and some additional mouse sets were used for the current study. All mice used were on their respective EDD and control diets for 30 weeks. The metabolic profiles and histological findings in organs were highlighted in Chapter 4 and summarised here in Table 5.2. Mice in the current study were considered T2D if they demonstrated a raised FBG level and AUC-GTT with evidence of glucose intolerance at levels higher than the upper 99% confidence interval for the mean of the age-matched control group (Appendix 2). As the mice fed on EDD showed the metabolic and histologic characteristic of T2D (Chapter 4), hereafter they will be termed 'diabetic mice'.

Table 5.2 Metabolic profiles and histological features of mice used in the study described in this Chapter

Parameters	Control (mean±SEM)	Diabetic (mean±SEM)	p-value
Body mass (g)	27.86 ±0.29	46.31±0.69	**** <0.0001
Blood glucose (mmol/L)	8.61±0.27	11.07±0.43	**** <0.0001
Insulin resistance (GTT-AUC)	1374±29.56	1657±42.81	**** <0.0001
Glycosylated haemoglobin (% HbA1c)	2.40±0.44	2.61±0.38	*0.0115
Renal profile			
Microalbumin (mg/L)	4.08±1.60	10.39±0.65	*** 0.0005
Creatinine (mmol/L)	4.51±0.21	3.15±0.17	*** 0.0003
ACR (mg/mmol)	0.91±0.14	3.34±0.69	**** <0.0001
Urine glucose (mmol/L)	1.38±0.06	1.57±0.15	ns >0.9999
Histological features			
Herxheimer's stained area (%)	0.19±0.91	28.26±2.20	**** <0.0001
Adipocyte size (μm^2)	496.5±55.54	1980±130.0	**** <0.0001
Pancreatic islet area/total pancreatic area (%)	0.62±0.06	1.46±0.14	**** <0.0001
Glomerular area (μm^2) in kidneys	1425±79.52	2275±89.27	**** <0.0001
PAS positive stain within glomeruli (%) in kidneys	17.14±1.48	25.23±1.34	*** 0.0005

GTT; glucose tolerance test, AUC; area under the curve, ACR; albumin creatinine ratio, PAS; periodic acid schiff; * level of significance and ns=non-significant

5.4.2 Phagocytosis of mycolic acid coated beads by the macrophages

The phagocytic capability of peritoneal exudate macrophages (PEM) from elicited peritoneal exudate cells (PEC; section 5.2.2.2), resident peritoneal macrophages (RPM) from non-elicited resident peritoneal cells (RPEC, section 5.2.2.2) and alveolar macrophages (AM) from alveolar leucocytes (AL; section 5.2.2.3) was assessed following 4 hours of co-culture with polystyrene beads (fresh beads; FB), whole mycolic acid coated beads (MACB), trehalose 6, 6′-dimycolate coated beads (TDMCB) and control beads (CB) (Figure 5.6).

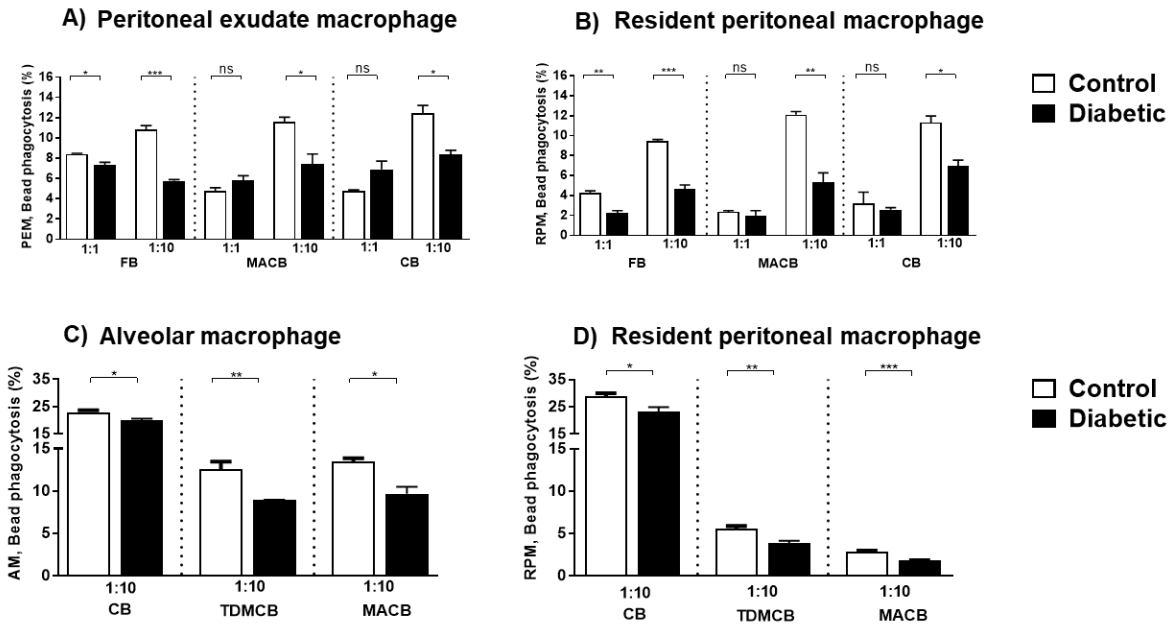

Figure 5.6 Mycolic acid coated bead phagocytosis by peritoneal, resident peritoneal and alveolar macrophages

Phagocytosis of beads by peritoneal (PEM, elicited) and resident peritoneal macrophages (RPM, non-elicited) and alveolar macrophages (AM, non-elicited) was assessed after 4 hours of co-culture with beads at ratios of 1:1 and 1:10. At MOI 1:10, the PEM and RPM from diabetic mice were less efficient in uptake of polystyrene beads as fresh beads (FB), mycolic acid coated beads (MACB) and control beads (CB) compared to controls (A & B). The trehalose 6, 6′-dimycolate coated beads (TDMCB), MACB and CB phagocytosis were also significantly lower in AM (C) and RPM (D) from the same group of diabetic mice compared to controls. Data presented as mean±SEM; n=3-5 replicates/group. The significant differences for non-normally distributed data were determined using the Mann-Whitney U test (A & B, CB of PEM and RPM) and the independent samples *t*-test for normally distributed data (A, B, C & D) (Appendix 3). The level of significance was indicated as *p≤0.05, **p≤0.01, ****p≤0.0001 and ns=non-significant.

Initially, the uptake of FB, MACB and CB by PEM and RPM at ratios of 1:1 and 1:10 (cell: bead) was assessed. Results showed that there was no consistent trend for bead phagocytosis by PEM from diabetic and control mice at MOI 1:1 (Figure 5.6 A). At MOI 1:10, the PEM and RPM from diabetic mice were less efficient in taking up the beads in comparison to controls

(Figure 5.6 A & B). The uptake of beads by the elicited PEM was higher than the non-elicited RPM from both groups of mice (Figure 5.6 A & B).

Furthermore, phagocytosis of TDMCB at MOI 1:10 by the AM and RPM collected from the same group of diabetic and control mice were also assessed. The internalisation of TDMCB and MACB was significantly lower in both AM (Figure 5.6 C) and RPM (Figure 5.6 D) from diabetic mice compared to control mice. Overall, AM had a higher capability of phagocytosis than RPM collected from diabetic and control mice (Figure 5.6 C & D).

In addition, the percentage of F4/80 and CD11b+ cells in PEC and RPEC and CD11c+ cells in AL were also evaluated during the assessment of phagocytosis using flow cytometry (as described in Figure 5.3 and 5.4) presented in Table 5.3. The PEC from diabetic mice contained lower number of F4/80+ and CD11b+ cells (PEM and RPM) compared to the controls. A similar trend was observed in RPEC from diabetic mice compared to controls. The AL from diabetic mice contained less number of CD11c+ cells (AM) compared to the controls. Although the viability of the PEC and RPEC after 4 hours of co-culture was found to be significantly higher in diabetic mice compared to controls, there were no significant differences in the viability of the AL at the same timepoint of co-culture.

Table 5.3 Percentage of macrophages in peritoneal exudates and broncho-alveolar lavage fluid

Cell types	Control Mean (%)±SEM)	Diabetic Mean (%)±SEM)	p-value
	F4/80 and CD11b+ cells (PEM/RPM)		
PEC (elicited)	66.65±1.55	44.72±1.25	**** 0.0000
RPEC	58.30±2.26	46.02±1.84	*** 0.0002
	CD11c+ cells (AM)		
AL (BALF)	58.06±1.29	33.47±1.44	**** 0.0000
	Viability		
PEC (elicited)	89.28±0.68	95.63±0.0.73	**** 0.0000
RPEC	87.02±0.96	94.75±0.44	**** 0.0000
AL (BALF)	67.33±2.90	65.47±2.00%,	ns 0.6046

n=13-19 replicates/group, PEC; peritoneal exudate cells, RPEC; resident peritoneal exudate cells, AL; alveolar leucocytes, BALF; broncho-alveolar lavage fluid, PEM; peritoneal exudate macrophages, RPM; resident peritoneal macrophages, AM; alveolar macrophages, * level of significance and ns=non-significant

5.4.2.1 Cytokine production by alveolar and resident peritoneal cells co-cultured with mycolic acid coated beads

Inflammatory cytokines were measured from the supernatant samples collected following co-culture with mycolic acid coated beads. After 4 hours of co-culture with the beads at a ratio of 1:10 (section 5.2.2.4), TNF-α and IL-6 were detected in both stimulated (AL/RPEC: beads) and unstimulated cells [AL/RPEC (cells)]. TNF-α (Figure 5.7 A) and IL-6 (Figure 5.7 E) were significantly lower in all diabetic AL compared to control AL. Importantly, mycolic acid coated bead (TDMCB and MACB) stimulation further impaired both TNF-α and IL-6 secretion in diabetic AL. TNF-α and IL-6 secretion by control AL in response to TDMCB and MACB was similar to unstimulated and CB treatments. TNF-α (Figure 5.7 B) and IL-6 (Figure 5.7 F) were also significantly lower in diabetic RPEC compared to control RPEC although there was no significant difference compared to unstimulated diabetic or control RPEC. The production of MCP-1, IL-12, IFN-γ and IL-10 were not detected in either bead stimulated or unstimulated AL and RPEC of diabetic or control mice (Figure 5.7 C, D, G, H, I, J, K & L).

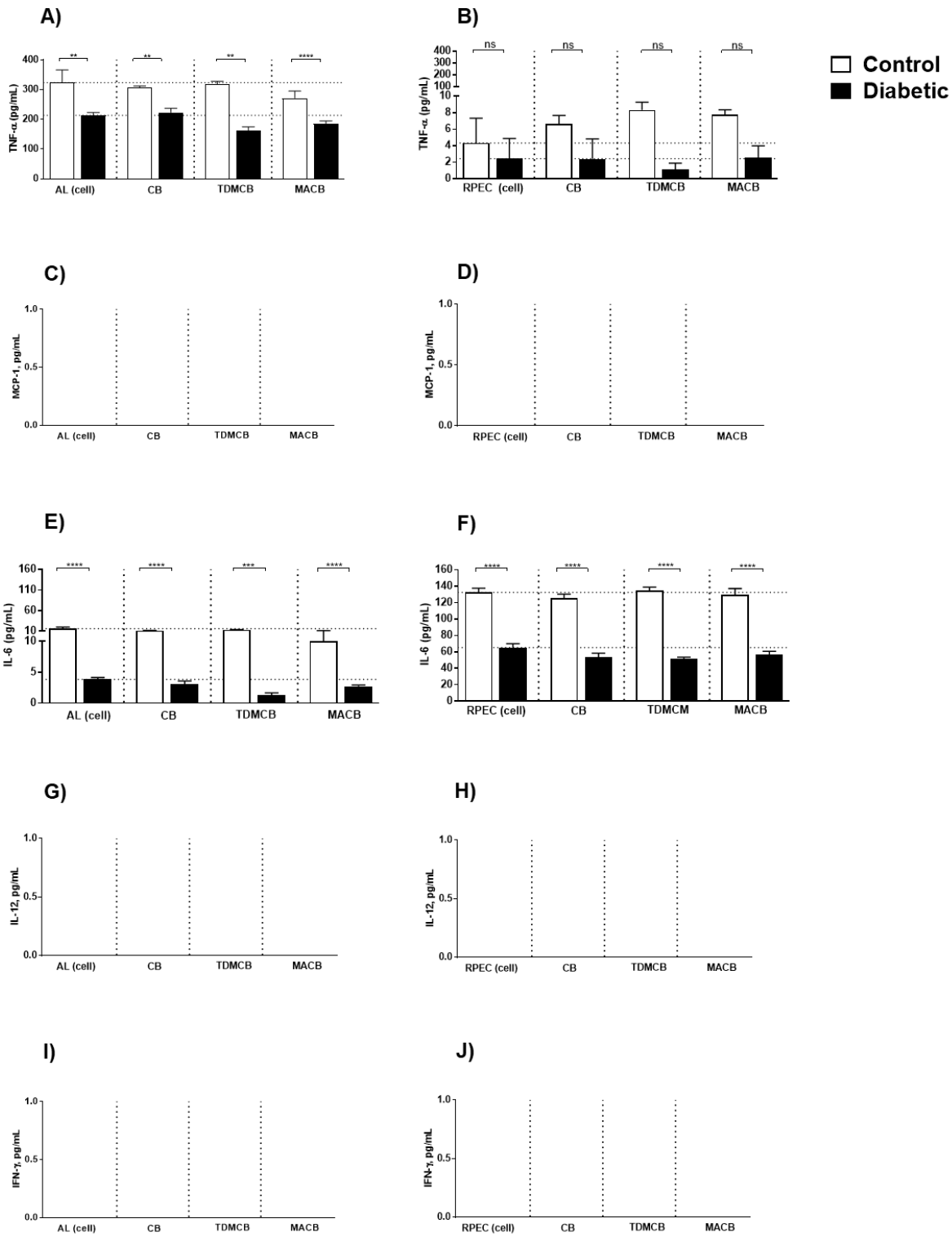
Alveolar leukocytes
Resident peritoneal exudate cells
A)
B)
C)
D)
E)
F)
G)
H)
I)
J)
Control
Diabetic
TNF-α (pg/mL)
MCP-1, pg/mL
IL-6 (pg/mL)
IL-12, pg/mL
IFN-γ, pg/mL
AL (cell)
RPEC (cell)
CB
TDMCB
TDMCM
MACB
ns

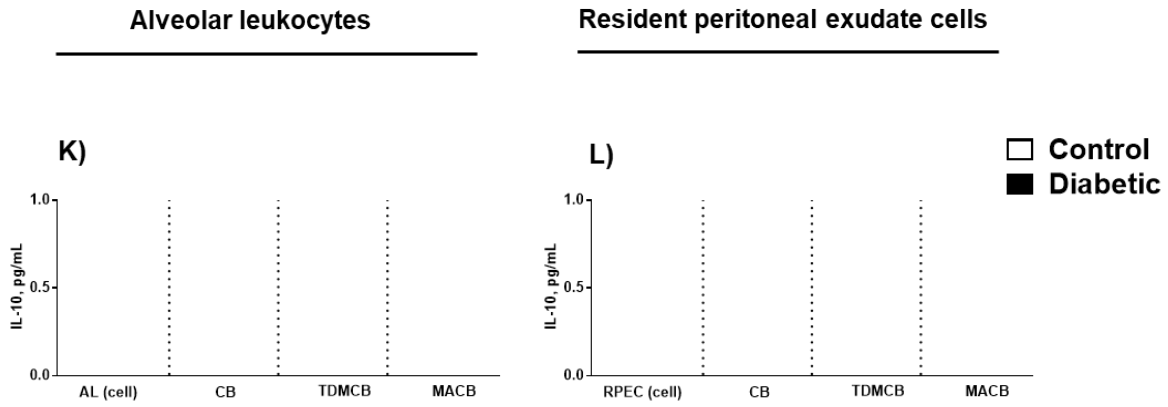

Figure 5.7 Cytokine production by alveolar leucocytes and resident peritoneal exudate cells co-cultured with mycolic acid coated beads

Alveolar leucocytes (AL) and resident peritoneal exudate cells (RPEC, non-elicited) were co-cultured with mycolic acid coated beads as control beads (CB), trehalose 6,6′-dimycolate (TDMCB) and whole mycolic acid coated beads (MACB) at a ratio of 1:10. Cytokine production was measured after 4 hours of co-culture. The production of TNF-α (A & B) and IL-6 (E & F) was detected in AL and RPEC. Although there was a significant difference in the production of TNF-α and IL-6 in AL and RPEC from diabetic mice compared to controls, they were not significant compared to their unstimulated control cells (not shown in the graphs). The production of MCP-1 (C & D), IL-12 (G & H), IFN-γ (I & J) and IL-10 (K & L) was not detected in either AL and RPEC from diabetic and control mice during co-culture. Data presented as mean±SEM; n=3-5 replicates/group. The significant differences were determined using the ordinary one-way ANOVA with Holm-Sidak's multiple comparisons test (Appendix 3). The level of significance was indicated as **p≤0.01, ***p≤0.001, ****p≤0.0001 and ns=non-significant.

5.4.3 Phagocytosis and bactericidal capacity of macrophages

5.4.3.1 Internalisation and killing of *M. fortuitum* by resident peritoneal cells

Counts of *M. fortuitum* were determined after 4 hours of MOI 1:1 and 1:10 co-culture with resident peritoneal exudate cells (RPEC, non-elicited, without CD11b+ cells isolation). The internalised and cell-associated bacteria were lower in RPEC from diabetic mice compared to the control mice, although the difference was not statistically significant (Figure 5.8 A). At MOI 1:10, the bacteria taken up/cell-associated was 1.35 times lower in RPEC from diabetic compared to control mice. The killing of internalised bacteria (extracellular bacteria were killed by treating with amikacin) by RPEC from diabetic mice was 1.50 times lower than RPEC from control mice (Figure 5.8 B).

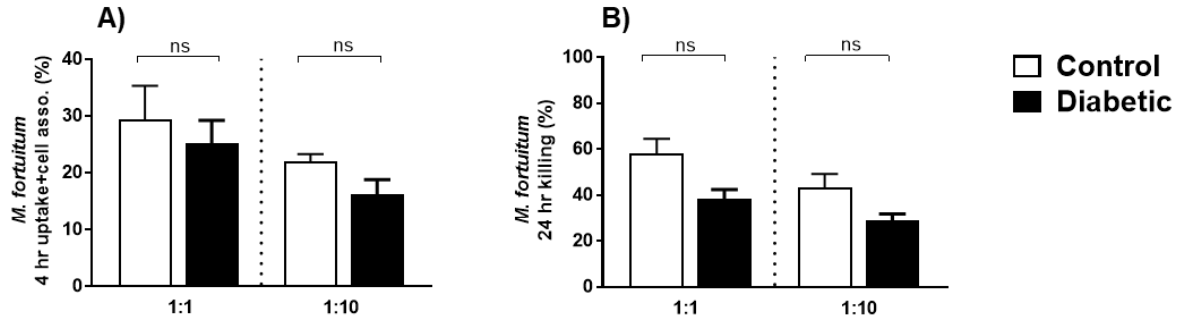

Figure 5.8 Internalisation and cell-associated *M. fortuitum* and killing by resident peritoneal exudate cells

Internalised and cell-associated bacterial number were quantified after 4 hours of co-culture of the resident peritoneal exudate cells (RPEC) with *M. fortuitum* at MOI 1:1 and 1:10 (cell: bacteria). After 4 hours of co-culture, the number of internalised and cell-associated bacteria were reduced in RPEC from diabetic mice compared to controls. The killing of internalised *M. fortuitum* by RPEC from diabetic mice was also lower after 24 hours of co-culture compared to the controls (B). The experiment was repeated thrice and result of a representative experiment was presented here. Data presented as mean±SEM; n=3 replicates/group. The significant differences were determined using the unpaired *t*-test with Welch's correction (Appendix 3). The level of significance was indicated as ns=non-significant ($p \geq 0.05$).

5.4.3.2 Internalisation and killing of *M. fortuitum* by alveolar and resident peritoneal macrophages

The uptake and killing capabilities of CD11c+ alveolar macrophages (AM) and CD11b+ resident peritoneal macrophages (RPM) were assessed by co-culture with *M. fortuitum* (*Mft*) at MOI 1:10 (cell: bacteria). The internalisation of *Mft* by AM from diabetic mice was 1.66 times lower compared to control mice after 4 hours of co-culture (Figure 5.9 A). The killing of *Mft* in AM from diabetic mice after 24 hours of co-culture was 1.46 times lower compared to controls (Figure 5.9 B). A similar trend for uptake and killing was observed for RPM (Figure 5.9 C & D). Overall, the uptake and killing capability of AM was greater than RPM for both diabetic and control mice (Figure 5.9).

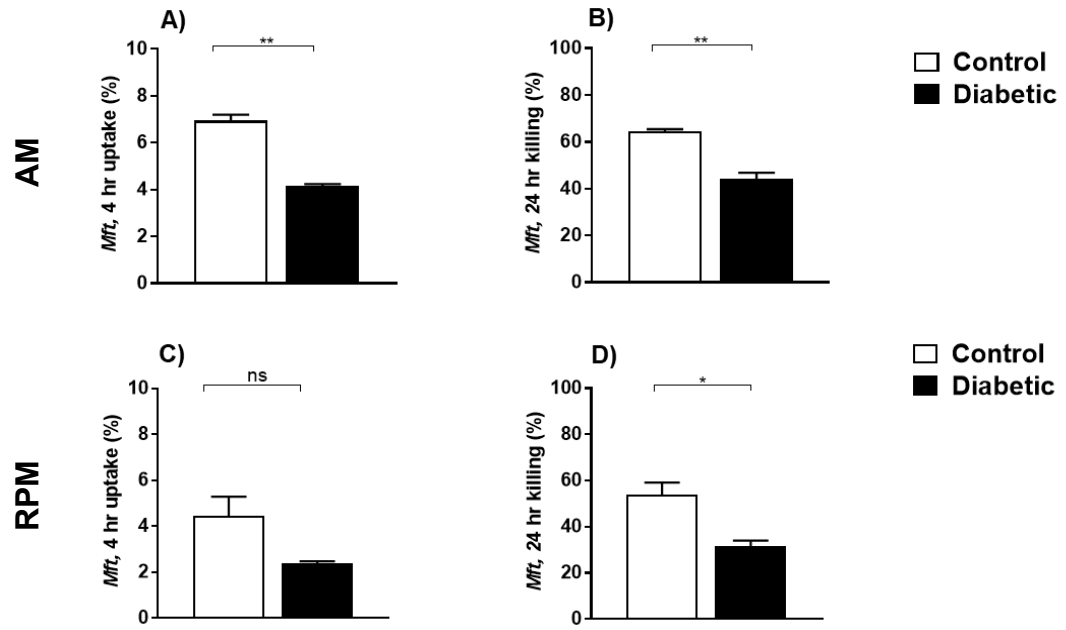

Figure 5.9 Internalisation and killing of *M. fortuitum* by alveolar and resident peritoneal macrophages

Following 4 hours of uptake and 24 hours of killing capability of the alveolar macrophages (AM, CD11c+ cells) resident peritoneal macrophages (RPM, CD11b+ cells) were assessed by co-culture with *M. fortuitum* (*Mft*) at MOI 1:10 (cell: bacteria). *M. fortuitum* uptake after 4 hours (A) and killing of the internalised bacteria after 24 hours (B) was reduced significantly in AM from diabetic mice compared to controls. There was a reduction in *Mft* uptake by RPM from diabetic mice co-cultured with the bacterium at 4 hours (C) and a significant reduction in the killing of the bacterium after 24 hours of co-culture (D). The experiment was repeated thrice and result of a representative experiment was presented here. Data presented as mean±SEM; n=3 replicates/group. The significant differences were determined using the unpaired *t*-test with Welch's correction (Appendix 3). The level of significance was indicated as *p≤0.05, **p≤0.01 and ns=non-significant.

5.4.3.2.1 Cytokine production by alveolar and resident peritoneal macrophages following co-culture with *M. fortuitum*

Alveolar macrophages (AM) from diabetic mice produced significantly lower amounts of TNF-α after 4 hours and 24 hours of co-culture with *Mft* compared to control mice (Figure 5.10 A & B). There was no difference between the groups in MCP-1 production by AM following 4 hours of co-culture although it was significantly reduced in AM from diabetic mice compared to controls after 24 hours of co-culture (Figure 5.10 C & D). A similar trend of IL-6 production was observed in AM from diabetic mice after 4 hours and 24 hours of incubation with *Mft* (Figure 5.10 E & F). Interleukin-12, IFN-γ and IL-10 were not detected in AM from either diabetic or control mice following either 4 or 24 hours of co-culture (5.10 G, H, I, J, K & L). IL-1β assays were not done in this experiment.

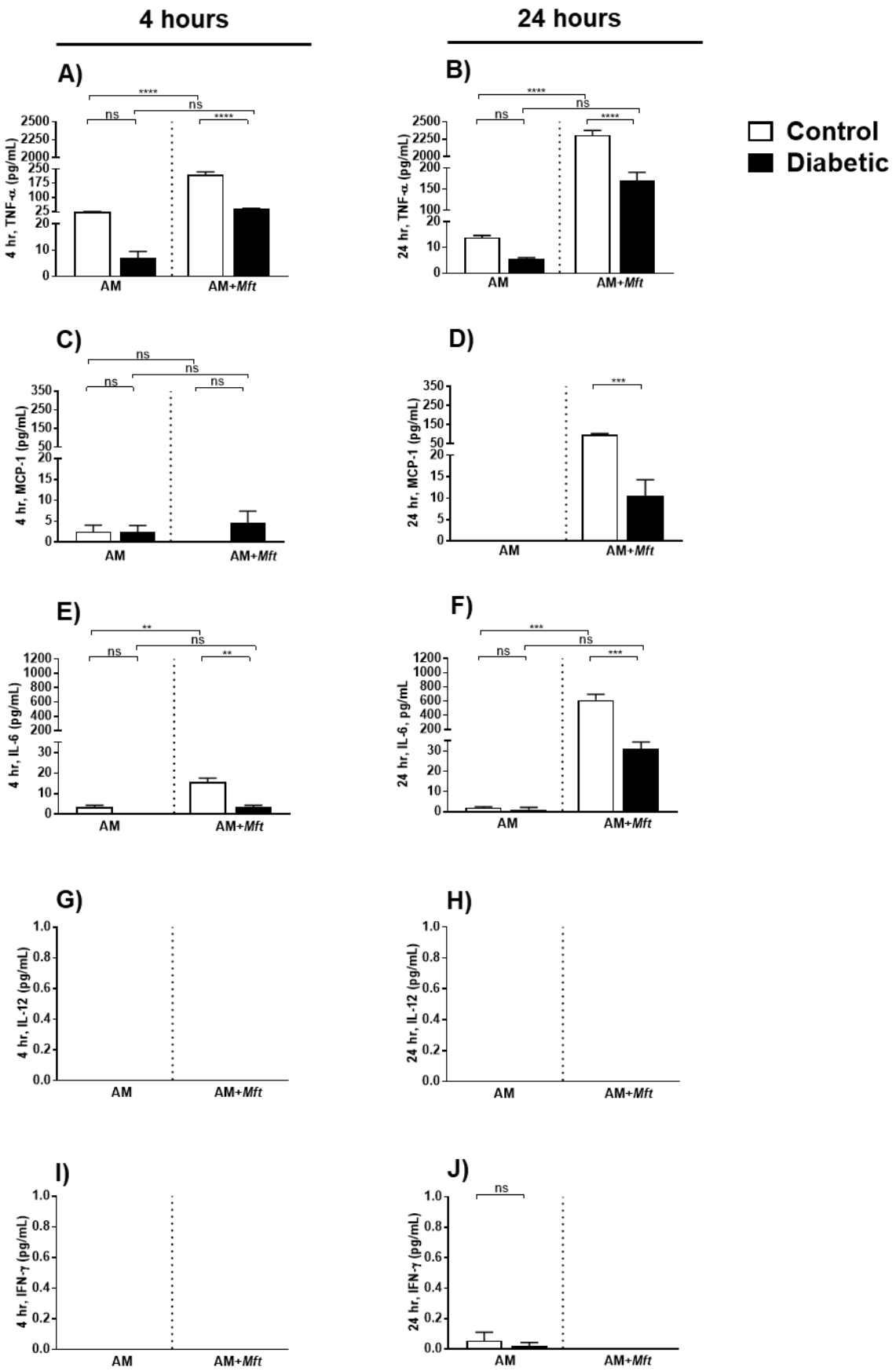
4 hours
24 hours
A)
B)
C)
D)
E)
F)
G)
H)
I)
J)
Control
Diabetic
4 hr, TNF-α (pg/mL)
24 hr, TNF-α (pg/mL)
4 hr, MCP-1 (pg/mL)
24 hr, MCP-1 (pg/mL)
4 hr, IL-6 (pg/mL)
24 hr, IL-6, pg/mL
4 hr, IL-12 (pg/mL)
24 hr, IL-12 (pg/mL)
4 hr, IFN-γ (pg/mL)
24 hr, IFN-γ (pg/mL)
AM
AM+Mft
ns
****
***
**

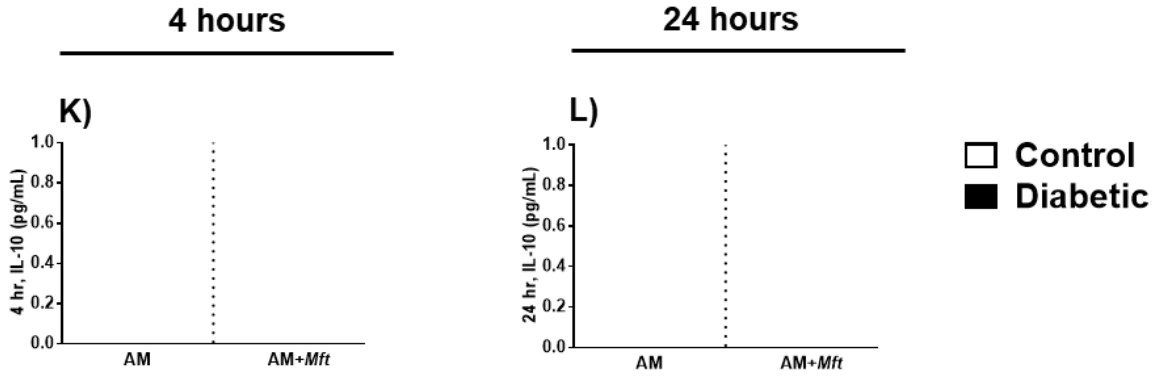

Figure 5.10 Cytokine production by alveolar macrophages co-cultured with *M. fortuitum*

Alveolar macrophages (AM, CD11c+ cells) were co-cultured with *M. fortuitum* (*Mft*) at MOI 1:10 (cell: bacteria). Cytokine production was measured after 4 and 24 hours of co-culture with *Mft*. There was a significant reduction in the production of TNF-α by AM from diabetic mice compared to controls after 4 (A) and 24 hours (B) of co-culture with the bacteria. The production of MCP-1 by AM from diabetic and control mice was negligible after 4 hours of co-culture (C) although it was significantly reduced in AM from diabetic mice compared to controls after 24 hours (D). The production of IL-6 by AM from diabetic mice was significantly decreased in both 4 (E) and 24 hours (F) of co-culture. Little or no cytokine production was detected for IL-12 (G & H), IFN-γ (I & J) and IL-10 (K & L) by AM from both diabetic and control mice after 4 and 24 hours of co-culture. Data presented as mean±SEM; n=2-6 replicates/group. The significant differences were determined using the ordinary one-way ANOVA with Holm-Sidak's multiple comparisons test (A-L except D) and the unpaired *t*-test with Welch's correction (D) (Appendix 3). The level of significance was indicated as **p≤0.01, ***p≤0.001, ****p≤0.0001 and ns=non-significant.

The production of TNF-α was significantly reduced in resident peritoneal macrophages (RPM) from diabetic mice after 4 hours and 24 hours of co-culture compared to controls (Figure 5.11 A & B). There were no differences in the levels of MCP-1 secretion by RPM at 4 hours of co-culture although a significantly reduced production was found in RPM from diabetic mice compared to control after 24 hours of co-culture (Figure 5.11 C & D). The production of IL-6 was lower in RPM from diabetic mice compared to control mice at both timepoints of co-culture (Figure 5.11 E & F). Furthermore, the overall IL-6 production was higher by the RPM compared to AM (Figure 5.10 and 5.11 E & F). The secretion of IL-10 was higher in RPM from control mice compared to the diabetic mice after 4 hours of co-culture although its level was not sustained at the later timepoint of infection (Figure 5.11 K & L). The production of IL-12 and IFN-γ by RPM was minimal at both 4 and 24 hours of co-culture with the bacteria (Figure 5.11 G, H, I & J). IL-1β assays were not done in this experiment.

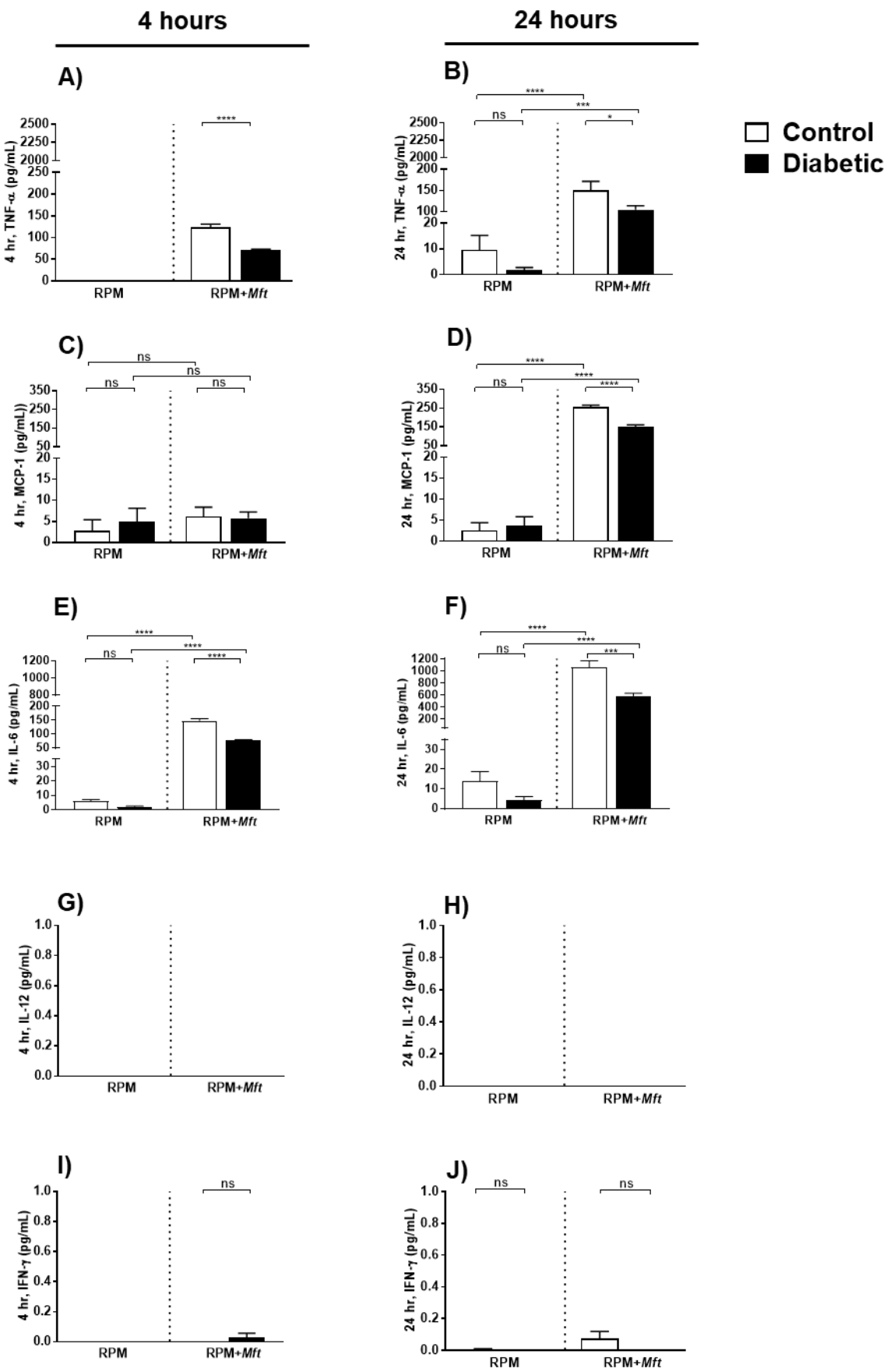
4 hours
24 hours
A)
B)
C)
D)
E)
F)
G)
H)
I)
J)
Control
Diabetic
4 hr, TNF-α (pg/mL)
24 hr, TNF-α (pg/mL)
4 hr, MCP-1 (pg/mL))
24 hr, MCP-1 (pg/mL)
4 hr, IL-6 (pg/mL)
24 hr, IL-6 (pg/mL)
4 hr, IL-12 (pg/mL)
24 hr, IL-12 (pg/mL)
4 hr, IFN-γ (pg/mL)
24 hr, IFN-γ (pg/mL)
RPM
RPM+Mft
ns
****
***
*

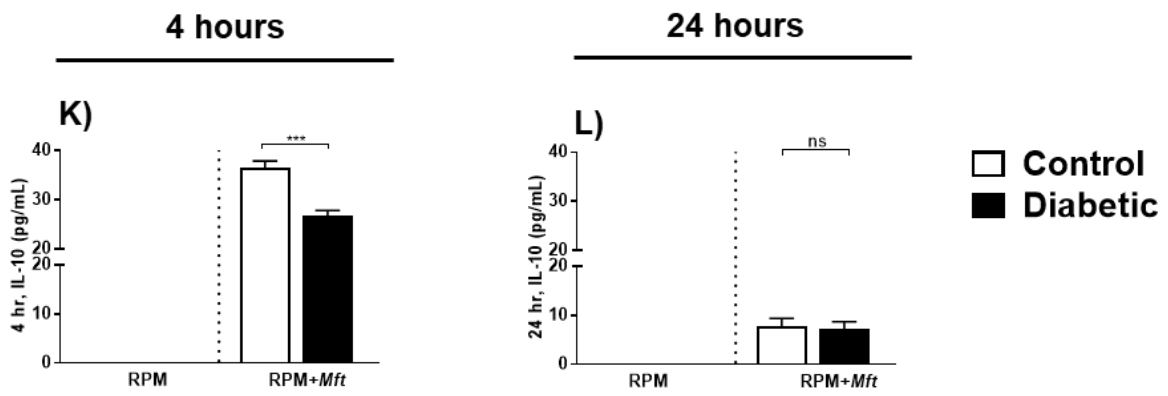

Figure 5.11 Cytokine production by resident peritoneal macrophages co-cultured with *M. fortuitum*

Resident peritoneal macrophages (RPM, CD11b+ cells) were co-cultured with *M. fortuitum* (*Mft*) at MOI 1:10 (cell: bacteria). Cytokine production was measured after 4 and 24 hours of co-culture with *Mft*. After 4 hours of co-culture, there was a significant reduction in the production of TNF-α by RPM from diabetic mice compared to controls after 4 (A) and 24 hours (B) of co-culture with the bacteria. The production of MCP-1 by RPM from both diabetic and control mice was negligible after 4 hours (C) although it was significantly reduced in RPM from diabetic mice compared to controls after 24 hours (D). The production of IL-6 by RPM from diabetic mice was significantly decreased compared to controls in both 4 (E) and 24 hours (F) of co-culture. The production of IL-10 by RPM from control mice was higher at 4 hours of co-culture (K) although its level was not sustained at the later timepoint (L). A minimum or no cytokine production was detected for IL-12 (G & H) and IFN-γ (I & J) by RPM from both diabetic and control mice after 4 and 24 hours of co-culture. Data presented as mean±SEM. The significant differences were determined using the ordinary one-way ANOVA with Holm-Sidak's multiple comparisons test (B, D-F and J), Kruskal-Wallis test with Dunn's multiple comparison tests (C) and the unpaired *t*-test (A & K) and Mann-Whitney U test (I & L) (Appendix 3). The level of significance was indicated as *p≤0.05, ***p≤0.001, ****p≤0.0001 and ns=non-significant.

5.4.3.3 Internalisation and killing of *M. bovis* (BCG) by alveolar and resident peritoneal macrophages

The internalisation of *M. bovis* (BCG) by alveolar macrophage (AM) from diabetic mice was 1.35 times lower compared to control mice after 4 hours of co-culture (Figure 5.12 A). The killing of same bacterium by AM from diabetic mice after 24 hours of co-culture was 1.04 times lower compared to controls (Figure 5.12 B). Similarly, the bacterial uptake by resident peritoneal macrophages (RPM) from diabetic mice was 1.51 times lower compared to control (Figure 5.12 C). Although the killing capability of the RPM increased over time, the killing efficiency after 24 and 48 hours of co-culture remained 1.04 and 1.02 times lower, respectively in RPM from diabetic mice compared to controls (Figure 5.12 D & E). Overall, the

internalisation and killing capability of AM was found to be comparatively higher than RPM from diabetic and control mice (Figure 5.12).

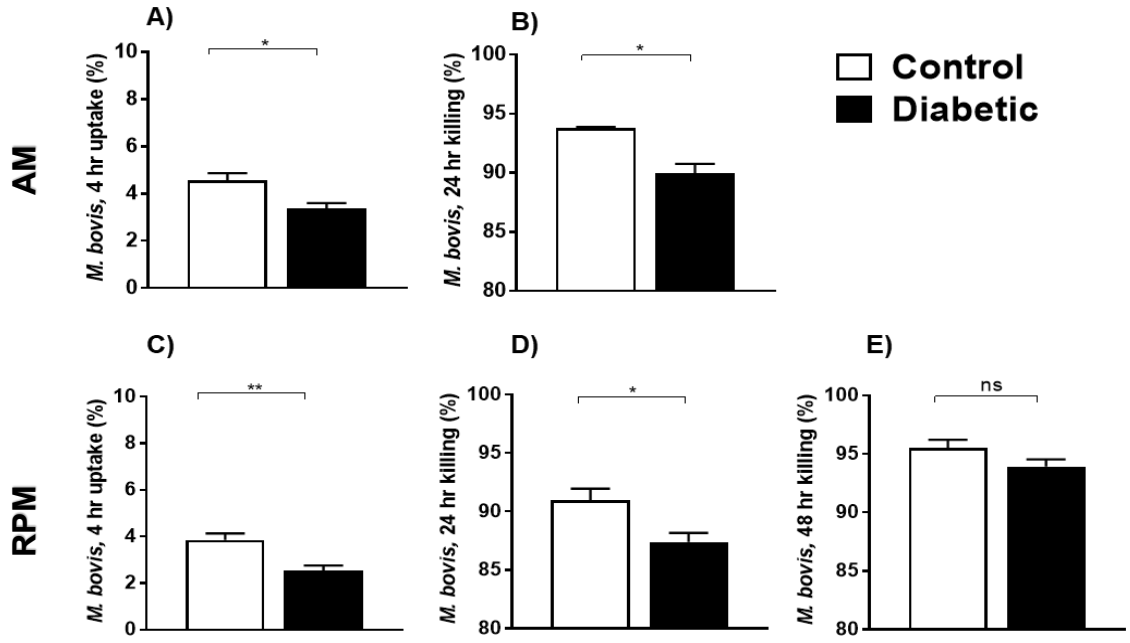

Figure 5.12 Internalisation and killing of *M. bovis* (BCG) by alveolar and resident peritoneal macrophages

Uptake after 4 hours and killing capability after 24/48 hours of alveolar macrophages (AM, CD11c+ cells) and resident peritoneal macrophages (RPM, CD11b+ cells) were assessed by co-culture with *M. bovis* (BCG) at MOI 1:10 (cell: bacteria). There was a significant reduction observed in the uptake (A) and killing of internalised (B) *M. bovis* (BCG) by the AM from the diabetic mice compared to the controls. A similar trend was observed in 4 hours uptake (C) and 24 (D) and 48 hours of killing (E) by the RPM from diabetic mice compared to controls. The experiment was repeated twice and result of a representative experiment was presented here. Data presented as mean±SEM; n=3-5 replicates/group. The significant differences were determined using the unpaired *t*-test with Welch's correction (Appendix 3). The level of significance was indicated as *p≤0.05, **p≤0.01 and ns=non-significant.

5.4.3.3.1 Cytokine production by alveolar and resident peritoneal macrophages following co-culture with *M. bovis* (BCG)

TNF-α production by alveolar macrophages (AM) increased between 4 and 24 hours of co-culture with *M. bovis* (BCG). Compared to the controls, AM from diabetic mice produced less TNF-α at both 4 and 24 hours timepoints (Figure 5.13 A & B). An opposite trend was observed in IL-6 production, where AM from diabetic mice released more IL-6 in response to *M. bovis* (BCG) at 4 and 24 hours (Figure 5.13 E & F). The production of IL-10 by AM from diabetic mice was higher after 4 and 24 hours of co-culture, although an elevated level of IL-10 was observed from the uninfected cells (Figure 5.13 M & N). The MCP-1, IL-1β, IL-12 and IFN-γ

production was undetectable in AM from both diabetic and control mice at both timepoints (Figure 5.13 C, D, G, H, I, J, K & L).

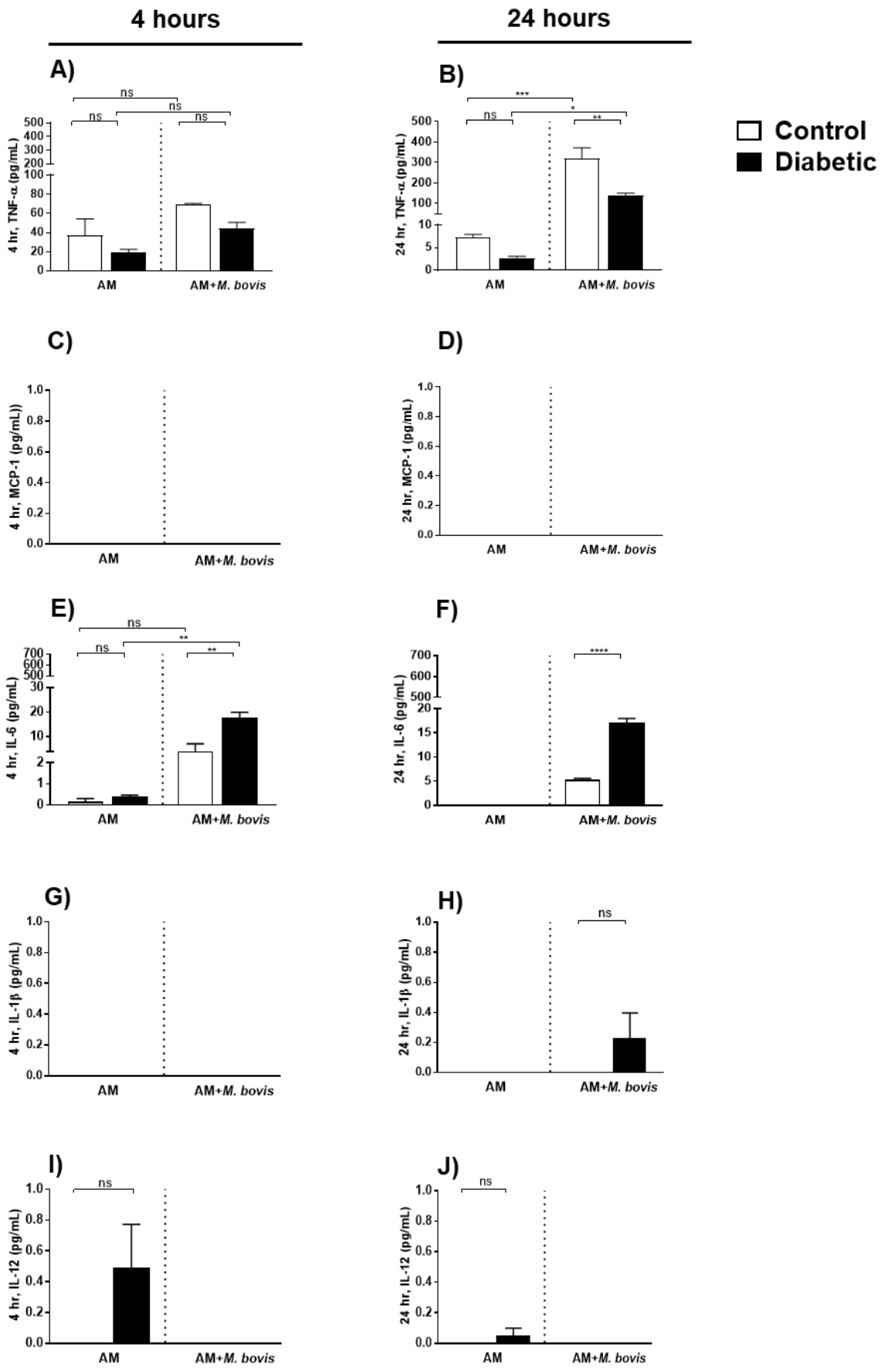

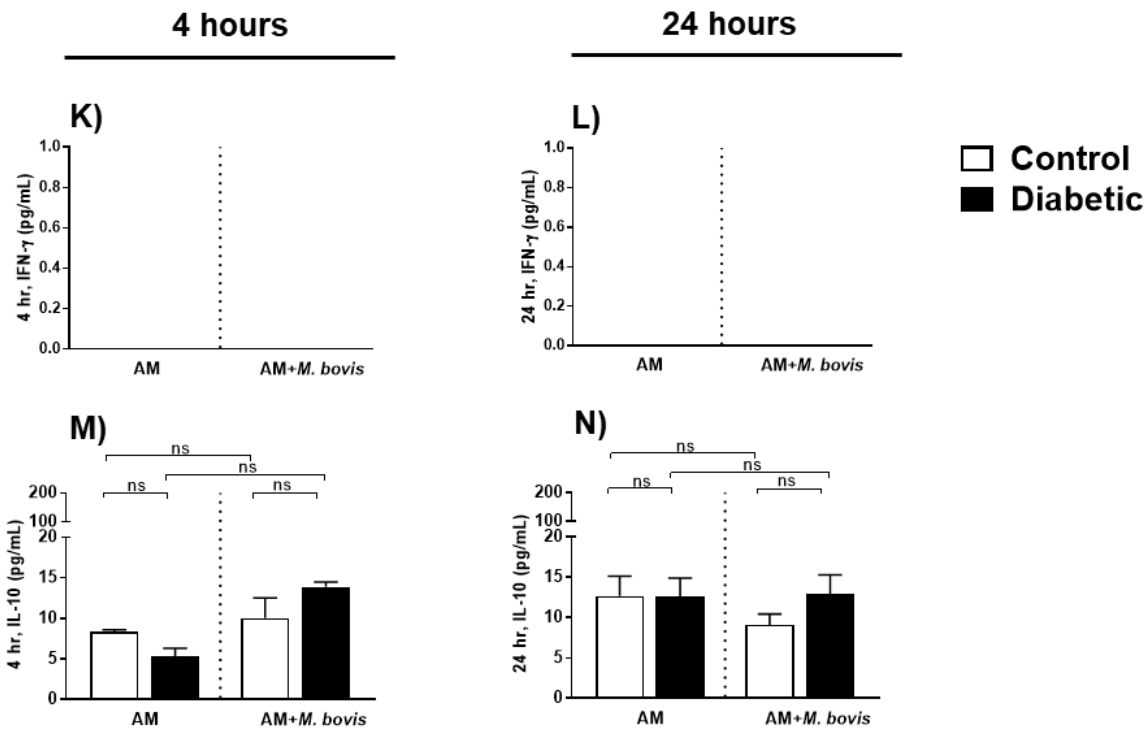

Figure 5.13 Cytokine production by alveolar macrophages co-cultured with *M. bovis* (BCG)

Alveolar macrophages (AM, CD11c+ cells) were co-cultured with *M. bovis* (BCG) at MOI 1:10 (cell: bacteria). Cytokine production was measured after 4 and 24 hours of co-culture with the bacterium. There was a significant reduction in the production of TNF-α by AM from diabetic mice compared to controls after 4 (A) and 24 hours (B) of co-culture. IL-6 production was increased by AM from diabetic mice compared to controls at both 4 (E) and 24 hours (F). Compared to control, IL-10 production by the AM from diabetic mice was higher at both 4 (M) and 24 hours (N) of co-culture. There was little or no MCP-1 (C & D), IL-1β (G & H), IL-12 (I & J) and IFN-γ (K & L) production by AM from both diabetic and control mice after 4 and 24 hours of co-culture. Data presented as mean±SEM; n=2-4 replicates/group. The significant differences were determined using the ordinary one-way ANOVA with Holm-Sidak's multiple comparisons test (A-B, E-F & M-N) and Mann-Whitney U test (H-J). (Appendix 3). The level of significance was indicated as *p≤0.05, **p≤0.01, ***p≤0.001, ****p≤0.0001 and ns=non-significant.

TNF-α production by resident peritoneal macrophages (RPM) from diabetic and control mice was detected following 4, 24 and 48 hours of co-culture with *M. bovis* (BCG) (Figure, 5.14 A & B and Table 5.4). There was an increasing trend in TNF-α production in RPM from control mice over time. The production of TNF-α was significantly lower in RPM from diabetic mice at 4 and 48 hours (Figure 5.14 A and Table 5.4) although its level was similar in RPM from both groups of mice at 24 hours (Figure 5.14 B). MCP-1 production by RPM from diabetic mice was significantly lower than controls at 24 and 48 hours (Figure 5.14 D and Table 5.2)

and was not detectable at 4 hours (Figure 5.14 C). Compared to controls, RPM from diabetic mice produced significantly reduced levels of IL-6 at all timepoints (Figure 5.14 E & F and Table 5.4). There was a reduced amount of IL-1β observed at 24 and 48 hours (Figure 5.14 H and Table 5.4) although its secretion was undetectable at 4 hours (Figure 5.14 G). A higher level of IL-10 was observed in the RPM from controls than diabetic mice at all the timepoints of co-culture (Figure 5.14 M & N and Table 5.4). The production of IL-12 and IFN-γ by the RPM from both diabetic and control mice was undetectable at all the timepoints (Figure 5.14 I, J, K & L and Table 5.4).

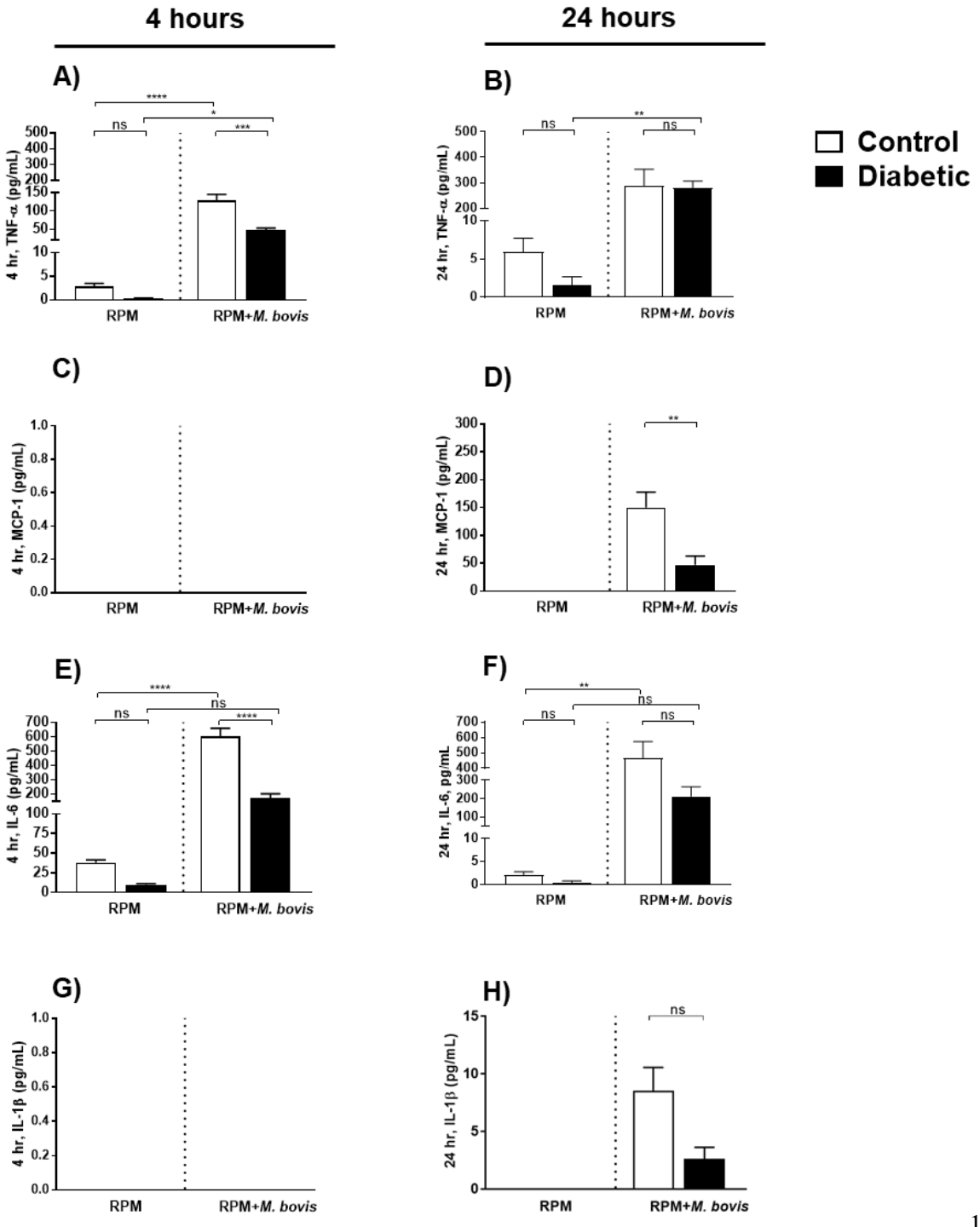

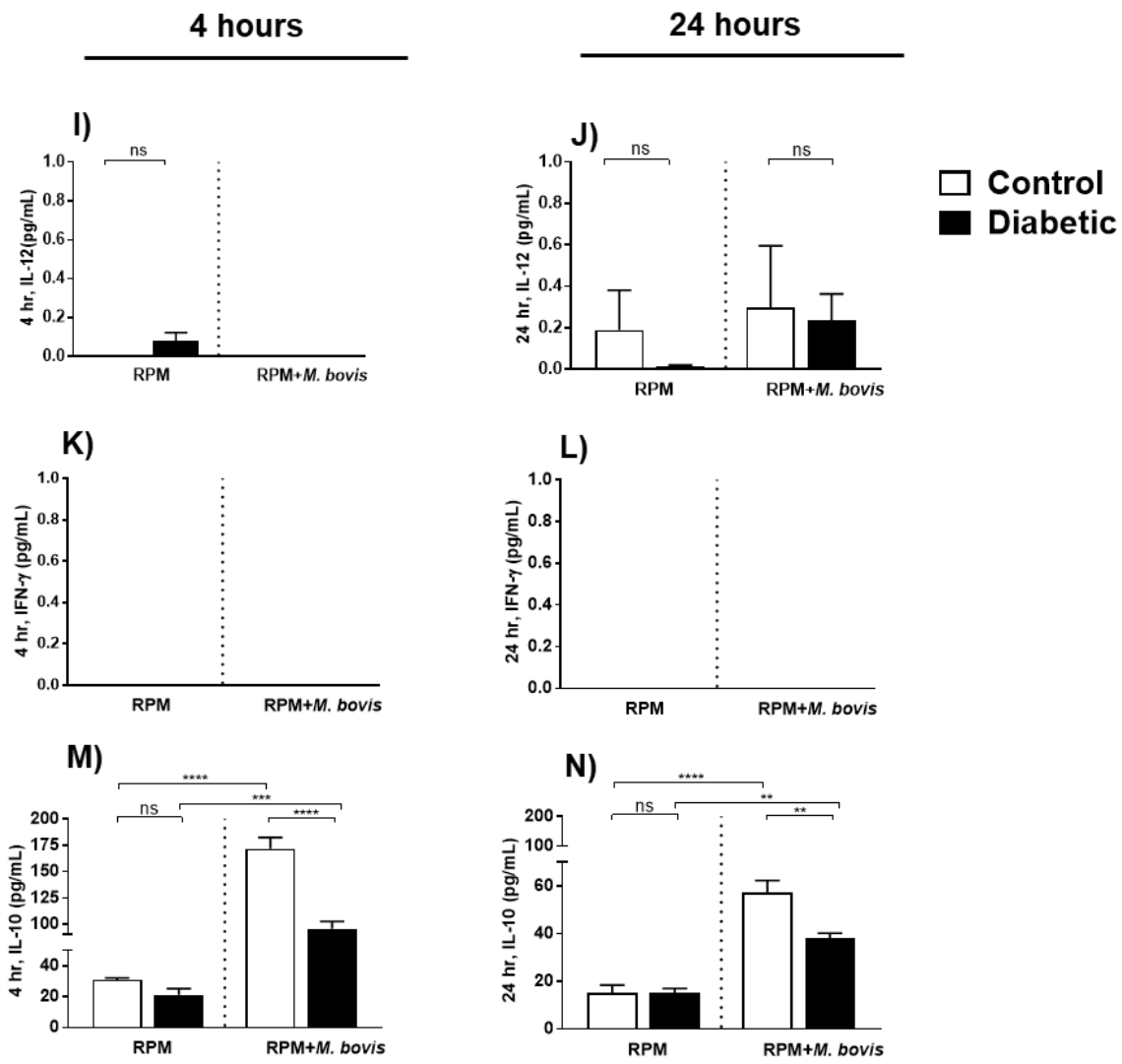

Figure 5.14 Cytokine production by resident peritoneal macrophages co-cultured with *M. bovis* (BCG)

Resident peritoneal macrophages (RPM, CD11b+ cells) were co-cultured with *M. bovis* (BCG) at MOI 1:10 (cell: bacteria). Cytokine production was measured after 4, 24 and 48 hours of co-culture with the bacterium. A significant reduction of TNF-α by RPM from diabetic mice compared to controls was observed after 4 hours of co-culture (A) although there was no difference of it after 24 hours (B). Although MCP-1 secretion by the RPM from both diabetic and control mice was undetectable after 4 hours (C), it was significantly reduced by RPM from diabetic mice after 24 hours (D). The production of IL-6 (E & F) and IL-10 (M & N) was higher by RPM from diabetic mice compared to controls. IL-1β production was lower by RPM from diabetic mice compared to controls after 24 hours (H) although its secretion by RPM from both diabetic and control mice was undetectable at the initial timepoint of co-culture (G). There were no or minimum production IL-12 (I & J) and IFN-γ (K & L) was observed in the RPM of both diabetic and control mice at both timepoints of infection. Data presented as mean±SEM; n=3-4 replicates/group. The significant differences were determined by the ordinary one-way ANOVA with Holm-Sidak's multiple comparisons test (A-B, E-F, J & M-N), unpaired *t*-test with Welch's correction (D & H) and Mann-Whitney U test (I) (Appendix 3). The level of significance was indicated as *p≤0.05, **p≤0.01, ***p≤0.001, ****p≤0.0001 and ns=non-significant.

Table 5.4 Cytokine production by resident peritoneal macrophages after 48 hours of co-culture with *M. bovis* (BCG)

	48 hours cytokines (pg/mL)					
	RPM (uninfected)			RPM: *M. bovis* (BCG)		
Cytokine	**Control**	**Diabetic**	**p-value**	**Control**	**Diabetic**	**p-value**
TNF-α	2.85±1.12	1.29±1.00	0.9750	415.00±53.27	78.48±10.28	**<0.0001**
MCP-1	0.00±0.00	0.00±0.00	-	238.44±40.20	30.54±12.32	**0.0105**
IL-6	0.00±0.00	0.00±0.00	-	439.08±70.62	81.80±21.72	**0.0112**
IL-1β	0.00±0.00	0.00±0.00	-	6.04±1.15	0.28±0.28	**0.0128**
IL-12	0.02±0.01	0.24±0.24	0.5233	0.00±0.00	0.00±0.00	-
IFN-γ	0.12±0.12	0.57±0.47	0.4016	0.00±0.00	0.00±0.00	-
IL-10	8.34±0.67	11.07±0.59	**0.0373**	56.82±4.51	18.89±1.32	**<0.0001**

Data presented as mean±SEM; n=3-4 replicates/group, RPM; resident peritoneal macrophages

5.4.3.4 Internalisation and killing of *M. tuberculosis* (H37Rv) by alveolar and resident peritoneal macrophages

The internalisation of *M. tuberculosis* (*Mtb* H37Rv) by alveolar macrophages (AM) from diabetic mice was 1.45 times lower compared to control mice after 4 hours of co-culture (Figure 5.15 A). The killing of *Mtb* by AM from diabetic mice after 24 hours of co-culture was 1.07 times lower compared to controls (Figure 5.15 B). A similar trend for uptake and killing was observed in resident peritoneal macrophages (RPM) (Figure 5.15 C & D). Overall, the uptake and killing capability of AM was higher than RPM from diabetic and control mice during co-culture with the *Mtb*.

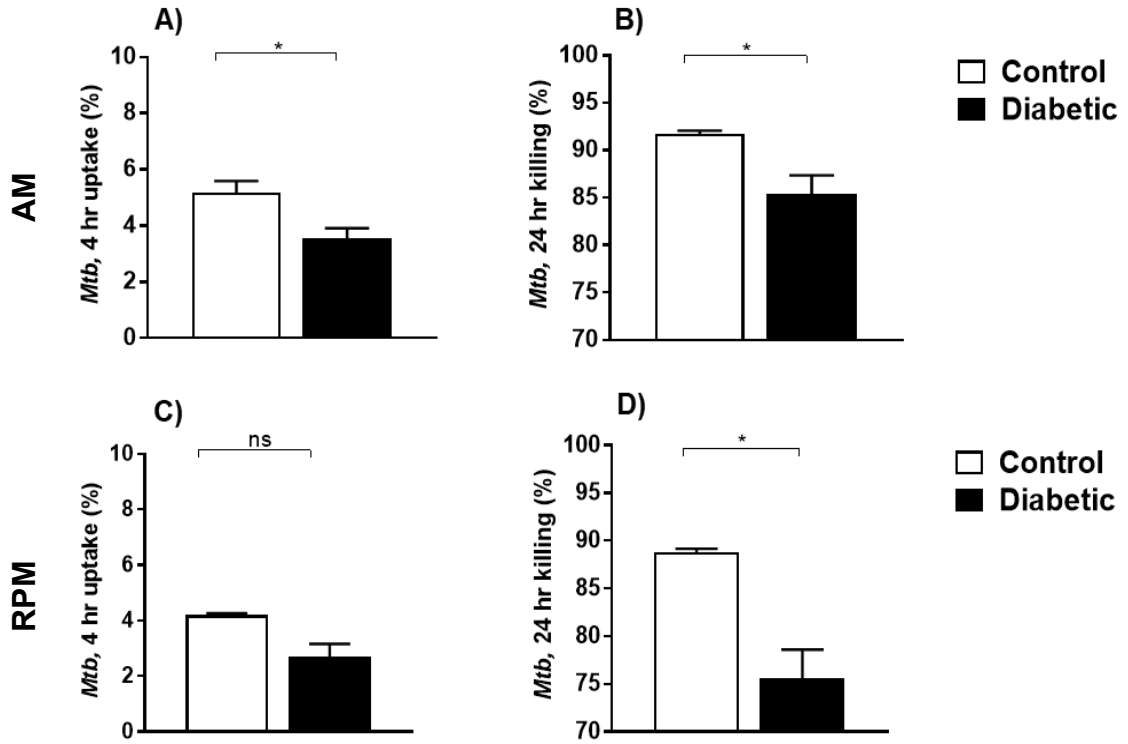

Figure 5.15 Internalisation and killing of *M. tuberculosis* (H37Rv) by alveolar and resident peritoneal macrophages

The uptake and killing capability of the alveolar macrophages (AM, CD11c+ cells) and resident peritoneal macrophages (RPM, CD11b+ cells) were assessed by co-culture with *M. tuberculosis* (*Mtb* H37Rv) at MOI 1:10 (cell: bacteria). There was a significant reduction in the uptake (A) and killing of internalised *Mtb* (B) by AM from diabetic mice compared to controls. A similar trend was observed in uptake (C) and killing (D) by the RPM from diabetic mice compared to controls. The experiment was repeated twice and result of a representative experiment was presented here. Data presented as mean±SEM; n=2-5 replicates/group. The significant differences were determined using the unpaired *t*-test with Welch's correction (Appendix 3). The level of significance was indicated as *p≤0.05 and ns=non-significant.

5.4.3.4.1 Cytokine production by alveolar and resident peritoneal macrophages following co-culture with *M. tuberculosis* (H37Rv)

Following co-culture with *M. tuberculosis* (*Mtb*), the secretion of TNF-α by AM was observed after 4 and 24 hours co-culture. There was a significantly lower level of TNF-α production by the AM from the diabetic mice compared to controls at both 4 and 24 hours timepoints (Figure 5.16 A & B). A similar trend was observed in the production of IL-6 by AM from diabetic mice compared to control at 4 and 24 hours (Figure 5.16 E & F). The secretion of MCP-1 and IL-1β was significantly lower from AM of diabetic mice compared to control mice after 24 hours (Figure 5.16 D & H), although the levels were negligible at 4 hours (Figure 5.16 C & G).

Moreover, there was no IL-12, IFN-γ and IL-10 production by AM from either diabetic or control mice (Figure 5.16 I, J, K, L, M & N).

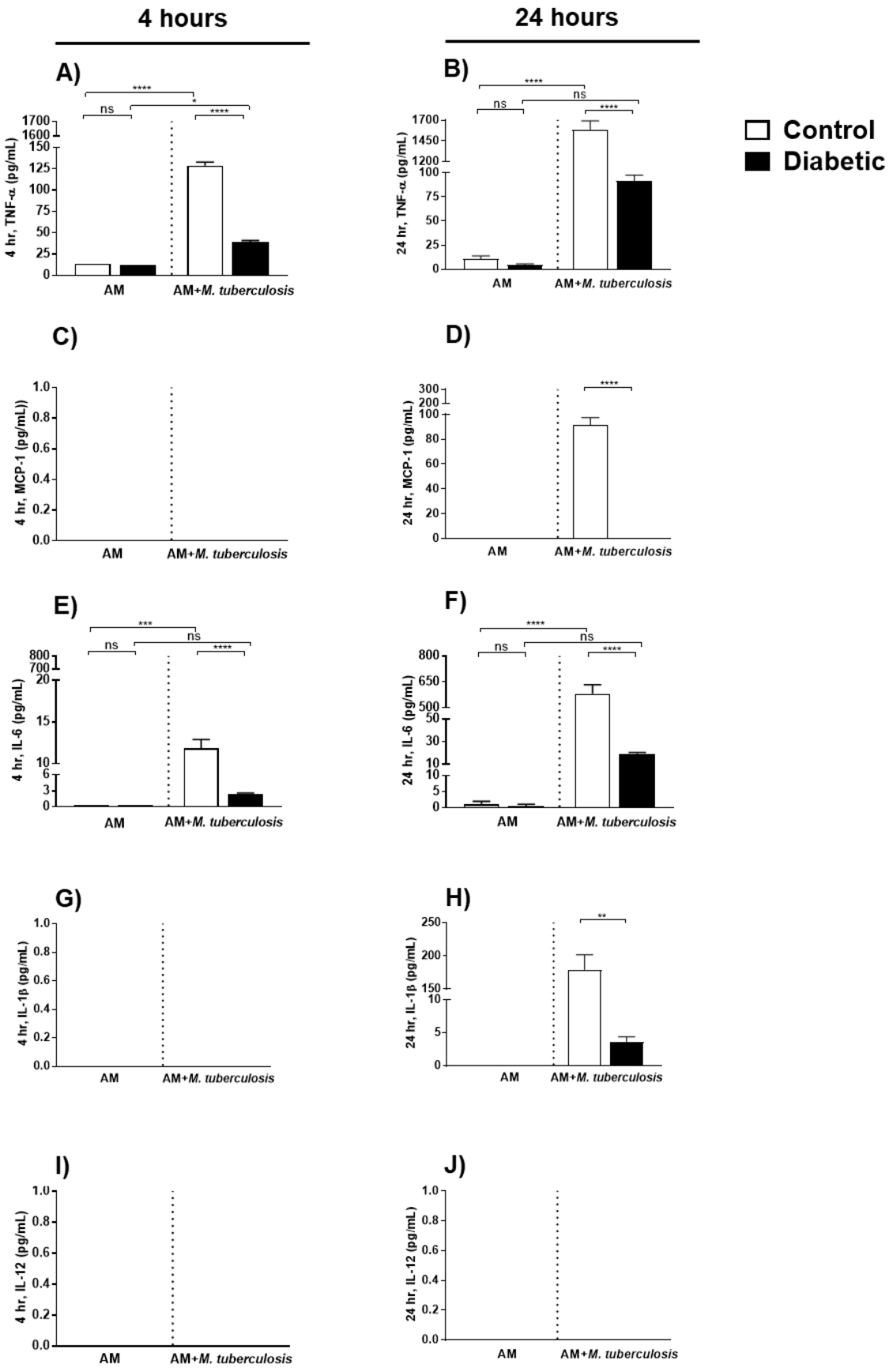

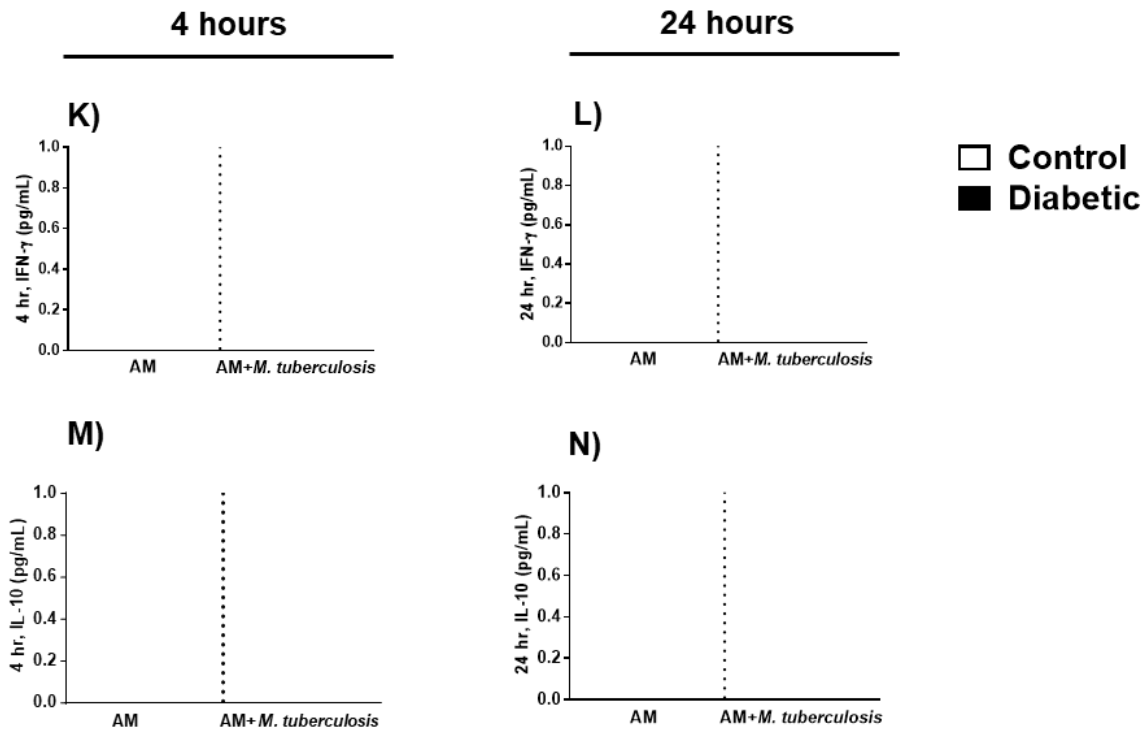

Figure 5.16 Cytokine production in alveolar macrophages co-cultured with *M. tuberculosis* (H37Rv)

Alveolar macrophages (AM, CD11c+ cells) were co-cultured with *M. tuberculosis* (*Mtb* H37Rv) at MOI 1:10. Cytokine production was measured after 4 and 24 hours of co-culture with *Mtb*. There was a significant reduction in the production of TNF-α (A & B) and IL-6 (E & F) by AM from diabetic mice compared to controls after 4 and 24 hours co-culture. A significantly reduced amount MCP-1 (D) was detected in AM from diabetic mice compared to controls after 24 hours, although they were negligible at 4 hours (C). A similar trend was found in the production of IL-1β production by the AM from diabetic mice compared to controls at 4 and 24 hours (G & H). There was no production of IL-12 (I & J), IFN-γ (K & L) and IL-10 (M & N) by the AM from both diabetic and control mice at 4 and 24 hours. Data presented as mean±SEM; n=1-4 replicates. The significant differences were determined using the ordinary one-way ANOVA with Holm-Sidak's multiple comparisons test (A-B & E-F) and unpaired *t*-test with Welch's correction (D & H) (Appendix 3). The level of significance was indicated as *p≤0.05, **p≤0.01, ***p≤0.001, ****p≤0.0001 and ns=non-significant.

A significantly reduced level of TNF-α was found in RPM supernatants from diabetic mice compared to controls at 4 and 24 hours timepoints (Figure 5.17 A & B). A similar trend was observed in the production of IL-6 by RPM from diabetic mice compared to controls at both 4 and 24 hours (Figure 5.17 E & F). MCP-1 and IL-1β production by RPM from diabetic mice was lower than controls at 24 hours (Figure 5.17 D & H) and these cytokines were undetectable at 4 hours timepoint (Figure 5.17 C & G). There was no detectable IL-12, IFN-γ and IL-10 produced by RPM from either diabetic or control mice during *Mtb* co-culture (Figure 5.17 I, J, K, L, M & N).

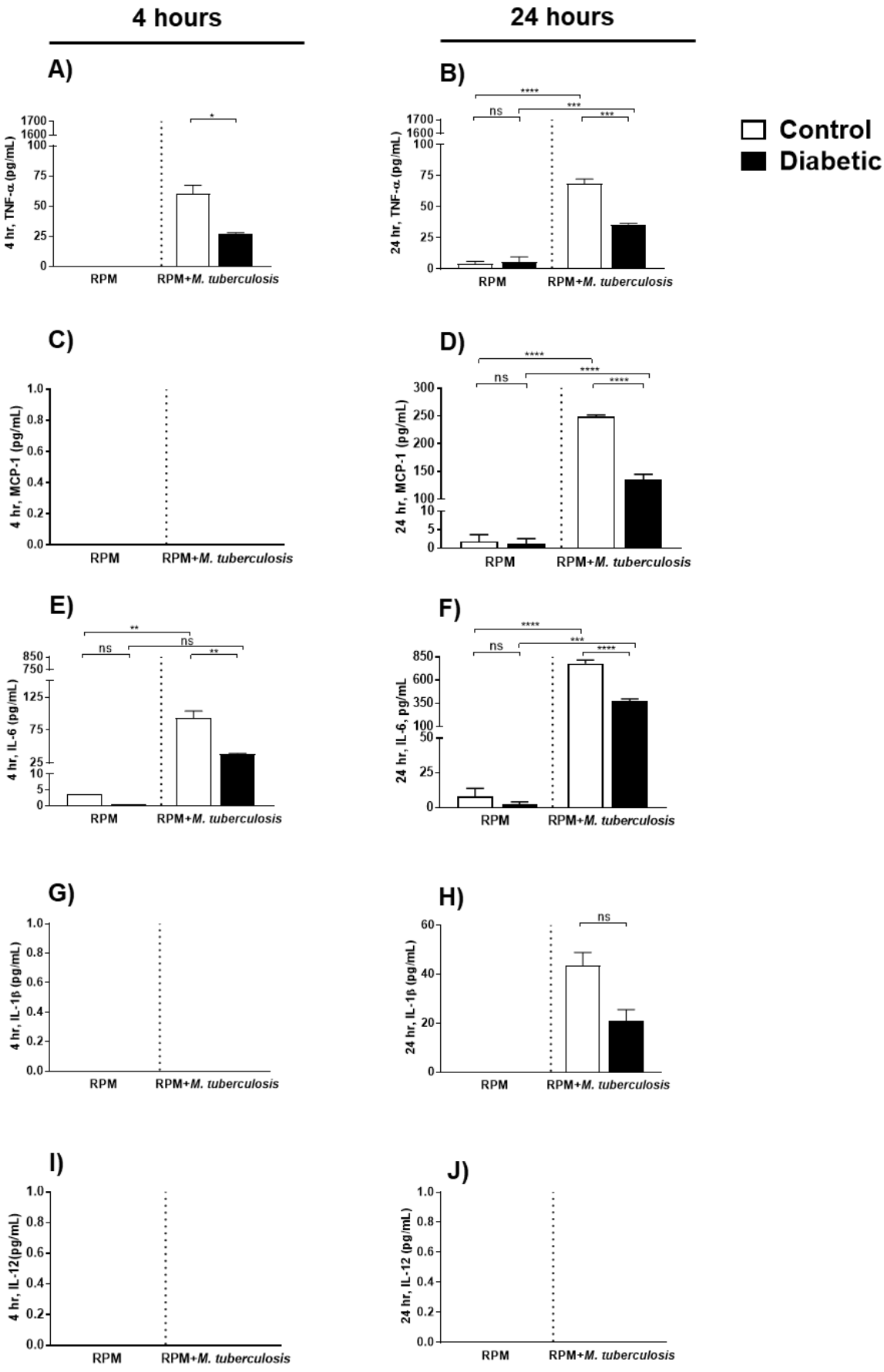
4 hours
24 hours
A)
B)
C)
D)
E)
F)
G)
H)
I)
J)
Control
Diabetic
4 hr, TNF-α (pg/mL)
24 hr, TNF-α (pg/mL)
4 hr, MCP-1 (pg/mL)
24 hr, MCP-1 (pg/mL)
4 hr, IL-6 (pg/mL)
24 hr, IL-6, pg/mL
4 hr, IL-1β (pg/mL)
24 hr, IL-1β (pg/mL)
4 hr, IL-12(pg/mL)
24 hr, IL-12 (pg/mL)
RPM
RPM+M. tuberculosis
ns

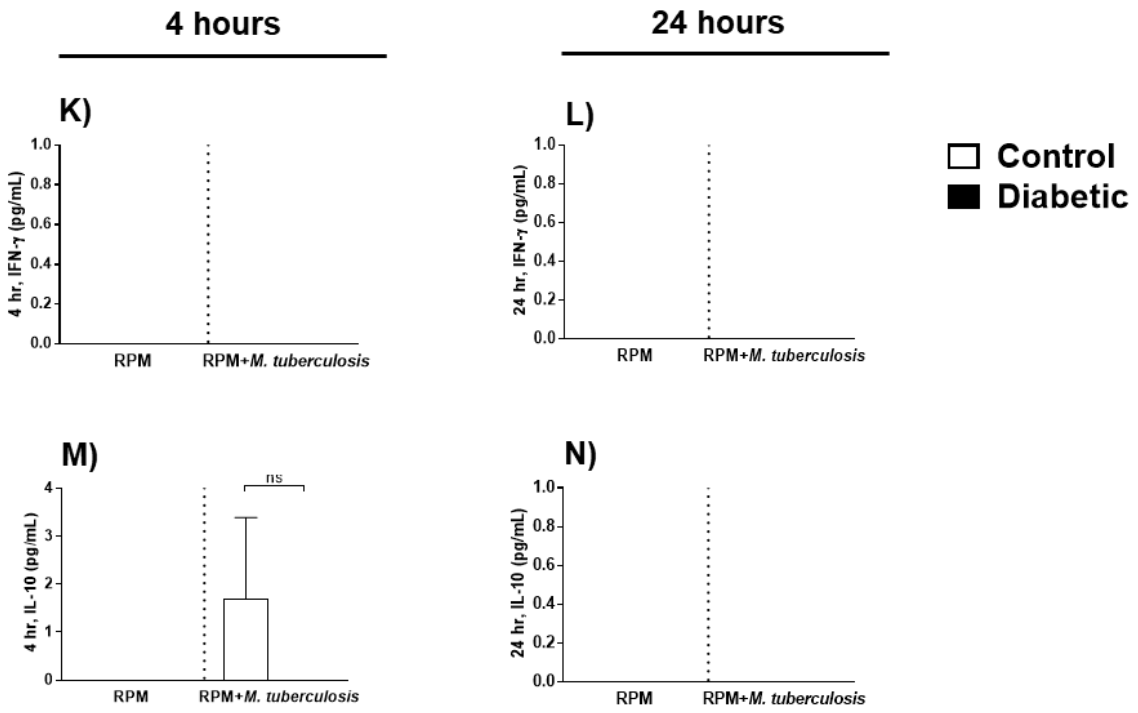

Figure 5.17 Cytokine production by resident peritoneal macrophages co-cultured with *M. tuberculosis* (H37Rv)

Resident peritoneal macrophages (RPM, CD11b+ cells) were co-cultured with *M. tuberculosis* (*Mtb* H37Rv) at MOI 1:10 (cell: bacteria). Cytokine production was measured after 4 and 24 hours of co-culture. There was a significant reduction in the production of TNF-α (A & B) and IL-6 (E & F) by RPM from diabetic mice compared to controls after 4 and 24 hours co-culture. A significantly reduced amount MCP-1 (D) was detected in RPM from diabetic mice compared to controls after 24 hours although it was negligible at 4 hours timepoint(C). A similar trend was found in the production of IL-1β production by the RPM from diabetic mice compared to controls at 4 and 24 hours (G & H). IL-12 (I & J), IFN-γ (K & L) and IL-10 production (M & N) by the RPM from both diabetic and control mice at 4 and 24 hours were below the limits of detection of the assay. Data presented as mean±SEM; n=1-4 replicates/group. The significant differences were determined using the ordinary one-way ANOVA with Holm-Sidak's multiple comparisons test (B & D-F) and the unpaired *t*-test with Welch's correction (A) and Mann-Whitney U test (H & M) (Appendix 3). The level of significance was indicated as *p≤0.05, **p≤0.01, ***p≤0.001, ****p≤0.0001 and ns=non-significant.

5.5 Discussion

In host-mycobacterial interactions, macrophages play the pivotal role in phagocytosis of the bacilli, secretion of chemical mediators, antigen presentation and subsequent activation of adaptive immune responses (Cooper, 2009). Previous studies have suggested that increased TB susceptibility in diabetic patients may be due to compromised macrophage function (Saiki et al., 1980, Martinez et al., 2016). We investigated the phagocytic capability, killing and cytokine

production in mouse alveolar macrophages (AM) and resident peritoneal macrophages (RPM) using mycolic acid coated beads, a non-tuberculous mycobacterium (NTM, *M. fortuitum*) and two species of *M. tuberculosis* complex (*M. bovis*, BCG and *M. tuberculosis*, H37Rv strain). We have shown that phagocytic function is impaired and cytokine production is dysregulated in macrophages from diabetic animals.

This study showed that the uptake of mycolic acid coated beads was reduced in AM and RPM of diabetic mice compared to controls (Figure 5.6). In previous studies using a streptozotocin (STZ)-induced diabetes model, polystyrene bead uptake was reduced in F4/80+ peritoneal macrophages (Saiki et al., 1980, Ma et al., 2008). This observation supported the findings of our study, where RPM from diabetic mice was less capable of internalising either mycolic acid coated beads or bacteria compared to controls. Ma and colleagues (2008) highlighted the alteration of macrophage phenotype and reduced numbers of F4/80+ cells in the peritoneal exudate as a reason for decreased uptake of beads in STZ-induced diabetic mice. We also observed a significantly lower number of F4/80+ and CD11b+ cells in both thioglycollate-elicited peritoneal (PEC) and resident peritoneal exudate cells (RPEC) of diabetic mice compared to controls (Table 5.3). Similar to the data presented here, impaired uptake of TDM coated latex beads was previously observed in AM from STZ-induced hyperglycaemic mice (Martinez et al., 2016). A significantly reduced uptake and killing of *M. fortuitum* (Figure 5.9), *M. bovis* (BCG) (Figure 5.12) and *M. tuberculosis* (H37Rv) (Figure 5.15) was observed in both AM and RPM from diabetic mice compared to controls. Martinez and colleagues (2016) demonstrated a lower uptake of *M. tuberculosis* (H37Rv/mCherry strain) in AM of hyperglycaemic mice which was in line with the findings of this study. Similar deficits in the phagocytic uptake function of macrophages have been reported in diabetic patient samples using other intracellular and extracellular bacteria including *Salmonella enterica* serovar *Typhimurium*, *Escherichia coli*, *Burkholderia pseudomallei, Streptococcus pneumoniae* and *Staphylococcus aureus* (Bagdade et al., 1972, Chanchamroen et al., 2009, Williams et al., 2011, Mathews et al., 2012).

The precise mechanisms underlying this decreased uptake and killing of mycobacteria by diabetic macrophages remain unclear. Ma and colleagues (2008) suggested the possibility of reduced macrophage numbers due to deficient differentiation of macrophage from bone marrow cells as one of the reasons of lower phagocytosis in diabetic mice. Defective and lower yields of macrophages (and stem cells) from bone marrow cells have also been observed in diabetes (Nikolic et al., 2004, Fu et al., 2006, Kuki et al., 2006, Rota et al., 2006). We have also observed

the lower number of F4/80+cells (considered as macrophages) from the broncho-alveolar lavage and resident peritoneal exudate cells from diabetic mice. Other reasons suggested for impaired phagocytosis in diabetes include reduced association (attachment) between bacteria and monocyte/macrophages, alteration of serum opsonins or complement proteins (C3b) and complement receptors (CR1 and CR3) (Schlesinger et al., 1990, Schlesinger, 1998, Gomez et al., 2013). Recent studies indicated that compromised phagocytosis of mycolic acid coated beads in diabetic macrophages was due to the lower expression of the macrophage receptors with collagenous structure (MARCO), Toll-like receptor 2 (TLR2) and the co-receptor for bacterial LPS (lipopolysaccharide), CD14 (Bowdish et al., 2009, Martinez et al., 2016). Advanced glycation end products accumulation in diabetes has also been shown to alter the expression of macrophage surface receptors (Lachmandas et al., 2015, Martinez et al., 2016). Impaired phagocytic activity of macrophages from diabetic mice leads to poor antigen presentation which in turns results in compromised T cell mediated immunity (Ma et al., 2008, Ahmad, 2011).

Significantly reduced killing (or higher survival) of *M. fortuitum* (Figure 5.9 B & D)*, M. bovis* (BCG) (Figure 5.12 B & D) and *M. tuberculosis* (H37Rv) (Figure 5.15 B & D) was observed in both AM and RPM from diabetic mice compared to controls in the current study. The reason for decreased killing or higher surviving numbers of bacteria in macrophages from diabetic mice may be due to the restricted secretion of antimycobacterial compounds (e.g. reactive oxygen species; ROS, inducible nitric oxide synthase; iNOS), delayed acidification of the phagosome and phagosome-lysosome fusion and inappropriate cytokine expression (Appelberg et al., 1994b, Da Silva et al., 2002, Jordao et al., 2008, Cooper, 2009, Cebula et al., 2012). Vallerskog and colleagues (2010) found decreased production of iNOS in the lungs of diabetic mice and suggested that this may explain the inability of diabetic macrophages to efficiently kill *Mtb*. The precise antimicrobial compounds deficient in diabetic macrophages in our model system were not undertaken as part of the current study. Future research is required to investigate this knowledge gap and identify the key defects and mediators in diabetic mice.

M. fortuitum survived better in both macrophages from diabetic and control mice as opposed to the survival of *M. bovis* (BCG) and *M. tuberculosis* (H37Rv). The increased survival of NTM including *M. fortuitum* has been described previously (Crowle et al., 1986, Da Silva et al., 2002, Parti et al., 2005, González-Pérez et al., 2013). Following infection, mycobacteria (pathogenic or non-pathogenic) are internalised into the macrophages. Although the non-pathogenic mycobacteria are invariably killed, the surviving bacteria can quickly multiply within the cells

(Da Silva et al., 2002, Jordao et al., 2008). Higher survival of *M. fortuitum* compared to *M. bovis* (BCG) and *M. tuberculosis* (H37Rv) within macrophages may be due to differences in the cell wall structure, composition of the phagosome, time required for phagosome-lysosome fusion, secretion of antimycobacterial compounds and the replication time of the bacteria (Orme and Collins, 1983, Appelberg et al., 1994b, Da Silva et al., 2002, Ahmed and Hasnain, 2011, Cebula et al., 2012, Honda et al., 2015). It has been reported that the inability of less or non-pathogenic bacteria (*M. smegmatis*, *M. fortuitum*) to cause disease despite their higher number in macrophages was due to their rapid induction of host cell apoptosis. The rapid induction of apoptosis of infected macrophages is followed by the rapid killing of internalised mycobacteria (Molloy et al., 1994, Keane et al., 2002, Bohsali et al., 2010). Whereas survival of the pathogenic bacteria in macrophages (*M. tuberculosis*) was due to their inhibition or evasion of the host cell apoptotic mechanisms (Keane et al., 2000). A higher survival of *M. fortuitum*, *M. bovis* (BCG) and *M. tuberculosis* (H37Rv) in macrophages in diabetic mice in our studies suggests a detailed investigation of the mechanisms of survival of bacteria inside the macrophages in diabetes by further research. The understanding of the mechanisms may help in designing therapeutic agents to increase killing of the bacteria in the early stages of infection thereby increasing antigen presentation to T cell.

Macrophage-mycobacterial interactions result in the secretion of various cytokines and chemokines which ultimately determine the fate of infection (Benoit et al., 2008). Classically activated macrophages (M1 macrophages) are pro-inflammatory and have a central role in host defence against infection. Upon activation of M1 macrophages exhibit antimicrobial pro-inflammatory properties via the production of many pro-inflammatory cytokines including TNF-α, IL- 1β, IL-12, IL-15, IL-23 and IFN-γ (Doherty et al., 1996, Wang et al., 1999, Verreck et al., 2004, Verreck et al., 2006). In contrast, the alternatively activated macrophage (M2) lacks significant antimicrobial activity and fails to produce inflammatory cytokines. M2 subsets have poor antigen presenting capability and suppress cellular immunity by producing anti-inflammatory cytokines (IL-10, IL-4, TGF-β) (VanHeyningen et al., 1997, Guyot-Revol et al., 2006, Verreck et al., 2006). Pro-inflammatory cytokines are essential for effective immune responses against mycobacterial infections, although dysregulated and/or excessive pro-inflammatory cytokines can also be detrimental in infection (Garlanda et al., 2007).

In the current study, we determined the cytokine production from supernatant samples collected following co-culture with mycolic acid coated beads, *M. fortuitum, M. bovis* (BCG) and *M. tuberculosis* (H37Rv). After 4 hours of co-culture with mycolic acid coated beads, TNF-α and

IL-6 were found in the supernatants of RPEC and AL (Figure 5.7 A, B, E & F). No other cytokines (MCP-1, IL-12, IL-6, IL-10, IFN-γ) were detected following bead co-culture. The production of both TNF-α and IL-6 by RPEC and AL of both diabetic and control mice wasn't significantly different when compared to unstimulated cells. Bowdish and colleagues (2009) stimulated bone marrow-derived macrophages (BMMφ) and RPM with TDM coated beads for 24 hours and found detectable amounts of TNF-α. The amount of cytokine produced depends on the size of the beads and the localisation of the beads (outside or inside macrophages). Previous studies have shown that BMMφ produce less pro-inflammatory cytokines in response to TDM coated beads on the cell surface that are too large to be phagocytosed. In contrast, RPM can produce higher amounts of TNF-α in response to smaller beads capable of being phagocytosed (Geisel et al., 2005, Bowdish et al., 2009). In our study, we used RPEC and AL. These cell populations do not contain purified macrophages which could be one of the reasons for lower cytokine production during co-culture with beads observed. The shortest stimulation time was another reason for lower secretion of cytokines by these cells. This study also didn't determine the size of the mycolic acid coated beads which also had some role in the production of cytokines.

TNF-α production was decreased in AM and RPM from diabetic mice compared to controls following co-culture with *M. fortuitum* (Figure 5.10 A & B and 5.11 A & B), *M. bovis* (BCG) (Figure 5.13 A & B, 5.14 A & B and Table 5.4) and *M. tuberculosis* (H37Rv) (Figure 5.16 A & B and 5.17 A & B). Previous studies have shown that mice lacking the ability to secrete TNF-α had increased susceptibility to mycobacterial infections (Flynn et al., 1995, Benoit et al., 2008). This cytokine is crucial for enhancing the capability of macrophages to secrete different antimycobacterial compounds for uptake and killing of the bacteria (Yu et al., 1999, Keane et al., 2000, Scanga et al., 2001). It is also crucial for the formation of the granuloma and its continued maintenance by controlling the growth of bacteria (Kindler et al., 1989, Flynn et al., 1995, Senaldi et al., 1996, Olleros et al., 2005, Saunders et al., 2005). Consistent with our findings, lower levels of TNF-α were observed in macrophages of type 1 and 2 diabetic animal models (Sugawara et al., 2004, Sugawara and Mizuno, 2008). Decreased production of TNF-α in macrophages from diabetic animals corresponded to the lower uptake and killing of the bacteria observed in the current study (Figure 5.9 A & B, 5.12 A & B and 5.15 A & B). In comparison to AM, the overall TNF-α secretion was lower in RPM resulting in lower bacterial uptake and higher survival. Sun and colleagues (2012) reported lower secretion of TNF-α from F4/80+ peritoneal exudate macrophages in STZ-induced mice which was similar to the findings of this study. Furthermore, increased IL-10 production by RPM is related to the downregulation

of the TNF-α production (Fulton et al., 1998). We also observed higher production of IL-10 in RPM compared to AM from both diabetic and control mice. This might be one of the reasons for an overall lower TNF-α production by RPM contributing to the comparatively lower uptake and killing of the bacteria.

M. fortuitum infected macrophages showed an overall higher production of TNF-α from both diabetic and control mice compared to *M. tuberculosis* (H37Rv) and *M. bovis* (BCG) infected cells. Falcone and colleagues (1994) reported a higher production of TNF-α in murine peritoneal macrophages cultured with live avirulent *M. tuberculosis* H37Ra and *M. smegmatis* compared to live virulent *M. tuberculosis* H37Rv. Another study using human macrophages with non-pathogenic (*M. smegmatis*, *M. phlei*) and other selected pathogenic mycobacteria (*M. tuberculosis*, *M. avium*, *M. kansasii*, *M. xenipi*) found differences in TNF-α production with non-pathogenic mycobacteria stimulating higher amounts of TNF-α production compared to pathogenic mycobacteria (Beltan et al., 2000). This observation was also true for the current study where the less pathogenic *M. fortuitum, avirulent M. bovis* (BCG) and pathogenic mycobacteria (*M. tuberculosis,* H37Rv) were used. Although it was not clear how TNF-α is triggered in pathogenic and non-pathogenic bacteria, possible reasons might be related to their differences in lipoarabinomannan (LAM) structure on the cell wall (Chatterjee et al., 1992b, Singh and Goyal, 2013). Chatterjee and colleagues (1992b) reported that LAM from avirulent *M. tuberculosis* was 100-fold more potent at inducing TNF-α than LAM from the virulent Erdman strain. Non-pathogenic mycobacteria possess extensive arabinose side-chains on LAM which is a potential inducer of cytokines. In contrast, pathogenic mycobacteria possess a short mannan chain which extensively masks the arabinose side chain (Chatterjee et al., 1991, Chatterjee et al., 1992b). Another possible mechanism for greater TNF-α production induced by non-pathogenic bacteria compared to pathogenic bacteria is the relative differences in phagolysosome fusion. Phagolysosome fusion is a pre-requisite to enhance the production of cytokines. Phosphatidylinositol 3-phosphate (PI3P) is a membrane trafficking regulatory lipid which is important for the phagosomal acquisition of lysosomal contents (Vergne et al., 2005b). Pathogenic mycobacteria (e.g. *M. tuberculosis* H37Rv) and *M. bovis* (BCG) secrete an acid phosphatase known as SapM which is required to hydrolyse PI3P, resulting in inhibition of phagos lysosomal fusion. Non-pathogenic mycobacteria (e.g. *M. fortuitum*) do not produce SapM, thus no inhibition of phagosome with lysosomes resulting in more cytokine production (Saleh and Belisle, 2000). The inherent toxicity of pathogenic mycobacteria on macrophages may be another reason for lower production of cytokines. The non-pathogenic or attenuated pathogenic bacteria (e.g. heat-killed *M. tuberculosis* H37Rv) is non-toxic and can induce a

significant amount of TNF-α compared to its live counterparts (Falcone et al., 1994). The current study found a lower production of TNF-α from *M. bovis* (BCG) and *M. tuberculosis* (H37Rv) infected macrophages compared to the *M. fortuitum* infected macrophages. This may be due to a higher cytotoxic effect on macrophages by the *M. bovis* (BCG) and *M. tuberculosis* (H37Rv) compared to *M. fortuitum*. This was not investigated in the current study.

MCP-1 (also known as CCL2) is crucial for the influx of the different immune cells (monocytes, dendritic cells, natural killer cells and activated T cells) to provide protection at sites of infection (Kipnis et al., 2003). Kipnis and colleagues (2003) observed that fewer macrophages entered the lungs of CCL2 knockout mice compared to wild type littermates in experimental *Mtb* infections. This allowed for increased lung bacterial load followed by a failure recruitment of antigen-specific effector T lymphocyte into the lung. Expression of this cytokine was well documented in both animal models (Rhoades et al., 1995, Peters et al., 2001) and patients with *M. tuberculosis* infection (Lin et al., 1998, Lee et al., 2003). In the current investigation, we observed a significantly lower production of MCP-1 in AM (Figure 5.10 D and 5.16 D) and RPM (Figure 5.11 D, 5.14 D, 5.17 D and Table 5.4) from diabetic mice compared to controls after 24/48 hours of co-culture with the mycobacteria. The diminished production of this cytokine could result in a defect in immune cells recruitment into the lungs during *Mtb* infections (Rhoades et al., 1995, Lin et al., 1998, Peters et al., 2001, Lee et al., 2003). Vallerskog and colleagues (2010) observed a reduced level of chemoattractant factors including MCP-1 (CCL2) as a cause of delayed recruitment of myeloid cells followed by delayed antigen presentation in STZ-induced diabetic mice infected with *Mtb*.

IL-6 has both pro- and anti-inflammatory roles in *Mtb* infection (VanHeyningen et al., 1997). There are conflicting reports in the literature as to the role of IL-6 in *Mtb* infection (Ladel et al., 1997a, Sodenkamp et al., 2012). IL-6 knockout mice were highly susceptible to *Mtb* infection and this cytokine also contributed to vaccine induced protective immunity in mice (Saunders et al., 2000, Leal et al., 2001). In the current study, higher levels of IL-6 were found in mycobacteria infected AM and RPM from diabetic mice compared to controls although overall concentrations were higher in RPM compared to AM (Figure 5.10 E & F, 5.11 E & F, 5.14 E & F, 5.16 E & F, 5.17 E & F and Table 5.4). Furthermore, an overall higher production of IL-6 was observed in RPM in *M. fortuitum* infection compared to *M. bovis* (BCG) and *M. tuberculosis* (H37Rv) at the later timepoint of infection. Singh and Goyal (2013) observed a higher IL-6 secretion in murine peritoneal macrophages using a heat killed, avirulent *M. tuberculosis* compared to live, virulent *M. tuberculosis*. The authors also found higher IL-6

secretion in the same macrophages using a non-pathogenic *M. smegmatis* compared to *M. tuberculosis* H37Ra/v. These findings were consistent with our observations. Beltan and colleagues (2000) also observed higher production of IL-6 by human macrophages co-cultured with various non-pathogenic mycobacteria (*M. smegmatis*, *M. phlei*) compared to pathogenic bacteria (*M. tuberculosis*, *M. avium*). The precise mechanism underlying the role of IL-6 production in response to pathogenic and non-pathogenic mycobacterial infection is not clear. Elevated production of IL-6 from less/non-pathogenic (e.g. *M. fortuitum*) mycobacteria compared to highly pathogenic bacteria (e.g. *M. tuberculosis*) might be due to the extensive LAM structure on the cell wall and less inhibition and fusion of the phagosome with late endosomes (Singh and Goyal, 2013). The reduced production of IL-6 in macrophages from diabetic animals of this study indicated higher bacterial survival. Martinez and colleagues (2013) also observed higher *M. tuberculosis* growth in macrophages of IL-6 knockout mice. Despite the lower IL-6 production in AM, a higher TNF-α production might compensate the situation to reduce bacterial growth compared to RPM as observed in this study.

IL-1β secretion was significantly lower in the AM and RPM of diabetic mice compared to controls following co-culture with *M. tuberculosis* (H37Rv) (Figure 5.16 H and 5.17 H). Although there was no IL-1β production by AM infected with *M. bovis* (BCG), a reduction of this cytokine was noticed in RPM from diabetic mice compared to controls (Figure 5.13 H, 5.14 H and Table 5.4). Previous studies have shown that IL-1β is required to stimulate macrophages to produce TNF-α and IL-6 (Toossi et al., 1990, Dinarello, 2005). This observation was consistent with our findings which suggests that IL-1β positively correlated with the secretion of TNF-α and IL-6. Reduced production of IL-1β section by macrophages from diabetic mice also related to the higher survival of the bacteria as it has a role in the activation of macrophages to increase secretion of antimycobacterial compounds to kill the bacteria (Dinarello, 2005). Other studies have demonstrated that IL-1 receptor or IL-1β gene knockout mice showed higher susceptibility to *M. tuberculosis* infection resulting in a higher bacterial burden in organs, defective granuloma formation and less production of IFN-γ leading to the death of the mice (Juffermans et al., 2000, Bourigault et al., 2013).

This study showed significantly higher production of IL-10 by RPM from control mice at the earliest timepoint of *M. fortuitum* infection although this wasn't observed at later timepoint (Figure 5.11 K & L). A similar trend was observed at all timepoints of infection during co-culture with *M. bovis* (BCG) (Figure 5.14 M & N and Table 5.4). There was no detectable IL-10 production by AM and RPM following co-culture with *M. tuberculosis* (H37Rv) (Figure

5.16 M & N and 5.17 M & N). The production IL-10 has the roles in limiting the immune responses during mycobacterial infections (Bermudez and Champsi, 1993, Murray and Young, 1999, Jacobs et al., 2000, Roque et al., 2007). Enhanced protection from *M. bovis* (BCG) mortality and reduced immune-mediated pathology was observed in IL-10 knockout mice (Murray and Young, 1999). Furthermore, addition of an IL-10 antagonist as an adjuvant during vaccination improved infection outcomes (Silva et al., 2001, Roberts et al., 2005, Stober et al., 2005). Increased production of IL-10 is associated with the down-regulation of pro-inflammatory cytokines (e.g. TNF-α) leading to lower uptake and killing of the organism (Gong et al., 1996, Fulton et al., 1998, Hirsch et al., 1999a). Although we detected a higher amount of IL-10 in macrophages of control mice, the survival of the organism inside the macrophages was low. The anti-inflammatory environment and the higher killing of the phagocytosed bacteria by the macrophages from control mice may be compensated by the higher secretion of other pro-inflammatory cytokines (TNF-α, MCP-1, IL-6, IL-1β) as observed in this investigation. Despite secretion of a lower amount of IL-10 in macrophages of diabetic mice, they are unable to secrete sufficient amounts of other pro-inflammatory cytokines leading to the higher survival of mycobacteria within macrophages. Higher secretion of IL-10 by RPM might also contribute to this lower production of pro-inflammatory cytokines.

In the current investigation, we observed a reduced uptake and killing of the mycobacteria by the AM and RPM from diabetic mice compared to non-diabetic controls. Bacterial uptake and killing were impaired in diabetic macrophages and this was associated with the reduced or impaired production of various cytokines. Findings of this *in vitro* study enhance our understanding of how macrophage functions are impaired in TB-T2D co-morbid infections. It is also important to understand how antimycobacterial immunity is impaired in diabetic individuals infected with TB. Therefore, in the subsequent three Chapters (Chapter 6, 7 and 8) antimycobacterial immunity will be studied *in vivo* in diabetic mice infected with *M. fortuitum*, *M. bovis* (BCG) and *M. tuberculosis* (H37Rv).

CHAPTER 6
EFFECT OF TYPE 2 DIABETES ON SURVIVAL AND ORGAN MYCOBACTERIAL KINETICS IN MICE

6.1 Introduction

Patients with co-morbid TB-DM (Diabetes Mellitus), have increased severity of infections and mortality (Oursler et al., 2002, Lindoso et al., 2008, Dooley et al., 2009, Wang et al., 2009). Studies have demonstrated a higher bacterial burden on sputum culture, reinfection and relapse during the time of treatment and a longer time required for bacterial clearance from sputum in TB-DM patients than in non-diabetic TB patients (Restrepo et al., 2008b, Dooley et al., 2009, Wang et al., 2009, Jimenez-Corona et al., 2013). There are controversies as to the impact of diabetes on the development of extrapulmonary TB, with some studies reporting a similar or even reduced relative risk of extrapulmonary TB progression in diabetic compared to non-diabetic patients (Long et al., 1997, Leung et al., 2008, Young et al., 2012). However, in parallel to the growing incidence of TB in diabetic patients, there is growing evidence of an increased incidence of non-tuberculous mycobacterial (NTM) infections in patients with AIDS (acquired immunodeficiency syndrome) and diabetes (Tortoli et al., 1995, Piersimoni et al., 1997, Gholizadeh et al., 1998, Uslan et al., 2006, Orme and Ordway, 2014, Bridson et al., 2016, Xu et al., 2016). Although the host-TB/NTM infections are well documented in the literature, there is lack of information on how T2D influences the outcomes of these infections.

Understanding the impact of T2D on mycobacterial dissemination and clearance in TB/NTM patients is crucial. Currently, the mouse model most often used to study the pathogenesis of TB-DM co-morbid infections is one in which animals are treated with high-doses of cytotoxic Streptozotocin (STZ)/ STZ+Nicotinamide (NA) to induce type 1 diabetes (T1D) (Saiki et al., 1980, Yamashiro et al., 2005, Martens et al., 2007, Vallerskog et al., 2010, Podell et al., 2014, Cheekatla et al., 2016). Some researchers have used Goto Kakizaki (GK) T1D and T2D rat models in TB-DM co-morbid infections (Sugawara et al., 2004, Sugawara and Mizuno, 2008). In the GK T1D rat model, animals are not obese and total insulin resistance develops due to severe insulitis which most closely models the features of T1D (Sugawara et al., 2004). The GK T2D rat model is also a non-obese and is less commonly used due to its limitations. The development of hyperglycaemia in this model is associated with increased secretion of corticosterone which differs significantly from the mechanism of hyperglycaemia development in T2D (Beddow and Samuel, 2012). Although the above-mentioned animal models have

provided important information as to how hyperglycaemia affects chronic TB disease, they did not model the effects of diet on the development and outcome of acute TB-DM co-morbid infections. To our knowledge, this is the first study examining mycobacterial susceptibility using tuberculous and non-tuberculous mycobacterial species in diet-induced murine model of T2D.

In this Chapter, we hypothesise that chronic persistent hyperglycaemia in a diet-induced murine model of T2D leads to higher bacterial burden in organs leading to decreased survival from mycobacterial infections. As mycobacterial susceptibility increases in poorly controlled diabetic patients (Restrepo et al., 2008a), the animals used is the current study were maintained on the energy-dense-diet (EDD; Chapter 4) for extended periods and monitored for energy intake, body weight loss and blood glucose level during acute mycobacterial infections. We investigated the survival and kinetics of bacillary burden in our T2D model following mycobacterial infections. We used non-tuberculous mycobacteria (*M. fortuitum*) and tuberculous (*M. bovis*; BCG and *M. tuberculosis*; H37Rv) mycobacteria throughout this study to investigate whether T2D influences the outcomes of diverse mycobacterial infection types.

The specific Aims of this research described in this Chapter are:

1. To investigate the survival of T2D mice following infection with a high-dose of *M. fortuitum*, *M. bovis* (BCG) and *M. tuberculosis* (H37Rv)
2. To determine the effect of T2D on kinetics of organ bacterial load following infection with a low-dose of *M. fortuitum*, *M. bovis* (BCG) and *M. tuberculosis* (H37Rv)

6.2 Materials and Methods

6.2.1 Animal ethics and institutional approvals

The details of animal ethics and institutional approvals are described in Chapter 3 (section 3.1.1).

6.2.2 Experimental animals and induction of diabetes

Six-week old male C57BL/6 mice were used for the induction of diabetes. Mice were received from SABU, James Cook University at 4 weeks of age and randomly housed in cages (5 mice/cage) within a temperature and light controlled environment. Ear marking was done for longitudinal characterisation of individual mouse. Three sets of mice (Table 6.1) were kept on diets for a period of 30 weeks. The diabetic groups were provided with an *ad libitum* access to

an energy-dense diet (EDD), whereas the non-diabetic control groups were fed a standard rodent diet (SRD). The body weight gain, glucose tolerance test and area under the curve as the measures of insulin resistance were determined after the end of the diet intervention period. Animal care and nutritional provisions, marking of individual mouse and methods for determining the metabolic parameters are described in Chapter 3 (section 3.1.3).

Table 6.1 Mice used for the induction of diabetes for infection studies

Infection studies	Mouse set	Diet (30 weeks)	
		EDD (n)	SRD (n)
M. fortuitum	1	33	33
M. bovis (BCG)	2	33	31
M. tuberculosis (H37Rv)	3	40	39

EDD; energy-dense diet, SRD; standard rodent diet, n; number of mice

6.2.3 Mycobacterial infections

6.2.3.1 Preparation of mycobacterial culture for infection

For the preparation of bacterial inocula for injection, frozen aliquots of the bacterial culture were thawed and washed twice with PBS at 4000 xg for 10 minutes. Bacterial pellets were then vortexed for several minutes. The bacterial clumps were further broken down by passing the suspension 10-15 times through 27-gauge needles followed by sonication for 10 seconds (50% maximum frequency). The diluted bacterial inoculum was plated on 7H11 agar plates to confirm the bacterial CFU/mL (Chapter 3, section 3.3.1 and 3.3.2).

For the infection studies using *M. fortuitum*, *M. bovis* (BCG) and *M. tuberculosis* (H37Rv), diabetic and control mice were injected intravenously via the lateral tail vein with an either a high-dose or a low-dose of bacteria in a final volume of 200 µL of PBS (Table 6.2).

Table 6.2 Infective doses for mycobacterial infections

Organism	Dose (CFU/mouse)		Mice number		Reference
			Diabetic	Control	
M. fortuitum	High	$3x10^8$	14	13	Parti et al. (2005)
	Low	$1x10^7$	30	33	
M. bovis (BCG)	High	$2x\ 10^6$	9	12	Orme and Roberts (2001) Pedras-Vasconcelos et al. (2002)
	Low	$1x10^6$	32	34	
M. tuberculosis (H37Rv)	High	$2x\ 10^7$	12	10	
	Low	$4x10^6$	40	39	

6.2.4 Monitoring and culling of infected mice

Following infections and throughout the infection period mice were monitored for survival and metabolic parameters (daily feed and energy intake, body weight loss and blood glucose level). Mice infected with a low-dose of bacteria were sacrificed at 1, 14 and 30/35 days post-infection (dpi) to determine the bacterial loads, histopathological changes (Chapter 7) and cytokine production (Chapter 8). Some low-dose *M. fortuitum* infected mice were monitored for their survival for 60 dpi although no metabolic parameters were recorded after 4 weeks.

Mice infected with a high-dose of mycobacteria were observed primarily for their survival at 60 dpi and metabolic parameters were monitored for 7 weeks. Some high-dose *M. fortuitum* infected mice were sacrificed at 14 dpi to investigate the kinetics of infection.

6.2.5 Preparation of organ homogenates

Three to five mice from each group were euthanised by CO_2 asphyxiation at 1, 14, 35 days post infection (dpi) (30 dpi for *M. tuberculosis* infection) for the collection of spleen, liver and lungs. All samples were processed according to previously published protocols (Da Silva et al., 2002, Parti et al., 2005, Yamashiro et al., 2005, Vallerskog et al., 2010, Ordway and Orme, 2011). Briefly, spleen (half total organ weight), liver (1 g), lungs (left lung) were homogenised separately in a stomacher bag containing 1 mL of PBS with 0.05% Tween 80. The homogenates were centrifuged (3000 xg for 5 minutes) and supernatants were collected and stored at -80^{0}C for cytokine assays (Chapter 7). The cell pellets were then lysed with 300 µL of 0.1% Triton X-100® for 10 minutes followed by sample dilution with 700 µL of PBS. Serial 10 or 5-fold dilutions were prepared from lysates and plated on 7H11 agar plates. Colonies were counted after 5-7 days (*M. fortuitum* infection) and from 16 days after (*M. bovis*; BCG and *M. tuberculosis;* H37Rv) infection of incubation at 37^{0}C with 5% CO_2. Organs from 2 moribund diabetic and 3 non-diabetic mice infected with high-dose *M. fortuitum* were also culled and samples were processed as described above.

6.3 Statistical analysis

Statistical analysis was performed using the SPSS version 24.0 and GraphPad Prism 7.03 software. All the data were checked for normality using the Shapiro-Wilk's test. Data passed the test of normality if $p \geq 0.05$. The normally distributed data were compared between diabetic and control groups using the independent samples *t*-test. The non-normally distributed data were compared between the groups using the non-parametric Mann-Whitney U test. Normally distributed data of multiple groups were compared using the ordinary one-way ANOVA with

Holm-Sidak's multiple comparisons test. The Kruskal-Wallis test with Dunn's multiple comparisons test was performed for non-normally distributed data of multiple groups. The two-way ANOVA with Sidak's multiple comparisons test was performed for repeated measures data (e.g. kinetics of feed and energy intake, body weight loss, changes in blood glucose level). The Kaplan Meier survival curves with log-rank (Mantel-Cox) tests were used to compare diabetic and control mouse survival post-infection. All data were expressed as mean±SEM. The level of significance was indicated as *p≤0.05, **p≤0.01, ***p≤0.001 and ****p≤0.0001.

6.4 Results

6.4.1 Assessment of metabolic parameters following diet intervention

Prior to the diet intervention, the starting body weight of mice on the energy-dense diet (EDD) and standard rodent diet (SRD) was similar in all the mouse sets (Figure 6.1 A, D & G). After 30 weeks of diet intervention, the body weight gain was significantly higher in mice on EDD compared to controls (Figure 6.1 A, D & G). For mouse set 1, the overall increase in the body weight was 58.21% in SRD group and 143.06% in EDD group. A similar trend of body weight gain was also observed in mouse set 2 (SRD, 8.97 *vs* EDD, 83.51, %) and mouse set 3 (SRD, 35.77 *vs* EDD, 137.73, %). The glucose tolerance test (GTT) demonstrated that mice on EDD were more glucose intolerant compared to control mice on SRD (Figure 6.1 B, E & H). In mouse set 1, the baseline fasting blood glucose (FBG) level (before the glucose challenge indicated as 0 minutes) was 6.66±0.13 and 9.11±0.20 mmol/L in mice on SRD and EDD, respectively. Compared to controls, diabetic mice were less efficient in clearing the glucose from the circulation even 2 hours after an intraperitoneal glucose challenge (SRD, 5.99±0.12 *vs* EDD, 10.00±0.24, mmol/L, p≤0.0001) (Figure 6.1 B). In mouse set 2 and 3, the baseline FBG concentration and 2 hours post-glucose challenge blood glucose level was also higher in mice on EDD compared to control mice on SRD (Figure 6.1 E & H). The area under the curve (AUC) based on GTT (AUC-GTT) was also significantly higher in EDD fed mice compared to controls (Figure 6.1 C, F & I), which also indicated a higher glucose intolerance by diabetic mice due to higher insulin resistance.

In the current study, EDD fed mice were considered T2D if they demonstrated an elevated FBG level and AUC-GTT with evidence of glucose intolerance higher than the upper 99% confidence interval for the mean of the age-matched control group (described in Chapter 4). Based on FBG level and AUC-GTT, a total of 96.97 to 100% mice on EDD became diabetic in mouse set 1 (Appendix 4) and mouse set 2 (Appendix 5). In mouse set 3, 100% of mice became

diabetic based on FBG and AUC-GTT after the diet intervention (Appendix 6). Those mice which failed to meet at least one of the above criteria mentioned were excluded from the infection study.

As the mice fed on EDD showed the characteristic features of T2D, hereafter they will be termed 'diabetic mice'.

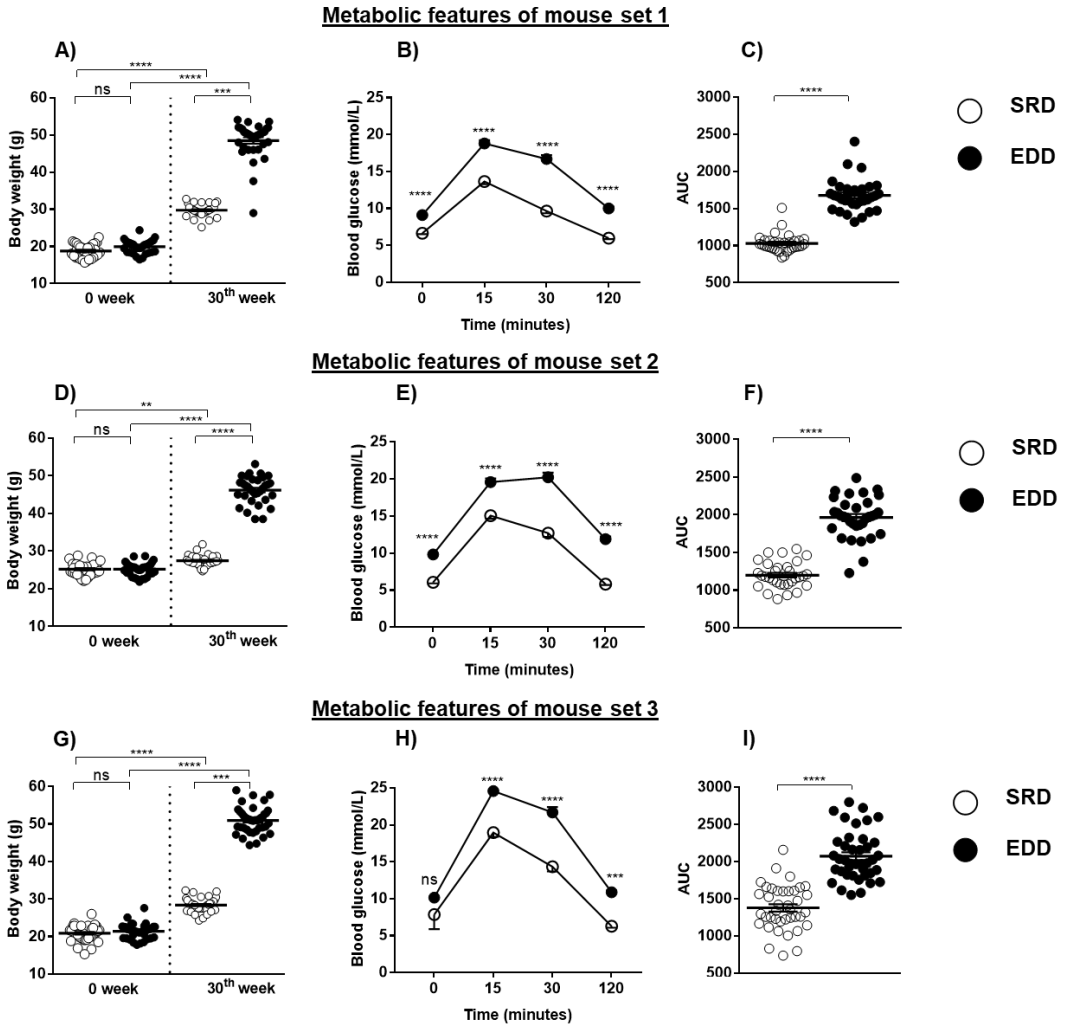

Figure 6.1 Metabolic profile of three sets of mice used in this study

C57BL/6 mice were kept on the energy-dense diet (EDD) and standard rodent diet (SRD) for a period of 30 weeks. After diet intervention, weight gain (A, D & G), glucose tolerance test (GTT) after 6 hours of morning fasting (B, E & H) and Area Under the Curve (AUC) based on GTT (C, F & I) were significantly higher in mice on EDD compared to control mice on SRD. The mice set 1 (A, B & C), 2 (D, E & F) and 3 (G, H & I) were used for *M. fortuitum*, *M. bovis* (BCG) and *M. tuberculosis* (H37Rv) infection study, respectively. Data presented as mean±SEM (Appendix 4; *M. fortuitum*, 5; *M. bovis* BCG and 6; *M. tuberculosis* H37Rv). Significant differences were determined using the Kruskal-Wallis test with Dunn's multiple comparisons test (A, D & G), the two-way ANOVA with Sidak's multiple comparisons test (B, E & H), Mann-Whitney U test (C, F) and the independent sample *t*-test (I). The level of significance was indicated as **p≤0.01, ***p≤0.001 and ****p≤0.0001.

6.4.2 Assessment of metabolic parameters following mycobacterial infections

6.4.2.1 Metabolic parameters following *M. fortuitum* infection

Following infection with *M. fortuitum* at a dose of $1x10^7$ CFU/mouse (low-dose), the daily feed (Appendix 4, Figure A4.1) and energy intake of diabetic mice was reduced during the first 2 weeks of infection, compared to the later weeks post-infection (pi) (Figure 6.2 A). In contrast, the feed (Appendix 4, Figure A4.1) and energy intake (Figure 6.2 A) of control mice fluctuated throughout the infection period. Four weeks pi, the overall energy intake/mouse/day was reduced in control mice by 3.76% compared to pre-infection (baseline; 0 week) intake. However, in diabetic mice, daily energy intake increased by 10.83% pi which might be due to feed waste. It was observed that when HFD feed was supplied for 7-days, pellets softened and dropped down to the bottom of the cages. Infected diabetic mice showed a gradual loss in body weight over the infection period, whereas fluctuations in weight of the control group were observed (Figure 6.2 B). Overall diabetic mice lost 13.58% body weight, whereas control mice gain 8.94% in the same period pi. Prior to infection, the blood glucose level of diabetic mice was significantly higher than the control group (control, 6.65±0.13 *vs* diabetic, 9.23±0.20, mmol/L, $p \leq 0.001$). Following infection and for the first 3 weeks pi, we observed an initial decrease in blood glucose level in diabetic mice. In the control mice, a fall in blood glucose level was not seen after the second week pi. During the final week of the infection study (day 35), the blood glucose level of both groups was elevated (control, 7.70±0.36 *vs* diabetic, 11.07±0.54, mmol/L) and significantly higher than their pre-infection blood glucose levels.

When the mice were infected with high-dose ($3x10^8$ CFU/mouse) bacteria, diabetic mice were observed to be considerably more inactive and lethargic compared to control mice. The daily feed (Appendix 4, Figure A4.10) and energy intake, weekly body weight and blood glucose level were reduced significantly in both diabetic and control mice (Figure 6.2 D, E & F) following high-dose infection. The overall daily energy intake/mouse/day was reduced by 28.43% in control and 66.01% in diabetic mice, which also corresponded to their body weight loss. At 2 weeks pi, control and diabetic mice had lost 10% and 33.33% of their body weight respectively. In contrast to the low-dose infection, the blood glucose level of both control and diabetic mice dropped sharply following infection and failed to return to pre-infection levels (Figure 6.2 C *vs* Figure 6.2 F).

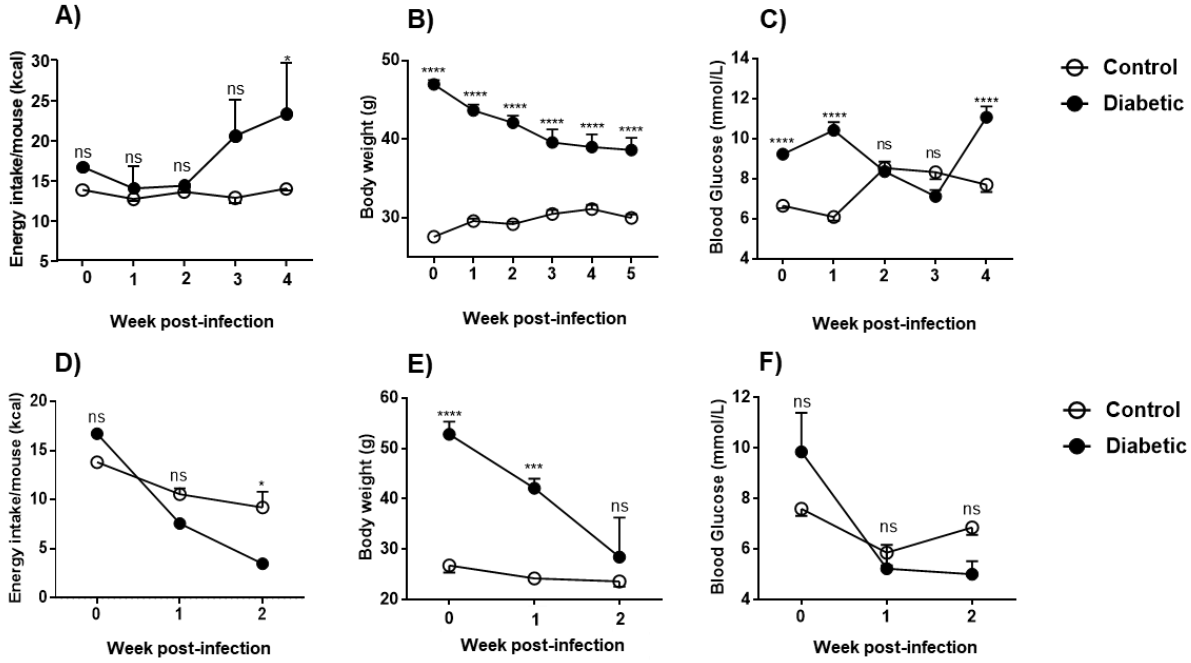

Figure 6.2 Metabolic parameters of mice following *M. fortuitum* infection

Diabetic and control mice were infected with a dose of $1x10^7$ CFU/mouse intravenously (A-C). Following infection, the daily energy intake (A), weekly body weight (B) and blood glucose level (C) were monitored for a period of 35 days. Whereas some mice were infected at a high-dose of $3x10^8$ CFU/mouse (D-F). The daily energy intake (D), weekly body weight (E) and blood glucose level (F) were also monitored for a period of 2 weeks (until the death of the mice). In both low and high-dose infection groups, the overall reduction of energy intake, body weight and blood glucose level were observed in both diabetic and control mice. Data presented as mean±SEM; n=30-33 (low-dose) and 13-14 (high-dose) mice/group. The significant differences were determined using the two-way ANOVA with Sidak's multiple comparisons test (Appendix 4). The level of significance was indicated as *p≤0.05, ***p≤0.001, ****p≤0.0001 and ns=non-significant.

6.4.2.2 Metabolic parameters following *M. bovis* (BCG) infection

In mice infected with $1x10^6$ CFU *M. bovis* (BCG), the daily feed (Appendix 5, Figure A5.1) and energy intake (Figure 6.3 A) fell progressively in the first 2 weeks of infection in both diabetic and control mice followed by a gradual rise until the last week of the infection study. After 4 weeks, the energy intake/mouse/day was reduced by 14.70% for diabetic mice compared to pre-infection. In the control group, the overall reduction of energy intake/mouse/day was 31.33%. Weight loss was gradual in diabetic mice (22.05% weight loss compared to pre-infection), whereas control mice maintained their weight over the study period (Figure 6.3 B). The pre-infection (indicated as '0 week') blood glucose level of the diabetic

mice was significantly higher than the control group (control, 7.35±0.20 *vs* diabetic, 8.54±0.29, mmol/L, p=0.0012). Following infection, blood glucose levels decreased from the second to 4th week pi (Figure 6.3 C). At the end of the infection study, the blood glucose levels in both groups were elevated compared to pre-infection levels, although these increases were not statistically significant (control, 8.39±0.22 *vs* diabetic, 9.01±0.53, mmol/L, p=0.2632).

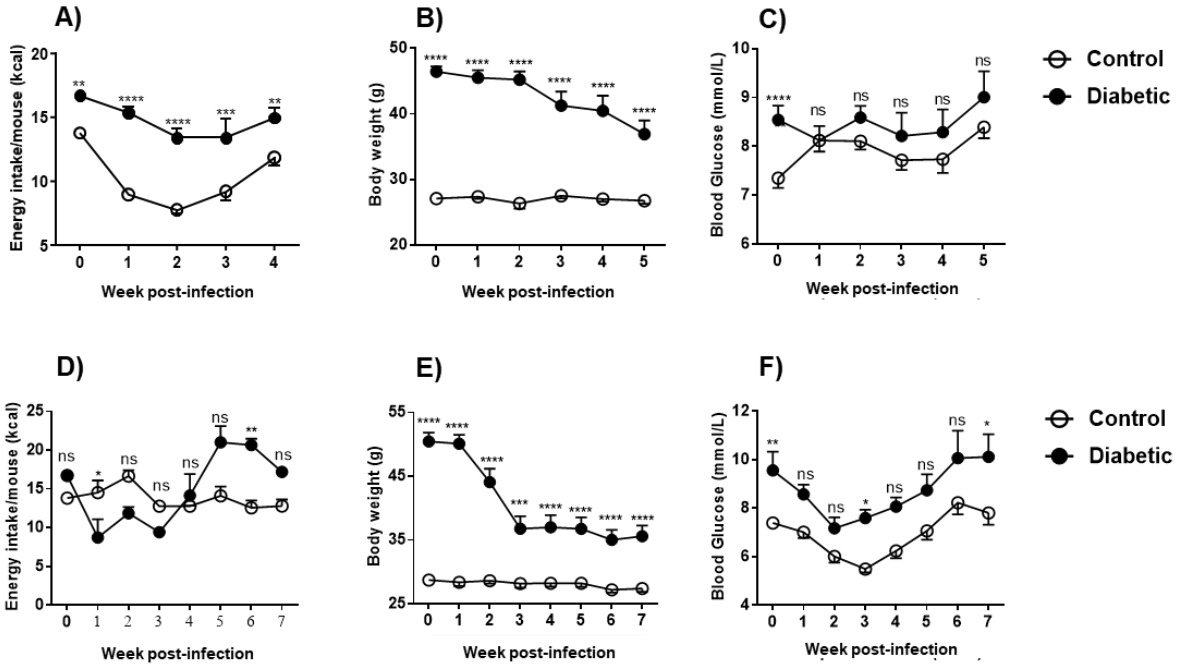

Figure 6.3 Metabolic parameters of mice following *M. bovis* (BCG) infection

Diabetic and control mice were infected with a low-dose of ($1x10^6$ CFU/mouse) *M. bovis* (BCG) to observe the kinetics of infection (A-C). Following infection, the daily energy intake (A), weekly body weight loss (B) and blood glucose level (C) were monitored for a period of 35 days. Whereas mice infected with a high-dose ($2x10^6$ CFU/mouse) of the same bacteria were monitored for the daily energy intake (D), weekly body weight loss (E) and blood glucose level (F) for 7 weeks during determining the survial. In both groups, the overall reduction of energy intake, body weight and blood glucose level was higher in the diabetic group compared to controls. Data presented as mean±SEM; n=32-34 (low-dose) and 09-12 (high-dose) mice/group. The significant differences were determined using the two-way ANOVA with Sidak's multiple comparisons test (Appendix 5). The level of significance was indicated as *p≤0.05, **p≤0.01, ***p≤0.001 and ****p≤0.0001 and ns=non-significant.

Both diabetic and control mice infected with high-dose *M. bovis* BCG ($2x10^6$ CFU/mouse), showed an erratic trend of daily feed (Appendix 5, Figure A5.10) and energy intake (Figure 6.3 D) throughout the infection period. Compared to their pre-infection energy intake/day/mouse, a 12.01% and 0.5% reduction of energy intake/mouse/day was observed in diabetic mice and controls, respectively. A sharp decrease in body weight was observed in diabetic mice at weeks

1-3 pi and then body weight stabilised until the end of the infection period (Figure 6.3 E). In control mice, the body weight was generally stable throughout the infection study (Figure 6.3 E). After the end of 7th week of infection, we observed a 29.44% and 4.66% body weight reduction in diabetic and control mice, respectively. Furthermore, the blood glucose level in both diabetic and control mice fell in the first 2 weeks of infection but after this time glucose levels gradually increased to pre-infection levels (Figure 6.3 F).

6.4.2.3 Metabolic parameters following *M. tuberculosis* (H37Rv) infection

The daily feed (Appendix 6, Figure A6.1) and energy intake (Figure 6.4 A) of diabetic mice infected with low-dose (4x10^6 CFU) *M. tuberculosis* (H37Rv), reduced dramatically in the first 2 weeks followed by a gradual increase at later weeks of the infection period. In control mice, the feed (Appendix 6, Figure A6.1) and the energy intake was lower in the first 2 weeks pi and then slowly increased until the last week (Figure 6.4 A). At 4 weeks pi, the energy intake/mouse/day of diabetic mice decreased by 26.06% compared to pre-infection intake. In the control group, the opposite trend was observed i.e. energy intake/mouse/day increased by 19.39% compared to pre-infection intake (Figure 6.4 A). A gradual decrease in the body weight of diabetic mice was observed during the entire period of infection. In contrast, the body weight of the control mice was maintained (Figure 6.4 B). At 4 weeks pi, diabetic mice lost an average of 15.39% of their body weight which contrasted with the minor (1.56%) body weight reduction measured from control mice. Pre-infection blood glucose level in diabetics was significantly higher than the control group (control, 5.68±0.30 *vs* diabetic, 9.78±0.30, mmol/L, p=0.0000). In diabetic mice, the pi blood glucose level dropped until the second week of infection followed by a gradual rise until the last week of infection (Figure 6.4 C). The pi blood glucose level of the control group was higher than the pre-infection level throughout the infection (Figure 6.4 C) with some control animals even showing higher blood glucose than diabetic animals during the last 2 weeks of infection, although this was not statistically significant.

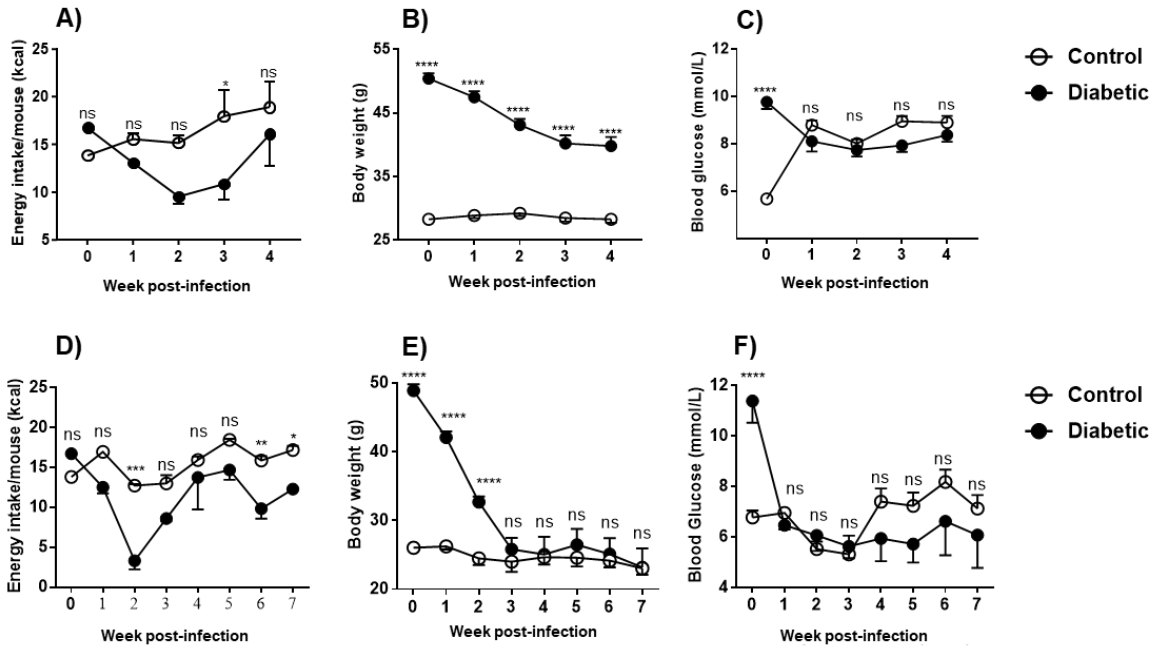

Figure 6.4 Metabolic parameters of mice following *M. tuberculosis* (H37Rv) infection

Diabetic and control mice were infected with a low-dose of ($4x10^6$ CFU/mouse) *M. tuberculosis* (H37Rv) to observe the kinetics of infection (A-C). Following infection, the daily energy intake (A), weekly body weight loss (B) and blood glucose level (C) were monitored for a period of 30 days. Whereas mice infected with a high-dose ($2x10^7$CFU/mouse) of the same bacteria were monitored them for the daily energy intake (D), weekly body weight loss (E) and blood glucose level (F) for 7 weeks during determining the survial. In both low- and high-dose groups, the overall reduction of energy intake, body weight and blood glucose level was higher in the diabetic group compared to control group. Data presented as mean±SEM; n=39-40 (low-dose) and 10-12 (high-dose) mice/group. The significant differences were determined using the two-way ANOVA with Sidak's multiple comparisons test (Appendix 6). The level of significance was indicated as *p≤0.05, **p≤0.01, ***p≤0.001 and ****p≤0.0001 and ns=non-significant.

Diabetic and control mice infected with high-dose ($2x10^7$ CFU) *M. tuberculosis* (H37Rv) both showed inactivity, lethargy, decreased responsiveness to external stimuli and rough hair coats, although the signs were more apparent in diabetic mice. Moribund animals were found emaciated and their movement was diminished with a sign of dyspnoea. A dramatic fall in feed (Appendix 6, Figure A6.10) and energy intake (Figure 6.4 D) was recorded for diabetic mice until the second week of infection, whereas slight reduction of energy intake (Figure 6.4 D) was observed in control mice. After the second week pi, feed and energy intake increased gradually in both control and diabetic mice although some fluctuation was noticed during the last 3 weeks of the study period (Figure 6.4 D). Compared to the pre-infection values, a 35.92% reduction of energy intake/mouse/day was observed in diabetic mice, whereas a 13.89% increase was measured for control mice. A significant reduction in body weight loss was observed in diabetic mice during the first 3 weeks pi followed by a gradual loss until the end of the infection period

(Figure 6.4 E). In control mice, a slow reduction in the body weight was observed during the first few weeks of infection although it remained static in the subsequent weeks (Figure 6.4 E). An overall 52.56% and 10.65% body weight reduction was measured in diabetic and control mice respectively after 7 weeks of infection. Furthermore, the blood glucose level dropped sharply in the first 3 weeks of infection in both diabetic and control mice followed by a slightly rising trend which continued until the end of infection (Figure 6.4 F).

6.4.3 Survival of mice following mycobacterial infections

In *M. fortuitum* infection with a dose of $1x10^7$ CFU/mouse (low-dose), there was no mortality observed after 60 days post-infection (dpi) (Appendix 4, Figure A4.2). When the mice were infected with a high-dose ($3x10^8$ CFU/mouse) of the same bacteria, a higher mortality was found in diabetic mice compared to controls (Figure 6.5, A). After 14 dpi, 41.67% of the control and 20% of diabetic mice were survived although the difference was not statistically significant (p=0.0601).

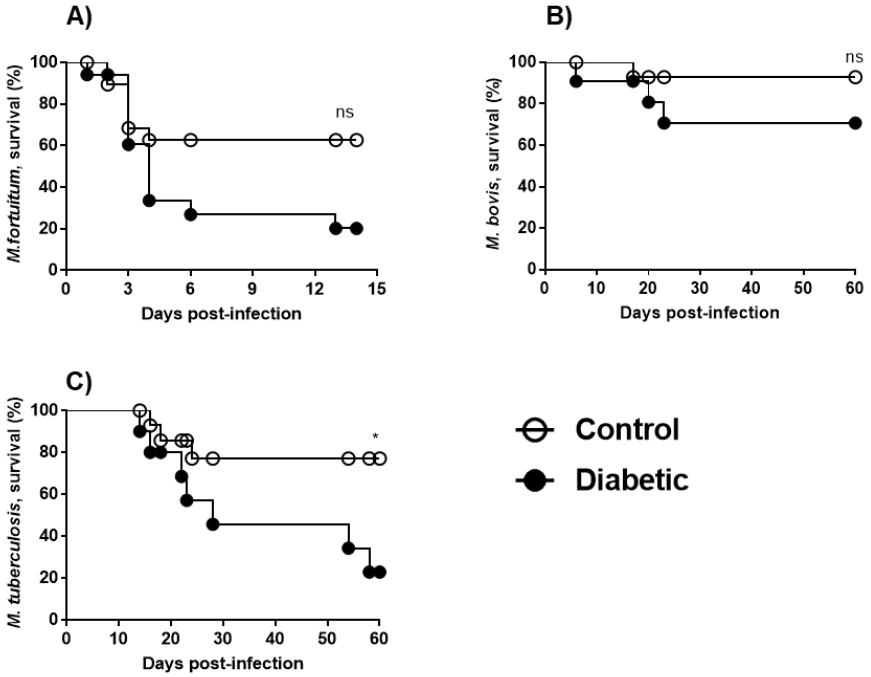

Figure 6.5 Survival of mice following mycobacterial infections

Mice were infected with a high-dose of *M. fortuitum* ($3x10^8$ CFU/mouse), *M. bovis* BCG ($2x10^6$ CFU/mouse) and *M. tuberculosis* (H37Rv, $2x10^7$ CFU/mouse) to observe the survival of mice. Following infection, a lower survival (higher mortality) was observed in diabetic mice compared to control mice (A, B & C). The Kaplan Meier survival curves with Log-rank (Mantel-Cox) tests were used to compare susceptibility between the groups. A total of 14 diabetic, 13 control mice were infected for *M. fortuitum*, 9 diabetic and 12 controls for *M. bovis* (BCG) and 12 diabetic and 10 controls for *M. tuberculosis* (H37Rv) study. The level of significance was indicated as *p≤0.05 and ns=non-significant.

In *M. bovis* (BCG, $1x10^6$ CFU/mouse) and *M. tuberculosis* (H37Rv, $4x10^6$ CFU/mouse) infection with a low-dose, there was no mortality observed in both diabetic and control mice after 35/30 dpi (data not shown). When the mice were infected with a high-dose *M. bovis* (BCG, $2x10^6$ CFU/mouse), a total of 70% of the diabetic mice were survived, whereas 92.31% control mice survived after 60 dpi (Figure 6.5 B). Similarly, a significantly lower survival of diabetic mice compared to controls infected with a high-dose of *M. tuberculosis* (H37Rv, $2x10^7$ CFU/mouse) was observed (control, 66.66 *vs* diabetic, 22.22, %, p=0.0246) (Figure 6.5 C). Overall, the survival of diabetic mice was lower compared to controls infected with a high-dose of mycobacteria.

6.4.4 Kinetics of organ bacterial load following mycobacterial infections

6.4.4.1 Organ bacterial load in *M. fortuitum* infected mice

Diabetic mice infected with *M. fortuitum* ($1x10^7$ CFU/mouse), were less efficient in controlling organ bacterial loads compared to control mice (Figure 6.6). Overall, a high *M. fortuitum* load was observed in the organs of diabetic mice at 14 and 35 days post-infection (dpi) compared to controls. The *M. fortuitum* burden in the spleen of diabetic mice was 1.33 times higher at 1 dpi compared to controls albeit it was not statistically significant (Figure 6.6 A). A declining trend of *M. fortuitum* organ load was observed at the later timepoints of infection. The *M. fortuitum* burden in the spleen of diabetic *versus* control mice was significantly different at 35 dpi (Figure 6.6 A) with diabetic mice showing 1.79 times higher load than control mice. There was no difference in the *M. fortuitum* burden in the liver at 1 dpi. However, the liver load in diabetic mice was 2 times higher at 14 dpi and 2.43 times higher at 35 dpi compared to controls (Figure 6.6 B). There was no significant difference in *M. fortuitum* load in the lungs at 1 dpi (Figure 6.6 C). However as observed for liver, the lung counts for diabetic mice were 4.26 times higher at 14 dpi and 3.69 times higher at 35 dpi compared to controls. An increasing trend of *M. fortuitum* burden was observed in kidneys following infection (Figure 6.6 D). Compared to controls, the kidney *M. fortuitum* counts at 14 and 35 dpi in diabetic mice were 2.93 and 5.42 times higher, respectively.

Diabetic mice infected with high-dose ($3x10^8$ CFU/mouse) *M. fortuitum*, had higher counts at 14 dpi than controls in all organs examined (Figure 6.6 D). Organ *M. fortuitum* burden was 6.51 times higher in the spleen of diabetic mice compared to controls. In liver, the bacterial burden was 16.94 times higher in diabetic mice in comparison to control mice. Compared to controls, diabetic mice demonstrated a 14.79 and 3.78 times higher bacterial burden in lungs and kidneys,

respectively, although these were not statistically significant as only small group sizes were used for these high-dose experiments.

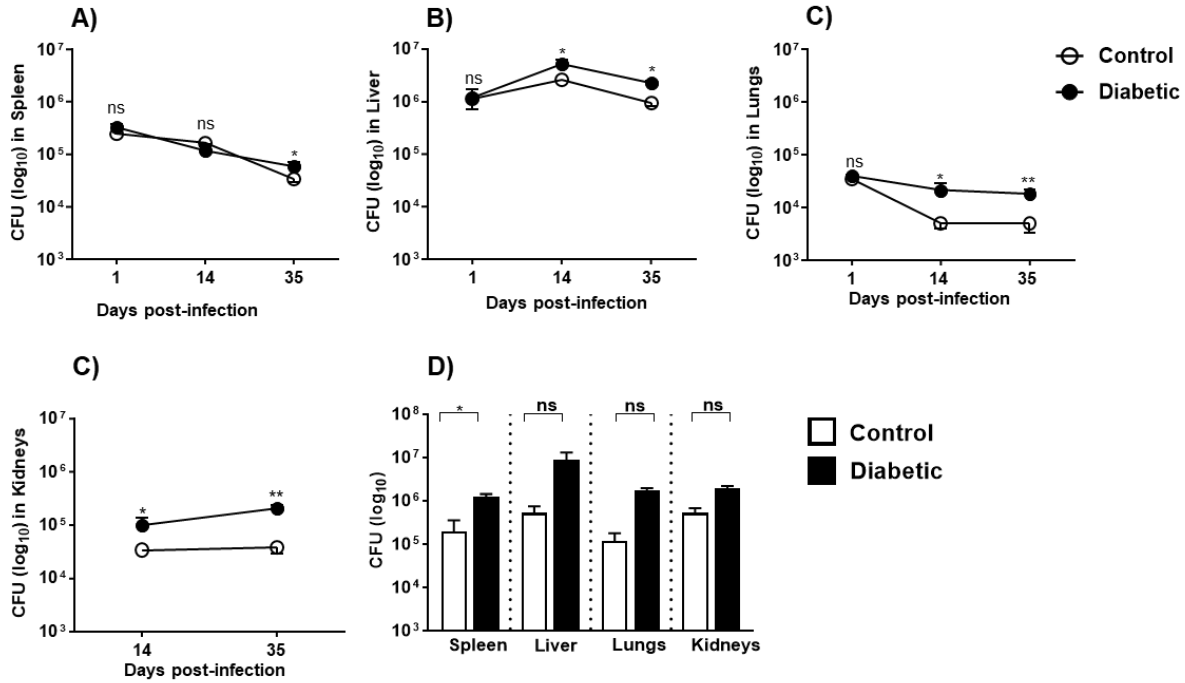

Figure 6.6 Organ bacterial load following *M. fortuitum* infection

Mice were infected with a dose of $1x10^7$ CFU/mouse were sacrificed at 1, 14 and 35 days post-infection (dpi). *M. fortuitum* load was higher in spleen (A), liver (B), lungs (C) and kidneys (D) of diabetic mice compared to controls at 14 and 35 dpi. Moreover, some moribund diabetic and control mice infected with a high-dose of *M. fortuitum* ($3x10^8$ CFU/mouse) were also sacrificed at 14 dpi to observe the organ bacterial load. In this group, bacterial load was also recorded higher in spleen, liver, lungs and kidneys of the diabetic mice compared to controls (D). Data were mean Log_{10} CFU±SEM; n=3-5 (low-dose) and 2-3 (high-dose) mice/group. The significance differences were determined using the independent sample *t*-test except a few non-normally distributed data set (14 days organ load in liver and lungs), which were analysed using the Mann-Whitney U test (Appendix 4). The level of significance was indicated as *p≤0.05, **p≤0.01 and ns=non-significant.

6.4.4.2 Organ bacterial load in *M. bovis* (BCG) infected mice

Mice infected with *M. bovis* (BCG) were culled at 1, 14 and 35 days post-infection (dpi) to determine the organ *M. bovis* (BCG) load in spleen, liver and lungs. Following infection, a gradual rise in the *M. bovis* (BCG) counts was observed in the spleen, liver and lungs of both diabetic and control mice followed by a decline at later timepoints (Figure 6.7 A, B & C). The *M. bovis* (BCG) counts in the spleen at 1 dpi were 1.23 higher in diabetic mice compared to controls (Figure 6.7 A). Similarly, at 14 dpi spleen counts were 2.55 times higher in diabetic

mice compared to controls. A decreasing trend in *M. bovis* (BCG) load was observed in the spleen at 35 dpi in both groups although it was 1.81 times higher in diabetic mice. In liver, the *M. bovis* (BCG) burden was 2.44 times higher in diabetic mice at 1 dpi although it did not reach significance (Figure 6.7 B). Compared to controls, diabetic mice had 3.40 and 6.10 times higher *M. bovis* (BCG) counts in the liver at 14 and 35 dpi, respectively. In the lungs, the highest *M. bovis* (BCG) counts was found at 14 dpi which was 2.23 times higher in diabetic mice compared to controls (Figure 6.7 C). At 35 dpi, the lung *M. bovis* (BCG) burden remained high in diabetic mice (2.88 times higher) compared to controls. Overall, a higher *M. bovis* (BCG) load was observed in organs of diabetic mice at 14 and 35 dpi compared to controls. These findings indicated that diabetic mice were less efficient in clearing *M. bovis* (BCG) from all organs compared to controls.

6.4.4.3 Organ bacterial load in *M. tuberculosis* (H37Rv) infected mice

The counts of *M. tuberculosis* (H37Rv) in the spleen, liver and lungs of diabetic and control mice were determined at 1, 14 and 30 days post-infection (dpi). The trends for *M. tuberculosis* (H37Rv) burden in all organs were similar to those for *M. bovis* (BCG) (Figure 6.7). At 1 dpi, the spleen *M. tuberculosis* (H37Rv) counts were similar in control and diabetic mice (Figure 6.7 D). Compared to controls, diabetic mice had 5.80 and 4.95 times higher spleen *M. tuberculosis* (H37Rv) burden at 14 and 30 dpi, respectively. A similar trend was observed in the liver organ bacterial load, where diabetic mice had 1.79 and 2.62 times higher *M. tuberculosis* (H37Rv) burden at 14 and 30 dpi, respectively (Figure 6.7 E). In lungs, the *M. tuberculosis* (H37Rv) load was 1.26 times higher in control mice at 1 dpi although this was not statistically significant. A continuous rise in the counts of *M. tuberculosis* (H37Rv) in the lungs of both diabetic and control mice was seen at later timepoints of infection (Figure 6.7 F). At 14 and 30 dpi, the lung *M. tuberculosis* (H37Rv) load was 3.5 and 1.96 times higher in diabetic mice compared to controls, respectively.

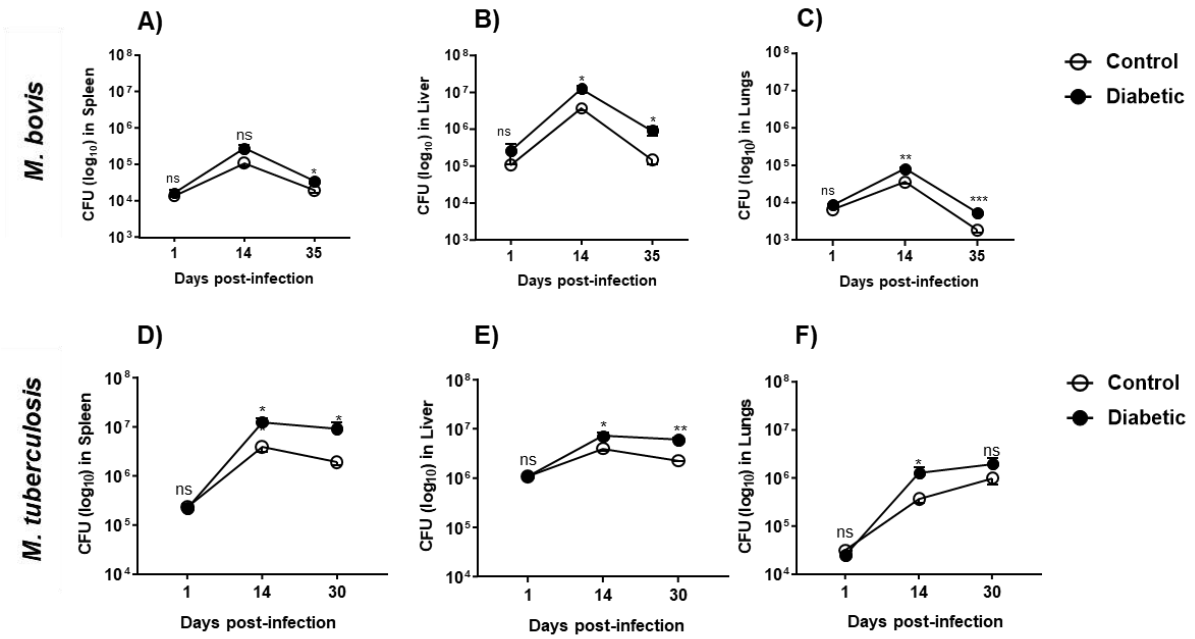

Figure 6.7 Organ bacterial load following *M. bovis* (BCG) and *M. tuberculosis* (H37Rv) infections

Mice were infected with *M. bovis* (BCG, 1x10^6 CFU/mouse) and *M. tuberculosis* (H37Rv, 4x10^6 CFU/mouse) were sacrificed 1, 14 and 35/30 days post-infection (dpi). The *M. bovis* load was higher in spleen (A), liver (B), lungs (C) of diabetic mice compared to control at 14 and 35 dpi. A similar trend of *M. tuberculosis* (H37Rv) load was observed in spleen (D) liver (E) and lungs (F) at the same timepoint of infection. Data presented as mean Log_{10} CFU±SEM; n=4-5 mice/group. The significance differences were compared between groups using the independent sample *t*-test except for few non-normally distributed data sets. The non-normally distributed data were compared between groups using the Mann-Whitney U test (*M. bovis*, Appendix 5 and *M. tuberculosis,* Appendix 6). The level of significance was indicated as *p≤0.05, **p≤0.01, ***p≤0.001 and ns=non-significant.

6.5 Discussion

Susceptibility to TB can be increased by type 2 diabetes mellitus with diabetic patients having an overall threefold increased risk of developing active TB (Jeon and Murray, 2008). There is also increasing evidence that the risk of non-tuberculous mycobacterial infections is elevated in patients with diabetes (Bridson et al., 2016). In this study, we investigated whether diabetic mice showed increased susceptibility to both TB complex and NTM infection compared to control non-diabetic mice. We demonstrated that indeed diabetic mice are more susceptible to these infections with severely impaired glucose regulation during infection, increased bacterial loads in the lungs and other organs and increased mortality.

Both low- and high-dose intravenous infections of *M. fortuitum*, *M. bovis* (BCG and *M. tuberculosis* (H37Rv) were used in this study. Low-dose infections were used to examine the

course of infection at 1, 14 and 30/35 days timepoints, whereas high-doses were used to determine mouse survival post-infection (pi). In the current Chapter, the metabolic parameters, mouse survival and organ mycobacterial loads following infections are described. Organ pathology and inflammatory cytokines are described in the following Chapters.

Following infection with all mycobacteria species examined, energy intake, body weight and blood glucose levels were monitored during the course of infection. Control mice infected with low-dose *M. fortuitum* and *M. bovis* (BCG) showed a minimal reduction in overall energy intake pi with a slight increase in body weight (Figure 6.2, 6.3 A & B). Control mice were provided with a controlled amount of feed (4.5 g/day/mouse) during the pre-infection period, whereas feed was given *ad libitum* during the pi period. The feed and energy intake were calculated on a weekly basis to reduce the frequency of animal handling during the time of infection. The explanation for the slightly higher body weight in control mice despite the small reduction of dietary energy intake may be due to the sudden exposure to *ad libitum* feed supply. Furthermore, mice infected with either low or high-dose of *M. tuberculosis* (H37Rv) infection, the overall energy intake by the control mice was higher although an overall body weight reduction was observed (Figure 6.4 A, B, D & E). The lower body weight gain (1.56%) of control mice against their calculated higher energy intake (19.39%) in low-dose of *M. tuberculosis* (H37Rv) infection suggested a feed waste. These findings were further supported by the observation in low-dose of *M. bovis* (BCG) infection, where the body weight of control mice was almost constant although 31.33% energy intake reduction was determined (Figure 6.3 A & B). However, control mice infected with the high-dose of mycobacteria lose more body weight which was contributed by both less energy intake and effect of the infections as mice were found lethargic during infection.

In diabetic mice, an overall reduction of energy intake was recorded following both high or low-doses *M. tuberculosis* (BCG) and *M. bovis* (BCG) infection. The decrease in body weight pi reflected this diminished feed intake (Figure 6.3 and 6.4 A, B, D & E). Diabetic mice infected with low-dose *M. fortuitum*, increased their feed and energy intake during the pi period (Figure 6.2 A). Mice on the EDD were provided with *ad libitum* feed during the pre-infection period and the amount consumed was determined weekly. The reason for the apparent higher feed intake may be due to feed wastage.

A reduction in body weight in *M. fortuitum*, *M. bovis* (BCG) and *M. tuberculosis* (H37Rv) infected mice was more noticeable in diabetic mice compared to control mice (Figure 6.2, 6.3 and 6.4 B & E). As expected weight reduction was higher in high-dose than low-dose infections.

The greatest reduction in body weight was in *M. tuberculosis* (H37Rv) infected animals. This may be related to organism virulence or differences in infectious doses. The overall reduction in body weight in diabetic mice is likely due to the impact of infection on the desire for feed consumption. Anorexia is a typical feature of infection-induced sickness behavior. During the infection period diabetic mice displayed more severe lethargy and sickness compared to controls (Parti et al., 2005).

Systemic blood glucose levels in diabetic animals decreased pi with low- and high-dose *M. fortuitum, M. bovis* (BCG) and *M. tuberculosis* (H37Rv) (Figure 6.2, 6.3 and 6.4 C & F). This drop-in blood glucose level corresponded to the overall reduced energy intake and body weight reduction. The blood glucose also fell in control mice infected with high-dose *M. fortuitum*, *M. bovis* (BCG) and *M. tuberculosis* (H37Rv) infection although in low-dose infected control animals the level actually increased above the pre-infection level (0 week). The sudden upward shift in glucose in the control group may be explained by the introduction of the *ad libitum* rather than controlled feed supply. For both control and diabetic mice infected with high-dose *M. fortuitum, M. bovis* (BCG) or *M. tuberculosis* (H37Rv) infection, the blood glucose level fell in the first few weeks pi and this corresponded with lower energy intake, body weight loss and increased mortality during this period. At the later timepoints of the infection period blood glucose levels in both diabetic and control mice were restored to, or surpassed, pre-infection levels, suggesting that mice had started to recover from the infections. Martens and colleagues (2007) found no significant difference in blood glucose level between control mice and streptozotocin (STZ)-induced diabetic mice following an aerosolised infection with *M. tuberculosis* (Erdman). This finding contradicted the findings of the current study however differences in dose, route of infection and the diabetes model used may explain these differences.

There was no difference in the 60 days survival of diabetic *versus* control mice infected with low-dose *M. fortuitum* (Appendix 4, Figure A4.2). Parti and colleagues (2005) found minimal mortality of BALB/c mice infected intravenously with $5x10^7$ *M. fortuitum*/mouse. In our study, we used a *M. fortuitum* dose 5 times lower than the dose used by Parti and co-workers (2005). Increased mortality was observed at 14 dpi following high-dose *M. fortuitum* infection (Figure 6.5 A). Parti and co-workers (2005) observed 40-50% mortality after 60 dpi when the mice were infected with $5x10^8$ CFU/mouse. This observation was consistent with the findings of the current study, in which 58.53% mortality was recorded for control mice infected with $3x10^8$ CFU/mouse.

No mortality was recorded in either diabetic or control mice infected with low-dose *M. bovis* (BCG, $1x10^6$ CFU) or *M. tuberculosis* (H37Rv, $4x10^6$ CFU) over 30/35 dpi (data not shown). Other study reports similar findings for 100 days survival following *M. bovis* (BCG; 10^7 CFU) or *M. tuberculosis* (H37Rv; 10^5 CFU) intravenous infections in non-diabetic mice (Olleros et al., 2005), which supported the findings of this study. In contrast, Maeurer and colleagues (2000) showed some BALB/c mice infected intravenously with $3x10^6$ *M. tuberculosis* succumbed to infection by 30 dpi with the majority of animals dead by 60 dpi. This finding supported the observations of high-doses *M. bovis* and *M. tuberculosis* infection, in which we observed a higher mortality of both diabetic and control mice by 60 dpi (Figure 6.5 B & C).

Several previous studies have investigated the survival of diabetic animals during *M. tuberculosis* infections (Saiki et al., 1980, Podell et al., 2014, Cheekatla et al., 2016), although to our knowledge, no studies have investigated mortality during *M. fortuitum* and *M. bovis* (BCG) infections. An overall higher mortality was observed in diabetic mice infected with *M. fortuitum*, *M. bovis* (BCG) and *M. tuberculosis* (H37Rv) (Figure 6.5 A, B & C). A recent study demonstrated that 100% of STZ+ NA-induced diabetic C57BL/6 mice infected with *M. tuberculosis* via the aerosol route, died after 10 months pi, whilst only 6.6% of the control mice died by this same timepoint (Cheekatla et al., 2016). Saiki and colleagues (1980) observed that 60 days mortality of *M. tuberculosis* infected STZ-induced ICR diabetic mice was higher compared to controls (>90 *vs* 30%). In the guinea pig model of TB-diabetes comorbidity, the survival time of *M. tuberculosis* infected STZ-induced diabetic guinea pigs was decreased compared to controls (Podell et al., 2014). These authors reported that 60% diabetic guinea pigs died by 45 dpi (aerosolised *M. tuberculosis*) compared to 50% death of control animals over 145 days. The early death of diabetic guinea pigs compared to diabetic mouse is likely to be due to differences in host-mycobacterial susceptibility, routes of infection, disease progression and immune responses (Gupta and Katoch, 2005, Ordway and Orme, 2011). Hodgson and colleagues (2013b) observed higher mortality in DID mice following infection with the intracellular Gram-negative *Burkholderia pseudomallei*. Overall, these previous studies support the findings of the current study with higher mortality in diabetic mice compared to controls. Studies on TB-T2D co-morbidity in humans showed that diabetics infected with TB have a 6.5-7% (Oursler et al., 2002, Dooley and Chaisson, 2009), 12.2% (Wang et al., 2009) or 16% (Lindoso et al., 2008) higher chance of death compared to non-diabetic individuals.

We also investigated the bacterial burden in different organs of diabetic and control mice following infection with *M. fortuitum, M. bovis* (BCG) and *M. tuberculosis* (H37Rv). Following

intravenous infection with all species, we observed a disseminated infection in both diabetic and control mice characterised by an initial increase in bacterial load in lungs, spleen and liver followed by a progressive reduction (Figure 6.6 and 6.7). The kinetics of *M. fortuitum* infection in our study was consistent with the trends described in previous reports (Parti et al., 2005, Silva et al., 2010). The *M. fortuitum* kinetics described in the current study were different from those reported by Orme and Collins (1983) for other NTM such as *M. kansaii* and *M. avium*, where a peak in bacterial burden was observed at 40 dpi. This difference may be due to the differences of surface lipid components of the cell wall and subsequent host recognition and responses by different NTM (Maeda et al., 2003, Honda et al., 2015). The kinetics of *M. bovis* (BCG) and *M. tuberculosis* (H37Rv) infection in the current study showed similar trends to those described previously (North and Izzo, 1993, North, 1995, Lagranderie et al., 1996, Beamer and Turner, 2005, Singhal et al., 2011). A higher bacterial burden in organs was observed in *M. tuberculosis* (H37Rv) infected mice compared to *M. bovis* (BCG) infected mice (Figure 6.7). The organ bacterial burden decreased slowly from 14 dpi to 30 dpi in *M. tuberculosis* (H37Rv) infected mice compared to *M. bovis* (BCG) infected mice. In the current investigation, a 4 times higher infective dose was used in *M. tuberculosis* (H37Rv) infected mice compared to *M. bovis* (BCG) infected mice. A higher organ bacterial load in *M. tuberculosis* (H37Rv) infected mice compared to *M. bovis* (BCG) infected mice might be due to the dose difference. However, the growth and survival of the bacteria in organs also depends on the nature and virulence of the organism, as well as organism specific immune responses (North and Izzo, 1993, Fulton et al., 2000, Sherman et al., 2004). Prior research demonstrated that mice infected with *M. tuberculosis* intravenously develop a chronic, progressive infection (North and Jung, 2004, Orme, 2005, Basaraba, 2008) with the presence of non-replicating bacilli (Munoz-Elias et al., 2005) and that bacterial numbers do not change appreciably over a long period of time (Rhoades et al., 1997, Ordway and Orme, 2011). Mice can control *M. bovis* (BCG) load more efficiently than virulent *M. tuberculosis* (H37Rv) with *M. tuberculosis* more able to evade host bactericidal immune responses (North and Izzo, 1993, Fulton et al., 2000).

One of the Aims (2) of this study was to compare the organ mycobacterial load in diabetic and control mice. We observed a significantly higher bacterial burden in the spleen, liver and lungs of diabetic mice compared to controls infected with *M. fortuitum*. *M. bovis* (BCG) and *M. tuberculosis* (H37Rv) at 14 and 30/35 dpi (Figure 6.6 and 6.7). Yamashiro and colleagues (2005) first observed a higher bacterial burden in the spleen, liver and lungs of STZ-induced diabetic mice compared to controls infected intravenously with *M. tuberculosis* (H37Rv) at 14 and 35 dpi. A similar pattern of bacterial burden in spleen, liver and lungs was observed in

STZ-induced diabetic mice compared to controls when the mice were infected via the aerosol route with *M. tuberculosis* (H37Rv) (Cheekatla et al., 2016). A higher *M. tuberculosis* burden in lungs was observed in STZ-induced diabetic mice infected aerogenically by the prior research (Martens et al., 2007, Vallerskog et al., 2010). Sugawara and colleagues (2004) observed a higher bacterial burden in lungs and spleen of spontaneously induced GK/Jcl diabetic rats compared to controls infected aerobically with *M. tuberculosis* (kurono strain) at 1, 3, 7 and 12 weeks of infection. A higher *M. tuberculosis* (kurono strain) burden was reported in the lungs and spleen of rats with T1D at 7 weeks of infection (Sugawara and Mizuno, 2008). In an STZ-induced pig model of TB-DM co-morbidity, a significantly higher bacterial burden was found in spleen, liver, lungs and lymph nodes of diabetic guinea pig compared to controls aerobically-infected with low-dose *M. tuberculosis* (H37Rv) at 30 dpi (Podell et al., 2014). Podell and colleagues (2014) also observed a higher organ bacterial load in mice with impaired glucose tolerance at 60 and 90 dpi compared to controls. Higher organ loads were demonstrated in DID mice infected with *Burkholderia pseudomallei* (Hodgson et al., 2011, Hodgson et al., 2013b). All these observations are consistent with our findings and suggest that diabetic individuals are less efficient in controlling and clearing infections and hence more susceptible to mycobacterial infection compared to non-diabetic patients. Impaired phagocytosis and dysregulated secretion of key cytokines may explain this phenomenon (as described in Chapter 5).

In this study, we observed lower survival (higher mortality) of diabetic mice compared to controls in high-dose infections with *M. fortuitum*, *M. bovis* (BCG) and *M. tuberculosis* (H37Rv). When mice were infected with low-dose mycobacteria to determine the kinetics of infection, we observed higher organ bacterial loads in spleen, liver and lungs of diabetic mice compared to controls. The precise defects responsible for this increased susceptibility to mycobacterial infection remain unclear. In Chapter 7 we will describe the gross and histological changes that occur in organs during these mycobacterial infections and explore differences that may underlie this increased susceptibility.

CHAPTER 7
EFFECT OF TYPE 2 DIABETES ON TISSUE INFLAMMATION DURING MYCOBACTERIAL INFECTIONS

7.1 Introduction

Inflammation is essential to the control of microorganisms, but excessive or dysregulated inflammatory responses can disrupt the function of tissues. Mycobacterial infections, particularly *M. tuberculosis* infection, are accompanied by intense local (primarily in the lungs) and chronic responses which are critical to the disease pathogenesis (Toossi, 2000). Following infection with mycobacteria, the primary encounter is mediated by phagocytosis of bacilli by macrophages (Dheda et al., 2010). During this process, macrophages trigger inflammation via the secretion of various cytokine and chemokines for attracting more inflammatory cells to the sites of infection (Dheda et al., 2010, Cooper et al., 2011). These inflammatory mediators activate the adaptive immune responses and determine the fate of infection. With the intricate interplay between the host innate and adaptive immune cells, granulomas are formed (Saunders and Britton, 2007, Korbel et al., 2008) which are considered the hallmark of TB infections (Silva Miranda et al., 2012). Immune cells within the granuloma prevent further bacterial dissemination as well as reactivation of bacilli (Saunders and Cooper, 2000, Ehlers, 2009).

Existing data suggest a role for inflammation in the pathogenesis of T2D which is now considered to be a chronic inflammatory disease characterised by an exaggerated and dysregulated inflammatory response. Components of the immune system are altered in obesity and T2D with the most significant changes occurring in adipose tissue, liver, pancreatic islet, the vasculature and in circulating leucocytes. Metabolic disturbances including impaired insulin secretion and sensitivity and resulting loss of glucose homeostasis are increasingly being attributed to the inflammatory process. Oxidative stress, lipid deposition in muscle, liver and pancreas, amyloid deposition in pancreas, lipotoxicity and glucotoxicity may induce an inflammatory response or are exacerbated by or associated with inflammation. Immune dysregulation in T2D is believed to play a significant role in the increased susceptibility of T2D individuals to infections (Hodgson et al., 2015).

Type 2 diabetes is considered one of the most significant co-morbidities associated with increased TB susceptibility (Jeon and Murray, 2008, Martinez and Kornfeld, 2014). Effective protective immunity against TB appears to be lost in individuals with T2D as a consequence of their dysregulated inflammatory and immune response networks (Sasindran and Torrelles,

2011). Hence individuals with T2D may mount inappropriate immune responses against the invading organism that cannot control the bacterium or its dissemination and at the same time tissues may become damaged and dysfunctional.

In the previous Chapters (5 and 6) of this thesis, it has been demonstrated that diabetic macrophage function is impaired, cytokines are dysregulated and diabetic hosts have increased susceptibility to mycobacterial infections compared to non-diabetic controls. What happens in tissues infected with mycobacteria is the subject of this Chapter.

Other studies have identified higher inflammatory lesions in the lungs of streptozotocin (STZ)/STZ+NA (Nicotinamide) induced type 1 diabetic (T1D) mice compared to controls following aerosol infection with *M. tuberculosis* (Martens et al., 2007, Vallerskog et al., 2010, Cheekatla et al., 2016). Similarly, Sugawara and Mizuno (2008) and Sugawara and colleagues (2004) observed larger lung granulomas in T1D and T2D Goto Kakizaki (GK) rats following *M. tuberculosis* infection. Only lung pathology was examined in these studies, although extrapulmonary TB is also an important clinical manifestation in patients with TB (Knechel, 2009). In a guinea pig model of diabetes induced by high-fat high-carbohydrate (HFHC)+STZ, lung and spleen inflammatory lesions were quantified at 30, 60 and 90 days post-infection (dpi) (Podell et al., 2014) although there was minimal detailed data regarding the size and numbers of granulomas in these tissues. The authors did not include any earlier timepoints. Many of the key immunological events that influence infection outcome and disease progression occur within 3-4 weeks of infections (Ordway and Orme, 2011), however, analysis of tissue inflammation at early timepoints post-infection is currently lacking.

Previous research has shown that in immunocompetent individuals with TB infection, granulomas are small, compact and characterised by the presence of a signfiicant number of IFN-γ producing CD4T cells. In contrast to immunodeficient individuals, the TB granuloma is larger in size, rich in activated macrophages and with few surrounding lymphocytes. These granulomas are unable to effectively control and confine the infection (Ulrichs et al., 2005). One of the key reasons for tissue injury and clinical manifestations of pulmonary TB is the large caseating granuloma and fibrotic scarring which is also driven by granulomatous inflammation (Sasindran and Torrelles, 2011). There are controversies as to the impact of diabetes in the development of extrapulmonary TB. The relative risk of extrapulmonary TB progression is similar or less to that of non-diabetic patients (Long et al., 1997, Leung et al., 2008, Knechel, 2009, Young et al., 2012). Clearly, there are many gaps in our knowledge of the precise relationships between diabetes and control of the tuberculosis organism within tissues.

We hypothesised that the reason for increased mortality and higher bacterial burden in organs of diabetic mice (Chapter 6) was due to dysregulated inflammation followed by defective/delayed granuloma formation. Therefore, in this Chapter, we studied the gross and histopathological lesions in lungs (pulmonary) and liver (extra-pulmonary) in diet-induced T2D mice during infections with *M. fortuitum, M. bovis* (BCG) and *M. tuberculosis* (H37Rv). Previous reports have indicated that in *M. fortuitum* infection, kidneys are one of the preferred niches above other organs (Saito and Tasaka, 1969, Parti et al., 2005). Therefore, kidneys were also included in the current study. The findings of this study will increase our understanding of the reasons for increased mycobacterial susceptibility in T2D patients with concomitant mycobacterial infections.

The specific Aims of this research described in this Chapter are:

1. To investigate the gross pathological changes in spleen, liver, lungs and kidney of T2D mice following infection with low- and high-dose *M. fortuitum*
2. To evaluate the histopathological changes in liver, lungs and kidneys of T2D mice following infection with low- and high-dose *M. fortuitum*
3. To assess the gross pathological changes in spleen, liver and lungs of T2D mice following infection with low-dose *M. bovis* (BCG) and *M. tuberculosis* (H37Rv)
4. To measure the histopathological changes in liver and lungs of T2D mice following infection with low-dose *M. bovis* (BCG) and *M. tuberculosis* (H37Rv)

7.2 Materials and Methods

7.2.1 Animal Ethics and institutional approvals

The details of animal ethics and institutional approvals are described in Chapter 3 (section 3.1.1).

7.2.2 Experimental animals and induction of diabetes

The details of experimental animals and induction of diabetes are described in Chapter 3 (section 3.1.3) and Chapter 6 (section 6.2.2).

7.2.3 Preparation of mycobacterial culture for infection

The details of the preparation of mycobacterial culture for infection are described in Chapter 3 (section 3.3.2) and Chapter 6 (section 6.2.3.1).

7.2.4 Monitoring and culling of infected mice

The details of monitoring and culling of infected mice are described in Chapter 6 (section 6.2.4).

7.2.5 Gross and histopathological examinations

Following infection with *M. fortuitum*, *M. bovis* (BCG) and *M. tuberculosis* (H37Rv), mice were monitored once daily until the end of the study. Infected mice were sacrificed at 1, 14 and 30 (for *M. tuberculosis* infection) or 35 days post-infection (dpi). The whole organs, namely spleen, liver, lungs and kidney (*M. fortuitum* only) were weighed, observed and photographed for the presence of gross lesions. For histopathological examination, liver (after removing 1 g for bacterial count), left lobe of lungs and both kidneys were collected in 10% neutral buffered formalin (NBF). Tissue sections; liver and lungs and kindneys (only for *M. fortuitum* infection study) were prepared from formalin fixed tissue for Haematoxylin and Eosin (H&E) staining (Chapter 3, section 3.5).

The relative percentage of the inflamed area on the liver sections were quantified according to previously described methods (Flynn et al., 1998, Chambers et al., 2006, Silva et al., 2010). Briefly, the number of inflammatory foci/granulomas was counted on 10 continuous microscopic fields (200x magnification) per slide. The relative percent of inflamed area with liver sections was calculated by measuring the total area of the inflammatory foci/granulomas over the total area of 10 microscopic fields (Chapter 3, section 3.5.5). The inflamed area within the lungs was evaluated on representative lung sections according to previously published methods (Schneider et al., 2010, Kupz et al., 2016). In short, the total area of a representative section was measured on images captured using 4x objectives (40x magnification). The inflamed area was calculated on the same lung sections by capturing images using 10x objectives (100x magnification). Inflammatory lesions in the kidney sections were not quantified. The CellSens® Image Analysis software (Olympus) was used for digital photography and quantitative analysis of the tissue sections (Chapter 3, section 3.5.5).

7.2.6 Tissue Ziehl-Neelsen staining for localisation of bacteria

Ziehl-Neelsen (ZN; acid-fast) staining of liver sections was performed at 14 and 30/35 days post-infection (dpi). Counting of acid-fast bacilli was done using previously published protocols (Chambers et al., 2006, Reynolds et al., 2009). In short, a representative liver section from each mouse was stained and visualised at 1000x magnification for counting the acid-fast bacilli within each of the inflammatory focus/granuloma. Individual ZN positive magenta

bacilli were counted in a total of first 10 positive inflammatory foci/ granulomas (presence of at least one bacterium) from each mouse section (Chapter 3, section 3.6).

7.3 Statistical analysis

The details of the statistical analysis are described in Chapter 6 (section 6.3).

7.4 Results

7.4.1 Organ pathology following mycobacterial infections

7.4.1.1 Gross pathological findings in organs of *M. fortuitum* infected mice

Thirty-five days after low-dose ($1x10^7$) *M. fortuitum* infection, diabetic mice were found inactive and lethargic compared to the control mice. Gross morphology at 35 days post-infection (dpi) showed obvious splenomegaly and hepatomegaly in both controls (Figure 7.1 A, B & C) and diabetic mice. (Figure 7.1 F, G & H). Spleen weight was 2.57 and 3.11 times higher than the initial weight at 1 dpi for diabetic and control mice, respectively (Figure 7.2 A). Liver weight increased gradually in diabetic and control mice at 14 and 35 dpi compared to the initial weight measured at 1 dpi (Figure 7.2 B). Lungs appeared larger in diabetic mice (Figure 7.1 I) although lungs weight remained similar for both groups throughout the infection period (Figure 7.2 C). Kidneys from diabetic mice were noticeably paler and appeared distended compared to those from control mice (Figure 7.1 E & J). Kidney weight at 35 dpi was significantly higher than weight at 14 dpi (1.13 and 1.09 times higher for diabetic and control mice, respectively) (Figure 7.2 D).

When mice were infected with high-dose ($3x10^8$) *M. fortuitum*, diabetic mice were observed to be more inactive and lethargic compared to control mice. Spleen, liver, lungs and kidneys were harvested from moribund mice at 14 dpi and weighed and observed for gross lesions. Splenomegaly was a common finding in both groups (Figure 7.3 B & G). Livers of both diabetic and control mice were enlarged and abscess-like lesions were found across the surface of liver lobes of both groups, although the numbers of lesions were higher in diabetic mice (Figure 7.3 C & H). Congested, haemorrhagic foci and distended lungs were observed in both groups of mice (Figure 7.3 D & I). Kidneys of diabetic mice were found more distended and were extremely pale compared to controls (Figure 7.3 E & J). Moreover, in some diabetic mice, pus-like semi-solid masses were revealed upon incision of the kidneys.

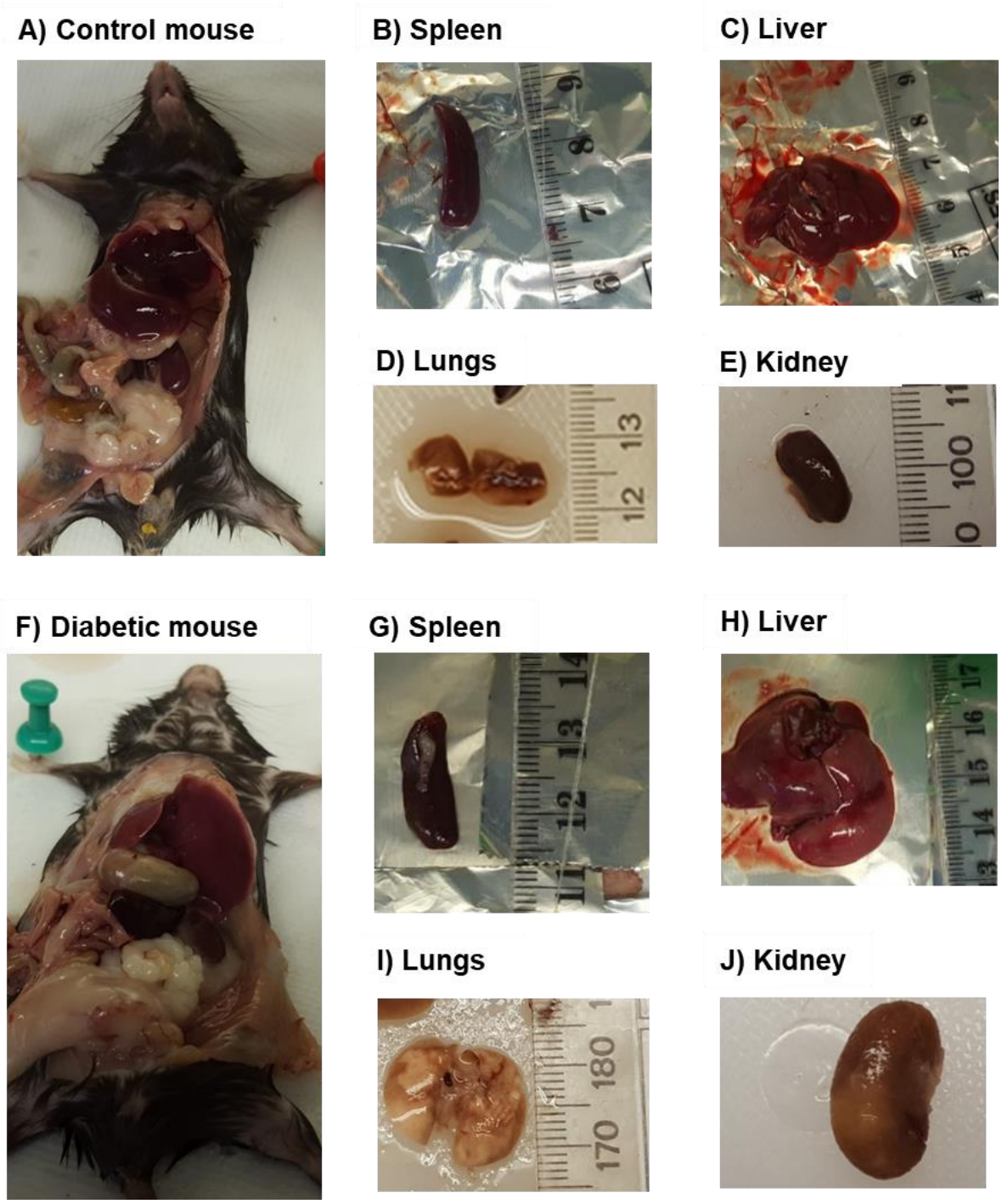

Figure 7.1 Gross pathological findings following low-dose *M. fortuitum* infection

Mice infected with low-dose ($1x10^7$) *M. fortuitum* were sacrificed at 1, 14, 35 days post-infection (dpi). Splenomegaly and hepatomegaly were evident in both control and diabetic mice at 14 (not shown in this figure) and 35 dpi. Images showed the dissection of a control mouse (A) at 35 dpi demonstrating splenomegaly (B), hepatomegaly (C), lungs (D) and distended kidney (E). Similar types of gross lesions were also observed in diabetic mice at 35 dpi (F, G, H, I & J).

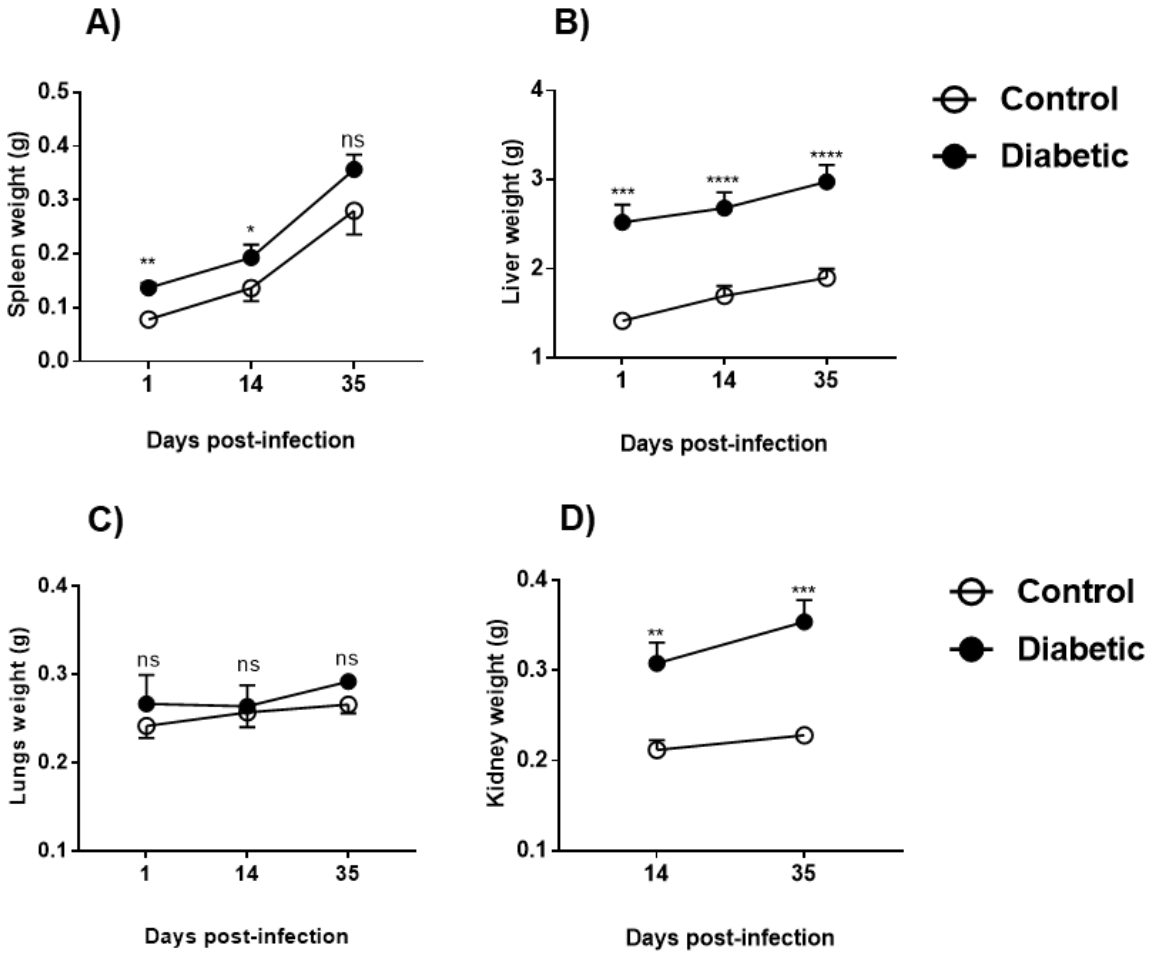

Figure 7.2 Weight of organs following low-dose *M. fortuitum* infection

Mice infected with low-dose ($1x10^7$) *M. fortuitum* were culled at 1, 14, 35 days post-infection (dpi). Spleen, liver, lungs and kidney (left) from both diabetic and control were weighed at all timepoints of infection. Splenomegaly (A) and hepatomegaly (B) were observed in both diabetic and control mice at 14 and 35 dpi. Lungs weight remained steady for both groups throughout the infection period (C). Moreover, an increasing trend of kidney weight was observed in both diabetic mice compared to controls (D). Data presented as mean±SEM; n=6-10 mice/group. Significant differences between the groups were determined using the independent sample *t*-test except for few non-normally distributed data sets. The non-normally distributed data were analysed using the Mann-Whitney U test (Appendix 4). The level of significance was indicated as *p≤0.05, **p≤0.01, ***p≤0.001,****p≤0.0001 and ns=non-significant.

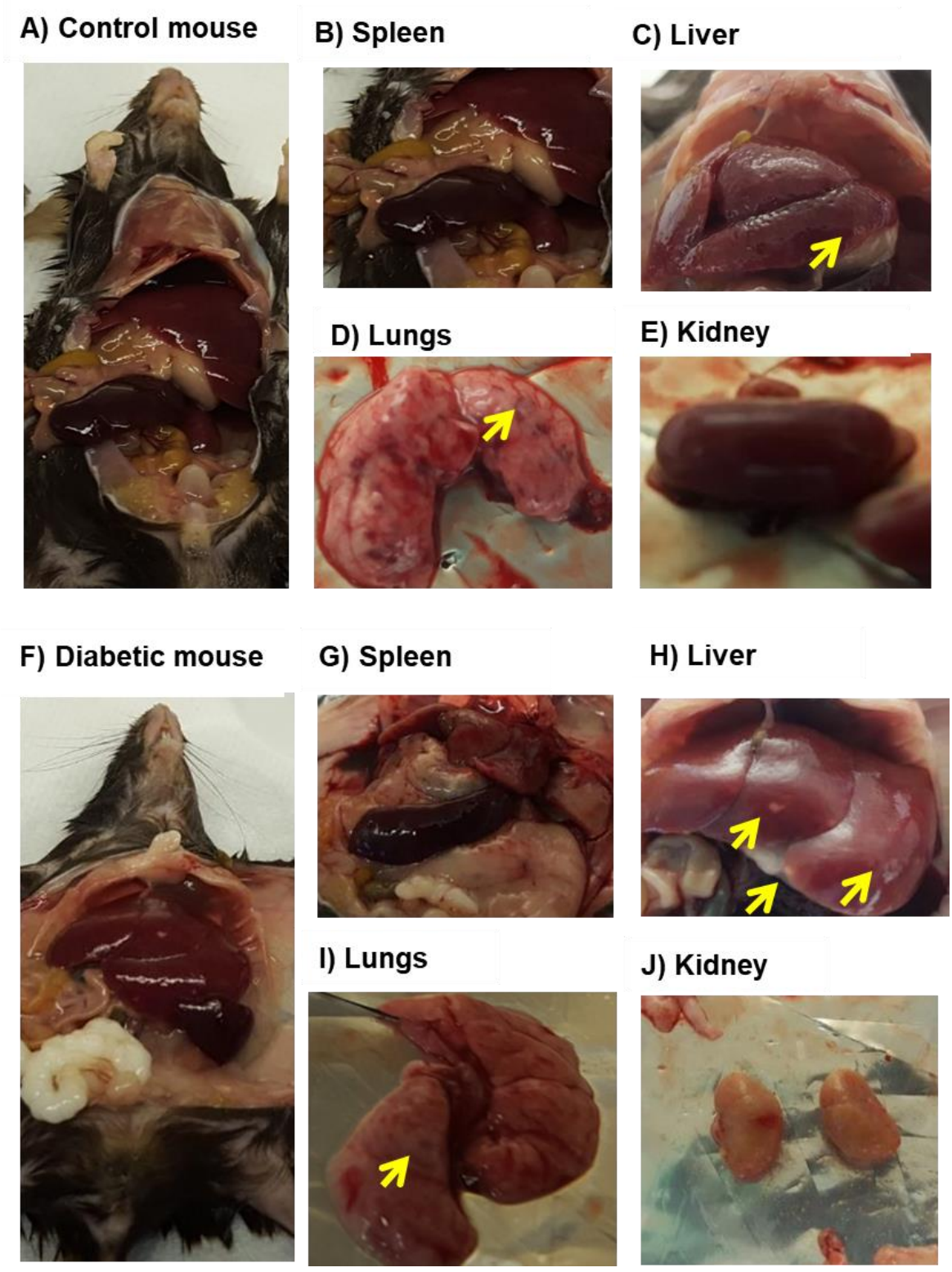

Figure 7.3 Gross pathological findings following high-dose *M. fortuitum* infection

Mice infected with high-dose ($3x10^8$) *M. fortuitum* were sacrificed at 14 days post-infection (dpi). Dissection of a control mouse was showing internal organs (A) along with marked splenomegaly (B), hepatomegaly (arrow indicates necrotic foci) (C), hemorrhagic and distended lungs (arrow indicates hemorrhagic foci) (D) and an enlarged kidney in control mice (E). Similar types of lesions were also observed in diabetic mice at the same timepoint of infection (F, G, H, I & J).

7.4.1.2 Gross pathological findings in organs of *M. bovis* (BCG) infected mice

Mice infected with 1x10^6 *M. bovis* (BCG) were sacrificed at 1, 14 and 35 days post-infection (dpi) and organs (spleen, liver and lungs) were weighed and visually observed for lesions. Splenomegaly and hepatomegaly was observed in both diabetic and control mice, however, there were no obvious lesions on the surface of the spleen and liver (Figure 7.4 A). The lungs of mice in both groups were found slightly congested and distended at 14 and 35 dpi (Figure 7.4 A).

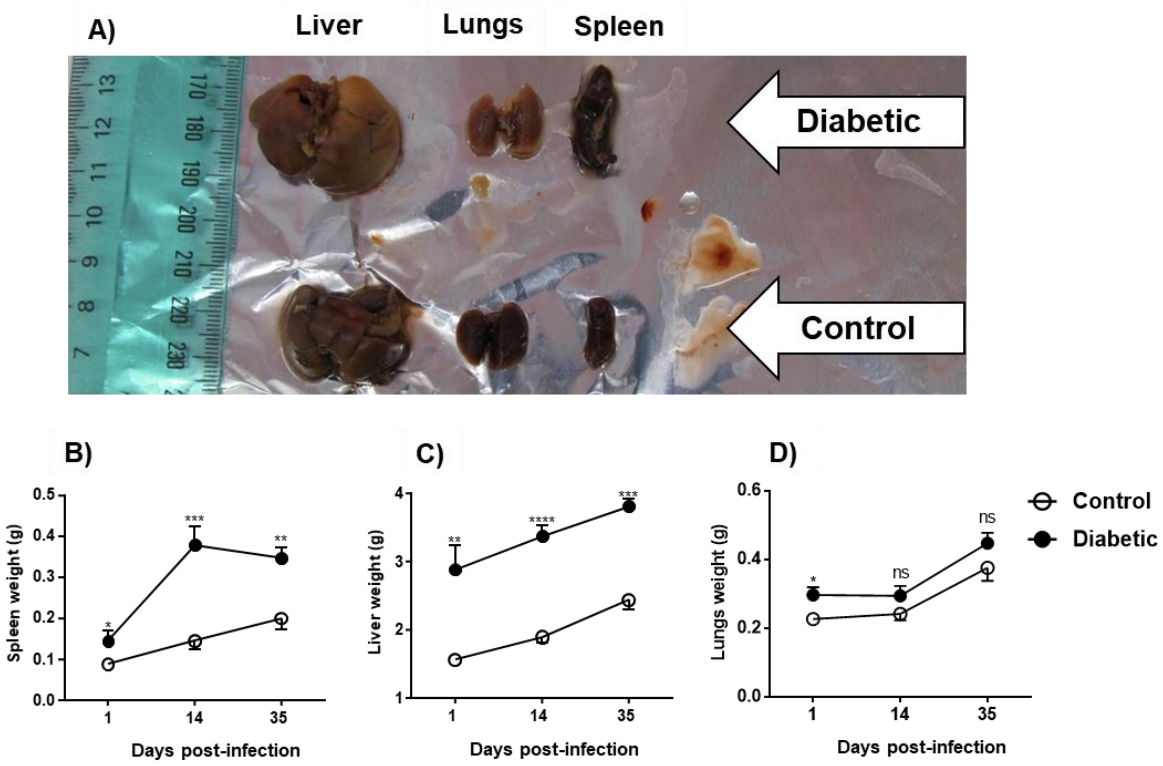

Figure 7.4 Gross pathological findings following *M. bovis* (BCG) infection

Mice infected with 1x10^6 *M. bovis* (BCG) were culled at 1, 14, 35 days post-infection (dpi). Splenomegaly and hepatomegaly were evident in both control and diabetic mice at 14 (not shown in this figure) and 35 dpi (A). Weighing of the spleen and liver demonstrated a marked splenomegaly (B) and hepatomegaly (C) in diabetic and control mice at 14 and 35 dpi compared to controls. The lungs weight slightly increased in both diabetic and control mice at the later timepoint of infection compared to 1 and 14 dpi (D). Data presented as mean±SEM; n=4-10 mice/group. The significant differences between the groups were determined using the independent sample *t*-test except for non-normally distributed data sets. The non-normally distributed data were analysed using the Mann-Whitney U test (Appendix 5). The level of significance was indicated as *p≤0.05, **p≤0.01, ***p≤0.001, ****p≤0.0001 and ns=non-significant.

Spleen and liver weights confirmed splenomegaly and hepatomegaly in both control and diabetic mice. (Figure 7.4 B & C). The highest weight increase of the spleen was recorded at 14 dpi with spleen from diabetic and control mice weighing 2.53 and 1.67 times more than their initial weights at 1 dpi (Figure 7.4 B). The liver weight increased gradually in both diabetic and control mice over the infection period (Figure 7.4 C). At 35 dpi, the weight of the liver increased 1.31 and 1.53 times in diabetic and control mice, respectively compared to the initial weight at 1 dpi (Figure 7.4 C). Lungs weight had increased by 35 dpi compared to 1 dpi although this did not reach significance (Figure 7.4 D).

7.4.1.3 Gross pathological findings in organs of *M. tuberculosis* (H37Rv) infected mice

Similar to *M. fortuitum* and *M. bovis* (BCG) infections, mice infected with $4x10^6$ *M. tuberculosis* (H37Rv) were monitored once daily. Mice were culled and organs samples were collected at 1, 14 and 30 days post-infection (dpi). Splenomegaly, hepatomegaly and distention and congestion of the lungs were common observations at necropsy of both diabetic and control mice (Figure 7.5). An abscess-like lesion was found on the surface of livers of all diabetic mice (Figure 7.5 D). Spleen and liver weight confirmed splenomegaly and hepatomegaly in both control and diabetic mice. (Figure 7.5 E & F). The highest weight increase of the spleen was found at 14 dpi, where spleen weight was 2.65 and 5 times higher than the initial weight at 1 dpi for diabetic and control mice, respectively. Liver weight increased gradually in diabetic mice although a decreasing trend was noticed for control mice after 14 dpi (Figure 7.4 F). At 35 dpi, the weight of the liver increased 1.42 and 1.35 times in diabetic and control mice, respectively compared to the initial weight at 1 dpi. The weight of diabetic and control mice lungs remained steady throughout the infection period. Although an increase in lungs weight was observed in diabetic mice at 14 dpi, this did not reach significance (Figure 7.5 G).

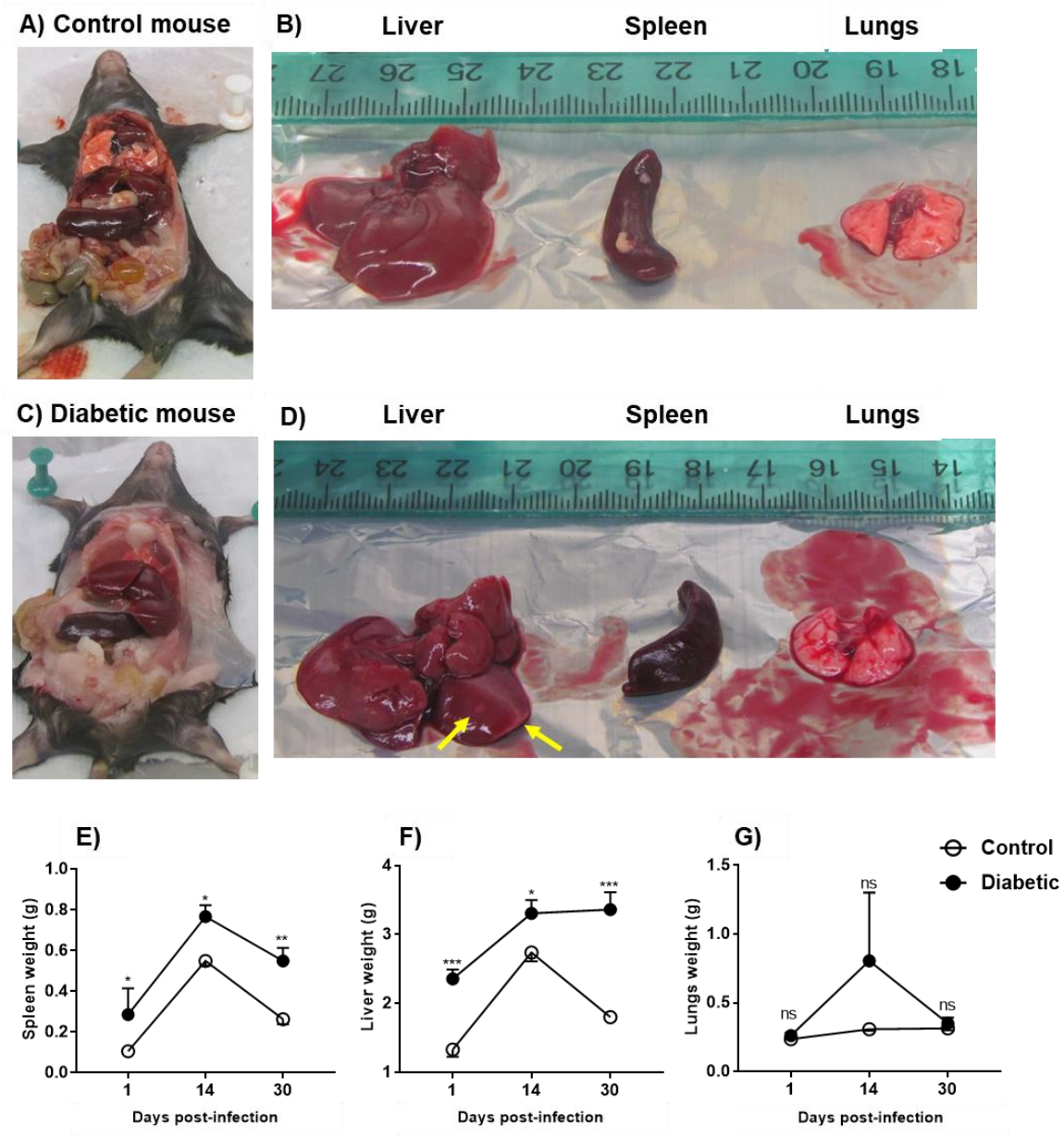

Figure 7.5 Gross pathological findings following *M. tuberculosis* (H37Rv) infection

Mice infected with $4x10^6$ *M. tuberculosis* (H37Rv) were sacrificed at 1, 14, 30 days post-infection (dpi). Splenomegaly and hepatomegaly were evident in both control and diabetic mice at 14 (A, B, C & D) and 35 dpi (not shown in this figure). In livers of all diabetic mice, abscess-like (yellow arrows) whitish spots were seen (D). Lungs of both control and diabetic mice were found slightly distended at later timepoints (B & D). Spleen and liver weights demonstrated a marked splenomegaly (E) and hepatomegaly (F) in both diabetic and control mice at 14 and 35 dpi. The lungs weight was remained steady throughout the infection period although a fluctuation was observed at 14 dpi in diabetic mice (G). Data presented as mean±SEM; n=5 mice/group. The significant differences between the groups were determined using the independent sample *t*-test except for non-normally distributed data sets. The non-normally distributed data were determined using the Mann-Whitney U test (Appendix 6). The level of significance was indicated as *p≤0.05, **p≤0.01, ***p≤0.001 and ns=non-significant.

7.4.1.4 Inflammatory lesions in liver following mycobacterial infections

7.4.1.4.1 Inflammation in liver of *M. fortuitum* infected mice

Following infection with low-dose *M. fortuitum* (*Mft*), histopathological examination revealed inflammatory cells and foci in the liver of both diabetic and control mice (Figure 7.7). At 1 day post-infection (dpi), a diffuse accumulation of inflammatory cells was observed in both diabetic and control groups (Figure 7.7 A & B). At 14 dpi, the number of inflammatory foci/granulomas was 2.21 times higher in diabetic mice than control mice (Figure 7.6 A and 7.7 C, D). The percent inflamed area in the liver was 2.78 times higher in diabetic mice compared to controls (Figure 7.6 B). At 35 dpi, a similar trend was observed for inflammatory foci/granuloma and percent inflamed area in the liver of diabetic mice compared to controls (Figure 7.6 A, B and Figure 7.7 E & F). The mean area of individual liver inflammatory focus at 14 and 35 dpi was higher in diabetic mice compared to controls (Figure 7.6 C and Figure 7.7 C, D, E & F).

At high-dose of infection, severe inflammatory responses were observed in the liver of both diabetic and control mice at 14 dpi (Figure 7.8 E & F). The number of inflammatory foci/granulomas was 2.10 times higher in the liver of diabetic mice compared to controls (Figure 7.8 A). The percent area of inflammation in the liver was 1.92 times higher in diabetic mice compared to controls (Figure 7.8 B). Furthermore, slightly smaller inflammatory foci/granulomas were found in the liver of diabetic mice compared to control although it was not statistically significant (Figure 7.8 C).

7.4.1.4.2 *M. fortuitum* in the inflammatory foci/granulomas

Ziehl-Neelsen staining of 35 dpi liver sections of infected mice demonstrated a higher number of bacilli per inflammatory focus/granuloma for diabetic mice compared to controls (Figure 7.6 D and Figure 7.7 G & H). Similar findings were noted in liver of diabetic and control mice 14 dpi with high-dose of *Mft* infection (Figure 7.8 D, G & H).

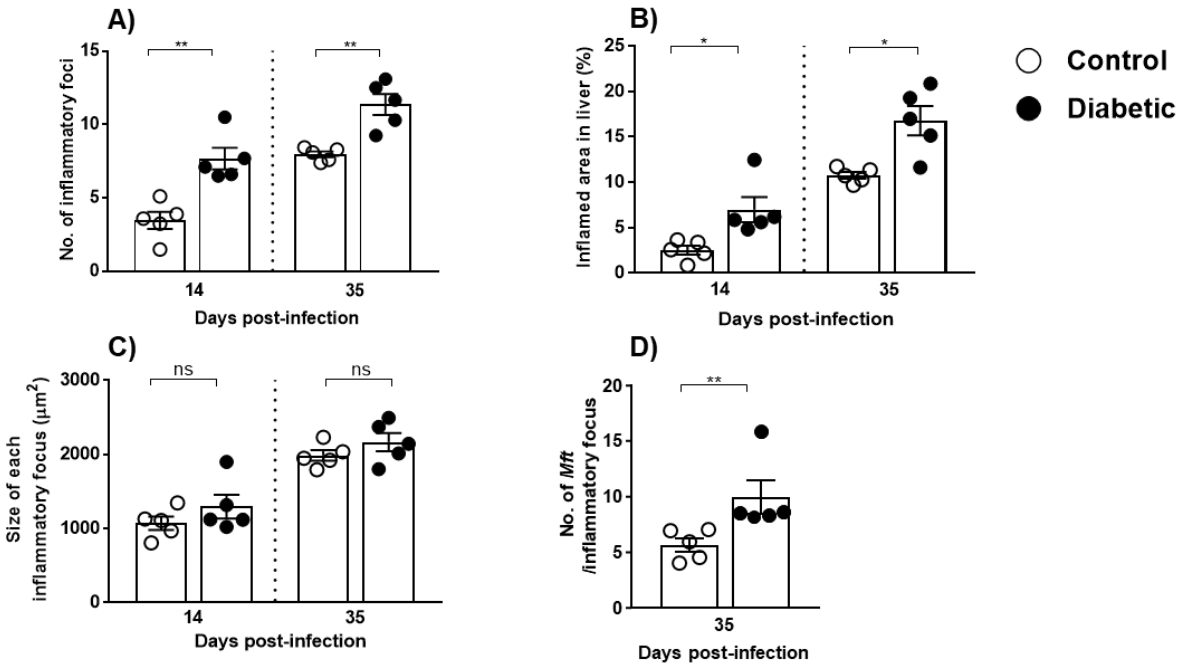

Figure 7.6 Inflammatory lesions in liver following low-dose *M. fortuitum* infection

H&E stained liver sections infected with low-dose *M. fortuitum* were used to assess the inflammatory lesions at 1, 14 and 35 days post-infection (dpi). Quantification of liver lesions demonstrated a significantly higher number of inflammatory foci (A) and percent inflamed area (B) in the liver of diabetic mice compared to control at both timepoints. The relative size of each inflammatory focus was higher in diabetic mice compared to controls (C). Ziehl-Neelsen staining demonstrated a higher number of acid-fast bacilli in each of inflammatory focus/granuloma of diabetic mice compared to controls (D). Data presented as mean±SEM, n=5 mice/group. The significant differences between the groups were determined using the independent sample *t*-test (A, B & C) and Mann-Whitney U test (D) (Appendix 4). The level of significance was indicated as *p≤0.05, **p≤0.01 and ns=non-significant.

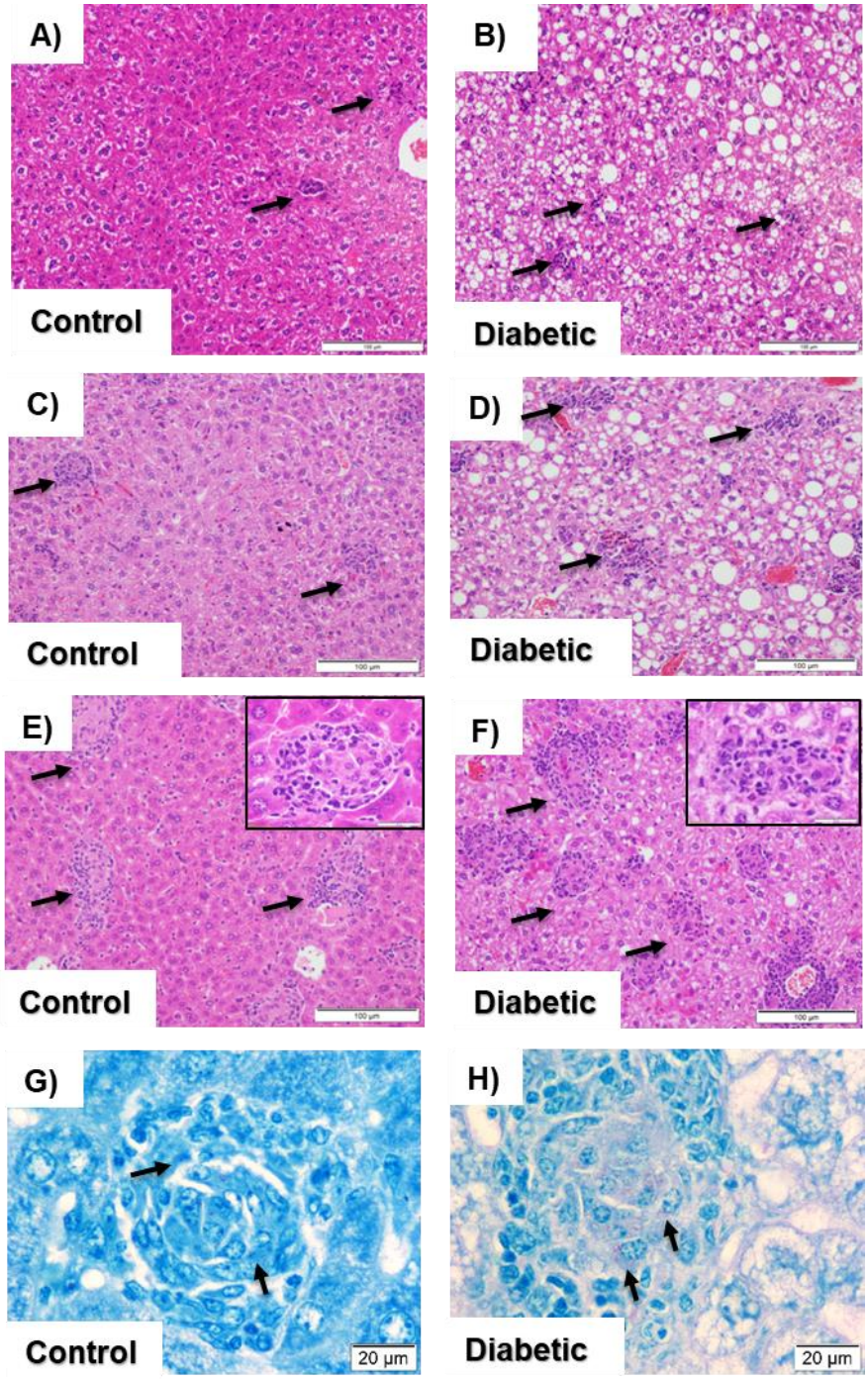

Figure 7.7 Inflammatory lesions and acid-fast bacill in the inflammatory foci of liver following low-dose *M. fortuitum* infection

H&E stained liver sections was used to assess the inflammation following infection with low-dose ($1x10^7$) *M. fortuitum*. A diffuse infiltration of inflammatory cells was observed in the liver of both diabetic and control mice at 1 day post-infection (dpi) (A & B; arrow indicates inflammatory cells). Compared to controls, a higher number of inflammatory foci/granuloma formation (arrow and insert image) in the liver of diabetic mice was evident in both 14 (C & D) and 35 dpi (E & F). Ziehl-Neelsen staining demonstrated a higher bacillary burden in each inflammatory focus/granuloma in liver of diabetic mice compared to controls (G & H). Images are representative of n=5 mice/group. Magnification of photomicrographs: A-F; 200x (scale bar 100 µm), insert images at 1000x (scale bar 20 µm). Images from other animals are in Appendix 4, Figure A4.3-A4.6.

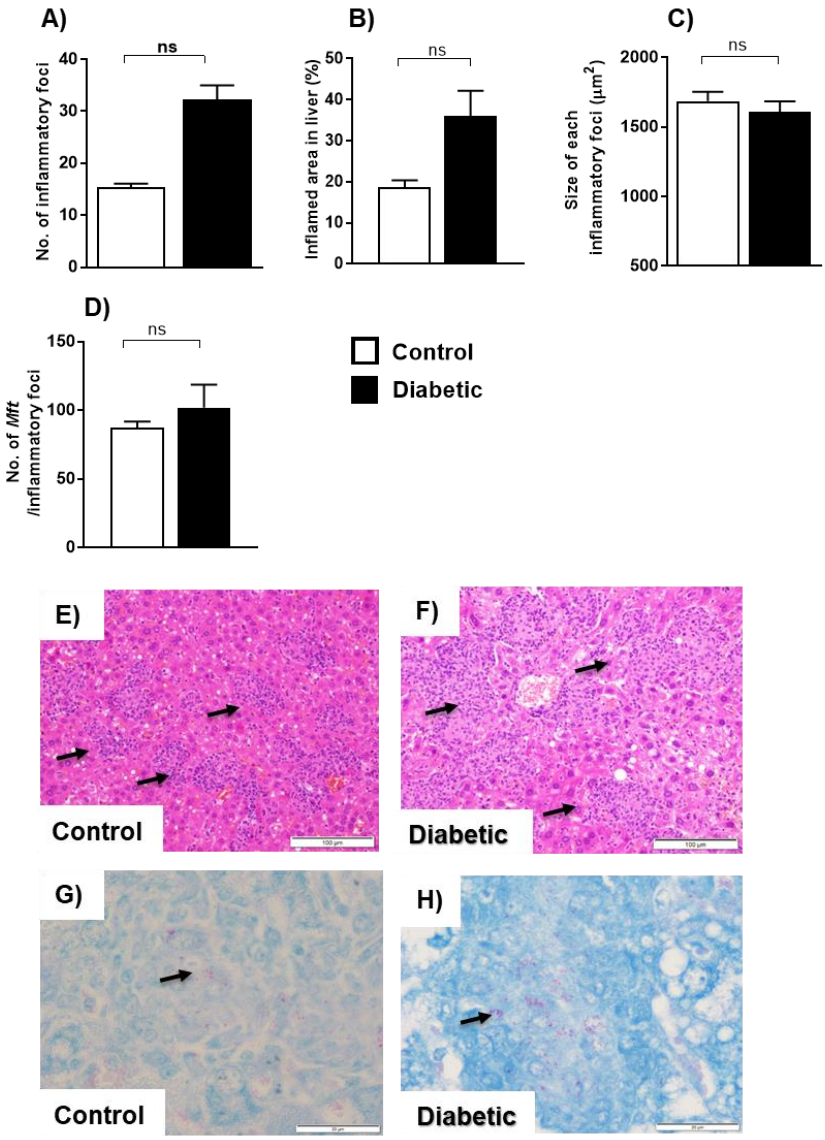

Figure 7.8 Inflammatory lesions and acid-fast bacill in the inflammatory foci of liver following high-dose *M. fortuitum* infection

H&E stained liver sections infected with high-dose *M. fortuitum* were used to assess the inflammatory lesions at 14 days post-infection (dpi). Quantification of liver lesions demonstrated a significantly higher number of inflammatory foci/granulomas (A) and percent inflamed area in the liver of diabetic mice compared to controls (B). The relative size of each inflammatory focus/granuloma was slightly lower in diabetic mice compared to controls (C). Ziehl-Neelsen (ZN) staining showed the presence of higher number of acid-fast bacilli in each inflammatory focus/granuloma of liver of diabetic mice compared to controls (D). However, the photomicrographs demonstrated the inflammatory aggregates (arrow) on liver section of both control (E) and diabetic mice (F) at 14 dpi. ZN stained liver sections demonstrated the presence of acid-fast bacilli (magenta) in an inflammatory focus/granuloma in liver of control (G) and diabetic mice (H) at the same timepoint of infection. Magnification of photomicrographs: E-F; 200x (scale bar 100 µm) and G-H; 1000x (scale bar 20 µm). Data presented as mean±SEM; n=2-3 mice/group. The significant differences between the groups were determined using the independent sample *t*-test (A, B, C & D) (Appendix 4). The level of significance was indicated as ns=non-significant. Images from other animals are in Appendix 4, Figure A4.11-A4.12.

7.4.1.4.3 Inflammation in liver of *M. bovis* (BCG) infected mice

Similar to *M. fortuitum* infection, histopathological examination revealed marked inflammation in the liver of *M. bovis* infected diabetic and control mice (Figure 7.9 D, E, F & G). At 1 day post-infection (dpi), a diffuse infiltration of inflammatory cells was observed in both diabetic and control groups (Appendix 5, Figure A5.2). The number of inflammatory foci/granulomas and inflamed area increased at later timepoints of infection (Figure 7.9 A & B). At 14 and 35 dpi, the number of inflammatory foci/granulomas in the liver was higher in diabetic mice compared to controls (Figure 7.9 A, D, E, F & G). The percent area of inflammation in the liver was 1.83 and 1.32 times higher in diabetic compared to controls at both 14 and 35 dpi, respectively (Figure 7.9 B, D, E, F & G). Moreover, the mean area of each inflammatory focus/granuloma at 14 and 35 dpi were greater in the liver of diabetic mice compared to controls (Figure 7.9 C).

7.4.1.4.4 *M. bovis* (BCG) in the inflammatory foci/granulomas

The Ziehl-Neelsen staining of the liver sections demonstrated the presence of higher number of bacilli in each of the inflammatory focus/granuloma of diabetic mice at both 14 and 35 days post-infection (dpi) compared to controls (Figure 7.10 A, B & C). This was not however statistically significant. Inflammatory cells in the foci/granulomas in liver of diabetic mice appeared to be more diffuse and less compact than those of control mice (Figure 7.10 B & C; dotted line indicates the area of a granuloma/inflammatory focus). In diabetic mice, bacilli were not only localised within the inflammatory foci/granuloma but were also found dispersed throughout the liver parenchyma and within cells (Figure 7.10 D). This localisation was quite different to what was observed for control mice, in which the majority of bacteria appeared to be contained within inflammatory foci (Figure 7.10 B). In diabetic liver, a higher number of bacilli was observed per infected cell compared to control liver, although bacilli/cell were not directly quantified (Figure 7.10 E).

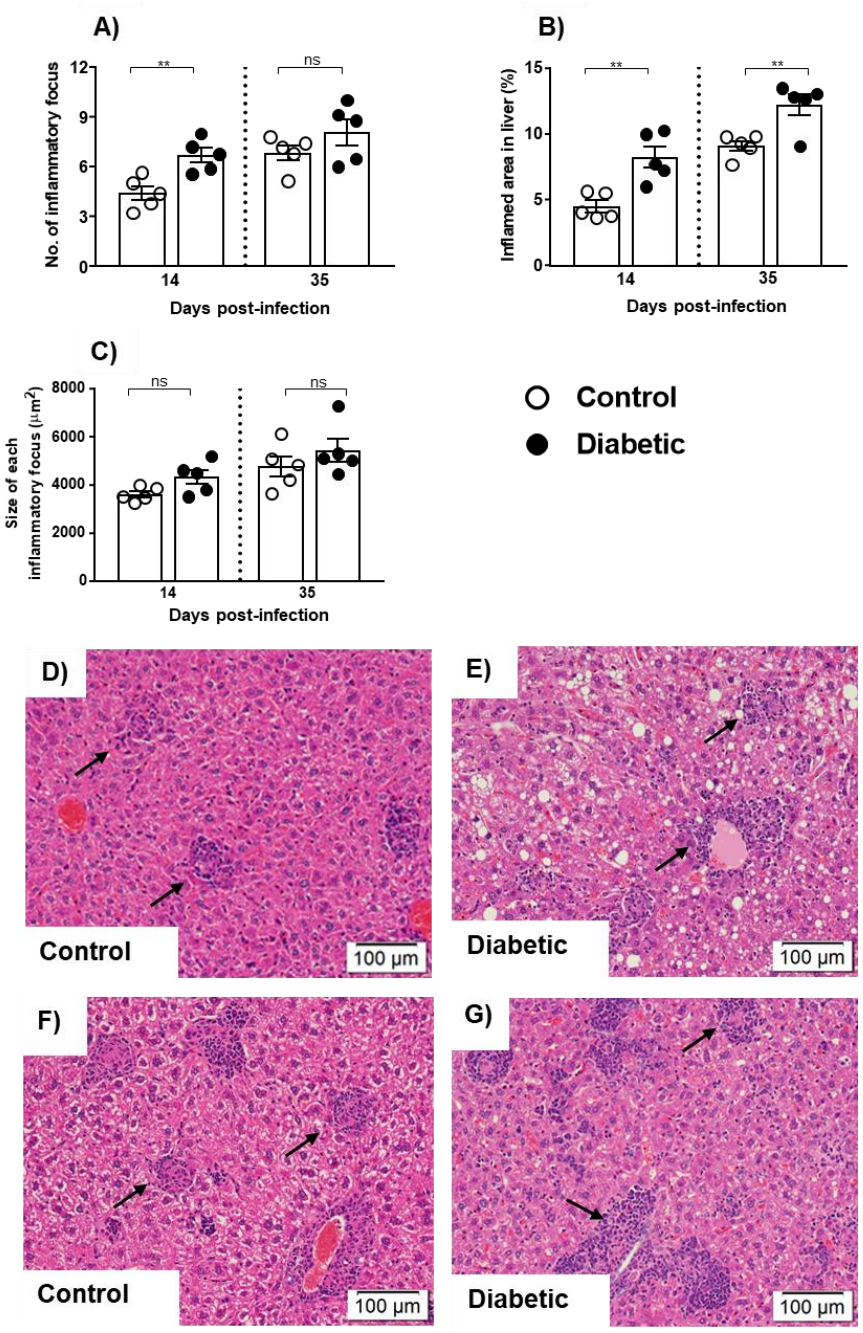

Figure 7.9 Inflammatory lesions in liver following *M. bovis* (BCG) infection

H&E stained liver sections infected with low-dose *M. bovis* (BCG) were used to assess the inflammatory lesions at 1, 14 and 35 days post-infection (dpi). Quantification of liver lesions at 14 and 35 dpi demonstrated a higher number of inflammatory foci/granulomas (A) and percent inflamed area (B) in the liver of diabetic mice compared to controls. The relative size of each inflammatory focus/granuloma was higher in diabetic mice compared to controls (C). Photomicrographs of the liver sections demonstrated inflammatory foci/granulomas at 14 (D & E) and 35 dpi (F & G) in diabetic and control mice. Magnification of photomicrographs: D-G; 200x (scale bar 100 µm). Data presented as mean±SEM; n=5 mice/group. The significant differences between the groups were determined using the independent sample *t*-test (A, B, & C) (Appendix 5). The level of significance was indicated as *p≤0.05, **p≤0.01 and ns=non-significant. Images of other animals are given in Appendix 5, Figure A5.2-A5.4.

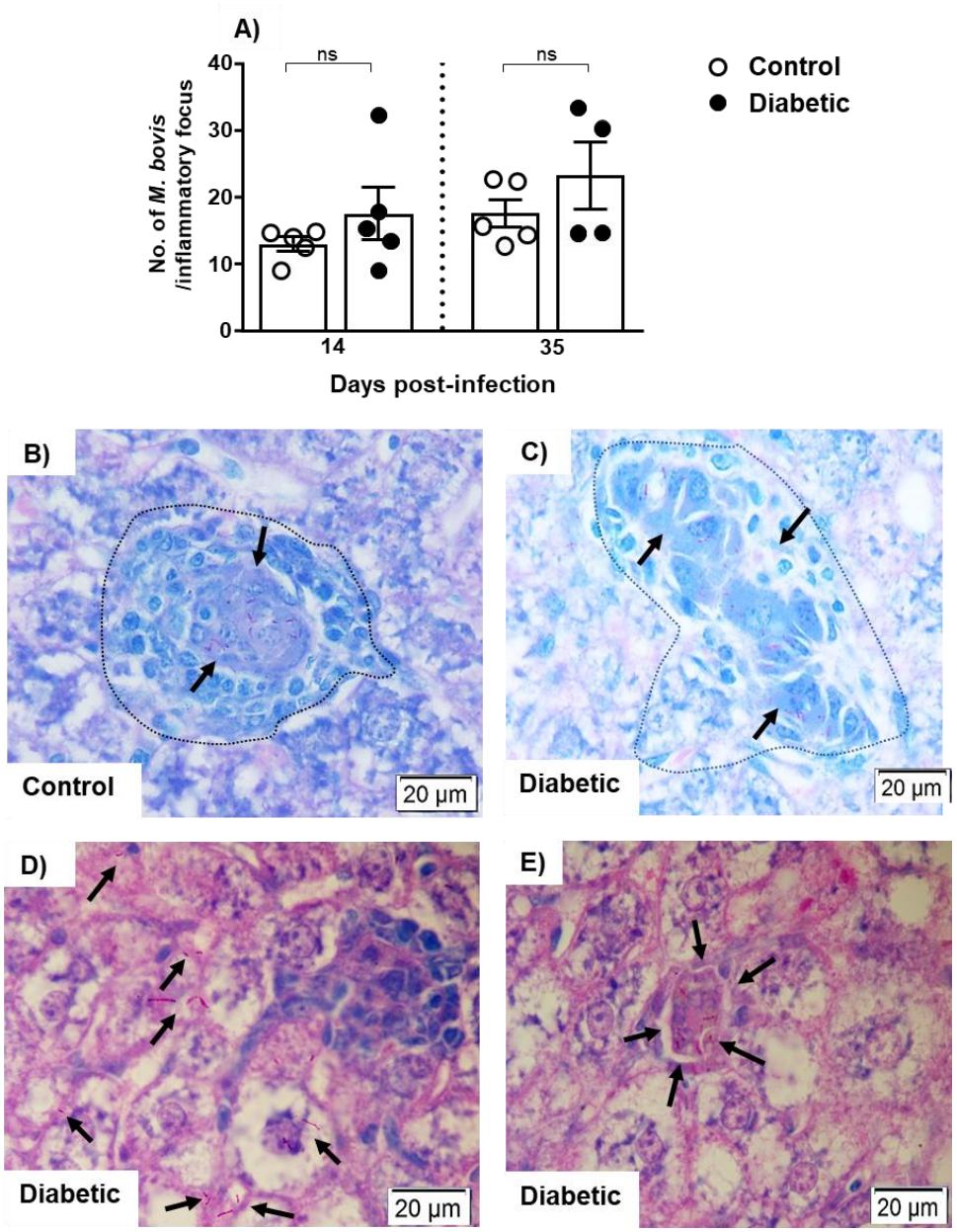

Figure 7.10 Acid-fast bacilli in inflammatory foci of *M. bovis* (BCG) infected mice

The Ziehl-Neelsen staining of liver sections infected with *M. bovis* (BCG) was performed at 1, 14 and 35 days post-infection (dpi). Quantification of the acid-fast bacilli demonstrated a higher number of *M. bovis* (BCG) in each inflammatory focus/granuloma in liver section of diabetic mice compared to controls (A). The photomicrographs demonstrated a relatively well-organised inflammatory or granuloma (demarcated by a dotted line) in the liver section of control mice with a lower number of bacilli (B). Whereas inflammatory cells in the granuloma/inflammatory foci of diabetic mice were loosely associated with a higher number of bacilli (C). In liver section of diabetic mice, bacilli were found more scattered across the liver parenchyma (outside of the granuloma/inflammatory foci) (D) and a higher number of the bacilli were also found in each infected cell (E). Magnification of photomicrographs: B-E; 1000x (scale bar 200 µm). Data presented as mean±SEM; n=4-5 mice/group. The significant differences between the groups were determined using the Mann-Whitney U test (A) (Appendix 5). The level of significance was indicated as ns=non-significant. Images from other animals are in Appendix 5, Figure A5.5-A5.6.

7.4.1.4.5 Inflammation in liver of *M. tuberculosis* (H37Rv) infected mice

In *M. tuberculosis* (H37Rv) infection, a strong inflammatory response was observed in the liver. At 1 day post infection (dpi), accumulation of inflammatory cells was evident throughout the liver sections of both diabetic and control mice (Appendix 6, Figure A6.2). This was similar to *M. fortuitum* and *M. bovis* (BCG) infection. At 14 dpi, there was no significant difference in the number of inflammatory foci/granulomas formation in the liver of diabetic mice compared to controls (Figure 7.11 A, D & E). The inflamed area was 1.38 times higher in the liver of diabetic mice compared to the control mice at the same timepoint (Figure 7.11 B, D & E). At 30 dpi, the number of inflammatory foci/granulomas in liver was higher in diabetic mice compared to controls although this was not statistically significant (Figure 7.11 A, F & G). Diabetic mice had 1.32 times higher inflamed area in the liver of diabetic mice compared to controls at 30 dpi (Figure 7.11 B, F & G). The area of each inflammatory focus/granuloma was greater in diabetic mice at both 14 and 30 dpi (Figure 7.11 C).

7.4.1.4.6 *M. tuberculosis* (H37Rv) in the inflammatory foci/granuloma

Similar to *M. fortuitum* and *M. bovis* (BCG) infection, a higher number of bacilli per inflammatory focus/granuloma of the liver of diabetic mice were observed at both 14 and 30 dpi compared to controls (Figure 7.12 A, B & C). Similar to *M. bovis* (BCG) infection, the inflammatory cells involved in the formation of foci of inflammation/granuloma were more loosely associated in diabetic mice compared to control mice at both timepoints of infection (Figure 7.12 B & C). The bacilli were also seen dispersed in the liver parenchyma of diabetic mice compared to control (Figure 7.12 D). A higher number of bacilli were observed per infected cell compared to control, although bacilli/cell were not directly quantified (Figure 7.12 E).

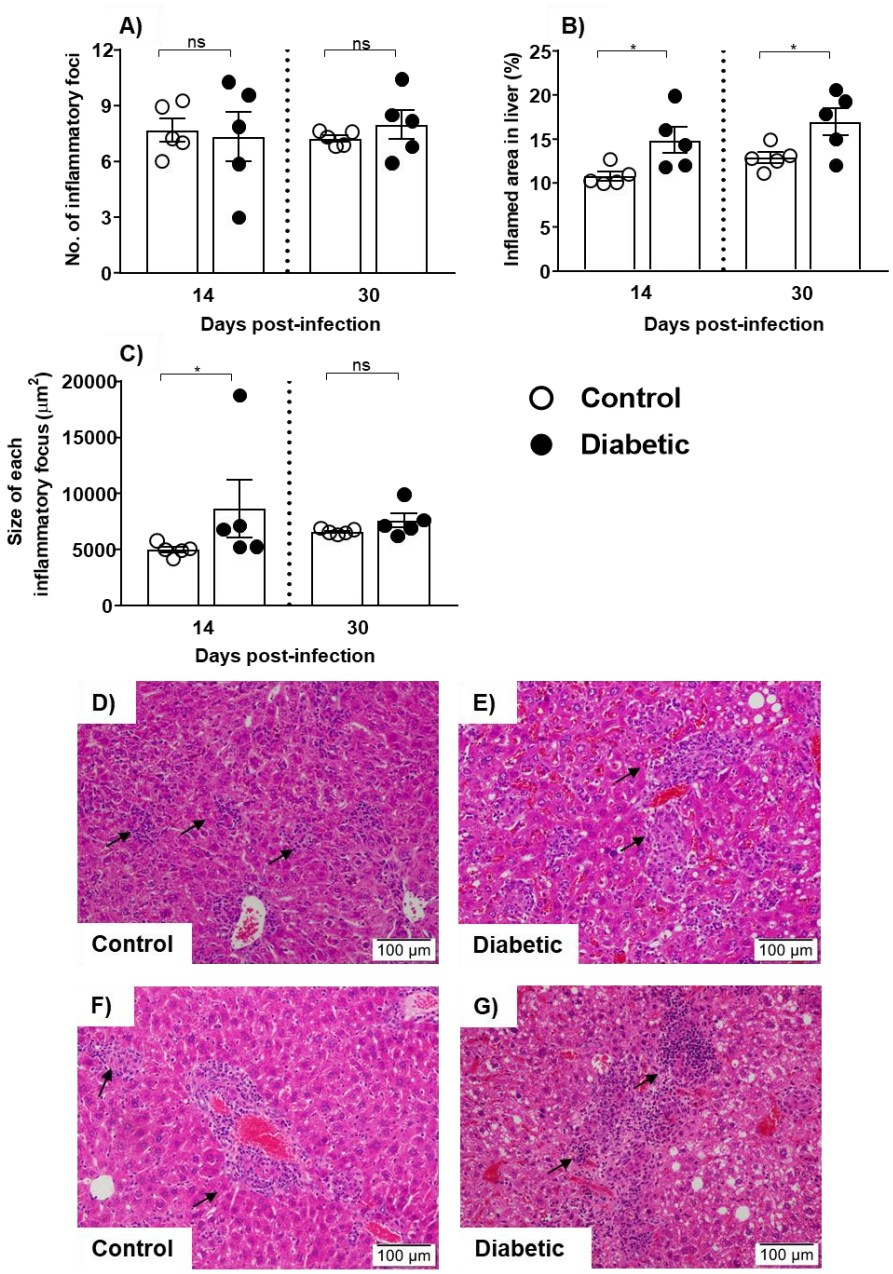

Figure 7.11 Inflammatory lesions in liver following *M. tuberculosis* (H37Rv) infection

H&E stained liver sections infected with low-dose *M. tuberculosis* (H37Rv) were used to assess the inflammatory lesions at 1, 14 and 30 days post-infection (dpi). Quantification of liver lesions at 14 and 30 dpi demonstrated that there was no significant different in number of inflammatory foci/granulomas in liver of diabetic mice compared to controls (A). The percent inflamed area in the liver was higher in diabetic mice compared to controls at the same timepoints of infection (B). The relative size of each inflammatory focus/granuloma on liver section was found higher in diabetic mice comparted to controls at both timepoints of infection (C). The photomicrographs of liver sections demonstrated inflammatory area at 14 (D & E) and 35 dpi (F & G) in diabetic and control mice. Magnification of the photomicrographs: D-G; 200x (scale bar 100 µm). Data presented as mean±SEM; n=5 mice/group. The significant differences between the groups were determined using the independent sample *t*-test (A & B), Mann-Whitney U test (C) (Appendix 6). The level of significance was indicated as *p≤0.05 and ns=non-significant. Images from other animals are in Appendix 6, Figure A6.2-A6.4.

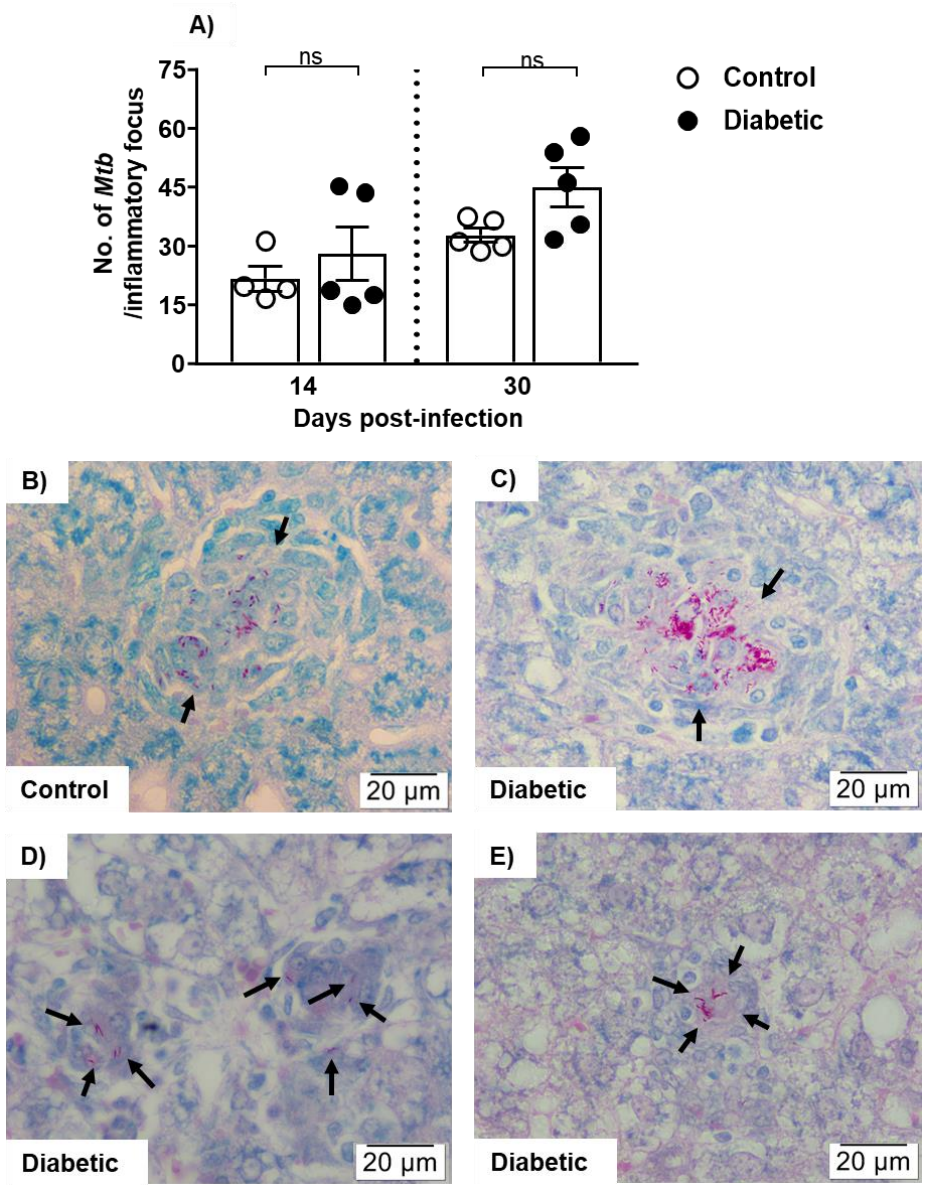

Figure 7.12 Acid-fast bacilli in the granuloma of *M. tuberculosis* (H37Rv) infected mice

The Ziehl-Neelsen staining of liver sections infected with *M. tuberculosis* (H37Rv) was performed at 1, 14 and 30 days post-infection (dpi). Quantification of acid-fast bacilli demonstrated a higher number of *M. tuberculosis* (*Mtb*) in each inflammatory focus/granuloma from diabetic mice compared to control mice at both 14 and 30 dpi. Photomicrographs demonstrated a relatively well-organised granuloma/inflammatory foci in the liver section of control mice with a lower number of bacilli (magenta) (B). Whereas inflammatory cells in inflammatory foci/granulomas of the diabetic mice were more loosely associated with a higher number of bacilli (C). In liver section of diabetic mice, bacilli were also found more disperse (outside of inflammatory focus/granuloma) (D). A higher number of bacilli was found in each infected cell of diabetic mice comparted to controls (E). Magnification of the photomicrographs: B-E; 200x (scale bar 100 µm). Data presented as mean±SEM; n=4-5 mice/group. The significant differences between the groups were determined using the Mann-Whitney U test (14 dpi) and the independent sample *t*-test (30 dpi) (Appendix 6). The level of significance was indicated as *p≤0.05, and ns=non-significant. Images from other animals are in Appendix 6, Figure A6.5-A6.6.

7.4.1.5 Inflammatory lesions in lungs following mycobacterial infections

7.4.1.5.1 Inflammation in lungs of *M. fortuitum* infected mice

Lung sections from diabetic and control mice infected with low-dose ($1x10^7$) *M. fortuitum* showed a marked inflammatory response (Figure 7.13 A, C, D, E & F). At 1 day post-infection (dpi), a diffuse accumulation of inflammatory cells was observed in both diabetic and control groups (Appendix 4, Figure A4.7). At 14 dpi, the inflamed area in the lungs was 1.38 times more in diabetic mice compared to controls although this difference was not significant (Figure 7.13, A, C & D). At 35 dpi, diabetic mice had a significantly 1.21 times higher inflamed lung area compared to control mice (Figure 7.13 A, E & F).

When the mice were infected with high-dose ($3x10^8$) *M. fortuitum*, extensive inflammation was observed in the lungs of both diabetic and control mice (Figure 7.13 B, G & H). Compared to control mice, diabetic mice had a 1.29 times higher inflamed area across the lung sections at 14 dpi (Figure 7.13 B).

7.4.1.5.2 Inflammation in lungs of *M. bovis* (BCG) infected mice

Examination of H&E stained lung sections from *M. bovis* infected mice revealed similar findings as those of *M. fortuitum* infection, with inflammation in both diabetic and control lungs (Figure 7.14). A diffuse accumulation of inflammatory cells was observed in both diabetic and control groups at 1 day post-infection (dpi) (Figure 7.14 B & C). At 14 dpi, diabetic mice had 1.65 times higher inflamed area across the lung sections compared to controls (Figure 7.14 A, D & E). A similar trend was observed at 35 dpi where diabetic mice had a 1.12 times more inflamed area in lungs compared to controls (Figure 7.14 A, F & G).

7.4.1.5.3 Inflammation in lungs of *M. tuberculosis* (H37Rv) infected mice

A strong inflammatory response was also evident in *M. tuberculosis* (H37Rv) infected mice (Figure 7.15). At 1 day post-infection (dpi), a diffuse inflammatory infiltrate was observed in the lungs of diabetic and control mice (Figure 7.15 B & C). Compared to controls, diabetic mice demonstrated a 1.43 times higher inflamed area across the lungs at 14 dpi (Figure 7.15 A, D & E). A similar trend was observed at 30 dpi (Figure 7.15 A, F & G).

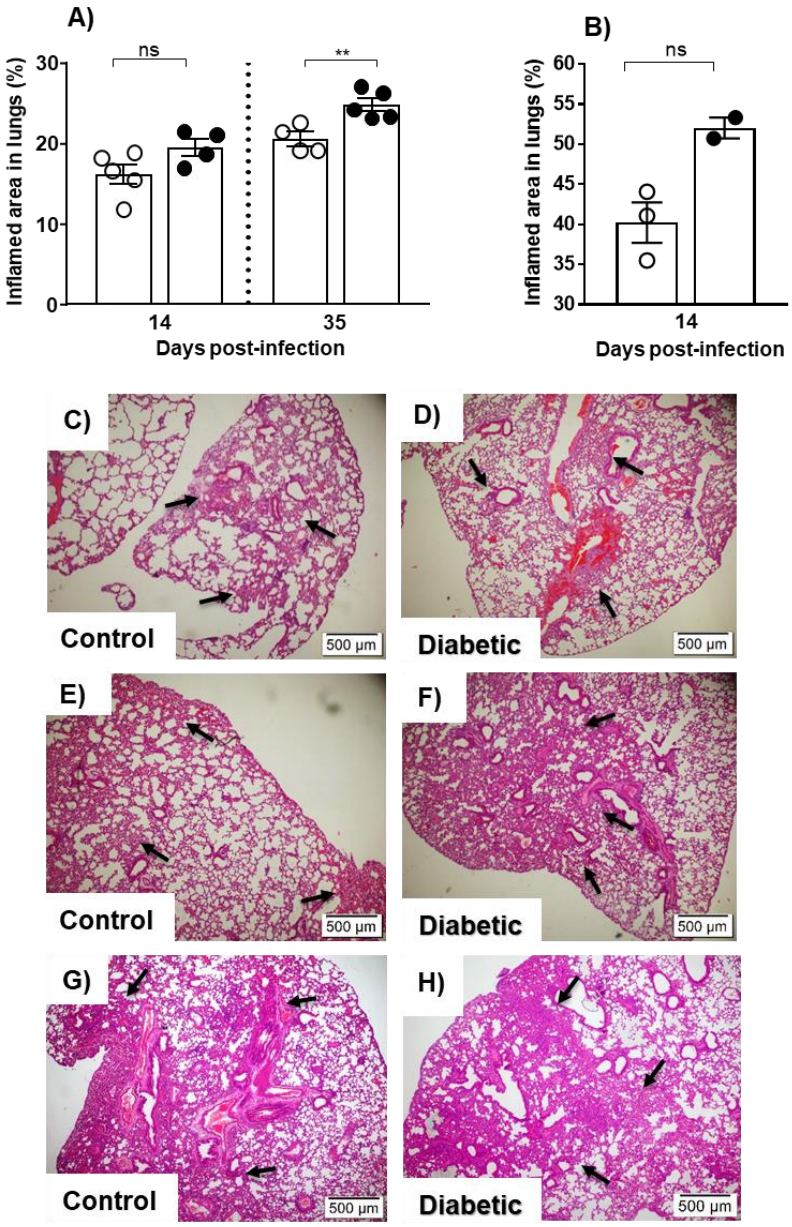

Figure 7.13 Inflammatory lesions in lungs following *M. fortuitum* infection

H&E stained lung sections of diabetic and control mice infected with low-dose ($1x10^7$) *M. fortuitum* were assessed for inflammation at 1, 14 and 35 days post-infection (dpi). Some moribund animals infected with high-dose ($3x10^8$) *M. fortuitum* were considered to quantify the lung lesions at 14 dpi. Quantification of the lungs lesions demonstrated a significantly higher inflamed area in lungs of diabetic mice compared to controls infected with low-dose of bacteria at both 14 and 35 dpi (A). Mice infected with a high-dose of bacteria showed a similar trend of inflammation in lungs at 14 dpi (B). Photomicrographs were representing the inflamed area in lungs at 14 (C & D) and 35 dpi (E & F) of mice infected with a low-dose of *M. fortuitum* and 14 dpi (G & H) of high-dose group. Magnification of photomicrographs: C-H; 40x (scale bar 500 µm). Data presented as mean±SEM; n=5 (low-dose) and 2-3 (high-dose) mice/group. The significant differences between the groups were determined using the independent sample *t*-test (Appendix 4). The level of significance was indicated as **p≤0.01 and ns=non-significant. Images from other animals are in given in Appendix 4, Figure A4.7-A4.9 and A4.13.

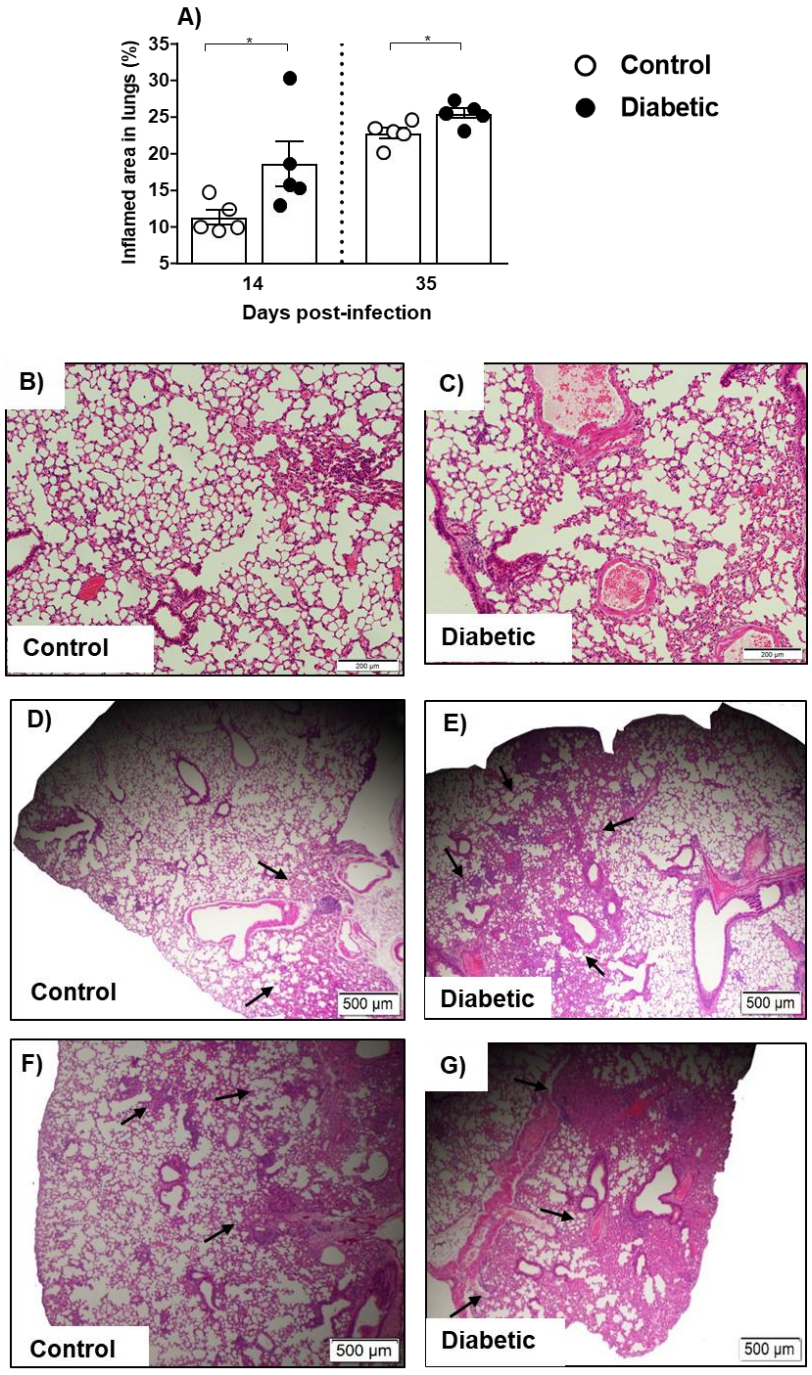

Figure 7.14 Inflammatory lesions in lungs following *M. bovis* (BCG) infection

H&E stained lung sections of diabetic and control mice infected with low-dose *M. bovis* (BCG) were assessed for inflammation at 1, 14 and 35 days post-infection (dpi). Quantification of the lesions demonstrated a significantly higher inflamed area in lungs of diabetic mice compared to controls at both 14 and 35 dpi (A). The photomicrographs represented the inflamed area in lungs of diabetic and control mice at 1 (B & C) 14 (D & E) and 35 dpi (F & G). Magnification of the photomicrographs: B-C; 100x (scale bar 200 µm) and D-G; 40x (scale bar 500 µm). Data presented as mean±SEM; n=5 mice/group. The significant differences between the groups were determined using the independent sample *t*-test (Appendix 5). The level of significance was indicated as *p≤0.05. Images from other animals are in Appendix 5, Figure A5.7-A5.9.

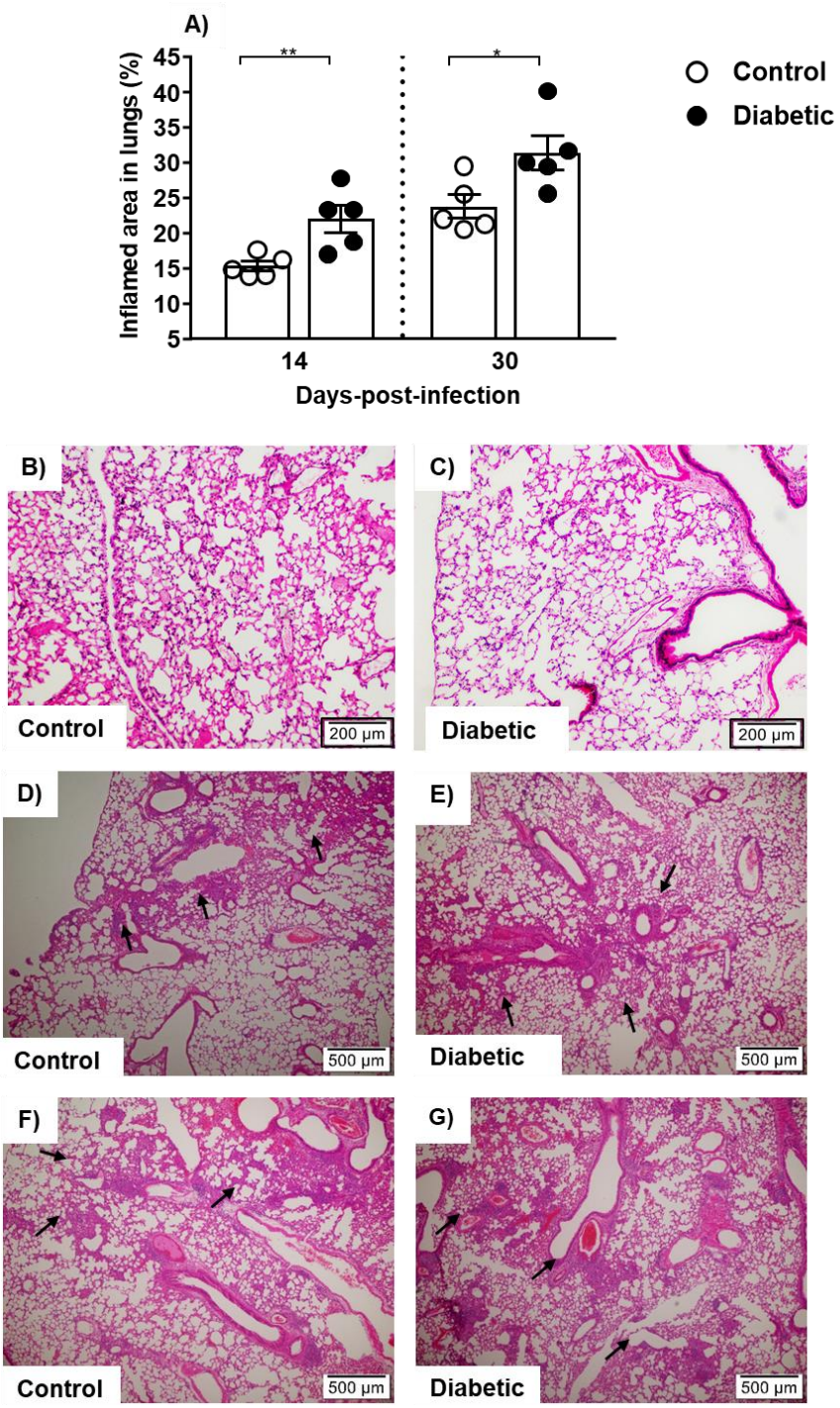

Figure 7.15 Inflammatory lesions in lungs following *M. tuberculosis* (H37Rv) infection

H&E stained lung sections of diabetic and control mice infected with low-dose *M. tuberculosis* (H37Rv) were assessed for inflammation at 1, 14 and 30 days post-infection (dpi). Quantification of the lesions demonstrated a significantly higher inflamed area in lungs of diabetic mice compared to controls (A). The photomicrographs represented the inflamed area in lungs of diabetic and control mice at 1 (B & C) 14 (D & E) and 30 dpi (F & G). Magnification of the photomicrographs: B-C; 100x (scale bar 200 µm) and D-G; 40x (scale bar 500 µm). Data presented as mean±SEM; n=5 mice/group. The significant differences between the groups were determined using the independent sample *t*-test (Appendix 6). The level of significance was indicated as *p≤0.05 and **p≤0.01. Images from other animals are in Appendix 6, Figure A6.7-A6.9.

7.4.1.6 Inflammation in kidneys of *M. fortuitum* infected mice

Histopathological examination of kidney sections of mice infected with low-dose of *M. fortuitum* demonstrated a gradual increase in inflammatory cells in both the cortex and medullary regions of kidneys of both diabetic and control mice (Figure 7.16 A, B, C, D, E & F). Inflammation was increased at 35 dpi compared to 14 dpi. The numbers of inflammatory cells appeared higher in the kidneys of diabetic mice compared to the controls, although inflammatory lesions were not quantified directly. Granuloma-like structures were predominantly observed in the kidneys of diabetic mice at 35 dpi (Figure 7.16 E & F).

In mice infected with high-dose *M. fortuitum* inflammatory infiltrates were found in the cortex and medullary regions of kidneys of both diabetic and control mice at 14 dpi. (Figure 7.16 G & H). Granuloma like structures and hypertrophy of the glomeruli were mainly observed in diabetic mice compared to controls, albeit lesions were not quantified.

As kidneys are known to be one of the initial organs affected following *M. fortuitum* infection, they were collected for analysis for this species only. Kidney samples of mice infected with *M. bovis* (BCG) and *M. tuberculosis* (H37Rv) were not considered as they are not under the area interest of this investigation.

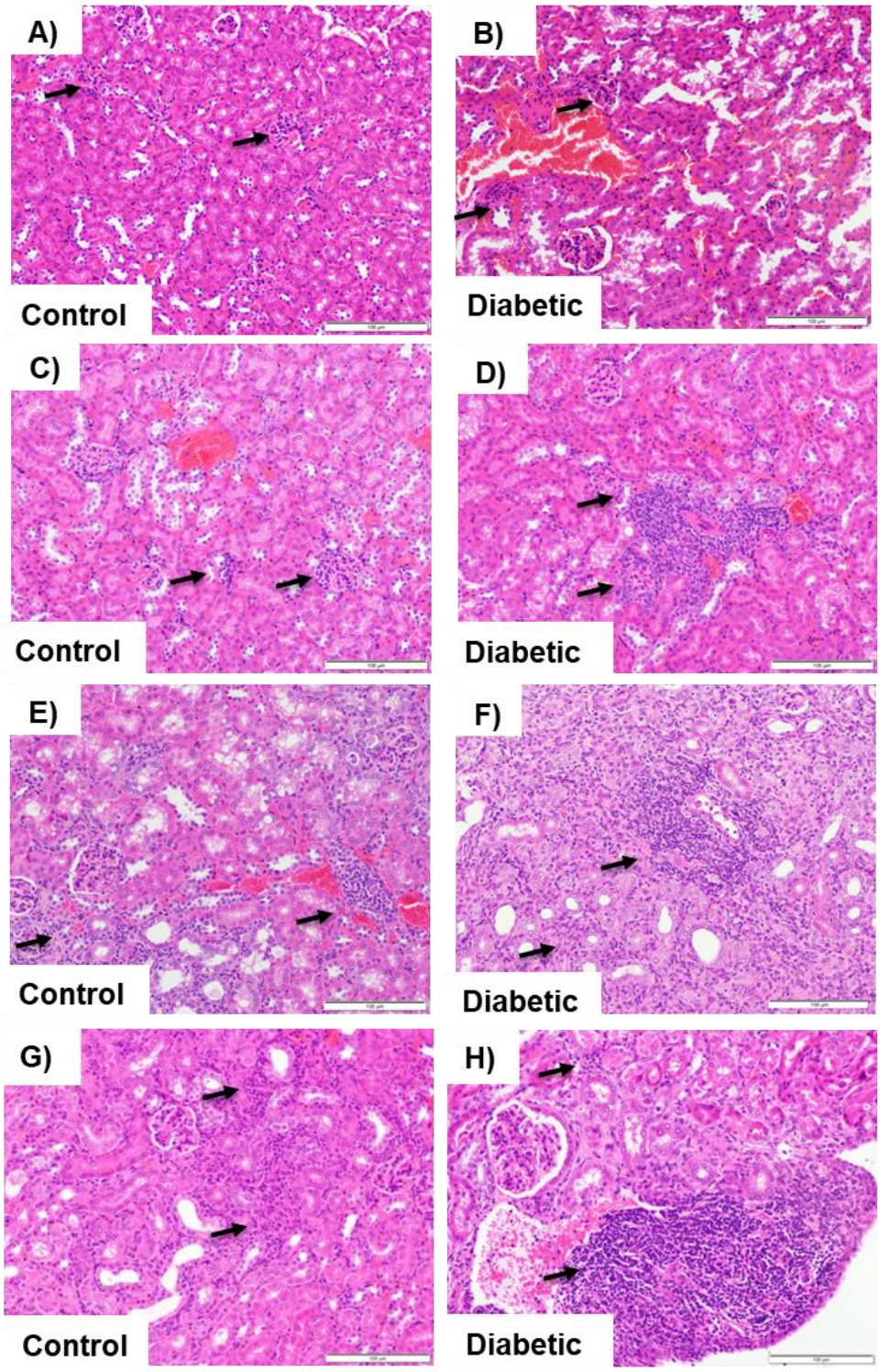

Figure 7.16 Inflammatory lesions in kidneys following *M. fortuitum* infection

H&E stained kidney sections were used to assess kidney inflammation. Mice infected with low-dose ($1x10^7$) *M. fortuitum* showed inflammatory infiltrates in kidneys. More inflammation (arrow indicated inflammatory infiltrates) was observed in kidneys of diabetic mice at 1 (A & B), 14 (C & D) and 35 days post-infection (dpi) (E & F) compared to controls, although lesions were not quantified. Diabetic mice infected with high-dose ($3x10^8$) *M. fortuitum* had marked kidney inflammation including large granuloma-like structures (G & H). Magnification of photomicrographs: A-H; 200x (scale bar 100 µm).

7.5 Discussion

In Chapter 6 we investigated the susceptibility of diabetic mice to mycobacterial infections. Following *M. fortuitum*, *M. bovis* (BCG) and *M. tuberculosis* (H37Rv) infections, we observed alterations in metabolic parameters, higher mortality and increased bacterial burden in the spleen, liver and lungs of diabetic mice compared to non-diabetic mice. Bacterial infection of tissues leads to inflammatory responses with the aim of effective control of bacterial replication. In mycobacterial infections, the granuloma plays an important role in killing and containment of the organism. In this Chapter, we examined the gross changes to organs and tissue inflammation in diabetic and control mice infected with *M. fortuitum, M. bovis* (BCG) and *M. tuberculosis* (H37Rv). Furthermore, the bacillary burden in each granuloma/inflammatory foci was quantified during infection. This study showed that inflammation was exaggerated and the structure of the mycobacterial granuloma altered in diabetic hosts.

Following infection with *M. fortuitum, M. bovis* (BCG) and *M. tuberculosis* (H37Rv) infections, splenomegaly and hepatomegaly were common observations in both diabetic and control mice (Figure 7.1-7.5). Diabetic mice infected with *M. fortuitum* (high-dose) and *M. tuberculosis* (H37Rv) showed abscess-like lesions and significant distention and congestion of the lungs (Figure 7.3 and 7.5). Histological examination demonstrated inflammation in liver (Figure 7.6-7.9 and 7.11) and lungs (Figure 7.13, 7.14 and 7.15) of both diabetic and control mice. In liver, diffuse inflammatory infiltrates were evident following *M. fortuitum*, *M. bovis* (BCG) and *M. tuberculosis* (H37Rv) infections. The inflammatory aggregates increased in mice during the infection period. Ziehl-Neelsen staining of liver sections also demonstrated the presence of higher numbers of bacilli per inflammatory focus/granuloma in diabetic mice compared to controls (Figure 7.6-7.8, 7.10 and 7.12). Previous studies in animal models have described poorly structured inflammatory aggregates early in mycobacterial infection. Whereas the granulomatous response becomes more conspicuous later in the course of infection (Ueda et al., 1972, Parti et al., 2005, Silva et al., 2010, Singhal et al., 2011). Silva and colleagues (2010) showed that the number of granulomas and their relative size increased at 14, 28 and 60 dpi during *M. fortuitum* and *M. avium intracellulare* infection in BALB/c mice. A higher number of inflammatory foci containing a higher number of *M. bovis* per aggregate were found at 27 and 117 dpi compared to 2 and 14 dpi (Chambers et al., 2006). These observations were in line with the findings of the current study in which we observed a higher number of inflammatory foci with a higher number of acid-fast bacilli at later timepoints.

Similar to the inflammatory lesions in the liver, diffuse inflammation was seen in lungs early in infection with increasing number of lesions observed at later in infection (Figure 7.13-7.15). Rhoades and co-workers (1997) demonstrated a gradual progression of pulmonary lesions in mice infected with *M. tuberculosis*. Another study using *M. bovis* infected mice demonstrated increased numbers of inflammatory lesions at 27 dpi compared to 1 dpi (Chambers et al., 2006). These findings are consistent with the current study in which the inflammatory or granulomatous response in lungs was more evident in later timepoints. Previous investigators have characterised and enumerated specific cell types during the establishment of the mycobacterial granuloma in order to more fully understand the respective roles of immune cells in protective immunity and immunopathogenesis (Rhoades et al., 1997, Parti et al., 2005, Chambers et al., 2006, Costa et al., 2010). A detailed characterisation of lung-infiltrating cells was beyond the scope of the current study, however, future studies examining the cell phenotypes and numbers and detailed kinetics of lung inflammation in diabetic *versus* non-diabetic mice may elucidate the cellular defects influencing the antimycobacterial immunity in diabetic animals.

Previous reports documented that the kidney is a preferred niche for *M. fortuitum* growth (Saito and Tasaka, 1969, Parti et al., 2005). We examined the kidneys of *M. fortuitum* infected diabetic and control mice, determined the bacterial load in kidneys (Chapter 6) and examined H&E stained sections for inflammatory changes. We observed pale and distended kidneys in the diabetic mice infected with low-dose *M. fortuitum* (Figure 7.1 E & J). In animals receiving high-dose *M. fortuitum*, similar lesions were observed but in addition pus-filled kidneys were revealed upon incision (Figure 7.3 E & J). These findings were consistent with the previous reports (Saito and Tasaka, 1969, Parti et al., 2005). Histological staining revealed apparently higher inflammatory infiltrates in kidneys of diabetic mice compared to control (Figure 7.16 A, B, C, D E & F). Granuloma like inflammatory aggregates was also seen in the kidney sections of diabetic mice infected with a high-dose of *M. fortuitum* (Figure 7.16 H). Parti and his colleagues (2005) observed white spots on the external surface of the kidneys and renal enlargement in BALB/c mice infected with *M. fortuitum*. The authors also reported clustering of inflammatory aggregates in the interstitial tissue and abscess formation in the renal parenchyma of the kidneys at 15 dpi. A granuloma-like structure with densely packed lymphocytes surrounded by the fibrous tissue was also described by the same authors at 30 dpi. It is worth mentioning that during characterisation of the T2D mouse model (Chapter 4), we found features of nephropathy (section 4.4.2.4.). Precisely how pre-existing renal impairment compromised immunity to *M. fortuitum* is unclear. However, our initial findings showing renal

functional impairment in our T2D model will be a useful baseline for future studies on the influence of T2D on non-mycobacterial and tuberculous kidney infections.

The primary Aims of the current study (Aim 2 to 4) were the quantification of inflammatory lesions in liver and lungs of diabetic and control mice infected with *M. fortuitum*, *M. bovis* (BCG) and *M. tuberculosis* (H37Rv). Increased areas of inflammation were observed in the liver of diabetic mice compared to controls following infection with *M. fortuitum* (Figure 7.6 B and 7.8 B), *M. bovis* (BCG) (Figure 7.9 B) and *M. tuberculosis* (H37Rv) (Figure 7.11 B). The number (Figure 7.6 A, 7.8 A, 7.9 A and 7.11 A) and size (Figure 7.6 C, 7.9 C and 7.11 C) of inflammatory foci/granulomas were also increased in diabetic mice. Furthermore, we observed higher number of acid-fast bacilli per inflammatory focus/granuloma in diabetic mice (Figure 7.6 D, 7.8 D, 7.10 A and 7.12 A). The cells involved in the formation of inflammatory foci/granuloma in diabetics were loosely associated, resulting in diffuse cellular aggregates of increased size. This contrasted with the more compact lesions observed in liver sections from control mice (Figure 7.7 G & H, 7.10 B & C and 7.12 B & C). In diabetic mice, bacilli were also found scattered throughout the liver parenchyma and we observed higher number of bacilli per cell (Figure 7.10 D, E and 7.12 D, E). Only a few previous studies using T1D and T2D rat models have reported large granulomas in the liver and other organs in *M. tuberculosis* infection (Sugawara et al., 2004, Sugawara and Mizuno, 2008). The findings of our study are consistent with these previous studies. However, a higher number of bacilli in the inflammatory foci/granulomas in liver of diabetic mice indicated higher bacillary burden (Chapter 6). These findings further suggested that diabetic mice were less efficient in arresting and controlling the bacilli, resulting in a defective or delayed granuloma formation. Another important extrapolation of these findings may be that due to the loose, unorganised nature of the diabetic granuloma, granuloma breakdown may readily occur in diabetics with latent TB infection, resulting in more frequent reactivation events.

In lungs, we observed increased numbers of inflammatory lesions in diabetic mice compared to controls infected with *M. fortuitum* (Figure 7.13), *M. bovis* (BCG) (Figure 7.14) and *M. tuberculosis* (H37Rv) (Figure 7.15). Several studies quantified the inflammatory lesions in lungs of STZ/STZ+NA- induced diabetic animal models following infection with *M. tuberculosis*. Martens and colleagues (2007) observed a gradual rise of inflammatory lesions in the lungs of STZ-induced diabetic mice suffered from an acute (4 weeks) to chronic (8 and 16 weeks) *M. tuberculosis* (Erdman) infection. This research group also demonstrated a higher inflamed area in chronic infection in comparison to acute infection. In this study, mice were

infected intravenously which resulted in a rapid dissemination of the mycobacteria in lungs which might be a probable reason for higher inflammatory lesions development at 4-5 weeks of infection (acute). In a guinea pig model of TB-DM co-morbidity, a significantly higher inflamed area was detected in the of lungs of diabetic mice compared to controls at 30 dpi with a low-dose of *M. tuberculosis* infection (Podell et al., 2014). A higher lung inflammatory score was observed in STZ+NA-induced diabetic mice compared to controls at 6 months pi with *M. tuberculosis* (Cheekatla et al., 2016). Findings of this study were in agreement with the previous studies described above. Higher inflammation in lungs of diabetic mice indicates higher bacterial burden (Chapter 6) due to failure to control and confined the bacilli in the inflammatory foci/granuloma. Studies in human TB patients have shown that immunocompetent patients develop small, compact lung granulomas containing a large number of IFN-γ producing CD4 T cells, whereas immunocompromised patients, tend to have larger granulomas that are rich in macrophages but containing few lymphocytes (Ulrichs et al., 2005, Sasindran and Torrelles, 2011). In human tuberculosis, one of the reasons for tissue damage is the presence of large caseating granulomas with areas of central necrosis and fibrotic scarring driven by chronic granulomatous inflammatory responses (Sasindran and Torrelles, 2011). Whereas murine model of tuberculosis, granulomas are formed by loose non-necrotic cellular aggregates, lymphocytes, but lacking the encapsulation seen in human tuberculosis granulomas (Gupta and Katoch, 2005). Although replicating the human tuberculosis granuloma in a mouse model is challenging, the study of cellular involvement in this T2D model by future research will further extend our understanding in immunopathology in this co-morbid infection.

Overall, increased liver and lung inflammation in diabetic mice compared to controls suggested impaired control of *M. fortuitum*, *M. bovis* (BCG) and *M. tuberculosis* (H37Rv) infection and furthermore indicated aberrant inflammation may indeed be responsible for increased infection susceptibility and mortality was seen in diabetic mice. This increased inflammation is likely to drive by the higher bacillary load (Chapter 6) which was further confirmed by the presence of increased numbers of acid-fast bacilli in each inflammatory focus/granuloma. In this study, we found inflammatory cells involved in the formation of granuloma were more loosely associated along and bacteria were scattered throughout the liver parenchyma in diabetic mice. These findings indicated that diabetic mice were less efficient in arresting and controlling the bacilli resulting in a defective or delayed formation of granuloma. Exaggerated inflammatory responses as seen here in diabetic mice may also impair mycobacterial phagocytosis, leading to impaired and dysregulated cytokine production as shown in our *in vitro* study (Chapter 5). Pro- and anti-inflammatory cytokine networks play key roles in protective immunity in

mycobacterial infections (Cooper, 2009, Cooper et al., 2011). Examining whether cytokine production is dysregulated in infected diabetic animals may advance our understanding of the reasons for increased bacterial burden and inflammatory responses and abnormal granuloma formation in diabetics in mycobacterial infections. Hence, in Chapter 8, we will determine and discuss the role of different pro- and anti-inflammatory cytokines in our T2D model following mycobacterial infections.

CHAPTER 8
EFFECT OF TYPE 2 DIABETES ON CYTOKINE PRODUCTION IN MYCOBACTERIAL INFECTIONS

8.1 Introduction

Cytokines orchestrate the immune response in host-mycobacterial infections. Diverse cells involved in mediating the innate and adaptive immune response following mycobacterial infections secrete various pro-inflammatory (e.g. TNF-α, MCP-1, IL-1β, IL-18, IL-12, IL-17, IFN-γ, IL-6, IL-2) and anti-inflammatory cytokines (e.g. IL-10, IL-4, TGF-β) (Cooper, 2009, Cooper et al., 2011). The cytokine networks and combinations involved in mycobacterial immunity are complex, however certain cytokines have been identified in both human studies and animal models as key mediators of anti-TB immunity. Previous research has highlighted the essential role of TNF-α in mycobacterial immunity, maintaining latency and preventing reactivation. Mice lacking TNF-α are more prone to lethal mycobacterial infections with very high bacterial loads in multiple organs (Flynn et al., 1995, Benoit et al., 2008). TNF-α is also essential for the activation of endothelial cells, macrophages and neutrophils (Orme and Cooper, 1999, Tsenova et al., 1999, Gan et al., 2005) followed by granuloma formation and its maintenance (Kindler et al., 1989, Flynn et al., 1995, Senaldi et al., 1996). Interleukin-1β (IL-1β) and IL-18 enhance macrophage secretion of TNF-α, IL-6, IFN-γ leading to granuloma formation (Toossi et al., 1990, Juffermans et al., 2000). IL-12 and IL-18 are required for Th1 cells differentiation and IFN-γ secretion required to restrict mycobacterial growth within macrophages (Sieling et al., 1994, Cooper et al., 1995, Trinchieri, 1995, O'Neill and Greene, 1998). Human studies have documented that defects in components of IL-12 and IFN-γ pathways increase susceptibility to mycobacteria (Altare et al., 1998a, de Jong et al., 1998, Ottenhoff et al., 2002). IL-2 is associated with the activation and expansion of T cell (Johnson et al., 2003). This cytokine has been shown to reduce bacterial replication by the activation of macrophages through IFN-γ mediated pathways or by the development of cytotoxic T cells (Toossi et al., 1986, Jeevan and Asherson, 1988). Patients with TB often have deficient IL-2 induced cell proliferation (Toossi et al., 1986). IL-10 is made by many hematopoietic cells and plays a major role in modulating macrophage and dendritic cells function, required for the phagocytosis and killing of bacteria and the initiation of adaptive immune responses to mycobacteria. Similarly, high levels of IL-4 made by Th2 cells, innate lymphoid cells (ILCs) and other cells may be responsible for the downregulation of IFN-γ, TNF-α and IL-12 expression and suppressing essential Th1 cell protective immune functions (Redford et al.,

2011). These inhibitory cytokines however also play essential roles in limiting host-mediated tissue damage induced by the pro-inflammatory cytokines. Hence it is the intricate interplay of multiple cytokines that orchestrates appropriate innate and adaptive immune responses for effective control of mycobacteria.

The few studies that investigated cellular immune response in diabetic TB patients showed that cellular immunity was impaired (Goonetilleke et al., 2003, Niazi and Kalra, 2012). Fewer T lymphocytes with reduced production of IFN-γ, TNF-α, IL-1β and IL-6 were also seen in individuals with concomitant diabetes and TB compared to non-diabetics (Tsukaguchi et al., 1997, Geerlings and Hoepelman, 1999). Conflicting reports however have suggested that there is either no difference (Zhang et al., 2012), decreased (Stalenhoef et al., 2008) or increased (Legesse et al., 2013) production of Th1 cell specific IFN-γ by diabetics compared to non-diabetic TB patients. Kumar and colleagues (2013) reported that there was heightened production of type 1 (IFN-γ, IL-2, TNF-α), type 2 (IL-5) type 17 (IL-17A), other pro-inflammatory cytokines (IL-1β, IL-6, IL-18) and decreased production of IL-10 in TB patients with diabetes. Whereas there was a diminished production of systemic and antigen specific type 1 (IFN-γ, IL-2, TNF-α), type 17 (IL-17F) and other pro-inflammatory cytokines (IL-1β, IL-18) in diabetics and pre-diabetic individuals with latent TB infection (Kumar et al., 2014).

In animal models of TB-diabetes comorbidity, the pattern of pro- and anti-inflammatory cytokine production is unclear. Martens and colleagues (2007) observed higher expression of pro-inflammatory cytokines (IFN-γ, IL-12, TNF-α) in the lungs of aerosol infected STZ-induced diabetic mice at 8 and 16 weeks post-infection (pi) although IFN-γ expression was lower in their chronic diabetic mouse model during the first 3 weeks of infection. Decreased expression of pro-inflammatory cytokines (TNF-α, IL-1β, IL-2, IL-12) was seen at 3-4 weeks pi infection in the lungs of Goto Kakizaki (GK) rats infected with *M. tuberculosis* although the opposite trend was found at 12 weeks pi. (Sugawara et al., 2004). Cheekalta and colleagues (2016) found a significantly higher production of TNF-α, IL-6, IFN-γ, IL-1β, MCP-1 and IL-10 in the lungs of STZ+NA-induced diabetic mice infected with *M. tuberculosis* at 6 months pi although lower production of IL-6, TNF-α, IFN-γ was found at 4 weeks pi. The aforementioned studies determined cytokine production mostly in lungs but not other organs and didn't examine cytokines produced in early infection. Only one study measured cytokine production at 14 and 35 dpi in spleen, liver and lungs after iv infection of STZ-induced diabetic mice with *M. tuberculosis* (Yamashiro et al., 2005).The authors observed reduced expression of IFN-γ and IL-12 and increased expression IL-4 at these timepoints.

Both human and animal studies have indicated a dysregulated cytokine production in TB-diabetes co-morbid infections. Data presented in Chapter 6 of this thesis showed increased mortality and increased bacterial burden in spleen, liver and lungs of diabetic mice compared to controls. Furthermore, increased inflammation was found in the liver and lungs of diabetic mice compared to controls (Chapter 7).

The study described in Chapter 8 was designed to investigate the relationships between mortality, bacterial burden and inflammation and organ pro-inflammatory and anti-inflammatory cytokine production. This data will enhance our understanding of which, if any, cytokines are dysregulated in diabetics infected with mycobacteria.

The specific Aims of this research described in this Chapter are:

1. To measure cytokines in spleen, liver and lungs of diabetic mice following infection with low- and high-dose *M. fortuitum*
2. To measure cytokines in spleen, liver and lungs of diabetic mice following infection with *M. bovis* (BCG) and *M. tuberculosis* (H37Rv)

8.2 Materials and Methods

8.2.1 Animal ethics and institutional approvals

The details of animal ethics and all institutional approvals are described in Chapter 3 (section 3.1.1).

8.2.2 Experimental animals and induction of diabetes

The details of experimental animals and induction of diabetes are described in Chapter 3 (section 3.1.3) and Chapter 6 (section 6.2.2).

8.2.3 Preparation of mycobacterial culture for infection

The details of the preparation of mycobacterial culture for infection are described in Chapter 3 (section 3.3.2) and Chapter 6 (section 6.2.3.1).

8.2.4 Organ collection

The details of organ collection from the mycobacteria infected mice are described in Chapter 6 (section 6.2.4 and 6.2.5).

8.2.5 Cytokine assays

Supernatants from spleen, liver and lungs homogenates' were prepared at 1, 14, 35 days post-infection (dpi) (low-dose) and 14 dpi (high-dose) with *M. fortuitum*. Cytokine concentrations in tissue supernatants were determined using the BD Cytometric Bead Array Mouse Inflammation Kit® (TNF-α, MCP-1, IL-6, IFN-γ, IL-12p70, IL-10; cat. no. 552364, BD Biosciences, Australia). For *M. bovis* (BCG) and *M. tuberculosis* (H37Rv) infections, organs were collected at 1, 14 and 35 dpi (30 dpi for *M. tuberculosis*) and cytokine concentrations determined as above and using the Mouse Th1/Th2/Th17 Cytokine Kit® (IL-2, IL-4, IL-17A; cat. no. 60485) and Mouse IL-1β Flex Set® (IL-1β; cat. no. 560232). Manufacturer's instructions were followed. Samples were acquired using the BD FACS Calibur™ flow cytometer and analysed using BD FCAP Array™ software (version 3) (Chapter 3, section 3.8). Cytokine levels that were below the limit of detection (Chapter 3, Table 3.2) are shown as zero ('0').

8.3 Statistical analysis

The details of the statistical analysis are described in Chapter 6 (section 6.3).

8.4 Results

8.4.1 Cytokine production following *M. fortuitum* infection

8.4.1.1 Cytokine production in spleen

At 1 day post-infection (dpi) with low-dose *M. fortuitum*, the only significant difference in spleen cytokine concentration between diabetic and control mice was in IL-6, albeit its concentration was extremely low (Table 8.1). TNF-α, IL-10 etc., were decreased in diabetic spleen however the differences were not statistically significant. No significant differences were observed for any splenic cytokines in day 14 or day 35 samples (Table 8.1). MCP-1 peaked at day 14, IL-10 and TNF-α concentrations were similar at all timepoints, whereas the production of IFN-γ increased gradually in the spleen of both control and diabetic mice. No IL-12 was detected during infection period (Table 8.1).

In mice infected with high-dose *M. fortuitum*, decreased concentrations of TNF-α, MCP-1, IL-6, IFN-γ and IL-10 were found in the spleen of diabetic mice compared to controls at 14 dpi although these differences were not significant (Table 8.1). There was no production of IL-12 in the spleen of both control and diabetic mice during high-dose of *M. fortuitum* infection (Table 8.1).

Table 8.1 Cytokine production in spleen following *M. fortuitum* infection

Spleen		Days post-infection					
		1		14		35	
Cytokine	Mouse	Mean±SEM (pg/mL)	p-value	Mean±SEM (pg/mL)	p-value	Mean±SEM (pg/mL)	p-value
Low-dose ($1x10^7$)							
TNF-α	Control	30.77±3.41	0.0976	13.16±3.59	0.4104	36.13±15.33	0.4958
	Diabetic	17.05±2.08		22.35±9.74		23.63±8.48	
MCP-1	Control	39.94±5.08	0.9295	58.71±5.63	0.8471	60.52±15.83	0.7859
	Diabetic	38.38±13.74		63.96±22.72		55.52±8.13	
IL-6	Control	1.63±0.03	**0.0495**	0.99±0.59	0.8023	1.38±0.74	0.2898
	Diabetic	0.76±0.44		1.32±1.01		0.64±0.64	
IL-12	Control	0.68±0.15	0.1382	0.31±0.31	1.000	0.23±0.23	1.000
	Diabetic	0.00		0.33±0.33		0.47±0.47	
IFN-γ	Control	6.63±0.48	0.1269	11.14±3.72	0.3336	15.77±5.14	0.4958
	Diabetic	2.85±1.04		6.74±1.44		9.84±4.94	
IL-10	Control	38.18±4.92	0.1037	14.24±1.66	0.0790	10.67±2.91	0.8820
	Diabetic	16.41±5.68		9.19±1.75		11.32±3.07	
High-dose ($3x10^8$)							
TNF-α	Control			121.02±5.55	0.1233		
	Diabetic			51.20±16.92			
MCP-1	Control			113.80±11.19	0.3011		
	Diabetic			88.10±19.73			
IL-6	Control			17.68±9.32	0.4614		
	Diabetic			7.31±3.41			
IL-12	Control			0.00±0.00	-		
	Diabetic			0.00±0.00	-		
IFN-γ	Control			44.12±8.22	**0.0752**		
	Diabetic			14.84±3.52			
IL-10	Control			13.79±2.74	0.4171		
	Diabetic			10.38±1.13			

Data presented as mean±SEM; n=4-5 mice/group (low-dose) and 2-3 mice/group (high-dose)

8.4.1.2 Cytokine production in liver

Following infection with low-dose *M. fortuitum*, TNF-α concentrations in diabetic liver appeared 3 times higher than control liver at 1 dpi, although this difference was not statistically significant (Table 8.2). However, at 14 and 35 dpi, TNF-α levels were lower in diabetic mice compared to controls (Table 8.2). A similar trend for MCP-1 levels were observed with higher initial levels in diabetic followed by decreased liver concentrations over time (Table 8.2). Liver IL-6 was relatively unchanged over time. IL-12 production was higher in the liver of diabetic mice compared to control mice at 1 dpi (Table 8.2) but lower at 14 and 35 dpi. IFN-γ production was similar in diabetic and control liver early in infection but was decreased compared to control liver at both 14 and 35 dpi (Table 8.2). The levels of IL-10 in the liver of diabetic mice were higher at 1 dpi although an opposite trend of was observed at 14 dpi (Table 8.2). At 35

dpi, a 1.03 times higher production of IL-10 was found in the liver of diabetic mice although this difference was not significant.

Liver from diabetic mice infected with high-dose of *M. fortuitum* showed decreased TNF-α and IL-6 production compared to controls at 14 dpi although they did not reach significance (Table 8.2). Increased MCP-1 and IL-10 production were found in liver of diabetic mice compared to controls at 14 dpi (Table 8.2). IFN-γ level was decreased in liver from diabetic mice compared to controls (Table 8.2). The level of IL-12 was undetectable in liver of both diabetic and control mice (Table 8.2).

Table 8.2 Cytokine production in liver following *M. fortuitum* infection

Liver		**Days post-infection**					
		1		**14**		**35**	
Cytokine	**Mouse**	**Mean±SEM (pg/mL)**	**p-value**	**Mean±SEM (pg/mL)**	**p-value**	**Mean±SEM (pg/mL)**	**p-value**
Low-dose ($1x10^7$)							
TNF-α	Control	63.39±19.74	0.1742	137.93±32.32	**0.0388**	177.19±26.09	0.1616
	Diabetic	191.96±75.35		56.89±11.23		129.90±14.31	
MCP-1	Control	152.97±26.26	0.0986	431.28±86.27	0.2652	347.19±16.87	**0.0002**
	Diabetic	245.58±34.28		311.92±49.85		182.18±17.89	
IL-6	Control	13.04±4.34	0.3998	11.66±5.02	0.5136	20.25±7.44	0.8065
	Diabetic	20.08±6.09		8.05±1.63		14.81±4.28	
IL-12	Control	24.32±6.17	0.1866	25.50±9.74	0.2248	62.90±0.75	**0.0425**
	Diabetic	52.10±10.79		10.33±5.55		39.19±7.03	
IFN-γ	Control	11.72±3.59	0.7888	57.39±18.67	0.0928	61.18±13.65	0.1604
	Diabetic	13.18±3.60		19.84±2.18		33.72±10.26	
IL-10	Control	94.71±11.90	0.5708	73.87±4.24	**0.0300**	89.17±26.35	0.9121
	Diabetic	110.20±22.11		55.32±5.01		92.23±5.32	
High-dose ($3x10^8$)							
TNF-α	Control			330.08±42.43	0.4295		
	Diabetic			225.11±136.04			
MCP-1	Control			433.29±192.66	0.6579		
	Diabetic			574.35±194.76			
IL-6	Control			40.24±20.88	0.5472		
	Diabetic			21.41±9.35			
IL-12	Control			0.00±0.00	0.2722		
	Diabetic			0.64±0.64			
IFN-γ	Control			104.57±12.39	**0.0559**		
	Diabetic			34.50±22.30			
IL-10	Control			27.76±1.86	0.1108		
	Diabetic			42.51±8.22			

Data presented as mean±SEM; n=4-5 mice/group (low-dose) and 2-3 mice/group (high-dose)

8.4.1.3 Cytokine production in lungs

The only notable difference between diabetic and control lungs cytokines following infection with low-dose *M. fortuitum* was decreased TNF-α in diabetic lungs at 1 dpi and decreased IL-6 at 35 dpi. Lungs from diabetic mice infected with high-dose *M. fortuitum* had lower levels of TNF-α and IL-6 compared to control mice at 14 dpi. IFN-γ concentration was markedly reduced in lungs of diabetic mice compared to controls during the infection. No IL-12 was detected in any sample at any timepoint.

Table 8.3 Cytokine production in lungs following *M. fortuitum* infection

Lungs		Days post-infection					
		1		14		35	
Cytokine	**Mouse**	**Mean±SEM (pg/mL)**	**p-value**	**Mean±SEM (pg/mL)**	**p-value**	**Mean±SEM (pg/mL)**	**p-value**
Low-dose ($1x10^7$)							
TNF-α	Control	15.09±4.49	0.2890	1.06±0.81	0.2896	15.04±2.99	0.3083
	Diabetic	7.62±0.46		0.76±0.76		10.41±3.02	
MCP-1	Control	75.09±2.62	0.8969	62.14±9.95	0.7315	67.60±11.81	0.7665
	Diabetic	72.60±15.22		66.96±9.22		71.94±7.75	
IL-6	Control	3.83±3.35	0.6818	1.32±1.12	0.8139	8.46±2.27	**0.0432**
	Diabetic	6.40±4.94		1.82±1.34		2.42±1.09	
IL-12	Control	0.00	0.2207	0.14	0.3739	0.00	0.3473
	Diabetic	0.04±0.04		0.00		0.46±0.46	
IFN-γ	Control	5.17±2.03	0.9681	11.36±8.65	0.3470	7.86±2.31	0.4395
	Diabetic	5.05±1.47		2.13±0.87		5.89±0.74	
IL-10	Control	40.44±5.42	0.4807	31.08±9.20	0.9163	45.69±10.30	0.4776
	Diabetic	34.76±1.44		30.29±7.69		35.73±8.51	
High-dose ($3x10^8$)							
TNF-α	Control			374.81±155.59	0.2895		
	Diabetic			126.57±77.57			
MCP-1	Control			502.20±75.84	0.7739		
	Diabetic			412.17±263.55			
IL-6	Control			58.15±36.28	0.4972		
	Diabetic			20.72±17.34			
IL-12	Control			0.00±0.00	-		
	Diabetic			0.00±0.00			
IFN-γ	Control			94.60±0.00	**0.0042**		
	Diabetic			8.95±5.59			
IL-10	Control			24.06±4.51	0.6524		
	Diabetic			20.74±4.34			

Data presented as mean±SEM; n=4-5 mice/group (low-dose) and 2-3 mice/group (high-dose)

8.4.2 Cytokine production following *M. bovis* (BCG) infection

8.4.2.1 Cytokine production in spleen

IL-1β concentration in the spleen of diabetic mice was higher than control spleen at all timepoints of infection (Figure 8.1 A) with the peak level detected at 14 days post-infection (dpi). TNF-α concentration in diabetic spleen was lower at 1 dpi and 35 dpi compared to controls (Figure 8.1 B).

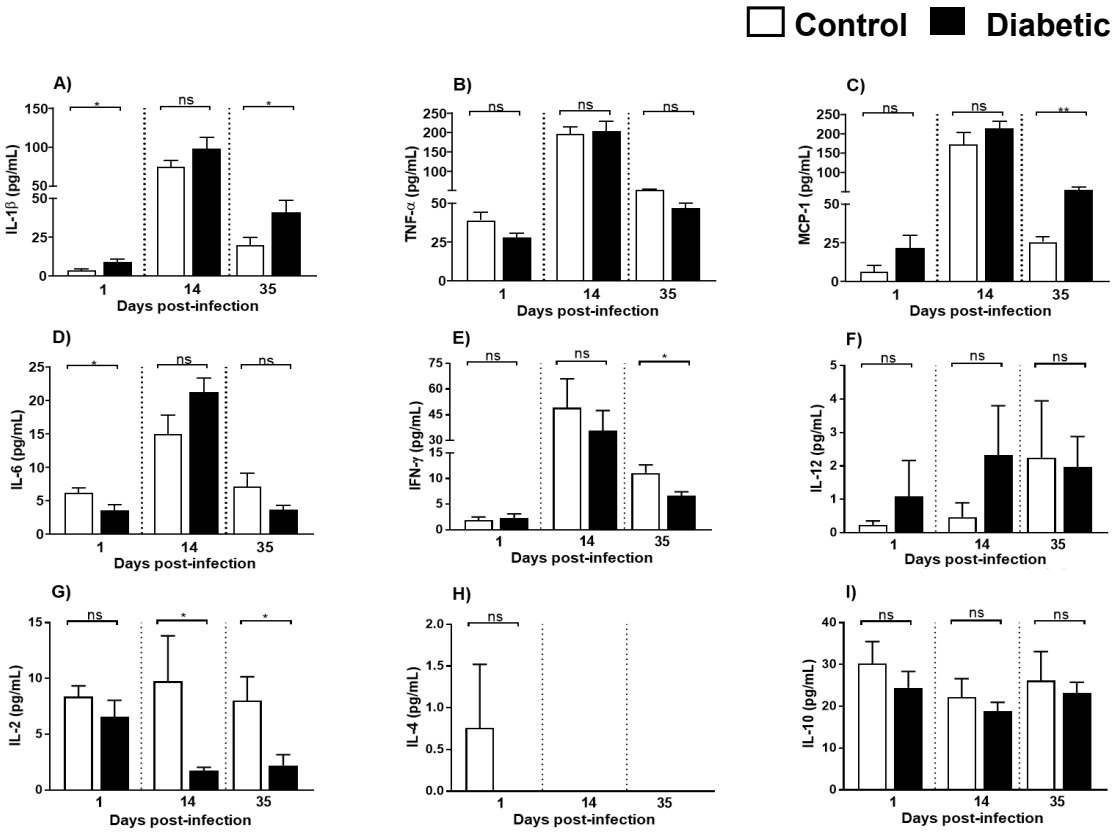

Figure 8.1 Cytokine production in spleen following *M. bovis* (BCG) infection

Mice infected with *M. bovis* (BCG) were assessed for cytokine production in spleen. Figure illustrates the kinetics of IL-1β (A), TNF-α (B), MCP-1 (C), IL-6 (D), IFN-γ (E), IL-12 (F), IL-2 (G), IL-4 (H) and IL-10 (I) production in control and diabetic mice at 1, 14 and 35 days post-infection (dpi). Overall, a higher production of IL-1β (A), TNF-α (B), MCP-1 (C), IL-6 (D) was observed in diabetic mice compared to controls. Whereas the production of IFN-γ (E), IL-2 (G) and IL-10 (I) was lower in diabetic mice compared to controls. The production of IL-12 (F) and IL-4 (H) was minimum or negligible in both of the groups throughout infection period. Data presented as mean±SEM; n=4-5 mice/group. The significant differences between the groups were determined using the independent sample *t*-test for the normally distributed data. The non-normally distributed data were analysed using the Mann-Whitney U test (Appendix 5). The level of significance was indicated as *p≤0.05, **p≤0.01 and ns=non-significant.

MCP-1 levels were higher in diabetic spleen at all timepoints (Figure 8.1 C). IL-6 was higher in diabetic spleen at 14 dpi although it was lower at both 1 dpi and 35 dpi compared to controls (Figure 8.1 D). IFN-γ concentration was lower in spleen of diabetic mice compared to controls

at 14 dpi and 35 dpi (Figure 8.1 E). IL-12 levels were negligible in both diabetic and control mice throughout the infection period (Figure 8.1 F). The production of IL-2 was lower in diabetic mice at 1, 14 and 35 dpi (Figure 8.1 G). A reduced level of interleukin-10 was observed in diabetic mice compared to controls at all the timepoints of infection although they did not reach a significant level (Figure 8.1 I). IL-4 (Figure 8.1 H) and IL-17A (Appendix 5, Table A5.12) were below the limits of detection in all samples.

8.4.2.2 Cytokine production in liver

IL-1β level was significantly higher in the liver of diabetic mice compared to controls at 1 day post-infection (dpi) (Figure 8.2 A). At 14 dpi and 35 dpi, the level of TNF-α in diabetic liver was approximately half the concentration measured in control liver (Figure 8.2 B). MCP-1 secretion peaked at 14 dpi however no significant differences were seen between diabetic and control mice (Figure 8.2 C). The concentration of IL-6 was significantly reduced in liver from diabetics at 35 dpi (Figure 8.2 D). IFN-γ production was significantly lower in diabetic mice at 14 and 35 dpi compared to controls (Figure 8.2 E). IL-12 secretion was higher at 1 and 14 dpi although this was not statistically significant, however, at 35 dpi IL-12 level in diabetic liver was lower than controls (Figure 8.2 F). IL-2 was slightly higher in the liver of diabetic mice compared to controls at 14 dpi and 35 dpi but these did not reach significance (Figure 8.2 G). The production of IL-4 was 3.44 and 6.53 times higher in diabetic mice compared to controls at 1 and 14 dpi, respectively (Figure 8.2 H). At 35 dpi, no IL-4 was detected in liver of diabetic or control mice (Figure 8.2 H). IL-10 level was higher in diabetic liver compared to controls at 1 and 14 dpi but reduced at 35 dpi (Figure 8.2 I). IL-17A was not detected (Appendix 5, Table A5.13).

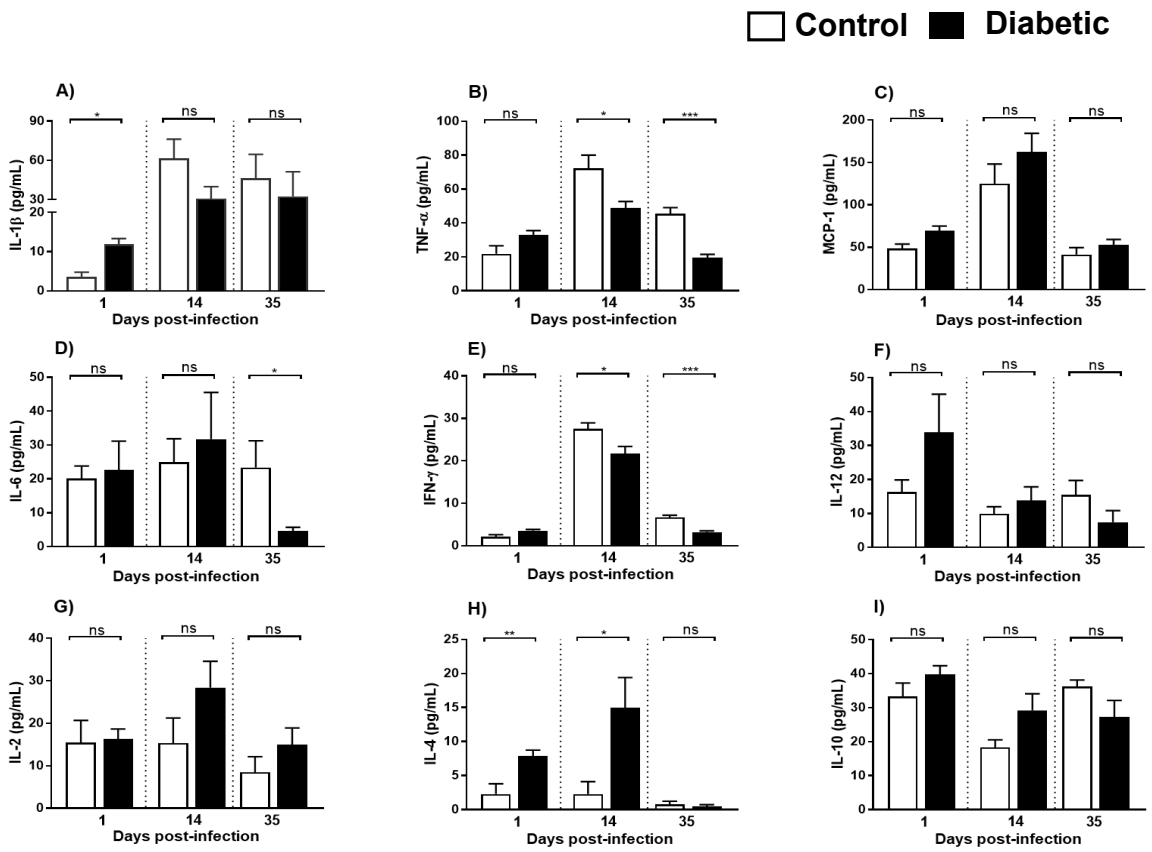

Figure 8.2 Cytokine production in liver following *M. bovis* (BCG) infection

Mice infected with *M. bovis* (BCG) were assessed for cytokine production in liver. Figure illustrates the kinetics of IL-1β (A), TNF-α (B), MCP-1 (C), IL-6 (D), IFN-γ (E), IL-12 (F), IL-2 (G), IL-4 (H) and IL-10 (I) production in control and diabetic mice at 1, 14 and 35 days post-infection (dpi). Overall, the production of IL-1β (A), TNF-α (B) and IFN-γ (E) was lower in diabetic liver compared to controls. The production of MCP-1 (C), IL-2 (G), IL-4 (H) was higher in liver of diabetic mice compared to controls. A higher production of IL-12 was observed in diabetic mice at 1 and 14 dpi although the level did not sustain to 35 dpi. The production of IL-10 (I) was higher in diabetic mice compared to controls at 1 and 14 dpi although its level was higher in control mice at the end timepoint of infection. Data presented as mean±SEM; n=4-5 mice/group. The significant differences between the groups were determined using the independent sample *t*-test for the normally distributed data. The non-normally distributed data were analysed using the Mann-Whitney U test (Appendix 5). The level of significance was indicated as *p≤0.05, **p≤0.01, ***p≤0.001 and ns=non-significant.

8.4.2.3 Cytokine production in lungs

Early after infection with *M. bovis* (BCG), higher concentration of IL-1β was found in the lungs of diabetic mice compared to controls (Figure 8.3 A). No differences were observed at 14 days post-infection (dpi) or 35 dpi (Figure 8.3 A). At 14 dpi and 35 dpi, TNF-α level in the lungs of diabetic mice was lower than controls (Figure 8.5 B).

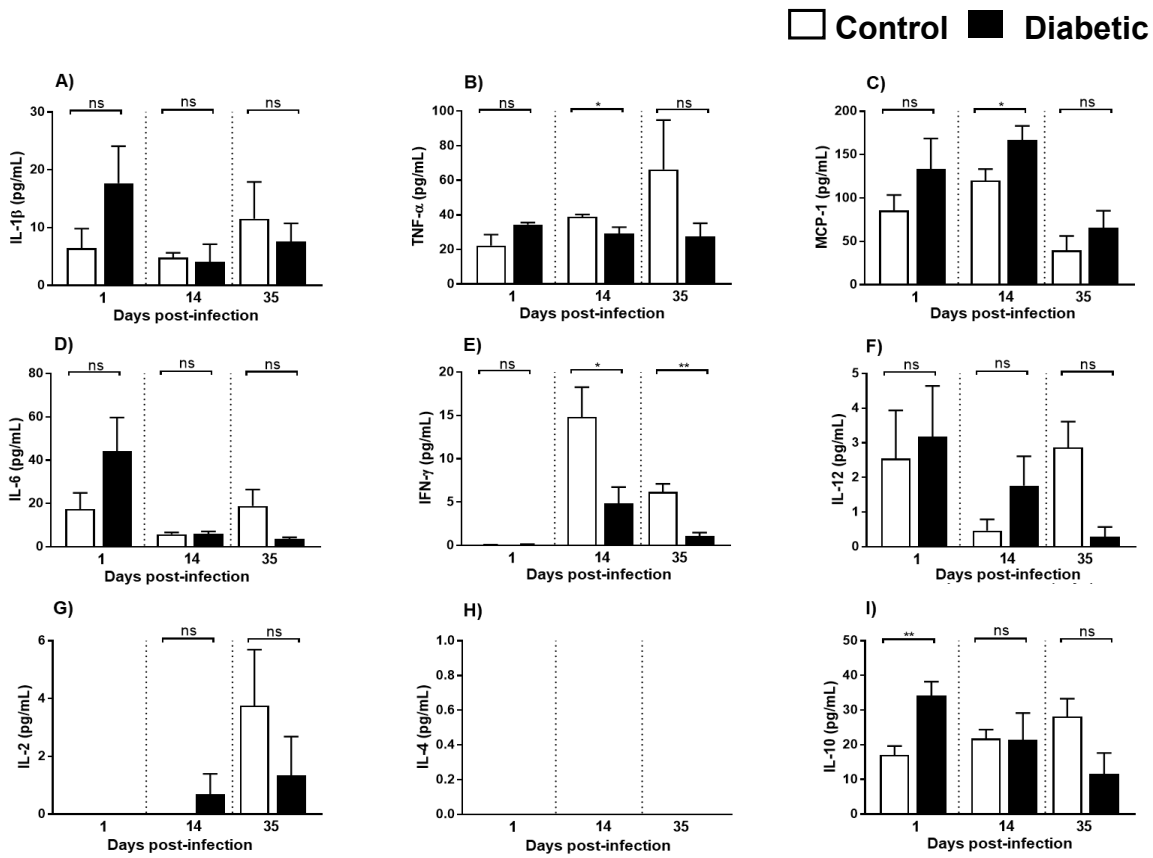

Figure 8.3 Cytokine production in lungs following *M. bovis* (BCG) infection

Mice infected with *M. bovis* (BCG) were assessed for cytokine production in lungs. Figure illustrates the kinetics of IL-1β (A), TNF-α (B), MCP-1 (C), IL-6 (D), IFN-γ (E), IL-12 (F), IL-2 (G), IL-4 (H) and IL-10 (I) production in control and diabetic mice at 1, 14 and 35 days post-infection (dpi). A lower production of IL-1β (A), IL-6 (D), IL-12 (F), IL-2 (G) was observed in the diabetic mice compared to controls at 35 dpi. The production of MCP-1 was found higher in diabetic mice compared to controls at all timepoints of infection. A significantly lower production of TNF-α (B) was observed in diabetic mice at 14 dpi compared to controls which maintained the same trend at the end timepoint of infection. The production of IFN-γ (E) was significantly lower in diabetic mice at both 14 and 35 dpi although its secretion was minimum 1 dpi. IL-4 production was negligible throughout the infection in both control and diabetic mice (H). Although IL-10 production was higher in lungs of diabetic mice compared to controls at 1 dpi, it was opposite at 35 dpi (I). Data presented as mean±SEM; n=4-5 mice/group. The significant differences between the groups were determined using the independent sample *t*-test for the normally distributed data. The non-normally distributed data were analysed using the Mann-Whitney U test (Appendix 5). The level of significance was indicated as *p≤0.05, **p≤0.01, and ns=non-significant.

MCP-1 production however was higher in diabetic lungs at all timepoints (Figure 8.3 C). IL-6 was initially slightly higher in diabetic but by 35 dpi was lower than controls (Figure 8.3 D). IFN-γ was undetectable at 1 dpi but it was significantly decreased in diabetic lungs compared to control lungs at 14 dpi and 35 dpi (Figure 8.3 E).

IL-12 concentration was slightly elevated in the lungs of diabetic mice compared to control mice at 1 and 14 dpi (Figure 8.3 F) but lower at 35 dpi (Figure 8.3 F). IL-10 level was higher at 1 dpi, similar at 14 dpi and lower at 35 dpi in lungs of diabetic mice compared to controls (Figure 8.3 I). IL-2 (Figure 8.3 G), IL-4 (Figure 8.3 H) and IL-17A (Appendix 5, Table A5.14) were undetectable in the lungs of both diabetic and control mice at all timepoints of infection.

8.4.3 Cytokine production following *M. tuberculosis* (H37Rv) infection

8.4.3.1 Cytokine production in spleen

In *M. tuberculosis* (H37Rv) infection at 1 day post infection (dpi), IL-1β level in the spleen of both diabetic and control mice was comparable (Figure 8.4 A). The secretion of IL-1β peaked at 14 dpi and was 3.30 times higher in diabetic mice compared to controls. Although the production of this cytokine was reduced by 30 dpi in both groups, the level in diabetic spleen was slightly higher than controls (Figure 8.4 A). TNF-α and MCP-1 production were initially lower in diabetic mice but higher at later timepoints (Figure 8.4 B & C). IL-6 production was significantly higher in diabetic mice at 14 dpi although there were no differences in the production of this cytokine in both groups at 1 and 30 dpi (Figure 8.4 D). IFN-γ concentration was consistently lower in diabetic spleen compared to control mice at all timepoints of infection (Figure 8.4 E). IL-2 level in diabetics and control was similar early in infection but level in diabetics were significantly lower at 14 and 30 dpi (Figure 8.4 G). IL-10 concentration was slightly higher in diabetic at 14 dpi although a reverse trend was found in 30 dpi (Figure 8.3 I). IL-12 (Figure 8.4 F), IL-4 (Figure 8.4 H) and IL-17A (Appendix 6, Table A6.12) were not detected in any spleen supernatants.

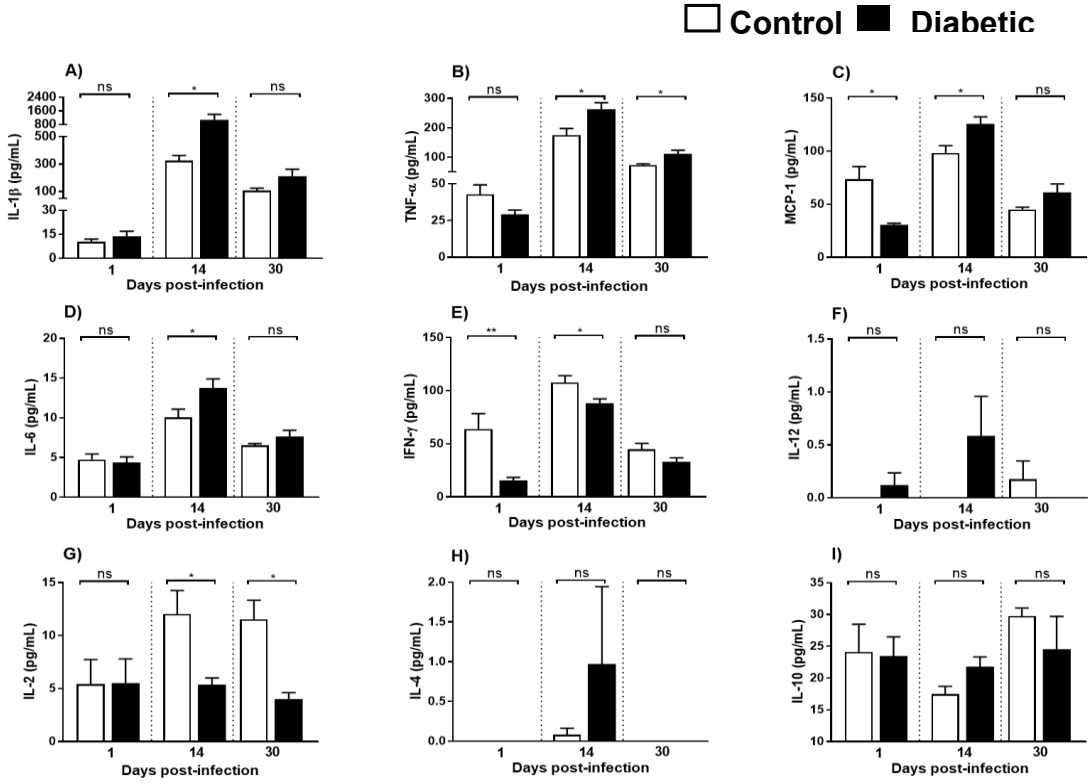

Figure 8.4 Cytokine production in spleen following *M. tuberculosis* (H37Rv) infection

Mice infected with *M. tuberculosis* (H37Rv) were assessed for cytokine production in spleen. Figure illustrates the kinetics of IL-1β (A), TNF-α (B), MCP-1 (C), IL-6 (D), IFN-γ (E), IL-12 (F), IL-2 (G), IL-4 (H) and IL-10 (I) production in control and diabetic mice at 1, 14 and 30 days post-infection (dpi). Overall, a higher production of IL-1β (A), TNF-α (B), MCP-1 (C), IL-6 (D) was observed in diabetic mice compared to controls at 14 and 30 dpi. Whereas the production of IFN-γ (E) was significantly lower in diabetic mice compared to controls at both 1 and 14 dpi although its level did not sustain at 30 dpi. A significantly lower production of IL-2 (G) was observed at 14 and 30 dpi although there was no difference at 1 dpi. The production of IL-10 (I) was higher in diabetic at 14 dpi although a reverse trend was found in 30 dpi. IL-12 (F) and IL-4 (H) secretion was minimum throughout the infection in both groups. Data presented as mean±SEM; n=4-5 mice/group. The significant differences between the groups were determined using the independent sample *t*-test for the normally distributed data. The non-normally distributed data were analysed using the Mann-Whitney U test (Appendix 6). The level of significance was indicated as *p≤0.05, **p≤0.01 and ns=non-significant.

8.4.3.2 Cytokine production in liver

Liver IL-1β level in diabetic was lower at all timepoints compared to controls following *M. tuberculosis* (H37Rv) infection (Figure 8.5 A). The TNF-α concentration was consistently lower in diabetic liver compared to controls at all the timepoints of infection (Figure 8.5 B). MCP-1 was lower in diabetic liver at 1 and 35 dpi although it was opposite at 14 dpi (Figure 8.5 C). Secretion of IL-6 was variable during the infection (Figure 8.5 D). IFN-γ and IL-12 concentrations in the liver of diabetic mice were lower than control mice at all the timepoints post infection (Figure 8.5 E & F). IL-2 level was comparable at 1 and 14 dpi, but significantly

decreased in diabetic mice at 30 dpi (Figure 8.5 G). IL-4 level was slightly increased in diabetic liver compared to controls at 1 dpi although level was minimal at 14 and 30 dpi (Figure 8.5 H). IL-10 secretion was found slightly higher in liver of diabetic mice compared to controls at 1 and 14 dpi although a reverse trend was observed at 30 dpi (Figure 8.5 I). IL-17A was slightly higher in the liver of control mice at 1 (control, 2.03±1.27 *vs* diabetic, 0.97±0.77, pg/mL, p=0.9113) and 30 dpi (control, 4.99±2.85 *vs* diabetic, 0.0.38±0.0.30, pg/mL, p=0.1955) although it was undetectable in either group at 14 dpi.

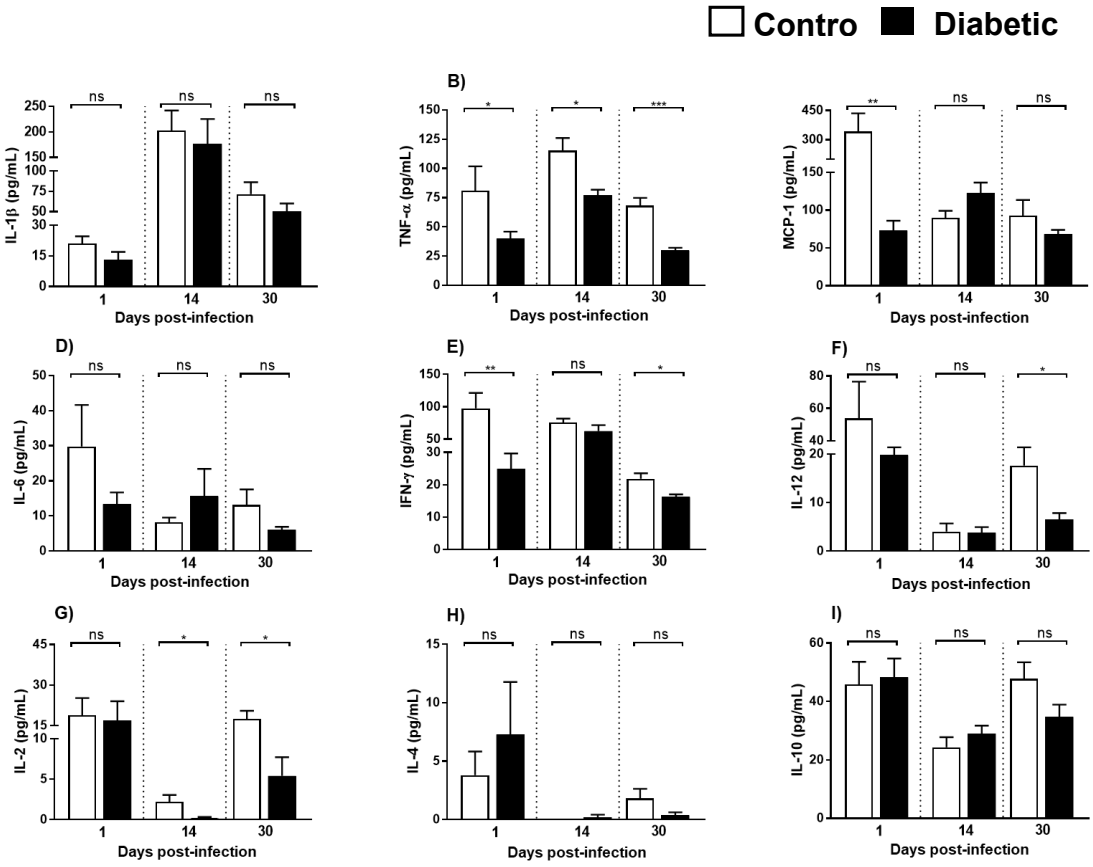

Figure 8.5 Cytokine production in liver following *M. tuberculosis* (H37Rv) infection

Mice infected with *M. tuberculosis* (H37Rv) were assessed for cytokine production in liver. Figure illustrates the kinetics of IL-1β (A), TNF-α (B), MCP-1 (C), IL-6 (D), IFN-γ (E), IL-12 (F), IL-2 (G), IL-4 (H) and IL-10 (I) production in control and diabetic mice at 1, 14 and 30 days post-infection (dpi). Overall, the production of IL-1β (A), TNF-α (B), IL-6 (D), IFN-γ (E), IL-12 (F) and IL-2 (G) was lower in diabetic mice compared to controls. The production of MCP-1 (C) was significantly lower in diabetic mice compared to controls at 1 dpi although a reverse trend was found at 30 dpi. A slightly higher production of IL-4 (H) was observed at 1 dpi although its level was minimum in both groups at later timepoints of infections. A slightly higher production of IL-10 (I) was found in diabetic mice at 1 and 14 dpi although a reverse trend was found at 30 dpi. Data presented as mean±SEM; n=4-5 mice/group. The significant differences between the groups were determined using the independent sample *t*-test for the normally distributed data. The non-normally distributed data were analysed using the Mann-Whitney U test (Appendix 6). The level of significance was indicated as *p≤0.05, **p≤0.01, and ns=non-significant.

8.4.3.3 Cytokine production in lungs

One day after iv infection with *M. tuberculosis* (H37Rv) no IL-1β was detected in either diabetic and control mice (Figure 8.6 A). Later in infection, there was no difference in IL-1β level. The TNF-α concentration was slightly lower in diabetic mice compared to controls at all timepoints of infections (Figure 8.6 B).

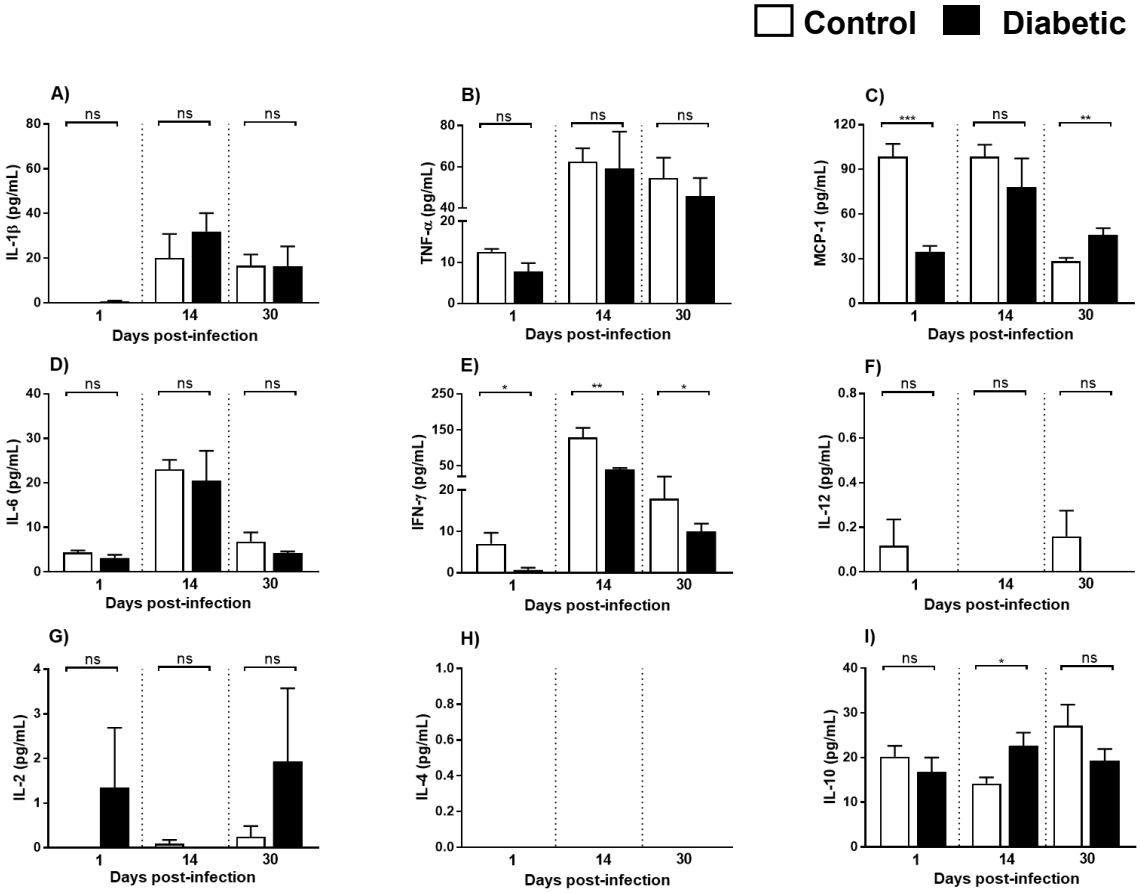

Figure 8.6 Cytokine production in lungs following *M. tuberculosis* (H37Rv) infection

Mice infected with *M. tuberculosis* (H37Rv) were assessed for cytokine production in lungs. Figure illustrates the kinetics of IL-1β (A), TNF-α (B), MCP-1 (C), IL-6 (D), IFN-γ (E), IL-12 (F), IL-2 (G), IL-4 (H) and IL-10 (I) production in control and diabetic mice at 1, 14 and 30 days post-infection (dpi). The production of IL-1β (A) was slightly higher in the diabetic mice compared to controls at 14 dpi although the level was almost same at both 1 and 30 dpi in both groups. The production of MCP-1 was observed lower in diabetic mice compared to controls at 1 and 14 dpi although a reverse trend was found at 30 dpi. An overall lower production of TNF-α (B), IL-6 (D) and IFN-γ (E) was observed in diabetic mice compared to controls. A significantly higher production of IL-10 was observed in diabetic mice compared to controls at 14 dpi although an opposite trend was found at 1 and 30 dpi. The production of IL-12 (F), IL-2 (G), IL-4 (H) was negligible or undetectable in both groups. Data presented as mean±SEM; n=4-5 mice/group. The significant differences between the groups were determined using the independent sample *t*-test for the normally distributed data. The non-normally distributed data were analysed using the Mann-Whitney U test (Appendix 6). The level of significance was indicated as *p≤0.05, **p≤0.01, ***p≤0.001, and ns=non-significant.

MCP-1 concentration was lower in diabetic lungs at 1 and 14 dpi but higher at 30 dpi (Figure 8.6 C). IL-6 production was almost similar between groups at all timepoints (Figure 8.6 D). The production of IFN-γ was significantly lower in the lungs of diabetic mice compared to control at all the timepoints (Figure 8.6 E). It was 10, 3.20 and 1.80 times lower in the lungs of diabetic mice compared to controls at 1, 14 and 30 dpi, respectively (Figure 8.6 E). IL-10 concentration in diabetic lungs was increased significantly at 14 dpi compared to controls but decreased by 30 dpi (Figure 8.6 I). IL-12 (Figure 8.6 F), IL-2 (Figure 8.6 G), IL-4 (Figure 8.6 H) and IL-17A (Appendix 6, Table A6.14) were low or undetectable.

8.5 Discussion

Increased bacillary loads (Chapter 6) and increased tissue inflammation (Chapter 7) in diabetic mice suggest defective and/or dysregulated immune responses in these hosts. Furthermore, we have demonstrated that cellular function and cytokine secretion in mycobacteria-activated diabetic macrophages is abnormal (Chapter 5). To further investigate these phenomena, we measured tissue cytokines secreted in response to different mycobacterial infections.

The roles of specific pro- and anti-inflammatory cytokines in mycobacterial infections have been widely studied and reviewed (Orme and Cooper, 1999, Cooper et al., 2011, Orme and Ordway, 2014). In both tuberculous and NTM infections, previous studies have shown that mice lacking TNF-α promptly succumb to infections (Appelberg et al., 1994b, Parti et al., 2005, Benoit et al., 2008) by failure to activate macrophages and neutrophils (Orme and Cooper, 1999, Tsenova et al., 1999, Gan et al., 2005), leading to higher organ bacterial loads (Flynn et al., 1995) and ineffective granuloma formation (Kindler et al., 1989, Flynn et al., 1995, Senaldi et al., 1996). Mice with defective IL-1 signalling showed decreased IFN-γ and IL-6 production during *M. tuberculosis* infection, leading to defective granuloma formation (Toossi et al., 1990, Juffermans et al., 2000). MCP- 1 (also called CCL2) is essential for recruitment of various immune cells and activated T cells into tissues (Kipnis et al., 2003). Kipnis and colleagues (2003) reported fewer macrophages in lungs, an increased bacterial load and failure to recruit antigen-specific T lymphocytes into the lungs of CCL2 knockout mice.

In the current study, we measured less IL-1β and TNF-α in the liver and lungs of diabetic mice compared to controls following both *M. bovis* (BCG) and *M. tuberculosis* (H37Rv) infections although the opposite trend was observed in the spleen (Figure 8.1-8.6 A & B). In *M. fortuitum* infection studies, we reported a trend for decreased TNF-α in liver, lungs and spleen of diabetic mice compared to controls (Table 8.1-8.3). MCP-1 concentration in spleen, liver and lungs of

the diabetic mice tended to be higher than controls in *M. bovis* infection (Figure 8.1-8.3 C). In *M. tuberculosis* (H37Rv) infection, overall MCP-1 production in spleen, liver and lungs was lower at the earliest timepoint of infection although an opposite trend was observed at later timepoint of infection in diabetics compared to controls (Figure 8.4-8.6 C). In *M. fortuitum* infection (low-dose), there was no significance difference in the secretion of MCP-1 in spleen and lungs of both diabetic and control mice although it was lower in the liver of diabetic mice (Table 8.1-8.3).

Previous studies examining TNF-α, IL-1β and MCP-1 levels in different animal models have produced conflicting results. A recent investigation demonstrated significantly lower TNF-α levels in the lungs of STZ+NA-induced diabetic mice compared to non-diabetic controls 1 month pi although by 6-month pi TNF-α levels was far in excess of both 1 month levels and non-diabetic controls (Cheekatla et al., 2016). Martens and co-workers (2007) reported an increased level of IL-1β and TNF-α in the lungs of chronic diabetic mice (>16 weeks) compared to controls. Cytokine gene expression analysis showed lungs TNF-α and IL-1β mRNA expression was delayed in *M. tuberculosis* infected diabetic rats compared to control rats with decreased expression at 3-5 weeks post-infection (pi) but increased expression by 12 weeks pi (Sugawara et al., 2004). Sugawara and colleagues (2008) found increased expression of the TNF-α genes in the lungs of T2D rat compared to controls at 7 weeks pi in *M. tuberculosis* infection. In a guinea pig model of TB-diabetes co-morbidity, TNF-α and MCP-1 were more highly expressed in the spleen of diabetic guinea pigs 30 days after aerosol *M. tuberculosis* infection compared to controls (Podell et al., 2014). They also reported higher expression of IL-1β and MCP-1 and decreased expression of TNF-α in infected diabetic Guinea pig lungs compared to controls.

Our data i.e. decreased IL-1β, TNF-α, MCP-1 concentrations early in *M. tuberculosis* (H37Rv) infection in diabetics is in general agreement with those studies that have used acute diabetic animal models infected. Collectively, the data indicate that IL-1β, TNF-α, MCP-1 are crucial in acute infections. These data suggested that an overall lower production of TNF-α, IL-1β and MCP-1 at the earliest time of infection in diabetic mice failed to activate and recruit macrophages to secrete bactericidal compounds such as ROS and iNOS. Although it was beyond the scope of the current study to measure these compounds, previous studies report that decreased production of such compounds in diabetic mice during mycobacterial infections leads to higher bacterial burdens and increased inflammation in infected organs (Yamashiro et al., 2005, Vallerskog et al., 2010). Moreover, a higher production of MCP-1 in diabetic organs at

later timepoints of this study further suggested failure to control bacterial loads (as seen in Chapter 6) resulting in more tissue inflammation as observed in other diabetic animal models (Vallerskog et al., 2010, Podell et al., 2014, Cheekatla et al., 2016).

The role of IL-6 in TB defence is conflicting (Nagabhushanam et al., 2003, Cooper et al., 2011, Dutta et al., 2012, Martinez et al., 2013, Singh and Goyal, 2013). In the current study, we observed slightly reduced IL-6 levels in organs of diabetic mice compared to controls infected with *M fortuitum* (Table 8.1-8.3), *M. bovis* (BCG) and *M. tuberculosis* (H37Rv) (Figure 8.1-8.6 D). In the STZ+NA-induced mouse model, Cheekatla and co-workers (2016) demonstrated a significantly reduced production of IL-6 in the lungs of diabetic mice compared to controls during acute *M. tuberculosis* infection (1 month), whereas the reverse was true in chronic infections (6 months). These investigators suggested that IL-6 was responsible for driving inflammation in the lungs of chronically infected diabetic mice. When they treated chronically infected diabetic mice with anti-IL-6 antibodies, the expression of all pro-inflammatory cytokines (IFN-γ, TNF-α, IL-1β and MCP-1) was abolished in lungs compared to controls, suggesting that IL-6 has a primary role in driving the expression of many pro-inflammatory cytokines. The findings of the current study suggested that IL-6 has a protective role in acute infection to control the infections by inducing increase expression of pro-inflammatory cytokines. It would be interesting to evaluate the effect of IL-6 in this T2D model during chronic mycobacterial infections.

Th1 cell responses are crucial in developing resistance and protective immunity in mycobacterial infections which is driven by IL-12 (Cooper et al., 1995, Cooper, 2009, Jasenosky et al., 2015). In the current investigation, we observed decreased concentrations of IL-12 in organs of diabetic mice compared to controls during *M. fortuitum* (Table 8.1-8.3), *M. bovis* (BCG) (Figure 8.1-8.3 F) and *M. tuberculosis* (H37Rv) infections (Figure 8.4-8.6 F). Previous studies observed a decreased expression of IL-12 in the lungs of diabetic rats compared to controls(Sugawara et al., 2004, Sugawara and Mizuno, 2008). Reduced IL-12 production was observed in peritoneal exudate cells stimulated with *M. bovis* (Yamashiro et al., 2005). These authors demonstrated decreased production of both IL-12 in the spleen, liver and lungs of STZ-induced diabetic mice compared to controls infected intravenously with *M. tuberculosis.* Reduced secretion of IL-12 in diabetic mice of this study suggests poor antigen presentation and Th1 cells differentiation resulting in higher mycobacterial susceptibility.

Another key cytokine for TB protection is IFN-γ which is secreted by Th1 cell-mediated responses (Cooper, 2009). In the current study, we have observed an overall reduced production

of IFN-γ in organs of diabetic mice compared to controls during *M. fortuitum* (Table 8.1-8.3), *M. bovis* (BCG) (Figure 8.1-8.3 E) and *M. tuberculosis* (H37Rv) infections (Figure 8.4-8.6 E). The necessity for IFN-γ and its role in at the earliest timepoints after *M. tuberculosis* infection in hyperglycaemic mice was described by Martens and co-workers (2007). These authors observed decreased production of IFN-γ in lung lysates collected from hyperglycaemic mice at 7, 14 and 21 dpi. A lower production of IFN-γ was recoded in spleen, liver and lungs of STZ-induced diabetic mice (Yamashiro et al., 2005). Vallerskog and colleagues (2010) showed delayed priming of T cell responses in diabetic mice following aerosol *M. tuberculosis* infection compared to controls due to delayed appearance of IFN-γ producing T cells in the lungs and draining lymph nodes of diabetic mice. Other investigators have shown a marked reduction in IFN-γ secretion by spleen cells of diabetic mice stimulated with PPD (purified protein derivatives) and CFP (culture filtrate proteins) and ESAT-6 (early secretory antigenic target-6) antigens (Yamashiro et al., 2005). Our data are in agreement with the above studies suggesting an impaired or delayed Th1 cell responses in diabetic mice leading to higher susceptibility to mycobacterial infections. This study did not examine IFN-γ producing T cells in lungs and other organs, however, future studies could determine the contribution of these cells in TB-diabetes co-morbid infections and how the observed lack of IFN-γ in these diabetic mice influences infection outcome.

In the current study, we observed minor decreases in IL-2 in the spleen and liver of diabetic mice compared to controls during *M. bovis* (BCG) and *M. tuberculosis* (H37Rv) infections (Figure 8.1, 8.2, 8.4 and 8.5 G). IL-2 has an important role in the activation and expansion of T cells (Johnson et al., 2003). This cytokine has been shown to reduce bacterial replication by its effects on IFN-γ mediated macrophage activation and in the expansion of cytotoxic T cells (Toossi et al., 1986, Jeevan and Asherson, 1988). Deficits in IL-2 induced cell proliferation are common in TB patients (Toossi et al., 1986). In diabetic rats infected with *M. tuberculosis* decreased IL-2 gene expression was observed at 3-5 weeks pi although expression was increased by 12 weeks pi (Sugawara et al., 2004). The differences in the secretion of IL-2 in the diabetic and control mice of this study further suggested the possibility of diminished or delayed T cell expansion and IFN-γ-producing effector T cell differentiation.

In this investigation, we observed minor increases in IL-4 in the liver of diabetic mice early in infections (Figure 8.2 and 8.5 H) suggesting the possibility of immune responses (innate and adaptive) skewed to a type 2 response. Although type 2 cytokines can increase host resistance to some specific pathogens (e.g. Leishmania, Cryptococcus) (Kopf et al., 1996, Blackstock et

al., 1999), alterations in the Th1/Th2 balance toward a Th2- dominant response has been linked to adverse disease outcomes (Heinzel et al., 1989, Heinzel et al., 1995). Yamashiro and co-workers (2005) observed increased IL-4 in the lungs and liver of STZ-induced ICR mice compared to controls infected intravenously with *M. tuberculosis*. This finding suggested that *M. tuberculosis* immune responses in diabetics may be skewed to IL-4 driven Th2 responses rather than the protective IL-12/IFN-γ driven Th1 responses. However, the role of this cytokine is still controversial and whether elevated tissue IL-4 skews immune responses in mycobacterial (and other) infections is far from clear (Hernandez-Pando et al., 1996, North, 1998, Flynn and Chan, 2001a, Jung et al., 2002, Hernandez-Pando et al., 2004).

There was no constant trend for IL-10 production in the organs of diabetic mice compared to controls during mycobacterial infections (Table 8.1-8.3, Figure 8.1-8.6 I). Although we observed minor increases in IL-10 in the organs of diabetic mice compared to controls at the earliest timepoint of *M. bovis* (BCG) and *M. tuberculosis* (H37Rv) infection. In line with the findings of the current investigation, higher IL-10 production was observed in lungs of STZ-induced diabetic mice during *M. tuberculosis* infection at 4 weeks pi although an opposite trend was found at 24 weeks pi (Cheekatla et al., 2016). IL-10 plays an important role in limiting potentially harmful inflammatory immune responses during mycobacterial infections (Bermudez and Champsi, 1993, Murray and Young, 1999, Jacobs et al., 2000, Roque et al., 2007). Increased production of this cytokine in the current study suggested a decrease production of pro-inflammatory cytokines (e.g. TNF-α, IFN-γ) as observed in TB research (Gong et al., 1996, Fulton et al., 1998, Hirsch et al., 1999a) and diabetic animal model research (Cheekatla et al., 2016). Future research can be directed to determine the role of IL-10 in TB-diabetes co-morbid study in IL-10 knockout diabetic mice.

In the current investigation, the dysregulation of several pro-inflammatory cytokines (TNF-α, IL-1β, IL-6, IFN-γ, IL-12, IL-2) in organs from diabetic mice during acute infection with *M. fortuitum*, *M. bovis* and *M. tuberculosis* is likely to contribute to dysregulated immune responses. Some of the cytokine data presented here shows discrepancies with data from chronic mycobacterial infection models discussed above. The current research focused primarily on comparing early inflammatory responses (i.e. 4-5 weeks) in diabetic and non-diabetic hosts following intravenous infections. Many of the aforementioned diabetic animal models are chronic infection model, often using an aerosol infection route. Future studies could investigate the immune status of diabetics in chronic mycobacterial infections considering both routes of infection (aerosol and iv)

CHAPTER 9
GENERAL DISCUSSION

Type 2 diabetes (T2D) is considered to be one of the most significant risk factors for increased Tuberculosis (TB) susceptibility or its reactivation leading to higher mortality (Jeon and Murray, 2008, Martinez and Kornfeld, 2014, Hodgson et al., 2015). Understanding TB-T2D co-morbid infection has become a global public health issue. Whilst *M. tuberculosis* contributes to the majority of mycobacterial infections, there are more than 150 non-tuberculous mycobacterial (NTM) species which are capable of causing a wide spectrum of human diseases (Orme and Ordway, 2014). Epidemiological studies indicate a rising incidence in pulmonary and skin and soft tissue infections caused by NTM (e.g. *M. fortuitum*) (De Groote and Huitt, 2006, Jackson et al., 2007, Hoefsloot et al., 2013) particularly in patients with AIDS and diabetes (Tortoli et al., 1995, Piersimoni et al., 1997, Gholizadeh et al., 1998, Uslan et al., 2006, Orme and Ordway, 2014, Bridson et al., 2016, Xu et al., 2016). The precise mechanisms underlying this increased susceptibility of diabetics to TB or NTM infections are unclear and many critical questions remain to be answered. The studies presented in this thesis contribute to our understanding of some key differences between diabetics and non-diabetics in their respective responses to mycobacterial infections, identifying deficits in macrophage function and an inability to regulate tissue inflammation as potential reasons for increased susceptibility.

To date, relatively few studies have been done in either humans (Kumar Nathella and Babu, 2017) or animal models (Saiki et al., 1980, Sugawara et al., 2004, Yamashiro et al., 2005, Martens et al., 2007, Vallerskog et al., 2010, Podell et al., 2014, Cheekatla et al., 2016) to dissect the pathobiology in TB-T2D comorbid infections. Mimicking the key features of the pathology of human T2D in animal models has proven challenging with numerous models evaluated over many years, often producing contradictory results. Whilst diverse animal models of T2D exist, animal models used to investigate TB-diabetes have primarily utilised administration of high-dose of cytotoxic streptozotocin (STZ)/STZ+NA (Nicotinamide) to induce a T1D (type 1 diabetes)-like disease. Despite the rapid onset of hyperglycaemia in these models, they do no accurately model the chronic vascular and inflammatory complications associated with T2D. Although these studies have provided substantial information as to how hyperglycaemia affects active TB disease, the influence of diet, a key driver of human T2D had not been modelled, thereby limiting the utility of these models to investigate the pathogenesis of increased

mycobacterial susceptibility in diabetics (Gilbert et al., 2011, Hodgson et al., 2013a). To address this need, we first characterised a diet-induced murine model of T2D that mimics the overt signs of chronic T2D of human patients. We then assessed macrophage function, the kinetics of infection and inflammation and mortality in diabetic and non-diabetic animals infected with three different mycobacteria species. We showed that antimycobacterial activity in diabetics is significantly compromised.

In this thesis, we describe a detailed metabolic and biochemical characterisation of a diet-induced murine model of T2D for evaluating mycobacterial susceptibility. An energy-dense diet (EDD); a combination of refined carbohydrate with a moderate amount of fat was used to induced diabetes. Other researchers used a traditional high-fat diet (60% of energy from fat) which markedly exceed the typical dietary intake in developed nations (34% energy) (Harika et al., 2013). A sole source of energy from the high-fat diet does not represent the global dietary pattern. A range of parameters was evaluated after EDD intervention, as high consumption of EDD has been linked to high energy intake and excess weight gain (Hodgson et al., 2013a). The specially formulated EDD influenced glucose metabolism and resulted in obesity induced T2D in mice which are reflected through the higher body weight gain (almost double the weight of control mice). Hyperglycaemia and insulin resistance is one of the pathognomonic clinical features of T2D in human (ADA., 2010). Comparison of hyperglycaemic status in mice indicated that EDD fed mice suffered from chronic hyperglycaemia as they become more glucose intolerant due to insulin resistance. Chronic hyperglycaemia imposes glucose toxicity on numerous cell types (e.g. pancreatic β-cells and vascular endothelial cells) and correlates with many diabetes-related complications. Chronic hyperglycaemia (glucose toxicity) and insulin resistance; characteristics features of T2D in human patients (ADA., 2010, Quan et al., 2013), was observed in the mouse model we developed including elevated levels of HbA1c and hyperplasia of the pancreatic islets. Moreover, an overall adiposity in EDD fed mice also suggested dyslipidaemia although we didn't determine the relevant parameters such as triglyceride, High- (HDL) and Low-Density Lipoprotein (LDL)-cholesterol concentration in blood. As dyslipidaemia is associated with T2D and forms part of the diagnostic criteria for metabolic syndrome (Mullarkey et al., 1990, Sacks et al., 2002, Abraira et al., 2003), additional studies are required to assess the parameters related to dyslipidaemia.

We also determined the impact of EDD on renal function. Diabetic kidney disease is one of the most prevalent complications of T2D and is now the leading cause of end-stage renal disease (ESRD) in developed countries (Ghaderian et al., 2015). The pathogenesis of diabetic kidney

disease is multifactorial, with the interaction of both genetic and environmental factors that trigger a complex network of pathophysiological events. The main criteria to diagnose diabetic kidney disease is the presence of an increased urinary albumin excretion (microalbuminuria and macroalbuminuria), which is associated with an increased risk of decline in glomerular filtration rate and a high risk of kidney failure (Gross et al., 2005, Fowler, 2008, Dabla, 2010). Energy-dense diet fed mice showed microalbuminuria and higher urinary albumin creatinine ratio (ACR) than non-diabetic animals, indicating some level of glomerular damage. Furthermore, lower levels of urinary creatinine in EDD fed mice also suggested kidneys were unable to function properly to filter circulating creatinine. The current study did not measure plasma creatinine concentrations, therefore further studies are required to accurately determine creatinine clearance. The urine biochemical parameters together with observed changes in kidney structure (mesangial thickening in the glomeruli and glomerular hypertrophy) have demonstrated a prolonged EDD intervention can result in significant kidney damages.

Subclinical chronic inflammation is a hallmark of T2D and its associated vascular complications characterised by oxidative stress, elevated levels of acute phase proteins (e.g. C-reactive protein), accumulation of advanced glycation end products, inflammatory cytokines and changing the proportion of immune cell subsets and their functions (Jagannathan-Bogdan et al., 2011, Morris et al., 2016). Future studies can also be directed to determine these parameters in this T2D model to better understand the pathophysiology of T2D and interpretation of co-morbid infections.

Susceptibility to *M. fortuitum*, *M. bovis* (BCG) and *M. tuberculosis* (H37Rv) infections was determined using this T2D model (Chapter 5, 6, 7 and 8). To our knowledge, this was the first study to investigate host-*M. fortuitum* and *M. bovis* (BCG) interactions in diet-induced diabetic animal model. When the mice were challenged with high-doses of all species, increased mortality was observed in diabetic mice (Chapter 6). The lower survival of diabetic mice infected with all mycobacteria species indicated defective antimycobacterial immunity. In host-mycobacterial infections, the primary encounter is mediated by the macrophages, particularly the alveolar macrophages (Tascon et al., 2000, Gonzalez-Juarrero et al., 2001, Dheda et al., 2010). The primary function of the macrophage is phagocytosis (uptake and killing) of the bacilli (Henderson et al., 1997, Thurnher et al., 1997) followed by the production of the myriad of pro- and anti-inflammatory cytokines required for mounting an effective immune response. Assessment of the uptake and killing capability of alveolar (AM) and resident peritoneal macrophages (RPM) revealed decreased uptake and killing of all mycobacteria species by

diabetic macrophages (Chapter 5). Further, the uptake of mycolic acid coated beads by both diabetic AM and RPM was also reduced compared to uncoated beads suggestive of modulation of phagocytic uptake mediated, at least in part, by components of mycolic acid. The higher bacterial burden in the organs of mycobacteria-infected diabetic mice also suggested that macrophage phagocytic functions were impaired in diabetes (Figure 9.1). Although the precise mechanisms underlying this decreased phagocytic function in diabetic macrophages remains unclear, previous studies have suggested the following as possible reasons: (i) impairment of pattern recognition receptors (PRRs) signalling; (ii) lower expression of scavenging receptors (e.g. macrophage receptors with collagenase structure; MARCO, mannose, mincle receptors); (iii) reduced activation of co-stimulatory molecules (e.g. major histocompatibility complex Class II, CD14); (iv) reduced association (attachment), alteration of complement (C3b) and complement receptors (CR1 and CR3) with macrophages; (v) differentiation and reduction of macrophage number and; (vi) impaired cytokine production. It is also possible that a combination of these processes contributes to the defective immune responses in diabetics. In TB defence, host recognition by the different PRRs (mannosylated lipoarabinomannan, ManLAM, toll like receptors 2; TLR-2, C-type lectin) is a primary immune event that not only activates innate immune mechanisms, but also assists in the development of antigen specific adaptive immunity (Ahmad, 2011). In this host recognition process, many scavenging receptors are involved in phagocytosis of the bacilli, with one of the major receptors, being MARCO. Bowdish and colleagues (2009) demonstrated that phagocytosis by macrophages is reduced due to lower expression of MARCO receptors and CD14, a co-stimulatory molecule that acts with MARCO in the recognition of the mycobacterial cell wall components (e.g. trehalose 6,6′-dimycolate). Amongst the receptors that mediate phagocytosis, complement receptors 1 and 3 (CR1 and CR3) are essential, with 80% of *M. tuberculosis* phagocytosis being associated with CR3. Future studies could be directed to explore the roles of these different PRRs, scavenging receptors and co-stimulatory molecules in diabetic animal models to better understand their respective roles in host recognition, mycobacterial uptake and killing.

In our study, an overall decreased production of pro-inflammatory cytokines (TNF-α, MCP-1 and IL-6, IL-1β) by diabetic macrophages was associated with impaired killing of mycobacteria (Figure 9.1). Among these cytokines, TNF-α enables macrophages to secrete more antimycobacterial compounds (e.g. ROS and iNOS) to kill internalised bacteria (Schlesinger et al., 1990, Ahmad, 2011). The production of IL-1β and IL-6 further enhances the production of TNF-α (also IFN-γ) from macrophages (Saunders et al., 2000, Cooper, 2009, Cooper et al., 2011). Decreased production of these cytokines in this study suggested that lower secretion of

antimycobacterial compounds by the mycobacteria infected macrophages leading to higher bacterial burden in the diabetic host. Future studies could determine whether the production of specific antimicrobial compounds is impaired in diabetic macrophages in *vivo*. Abnormal differentiation and egress of macrophage precursors from bone marrow have been observed in diabetic animals (Nikolic et al., 2004, Ma et al., 2008). Consistent with these findings, we observed decreased numbers of macrophages in peritoneal exudates and broncho-alveolar fluid from diabetic mice; potentially contributing to the impaired phagocytosis observed in diabetes.

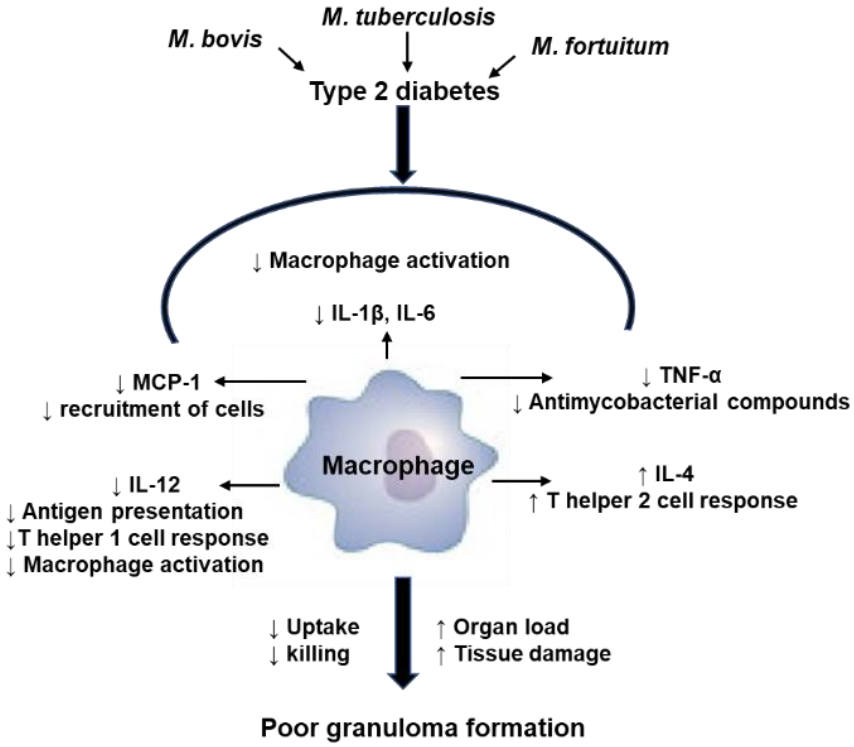

Figure 9.1 Impairment of macrophage functions in type 2 diabetes-mycobacterial co-morbid infections

In *M. tuberculosis* infection, the transition from innate immune to adaptive responses requires phagocytic antigen presenting cells (dendritic cells and macrophages) to deliver peptides of the bacilli from the alveolar space to lung-draining lymph nodes for naïve T cell priming (Cooper, 2009). Although the current study used an intravenous route of infections and didn't determine the function of antigen presenting cells *per se*, our results suggest that antigen presentation may be delayed, followed by delayed or impaired T cell priming. IL-12 is a crucial cytokine (signal 3) associated with antigen presentation and Th1 cells differentiation from naïve CD4 T cells. IL-2 enhances Th1 cell clonal expansion. IFN-γ is a key cytokine secreted mostly by activated

Th1 cells and involved in the macrophage-activating effector function (Cooper, 2009, Cooper et al., 2011). The central role of Th1 cells in the defence against TB has been attributed to the ability of Th1 cell-derived IFN-γ to activate macrophages and stimulate phagocytosis, phagosome maturation, production of antimycobacterial compouds, killing of bacteria and antigen presentation. Th1 cells secrete IFN-γ to promote macrophage M1 polarisation and enhance its pro-inflammatory functions by inducing the release of IL-1β, IL-6 and TNF-α. In the absence of effective IFN-γ signalling, increased TB susceptibility as a result of reduced production of antimycobacterial compounds by the macrophages and failure to restrict the growth of the bacilli was observed (Cooper et al., 1993, Flynn et al., 1993). We observed decreased levels of IFN-γ in diabetic animals in response to mycobacterial infections suggesting impaired/delayed Th1 cell responses in early infection. This result may be further explained by the decreased production of IL-12 and the lower production of IL-2 that could further reduce, or at least, delayed Th1 cell differentiation and expansion in acute TB-T2D co-morbid infections (Cooper, 2009, Cooper et al., 2011). However, some prior studies demonstrated a high pro-inflammatory responses (e.g. TNF-α, IL-6, MCP-1, IFN-γ) in chronic TB-diabetes co-morbid patients (Kumar Nathella and Babu, 2017), although there are also conflicting reports (Tsukaguchi et al., 1992, Tsukaguchi et al., 1997, Tsukaguchi et al., 2002, Kumar et al., 2014). The possible explanations of these paradoxical findings in chronic TB-diabetes suggested by the previous research are (i) persistent higher bacterial burden (ii) alteration of downstream signal transduction and regulation (iii) inactivity of the cytokines (iv) an increased half-life of cytokine due to delayed proteolysis. All these events are resulted in with the accumulation of AGEs in diabetes (Greenhalgh and Hilton, 2001, Tamarat et al., 2003, Restrepo et al., 2008a, Uribarri et al., 2010) and mechanisms need to be addressed by future studies.

Our findings also suggested the possibility of a shift of the immune system towards Th2 cell responses in diabetics (Figure 9.1). We observed increases in the Th2 cell associated cytokine IL-4 in response to early mycobacterial infections. IL-4 may induce macrophages to take on an M2 phenotype in order to resolve inflammation (Cooper, 2009, Cooper et al., 2011). Furthermore, IL-4 down-regulates Th1 responses by inhibiting Th1 cell differentiation and inducing a reversion of developing Th1 cells to the Th2 lineage and further influencing the transcription of the IFN-γ gene in Th1 effector cells (Wurtz et al. 2004).

To overcome the limitation of these studies, future studies can be directed towards evaluating: (i) whether delayed antigen presenting cell trafficking from the alveolar airspace to regional lymph nodes impairs/delays antigen presentation; (ii) macrophage differentiation (pro or anti-

inflammatory) and (iii) T cell differentiation and phenotypes (iv) and cytokine gene expression in diabetics infected with mycobacteria in both acute and chronic mycobacterial infections. Such studies will widen our understanding of T cell mediated responses in diabetic individuals. The current study highlighted the diminished antimycobacterial functions during acute mycobacterial infections. It would however be interesting to determine whether our findings would be replicated using chronic infection models (e.g. aerosol infections).

The granuloma is considered a hallmark of TB infection. The granuloma is a type IV hypersensitivity reaction characterised by (i) infiltration of leucocytes; (ii) tissue destruction induced by persistent organisms or inflammatory cells and (iii) attempted healing by connective tissue replacement of damaged tissue and fibrosis. It contains live bacilli and prevents bacterial dissemination and reactivation of disease (Saunders and Cooper, 2000, Ehlers, 2009). Formation of the granuloma is one of the important outcomes of TB defence but its effectiveness in containing live microorganisms relies on appropriate innate and adaptive immune responses involved in its formation (Korbel et al., 2008). Macrophages are the principal cells found in the TB granuloma (Jo et al., 2007, Cooper et al., 2011). The granuloma is mainly composed of centrally infected macrophages surrounded by epithelioid cells, foamy macrophages, multinucleated giant cells of the Langhans type which are peripherally surrounded by CD4+ and CD8+ T cells (Gonzalez-Juarrero and Orme, 2001, Puissegur et al., 2004). A mature granuloma is compact, highly stratified, becomes vascularised and develops a fibrotic capsule (Russell, 2007). However, the granuloma-associated cells aggregate in response to different cytokines (e.g. TNF-α, IL-12, IFN-γ) and chemokines (e.g. MCP-1) during host-mycobacterial interactions (Saunders and Cooper, 2000, Saunders et al., 2005, Guirado and Schlesinger, 2013). Our findings suggest that there is defective or delayed formation of the granuloma/inflammatory foci possibly due to impaired macrophage antimycobacterial functions and Th1 cell responses. In diabetic mice infected with mycobacteria, inflammatory foci in liver were more diffuse with loosely associated cells containing higher numbers of bacilli. The presence of bacilli scattered throughout liver parenchyma rather than being contained within inflammatory foci, suggests that leucocyte recruitment in response to higher numbers of bacteria may also be impaired. Consequently, bacilli were diffusely spread and poorly confined within the tissue which was indicative of poor granuloma formation in diabetic mice. In contrast, the granulomas of non-diabetic mice were more compact with a lower number of bacteria. Previous research has shown that granulomas are larger in size, rich in activated macrophages and with few surrounding lymphocytes in immunodeficient patients with TB, whereas they are small, compact with more IFN-γ producing CD4 T cell in immunocompetent

individuals with TB infection (Ulrichs et al., 2005). Although this study didn't determine the involvement of specific cells in the formation of granuloma, it would be interesting to explore cell phenotypes in future research.

The current study also suggested another possibility: the breakdown of this defective granuloma increases the risk of reactivation of disease. Understanding the cellular basis of latent TB infection (LTBI) is an area of research that requires special attention as an estimated one third of the world population (approximately 2.5 billion) is currently considered to be latently infected with TB. Due to the increase in T2D and an ageing population, a considerable proportion of those cases could reactivate presenting a major worldwide public health crisis (Martinez and Kornfeld, 2014). The development of a good, tractable LTBI model is a prerequisite to investigate how T2D influences the risk to reactivation of latent disease. The use of the EDD animal model described in this study combined with novel LTBI animal models will certainly enhance our understanding of the true risk that T2D poses in infected people throughout the world. As highlighted throughout this thesis TB-T2D coinfection has the potential to become a major public health problem. Research into the immune mechanisms of TB-T2D coinfection should pave the way for the development of effective treatment and preventive options that reach the world's most vulnerable populations.

REFERENCES

AAGAARD, C., HOANG, T., DIETRICH, J., CARDONA, P. J., IZZO, A., DOLGANOV, G., SCHOOLNIK, G. K., CASSIDY, J. P., BILLESKOV, R. & ANDERSEN, P. 2011. A multistage tuberculosis vaccine that confers efficient protection before and after exposure. *Nat Med,* 17**,** 189-94.

AAGAARD, C., HOANG, T. T., IZZO, A., BILLESKOV, R., TROUDT, J., ARNETT, K., KEYSER, A., ELVANG, T., ANDERSEN, P. & DIETRICH, J. 2009. Protection and polyfunctional T cells induced by Ag85B-TB10.4/IC31 against *Mycobacterium tuberculosis* is highly dependent on the antigen dose. *PLoS One,* 4**,** e5930.

ABEBE, F. & BJUNE, G. 2009. The protective role of antibody responses during *Mycobacterium tuberculosis* infection. *Clin Exp Immunol,* 157**,** 235-43.

ABEL, B., TAMERIS, M., MANSOOR, N., GELDERBLOEM, S., HUGHES, J., ABRAHAMS, D., MAKHETHE, L., ERASMUS, M., DE KOCK, M., VAN DER MERWE, L., HAWKRIDGE, A., VELDSMAN, A., HATHERILL, M., SCHIRRU, G., PAU, M. G., HENDRIKS, J., WEVERLING, G. J., GOUDSMIT, J., SIZEMORE, D., MCCLAIN, J. B., GOETZ, M., GEARHART, J., MAHOMED, H., HUSSEY, G. D., SADOFF, J. C. & HANEKOM, W. A. 2010. The novel tuberculosis vaccine, AERAS-402, induces robust and polyfunctional CD4+ and CD8+ T cells in adults. *Am J Respir Crit Care Med,* 181**,** 1407-17.

ABRAIRA, C., DUCKWORTH, W., MCCARREN, M., EMANUELE, N., ARCA, D., REDA, D. & HENDERSON, W. 2003. Design of the cooperative study on glycemic control and complications in diabetes mellitus type 2: Veterans Affairs Diabetes Trial. *J Diabetes Complications,* 17**,** 314-22.

ABRASS, C. K. 1991. Fc-receptor-mediated phagocytosis: abnormalities associated with diabetes mellitus. *Clin Immunol Immunopathol,* 58**,** 1-17.

ADA. 2009a. American Diabetes Association: Executive summary: standards of medical care in diabetes-2009. *Diabetes Care,* 32 Suppl 1**,** S6-12.

ADA. 2009b. American Diabetes Association: International Expert Committee report on the role of the A1C assay in the diagnosis of diabetes *Diabetes Care,* 32**,** 1327-34.

ADA. 2010. American Diabetes Association: Diagnosis and classification of diabetes mellitus. *Diabetes Care,* 33**,** 62-69.

ADAMS, D. O. 1976. The granulomatous inflammatory response. A review. *Am J Pathol,* 84**,** 164-92.

ADAMS, D. O. 1989. Molecular interactions in macrophage activation. *Immunol Today,* 10**,** 33-5.

ADEYI, A. O., IDOWU, B. A., MAFIANA, C. F., OLUWALANA, S. A., AJAYI, O. L. & AKINLOYE, O. A. 2012. Rat model of food-induced non-obese-type 2 diabetes mellitus: comparative pathophysiology and histopathology. *Int J Physiol Pathophysiol Pharmacol,* 4**,** 51-8.

AHMAD, S. 2011. Pathogenesis, immunology, and diagnosis of latent *Mycobacterium tuberculosis* infection. *Clin Dev Immunol,* 2011**,** 814943.

AHMED, N. & HASNAIN, S. E. 2011. Molecular epidemiology of tuberculosis in India: moving forward with a systems biology approach. *Tuberculosis (Edinb),* 91**,** 407-13.

AKERBLOM, H. K., VAARALA, O., HYOTY, H., ILONEN, J. & KNIP, M. 2002. Environmental factors in the etiology of type 1 diabetes. *Am J Med Genet,* 115**,** 18-29.

AKINMOKUN, A., HARRIS, P., HOME, P. D. & ALBERTI, K. G. 1992. Is diabetes always diabetes? *Diabetes Res Clin Pract,* 18**,** 131-6.

AKIRA, S., UEMATSU, S. & TAKEUCHI, O. 2006. Pathogen recognition and innate immunity. *Cell,* 124**,** 783-801.

AL-ORAINEY, I. O. 2009. Diagnosis of latent tuberculosis: Can we do better? *Ann Thorac Med,* 4**,** 5-9.

ALBA-LOUREIRO, T. C., HIRABARA, S. M., MENDONCA, J. R., CURI, R. & PITHON-CURI, T. C. 2006. Diabetes causes marked changes in function and metabolism of rat neutrophils. *J Endocrinol,* 188**,** 295-303.

ALISJAHBANA, B., VAN CREVEL, R., SAHIRATMADJA, E., DEN HEIJER, M., MAYA, A., ISTRIANA, E., DANUSANTOSO, H., OTTENHOFF, T., NELWAN, R. & VAN DER MEER, J. 2006. Diabetes mellitus is strongly associated with tuberculosis in Indonesia. *Int J Tuberc Lung Dis,* 10**,** 696-700.

ALTARE, F., DURANDY, A., LAMMAS, D., EMILE, J. F., LAMHAMEDI, S., LE DEIST, F., DRYSDALE, P., JOUANGUY, E., DOFFINGER, R., BERNAUDIN, F., JEPPSSON, O., GOLLOB, J. A., MEINL, E., SEGAL, A. W., FISCHER, A., KUMARARATNE, D. & CASANOVA, J. L. 1998a. Impairment of mycobacterial immunity in human interleukin-12 receptor deficiency. *Science,* 280**,** 1432-5.

ALTARE, F., LAMMAS, D., REVY, P., JOUANGUY, E., DOFFINGER, R., LAMHAMEDI, S., DRYSDALE, P., SCHEEL-TOELLNER, D., GIRDLESTONE, J., DARBYSHIRE, P., WADHWA, M., DOCKRELL, H., SALMON, M., FISCHER, A., DURANDY, A., CASANOVA, J. L. & KUMARARATNE, D. S. 1998b. Inherited interleukin 12 deficiency in a child with bacille Calmette-Guerin and Salmonella enteritidis disseminated infection. *J Clin Invest,* 102**,** 2035-40.

ALY, S., WAGNER, K., KELLER, C., MALM, S., MALZAN, A., BRANDAU, S., BANGE, F. C. & EHLERS, S. 2006. Oxygen status of lung granulomas in *Mycobacterium tuberculosis*-infected mice. *J Pathol,* 210**,** 298-305.

AMOS, A. F., MCCARTY, D. J. & ZIMMET, P. 1997. The rising global burden of diabetes and its complications: estimates and projections to the year 2010. *Diabet Med,* 14 Suppl 5**,** S1-85.

ANDERSEN, B., GOLDSMITH, G. H. & SPAGNUOLO, P. J. 1988. Neutrophil adhesive dysfunction in diabetes mellitus; the role of cellular and plasma factors. *J Lab Clin Med,* 111**,** 275-85.

ANDERSEN, P. 1997. Host responses and antigens involved in protective immunity to *Mycobacterium tuberculosis*. *Scand J Immunol,* 45**,** 115-31.

ANDERSEN, P. & KAUFMANN, S. H. 2014. Novel Vaccination Strategies against Tuberculosis. *Cold Spring Harb Perspect Med,* 4.

ANONYMOUS 2014. Clinicians Guide to Quantiferon-TB Gold (cited in 2004). Available from: http://www.cellestis.com/IRM/contentAU/gold/cliniciansguide.pdf.

APPELBERG, R., CASTRO, A. G., PEDROSA, J. & MINOPRIO, P. 1994a. Role of interleukin-6 in the induction of protective T cells during mycobacterial infections in mice. *Immunology,* 82**,** 361-4.

APPELBERG, R., CASTRO, A. G., PEDROSA, J., SILVA, R. A., ORME, I. M. & MINÓPRIO, P. 1994b. Role of gamma interferon and tumor necrosis factor alpha during T-cell-independent and -dependent phases of *Mycobacterium avium* infection. *Infect Immun,* 62**,** 3962-3971.

APPELBERG, R., ORME, I. M., PINTO DE SOUSA, M. I. & SILVA, M. T. 1992. In vitro effects of interleukin-4 on interferon-gamma-induced macrophage activation. *Immunology,* 76**,** 553-9.

ARBUES, A., AGUILO, J. I., GONZALO-ASENSIO, J., MARINOVA, D., URANGA, S., PUENTES, E., FERNANDEZ, C., PARRA, A., CARDONA, P. J., VILAPLANA, C.,

AUSINA, V., WILLIAMS, A., CLARK, S., MALAGA, W., GUILHOT, C., GICQUEL, B. & MARTIN, C. 2013. Construction, characterization and preclinical evaluation of MTBVAC, the first live-attenuated *M. tuberculosis*-based vaccine to enter clinical trials. *Vaccine,* 31**,** 4867-73.

ARITA, Y., KIHARA, S., OUCHI, N., TAKAHASHI, M., MAEDA, K., MIYAGAWA, J., HOTTA, K., SHIMOMURA, I., NAKAMURA, T., MIYAOKA, K., KURIYAMA, H., NISHIDA, M., YAMASHITA, S., OKUBO, K., MATSUBARA, K., MURAGUCHI, M., OHMOTO, Y., FUNAHASHI, T. & MATSUZAWA, Y. 1999. Paradoxical decrease of an adipose-specific protein, adiponectin, in obesity. *Biochem Biophys Res Commun,* 257**,** 79-83.

ARMSTRONG, J. A. & HART, P. D. 1975. Phagosome-lysosome interactions in cultured macrophages infected with virulent tubercle bacilli. Reversal of the usual nonfusion pattern and observations on bacterial survival. *J Exp Med,* 142**,** 1-16.

ARNER, P. 2003. The adipocyte in insulin resistance: key molecules and the impact of the thiazolidinediones. *Trends Endocrinol Metab,* 14**,** 137-45.

ARONSON, N. E., SANTOSHAM, M., COMSTOCK, G. W., HOWARD, R. S., MOULTON, L. H., RHOADES, E. R. & HARRISON, L. H. 2004. Long-term efficacy of BCG vaccine in American Indians and Alaska Natives: A 60-year follow-up study. *Jama,* 291**,** 2086-91.

ATKINSON, M. A. & EISENBARTH, G. S. 2001. Type 1 diabetes: new perspectives on disease pathogenesis and treatment. *Lancet,* 358**,** 221-9.

AYALA, J. E., SAMUEL, V. T., MORTON, G. J., OBICI, S., CRONIGER, C. M., SHULMAN, G. I., WASSERMAN, D. H. & MCGUINNESS, O. P. 2010. Standard operating procedures for describing and performing metabolic tests of glucose homeostasis in mice. *Dis Model Mech,* 3**,** 525-34.

BAETENS, D., STEFAN, Y., RAVAZZOLA, M., MALAISSE-LAGAE, F., COLEMAN, D. L. & ORCI, L. 1978. Alteration of islet cell populations in spontaneously diabetic mice. *Diabetes,* 27**,** 1-7.

BAFICA, A., SCANGA, C. A., FENG, C. G., LEIFER, C., CHEEVER, A. & SHER, A. 2005. TLR9 regulates Th1 responses and cooperates with TLR2 in mediating optimal resistance to *Mycobacterium tuberculosis*. *J Exp Med,* 202**,** 1715-24.

BAGDADE, J. D., NIELSON, K. L. & BULGER, R. J. 1972. Reversible abnormalities in phagocytic function in poorly controlled diabetic patients. *Am J Med Sci,* 263**,** 451-6.

BAGDADE, J. D., STEWART, M. & WALTERS, E. 1978. Impaired granulocyte adherence. A reversible defect in host defense in patients with poorly controlled diabetes. *Diabetes,* 27**,** 677-81.

BAGDADE, J. D. & WALTERS, E. 1980. Impaired granulocyte adherence in mildly diabetic patients: effects of tolazamide treatment. *Diabetes,* 29**,** 309-11.

BALAKRISHNAN, S., VIJAYAN, S., NAIR, S., SUBRAMONIAPILLAI, J., MRITHYUNJAYAN, S., WILSON, N., SATYANARAYANA, S., DEWAN, P. K., KUMAR, A. M., KARTHICKEYAN, D., WILLIS, M., HARRIES, A. D. & NAIR, S. A. 2012. High diabetes prevalence among tuberculosis cases in Kerala, India. *PLoS One,* 7**,** e46502.

BANYAI, A. L. 1931. Diabetes and pulmonary tuberculosis. Am Rev Tuberc ;24:650–67.

BARLOW, S. E. 2007. Expert committee recommendations regarding the prevention, assessment, and treatment of child and adolescent overweight and obesity: summary report. *Pediatrics,* 120 Suppl 4**,** S164-92.

BARNES, P. F., ABRAMS, J. S., LU, S., SIELING, P. A., REA, T. H. & MODLIN, R. L. 1993. Patterns of cytokine production by mycobacterium-reactive human T-cell clones. *Infect Immun,* 61**,** 197-203.

BARNETT, A. H., EFF, C., LESLIE, R. D. & PYKE, D. A. 1981. Diabetes in identical twins. A study of 200 pairs. *Diabetologia,* 20**,** 87-93.

BARRAL, D. C. & BRENNER, M. B. 2007. CD1 antigen presentation: how it works. *Nat Rev Immunol,* 7**,** 929-41.

BARRETT-CONNOR, E. & KHAW, K. T. 1989. Cigarette smoking and increased central adiposity. *Ann Intern Med,* 111**,** 783-7.

BARROW, W. W., DE SOUSA, J. P., DAVIS, T. L., WRIGHT, E. L., BACHELET, M. & RASTOGI, N. 1993. Immunomodulation of human peripheral blood mononuclear cell functions by defined lipid fractions of *Mycobacterium avium*. *Infect Immun,* 61**,** 5286-5293.

BASARABA, R. J. 2008. Experimental tuberculosis: the role of comparative pathology in the discovery of improved tuberculosis treatment strategies. *Tuberculosis (Edinb),* 88 Suppl 1**,** S35-47.

BAYRY, J., TCHILIAN, E. Z., DAVIES, M. N., FORBES, E. K., DRAPER, S. J., KAVERI, S. V., HILL, A. V., KAZATCHKINE, M. D., BEVERLEY, P. C., FLOWER, D. R. & TOUGH, D. F. 2008. In silico identified CCR4 antagonists target regulatory T cells and exert adjuvant activity in vaccination. *Proc Natl Acad Sci U S A,* 105**,** 10221-6.

BAYS, H., MANDARINO, L. & DEFRONZO, R. A. 2004. Role of the adipocyte, free fatty acids, and ectopic fat in pathogenesis of type 2 diabetes mellitus: peroxisomal proliferator-activated receptor agonists provide a rational therapeutic approach. *J Clin Endocrinol Metab,* 89**,** 463-78.

BEAMER, G. L. & TURNER, J. 2005. Murine models of susceptibility to tuberculosis. *Arch Immunol Ther Exp (Warsz),* 53**,** 469-83.

BEAN, A. G., ROACH, D. R., BRISCOE, H., FRANCE, M. P., KORNER, H., SEDGWICK, J. D. & BRITTON, W. J. 1999. Structural deficiencies in granuloma formation in TNF gene-targeted mice underlie the heightened susceptibility to aerosol *Mycobacterium tuberculosis* infection, which is not compensated for by lymphotoxin. *J Immunol,* 162**,** 3504-11.

BEDDOW, S. A. & SAMUEL, V. T. 2012. Fasting hyperglycemia in the Goto-Kakizaki rat is dependent on corticosterone: a confounding variable in rodent models of type 2 diabetes. *Dis Model Mech,* 5**,** 681-685.

BEETZ, S., WESCH, D., MARISCHEN, L., WELTE, S., OBERG, H. H. & KABELITZ, D. 2008. Innate immune functions of human gammadelta T cells. *Immunobiology,* 213**,** 173-82.

BEHR, M. A., WILSON, M. A., GILL, W. P., SALAMON, H., SCHOOLNIK, G. K., RANE, S. & SMALL, P. M. 1999. Comparative genomics of BCG vaccines by whole-genome DNA microarray. *Science,* 284**,** 1520-3.

BELL, A. C., GE, K. & POPKIN, B. M. 2002. The road to obesity or the path to prevention: motorized transportation and obesity in China. *Obes Res,* 10**,** 277-83.

BELTAN, E., HORGEN, L. & RASTOGI, N. 2000. Secretion of cytokines by human macrophages upon infection by pathogenic and non-pathogenic mycobacteria. *Microb Pathog,* 28.

BELVIN, M. P. & ANDERSON, K. V. 1996. A conserved signaling pathway: the Drosophila toll-dorsal pathway. *Annu Rev Cell Dev Biol,* 12**,** 393-416.

BENOIT, M., DESNUES, B. & MEGE, J. L. 2008. Macrophage polarization in bacterial infections. *J Immunol,* 181**,** 3733-9.

BERGMAN, M. 2013. Pathophysiology of prediabetes and treatment implications for the prevention of type 2 diabetes mellitus. *Endocrine,* 43**,** 504-13.

BERMUDEZ, L. E. & CHAMPSI, J. 1993. Infection with *Mycobacterium avium* induces production of interleukin-10 (IL-10), and administration of anti-IL-10 antibody is associated with enhanced resistance to infection in mice. *Infect Immun,* 61**,** 3093-7.

BERMUDEZ, L. E., WU, M., PETROFSKY, M. & YOUNG, L. S. 1992. Interleukin-6 antagonizes tumor necrosis factor-mediated mycobacteriostatic and mycobactericidal activities in macrophages. *Infect Immun,* 60**,** 4245-52.

BERNARD, C., DELLA ZUANA, O. & KTORZA, A. 2013. Interaction between environment and genetic background in type 2 diabetes: lessons from animal models. *Med Sci (Paris),* 29**,** 791-9.

BERRINGTON, W. R. & HAWN, T. R. 2007. *Mycobacterium tuberculosis*, macrophages, and the innate immune response: does common variation matter? *Immunol Rev,* 219**,** 167-86.

BERTAGNOLLI, M. M., LIN, B. Y., YOUNG, D. & HERRMANN, S. H. 1992. IL-12 augments antigen-dependent proliferation of activated T lymphocytes. *J Immunol,* 149**,** 3778-83.

BERTHOLET, S., IRETON, G. C., ORDWAY, D. J., WINDISH, H. P., PINE, S. O., KAHN, M., PHAN, T., ORME, I. M., VEDVICK, T. S., BALDWIN, S. L., COLER, R. N. & REED, S. G. 2010. A defined tuberculosis vaccine candidate boosts BCG and protects against multidrug-resistant *Mycobacterium tuberculosis*. *Sci Transl Med,* 2**,** 53ra74.

BERTOLA, A., CIUCCI, T., ROUSSEAU, D., BOURLIER, V., DUFFAUT, C., BONNAFOUS, S., BLIN-WAKKACH, C., ANTY, R., IANNELLI, A., GUGENHEIM, J., TRAN, A., BOULOUMIÉ, A., GUAL, P. & WAKKACH, A. 2012. Identification of Adipose Tissue Dendritic Cells Correlated With Obesity-Associated Insulin-Resistance and Inducing Th17 Responses in Mice and Patients. *Diabetes,* 61**,** 2238-2247.

BEVERIDGE, N. E., PRICE, D. A., CASAZZA, J. P., PATHAN, A. A., SANDER, C. R., ASHER, T. E., AMBROZAK, D. R., PRECOPIO, M. L., SCHEINBERG, P., ALDER, N. C., ROEDERER, M., KOUP, R. A., DOUEK, D. C., HILL, A. V. & MCSHANE, H. 2007. Immunisation with BCG and recombinant MVA85A induces long-lasting, polyfunctional *Mycobacterium tuberculosis*-specific CD4+ memory T lymphocyte populations. *Eur J Immunol,* 37**,** 3089-100.

BIEDERMANN, T., MAILHAMMER, R., MAI, A., SANDER, C., OGILVIE, A., BROMBACHER, F., MAIER, K., LEVINE, A. D. & ROCKEN, M. 2001. Reversal of established delayed type hypersensitivity reactions following therapy with IL-4 or antigen-specific Th2 cells. *Eur J Immunol,* 31**,** 1582-91.

BILLESKOV, R., ELVANG, T. T., ANDERSEN, P. L. & DIETRICH, J. 2012. The HyVac4 subunit vaccine efficiently boosts BCG-primed anti-mycobacterial protective immunity. *PLoS One,* 7**,** e39909.

BLACK, B. L., CROOM, J., EISEN, E. J., PETRO, A. E., EDWARDS, C. L. & SURWIT, R. S. 1998. Differential effects of fat and sucrose on body composition in A/J and C57BL/6 mice. *Metabolism,* 47**,** 1354-9.

BLACKSTOCK, R., BUCHANAN, K. L., ADESINA, A. M. & MURPHY, J. W. 1999. Differential regulation of immune responses by highly and weakly virulent Cryptococcus neoformans isolates. *Infect Immun,* 67**,** 3601-9.

BOCK, T., PAKKENBERG, B. & BUSCHARD, K. 2003. Increased islet volume but unchanged islet number in ob/ob mice. *Diabetes,* 52**,** 1716-22.

BODEN, G. 1999. Free fatty acids, insulin resistance, and type 2 diabetes mellitus. *Proc Assoc Am Physicians,* 111**,** 241-8.

BOEHME, C. C., NABETA, P., HILLEMANN, D., NICOL, M. P., SHENAI, S., KRAPP, F., ALLEN, J., TAHIRLI, R., BLAKEMORE, R., RUSTOMJEE, R., MILOVIC, A., JONES, M., O'BRIEN, S. M., PERSING, D. H., RUESCH-GERDES, S., GOTUZZO, E., RODRIGUES, C., ALLAND, D. & PERKINS, M. D. 2010. Rapid molecular detection of tuberculosis and rifampin resistance. *N Engl J Med,* 363**,** 1005-15.

BOHSALI, A., ABDALLA, H., VELMURUGAN, K. & BRIKEN, V. 2010. The non-pathogenic mycobacteria *M. smegmatis* and *M. fortuitum* induce rapid host cell apoptosis via a caspase-3 and TNF dependent pathway. *BMC Microbiol,* 10**,** 237.

BORING, L., GOSLING, J., CHENSUE, S. W., KUNKEL, S. L., FARESE, R. V., JR., BROXMEYER, H. E. & CHARO, I. F. 1997. Impaired monocyte migration and reduced type 1 (Th1) cytokine responses in C-C chemokine receptor 2 knockout mice. *J Clin Invest,* 100**,** 2552-61.

BOSIO, C. M., GARDNER, D. & ELKINS, K. L. 2000. Infection of B cell-deficient mice with CDC 1551, a clinical isolate of *Mycobacterium tuberculosis*: delay in dissemination and development of lung pathology. *J Immunol,* 164**,** 6417-25.

BOUCOT, K. R., DILLON, E. S., COOPER, D. A., MEIER, P. & RICHARDSON, R. 1952. Tuberculosis among diabetics: the Philadelphia survey. *Am Rev Tuberc,* 65**,** 1-50.

BOURIGAULT, M. L., SEGUENI, N., ROSE, S., COURT, N., VACHER, R., VASSEUR, V., ERARD, F., LE BERT, M., GARCIA, I., IWAKURA, Y., JACOBS, M., RYFFEL, B. & QUESNIAUX, V. F. 2013. Relative contribution of IL-1alpha, IL-1beta and TNF to the host response to *Mycobacterium tuberculosis* and attenuated *M. bovis* BCG. *Immun Inflamm Dis,* 1**,** 47-62.

BOUSSIOTIS, V. A., TSAI, E. Y., YUNIS, E. J., THIM, S., DELGADO, J. C., DASCHER, C. C., BEREZOVSKAYA, A., ROUSSET, D., REYNES, J. M. & GOLDFELD, A. E. 2000. IL-10-producing T cells suppress immune responses in anergic tuberculosis patients. *J Clin Invest,* 105**,** 1317-25.

BOUTAYEB, A. 2006. The double burden of communicable and non-communicable diseases in developing countries. *Trans R Soc Trop Med Hyg,* 100**,** 191-9.

BOWDISH, D. M., SAKAMOTO, K., KIM, M. J., KROOS, M., MUKHOPADHYAY, S., LEIFER, C. A., TRYGGVASON, K., GORDON, S. & RUSSELL, D. G. 2009. MARCO, TLR2, and CD14 are required for macrophage cytokine responses to mycobacterial trehalose dimycolate and *Mycobacterium tuberculosis*. *PLoS Pathog,* 5**,** e1000474.

BREEN, R. A., LEONARD, O., PERRIN, F. M., SMITH, C. J., BHAGANI, S., CROPLEY, I. & LIPMAN, M. C. 2008. How good are systemic symptoms and blood inflammatory markers at detecting individuals with tuberculosis? *Int J Tuberc Lung Dis,* 12**,** 44-9.

BRIDSON, T., GOVAN, B., KETHEESAN, N. & NORTON, R. 2016. Overrepresentation of Diabetes in Soft Tissue Nontuberculous Mycobacterial Infections. *Am J Trop Med Hyg,* 95**,** 528-30.

BRIDSON, T., L 2015. The impact of type 2 diabetes on mycobacterial infections. In fulfillment of the requirements for the Degree of Bachelor of Medical Science, James Cook University,Australia.

BRIDSON, T. L., GOVAN, B. L., NORTON, R. E., SCHOFIELD, L. & KETHEESAN, N. 2014. The double burden: a new-age pandemic meets an ancient infection. *Trans R Soc Trop Med Hyg,* 108**,** 676-8.

BRIGHENTI, S. & ANDERSSON, J. 2010. Induction and regulation of CD8+ cytolytic T cells in human tuberculosis and HIV infection. *Biochem Biophys Res Commun,* 396**,** 50-7.

BRIKEN, V., PORCELLI, S. A., BESRA, G. S. & KREMER, L. 2004. Mycobacterial lipoarabinomannan and related lipoglycans: from biogenesis to modulation of the immune response. *Mol Microbiol,* 53**,** 391-403.

BRITO, P. L., FIORETTO, P., DRUMMOND, K., KIM, Y., STEFFES, M. W., BASGEN, J. M., SISSON-ROSS, S. & MAUER, M. 1998. Proximal tubular basement membrane width in insulin-dependent diabetes mellitus. *Kidney Int,* 53**,** 754-61.

BROCK, I., MUNK, M. E., KOK-JENSEN, A. & ANDERSEN, P. 2001. Performance of whole blood IFN-gamma test for tuberculosis diagnosis based on PPD or the specific antigens ESAT-6 and CFP-10. *Int J Tuberc Lung Dis,* 5**,** 462-7.

BROOKS, M. N., RAJARAM, M. V., AZAD, A. K., AMER, A. O., VALDIVIA-ARENAS, M. A., PARK, J. H., NUNEZ, G. & SCHLESINGER, L. S. 2011. NOD2 controls the nature of the inflammatory response and subsequent fate of *Mycobacterium tuberculosis* and M. bovis BCG in human macrophages. *Cell Microbiol,* 13**,** 402-18.

BROSCH, R., GORDON, S. V., MARMIESSE, M., BRODIN, P., BUCHRIESER, C., EIGLMEIER, K., GARNIER, T., GUTIERREZ, C., HEWINSON, G., KREMER, K., PARSONS, L. M., PYM, A. S., SAMPER, S., VAN SOOLINGEN, D. & COLE, S. T. 2002. A new evolutionary scenario for the *Mycobacterium tuberculosis* complex. *Proc Natl Acad Sci U S A,* 99**,** 3684-9.

BROSIUS, F. C., ALPERS, C. E., BOTTINGER, E. P., BREYER, M. D., COFFMAN, T. M., GURLEY, S. B., HARRIS, R. C., KAKOKI, M., KRETZLER, M., LEITER, E. H., LEVI, M., MCINDOE, R. A., SHARMA, K., SMITHIES, O., SUSZTAK, K., TAKAHASHI, N. & TAKAHASHI, T. 2009. Mouse Models of Diabetic Nephropathy. *J Am Soc Nephrol,* 20**,** 2503-2512.

BRUIN, J. E., PETRE, M. A., RAHA, S., MORRISON, K. M., GERSTEIN, H. C. & HOLLOWAY, A. C. 2008. Fetal and neonatal nicotine exposure in Wistar rats causes progressive pancreatic mitochondrial damage and beta cell dysfunction. *PLoS One,* 3**,** e3371.

BUTLER, A. E., JANSON, J., BONNER-WEIR, S., RITZEL, R., RIZZA, R. A. & BUTLER, P. C. 2003. Beta-cell deficit and increased beta-cell apoptosis in humans with type 2 diabetes. *Diabetes,* 52**,** 102-10.

CALMETTE, A., GUE´RIN, C., BOQUET, A., NE´GRE, L., 1927. La vaccination pre´ventive contre la tuberculose par le “BCG”. Masson, Paris.

CALMETTE, A. & PLOTZ, H. 1929. Protective inoculation against tuberculosis with BCG. *Am Rev Tuberc*, 19, 567–572.

CAMERON, S. J. 1974. Tuberculosis and the blood-a special relationship? *Tubercle,* 55**,** 55-72.

CAPIZZI, S., DE WAURE, C. & BOCCIA, S. 2015. Global Burden and Health Trends of Non-Communicable Diseases. *In:* BOCCIA, S., VILLARI, P. & RICCIARDI, W. (eds.) *A Systematic Review of Key Issues in Public Health.* Cham: Springer International Publishing.

CARDONA, P. J. 2006. RUTI: a new chance to shorten the treatment of latent tuberculosis infection. *Tuberculosis (Edinb),* 86**,** 273-89.

CARDONA, P. J. 2009. A dynamic reinfection hypothesis of latent tuberculosis infection. *Infection,* 37**,** 80-6.

CARDONA, P. J. 2010. Revisiting the natural history of tuberculosis. The inclusion of constant reinfection, host tolerance, and damage-response frameworks leads to a better understanding of latent infection and its evolution towards active disease. *Arch Immunol Ther Exp (Warsz),* 58**,** 7-14.

CAREY, D. G., JENKINS, A. B., CAMPBELL, L. V., FREUND, J. & CHISHOLM, D. J. 1996. Abdominal fat and insulin resistance in normal and overweight women: Direct measurements reveal a strong relationship in subjects at both low and high risk of NIDDM. *Diabetes,* 45**,** 633-8.

CARON, E. & HALL, A. 1998. Identification of two distinct mechanisms of phagocytosis controlled by different Rho GTPases. *Science,* 282**,** 1717-21.

CARRERA BOADA, C. A. & MARTINEZ-MORENO, J. M. 2013. Pathophysiology of diabetes mellitus type 2: beyond the duo "insulin resistance-secretion deficit". *Nutr Hosp,* 28 Suppl 2**,** 78-87.

CARTER, J. S., PUGH, J. A. & MONTERROSA, A. 1996. Non-insulin-dependent diabetes mellitus in minorities in the United States. *Ann Intern Med,* 125**,** 221-32.

CDC, O. 2000. Diagnostic Standards and Classification of Tuberculosis in Adults and Children. This official statement of the American Thoracic Society and the Centers for Disease Control and Prevention was adopted by the ATS Board of Directors, July 1999. This statement was endorsed by the Council of the Infectious Disease Society of America, September 1999. *Am J Respir Crit Care Med,* 161**,** 1376-95.

CEBULA, B. R., ROCCO, J. M., MASLOW, J. N. & IRANI, V. R. 2012. *Mycobacterium avium* serovars 2 and 8 infections elicit unique activation of the host macrophage immune responses. *Eur J Clin Microbiol Infect Dis,* 31**,** 3407-12.

CEFALU, W. T. 2006. Animal models of type 2 diabetes: clinical presentation and pathophysiological relevance to the human condition. *Ilar j,* 47**,** 186-98.

CELLA, M., SCHEIDEGGER, D., PALMER-LEHMANN, K., LANE, P., LANZAVECCHIA, A. & ALBER, G. 1996. Ligation of CD40 on dendritic cells triggers production of high levels of interleukin-12 and enhances T cell stimulatory capacity: T-T help via APC activation. *J Exp Med,* 184**,** 747-52.

CHAMBERS, M. A., GAVIER-WIDEN, D. & HEWINSON, R. G. 2006. Histopathogenesis of experimental *Mycobacterium bovis* infection in mice. *Res Vet Sci,* 80**,** 62-70.

CHAN, J. & FLYNN, J. 2004. The immunological aspects of latency in tuberculosis. *Clin Immunol,* 110**,** 2-12.

CHANCHAMROEN, S., KEWCHAROENWONG, C., SUSAENGRAT, W., ATO, M. & LERTMEMONGKOLCHAI, G. 2009. Human polymorphonuclear neutrophil responses to *Burkholderia pseudomallei* in healthy and diabetic subjects. *Infect Immun,* 77**,** 456-63.

CHANG, F. Y. & SHAIO, M. F. 1995. Decreased cell-mediated immunity in patients with non-insulin-dependent diabetes mellitus. *Diabetes Res Clin Pract,* 28**,** 137-46.

CHAPARAS, S. D., VANDIVIERE, H. M., MELVIN, I., KOCH, G. & BECKER, C. 1985. Tuberculin test. Variability with the Mantoux procedure. *Am Rev Respir Dis,* 132**,** 175-7.

CHAPMAN, A. L., MUNKANTA, M., WILKINSON, K. A., PATHAN, A. A., EWER, K., AYLES, H., REECE, W. H., MWINGA, A., GODFREY-FAUSSETT, P. & LALVANI, A. 2002. Rapid detection of active and latent tuberculosis infection in HIV-positive individuals by enumeration of *Mycobacterium tuberculosis*-specific T cells. *Aids,* 16**,** 2285-93.

CHATTERJEE, D., BOZIC, C. M., MCNEIL, M. & BRENNAN, P. J. 1991. Structural features of the arabinan component of the lipoarabinomannan of *Mycobacterium tuberculosis*. *J Biol Chem,* 266**,** 9652-60.

CHATTERJEE, D. & KHOO, K. H. 1998. Mycobacterial lipoarabinomannan: an extraordinary lipoheteroglycan with profound physiological effects. *Glycobiology,* 8**,** 113-20.

CHATTERJEE, D., ROBERTS, A., LOWELL, K., BRENNAN, P. & ORME, I. 1992a. Structural basis of capacity of lipoarabinomannan to induce secretion of tumor necrosis factor. *Infect Immun,* 60.

CHATTERJEE, D., ROBERTS, A. D., LOWELL, K., BRENNAN, P. J. & ORME, I. M. 1992b. Structural basis of capacity of lipoarabinomannan to induce secretion of tumor necrosis factor. *Infect Immun,* 60**,** 1249-53.

CHAWLA, A., CHAWLA, R. & JAGGI, S. 2016. Microvasular and macrovascular complications in diabetes mellitus: Distinct or continuum? *Indian J Endocrinol Metab,* 20**,** 546-551.

CHEEKATLA, S. S., TRIPATHI, D., VENKATASUBRAMANIAN, S., NATHELLA, P. K., PAIDIPALLY, P., ISHIBASHI, M., WELCH, E., TVINNEREIM, A. R., IKEBE, M., VALLURI, V. L., BABU, S., KORNFELD, H. & VANKAYALAPATI, R. 2016. NK-CD11c+ Cell Crosstalk in Diabetes Enhances IL-6-Mediated Inflammation during *Mycobacterium tuberculosis* Infection. *PLoS Pathog,* 12**,** e1005972.

CHEN, H., CHARLAT, O., TARTAGLIA, L. A., WOOLF, E. A., WENG, X., ELLIS, S. J., LAKEY, N. D., CULPEPPER, J., MOORE, K. J., BREITBART, R. E., DUYK, G. M., TEPPER, R. I. & MORGENSTERN, J. P. 1996. Evidence that the diabetes gene encodes the leptin receptor: identification of a mutation in the leptin receptor gene in db/db mice. *Cell,* 84**,** 491-5.

CHEN, H. D., SHAW, C. K., TSENG, W. P., CHEN, H. I. & LEE, M. L. 1997. Prevalence of diabetes mellitus and impaired glucose tolerance in Aborigines and Chinese in eastern Taiwan. *Diabetes Res Clin Pract,* 38**,** 199-205.

CHENSUE, S. W., WARMINGTON, K. S., ALLENSPACH, E. J., LU, B., GERARD, C., KUNKEL, S. L. & LUKACS, N. W. 1999. Differential expression and cross-regulatory function of RANTES during mycobacterial (type 1) and schistosomal (type 2) antigen-elicited granulomatous inflammation. *J Immunol,* 163**,** 165-73.

CHO, S., MEHRA, V., THOMA-USZYNSKI, S., STENGER, S., SERBINA, N., MAZZACCARO, R. J., FLYNN, J. L., BARNES, P. F., SOUTHWOOD, S., CELIS, E., BLOOM, B. R., MODLIN, R. L. & SETTE, A. 2000. Antimicrobial activity of MHC class I-restricted CD8+ T cells in human tuberculosis. *Proc Natl Acad Sci U S A,* 97**,** 12210-5.

COHEN, M. P., LAUTENSLAGER, G. T. & SHEARMAN, C. W. 2001. Increased urinary type IV collagen marks the development of glomerular pathology in diabetic d/db mice. *Metabolism,* 50**,** 1435-40.

COLDITZ, G. A., BREWER, T. F., BERKEY, C. S., WILSON, M. E., BURDICK, E., FINEBERG, H. V. & MOSTELLER, F. 1994. Efficacy of BCG vaccine in the prevention of tuberculosis. Meta-analysis of the published literature. *Jama,* 271**,** 698-702.

COLE, S. T., BROSCH, R., PARKHILL, J., GARNIER, T., CHURCHER, C., HARRIS, D., GORDON, S. V., EIGLMEIER, K., GAS, S., BARRY, C. E., 3RD, TEKAIA, F., BADCOCK, K., BASHAM, D., BROWN, D., CHILLINGWORTH, T., CONNOR, R., DAVIES, R., DEVLIN, K., FELTWELL, T., GENTLES, S., HAMLIN, N., HOLROYD, S., HORNSBY, T., JAGELS, K., KROGH, A., MCLEAN, J., MOULE, S., MURPHY, L., OLIVER, K., OSBORNE, J., QUAIL, M. A., RAJANDREAM, M. A., ROGERS, J., RUTTER, S., SEEGER, K., SKELTON, J., SQUARES, R., SQUARES, S., SULSTON, J. E., TAYLOR, K., WHITEHEAD, S. & BARRELL, B. G. 1998. Deciphering the biology of *Mycobacterium tuberculosis* from the complete genome sequence. *Nature,* 393**,** 537-44.

COLER, R. N., BERTHOLET, S., PINE, S. O., ORR, M. T., REESE, V., WINDISH, H. P., DAVIS, C., KAHN, M., BALDWIN, S. L. & REED, S. G. 2013. Therapeutic

immunization against *Mycobacterium tuberculosis* is an effective adjunct to antibiotic treatment. *J Infect Dis,* 207**,** 1242-52.

COLLINS, A. M., RYLANCE, J., WOOTTON, D. G., WRIGHT, A. D., WRIGHT, A. K., FULLERTON, D. G. & GORDON, S. B. 2014. Bronchoalveolar lavage (BAL) for research; obtaining adequate sample yield. *J Vis Exp*.

COLLISON, K. S., PARHAR, R. S., SALEH, S. S., MEYER, B. F., KWAASI, A. A., HAMMAMI, M. M., SCHMIDT, A. M., STERN, D. M. & AL-MOHANNA, F. A. 2002. RAGE-mediated neutrophil dysfunction is evoked by advanced glycation end products (AGEs). *J Leukoc Biol,* 71**,** 433-44.

COMSTOCK, G. W. 1975. False tuberculin test results. *Chest,* 68**,** 465-9.

COOKE, D. W. & PLOTNICK, L. 2008. Type 1 diabetes mellitus in pediatrics. *Pediatr Rev,* 29**,** 374-84; quiz 385.

COOPER, A. M. 2009. Cell-mediated immune responses in tuberculosis. *Annu Rev Immunol,* 27**,** 393-422.

COOPER, A. M., DALTON, D. K., STEWART, T. A., GRIFFIN, J. P., RUSSELL, D. G. & ORME, I. M. 1993. Disseminated tuberculosis in interferon gamma gene-disrupted mice. *J Exp Med,* 178**,** 2243-7.

COOPER, A. M., MAYER-BARBER, K. D. & SHER, A. 2011. Role of innate cytokines in mycobacterial infection. *Mucosal Immunol,* 4**,** 252-60.

COOPER, A. M., ROBERTS, A. D., RHOADES, E. R., CALLAHAN, J. E., GETZY, D. M. & ORME, I. M. 1995. The role of interleukin-12 in acquired immunity to *Mycobacterium tuberculosis* infection. *Immunology,* 84**,** 423-32.

CORRIS, V., UNWIN, N. & CRITCHLEY, J. 2012. Quantifying the association between tuberculosis and diabetes in the US: a case-control analysis. *Chronic Illn,* 8**,** 121-34.

COSTA, J. T., SILVA, R., SA, R., CARDOSO, M. J., RIBEIRO, C. & NIENHAUS, A. 2010. Comparison of interferon-gamma release assay and tuberculin test for screening in healthcare workers. *Rev Port Pneumol,* 16**,** 211-21.

COWLEY, S. C. & ELKINS, K. L. 2003. CD4+ T cells mediate IFN-gamma-independent control of *Mycobacterium tuberculosis* infection both in vitro and in vivo. *J Immunol,* 171**,** 4689-99.

CROWLE, A. J., TSANG, A. Y., VATTER, A. E. & MAY, M. H. 1986. Comparison of 15 laboratory and patient-derived strains of *Mycobacterium avium* for ability to infect and multiply in cultured human macrophages. *J Clin Microbiol,* 24**,** 812-21.

CUNNINGHAM, A. F. & SPREADBURY, C. L. 1998. Mycobacterial stationary phase induced by low oxygen tension: cell wall thickening and localization of the 16-kilodalton alpha-crystallin homolog. *J Bacteriol,* 180**,** 801-8.

CUSI, K. 2010. The role of adipose tissue and lipotoxicity in the pathogenesis of type 2 diabetes. *Curr Diab Rep,* 10**,** 306-15.

CYWES, C., GODENIR, N. L., HOPPE, H. C., SCHOLLE, R. R., STEYN, L. M., KIRSCH, R. E. & EHLERS, M. R. 1996. Nonopsonic binding of *Mycobacterium tuberculosis* to human complement receptor type 3 expressed in Chinese hamster ovary cells. *Infect Immun,* 64**,** 5373-83.

CYWES, C., HOPPE, H. C., DAFFE, M. & EHLERS, M. R. 1997. Nonopsonic binding of *Mycobacterium tuberculosis* to complement receptor type 3 is mediated by capsular polysaccharides and is strain dependent. *Infect Immun,* 65**,** 4258-66.

D'EMDEN, M. C., SHAW, J. E., COLMAN, P. G., COLAGIURI, S., TWIGG, S. M., JONES, G. R., GOODALL, I., SCHNEIDER, H. G. & CHEUNG, N. W. 2012. The role of HbA1c in the diagnosis of diabetes mellitus in Australia. *Med J Aust,* 197**,** 220-1.

DA SILVA, T. R., DE FREITAS, J. R., SILVA, Q. C., FIGUEIRA, C. P., ROXO, E., LEAO, S. C., DE FREITAS, L. A. & VERAS, P. S. 2002. Virulent *Mycobacterium fortuitum* restricts NO production by a gamma interferon-activated J774 cell line and phagosome-lysosome fusion. *Infect Immun,* 70**,** 5628-34.

DABLA, P. K. 2010. Renal function in diabetic nephropathy. *World J Diabetes,* 1**,** 48-56.

DAHL, K. E., SHIRATSUCHI, H., HAMILTON, B. D., ELLNER, J. J. & TOOSSI, Z. 1996. Selective induction of transforming growth factor beta in human monocytes by lipoarabinomannan of *Mycobacterium tuberculosis*. *Infect Immun,* 64**,** 399-405.

DAN, K., FUJITA, H., SETO, Y. & KATO, R. 1997. Relation between stable glycated hemoglobin A1C and plasma glucose levels in diabetes-model mice. *Exp Anim,* 46**,** 135-40.

DANDA, R. S., HABIBA, N. M., RINCON-CHOLES, H., BHANDARI, B. K., BARNES, J. L., ABBOUD, H. E. & PERGOLA, P. E. 2005. Kidney involvement in a nongenetic rat model of type 2 diabetes. *Kidney Int,* 68**,** 2562-71.

DAO, D. N., KREMER, L., GUERARDEL, Y., MOLANO, A., JACOBS, W. R., JR., PORCELLI, S. A. & BRIKEN, V. 2004. *Mycobacterium tuberculosis* lipomannan induces apoptosis and interleukin-12 production in macrophages. *Infect Immun,* 72**,** 2067-74.

DE BRUYN, G. & GARNER, P. 2003. *Mycobacterium vaccae* immunotherapy for treating tuberculosis. *Cochrane Database Syst Rev***,** Cd001166.

DE GROOTE, M. A. & HUITT, G. 2006. Infections due to rapidly growing mycobacteria. *Clin Infect Dis,* 42**,** 1756-63.

DE JONG, R., ALTARE, F., HAAGEN, I. A., ELFERINK, D. G., BOER, T., VAN BREDA VRIESMAN, P. J., KABEL, P. J., DRAAISMA, J. M., VAN DISSEL, J. T., KROON, F. P., CASANOVA, J. L. & OTTENHOFF, T. H. 1998. Severe mycobacterial and Salmonella infections in interleukin-12 receptor-deficient patients. *Science,* 280**,** 1435-8.

DE MELLO, K. G., MELLO, F. C., BORGA, L., ROLLA, V., DUARTE, R. S., SAMPAIO, E. P., HOLLAND, S. M., PREVOTS, D. R. & DALCOLMO, M. P. 2013. Clinical and therapeutic features of pulmonary nontuberculous mycobacterial disease, Brazil, 1993-2011. *Emerg Infect Dis,* 19**,** 393-9.

DE MUNTER, J. S., HU, F. B., SPIEGELMAN, D., FRANZ, M. & VAN DAM, R. M. 2007. Whole grain, bran, and germ intake and risk of type 2 diabetes: a prospective cohort study and systematic review. *PLoS Med,* 4**,** e261.

DE REKENEIRE, N., PEILA, R., DING, J., COLBERT, L. H., VISSER, M., SHORR, R. I., KRITCHEVSKY, S. B., KULLER, L. H., STROTMEYER, E. S., SCHWARTZ, A. V., VELLAS, B. & HARRIS, T. B. 2006. Diabetes, hyperglycemia, and inflammation in older individuals: the health, aging and body composition study. *Diabetes Care,* 29**,** 1902-8.

DE VALLIERE, S., ABATE, G., BLAZEVIC, A., HEUERTZ, R. M. & HOFT, D. F. 2005. Enhancement of innate and cell-mediated immunity by antimycobacterial antibodies. *Infect Immun,* 73**,** 6711-20.

DE WAAL MALEFYT, R., FIGDOR, C. G. & DE VRIES, J. E. 1993. Effects of interleukin 4 on monocyte functions: comparison to interleukin 13. *Res Immunol,* 144**,** 629-33.

DEEDS, M. C., ANDERSON, J. M., ARMSTRONG, A. S., GASTINEAU, D. A., HIDDINGA, H. J., JAHANGIR, A., EBERHARDT, N. L. & KUDVA, Y. C. 2011. Single dose streptozotocin-induced diabetes: considerations for study design in islet transplantation models. *Lab Anim,* 45**,** 131-40.

DEFRONZO, R. A. 1988. Lilly lecture 1987. The triumvirate: beta-cell, muscle, liver. A collusion responsible for NIDDM. *Diabetes,* 37**,** 667-87.

DEFRONZO, R. A., BONADONNA, R. C. & FERRANNINI, E. 1992. Pathogenesis of NIDDM. A balanced overview. *Diabetes Care,* 15**,** 318-68.

DEFRONZO, R. A. & FERRANNINI, E. 1991. Insulin resistance. A multifaceted syndrome responsible for NIDDM, obesity, hypertension, dyslipidemia, and atherosclerotic cardiovascular disease. *Diabetes Care,* 14**,** 173-94.

DEL PRATO, S. 2009. Role of glucotoxicity and lipotoxicity in the pathophysiology of Type 2 diabetes mellitus and emerging treatment strategies. *Diabet Med,* 26**,** 1185-92.

DELAMAIRE, M., MAUGENDRE, D., MORENO, M., LE GOFF, M. C., ALLANNIC, H. & GENETET, B. 1997. Impaired leucocyte functions in diabetic patients. *Diabet Med,* 14**,** 29-34.

DENIS, M. & GREGG, E. O. 1991. Recombinant interleukin-6 increases the intracellular and extracellular growth of *Mycobacterium avium*. *Can J Microbiol,* 37**,** 479-83.

DHEDA, K., SCHWANDER, S. K., ZHU, B., VAN ZYL-SMIT, R. N. & ZHANG, Y. 2010. The immunology of tuberculosis: from bench to bedside. *Respirology,* 15**,** 433-50.

DIETRICH, J., AAGAARD, C., LEAH, R., OLSEN, A. W., STRYHN, A., DOHERTY, T. M. & ANDERSEN, P. 2005. Exchanging ESAT6 with TB10.4 in an Ag85B fusion molecule-based tuberculosis subunit vaccine: efficient protection and ESAT6-based sensitive monitoring of vaccine efficacy. *J Immunol,* 174**,** 6332-9.

DINADAYALA, P., LEMASSU, A., GRANOVSKI, P., CERANTOLA, S., WINTER, N. & DAFFE, M. 2004. Revisiting the structure of the anti-neoplastic glucans of *Mycobacterium bovis* Bacille Calmette-Guerin. Structural analysis of the extracellular and boiling water extract-derived glucans of the vaccine substrains. *J Biol Chem,* 279**,** 12369-78.

DINARELLO, C. A. 1996. Biologic basis for interleukin-1 in disease. *Blood,* 87**,** 2095-147.

DINARELLO, C. A. 2005. Interleukin-1beta. *Crit Care Med,* 33**,** S460-2.

DING, E. L. & MALIK, V. S. 2008. Convergence of obesity and high glycemic diet on compounding diabetes and cardiovascular risks in modernizing China: an emerging public health dilemma. *Global Health,* 4**,** 4.

DIVANGAHI, M., MOSTOWY, S., COULOMBE, F., KOZAK, R., GUILLOT, L., VEYRIER, F., KOBAYASHI, K. S., FLAVELL, R. A., GROS, P. & BEHR, M. A. 2008. NOD2-deficient mice have impaired resistance to *Mycobacterium tuberculosis* infection through defective innate and adaptive immunity. *J Immunol,* 181**,** 7157-65.

DIVEU, C., MCGEACHY, M. J. & CUA, D. J. 2008. Cytokines that regulate autoimmunity. *Curr Opin Immunol,* 20**,** 663-8.

DOHERTY, T. M., SEDER, R. A. & SHER, A. 1996. Induction and regulation of IL-15 expression in murine macrophages. *J Immunol,* 156**,** 735-41.

DONG, C. 2008. Regulation and pro-inflammatory function of interleukin-17 family cytokines. *Immunol Rev,* 226**,** 80-6.

DONOVAN, J. & BROWN, P. 2005. Care and Handling of Laboratory Mice. *Curr Protoc Microbiol.* John Wiley & Sons, Inc.

DOOLEY, K. E. & CHAISSON, R. E. 2009. Tuberculosis and diabetes mellitus: convergence of two epidemics. *Lancet Infect Dis,* 9**,** 737-46.

DOOLEY, K. E., TANG, T., GOLUB, J. E., DORMAN, S. E. & CRONIN, W. 2009. Impact of diabetes mellitus on treatment outcomes of patients with active tuberculosis. *Am J Trop Med Hyg,* 80**,** 634-9.

DORHOI, A. & KAUFMANN, S. H. 2009. Fine-tuning of T cell responses during infection. *Curr Opin Immunol,* 21**,** 367-77.

DORMAN, S. E. & HOLLAND, S. M. 1998. Mutation in the signal-transducing chain of the interferon-gamma receptor and susceptibility to mycobacterial infection. *J Clin Invest,* 101**,** 2364-9.

DUCATI, R. G., RUFFINO-NETTO, A., BASSO, L. A. & SANTOS, D. S. 2006. The resumption of consumption -- a review on tuberculosis. *Mem Inst Oswaldo Cruz,* 101**,** 697-714.

DUTTA, R. K., KATHANIA, M., RAJE, M. & MAJUMDAR, S. 2012. IL-6 inhibits IFN-gamma induced autophagy in *Mycobacterium tuberculosis* H37Rv infected macrophages. *Int J Biochem Cell Biol,* 44**,** 942-54.

DYCK, R. F., KLOMP, H., MARCINIUK, D. D., TAN, L., STANG, M. R., WARD, H. A. & HOEPPNER, V. H. 2007. The relationship between diabetes and tuberculosis in Saskatchewan: comparison of registered Indians and other Saskatchewan people. *Can J Public Health,* 98**,** 55-9.

DYE, C., BOURDIN TRUNZ, B., LONNROTH, K., ROGLIC, G. & WILLIAMS, B. G. 2011. Nutrition, diabetes and tuberculosis in the epidemiological transition. *PLoS One,* 6**,** e21161.

ECKEL, R. H., KAHN, S. E., FERRANNINI, E., GOLDFINE, A. B., NATHAN, D. M., SCHWARTZ, M. W., SMITH, R. J. & SMITH, S. R. 2011. Obesity and type 2 diabetes: what can be unified and what needs to be individualized? *J Clin Endocrinol Metab,* 96**,** 1654-63.

EHLERS, S. 2009. Lazy, dynamic or minimally recrudescent? On the elusive nature and location of the mycobacterium responsible for latent tuberculosis. *Infection,* 37**,** 87-95.

EL-ETR, S. H. & CIRILLO, J. D. 2001. Entry mechanisms of mycobacteria. *Front Biosci,* 6**,** D737-47.

ENVIGO RESEARCH LABORATORY. 2015. C57BL/6 inbred mice data sheet. Accessed in 2016.

ERNST, J. D. 1998. Macrophage receptors for *Mycobacterium tuberculosis*. *Infect Immun,* 66**,** 1277-81.

ERUSLANOV, E. B., LYADOVA, I. V., KONDRATIEVA, T. K., MAJOROV, K. B., SCHEGLOV, I. V., ORLOVA, M. O. & APT, A. S. 2005. Neutrophil responses to Mycobacterium tuberculosis infection in genetically susceptible and resistant mice. *Infect Immun,* 73**,** 1744-53.

ESPOSITO, K., NAPPO, F., MARFELLA, R., GIUGLIANO, G., GIUGLIANO, F., CIOTOLA, M., QUAGLIARO, L., CERIELLO, A. & GIUGLIANO, D. 2002. Inflammatory cytokine concentrations are acutely increased by hyperglycemia in humans: role of oxidative stress. *Circulation,* 106**,** 2067-72.

FALCONE, V., BASSEY, E. B., TONIOLO, A., CONALDI, P. G. & COLLINS, F. M. 1994. Differential release of tumor necrosis factor-[alpha] from murine peritoneal macrophages stimulated with virulent and avirulent species of mycobacteria. *FEMS Immunol Med Microbiol,* 8.

FALKINHAM, J. O., 3RD 1996. Epidemiology of infection by nontuberculous mycobacteria. *Clin Microbiol Rev,* 9**,** 177-215.

FANTUZZI, G. & DINARELLO, C. A. 1996. The inflammatory response in interleukin-1 beta-deficient mice: comparison with other cytokine-related knock-out mice. *J Leukoc Biol,* 59**,** 489-93.

FAURHOLT-JEPSEN, D., RANGE, N., PRAYGOD, G., JEREMIAH, K., FAURHOLT-JEPSEN, M., AABYE, M. G., CHANGALUCHA, J., CHRISTENSEN, D. L., PIPPER,

C. B., KRARUP, H., WITTE, D. R., ANDERSEN, A. B. & FRIIS, H. 2011. Diabetes Is a Risk Factor for Pulmonary Tuberculosis: A Case-Control Study from Mwanza, Tanzania. *PLoS ONE,* 6**,** e24215.

FAURSCHOU, M. & BORREGAARD, N. 2003. Neutrophil granules and secretory vesicles in inflammation. *Microbes Infect,* 5**,** 1317-27.

FEINGLOS, M. N., ANGELYN, M., 2008. Type 2 diabetes mellitus: an evidence-based approach to practical management. Totowa, NJ: Humana Press. p. 462. ISBN 978-1-58829-794-5.

FERRANNINI, E. 1998. Insulin resistance versus insulin deficiency in non-insulin-dependent diabetes mellitus: problems and prospects. *Endocr Rev,* 19**,** 477-90.

FINE, P. E. 1995. Variation in protection by BCG: implications of and for heterologous immunity. *Lancet,* 346**,** 1339-45.

FINEGOOD, D. T., MCARTHUR, M. D., KOJWANG, D., THOMAS, M. J., TOPP, B. G., LEONARD, T. & BUCKINGHAM, R. E. 2001. Beta-cell mass dynamics in Zucker diabetic fatty rats. Rosiglitazone prevents the rise in net cell death. *Diabetes,* 50**,** 1021-9.

FLETCHER, B., GULANICK, M. & LAMENDOLA, C. 2002. Risk factors for type 2 diabetes mellitus. *J Cardiovasc Nurs,* 16**,** 17-23.

FLOTO, R. A., MACARY, P. A., BONAME, J. M., MIEN, T. S., KAMPMANN, B., HAIR, J. R., HUEY, O. S., HOUBEN, E. N., PIETERS, J., DAY, C., OEHLMANN, W., SINGH, M., SMITH, K. G. & LEHNER, P. J. 2006. Dendritic cell stimulation by mycobacterial Hsp70 is mediated through CCR5. *Science,* 314**,** 454-8.

FLYNN, J. L. & CHAN, J. 2001a. Immunology of tuberculosis. *Annu Rev Immunol,* 19**,** 93-129.

FLYNN, J. L. & CHAN, J. 2001b. Tuberculosis: latency and reactivation. *Infect Immun,* 69**,** 4195-201.

FLYNN, J. L., CHAN, J. & LIN, P. L. 2011. Macrophages and control of granulomatous inflammation in tuberculosis. *Mucosal Immunol,* 4**,** 271-8.

FLYNN, J. L., CHAN, J., TRIEBOLD, K. J., DALTON, D. K., STEWART, T. A. & BLOOM, B. R. 1993. An essential role for interferon gamma in resistance to *Mycobacterium tuberculosis* infection. *J Exp Med,* 178**,** 2249-54.

FLYNN, J. L., GOLDSTEIN, M. M., CHAN, J., TRIEBOLD, K. J., PFEFFER, K., LOWENSTEIN, C. J., SCHREIBER, R., MAK, T. W. & BLOOM, B. R. 1995. Tumor necrosis factor-alpha is required in the protective immune response against *Mycobacterium tuberculosis* in mice. *Immunity,* 2**,** 561-72.

FLYNN, J. L., SCANGA, C. A., TANAKA, K. E. & CHAN, J. 1998. Effects of aminoguanidine on latent murine tuberculosis. *J Immunol,* 160**,** 1796-803.

FOSSIEZ, F., DJOSSOU, O., CHOMARAT, P., FLORES-ROMO, L., AIT-YAHIA, S., MAAT, C., PIN, J. J., GARRONE, P., GARCIA, E., SAELAND, S., BLANCHARD, D., GAILLARD, C., DAS MAHAPATRA, B., ROUVIER, E., GOLSTEIN, P., BANCHEREAU, J. & LEBECQUE, S. 1996. T cell interleukin-17 induces stromal cells to produce proinflammatory and hematopoietic cytokines. *J Exp Med,* 183**,** 2593-603.

FOWLER, M. J. 2008. Microvascular and Macrovascular Complications of Diabetes. *Clin Diabetes,* 26**,** 77-81.

FREEMAN, D. J., NORRIE, J., CASLAKE, M. J., GAW, A., FORD, I., LOWE, G. D., O'REILLY, D. S., PACKARD, C. J. & SATTAR, N. 2002. C-reactive protein is an independent predictor of risk for the development of diabetes in the West of Scotland Coronary Prevention Study. *Diabetes,* 51**,** 1596-600.

FRICK, M. 2013. Where are we going, where have we been? In The HIV, HCV, TB pipeline report, pp. 263–283. http://www.pipelinereport.org.

FRIEDEN, T. R., STERLING, T. R., MUNSIFF, S. S., WATT, C. J. & DYE, C. 2003. Tuberculosis. *Lancet,* 362**,** 887-99.

FRUCHT, D. M. & HOLLAND, S. M. 1996. Defective monocyte costimulation for IFN-gamma production in familial disseminated *Mycobacterium avium* complex infection: abnormal IL-12 regulation. *J Immunol,* 157**,** 411-6.

FU, J., TAY, S. S., LING, E. A. & DHEEN, S. T. 2006. High glucose alters the expression of genes involved in proliferation and cell-fate specification of embryonic neural stem cells. *Diabetologia,* 49**,** 1027-38.

FUJIWARA, N. & KOBAYASHI, K. 2005. Macrophages in inflammation. *Curr Drug Targets Inflamm Allergy,* 4**,** 281-6.

FULTON, S. A., CROSS, J. V., TOOSSI, Z. T. & BOOM, W. H. 1998. Regulation of interleukin-12 by interleukin-10, transforming growth factor-beta, tumor necrosis factor-alpha, and interferon-gamma in human monocytes infected with *Mycobacterium tuberculosis* H37Ra. *J Infect Dis,* 178**,** 1105-14.

FULTON, S. A., MARTIN, T. D., REDLINE, R. W. & HENRY BOOM, W. 2000. Pulmonary immune responses during primary *Mycobacterium bovis*- Calmette-Guerin bacillus infection in C57Bl/6 mice. *Am J Respir Cell Mol Biol,* 22**,** 333-43.

FULTON, S. A., REBA, S. M., PAI, R. K., PENNINI, M., TORRES, M., HARDING, C. V. & BOOM, W. H. 2004. Inhibition of major histocompatibility complex II expression and antigen processing in murine alveolar macrophages by *Mycobacterium bovis* BCG and the 19-kilodalton mycobacterial lipoprotein. *Infect Immun,* 72**,** 2101-10.

GAN, H., HE, X., DUAN, L., MIRABILE-LEVENS, E., KORNFELD, H. & REMOLD, H. G. 2005. Enhancement of antimycobacterial activity of macrophages by stabilization of inner mitochondrial membrane potential. *J Infect Dis,* 191**,** 1292-300.

GAN, Y. H. 2013. Host susceptibility factors to bacterial infections in type 2 diabetes. *PLoS Pathog,* 9**,** e1003794.

GARCIA-PEREZ, B. E., MONDRAGON-FLORES, R. & LUNA-HERRERA, J. 2003. Internalization of *Mycobacterium tuberculosis* by macropinocytosis in non-phagocytic cells. *Microb Pathog,* 35**,** 49-55.

GARDNER, D. G. & SHOBACK, D. M. 2011. Greenspan's basic & clinical endocrinology, 9th Edn., chapter-17 New York: McGraw-Hill Medical, ISBN 0-07-162243-8.

GARLANDA, C., DI LIBERTO, D., VECCHI, A., LA MANNA, M. P., BURACCHI, C., CACCAMO, N., SALERNO, A., DIELI, F. & MANTOVANI, A. 2007. Damping excessive inflammation and tissue damage in *Mycobacterium tuberculosis* infection by Toll IL-1 receptor 8/single Ig IL-1-related receptor, a negative regulator of IL-1/TLR signaling. *J Immunol,* 179**,** 3119-25.

GAYNOR, C. D., MCCORMACK, F. X., VOELKER, D. R., MCGOWAN, S. E. & SCHLESINGER, L. S. 1995. Pulmonary surfactant protein A mediates enhanced phagocytosis of *Mycobacterium tuberculosis* by a direct interaction with human macrophages. *J Immunol,* 155**,** 5343-51.

GEERLINGS, S. E. & HOEPELMAN, A. I. 1999. Immune dysfunction in patients with diabetes mellitus (DM). *FEMS Immunol Med Microbiol,* 26**,** 259-65.

GEIJTENBEEK, T. B., KROOSHOOP, D. J., BLEIJS, D. A., VAN VLIET, S. J., VAN DUIJNHOVEN, G. C., GRABOVSKY, V., ALON, R., FIGDOR, C. G. & VAN KOOYK, Y. 2000a. DC-SIGN-ICAM-2 interaction mediates dendritic cell trafficking. *Nat Immunol,* 1**,** 353-7.

GEIJTENBEEK, T. B., TORENSMA, R., VAN VLIET, S. J., VAN DUIJNHOVEN, G. C., ADEMA, G. J., VAN KOOYK, Y. & FIGDOR, C. G. 2000b. Identification of DC-SIGN, a novel dendritic cell-specific ICAM-3 receptor that supports primary immune responses. *Cell,* 100**,** 575-85.

GEIJTENBEEK, T. B., VAN VLIET, S. J., KOPPEL, E. A., SANCHEZ-HERNANDEZ, M., VANDENBROUCKE-GRAULS, C. M., APPELMELK, B. & VAN KOOYK, Y. 2003. Mycobacteria target DC-SIGN to suppress dendritic cell function. *J Exp Med,* 197**,** 7-17.

GEISEL, R. E., SAKAMOTO, K., RUSSELL, D. G. & RHOADES, E. R. 2005. In vivo activity of released cell wall lipids of *Mycobacterium bovis* bacillus Calmette-Guerin is due principally to trehalose mycolates. *J Immunol,* 174**,** 5007-15.

GEISLER, C., ALMDAL, T., BENNEDSEN, J., RHODES, J. M. & KOLENDORF, K. 1982. Monocyte functions in diabetes mellitus. *Acta Pathol Microbiol Immunol Scand C,* 90**,** 33-7.

GELUK, A., VAN MEIJGAARDEN, K. E., FRANKEN, K. L., DRIJFHOUT, J. W., D'SOUZA, S., NECKER, A., HUYGEN, K. & OTTENHOFF, T. H. 2000. Identification of major epitopes of *Mycobacterium tuberculosis* AG85B that are recognized by HLA-A*0201-restricted CD8+ T cells in HLA-transgenic mice and humans. *J Immunol,* 165**,** 6463-71.

GERCKEN, J., PRYJMA, J., ERNST, M. & FLAD, H. D. 1994. Defective antigen presentation by *Mycobacterium tuberculosis*-infected monocytes. *Infect Immun,* 62**,** 3472-8.

GERICH, J. E. 1998. The genetic basis of type 2 diabetes mellitus: impaired insulin secretion versus impaired insulin sensitivity. *Endocr Rev,* 19**,** 491-503.

GHADERIAN, S. B., HAYATI, F., SHAYANPOUR, S. & BELADI MOUSAVI, S. S. 2015. Diabetes and end-stage renal disease; a review article on new concepts. *J Renal Inj Prev,* 4**,** 28-33.

GHOLIZADEH, Y., VARNEROT, A., MASLO, C., SALAUZE, B., BADAOUI, H., VINCENT, V. & BURE-ROSSIER, A. 1998. *Mycobacterium celatum* infection in two HIV-infected patients treated prophylactically with rifabutin. *Eur J Clin Microbiol Infect Dis,* 17**,** 278-81.

GILBERT, E. R., FU, Z. & LIU, D. 2011. Development of a nongenetic mouse model of type 2 diabetes. *Exp Diabetes Res,* 2011**,** 416254.

GINSBERG, H. N. 2000. Insulin resistance and cardiovascular disease. *J Clin Invest,* 106**,** 453-8.

GLASS, E. J., STEWART, J., MATTHEWS, D. M., COLLIER, A., CLARKE, B. F. & WEIR, D. M. 1987. Impairment of monocyte "lectin-like" receptor activity in type 1 (insulin-dependent) diabetic patients. *Diabetologia,* 30**,** 228-31.

GOLDBERG, R. B. 2009. Cytokine and cytokine-like inflammation markers, endothelial dysfunction, and imbalanced coagulation in development of diabetes and its complications. *J Clin Endocrinol Metab,* 94**,** 3171-82.

GOLDEN, M. P. & VIKRAM, H. R. 2005. Extrapulmonary tuberculosis: an overview. *Am Fam Physician,* 72**,** 1761-8.

GOLDSTEIN, B. J. 2002. Insulin resistance as the core defect in type 2 diabetes mellitus. *Am J Cardiol,* 90**,** 3g-10g.

GOMEZ, D. I., TWAHIRWA, M., SCHLESINGER, L. S. & RESTREPO, B. I. 2013. Reduced *Mycobacterium tuberculosis* association with monocytes from diabetes patients that have poor glucose control. *Tuberculosis (Edinb),* 93**,** 192-7.

GONG, J. H., ZHANG, M., MODLIN, R. L., LINSLEY, P. S., IYER, D., LIN, Y. & BARNES, P. F. 1996. Interleukin-10 downregulates *Mycobacterium tuberculosis*-induced Th1 responses and CTLA-4 expression. *Infect Immun,* 64**,** 913-8.

GONZALEZ-JUARRERO, M. & ORME, I. M. 2001. Characterization of murine lung dendritic cells infected with *Mycobacterium tuberculosis*. *Infect Immun,* 69**,** 1127-33.

GONZALEZ-JUARRERO, M., TURNER, O. C., TURNER, J., MARIETTA, P., BROOKS, J. V. & ORME, I. M. 2001. Temporal and spatial arrangement of lymphocytes within lung granulomas induced by aerosol infection with *Mycobacterium tuberculosis*. *Infect Immun,* 69**,** 1722-8.

GONZÁLEZ-PÉREZ, M., MARIÑO-RAMÍREZ, L., PARRA-LÓPEZ, C. A., MURCIA, M. I., MARQUINA, B., MATA-ESPINOZA, D., RODRIGUEZ-MÍGUEZ, Y., BAAY-GUZMAN, G. J., HUERTA-YEPEZ, S. & HERNANDEZ-PANDO, R. 2013. Virulence and Immune Response Induced by *Mycobacterium avium* Complex Strains in a Model of Progressive Pulmonary Tuberculosis and Subcutaneous Infection in BALB/c Mice. *Infect Immun,* 81**,** 4001-4012.

GOONETILLEKE, N. P., MCSHANE, H., HANNAN, C. M., ANDERSON, R. J., BROOKES, R. H. & HILL, A. V. 2003. Enhanced immunogenicity and protective efficacy against *Mycobacterium tuberculosis* of bacille Calmette-Guerin vaccine using mucosal administration and boosting with a recombinant modified vaccinia virus Ankara. *J Immunol,* 171**,** 1602-9.

GORDON, S. 2003. Alternative activation of macrophages. *Nat Rev Immunol,* 3**,** 23-35.

GREENHALGH, C. J. & HILTON, D. J. 2001. Negative regulation of cytokine signaling. *J Leukoc Biol,* 70**,** 348-56.

GRODE, L., GANOZA, C. A., BROHM, C., WEINER, J., 3RD, EISELE, B. & KAUFMANN, S. H. 2013. Safety and immunogenicity of the recombinant BCG vaccine VPM1002 in a phase 1 open-label randomized clinical trial. *Vaccine,* 31**,** 1340-8.

GRODE, L., SEILER, P., BAUMANN, S., HESS, J., BRINKMANN, V., NASSER EDDINE, A., MANN, P., GOOSMANN, C., BANDERMANN, S., SMITH, D., BANCROFT, G. J., REYRAT, J. M., VAN SOOLINGEN, D., RAUPACH, B. & KAUFMANN, S. H. 2005. Increased vaccine efficacy against tuberculosis of recombinant *Mycobacterium bovis* bacille Calmette-Guerin mutants that secrete listeriolysin. *J Clin Invest,* 115**,** 2472-9.

GROOP, L. C., WIDEN, E. & FERRANNINI, E. 1993. Insulin resistance and insulin deficiency in the pathogenesis of type 2 (non-insulin-dependent) diabetes mellitus: errors of metabolism or of methods? *Diabetologia,* 36**,** 1326-31.

GROSS, J. L., DE AZEVEDO, M. J., SILVEIRO, S. P., CANANI, L. H., CARAMORI, M. L. & ZELMANOVITZ, T. 2005. Diabetic nephropathy: diagnosis, prevention, and treatment. *Diabetes Care,* 28**,** 164-76.

GROTZKE, J. E. & LEWINSOHN, D. M. 2005. Role of CD8+ T lymphocytes in control of *Mycobacterium tuberculosis* infection. *Microbes Infect,* 7**,** 776-88.

GUIRADO, E. & SCHLESINGER, L. S. 2013. Modeling the *Mycobacterium tuberculosis* Granuloma - the Critical Battlefield in Host Immunity and Disease. *Front Immunol,* 4**,** 98.

GUPTA, A., AHMAD, F. J., AHMAD, F., GUPTA, U. D., NATARAJAN, M., KATOCH, V. & BHASKAR, S. 2012. Efficacy of *Mycobacterium indicus pranii* immunotherapy as an adjunct to chemotherapy for tuberculosis and underlying immune responses in the lung. *PLoS One,* 7**,** e39215.

GUPTA, U. D. & KATOCH, V. M. 2005. Animal models of tuberculosis. *Tuberculosis (Edinb),* 85**,** 277-93.

GUTIERREZ, M. C., BRISSE, S., BROSCH, R., FABRE, M., OMAIS, B., MARMIESSE, M., SUPPLY, P. & VINCENT, V. 2005. Ancient origin and gene mosaicism of the progenitor of *Mycobacterium tuberculosis*. *PLoS Pathog,* 1**,** e5.

GUYOT-REVOL, V., INNES, J. A., HACKFORTH, S., HINKS, T. & LALVANI, A. 2006. Regulatory T cells are expanded in blood and disease sites in patients with tuberculosis. *Am J Respir Crit Care Med,* 173**,** 803-10.

HALES, C. N. & OZANNE, S. E. 2003. For debate: Fetal and early postnatal growth restriction lead to diabetes, the metabolic syndrome and renal failure. *Diabetologia,* 46**,** 1013-9.

HAN, J., WEI, L., XU, W., LU, J., WANG, C., BAO, Y. & JIA, W. 2015. CTSK inhibitor exert its anti-obesity effects through regulating adipocyte differentiation in high-fat diet induced obese mice. *Endocr J,* 62**,** 309-17.

HARDING, C. V. & BOOM, W. H. 2010. Regulation of antigen presentation by *Mycobacterium tuberculosis*: a role for Toll-like receptors. *Nat Rev Microbiol,* 8**,** 296-307.

HARIKA, R. K., EILANDER, A., ALSSEMA, M., OSENDARP, S. J. & ZOCK, P. L. 2013. Intake of fatty acids in general populations worldwide does not meet dietary recommendations to prevent coronary heart disease: a systematic review of data from 40 countries. *Ann Nutr Metab,* 63**,** 229-38.

HARISHANKAR, N., KUMAR, P. U., SESIKERAN, B. & GIRIDHARAN, N. 2011. Obesity associated pathophysiological & histological changes in WNIN obese mutant rats. *Indian J Med Res,* 134**,** 330-40.

HARRIS, M. I., FLEGAL, K. M., COWIE, C. C., EBERHARDT, M. S., GOLDSTEIN, D. E., LITTLE, R. R., WIEDMEYER, H. M. & BYRD-HOLT, D. D. 1998. Prevalence of diabetes, impaired fasting glucose, and impaired glucose tolerance in U.S. adults. The Third National Health and Nutrition Examination Survey, 1988-1994. *Diabetes Care,* 21**,** 518-24.

HATANAKA, E., MONTEAGUDO, P. T., MARROCOS, M. S. & CAMPA, A. 2006. Neutrophils and monocytes as potentially important sources of proinflammatory cytokines in diabetes. *Clin Exp Immunol,* 146**,** 443-7.

HATHERILL, M. 2011. Prospects for elimination of childhood tuberculosis: the role of new vaccines. *Arch Dis Child,* 96**,** 851-6.

HEINZEL, F. P., AHMED, F., HUJER, A. M. & RERKO, R. M. 1995. Immunoregulation of murine leishmaniasis by interleukin-12. *Res Immunol,* 146**,** 575-81.

HEINZEL, F. P., SADICK, M. D., HOLADAY, B. J., COFFMAN, R. L. & LOCKSLEY, R. M. 1989. Reciprocal expression of interferon gamma or interleukin 4 during the resolution or progression of murine leishmaniasis. Evidence for expansion of distinct helper T cell subsets. *J Exp Med,* 169**,** 59-72.

HELGUERA-REPETTO, A. C., CHACON-SALINAS, R., CERNA-CORTES, J. F., RIVERA-GUTIERREZ, S., ORTIZ-NAVARRETE, V., ESTRADA-GARCIA, I. & GONZALEZ-Y-MERCHAND, J. A. 2014. Differential Macrophage Response to Slow- and Fast-Growing Pathogenic Mycobacteria. *Biomed Res Int,* 2014**,** 916521.

HENDERSON, R. A., WATKINS, S. C. & FLYNN, J. L. 1997. Activation of human dendritic cells following infection with *Mycobacterium tuberculosis*. *J Immunol,* 159**,** 635-43.

HENRY, R. R., SCHEAFFER, L. & OLEFSKY, J. M. 1985. Glycemic effects of intensive caloric restriction and isocaloric refeeding in noninsulin-dependent diabetes mellitus. *J Clin Endocrinol Metab,* 61**,** 917-25.

HERBERG, L. 1998. Insulin resistance in abdominal and subcutaneous obesity: comparison of C57BL/6J-ob/ob with New Zealand obese mice.In Frontiers in Diabetes Research:

Lessons from Animal Diabetes II. Shafrir E, Renold A, Eds. London, John Libbey, p. 367-373.

.

HERBST, S., SCHAIBLE, U. E. & SCHNEIDER, B. E. 2011. Interferon gamma activated macrophages kill mycobacteria by nitric oxide induced apoptosis. *PLoS One,* 6**,** e19105.

HERDER, C. & RODEN, M. 2011. Genetics of type 2 diabetes: pathophysiologic and clinical relevance. *Eur J Clin Invest,* 41**,** 679-92.

HERNANDEZ-PANDO, R., AGUILAR, D., HERNANDEZ, M. L., OROZCO, H. & ROOK, G. 2004. Pulmonary tuberculosis in BALB/c mice with non-functional IL-4 genes: changes in the inflammatory effects of TNF-alpha and in the regulation of fibrosis. *Eur J Immunol,* 34**,** 174-83.

HERNANDEZ-PANDO, R., JEYANATHAN, M., MENGISTU, G., AGUILAR, D., OROZCO, H., HARBOE, M., ROOK, G. A. & BJUNE, G. 2000. Persistence of DNA from *Mycobacterium tuberculosis* in superficially normal lung tissue during latent infection. *Lancet,* 356**,** 2133-8.

HERNANDEZ-PANDO, R., OROZCOE, H., SAMPIERI, A., PAVON, L., VELASQUILLO, C., LARRIVA-SAHD, J., ALCOCER, J. M. & MADRID, M. V. 1996. Correlation between the kinetics of Th1, Th2 cells and pathology in a murine model of experimental pulmonary tuberculosis. *Immunology,* 89**,** 26-33.

HESSELING, A. C., SCHAAF, H. S., GIE, R. P., STARKE, J. R. & BEYERS, N. 2002. A critical review of diagnostic approaches used in the diagnosis of childhood tuberculosis. *Int J Tuberc Lung Dis,* 6**,** 1038-45.

HILL, H. R., AUGUSTINE, N. H., RALLISON, M. L. & SANTOS, J. I. 1983. Defective monocyte chemotactic responses in diabetes mellitus. *J Clin Immunol,* 3**,** 70-7.

HILLEMANN, D., RUSCH-GERDES, S. & RICHTER, E. 2007. Evaluation of the GenoType MTBDRplus assay for rifampin and isoniazid susceptibility testing of *Mycobacterium tuberculosis* strains and clinical specimens. *J Clin Microbiol,* 45**,** 2635-40.

HIMSWORTH, H. P. 1936. Diabetes mellitus: its differentiation into insulin-sensitive and insulin-insensitive types. *Lancet* 1936; 1:127.

HIROSUMI, J., TUNCMAN, G., CHANG, L., GORGUN, C. Z., UYSAL, K. T., MAEDA, K., KARIN, M. & HOTAMISLIGIL, G. S. 2002. A central role for JNK in obesity and insulin resistance. *Nature,* 420**,** 333-6.

HIRSCH, C. S., ELLNER, J. J., BLINKHORN, R. & TOOSSI, Z. 1997. In vitro restoration of T cell responses in tuberculosis and augmentation of monocyte effector function against *Mycobacterium tuberculosis* by natural inhibitors of transforming growth factor beta. *Proc Natl Acad Sci U S A,* 94**,** 3926-31.

HIRSCH, C. S., ELLNER, J. J., RUSSELL, D. G. & RICH, E. A. 1994. Complement receptor-mediated uptake and tumor necrosis factor-alpha-mediated growth inhibition of *Mycobacterium tuberculosis* by human alveolar macrophages. *J Immunol,* 152**,** 743-53.

HIRSCH, C. S., TOOSSI, Z., JOHNSON, J. L., LUZZE, H., NTAMBI, L., PETERS, P., MCHUGH, M., OKWERA, A., JOLOBA, M., MUGYENYI, P., MUGERWA, R. D., TEREBUH, P. & ELLNER, J. J. 2001. Augmentation of apoptosis and interferon-gamma production at sites of active *Mycobacterium tuberculosis* infection in human tuberculosis. *J Infect Dis,* 183**,** 779-88.

HIRSCH, C. S., TOOSSI, Z., OTHIENO, C., JOHNSON, J. L., SCHWANDER, S. K., ROBERTSON, S., WALLIS, R. S., EDMONDS, K., OKWERA, A., MUGERWA, R., PETERS, P. & ELLNER, J. J. 1999a. Depressed T-cell interferon-gamma responses in pulmonary tuberculosis: analysis of underlying mechanisms and modulation with therapy. *J Infect Dis,* 180**,** 2069-73.

HIRSCH, C. S., TOOSSI, Z., VANHAM, G., JOHNSON, J. L., PETERS, P., OKWERA, A., MUGERWA, R., MUGYENYI, P. & ELLNER, J. J. 1999b. Apoptosis and T cell hyporesponsiveness in pulmonary tuberculosis. *J Infect Dis,* 179**,** 945-53.

HMAMA, Z., SENDIDE, K., TALAL, A., GARCIA, R., DOBOS, K. & REINER, N. E. 2004. Quantitative analysis of phagolysosome fusion in intact cells: inhibition by mycobacterial lipoarabinomannan and rescue by an 1alpha,25-dihydroxyvitamin D3-phosphoinositide 3-kinase pathway. *J Cell Sci,* 117**,** 2131-40.

HODGSON, K., GOVAN, B., KETHEESAN, N. & MORRIS, J. 2013a. Dietary composition of carbohydrates contributes to the development of experimental type 2 diabetes. *Endocrine,* 43**,** 447-51.

HODGSON, K., MORRIS, J., BRIDSON, T., GOVAN, B., RUSH, C. & KETHEESAN, N. 2015. Immunological mechanisms contributing to the double burden of diabetes and intracellular bacterial infections. *Immunology,* 144**,** 171-85.

HODGSON, K. A., GOVAN, B. L., WALDUCK, A. K., KETHEESAN, N. & MORRIS, J. L. 2013b. Impaired early cytokine responses at the site of infection in a murine model of type 2 diabetes and melioidosis comorbidity. *Infect Immun,* 81**,** 470-7.

HODGSON, K. A., MORRIS, J. L., FETERL, M. L., GOVAN, B. L. & KETHEESAN, N. 2011. Altered macrophage function is associated with severe *Burkholderia pseudomallei* infection in a murine model of type 2 diabetes. *Microbes Infect,* 13**,** 1177-84.

HOEFSLOOT, W., VAN INGEN, J., ANDREJAK, C., ANGEBY, K., BAURIAUD, R., BEMER, P., BEYLIS, N., BOEREE, M. J., CACHO, J., CHIHOTA, V., CHIMARA, E., CHURCHYARD, G., CIAS, R., DAZA, R., DALEY, C. L., DEKHUIJZEN, P. N., DOMINGO, D., DROBNIEWSKI, F., ESTEBAN, J., FAUVILLE-DUFAUX, M., FOLKVARDSEN, D. B., GIBBONS, N., GOMEZ-MAMPASO, E., GONZALEZ, R., HOFFMANN, H., HSUEH, P. R., INDRA, A., JAGIELSKI, T., JAMIESON, F., JANKOVIC, M., JONG, E., KEANE, J., KOH, W. J., LANGE, B., LEAO, S., MACEDO, R., MANNSAKER, T., MARRAS, T. K., MAUGEIN, J., MILBURN, H. J., MLINKO, T., MORCILLO, N., MORIMOTO, K., PAPAVENTSIS, D., PALENQUE, E., PAEZ-PENA, M., PIERSIMONI, C., POLANOVA, M., RASTOGI, N., RICHTER, E., RUIZ-SERRANO, M. J., SILVA, A., DA SILVA, M. P., SIMSEK, H., VAN SOOLINGEN, D., SZABO, N., THOMSON, R., TORTOLA FERNANDEZ, T., TORTOLI, E., TOTTEN, S. E., TYRRELL, G., VASANKARI, T., VILLAR, M., WALKIEWICZ, R., WINTHROP, K. L. & WAGNER, D. 2013. The geographic diversity of nontuberculous mycobacteria isolated from pulmonary samples: an NTM-NET collaborative study. *Eur Respir J,* 42**,** 1604-13.

HOLLAND, S. M., DORMAN, S. E., KWON, A., PITHA-ROWE, I. F., FRUCHT, D. M., GERSTBERGER, S. M., NOEL, G. J., VESTERHUS, P., BROWN, M. R. & FLEISHER, T. A. 1998. Abnormal regulation of interferon-gamma, interleukin-12, and tumor necrosis factor-alpha in human interferon-gamma receptor 1 deficiency. *J Infect Dis,* 178**,** 1095-104.

HONDA, J. R., KNIGHT, V. & CHAN, E. D. 2015. Pathogenesis and risk factors for nontuberculous mycobacterial lung disease. *Clin Chest Med,* 36**,** 1-11.

HORWITZ, O. & BUNCH-CHRISTENSEN, K. 1972. Correlation between tuberculin sensitivity after 2 months and 5 years among BCG vaccinated subjects. *Bull World Health Organ,* 47**,** 49-58.

HOTAMISLIGIL, G. S., SHARGILL, N. S. & SPIEGELMAN, B. M. 1993. Adipose expression of tumor necrosis factor-alpha: direct role in obesity-linked insulin resistance. *Science,* 259**,** 87-91.

HU, E. A., PAN, A., MALIK, V. & SUN, Q. 2012. White rice consumption and risk of type 2 diabetes: meta-analysis and systematic review. *Bmj,* 344**,** e1454.

HU, F. B. 2013. Resolved: There is sufficient scientific evidence that decreasing sugar-sweetened beverage consumption will reduce the prevalence of obesity and obesity-related diseases. *Obes Rev,* 14**,** 606-619.

HU, F. B., LI, T. Y., COLDITZ, G. A., WILLETT, W. C. & MANSON, J. E. 2003. Television watching and other sedentary behaviors in relation to risk of obesity and type 2 diabetes mellitus in women. *Jama,* 289**,** 1785-91.

HU, F. B., MANSON, J. E., STAMPFER, M. J., COLDITZ, G., LIU, S., SOLOMON, C. G. & WILLETT, W. C. 2001. Diet, lifestyle, and the risk of type 2 diabetes mellitus in women. *N Engl J Med,* 345**,** 790-7.

HU, F. B. & WILLETT, W. C. 2002. Optimal diets for prevention of coronary heart disease. *Jama,* 288**,** 2569-78.

HUEBNER, R. E., SCHEIN, M. F. & BASS, J. B., JR. 1993. The tuberculin skin test. *Clin Infect Dis,* 17**,** 968-75.

HULL, R. L., WESTERMARK, G. T., WESTERMARK, P. & KAHN, S. E. 2004. Islet amyloid: a critical entity in the pathogenesis of type 2 diabetes. *J Clin Endocrinol Metab,* 89**,** 3629-43.

IDF. 2013. International Diabetes Federation, IDF Diabetes Atlas, 6th Edn, 2013. © International Diabetes Federation, 2013.

IDF. 2017. International Diabetes Federation, Diabetes Atlas, 8th Edn, 2017. © International Diabetes Federation, 2017.

IHO, S., YAMAMOTO, T., TAKAHASHI, T. & YAMAMOTO, S. 1999. Oligodeoxynucleotides containing palindrome sequences with internal 5'-CpG-3' act directly on human NK and activated T cells to induce IFN-gamma production in vitro. *J Immunol,* 163**,** 3642-52.

INDIAN COUNCIL OF MEDICAL RESEARCH. 2013. Fifteen year follow up of trial of BCG vaccines in south India for tuberculosis prevention. 1999. *Indian J Med Res,* 137**,** 14 p following p571.

INDRIGO, J., HUNTER, R. L., JR. & ACTOR, J. K. 2002. Influence of trehalose 6,6'-dimycolate (TDM) during mycobacterial infection of bone marrow macrophages. *Microbiology,* 148**,** 1991-8.

INDRIGO, J., HUNTER, R. L., JR. & ACTOR, J. K. 2003. Cord factor trehalose 6,6'-dimycolate (TDM) mediates trafficking events during mycobacterial infection of murine macrophages. *Microbiology,* 149**,** 2049-59.

IONA, E., PARDINI, M., GAGLIARDI, M. C., COLONE, M., STRINGARO, A. R., TELONI, R., BRUNORI, L., NISINI, R., FATTORINI, L. & GIANNONI, F. 2012. Infection of human THP-1 cells with dormant *Mycobacterium tuberculosis*. *Microbes Infect,* 14**,** 959-67.

IZZEDINE, H., LAUNAY-VACHER, V., DEYBACH, C., BOURRY, E., BARROU, B. & DERAY, G. 2005. Drug-induced diabetes mellitus. *Expert Opin Drug Saf,* 4**,** 1097-109.

JABADO, N. & GROS, P. 2005. Tuberculosis: The genetics of vulnerability, *Nature* 434, 709-711(7), doi:10.1038/434709a.

JACKSON, E., STEWART, A., MAGUIRE, E. J. & NORTON, R. E. 2007. Mycobacterial soft tissue infections in North Queensland. *ANZ J Surg,* 77**,** 368-70.

JACKSON LABORATORY. 2015. Physiological and phenotypic data for many popular JAX® Mice strains. Accessed in 2016.

JACOBS, M., BROWN, N., ALLIE, N., GULERT, R. & RYFFEL, B. 2000. Increased resistance to mycobacterial infection in the absence of interleukin-10. *Immunology,* 100**,** 494-501.

JAGANNATHAN-BOGDAN, M., MCDONNELL, M. E., SHIN, H., REHMAN, Q., HASTURK, H., APOVIAN, C. M. & NIKOLAJCZYK, B. S. 2011. Elevated proinflammatory cytokine production by a skewed T cell compartment requires monocytes and promotes inflammation in type 2 diabetes. *J Immunol,* 186**,** 1162-72.

JAKOVLJEVIC, M. B. & MILOVANOVIC, O. 2015. Growing Burden of Non-Communicable Diseases in the Emerging Health Markets: The Case of BRICS. *Front Public Health,* 3**,** 65.

JANASZEK, W. 1991. [Evaluation of thermostability of lyophilized BCG vaccines by using an accelerated thermal degradation test]. *Med Dosw Mikrobiol,* 43**,** 43-9.

JANSON, J., ASHLEY, R. H., HARRISON, D., MCINTYRE, S. & BUTLER, P. C. 1999. The mechanism of islet amyloid polypeptide toxicity is membrane disruption by intermediate-sized toxic amyloid particles. *Diabetes,* 48**,** 491-8.

JARON, B., MARANGHI, E., LECLERC, C. & MAJLESSI, L. 2008. Effect of attenuation of Treg during BCG immunization on anti-mycobacterial Th1 responses and protection against *Mycobacterium tuberculosis*. *PLoS One,* 3**,** e2833.

JARZEMBOWSKI, J. A. & YOUNG, M. B. 2008. Nontuberculous mycobacterial infections. *Arch Pathol Lab Med,* 132**,** 1333-41.

JASENOSKY, L. D., SCRIBA, T. J., HANEKOM, W. A. & GOLDFELD, A. E. 2015. T cells and adaptive immunity to *Mycobacterium tuberculosis* in humans. *Immunol Rev,* 264**,** 74-87.

JEEVAN, A. & ASHERSON, G. L. 1988. Recombinant interleukin-2 limits the replication of *Mycobacterium lepraemurium* and *Mycobacterium bovis* BCG in mice. *Infect Immun,* 56**,** 660-4.

JEON, C. Y. & MURRAY, M. B. 2008. Diabetes mellitus increases the risk of active tuberculosis: a systematic review of 13 observational studies. *PLoS Med,* 5**,** e152.

JIMENEZ-CORONA, M. E., CRUZ-HERVERT, L. P., GARCIA-GARCIA, L., FERREYRA-REYES, L., DELGADO-SANCHEZ, G., BOBADILLA-DEL-VALLE, M., CANIZALES-QUINTERO, S., FERREIRA-GUERRERO, E., BAEZ-SALDANA, R., TELLEZ-VAZQUEZ, N., MONTERO-CAMPOS, R., MONGUA-RODRIGUEZ, N., MARTINEZ-GAMBOA, R. A., SIFUENTES-OSORNIO, J. & PONCE-DE-LEON, A. 2013. Association of diabetes and tuberculosis: impact on treatment and post-treatment outcomes. *Thorax,* 68**,** 214-20.

JO, E. K. 2008. Mycobacterial interaction with innate receptors: TLRs, C-type lectins, and NLRs. *Curr Opin Infect Dis,* 21**,** 279-86.

JO, E. K., YANG, C. S., CHOI, C. H. & HARDING, C. V. 2007. Intracellular signalling cascades regulating innate immune responses to Mycobacteria: branching out from Toll-like receptors. *Cell Microbiol,* 9**,** 1087-98.

JOHNSON, C. M., COOPER, A. M., FRANK, A. A., BONORINO, C. B., WYSOKI, L. J. & ORME, I. M. 1997. *Mycobacterium tuberculosis* aerogenic rechallenge infections in B cell-deficient mice. *Tuber Lung Dis,* 78**,** 257-61.

JOHNSON, J. L., SSEKASANVU, E., OKWERA, A., MAYANJA, H., HIRSCH, C. S., NAKIBALI, J. G., JANKUS, D. D., EISENACH, K. D., BOOM, W. H., ELLNER, J. J. & MUGERWA, R. D. 2003. Randomized trial of adjunctive interleukin-2 in adults with pulmonary tuberculosis. *Am J Respir Crit Care Med,* 168**,** 185-91.

JONES, B. W., MEANS, T. K., HELDWEIN, K. A., KEEN, M. A., HILL, P. J., BELISLE, J. T. & FENTON, M. J. 2001. Different Toll-like receptor agonists induce distinct macrophage responses. *J Leukoc Biol,* 69**,** 1036-44.

JORDAO, L., BLECK, C. K., MAYORGA, L., GRIFFITHS, G. & ANES, E. 2008. On the killing of mycobacteria by macrophages. *Cell Microbiol,* 10**,** 529-48.

JOUANGUY, E., ALTARE, F., LAMHAMEDI, S., REVY, P., EMILE, J. F., NEWPORT, M., LEVIN, M., BLANCHE, S., SEBOUN, E., FISCHER, A. & CASANOVA, J. L. 1996. Interferon-gamma-receptor deficiency in an infant with fatal bacille Calmette-Guerin infection. *N Engl J Med,* 335**,** 1956-61.

JUAREZ, E., CARRANZA, C., HERNANDEZ-SANCHEZ, F., LEON-CONTRERAS, J. C., HERNANDEZ-PANDO, R., ESCOBEDO, D., TORRES, M. & SADA, E. 2012. NOD2 enhances the innate response of alveolar macrophages to *Mycobacterium tuberculosis* in humans. *Eur J Immunol,* 42**,** 880-9.

JUFFERMANS, N. P., FLORQUIN, S., CAMOGLIO, L., VERBON, A., KOLK, A. H., SPEELMAN, P., VAN DEVENTER, S. J. & VAN DER POLL, T. 2000. Interleukin-1 signaling is essential for host defense during murine pulmonary tuberculosis. *J Infect Dis,* 182**,** 902-8.

JUFFERMANS, N. P., VERBON, A., VAN DEVENTER, S. J., VAN DEUTEKOM, H., BELISLE, J. T., ELLIS, M. E., SPEELMAN, P. & VAN DER POLL, T. 1999. Elevated chemokine concentrations in sera of human immunodeficiency virus (HIV)-seropositive and HIV-seronegative patients with tuberculosis: a possible role for mycobacterial lipoarabinomannan. *Infect Immun,* 67**,** 4295-7.

JULLIEN, D., SIELING, P. A., UYEMURA, K., MAR, N. D., REA, T. H. & MODLIN, R. L. 1997. IL-15, an immunomodulator of T cell responses in intracellular infection. *J Immunol,* 158**,** 800-6.

JUNG, Y. J., LACOURSE, R., RYAN, L. & NORTH, R. J. 2002. Evidence inconsistent with a negative influence of T helper 2 cells on protection afforded by a dominant T helper 1 response against *Mycobacterium tuberculosis* lung infection in mice. *Infect Immun,* 70**,** 6436-43.

JUNQUEIRA-KIPNIS, A. P., KIPNIS, A., JAMIESON, A., JUARRERO, M. G., DIEFENBACH, A., RAULET, D. H., TURNER, J. & ORME, I. M. 2003. NK cells respond to pulmonary infection with *Mycobacterium tuberculosis*, but play a minimal role in protection. *J Immunol,* 171**,** 6039-45.

KADOWAKI, T., YAMAUCHI, T., KUBOTA, N., HARA, K., UEKI, K. & TOBE, K. 2006. Adiponectin and adiponectin receptors in insulin resistance, diabetes, and the metabolic syndrome. *J Clin Invest,* 116**,** 1784-92.

KAHN, S. E., COOPER, M. E. & DEL PRATO, S. 2014. Pathophysiology and treatment of type 2 diabetes: perspectives on the past, present, and future. *Lancet,* 383**,** 1068-83.

KAHNERT, A., HOPKEN, U. E., STEIN, M., BANDERMANN, S., LIPP, M. & KAUFMANN, S. H. 2007. *Mycobacterium tuberculosis* triggers formation of lymphoid structure in murine lungs. *J Infect Dis,* 195**,** 46-54.

KAN-SUTTON, C., JAGANNATH, C. & HUNTER, R. L., JR. 2009. Trehalose 6,6'-dimycolate on the surface of *Mycobacterium tuberculosis* modulates surface marker expression for antigen presentation and costimulation in murine macrophages. *Microbes Infect,* 11**,** 40-8.

KANETSUNA, Y., TAKAHASHI, K., NAGATA, M., GANNON, M. A., BREYER, M. D., HARRIS, R. C. & TAKAHASHI, T. 2007. Deficiency of endothelial nitric-oxide synthase confers susceptibility to diabetic nephropathy in nephropathy-resistant inbred mice. *Am J Pathol,* 170**,** 1473-84.

KANG, B. K. & SCHLESINGER, L. S. 1998. Characterization of mannose receptor-dependent phagocytosis mediated by *Mycobacterium tuberculosis* lipoarabinomannan. *Infect Immun,* 66**,** 2769-77.

KANG, P. B., AZAD, A. K., TORRELLES, J. B., KAUFMAN, T. M., BEHARKA, A., TIBESAR, E., DESJARDIN, L. E. & SCHLESINGER, L. S. 2005. The human macrophage mannose receptor directs *Mycobacterium tuberculosis* lipoarabinomannan-mediated phagosome biogenesis. *J Exp Med,* 202**,** 987-99.

KAPUR, A. & HARRIES, A. D. 2013. The double burden of diabetes and tuberculosis - Public health implications. *Diabetes Res Clin Pract*.

KARAKOUSIS, P. C., BISHAI, W. R. & DORMAN, S. E. 2004. *Mycobacterium tuberculosis* cell envelope lipids and the host immune response. *Cell Microbiol,* 6**,** 105-16.

KASAHARA, K., TOBE, T., TOMITA, M., MUKAIDA, N., SHAO-BO, S., MATSUSHIMA, K., YOSHIDA, T., SUGIHARA, S. & KOBAYASHI, K. 1994. Selective expression of monocyte chemotactic and activating factor/monocyte chemoattractant protein 1 in human blood monocytes by *Mycobacterium tuberculosis*. *J Infect Dis,* 170**,** 1238-47.

KASSIM, I., RAY, CG., 2004. Sherris Medical Microbiology (4th ed.). McGraw Hill. ISBN 0-8385-8529-9.

KATZ, A., CARAMORI, M. L., SISSON-ROSS, S., GROPPOLI, T., BASGEN, J. M. & MAUER, M. 2002. An increase in the cell component of the cortical interstitium antedates interstitial fibrosis in type 1 diabetic patients. *Kidney Int,* 61**,** 2058-66.

KAUFMANN, S. H. 1991. Role of T-cell subsets in bacterial infections. *Curr Opin Immunol,* 3**,** 465-70.

KAUFMANN, S. H. 2004. New issues in tuberculosis. *Ann Rheum Dis,* 63 Suppl 2**,** ii50-ii56.

KAUFMANN, S. H. 2012. Tuberculosis vaccine development: strength lies in tenacity. *Trends Immunol,* 33**,** 373-9.

KAUFMANN, S. H. & PARIDA, S. K. 2008. Tuberculosis in Africa: learning from pathogenesis for biomarker identification. *Cell Host Microbe,* 4**,** 219-28.

KAWASAKI, F., MATSUDA, M., KANDA, Y., INOUE, H. & KAKU, K. 2005. Structural and functional analysis of pancreatic islets preserved by pioglitazone in db/db mice. *Am J Physiol Endocrinol Metab,* 288**,** E510-8.

KEANE, J. 2005. TNF-blocking agents and tuberculosis: new drugs illuminate an old topic. *Rheumatology (Oxford),* 44**,** 714-20.

KEANE, J., REMOLD, H. G. & KORNFELD, H. 2000. Virulent *Mycobacterium tuberculosis* strains evade apoptosis of infected alveolar macrophages. *J Immunol,* 164**,** 2016-20.

KEANE, J., SHURTLEFF, B. & KORNFELD, H. 2002. TNF-dependent BALB/c murine macrophage apoptosis following *Mycobacterium tuberculosis* infection inhibits bacillary growth in an IFNgamma independent manner. *Tuberculosis (Edinb),* 82.

KENNEDY, M. K. & PARK, L. S. 1996. Characterization of interleukin-15 (IL-15) and the IL-15 receptor complex. *J Clin Immunol,* 16**,** 134-43.

KEWCHAROENWONG, C., RINCHAI, D., UTISPAN, K., SUWANNASAEN, D., BANCROFT, G. J., ATO, M. & LERTMEMONGKOLCHAI, G. 2013. Glibenclamide reduces pro-inflammatory cytokine production by neutrophils of diabetes patients in response to bacterial infection. *Sci Rep,* 3**,** 3363.

KIM, S. J., HONG, Y. P., LEW, W. J., YANG, S. C. & LEE, E. G. 1995. Incidence of pulmonary tuberculosis among diabetics. *Tuber Lung Dis,* 76**,** 529-33.

KINDLER, V., SAPPINO, A. P., GRAU, G. E., PIGUET, P. F. & VASSALLI, P. 1989. The inducing role of tumor necrosis factor in the development of bactericidal granulomas during BCG infection. *Cell,* 56**,** 731-40.

KING, A. & BOWE, J. 2016. Animal models for diabetes: Understanding the pathogenesis and finding new treatments. *Biochem Pharmacol,* 99**,** 1-10.

KING, H., AUBERT, R. E. & HERMAN, W. H. 1998. Global burden of diabetes, 1995-2025: prevalence, numerical estimates, and projections. *Diabetes Care,* 21**,** 1414-31.

KIPNIS, A., BASARABA, R. J., ORME, I. M. & COOPER, A. M. 2003. Role of chemokine ligand 2 in the protective response to early murine pulmonary tuberculosis. *Immunology,* 109**,** 547-51.

KLEINNIJENHUIS, J., JOOSTEN, L. A., VAN DE VEERDONK, F. L., SAVAGE, N., VAN CREVEL, R., KULLBERG, B. J., VAN DER VEN, A., OTTENHOFF, T. H., DINARELLO, C. A., VAN DER MEER, J. W. & NETEA, M. G. 2009. Transcriptional and inflammasome-mediated pathways for the induction of IL-1beta production by *Mycobacterium tuberculosis*. *Eur J Immunol,* 39**,** 1914-22.

KNECHEL, N. A. 2009. Tuberculosis: pathophysiology, clinical features, and diagnosis. *Crit Care Nurse,* 29**,** 34-43; quiz 44.

KNEKT, P., LAAKSONEN, M., MATTILA, C., HARKANEN, T., MARNIEMI, J., HELIOVAARA, M., RISSANEN, H., MONTONEN, J. & REUNANEN, A. 2008. Serum vitamin D and subsequent occurrence of type 2 diabetes. *Epidemiology,* 19**,** 666-71.

KNOWLER, W. C., SAAD, M. F., PETTITT, D. J., NELSON, R. G. & BENNETT, P. H. 1993. Determinants of diabetes mellitus in the Pima Indians. *Diabetes Care,* 16**,** 216-27.

KOPF, M., BROMBACHER, F., KOHLER, G., KIENZLE, G., WIDMANN, K. H., LEFRANG, K., HUMBORG, C., LEDERMANN, B. & SOLBACH, W. 1996. IL-4-deficient Balb/c mice resist infection with Leishmania major. *J Exp Med,* 184**,** 1127-36.

KORBEL, D. S., SCHNEIDER, B. E. & SCHAIBLE, U. E. 2008. Innate immunity in tuberculosis: myths and truth. *Microbes Infect,* 10**,** 995-1004.

KOYA, D., HANEDA, M., NAKAGAWA, H., ISSHIKI, K., SATO, H., MAEDA, S., SUGIMOTO, T., YASUDA, H., KASHIWAGI, A., WAYS, D. K., KING, G. L. & KIKKAWA, R. 2000. Amelioration of accelerated diabetic mesangial expansion by treatment with a PKC beta inhibitor in diabetic db/db mice, a rodent model for type 2 diabetes. *Faseb j,* 14**,** 439-47.

KRODER, G., BOSSENMAIER, B., KELLERER, M., CAPP, E., STOYANOV, B., MUHLHOFER, A., BERTI, L., HORIKOSHI, H., ULLRICH, A. & HARING, H. 1996. Tumor necrosis factor-alpha- and hyperglycemia-induced insulin resistance. Evidence for different mechanisms and different effects on insulin signaling. *J Clin Invest,* 97**,** 1471-7.

KUBICA, G. 1976. *Mycobacterium tuberculosis* culture revealing organism's colonial morphology. Centre for Disease control and Prevention, Public Health Image Library (PHIL) Available at : http://phil.cdc.gov/phil/details.asp?pid=4428.

KUKI, S., IMANISHI, T., KOBAYASHI, K., MATSUO, Y., OBANA, M. & AKASAKA, T. 2006. Hyperglycemia accelerated endothelial progenitor cell senescence via the activation of p38 mitogen-activated protein kinase. *Circ J,* 70**,** 1076-81.

KUMAR NATHELLA, P. & BABU, S. 2017. Influence of diabetes mellitus on immunity to human tuberculosis. *Immunology,* 152**,** 13-24.

KUMAR, N. P., GEORGE, P. J., KUMARAN, P., DOLLA, C. K., NUTMAN, T. B. & BABU, S. 2014. Diminished systemic and antigen-specific type 1, type 17, and other proinflammatory cytokines in diabetic and prediabetic individuals with latent *Mycobacterium tuberculosis* infection. *J Infect Dis,* 210**,** 1670-8.

KUMAR, N. P., SRIDHAR, R., BANUREKHA, V. V., JAWAHAR, M. S., FAY, M. P., NUTMAN, T. B. & BABU, S. 2013. Type 2 diabetes mellitus coincident with

pulmonary tuberculosis is associated with heightened systemic type 1, type 17, and other proinflammatory cytokines. *Ann Am Thorac Soc,* 10**,** 441-9.

KUMAR, V. A., A.K.; FAUSTO, N; MITCHELL, R. N., 2007. Robbins Basic Pathology (8th Edn.). Saunders Elsevier. pp. 516-522

KUO, M. C., LIN, S. H., LIN, C. H., MAO, I. C., CHANG, S. J. & HSIEH, M. C. 2013. Type 2 diabetes: an independent risk factor for tuberculosis: a nationwide population-based study. *PLoS One,* 8**,** e78924.

KUPZ, A., ZEDLER, U., STABER, M., PERDOMO, C., DORHOI, A., BROSCH, R. & KAUFMANN, S. H. 2016. ESAT-6-dependent cytosolic pattern recognition drives noncognate tuberculosis control in vivo. *J Clin Invest,* 126**,** 2109-22.

KURSAR, M., KOCH, M., MITTRUCKER, H. W., NOUAILLES, G., BONHAGEN, K., KAMRADT, T. & KAUFMANN, S. H. 2007. Cutting Edge: Regulatory T cells prevent efficient clearance of *Mycobacterium tuberculosis*. *J Immunol,* 178**,** 2661-5.

LACHMANDAS, E., VRIELING, F., WILSON, L. G., JOOSTEN, S. A., NETEA, M. G., OTTENHOFF, T. H. & VAN CREVEL, R. 2015. The effect of hyperglycaemia on in vitro cytokine production and macrophage infection with *Mycobacterium tuberculosis*. *PLoS One,* 10**,** e0117941.

LADEL, C. H., BLUM, C., DREHER, A., REIFENBERG, K., KOPF, M. & KAUFMANN, S. H. E. 1997a. Lethal tuberculosis in interleukin-6-deficient mutant mice. *Infect Immun,* 65.

LADEL, C. H., SZALAY, G., RIEDEL, D. & KAUFMANN, S. H. 1997b. Interleukin-12 secretion by *Mycobacterium tuberculosis*-infected macrophages. *Infect Immun,* 65**,** 1936-8.

LAGRANDERIE, M. R., BALAZUC, A. M., DERIAUD, E., LECLERC, C. D. & GHEORGHIU, M. 1996. Comparison of immune responses of mice immunized with five different *Mycobacterium bovis* BCG vaccine strains. *Infect Immun,* 64**,** 1-9.

LALVANI, A., PATHAN, A. A., MCSHANE, H., WILKINSON, R. J., LATIF, M., CONLON, C. P., PASVOL, G. & HILL, A. V. 2001. Rapid detection of *Mycobacterium tuberculosis* infection by enumeration of antigen-specific T cells. *Am J Respir Crit Care Med,* 163**,** 824-8.

LARSEN, M. H., BIERMANN, K. & JACOBS, W. R., JR. 2007. Laboratory maintenance of *Mycobacterium tuberculosis*. *Curr Protoc Microbiol,* Chapter 10**,** Unit 10A.1.

LAVINE, R. L., VOYLES, N., PERRINO, P. V. & RECANT, L. 1977. Functional abnormalities of islets of Langerhans of obese hyperglycemic mouse. *Am J Physiol,* 233**,** E86-90.

LAWN, S. D. & ZUMLA, A. I. 2011. Tuberculosis. *Lancet,* 378**,** 57-72.

LE CABEC, V., EMORINE, L. J., TOESCA, I., COUGOULE, C. & MARIDONNEAU-PARINI, I. 2005. The human macrophage mannose receptor is not a professional phagocytic receptor. *J Leukoc Biol,* 77**,** 934-43.

LEAL, I. S., FLORIDO, M., ANDERSEN, P. & APPELBERG, R. 2001. Interleukin-6 regulates the phenotype of the immune response to a tuberculosis subunit vaccine. *Immunology,* 103.

LEBOVITZ, H. E. 1999. Type 2 diabetes: an overview. *Clin Chem,* 45**,** 1339-45.

LECUBE, A., PACHON, G., PETRIZ, J., HERNANDEZ, C. & SIMO, R. 2011. Phagocytic activity is impaired in type 2 diabetes mellitus and increases after metabolic improvement. *PLoS One,* 6**,** e23366.

LEE, E. T., HOWARD, B. V., SAVAGE, P. J., COWAN, L. D., FABSITZ, R. R., OOPIK, A. J., YEH, J., GO, O., ROBBINS, D. C. & WELTY, T. K. 1995. Diabetes and impaired

glucose tolerance in three American Indian populations aged 45-74 years. The Strong Heart Study. *Diabetes Care,* 18**,** 599-610.

LEE, I. M., SHIROMA, E. J., LOBELO, F., PUSKA, P., BLAIR, S. N. & KATZMARZYK, P. T. 2012. Effect of physical inactivity on major non-communicable diseases worldwide: an analysis of burden of disease and life expectancy. *Lancet,* 380**,** 219-29.

LEE, J. S., SONG, C. H., LIM, J. H., LEE, K. S., KIM, H. J., PARK, J. K., PAIK, T. H., JUNG, S. S. & JO, E. K. 2003. Monocyte chemotactic protein-1 production in patients with active pulmonary tuberculosis and tuberculous pleurisy. *Inflamm Res,* 52**,** 297-304.

LEE, Y., HIROSE, H., OHNEDA, M., JOHNSON, J. H., MCGARRY, J. D. & UNGER, R. H. 1994. Beta-cell lipotoxicity in the pathogenesis of non-insulin-dependent diabetes mellitus of obese rats: impairment in adipocyte-beta-cell relationships. *Proc Natl Acad Sci U S A,* 91**,** 10878-82.

LEGESSE, M., AMENI, G., MEDHIN, G., MAMO, G., FRANKEN, K. L., OTTENHOFF, T. H., BJUNE, G. & ABEBE, F. 2013. IgA response to ESAT-6/CFP-10 and Rv2031 antigens varies in patients with culture-confirmed pulmonary tuberculosis, healthy *Mycobacterium tuberculosis*-infected and non-infected individuals in a tuberculosis endemic setting, Ethiopia. *Scand J Immunol,* 78**,** 266-74.

LEITER, E. H. & REIFSNYDER, P. C. 2004. Differential levels of diabetogenic stress in two new mouse models of obesity and type 2 diabetes. *Diabetes,* 53 Suppl 1**,** S4-11.

LEROUX-ROELS, I., FORGUS, S., DE BOEVER, F., CLEMENT, F., DEMOITIE, M. A., METTENS, P., MORIS, P., LEDENT, E., LEROUX-ROELS, G. & OFORI-ANYINAM, O. 2013. Improved CD4(+) T cell responses to *Mycobacterium tuberculosis* in PPD-negative adults by M72/AS01 as compared to the M72/AS02 and Mtb72F/AS02 tuberculosis candidate vaccine formulations: a randomized trial. *Vaccine,* 31**,** 2196-206.

LESSING, M. P. & WALKER, M. M. 1993. Fatal pulmonary infection due to *Mycobacterium fortuitum*. *J Clin Pathol,* 46**,** 271-2.

LEUNG, C. C., LAM, T. H., CHAN, W. M., YEW, W. W., HO, K. S., LEUNG, G. M., LAW, W. S., TAM, C. M., CHAN, C. K. & CHANG, K. C. 2008. Diabetic control and risk of tuberculosis: a cohort study. *Am J Epidemiol,* 167**,** 1486-94.

LEUTHOLTZ, B. C. & RIPOLL, I. 2011. Exercise and disease management, 2nd Edn. Boca Raton: CRC Press. p. 25. ISBN 978-1-4398-2759-8.

LEWINSOHN, D. M., ALDERSON, M. R., BRIDEN, A. L., RIDDELL, S. R., REED, S. G. & GRABSTEIN, K. H. 1998. Characterization of human CD8+ T cells reactive with *Mycobacterium tuberculosis*-infected antigen-presenting cells. *J Exp Med,* 187**,** 1633-40.

LEWIS, G. F. 2013. Devastating metabolic consequences of a life of plenty: focus on the dyslipidemia of overnutrition. *Clin Invest Med,* 36**,** E242-7.

LI, S., SHIN, H. J., DING, E. L. & VAN DAM, R. M. 2009. Adiponectin levels and risk of type 2 diabetes: a systematic review and meta-analysis. *Jama,* 302**,** 179-88.

LIFSCHITZ, M. 1965. The value of the tuberculin skin test as a screening test for tuberculosis among BCG-vaccinated children. *Pediatrics,* 36**,** 624-7.

LIN, Y., GONG, J., ZHANG, M., XUE, W. & BARNES, P. F. 1998. Production of monocyte chemoattractant protein 1 in tuberculosis patients. *Infect Immun,* 66**,** 2319-22.

LINDOSO, A. A., WALDMAN, E. A., KOMATSU, N. K., FIGUEIREDO, S. M., TANIGUCHI, M. & RODRIGUES, L. C. 2008. Profile of tuberculosis patients progressing to death, city of Sao Paulo, Brazil, 2002. *Rev Saude Publica,* 42**,** 805-12.

LING, D. I., ZWERLING, A. A. & PAI, M. 2008. GenoType MTBDR assays for the diagnosis of multidrug-resistant tuberculosis: a meta-analysis. *Eur Respir J,* 32**,** 1165-74.

LIU, B. F., MIYATA, S., KOJIMA, H., URIUHARA, A., KUSUNOKI, H., SUZUKI, K. & KASUGA, M. 1999. Low phagocytic activity of resident peritoneal macrophages in diabetic mice: relevance to the formation of advanced glycation end products. *Diabetes,* 48**,** 2074-82.

LIU, H. F., ZHANG, H. J., HU, Q. X., LIU, X. Y., WANG, Z. Q., FAN, J. Y., ZHAN, M. & CHEN, F. L. 2012. Altered polarization, morphology, and impaired innate immunity germane to resident peritoneal macrophages in mice with long-term type 2 diabetes. *J Biomed Biotechnol,* 2012**,** 867023.

LIU, L. S., SPELLEKEN, M., ROHRIG, K., HAUNER, H. & ECKEL, J. 1998. Tumor necrosis factor-alpha acutely inhibits insulin signaling in human adipocytes: implication of the p80 tumor necrosis factor receptor. *Diabetes,* 47**,** 515-22.

LONG, R., O'CONNOR, R., PALAYEW, M., HERSHFIELD, E. & MANFREDA, J. 1997. Disseminated tuberculosis with and without a miliary pattern on chest radiograph: a clinical-pathologic-radiologic correlation. *Int J Tuberc Lung Dis,* 1**,** 52-8.

LOSKUTOFF, D. J., FUJISAWA, K. & SAMAD, F. 2000. The fat mouse. A powerful genetic model to study hemostatic gene expression in obesity/NIDDM. *Ann N Y Acad Sci,* 902**,** 272-81; discussion 281-2.

LU, B., RUTLEDGE, B. J., GU, L., FIORILLO, J., LUKACS, N. W., KUNKEL, S. L., NORTH, R., GERARD, C. & ROLLINS, B. J. 1998. Abnormalities in monocyte recruitment and cytokine expression in monocyte chemoattractant protein 1-deficient mice. *J Exp Med,* 187**,** 601-8.

LUCEY, D. R., CLERICI, M. & SHEARER, G. M. 1996. Type 1 and type 2 cytokine dysregulation in human infectious, neoplastic, and inflammatory diseases. *Clin Microbiol Rev,* 9**,** 532-62.

LUDWIG, D. S., MAJZOUB, J. A., AL-ZAHRANI, A., DALLAL, G. E., BLANCO, I. & ROBERTS, S. B. 1999. High glycemic index foods, overeating, and obesity. *Pediatrics,* 103**,** E26.

LUKACS, N. W., ADDISON, C. L., GAULDIE, J., GRAHAM, F., SIMPSON, K., STRIETER, R. M., WARMINGTON, K., CHENSUE, S. W. & KUNKEL, S. L. 1997. Transgene-induced production of IL-4 alters the development and collagen expression of T helper cell 1-type pulmonary granulomas. *J Immunol,* 158**,** 4478-84.

MA, H., LIU, G., DING, W., WU, Y., CAI, L. & ZHAO, Y. 2008. Diabetes-induced alteration of F4/80+ macrophages: a study in mice with streptozotocin-induced diabetes for a long term. *J Mol Med (Berl),* 86**,** 391-400.

MACK, U., MIGLIORI, G. B., SESTER, M., RIEDER, H. L., EHLERS, S., GOLETTI, D., BOSSINK, A., MAGDORF, K., HOLSCHER, C., KAMPMANN, B., AREND, S. M., DETJEN, A., BOTHAMLEY, G., ZELLWEGER, J. P., MILBURN, H., DIEL, R., RAVN, P., COBELENS, F., CARDONA, P. J., KAN, B., SOLOVIC, I., DUARTE, R. & CIRILLO, D. M. 2009. LTBI: latent tuberculosis infection or lasting immune responses to M. tuberculosis? A TBNET consensus statement. *Eur Respir J,* 33**,** 956-73.

MADIGAN, M., MARTINKO, J., PARKER, J., 2002. Brock Biology of Microorganisms (10th ed). Pearson Education, 2002.

MAEDA, N., NIGOU, J., HERRMANN, J. L., JACKSON, M., AMARA, A., LAGRANGE, P. H., PUZO, G., GICQUEL, B. & NEYROLLES, O. 2003. The cell surface receptor DC-SIGN discriminates between Mycobacterium species through selective recognition of the mannose caps on lipoarabinomannan. *J Biol Chem,* 278**,** 5513-6.

MAEURER, M. J., TRINDER, P., HOMMEL, G., WALTER, W., FREITAG, K., ATKINS, D. & STORKEL, S. 2000. Interleukin-7 or interleukin-15 enhances survival of *Mycobacterium tuberculosis*-infected mice. *Infect Immun,* 68**,** 2962-70.

MAGLIONE, P. J. & CHAN, J. 2009. How B cells shape the immune response against *Mycobacterium tuberculosis*. *Eur J Immunol,* 39**,** 676-86.

MAGNUS, K. & EDWARDS, L. B. 1955. The effect of repeated tuberculin testing on post-vaccination allergy; a preliminary note. *Lancet,* 269**,** 643-4.

MAHAIRAS, G. G., SABO, P. J., HICKEY, M. J., SINGH, D. C. & STOVER, C. K. 1996. Molecular analysis of genetic differences between *Mycobacterium bovis* BCG and virulent M. bovis. *J Bacteriol,* 178**,** 1274-82.

MALIK, V. S., POPKIN, B. M., BRAY, G. A., DESPRES, J. P. & HU, F. B. 2010. Sugar-sweetened beverages, obesity, type 2 diabetes mellitus, and cardiovascular disease risk. *Circulation,* 121**,** 1356-64.

MANSILLA BERMEJO, M. J., SANZ GIL, M. J., MORALEDA VELASCO, P., ALVAREZ PRADO, A., CARBAYO GARCIA, J. J. & MATA GUIJARRO, F. 1995. Tuberculin test in diabetic patients in a health center. *Aten Primaria,* 16**,** 154-7.

MANTZOROS, C. S., LI, T., MANSON, J. E., MEIGS, J. B. & HU, F. B. 2005. Circulating adiponectin levels are associated with better glycemic control, more favorable lipid profile, and reduced inflammation in women with type 2 diabetes. *J Clin Endocrinol Metab,* 90**,** 4542-8.

MARCHETTI, P., DEL GUERRA, S., MARSELLI, L., LUPI, R., MASINI, M., POLLERA, M., BUGLIANI, M., BOGGI, U., VISTOLI, F., MOSCA, F. & DEL PRATO, S. 2004. Pancreatic islets from type 2 diabetic patients have functional defects and increased apoptosis that are ameliorated by metformin. *J Clin Endocrinol Metab,* 89**,** 5535-41.

MARHOFFER, W., STEIN, M., MAESER, E. & FEDERLIN, K. 1992. Impairment of polymorphonuclear leukocyte function and metabolic control of diabetes. *Diabetes Care,* 15**,** 256-60.

MARKOWITZ, N., HANSEN, N. I., WILCOSKY, T. C., HOPEWELL, P. C., GLASSROTH, J., KVALE, P. A., MANGURA, B. T., OSMOND, D., WALLACE, J. M., ROSEN, M. J. & REICHMAN, L. B. 1993. Tuberculin and anergy testing in HIV-seropositive and HIV-seronegative persons. Pulmonary Complications of HIV Infection Study Group. *Ann Intern Med,* 119**,** 185-93.

MARTENS, G. W., ARIKAN, M. C., LEE, J., REN, F., GREINER, D. & KORNFELD, H. 2007. Tuberculosis susceptibility of diabetic mice. *Am J Respir Cell Mol Biol,* 37**,** 518-24.

MARTINEAU, A. R., NEWTON, S. M., WILKINSON, K. A., KAMPMANN, B., HALL, B. M., NAWROLY, N., PACKE, G. E., DAVIDSON, R. N., GRIFFITHS, C. J. & WILKINSON, R. J. 2007. Neutrophil-mediated innate immune resistance to mycobacteria. *J Clin Invest,* 117**,** 1988-94.

MARTINEZ, A. N., MEHRA, S. & KAUSHAL, D. 2013. Role of interleukin 6 in innate immunity to *Mycobacterium tuberculosis* infection. *J Infect Dis,* 207**,** 1253-61.

MARTINEZ, F. O., HELMING, L. & GORDON, S. 2009. Alternative activation of macrophages: an immunologic functional perspective. *Annu Rev Immunol,* 27**,** 451-83.

MARTINEZ, N., KETHEESAN, N., WEST, K., VALLERSKOG, T. & KORNFELD, H. 2016. Impaired Recognition of *Mycobacterium tuberculosis* by Alveolar Macrophages From Diabetic Mice. *J Infect Dis,* 214**,** 1629-1637.

MARTINEZ, N. & KORNFELD, H. 2014. Diabetes and immunity to tuberculosis. *Eur J Immunol,* 44**,** 617-26.

MATHEWS, C. E., BROWN, E. L., MARTINEZ, P. J., BAGARIA, U., NAHM, M. H., BURTON, R. L., FISHER-HOCH, S. P., MCCORMICK, J. B. & MIRZA, S. 2012. Impaired function of antibodies to pneumococcal surface protein A but not to capsular polysaccharide in Mexican American adults with type 2 diabetes mellitus. *Clin Vaccine Immunol,* 19**,** 1360-9.

MAUER, S. M., STEFFES, M. W. & BROWN, D. M. 1981. The kidney in diabetes. *Am J Med,* 70**,** 603-12.

MBOUSSA, J., MONABEKA, H., KOMBO, M., YOKOLO, D., YOKA-MBIO, A. & YALA, F. 2003. Course of pulmonary tuberculosis in diabetics. *Rev Pneumol Clin,* 59**,** 39-44.

MCCARTHY, M. I. 2010. Genomics, type 2 diabetes, and obesity. *N Engl J Med,* 363**,** 2339-50.

MCCARTY, D. & ZIMMET, P. 1994. Diabetes 1994 to 2010: Global Estimates and Projections. Melbourne: International Diabetes Institute. .

MCFADDEN, J. 1982. Encyclopedia of Microbiology. Vol. 3, copyright by American Press, Inc.

MCHUGH, T. D., NEWPORT, L. E. & GILLESPIE, S. H. 1997. IS6110 homologs are present in multiple copies in mycobacteria other than tuberculosis-causing mycobacteria. *J Clin Microbiol,* 35**,** 1769-71.

MCHUGH, T. D., POPE, C. F., LING, C. L., PATEL, S., BILLINGTON, O. J., GOSLING, R. D., LIPMAN, M. C. & GILLESPIE, S. H. 2004. Prospective evaluation of BDProbeTec strand displacement amplification (SDA) system for diagnosis of tuberculosis in non-respiratory and respiratory samples. *J Med Microbiol,* 53**,** 1215-9.

MCKENNA, K. & THOMPSON, C. 1997. Microalbuminuria: a marker to increased renal and cardiovascular risk in diabetes mellitus. *Scott Med J,* 42**,** 99-104.

MCNALLY, R. J., FELTBOWER, R. G., PARKER, L., BODANSKY, H. J., CAMPBELL, F. & MCKINNEY, P. A. 2006. Space-time clustering analyses of type 1 diabetes among 0- to 29-year-olds in Yorkshire, UK. *Diabetologia,* 49**,** 900-4.

MEANS, T. K., JONES, B. W., SCHROMM, A. B., SHURTLEFF, B. A., SMITH, J. A., KEANE, J., GOLENBOCK, D. T., VOGEL, S. N. & FENTON, M. J. 2001. Differential effects of a Toll-like receptor antagonist on *Mycobacterium tuberculosis*-induced macrophage responses. *J Immunol,* 166**,** 4074-82.

MEDZHITOV, R., PRESTON-HURLBURT, P. & JANEWAY, C. A., JR. 1997. A human homologue of the Drosophila Toll protein signals activation of adaptive immunity. *Nature,* 388**,** 394-7.

MEIGS, J. B., HU, F. B., RIFAI, N. & MANSON, J. E. 2004. Biomarkers of endothelial dysfunction and risk of type 2 diabetes mellitus. *Jama,* 291**,** 1978-86.

MEIKLE, A. W., LIU, X. H., TAYLOR, G. N. & STRINGHAM, J. D. 1988. Nicotine and cotinine effects on 3 alpha hydroxysteroid dehydrogenase in canine prostate. *Life Sci,* 43**,** 1845-50.

MENZIES, D., PAI, M. & COMSTOCK, G. 2007. Meta-analysis: new tests for the diagnosis of latent tuberculosis infection: areas of uncertainty and recommendations for research. *Ann Intern Med,* 146**,** 340-54.

MINGES, K. E., ZIMMET, P., MAGLIANO, D. J., DUNSTAN, D. W., BROWN, A. & SHAW, J. E. 2011. Diabetes prevalence and determinants in Indigenous Australian populations: A systematic review. *Diabetes Res Clin Pract,* 93**,** 139-49.

MIZUNO, K., CHIKAMATSU, K., AONO, A., AZUMA, Y., YAMADA, H. & MITARAI, S. 2009. Clinical evaluation of acid-fast smear examination with light emitting diode fluorescent microscopy. *Kekkaku,* 84**,** 627-9.

MOHAN, S., REDDICK, R. L., MUSI, N., HORN, D. A., YAN, B., PRIHODA, T. J., NATARAJAN, M. & ABBOUD-WERNER, S. L. 2008. Diabetic eNOS knockout mice develop distinct macro- and microvascular complications. *Lab Invest,* 88**,** 515-28.

MOHAN, V. P., SCANGA, C. A., YU, K., SCOTT, H. M., TANAKA, K. E., TSANG, E., TSAI, M. M., FLYNN, J. L. & CHAN, J. 2001. Effects of tumor necrosis factor alpha on host immune response in chronic persistent tuberculosis: possible role for limiting pathology. *Infect Immun,* 69**,** 1847-55.

MOLLOY, A., LAOCHUMROONVORAPONG, P. & KAPLAN, G. 1994. Apoptosis, but not necrosis, of infected monocytes is coupled with killing of intracellular bacillus Calmette-Guerin. *J Exp Med,* 180.

MONTAGNANI, C., CHIAPPINI, E., GALLI, L. & DE MARTINO, M. 2014. Vaccine against tuberculosis: what's new? *BMC Infect Dis,* 14 Suppl 1**,** S2.

MONTAGUE, C. T. & O'RAHILLY, S. 2000. The perils of portliness: causes and consequences of visceral adiposity. *Diabetes,* 49**,** 883-8.

MORI, M. A., LEONARDSON, G. & WELTY, T. K. 1992. The benefits of isoniazid chemoprophylaxis and risk factors for tuberculosis among Oglala Sioux Indians. *Arch Intern Med,* 152**,** 547-50.

MORIOKA, T., ASILMAZ, E., HU, J., DISHINGER, J. F., KURPAD, A. J., ELIAS, C. F., LI, H., ELMQUIST, J. K., KENNEDY, R. T. & KULKARNI, R. N. 2007. Disruption of leptin receptor expression in the pancreas directly affects beta cell growth and function in mice. *J Clin Invest,* 117**,** 2860-8.

MORRIS, J., WILLIAMS, N., RUSH, C., GOVAN, B., SANGLA, K., NORTON, R. & KETHEESAN, N. 2012. Burkholderia pseudomallei triggers altered inflammatory profiles in a whole-blood model of type 2 diabetes-melioidosis comorbidity. *Infect Immun,* 80**,** 2089-99.

MORRIS, J. L., BRIDSON, T. L., ALIM, M. A., RUSH, C. M., RUDD, D. M., GOVAN, B. L. & KETHEESAN, N. 2016. Development of a diet-induced murine model of diabetes featuring cardinal metabolic and pathophysiological abnormalities of type 2 diabetes. *Biol Open,* 5**,** 1149-62.

MORSY, A. M., ZAHER, H. H., HASSAN, M. H. & SHOUMAN, A. 2003. Predictors of treatment failure among tuberculosis patients under DOTS strategy in Egypt. *East Mediterr Health J,* 9**,** 689-701.

MOVASSAT, J., SAULNIER, C., SERRADAS, P. & PORTHA, B. 1997. Impaired development of pancreatic beta-cell mass is a primary event during the progression to diabetes in the GK rat. *Diabetologia,* 40**,** 916-25.

MOWAT, A. & BAUM, J. 1971. Chemotaxis of polymorphonuclear leukocytes from patients with diabetes mellitus. *N Engl J Med,* 284**,** 621-7.

MUGUSI, F., SWAI, A. B., ALBERTI, K. G. & MCLARTY, D. G. 1990. Increased prevalence of diabetes mellitus in patients with pulmonary tuberculosis in Tanzania. *Tubercle,* 71**,** 271-6.

MULLARKEY, C. J., EDELSTEIN, D. & BROWNLEE, M. 1990. Free radical generation by early glycation products: a mechanism for accelerated atherogenesis in diabetes. *Biochem Biophys Res Commun,* 173**,** 932-9.

MULLER, W. A., FALOONA, G. R., AGUILAR-PARADA, E. & UNGER, R. H. 1970. Abnormal alpha-cell function in diabetes. Response to carbohydrate and protein ingestion. *N Engl J Med,* 283**,** 109-15.

MUNOZ-ELIAS, E. J., TIMM, J., BOTHA, T., CHAN, W. T., GOMEZ, J. E. & MCKINNEY, J. D. 2005. Replication dynamics of *Mycobacterium tuberculosis* in chronically infected mice. *Infect Immun,* 73**,** 546-51.

MURRAY, P. J. & YOUNG, R. A. 1999. Increased antimycobacterial immunity in interleukin-10-deficient mice. *Infect Immun,* 67.

MUSILLI, C., PACCOSI, S., PALA, L., GERLINI, G., LEDDA, F., MUGELLI, A., ROTELLA, C. M. & PARENTI, A. 2011. Characterization of circulating and monocyte-derived dendritic cells in obese and diabetic patients. *Mol Immunol,* 49**,** 234-8.

MUYOYETA, M., SCHAAP, J. A., DE HAAS, P., MWANZA, W., MUVWIMI, M. W., GODFREY-FAUSSETT, P. & AYLES, H. 2009. Comparison of four culture systems for *Mycobacterium tuberculosis* in the Zambian National Reference Laboratory. *Int J Tuberc Lung Dis,* 13**,** 460-5.

NAGABHUSHANAM, V., SOLACHE, A., TING, L. M., ESCARON, C. J., ZHANG, J. Y. & ERNST, J. D. 2003. Innate inhibition of adaptive immunity: *Mycobacterium tuberculosis*-induced IL-6 inhibits macrophage responses to IFN-gamma. *J Immunol,* 171**,** 4750-7.

NAGATA, M., SUZUKI, W., IIZUKA, S., TABUCHI, M., MARUYAMA, H., TAKEDA, S., ABURADA, M. & MIYAMOTO, K. 2006. Type 2 diabetes mellitus in obese mouse model induced by monosodium glutamate. *Exp Anim,* 55**,** 109-15.

NATARAJAN, K., KUNDU, M., SHARMA, P. & BASU, J. 2011. Innate immune responses to M. tuberculosis infection. *Tuberculosis (Edinb),* 91**,** 427-31.

NATIONAL COMMITTEE FOR CLINICAL LABORATORY STANDARDS. 2002. Susceptibility testing of mycobacteria, nocardia, and other aerobic actinomycetes. Tentative standards, 2nd Edn. M24-T2, Wayne, PA, USA.

NATIONAL GLYCOHEMOGLOBIN STANDARDIZATION PROGRAM. 2010. HbA1c and eAG". www.ngsp.org. Retrieved 2016-02-24.

NATIONAL RESEARCH COUNCIL SUBCOMMITTEE ON LABORATORY ANIMAL NUTRITION. 1995. Nutrient Requirements of Laboratory Animals. 4th Rev Edn, 1995. Washington (DC): National Academies Press (US); 1995.

NG, M. C., LEE, S. C., KO, G. T., LI, J. K., SO, W. Y., HASHIM, Y., BARNETT, A. H., MACKAY, I. R., CRITCHLEY, J. A., COCKRAM, C. S. & CHAN, J. C. 2001. Familial early-onset type 2 diabetes in Chinese patients: obesity and genetics have more significant roles than autoimmunity. *Diabetes Care,* 24**,** 663-71.

NGAI, P., MCCORMICK, S., SMALL, C., ZHANG, X., ZGANIACZ, A., AOKI, N. & XING, Z. 2007. Gamma interferon responses of CD4 and CD8 T-cell subsets are quantitatively different and independent of each other during pulmonary *Mycobacterium bovis* BCG infection. *Infect Immun,* 75**,** 2244-52.

NIAZI, A. K. & KALRA, S. 2012. Diabetes and tuberculosis: a review of the role of optimal glycemic control. *J Diabetes Metab Disord,* 11**,** 28.

NICAS, M., NAZAROFF, W. W. & HUBBARD, A. 2005. Toward understanding the risk of secondary airborne infection: emission of respirable pathogens. *J Occup Environ Hyg,* 2**,** 143-54.

NIGOU, J., ZELLE-RIESER, C., GILLERON, M., THURNHER, M. & PUZO, G. 2001. Mannosylated lipoarabinomannans inhibit IL-12 production by human dendritic cells: evidence for a negative signal delivered through the mannose receptor. *J Immunol,* 166**,** 7477-85.

NIKOLIC, T., BUNK, M., DREXHAGE, H. A. & LEENEN, P. J. 2004. Bone marrow precursors of nonobese diabetic mice develop into defective macrophage-like dendritic cells in vitro. *J Immunol,* 173**,** 4342-51.

NISWENDER, K. D. & MAGNUSON, M. A. 2007. Obesity and the beta cell: lessons from leptin. *J Clin Invest,* 117**,** 2753-6.

NORTH, R. J. 1995. *Mycobacterium tuberculosis* is strikingly more virulent for mice when given via the respiratory than via the intravenous route. *J Infect Dis,* 172**,** 1550-3.

NORTH, R. J. 1998. Mice incapable of making IL-4 or IL-10 display normal resistance to infection with *Mycobacterium tuberculosis*. *Clin Exp Immunol,* 113**,** 55-8.

NORTH, R. J. & IZZO, A. A. 1993. Mycobacterial virulence. Virulent strains of *Mycobacteria tuberculosis* have faster in vivo doubling times and are better equipped to resist growth-inhibiting functions of macrophages in the presence and absence of specific immunity. *J Exp Med,* 177**,** 1723-33.

NORTH, R. J. & JUNG, Y. J. 2004. Immunity to tuberculosis. *Annu Rev Immunol,* 22.

NOSS, E. H., PAI, R. K., SELLATI, T. J., RADOLF, J. D., BELISLE, J., GOLENBOCK, D. T., BOOM, W. H. & HARDING, C. V. 2001. Toll-like receptor 2-dependent inhibition of macrophage class II MHC expression and antigen processing by 19-kDa lipoprotein of *Mycobacterium tuberculosis*. *J Immunol,* 167**,** 910-8.

O'BRIEN, D. P., FRIEDMAN, N. D., MCDONALD, A., CALLAN, P., HUGHES, A. & ATHAN, E. 2014. Clinical features and risk factors of oedematous *Mycobacterium ulcerans* lesions in an Australian population: beware cellulitis in an endemic area. *PLoS Negl Trop Dis,* 8**,** e2612.

O'GRADY, J., MAEURER, M., MWABA, P., KAPATA, N., BATES, M., HOELSCHER, M. & ZUMLA, A. 2011. New and improved diagnostics for detection of drug-resistant pulmonary tuberculosis. *Curr Opin Pulm Med,* 17**,** 134-41.

O'NEILL, L. A. & GREENE, C. 1998. Signal transduction pathways activated by the IL-1 receptor family: ancient signaling machinery in mammals, insects, and plants. *J Leukoc Biol,* 63**,** 650-7.

ODDO, M., RENNO, T., ATTINGER, A., BAKKER, T., MACDONALD, H. R. & MEYLAN, P. R. 1998. Fas ligand-induced apoptosis of infected human macrophages reduces the viability of intracellular *Mycobacterium tuberculosis*. *J Immunol,* 160**,** 5448-54.

OIL 2014. T Spot TB-Oxford Immunotec Limited (cited in 2014). Available from: http://www.oxfordimmunotec.com/products.htm.

OLEFSKY, J. M. & GLASS, C. K. 2010. Macrophages, inflammation, and insulin resistance. *Annu Rev Physiol,* 72**,** 219-46.

OLLEROS, M. L., GULER, R., VESIN, D., PARAPANOV, R., MARCHAL, G., MARTINEZ-SORIA, E., CORAZZA, N., PACHE, J. C., MUELLER, C. & GARCIA, I. 2005. Contribution of transmembrane tumor necrosis factor to host defense against *Mycobacterium bovis* bacillus Calmette-guerin and *Mycobacterium tuberculosis* infections. *Am J Pathol,* 166**,** 1109-20.

OLMOS, P., DONOSO, J., ROJAS, N., LANDEROS, P., SCHURMANN, R., RETAMAL, G., MEZA, M. & MARTINEZ, C. 1989. [Tuberculosis and diabetes mellitus: a longitudinal-retrospective study in a teaching hospital]. *Rev Med Chil,* 117**,** 979-83.

OLOKOBA, A. B., OBATERU, O. A. & OLOKOBA, L. B. 2012. Type 2 diabetes mellitus: a review of current trends. *Oman Med J,* 27**,** 269-73.

OPPMANN, B., LESLEY, R., BLOM, B., TIMANS, J. C., XU, Y., HUNTE, B., VEGA, F., YU, N., WANG, J., SINGH, K., ZONIN, F., VAISBERG, E., CHURAKOVA, T., LIU, M., GORMAN, D., WAGNER, J., ZURAWSKI, S., LIU, Y., ABRAMS, J. S., MOORE, K. W., RENNICK, D., DE WAAL-MALEFYT, R., HANNUM, C., BAZAN, J. F. & KASTELEIN, R. A. 2000. Novel p19 protein engages IL-12p40 to form a cytokine, IL-23, with biological activities similar as well as distinct from IL-12. *Immunity,* 13**,** 715-25.

ORDWAY, D. J. & ORME, I. M. 2011. Animal models of mycobacteria infection. *Curr Protoc Immunol,* Chapter 19**,** Unit19.5.

ORME, I. M. 2005. Mouse and guinea pig models for testing new tuberculosis vaccines. *Tuberculosis (Edinb),* 85**,** 13-7.

ORME, I. M. & COLLINS, F. M. 1983. Resistance of various strains of mycobacteria to killing by activated macrophages in vivo. *J Immunol,* 131**,** 1452-4.

ORME, I. M. & COOPER, A. M. 1999. Cytokine/chemokine cascades in immunity to tuberculosis. *Immunol Today,* 20**,** 307-12.

ORME, I. M. & ORDWAY, D. J. 2014. Host response to nontuberculous mycobacterial infections of current clinical importance. *Infect Immun,* 82**,** 3516-22.

ORME, I. M. & ROBERTS, A. D. 2001. Animal models of mycobacteria infection. *Curr Protoc Immunol,* Chapter 19**,** Unit 19.5.

OSCARSSON, P. N., SILWER, H. 1958. Incidence of pulmonary tuberculosis among diabetics. *Acta Med Scand,* 335.

OTHIENO, C., HIRSCH, C. S., HAMILTON, B. D., WILKINSON, K., ELLNER, J. J. & TOOSSI, Z. 1999. Interaction of *Mycobacterium tuberculosis*-induced transforming growth factor beta1 and interleukin-10. *Infect Immun,* 67**,** 5730-5.

OTTENHOFF, T. H., VERRECK, F. A., LICHTENAUER-KALIGIS, E. G., HOEVE, M. A., SANAL, O. & VAN DISSEL, J. T. 2002. Genetics, cytokines and human infectious disease: lessons from weakly pathogenic mycobacteria and salmonellae. *Nat Genet,* 32**,** 97-105.

OUCHI, N., PARKER, J. L., LUGUS, J. J. & WALSH, K. 2011. Adipokines in inflammation and metabolic disease. *Nat Rev Immunol,* 11**,** 85-97.

OURSLER, K. K., MOORE, R. D., BISHAI, W. R., HARRINGTON, S. M., POPE, D. S. & CHAISSON, R. E. 2002. Survival of patients with pulmonary tuberculosis: clinical and molecular epidemiologic factors. *Clin Infect Dis,* 34**,** 752-9.

OUYANG, W., KOLLS, J. K. & ZHENG, Y. 2008. The biological functions of T helper 17 cell effector cytokines in inflammation. *Immunity,* 28**,** 454-67.

PABLOS-MENDEZ, A., BLUSTEIN, J. & KNIRSCH, C. A. 1997. The role of diabetes mellitus in the higher prevalence of tuberculosis among Hispanics. *Am J Public Health,* 87**,** 574-9.

PAI, M., RILEY, L. W. & COLFORD, J. M., JR. 2004a. Interferon-gamma assays in the immunodiagnosis of tuberculosis: a systematic review. *Lancet Infect Dis,* 4**,** 761-76.

PAI, M., ZWERLING, A. & MENZIES, D. 2008. Systematic review: T-cell-based assays for the diagnosis of latent tuberculosis infection: an update. *Ann Intern Med,* 149**,** 177-84.

PAI, R. K., PENNINI, M. E., TOBIAN, A. A., CANADAY, D. H., BOOM, W. H. & HARDING, C. V. 2004b. Prolonged toll-like receptor signaling by *Mycobacterium tuberculosis* and its 19-kilodalton lipoprotein inhibits gamma interferon-induced regulation of selected genes in macrophages. *Infect Immun,* 72**,** 6603-14.

PALOMINO, J. C., MARTIN, A., VON GROLL, A. & PORTAELS, F. 2008. Rapid culture-based methods for drug-resistance detection in *Mycobacterium tuberculosis*. *J Microbiol Methods,* 75**,** 161-6.

PANCHOLI, P., MIRZA, A., BHARDWAJ, N. & STEINMAN, R. M. 1993. Sequestration from immune CD4+ T cells of mycobacteria growing in human macrophages. *Science,* 260**,** 984-6.

PARK, S. H. & BENDELAC, A. 2000. CD1-restricted T-cell responses and microbial infection. *Nature,* 406**,** 788-92.

PARRISH, N., DIONNE, K., SWEENEY, A., HEDGEPETH, A. & CARROLL, K. 2009. Differences in time to detection and recovery of *Mycobacterium* spp. between the MGIT 960 and the BacT/ALERT MB automated culture systems. *Diagn Microbiol Infect Dis,* 63**,** 342-5.

PARTI, R. P., SRIVASTAVA, S., GACHHUI, R., SRIVASTAVA, K. K. & SRIVASTAVA, R. 2005. Murine infection model for *Mycobacterium fortuitum*. *Microbes Infect,* 7**,** 349-55.

PASULA, R., DOWNING, J. F., WRIGHT, J. R., KACHEL, D. L., DAVIS, T. E., JR. & MARTIN, W. J., 2ND 1997. Surfactant protein A (SP-A) mediates attachment of *Mycobacterium tuberculosis* to murine alveolar macrophages. *Am J Respir Cell Mol Biol,* 17**,** 209-17.

PATHAK, S. K., BASU, S., BHATTACHARYYA, A., PATHAK, S., KUNDU, M. & BASU, J. 2005. *Mycobacterium tuberculosis* lipoarabinomannan-mediated IRAK-M induction negatively regulates Toll-like receptor-dependent interleukin-12 p40 production in macrophages. *J Biol Chem,* 280**,** 42794-800.

PATHAN, A. A., WILKINSON, K. A., KLENERMAN, P., MCSHANE, H., DAVIDSON, R. N., PASVOL, G., HILL, A. V. & LALVANI, A. 2001. Direct ex vivo analysis of antigen-specific IFN-gamma-secreting CD4 T cells in *Mycobacterium tuberculosis*-infected individuals: associations with clinical disease state and effect of treatment. *J Immunol,* 167**,** 5217-25.

PATLAK, M. 2002. New weapons to combat an ancient disease: treating diabetes. *Faseb j,* 16**,** 1853.

PAVKOV, M. E., HANSON, R. L., KNOWLER, W. C., BENNETT, P. H., KRAKOFF, J. & NELSON, R. G. 2007. Changing patterns of type 2 diabetes incidence among Pima Indians. *Diabetes Care,* 30**,** 1758-63.

PEDICINO, D., LIUZZO, G., TROTTA, F., GIGLIO, A. F., GIUBILATO, S., MARTINI, F., ZACCARDI, F., SCAVONE, G., PREVITERO, M., MASSARO, G., CIALDELLA, P., CARDILLO, M. T., PITOCCO, D., GHIRLANDA, G. & CREA, F. 2013. Adaptive immunity, inflammation, and cardiovascular complications in type 1 and type 2 diabetes mellitus. *J Diabetes Res,* 2013**,** 184258.

PEDRAS-VASCONCELOS, J. A., CHAPDELAINE, Y., DUDANI, R., VAN FAASSEN, H., SMITH, D. K. & SAD, S. 2002. *Mycobacterium bovis* BCG-Infected Mice Are More Susceptible to Staphylococcal Enterotoxin B-Mediated Toxic Shock than Uninfected Mice despite Reduced In Vitro Splenocyte Responses to Superantigens. *Infect Immun,* 70**,** 4148-4157.

PEPPER, T., JOSEPH, P., MWENYA, C., MCKEE, G. S., HAUSHALTER, A., CARTER, A., WARKENTIN, J., HAAS, D. W. & STERLING, T. R. 2008. Normal chest radiography in pulmonary tuberculosis: implications for obtaining respiratory specimen cultures. *Int J Tuberc Lung Dis,* 12**,** 397-403.

PERSSON, Y. A., BLOMGRAN-JULINDER, R., RAHMAN, S., ZHENG, L. & STENDAHL, O. 2008. *Mycobacterium tuberculosis*-induced apoptotic neutrophils trigger a pro-inflammatory response in macrophages through release of heat shock protein 72, acting in synergy with the bacteria. *Microbes Infect,* 10**,** 233-40.

PETERS, P. J., NEEFJES, J. J., OORSCHOT, V., PLOEGH, H. L. & GEUZE, H. J. 1991. Segregation of MHC class II molecules from MHC class I molecules in the Golgi complex for transport to lysosomal compartments. *Nature,* 349**,** 669-76.

PETERS, W., SCOTT, H. M., CHAMBERS, H. F., FLYNN, J. L., CHARO, I. F. & ERNST, J. D. 2001. Chemokine receptor 2 serves an early and essential role in resistance to *Mycobacterium tuberculosis*. *Proc Natl Acad Sci U S A,* 98**,** 7958-63.

PIERSIMONI, C., TORTOLI, E., DE LALLA, F., NISTA, D., DONATO, D., BORNIGIA, S. & DE SIO, G. 1997. Isolation of *Mycobacterium celatum* from patients infected with human immunodeficiency virus. *Clin Infect Dis,* 24**,** 144-7.

PIETERS, J. 2008. *Mycobacterium tuberculosis* and the macrophage: maintaining a balance. *Cell Host Microbe,* 3**,** 399-407.

PITTAS, A. G., DAWSON-HUGHES, B., LI, T., VAN DAM, R. M., WILLETT, W. C., MANSON, J. E. & HU, F. B. 2006. Vitamin D and calcium intake in relation to type 2 diabetes in women. *Diabetes Care,* 29**,** 650-6.

PLOUFFE, J. F., SILVA, J., JR., FEKETY, R. & ALLEN, J. L. 1978. Cell-mediated immunity in diabetes mellitus. *Infect Immun,* 21**,** 425-9.

PODELL, B. K., ACKART, D. F., OBREGON-HENAO, A., ECK, S. P., HENAO-TAMAYO, M., RICHARDSON, M., ORME, I. M., ORDWAY, D. J. & BASARABA, R. J. 2014. Increased severity of tuberculosis in Guinea pigs with type 2 diabetes: a model of diabetes-tuberculosis comorbidity. *Am J Pathol,* 184**,** 1104-18.

POLONSKY, K. S. 1995. Lilly Lecture 1994. The beta-cell in diabetes: from molecular genetics to clinical research. *Diabetes,* 44**,** 705-17.

POMPEI, L., JANG, S., ZAMLYNNY, B., RAVIKUMAR, S., MCBRIDE, A., HICKMAN, S. P. & SALGAME, P. 2007. Disparity in IL-12 release in dendritic cells and macrophages in response to *Mycobacterium tuberculosis* is due to use of distinct TLRs. *J Immunol,* 178**,** 5192-9.

POPKIN, B. M. & NIELSEN, S. J. 2003. The sweetening of the world's diet. *Obes Res,* 11**,** 1325-32.

POURSHAFIE, M. R., SONNENFELD, G. & BARROW, W. W. 1999. Immunological and ultrastructural disruptions of T lymphocytes following exposure to the glycopeptidolipid isolated from the *Mycobacterium avium* complex. *Scand J Immunol,* 49**,** 405-10.

POWRIE, F. & COFFMAN, R. L. 1993. Inhibition of cell-mediated immunity by IL4 and IL10. *Res Immunol,* 144**,** 639-43.

PRABOWO, S. A., GROSCHEL, M. I., SCHMIDT, E. D., SKRAHINA, A., MIHAESCU, T., HASTURK, S., MITROFANOV, R., PIMKINA, E., VISONTAI, I., DE JONG, B., STANFORD, J. L., CARDONA, P. J., KAUFMANN, S. H. & VAN DER WERF, T. S. 2013. Targeting multidrug-resistant tuberculosis (MDR-TB) by therapeutic vaccines. *Med Microbiol Immunol,* 202**,** 95-104.

PRADHAN, A. D., MANSON, J. E., RIFAI, N., BURING, J. E. & RIDKER, P. M. 2001. C-reactive protein, interleukin 6, and risk of developing type 2 diabetes mellitus. *Jama,* 286**,** 327-34.

PRANDO, R., CHELI, V., MELGA, P., GIUSTI, R., CIUCHI, E. & ODETTI, P. 1998. Is type 2 diabetes a different disease in obese and nonobese patients? *Diabetes Care,* 21**,** 1680-5.

PUISSEGUR, M. P., BOTANCH, C., DUTEYRAT, J. L., DELSOL, G., CARATERO, C. & ALTARE, F. 2004. An in vitro dual model of mycobacterial granulomas to investigate the molecular interactions between mycobacteria and human host cells. *Cell Microbiol,* 6**,** 423-33.

QI, L., MEIGS, J. B., LIU, S., MANSON, J. E., MANTZOROS, C. & HU, F. B. 2006. Dietary fibers and glycemic load, obesity, and plasma adiponectin levels in women with type 2 diabetes. *Diabetes Care,* 29**,** 1501-5.

QI, L., RIMM, E., LIU, S., RIFAI, N. & HU, F. B. 2005. Dietary glycemic index, glycemic load, cereal fiber, and plasma adiponectin concentration in diabetic men. *Diabetes Care,* 28**,** 1022-8.

QUAN, W., JO, E. K. & LEE, M. S. 2013. Role of pancreatic beta-cell death and inflammation in diabetes. *Diabetes Obes Metab,* 15 Suppl 3**,** 141-51.

RABINOVITCH, A. & SUAREZ-PINZON, W. L. 1998. Cytokines and their roles in pancreatic islet beta-cell destruction and insulin-dependent diabetes mellitus. *Biochem Pharmacol,* 55**,** 1139-49.

RADOSEVIC, K., WIELAND, C. W., RODRIGUEZ, A., WEVERLING, G. J., MINTARDJO, R., GILLISSEN, G., VOGELS, R., SKEIKY, Y. A., HONE, D. M., SADOFF, J. C., VAN DER POLL, T., HAVENGA, M. & GOUDSMIT, J. 2007. Protective immune responses to a recombinant adenovirus type 35 tuberculosis vaccine in two mouse strains: CD4 and CD8 T-cell epitope mapping and role of gamma interferon. *Infect Immun,* 75**,** 4105-15.

RAGHURAMAN, S., VASUDEVAN, K. P., GOVINDARAJAN, S., CHINNAKALI, P. & PANIGRAHI, K. C. 2014. Prevalence of Diabetes Mellitus among Tuberculosis Patients in Urban Puducherry. *N Am J Med Sci,* 6**,** 30-4.

RAHMAN, S., GUDETTA, B., FINK, J., GRANATH, A., ASHENAFI, S., ASEFFA, A., DERBEW, M., SVENSSON, M., ANDERSSON, J. & BRIGHENTI, S. G. 2009. Compartmentalization of immune responses in human tuberculosis: few CD8+ effector T cells but elevated levels of FoxP3+ regulatory t cells in the granulomatous lesions. *Am J Pathol,* 174**,** 2211-24.

RAJA, A. 2004. Immunology of tuberculosis. *Indian J Med Res,* 120**,** 213-32.

RAMAKRISHNAN, L. 2012. Revisiting the role of the granuloma in tuberculosis. *Nat Rev Immunol,* 12**,** 352-66.

REAVEN, G. M., LITHELL, H. & LANDSBERG, L. 1996. Hypertension and associated metabolic abnormalities--the role of insulin resistance and the sympathoadrenal system. *N Engl J Med,* 334**,** 374-81.

REC 1997. Report of the Expert Committee on the Diagnosis and Classification of Diabetes Mellitus. *Diabetes Care,* 20**,** 1183-97.

REDFORD, P. S., MURRAY, P. J. & O'GARRA, A. 2011. The role of IL-10 in immune regulation during M. tuberculosis infection. *Mucosal Immunol,* 4.

REED, S. G., COLER, R. N., DALEMANS, W., TAN, E. V., DELA CRUZ, E. C., BASARABA, R. J., ORME, I. M., SKEIKY, Y. A., ALDERSON, M. R., COWGILL, K. D., PRIEELS, J. P., ABALOS, R. M., DUBOIS, M. C., COHEN, J., METTENS, P. & LOBET, Y. 2009. Defined tuberculosis vaccine, Mtb72F/AS02A, evidence of protection in cynomolgus monkeys. *Proc Natl Acad Sci U S A,* 106**,** 2301-6.

REIFSNYDER, P. C. & LEITER, E. H. 2002. Deconstructing and reconstructing obesity-induced diabetes (diabesity) in mice. *Diabetes,* 51**,** 825-32.

RESTREPO, B. I. 2007. Convergence of the tuberculosis and diabetes epidemics: renewal of old acquaintances. *Clin Infect Dis,* 45**,** 436-8.

RESTREPO, B. I., CAMERLIN, A. J., RAHBAR, M. H., WANG, W., RESTREPO, M. A., ZARATE, I., MORA-GUZMAN, F., CRESPO-SOLIS, J. G., BRIGGS, J., MCCORMICK, J. B. & FISHER-HOCH, S. P. 2011. Cross-sectional assessment reveals high diabetes prevalence among newly-diagnosed tuberculosis cases. *Bull World Health Organ,* 89**,** 352-9.

RESTREPO, B. I., FISHER-HOCH, S. P., CRESPO, J. G., WHITNEY, E., PEREZ, A., SMITH, B. & MCCORMICK, J. B. 2007. Type 2 diabetes and tuberculosis in a dynamic bi-national border population. *Epidemiol Infect,* 135**,** 483-91.

RESTREPO, B. I., FISHER-HOCH, S. P., PINO, P. A., SALINAS, A., RAHBAR, M. H., MORA, F., CORTES-PENFIELD, N. & MCCORMICK, J. B. 2008a. Tuberculosis in poorly controlled type 2 diabetes: Altered cytokine expression in peripheral white blood cells. *Clin Infect Dis,* 47**,** 634-641.

RESTREPO, B. I., FISHER-HOCH, S. P., SMITH, B., JEON, S., RAHBAR, M. H. & MCCORMICK, J. B. 2008b. Mycobacterial clearance from sputum is delayed during the first phase of treatment in patients with diabetes. *Am J Trop Med Hyg,* 79**,** 541-4.

RETZINGER, G. S., MEREDITH, S. C., TAKAYAMA, K., HUNTER, R. L. & KEZDY, F. J. 1981. The role of surface in the biological activities of trehalose 6,6'-dimycolate. Surface properties and development of a model system. *J Biol Chem,* 256**,** 8208-16.

REYNOLDS, J., MOYES, R. B. & BREAKWELL, D. P. 2009. Differential staining of bacteria: acid fast stain. *Curr Protoc Microbiol,* Appendix 3**,** Appendix 3H.

RHOADES, E. R., COOPER, A. M. & ORME, I. M. 1995. Chemokine response in mice infected with *Mycobacterium tuberculosis*. *Infect Immun,* 63**,** 3871-7.

RHOADES, E. R., FRANK, A. A. & ORME, I. M. 1997. Progression of chronic pulmonary tuberculosis in mice aerogenically infected with virulent *Mycobacterium tuberculosis*. *Tuber Lung Dis,* 78**,** 57-66.

RICHARD 2011. Global health 101 (2nd ed.). Burlington, MA: Jones & Bartlett Learning. p. 253. ISBN 978-0-7637-9751-5.

RIPSIN, C. M., KANG, H. & URBAN, R. J. 2009. Management of blood glucose in type 2 diabetes mellitus. *Am Fam Physician,* 79**,** 29-36.

RISERUS, U., WILLETT, W. C. & HU, F. B. 2009. Dietary fats and prevention of type 2 diabetes. *Prog Lipid Res,* 48**,** 44-51.

ROACH, T. I., BARTON, C. H., CHATTERJEE, D. & BLACKWELL, J. M. 1993. Macrophage activation: lipoarabinomannan from avirulent and virulent strains of *Mycobacterium tuberculosis* differentially induces the early genes c-fos, KC, JE, and tumor necrosis factor-alpha. *J Immunol,* 150**,** 1886-96.

ROBERTS, M. T., STOBER, C. B., MCKENZIE, A. N. & BLACKWELL, J. M. 2005. Interleukin-4 (IL-4) and IL-10 collude in vaccine failure for novel exacerbatory antigens in murine Leishmania major infection. *Infect Immun,* 73**,** 7620-8.

ROECKLEIN, J. A., SWARTZ, R. P. & YEAGER, H., JR. 1992. Nonopsonic uptake of *Mycobacterium avium* complex by human monocytes and alveolar macrophages. *J Lab Clin Med,* 119**,** 772-81.

ROGLIC, G. & UNWIN, N. 2010. Mortality attributable to diabetes: estimates for the year 2010. *Diabetes Res Clin Pract,* 87**,** 15-9.

ROOT, H. 1934. The association of diabetes and tuberculosis. *N Eng J Med,* 210,1-13.

ROQUE, S., NOBREGA, C., APPELBERG, R. & CORREIA-NEVES, M. 2007. IL-10 underlies distinct susceptibility of BALB/c and C57BL/6 mice to *Mycobacterium avium* infection and influences efficacy of antibiotic therapy. *J Immunol,* 178**,** 8028-35.

ROSENKRANDS, I., SLAYDEN, R. A., CRAWFORD, J., AAGAARD, C., BARRY, C. E., 3RD & ANDERSEN, P. 2002. Hypoxic response of Mycobacterium tuberculosis studied by metabolic labeling and proteome analysis of cellular and extracellular proteins. *J Bacteriol,* 184**,** 3485-91.

ROSSI, S. E., FRANQUET, T., VOLPACCHIO, M., GIMENEZ, A. & AGUILAR, G. 2005. Tree-in-bud pattern at thin-section CT of the lungs: radiologic-pathologic overview. *Radiographics,* 25**,** 789-801.

ROTA, M., LECAPITAINE, N., HOSODA, T., BONI, A., DE ANGELIS, A., PADIN-IRUEGAS, M. E., ESPOSITO, G., VITALE, S., URBANEK, K., CASARSA, C., GIORGIO, M., LUSCHER, T. F., PELICCI, P. G., ANVERSA, P., LERI, A. & KAJSTURA, J. 2006. Diabetes promotes cardiac stem cell aging and heart failure, which are prevented by deletion of the p66shc gene. *Circ Res,* 99**,** 42-52.

ROTHER, K. I. 2007. Diabetes treatment--bridging the divide. *N Engl J Med,* 356**,** 1499-501.

ROTHFUCHS, A. G., BAFICA, A., FENG, C. G., EGEN, J. G., WILLIAMS, D. L., BROWN, G. D. & SHER, A. 2007. Dectin-1 interaction with *Mycobacterium tuberculosis* leads to enhanced IL-12p40 production by splenic dendritic cells. *J Immunol,* 179**,** 3463-71.

ROY, A., EISENHUT, M., HARRIS, R. J., RODRIGUES, L. C., SRIDHAR, S., HABERMANN, S., SNELL, L., MANGTANI, P., ADETIFA, I., LALVANI, A. & ABUBAKAR, I. 2014. Effect of BCG vaccination against Mycobacterium tuberculosis infection in children: systematic review and meta-analysis. *The BMJ,* 349**,** g4643.

ROY, S., BARNES, P. F., GARG, A., WU, S., COSMAN, D. & VANKAYALAPATI, R. 2008. NK cells lyse T regulatory cells that expand in response to an intracellular pathogen. *J Immunol,* 180**,** 1729-36.

RUDDY, M. J., WONG, G. C., LIU, X. K., YAMAMOTO, H., KASAYAMA, S., KIRKWOOD, K. L. & GAFFEN, S. L. 2004. Functional cooperation between interleukin-17 and tumor necrosis factor-alpha is mediated by CCAAT/enhancer-binding protein family members. *J Biol Chem,* 279**,** 2559-67.

RUSSELL, D. G. 2007. Who puts the tubercle in tuberculosis? *Nat Rev Microbiol,* 5**,** 39-47.

RUSSELL, M. S., DUDANI, R., KRISHNAN, L. & SAD, S. 2009. IFN-gamma expressed by T cells regulates the persistence of antigen presentation by limiting the survival of dendritic cells. *J Immunol,* 183**,** 7710-8.

SAAD, F. & GOOREN, L. 2009. The role of testosterone in the metabolic syndrome: a review. *J Steroid Biochem Mol Biol,* 114**,** 40-3.

SACKS, D. B., BRUNS, D. E., GOLDSTEIN, D. E., MACLAREN, N. K., MCDONALD, J. M. & PARROTT, M. 2002. Guidelines and recommendations for laboratory analysis in the diagnosis and management of diabetes mellitus. *Clin Chem,* 48**,** 436-72.

SAHA, B., DAS, G., VOHRA, H., GANGULY, N. K. & MISHRA, G. C. 1994. Macrophage-T cell interaction in experimental mycobacterial infection. Selective regulation of co-stimulatory molecules on *Mycobacterium*-infected macrophages and its implication in the suppression of cell-mediated immune response. *Eur J Immunol,* 24**,** 2618-24.

SAIKI, O., NEGORO, S., TSUYUGUCHI, I. & YAMAMURA, Y. 1980. Depressed immunological defence mechanisms in mice with experimentally induced diabetes. *Infect Immun,* 28**,** 127-31.

SAITO, H. & TASAKA, H. 1969. Comparison of the pathogenicity for mice of *Mycobacterium fortuitum* and *Mycobacterium abscessus*. *J Bacteriol,* 99**,** 851-5.

SAKAMOTO, K. 2012. The pathology of *Mycobacterium tuberculosis* infection. *Vet Pathol,* 49**,** 423-39.

SAKURABA, H., MIZUKAMI, H., YAGIHASHI, N., WADA, R., HANYU, C. & YAGIHASHI, S. 2002. Reduced beta-cell mass and expression of oxidative stress-related DNA damage in the islet of Japanese Type II diabetic patients. *Diabetologia,* 45**,** 85-96.

SALEH, M. T. & BELISLE, J. T. 2000. Secretion of an acid phosphatase (SapM) by *Mycobacterium tuberculosis* that is similar to eukaryotic acid phosphatases. *J Bacteriol,* 182**,** 6850-3.

SAMPSON, U. K., LINTON, M. F. & FAZIO, S. 2011. Are statins diabetogenic? *Curr Opin Cardiol,* 26**,** 342-7.

SANDOR, M., WEINSTOCK, J. V. & WYNN, T. A. 2003. Granulomas in schistosome and mycobacterial infections: a model of local immune responses. *Trends Immunol,* 24**,** 44-52.

SANGWAN, J., LATHWAL, S., KUMAR, S. & JUYAL, D. 2013. *Mycobacterium fortuitum* Peritonitis in a Patient on Continuous Ambulatory Peritoneal Dialysis (CAPD): A Case Report. *J Clin Diagn Res,* 7**,** 2950-1.

SANTOS, J. L., PEREZ-BRAVO, F., CARRASCO, E., CALVILLAN, M. & ALBALA, C. 2001. Low prevalence of type 2 diabetes despite a high average body mass index in the Aymara natives from Chile. *Nutrition,* 17**,** 305-9.

SASINDRAN, S. J. & TORRELLES, J. B. 2011. *Mycobacterium tuberculosis* Infection and Inflammation: what is Beneficial for the Host and for the Bacterium? *Front Microbiol,* 2**,** 2.

SAUNDERS, B. M. & BRITTON, W. J. 2007. Life and death in the granuloma: immunopathology of tuberculosis. *Immunol Cell Biol,* 85**,** 103-11.

SAUNDERS, B. M. & COOPER, A. M. 2000. Restraining mycobacteria: role of granulomas in mycobacterial infections. *Immunol Cell Biol,* 78**,** 334-41.

SAUNDERS, B. M., FRANK, A. A., ORME, I. M. & COOPER, A. M. 2000. Interleukin-6 induces early gamma interferon production in the infected lung but is not required for generation of specific immunity to *Mycobacterium tuberculosis* infection. *Infect Immun,* 68.

SAUNDERS, B. M., TRAN, S., RUULS, S., SEDGWICK, J. D., BRISCOE, H. & BRITTON, W. J. 2005. Transmembrane TNF is sufficient to initiate cell migration and granuloma formation and provide acute, but not long-term, control of *Mycobacterium tuberculosis* infection. *J Immunol,* 174**,** 4852-9.

SCANGA, C. A., MOHAN, V. P., TANAKA, K., ALLAND, D., FLYNN, J. L. & CHAN, J. 2001. The inducible nitric oxide synthase locus confers protection against aerogenic challenge of both clinical and laboratory strains of *Mycobacterium tuberculosis* in mice. *Infect Immun,* 69**,** 7711-7.

SCHAIBLE, U. E., WINAU, F., SIELING, P. A., FISCHER, K., COLLINS, H. L., HAGENS, K., MODLIN, R. L., BRINKMANN, V. & KAUFMANN, S. H. 2003. Apoptosis facilitates antigen presentation to T lymphocytes through MHC-I and CD1 in tuberculosis. *Nat Med,* 9**,** 1039-46.

SCHEEN, A. J. & LEFEBVRE, P. J. 1996. Insulin action in man. *Diabetes Metab,* 22**,** 105-10.

SCHEEN, A. J. & VAN GAAL, L. F. 2014. Combating the dual burden: therapeutic targeting of common pathways in obesity and type 2 diabetes. *Lancet Diabetes Endocrinol,* 2**,** 911-22.

SCHINDLER, R., MANCILLA, J., ENDRES, S., GHORBANI, R., CLARK, S. C. & DINARELLO, C. A. 1990. Correlations and interactions in the production of interleukin-6 (IL-6), IL-1, and tumor necrosis factor (TNF) in human blood mononuclear cells: IL-6 suppresses IL-1 and TNF. *Blood,* 75**,** 40-7.

SCHLESINGER, L. S. 1993. Macrophage phagocytosis of virulent but not attenuated strains of *Mycobacterium tuberculosis* is mediated by mannose receptors in addition to complement receptors. *J Immunol,* 150**,** 2920-30.

SCHLESINGER, L. S. 1998. *Mycobacterium tuberculosis* and the complement system. *Trends Microbiol,* 6**,** 47-9; discussion 49-50.

SCHLESINGER, L. S., BELLINGER-KAWAHARA, C. G., PAYNE, N. R. & HORWITZ, M. A. 1990. Phagocytosis of *Mycobacterium tuberculosis* is mediated by human monocyte complement receptors and complement component C3. *J Immunol,* 144**,** 2771-80.

SCHLUGER, N. W. 2001. Recent advances in our understanding of human host responses to tuberculosis. *Respir Res,* 2**,** 157-63.

SCHNEIDER, B. E., KORBEL, D., HAGENS, K., KOCH, M., RAUPACH, B., ENDERS, J., KAUFMANN, S. H., MITTRUCKER, H. W. & SCHAIBLE, U. E. 2010. A role for IL-18 in protective immunity against *Mycobacterium tuberculosis*. *Eur J Immunol,* 40**,** 396-405.

SCOTT-BROWNE, J. P., SHAFIANI, S., TUCKER-HEARD, G., ISHIDA-TSUBOTA, K., FONTENOT, J. D., RUDENSKY, A. Y., BEVAN, M. J. & URDAHL, K. B. 2007. Expansion and function of Foxp3-expressing T regulatory cells during tuberculosis. *J Exp Med,* 204**,** 2159-69.

SENALDI, G., YIN, S., SHAKLEE, C. L., PIGUET, P. F., MAK, T. W. & ULICH, T. R. 1996. *Corynebacterium parvum*- and *Mycobacterium bovis* bacillus Calmette-Guerin-induced granuloma formation is inhibited in TNF receptor I (TNF-RI) knockout mice and by treatment with soluble TNF-RI. *J Immunol,* 157**,** 5022-6.

SERBINA, N. V., LAZAREVIC, V. & FLYNN, J. L. 2001. CD4(+) T cells are required for the development of cytotoxic CD8(+) T cells during *Mycobacterium tuberculosis* infection. *J Immunol,* 167**,** 6991-7000.

SHAFRIR, E., ZIV, E. & KALMAN, R. 2006. Nutritionally induced diabetes in desert rodents as models of type 2 diabetes: Acomys cahirinus (spiny mice) and Psammomys obesus (desert gerbil). *Ilar j,* 47**,** 212-24.

SHAH, B. R. & HUX, J. E. 2003. Quantifying the risk of infectious diseases for people with diabetes. *Diabetes Care,* 26**,** 510-3.

SHARMA, K., MCCUE, P. & DUNN, S. R. 2003. Diabetic kidney disease in the db/db mouse. *Am J Physiol Renal Physiol,* 284**,** F1138-44.

SHARMA, P. K., SAHA, P. K., SINGH, A., SHARMA, S. K., GHOSH, B. & MITRA, D. K. 2009. FoxP3+ regulatory T cells suppress effector T-cell function at pathologic site in miliary tuberculosis. *Am J Respir Crit Care Med,* 179**,** 1061-70.

SHAW, T. C., THOMAS, L. H. & FRIEDLAND, J. S. 2000. Regulation of IL-10 secretion after phagocytosis of *Mycobacterium tuberculosis* by human monocytic cells. *Cytokine,* 12**,** 483-6.

SHERMAN, D. R., GUINN, K. M., HICKEY, M. J., MATHUR, S. K., ZAKEL, K. L. & SMITH, S. 2004. *Mycobacterium tuberculosis* H37Rv: Delta RD1 is more virulent than *M. bovis* bacille Calmette-Guerin in long-term murine infection. *J Infect Dis,* 190**,** 123-6.

SHIMOKATA, H., MULLER, D. C. & ANDRES, R. 1989. Studies in the distribution of body fat. III. Effects of cigarette smoking. *Jama,* 261**,** 1169-73.

SHOELSON, S. E., LEE, J. & GOLDFINE, A. B. 2006. Inflammation and insulin resistance. *J Clin Invest,* 116**,** 1793-801.

SHULDINER, A. R., YANG, R. & GONG, D. W. 2001. Resistin, obesity and insulin resistance--the emerging role of the adipocyte as an endocrine organ. *N Engl J Med,* 345**,** 1345-6.

SIELING, P. A., WANG, X. H., GATELY, M. K., OLIVEROS, J. L., MCHUGH, T., BARNES, P. F., WOLF, S. F., GOLKAR, L., YAMAMURA, M., YOGI, Y. & ET AL. 1994. IL-12 regulates T helper type 1 cytokine responses in human infectious disease. *J Immunol,* 153**,** 3639-47.

SILVA MIRANDA, M., BREIMAN, A., ALLAIN, S., DEKNUYDT, F. & ALTARE, F. 2012. The tuberculous granuloma: an unsuccessful host defence mechanism providing a safety shelter for the bacteria? *Clin Dev Immunol,* 2012**,** 139127.

SILVA, R. A., PAIS, T. F. & APPELBERG, R. 2001. Blocking the receptor for IL-10 improves antimycobacterial chemotherapy and vaccination. *J Immunol,* 167**,** 1535-41.

SILVA, T. R., PETERSEN, A. L., SANTOS TDE, A., ALMEIDA, T. F., FREITAS, L. A. & VERAS, P. S. 2010. Control of *Mycobacterium fortuitum* and *Mycobacterium intracellulare* infections with respect to distinct granuloma formations in livers of BALB/c mice. *Mem Inst Oswaldo Cruz,* 105**,** 642-8.

SINGH, A. K. & REYRAT, J. M. 2009. Laboratory maintenance of *Mycobacterium smegmatis*. *Curr Protoc Microbiol,* Chapter 10**,** Unit10C.1.

SINGH, P. P. & GOYAL, A. 2013. Interleukin-6: a potent biomarker of mycobacterial infection. *SpringerPlus,* 2**,** 1-8.

SINGHAL, A., ALIOUAT EL, M., HERVE, M., MATHYS, V., KIASS, M., CREUSY, C., DELAIRE, B., TSENOVA, L., FLEURISSE, L., BERTOUT, J., CAMACHO, L., FOO, D., TAY, H. C., SIEW, J. Y., BOUKHOUCHI, W., ROMANO, M., MATHEMA, B., DARTOIS, V., KAPLAN, G. & BIFANI, P. 2011. Experimental tuberculosis in the Wistar rat: a model for protective immunity and control of infection. *PLoS One,* 6**,** e18632.

SMAILL, F., JEYANATHAN, M., SMIEJA, M., MEDINA, M. F., THANTHRIGE-DON, N., ZGANIACZ, A., YIN, C., HERIAZON, A., DAMJANOVIC, D., PURI, L., HAMID, J., XIE, F., FOLEY, R., BRAMSON, J., GAULDIE, J. & XING, Z. 2013. A human type 5 adenovirus-based tuberculosis vaccine induces robust T cell responses in humans despite preexisting anti-adenovirus immunity. *Sci Transl Med,* 5**,** 205ra134.

SMYTH, S. & HERON, A. 2006. Diabetes and obesity: the twin epidemics. *Nat Med,* 12**,** 75-80.

SOBNGWI, E., CHOUKEM, S. P., AGBALIKA, F., BLONDEAU, B., FETITA, L. S., LEBBE, C., THIAM, D., CATTAN, P., LARGHERO, J., FOUFELLE, F., FERRE, P., VEXIAU, P., CALVO, F. & GAUTIER, J. F. 2008. Ketosis-prone type 2 diabetes mellitus and human herpesvirus 8 infection in sub-saharan africans. *Jama,* 299**,** 2770-6.

SODENKAMP, J., WAETZIG, G. H., SCHELLER, J., SEEGERT, D., GROTZINGER, J., ROSE-JOHN, S., EHLERS, S. & HOLSCHER, C. 2012. Therapeutic targeting of interleukin-6 trans-signaling does not affect the outcome of experimental tuberculosis. *Immunobiology,* 217**,** 996-1004.

SOUSA, A. O., MAZZACCARO, R. J., RUSSELL, R. G., LEE, F. K., TURNER, O. C., HONG, S., VAN KAER, L. & BLOOM, B. R. 2000. Relative contributions of distinct MHC class I-dependent cell populations in protection to tuberculosis infection in mice. *Proc Natl Acad Sci U S A,* 97**,** 4204-8.

SRINIVASAN, K. & RAMARAO, P. 2007. Animal models in type 2 diabetes research: an overview. *Indian J Med Res,* 125**,** 451-72.

SRINIVASAN, K., VISWANAD, B., ASRAT, L., KAUL, C. L. & RAMARAO, P. 2005. Combination of high-fat diet-fed and low-dose streptozotocin-treated rat: a model for type 2 diabetes and pharmacological screening. *Pharmacol Res,* 52**,** 313-20.

STALENHOEF, J. E., ALISJAHBANA, B., NELWAN, E. J., VAN DER VEN-JONGEKRIJG, J., OTTENHOFF, T. H., VAN DER MEER, J. W., NELWAN, R. H., NETEA, M. G. & VAN CREVEL, R. 2008. The role of interferon-gamma in the increased tuberculosis risk in type 2 diabetes mellitus. *Eur J Clin Microbiol Infect Dis,* 27**,** 97-103.

STEAD, W. W., EISENACH, K. D., CAVE, M. D., BEGGS, M. L., TEMPLETON, G. L., THOEN, C. O. & BATES, J. H. 1995. When did *Mycobacterium tuberculosis* infection first occur in the New World? An important question with public health implications. *Am J Respir Crit Care Med,* 151**,** 1267-8.

STEGENGA, M. E., VAN DER CRABBEN, S. N., BLUMER, R. M., LEVI, M., MEIJERS, J. C., SERLIE, M. J., TANCK, M. W., SAUERWEIN, H. P. & VAN DER POLL, T. 2008. Hyperglycemia enhances coagulation and reduces neutrophil degranulation, whereas hyperinsulinemia inhibits fibrinolysis during human endotoxemia. *Blood,* 112**,** 82-9.

STEPPAN, C. M., BAILEY, S. T., BHAT, S., BROWN, E. J., BANERJEE, R. R., WRIGHT, C. M., PATEL, H. R., AHIMA, R. S. & LAZAR, M. A. 2001. The hormone resistin links obesity to diabetes. *Nature,* 409**,** 307-12.

STEVENSON, C. R., CRITCHLEY, J. A., FOROUHI, N. G., ROGLIC, G., WILLIAMS, B. G., DYE, C. & UNWIN, N. C. 2007. Diabetes and the risk of tuberculosis: a neglected threat to public health? *Chronic Illn,* 3**,** 228-45.

STOBER, C. B., LANGE, U. G., ROBERTS, M. T., ALCAMI, A. & BLACKWELL, J. M. 2005. IL-10 from regulatory T cells determines vaccine efficacy in murine Leishmania major infection. *J Immunol,* 175**,** 2517-24.

STUART, R. L., BENNETT, N., FORBES, A. & GRAYSON, M. L. 2000. A paired comparison of tuberculin skin test results in health care workers using 5 TU and 10 TU tuberculin. *Thorax,* 55**,** 693-5.

STUBBINS, R. E., NAJJAR, K., HOLCOMB, V. B., HONG, J. & NUNEZ, N. P. 2012. Oestrogen alters adipocyte biology and protects female mice from adipocyte inflammation and insulin resistance. *Diabetes Obes Metab,* 14**,** 58-66.

STYBLO, K. & MEIJER, J. 1976. Impact of BCG vaccination programmes in children and young adults on the tuberculosis problem. *Tubercle,* 57**,** 17-43.

SUD, D., BIGBEE, C., FLYNN, J. L. & KIRSCHNER, D. E. 2006. Contribution of CD8+ T cells to control of *Mycobacterium tuberculosis* infection. *J Immunol,* 176**,** 4296-314.

SUGAWARA, I. & MIZUNO, S. 2008. Higher susceptibility of type 1 diabetic rats to *Mycobacterium tuberculosis* infection. *Tohoku J Exp Med,* 216**,** 363-70.

SUGAWARA, I., YAMADA, H., KANEKO, H., MIZUNO, S., TAKEDA, K. & AKIRA, S. 1999. Role of interleukin-18 (IL-18) in mycobacterial infection in IL-18-gene-disrupted mice. *Infect Immun,* 67**,** 2585-9.

SUGAWARA, I., YAMADA, H. & MIZUNO, S. 2004. Pulmonary tuberculosis in spontaneously diabetic goto kakizaki rats. *Tohoku J Exp Med,* 204**,** 135-45.

SUN, C., SUN, L., MA, H., PENG, J., ZHEN, Y., DUAN, K., LIU, G., DING, W. & ZHAO, Y. 2012. The phenotype and functional alterations of macrophages in mice with hyperglycemia for long term. *J Cell Physiol,* 227**,** 1670-9.

SURENDAR, J., MOHAN, V., PAVANKUMAR, N., BABU, S. & ARAVINDHAN, V. 2012. Increased levels of serum granulocyte-macrophage colony-stimulating factor is associated with activated peripheral dendritic cells in type 2 diabetes subjects (CURES-99). *Diabetes Technol Ther,* 14**,** 344-9.

SURWIT, R. S., KUHN, C. M., COCHRANE, C., MCCUBBIN, J. A. & FEINGLOS, M. N. 1988. Diet-induced type II diabetes in C57BL/6J mice. *Diabetes,* 37**,** 1163-7.

SUTHERLAND, I. & SPRINGETT, V. H. 1987. Effectiveness of BCG vaccination in England and Wales in 1983. *Tubercle,* 68**,** 81-92.

SUZUKI, W., IIZUKA, S., TABUCHI, M., FUNO, S., YANAGISAWA, T., KIMURA, M., SATO, T., ENDO, T. & KAWAMURA, H. 1999. A new mouse model of spontaneous diabetes derived from ddY strain. *Exp Anim,* 48**,** 181-9.

SWEET, L. & SCHOREY, J. S. 2006. Glycopeptidolipids from *Mycobacterium avium* promote macrophage activation in a TLR2- and MyD88-dependent manner. *J Leukoc Biol,* 80**,** 415-23.

TAKEGAKI, Y. 2000. Effect of serotype specific glycopeptidolipid (GPL) isolated from Mycobacterium avium complex (MAC) on phagocytosis and phagosome-lysosome fusion of human peripheral blood monocytes. *Kekkaku,* 75**,** 9-18.

TALUKDAR, S., OH, D. Y., BANDYOPADHYAY, G., LI, D., XU, J., MCNELIS, J., LU, M., LI, P., YAN, Q., ZHU, Y., OFRECIO, J., LIN, M., BRENNER, M. B. & OLEFSKY, J. M. 2012. Neutrophils mediate insulin resistance in high fat diet fed mice via secreted elastase. *Nature medicine,* 18**,** 1407-1412.

TAMARAT, R., SILVESTRE, J. S., HUIJBERTS, M., BENESSIANO, J., EBRAHIMIAN, T. G., DURIEZ, M., WAUTIER, M. P., WAUTIER, J. L. & LEVY, B. I. 2003. Blockade

of advanced glycation end-product formation restores ischemia-induced angiogenesis in diabetic mice. *Proc Natl Acad Sci U S A,* 100**,** 8555-60.

TAMERIS, M. D., HATHERILL, M., LANDRY, B. S., SCRIBA, T. J., SNOWDEN, M. A., LOCKHART, S., SHEA, J. E., MCCLAIN, J. B., HUSSEY, G. D., HANEKOM, W. A., MAHOMED, H. & MCSHANE, H. 2013. Safety and efficacy of MVA85A, a new tuberculosis vaccine, in infants previously vaccinated with BCG: a randomised, placebo-controlled phase 2b trial. *Lancet,* 381**,** 1021-8.

TAN, K. S., LEE, K. O., LOW, K. C., GAMAGE, A. M., LIU, Y., TAN, G. Y., KOH, H. Q., ALONSO, S. & GAN, Y. H. 2012. Glutathione deficiency in type 2 diabetes impairs cytokine responses and control of intracellular bacteria. *J Clin Invest,* 122**,** 2289-300.

TASCON, R. E., SOARES, C. S., RAGNO, S., STAVROPOULOS, E., HIRST, E. M. & COLSTON, M. J. 2000. *Mycobacterium tuberculosis*-activated dendritic cells induce protective immunity in mice. *Immunology,* 99**,** 473-80.

TAYLOR, J. L., ORDWAY, D. J., TROUDT, J., GONZALEZ-JUARRERO, M., BASARABA, R. J. & ORME, I. M. 2005. Factors associated with severe granulomatous pneumonia in *Mycobacterium tuberculosis*-infected mice vaccinated therapeutically with hsp65 DNA. *Infect Immun,* 73**,** 5189-93.

THOMA-USZYNSKI, S., STENGER, S., TAKEUCHI, O., OCHOA, M. T., ENGELE, M., SIELING, P. A., BARNES, P. F., ROLLINGHOFF, M., BOLCSKEI, P. L., WAGNER, M., AKIRA, S., NORGARD, M. V., BELISLE, J. T., GODOWSKI, P. J., BLOOM, B. R. & MODLIN, R. L. 2001. Induction of direct antimicrobial activity through mammalian toll-like receptors. *Science,* 291**,** 1544-7.

THURNHER, M., RAMONER, R., GASTL, G., RADMAYR, C., BOCK, G., HEROLD, M., KLOCKER, H. & BARTSCH, G. 1997. Bacillus Calmette-Guerin mycobacteria stimulate human blood dendritic cells. *Int J Cancer,* 70**,** 128-34.

TIEMESSEN, M. M., JAGGER, A. L., EVANS, H. G., VAN HERWIJNEN, M. J., JOHN, S. & TAAMS, L. S. 2007. CD4+CD25+Foxp3+ regulatory T cells induce alternative activation of human monocytes/macrophages. *Proc Natl Acad Sci U S A,* 104**,** 19446-51.

TOMITA, T., DOULL, V., POLLOCK, H. G. & KRIZSAN, D. 1992. Pancreatic islets of obese hyperglycemic mice (ob/ob). *Pancreas,* 7**,** 367-75.

TOOSSI, Z. 2000. The inflammatory response in *Mycobacterium tuberculosis* infection. *Arch Immunol Ther Exp (Warsz),* 48**,** 513-9.

TOOSSI, Z. & ELLNER, J. J. 1998. The role of TGF beta in the pathogenesis of human tuberculosis. *Clin Immunol Immunopathol,* 87**,** 107-14.

TOOSSI, Z., GOGATE, P., SHIRATSUCHI, H., YOUNG, T. & ELLNER, J. J. 1995. Enhanced production of TGF-beta by blood monocytes from patients with active tuberculosis and presence of TGF-beta in tuberculous granulomatous lung lesions. *J Immunol,* 154**,** 465-73.

TOOSSI, Z., KLEINHENZ, M. E. & ELLNER, J. J. 1986. Defective interleukin 2 production and responsiveness in human pulmonary tuberculosis. *J Exp Med,* 163**,** 1162-72.

TOOSSI, Z., SEDOR, J. R., LAPURGA, J. P., ONDASH, R. J. & ELLNER, J. J. 1990. Expression of functional interleukin 2 receptors by peripheral blood monocytes from patients with active pulmonary tuberculosis. *J Clin Invest,* 85**,** 1777-84.

TORRELLES, J. B., DESJARDIN, L. E., MACNEIL, J., KAUFMAN, T. M., KUTZBACH, B., KNAUP, R., MCCARTHY, T. R., GURCHA, S. S., BESRA, G. S., CLEGG, S. & SCHLESINGER, L. S. 2009. Inactivation of *Mycobacterium tuberculosis* mannosyltransferase pimB reduces the cell wall lipoarabinomannan and lipomannan

content and increases the rate of bacterial-induced human macrophage cell death. *Glycobiology,* 19**,** 743-55.

TORTOLI, E., PIERSIMONI, C., BACOSI, D., BARTOLONI, A., BETTI, F., BONO, L., BURRINI, C., DE SIO, G., LACCHINI, C., MANTELLA, A. & ET AL. 1995. Isolation of the newly described species *Mycobacterium celatum* from AIDS patients. *J Clin Microbiol,* 33**,** 137-40.

TRINCHIERI, G. 1995. Interleukin-12: a proinflammatory cytokine with immunoregulatory functions that bridge innate resistance and antigen-specific adaptive immunity. *Annu Rev Immunol,* 13**,** 251-76.

TSENOVA, L., BERGTOLD, A., FREEDMAN, V. H., YOUNG, R. A. & KAPLAN, G. 1999. Tumor necrosis factor alpha is a determinant of pathogenesis and disease progression in mycobacterial infection in the central nervous system. *Proc Natl Acad Sci U S A,* 96**,** 5657-62.

TSUKAGUCHI, K., OKAMURA, H., IKUNO, M., KOBAYASHI, A., FUKUOKA, A., TAKENAKA, H., YAMAMOTO, C., TOKUYAMA, T., OKAMOTO, Y., FU, A., YOSHIKAWA, M., YONEDA, T. & NARITA, N. 1997. [The relation between diabetes mellitus and IFN-gamma, IL-12 and IL-10 productions by CD4+ alpha beta T cells and monocytes in patients with pulmonary tuberculosis]. *Kekkaku,* 72**,** 617-22.

TSUKAGUCHI, K., OKAMURA, H., MATSUZAWA, K., TAMURA, M., MIYAZAKI, R., TAMAKI, S. & KIMURA, H. 2002. [Longitudinal assessment of IFN-gamma production in patients with pulmonary tuberculosis complicated with diabetes mellitus]. *Kekkaku,* 77**,** 409-13.

TSUKAGUCHI, K., YONEDA, T., YOSHIKAWA, M., TOKUYAMA, T., FU, A., TOMODA, K., NARITA, N., ENOKI, Y., TSUKAGUCHI, M., SHIRAI, F. & ET AL. 1992. [Case study of interleukin-1 beta, tumor necrosis factor alpha and interleukin-6 production peripheral blood monocytes in patients with diabetes mellitus complicated by pulmonary tuberculosis]. *Kekkaku,* 67**,** 755-60.

UEDA, H., IKEGAMI, H., KAWAGUCHI, Y., FUJISAWA, T., NOJIMA, K., BABAYA, N., YAMADA, K., SHIBATA, M., YAMATO, E. & OGIHARA, T. 2000. Age-dependent changes in phenotypes and candidate gene analysis in a polygenic animal model of Type II diabetes mellitus; NSY mouse. *Diabetologia,* 43**,** 932-8.

UEDA, K., YAMAZAKI, S. & SOMEYA, S. 1972. Studies on tubercle bacillus infection in germ-free mice. *J Reticuloendothel Soc,* 12**,** 545-63.

ULRICHS, T., KOSMIADI, G. A., JORG, S., PRADL, L., TITUKHINA, M., MISHENKO, V., GUSHINA, N. & KAUFMANN, S. H. 2005. Differential organization of the local immune response in patients with active cavitary tuberculosis or with nonprogressive tuberculoma. *J Infect Dis,* 192**,** 89-97.

ULUKANLIGIL, M., ASLAN, G. & TASCI, S. 2000. A comparative study on the different staining methods and number of specimens for the detection of acid fast bacilli. *Mem Inst Oswaldo Cruz,* 95**,** 855-8.

UNDERHILL, D. M., OZINSKY, A., SMITH, K. D. & ADEREM, A. 1999. Toll-like receptor-2 mediates mycobacteria-induced proinflammatory signaling in macrophages. *Proc Natl Acad Sci U S A,* 96**,** 14459-63.

UNDESA 2009. United Nations Department of Economic and Social Affairs. State of the World's Indigenous Peoples. UN: New York; 2009.

UNGER, R. H. & ZHOU, Y. T. 2001. Lipotoxicity of beta-cells in obesity and in other causes of fatty acid spillover. *Diabetes,* 50 Suppl 1**,** S118-21.

URIBARRI, J., WOODRUFF, S., GOODMAN, S., CAI, W., CHEN, X. U. E., PYZIK, R., YONG, A., STRIKER, G. E. & VLASSARA, H. 2010. Advanced Glycation End

Products in Foods and a Practical Guide to Their Reduction in the Diet. *Am Diet Assoc,* 110**,** 911-16.e12.

USLAN, D. Z., KOWALSKI, T. J., WENGENACK, N. L., VIRK, A. & WILSON, J. W. 2006. Skin and soft tissue infections due to rapidly growing mycobacteria: comparison of clinical features, treatment, and susceptibility. *Arch Dermatol,* 142**,** 1287-92.

UYSAL, K. T., WIESBROCK, S. M., MARINO, M. W. & HOTAMISLIGIL, G. S. 1997. Protection from obesity-induced insulin resistance in mice lacking TNF-alpha function. *Nature,* 389**,** 610-4.

VALLERSKOG, T., MARTENS, G. W. & KORNFELD, H. 2010. Diabetic mice display a delayed adaptive immune response to *Mycobacterium tuberculosis*. *J Immunol,* 184**,** 6275-82.

VALONE, S. E., RICH, E. A., WALLIS, R. S. & ELLNER, J. J. 1988. Expression of tumor necrosis factor in vitro by human mononuclear phagocytes stimulated with whole Mycobacterium bovis BCG and mycobacterial antigens. *Infect Immun,* 56**,** 3313-5.

VAN CREVEL, R., KARYADI, E., PREYERS, F., LEENDERS, M., KULLBERG, B. J., NELWAN, R. H. & VAN DER MEER, J. W. 2000. Increased production of interleukin 4 by CD4+ and CD8+ T cells from patients with tuberculosis is related to the presence of pulmonary cavities. *J Infect Dis,* 181**,** 1194-7.

VAN CREVEL, R., OTTENHOFF, T. H. & VAN DER MEER, J. W. 2002. Innate immunity to *Mycobacterium tuberculosis*. *Clin Microbiol Rev,* 15**,** 294-309.

VAN DISSEL, J. T., AREND, S. M., PRINS, C., BANG, P., TINGSKOV, P. N., LINGNAU, K., NOUTA, J., KLEIN, M. R., ROSENKRANDS, I., OTTENHOFF, T. H., KROMANN, I., DOHERTY, T. M. & ANDERSEN, P. 2010. Ag85B-ESAT-6 adjuvanted with IC31 promotes strong and long-lived *Mycobacterium tuberculosis* specific T cell responses in naive human volunteers. *Vaccine,* 28**,** 3571-81.

VAN PINXTEREN, L. A., CASSIDY, J. P., SMEDEGAARD, B. H., AGGER, E. M. & ANDERSEN, P. 2000. Control of latent *Mycobacterium tuberculosis* infection is dependent on CD8 T cells. *Eur J Immunol,* 30**,** 3689-98.

VANDANMAGSAR, B., YOUM, Y. H., RAVUSSIN, A., GALGANI, J. E., STADLER, K., MYNATT, R. L., RAVUSSIN, E., STEPHENS, J. M. & DIXIT, V. D. 2011. The NLRP3 inflammasome instigates obesity-induced inflammation and insulin resistance. *Nat Med,* 17**,** 179-88.

VANHEYNINGEN, T. K., COLLINS, H. L. & RUSSELL, D. G. 1997. IL-6 produced by macrophages infected with *Mycobacterium* species suppresses T cell responses. *J Immunol,* 158**,** 330-7.

VANKAYALAPATI, R., WIZEL, B., WEIS, S. E., SAMTEN, B., GIRARD, W. M. & BARNES, P. F. 2000. Production of interleukin-18 in human tuberculosis. *J Infect Dis,* 182**,** 234-9.

VENKATASWAMY, M. M., GOLDBERG, M. F., BAENA, A., CHAN, J., JACOBS, W. R., JR. & PORCELLI, S. A. 2012. In vitro culture medium influences the vaccine efficacy of *Mycobacterium bovis* BCG. *Vaccine,* 30**,** 1038-49.

VERGNE, I., CHUA, J. & DERETIC, V. 2003. *Mycobacterium tuberculosis* phagosome maturation arrest: selective targeting of PI3P-dependent membrane trafficking. *Traffic,* 4**,** 600-6.

VERGNE, I., CHUA, J., LEE, H. H., LUCAS, M., BELISLE, J. & DERETIC, V. 2005a. Mechanism of phagolysosome biogenesis block by viable *Mycobacterium tuberculosis*. *Proc Natl Acad Sci U S A,* 102**,** 4033-8.

VERGNE, I., CHUA, J., LEE, H. H., LUCAS, M., BELISLE, J. & DERETIC, V. 2005b. Mechanism of phagolysosome biogenesis block by viable *Mycobacterium tuberculosis*. *Proc Natl Acad Sci U S A,* 102.

VERRECK, F. A., DE BOER, T., LANGENBERG, D. M., HOEVE, M. A., KRAMER, M., VAISBERG, E., KASTELEIN, R., KOLK, A., DE WAAL-MALEFYT, R. & OTTENHOFF, T. H. 2004. Human IL-23-producing type 1 macrophages promote but IL-10-producing type 2 macrophages subvert immunity to (myco)bacteria. *Proc Natl Acad Sci U S A,* 101**,** 4560-5.

VERRECK, F. A., DE BOER, T., LANGENBERG, D. M., VAN DER ZANDEN, L. & OTTENHOFF, T. H. 2006. Phenotypic and functional profiling of human proinflammatory type-1 and anti-inflammatory type-2 macrophages in response to microbial antigens and IFN-gamma- and CD40L-mediated costimulation. *J Leukoc Biol,* 79**,** 285-93.

VERRECK, F. A., VERVENNE, R. A., KONDOVA, I., VAN KRALINGEN, K. W., REMARQUE, E. J., BRASKAMP, G., VAN DER WERFF, N. M., KERSBERGEN, A., OTTENHOFF, T. H., HEIDT, P. J., GILBERT, S. C., GICQUEL, B., HILL, A. V., MARTIN, C., MCSHANE, H. & THOMAS, A. W. 2009. MVA.85A boosting of BCG and an attenuated, phoP deficient *M. tuberculosis* vaccine both show protective efficacy against tuberculosis in rhesus macaques. *PLoS One,* 4**,** e5264.

VIJAN, S. 2010. Type 2 diabetes. *Ann Intern Med,* 152**,** ITC31-15; quiz ITC316.

VILLENEUVE, C., GILLERON, M., MARIDONNEAU-PARINI, I., DAFFE, M., ASTARIE-DEQUEKER, C. & ETIENNE, G. 2005. Mycobacteria use their surface-exposed glycolipids to infect human macrophages through a receptor-dependent process. *J Lipid Res,* 46**,** 475-83.

VISINTIN, A., MAZZONI, A., SPITZER, J. H., WYLLIE, D. H., DOWER, S. K. & SEGAL, D. M. 2001. Regulation of Toll-like receptors in human monocytes and dendritic cells. *J Immunol,* 166**,** 249-55.

VISTOLI, G., DE MADDIS, D., CIPAK, A., ZARKOVIC, N., CARINI, M. & ALDINI, G. 2013. Advanced glycoxidation and lipoxidation end products (AGEs and ALEs): an overview of their mechanisms of formation. *Free Radic Res,* 47 Suppl 1**,** 3-27.

VISWANATHAN, V., KUMPATLA, S., ARAVINDALOCHANAN, V., RAJAN, R., CHINNASAMY, C., SRINIVASAN, R., SELVAM, J. M. & KAPUR, A. 2012. Prevalence of diabetes and pre-diabetes and associated risk factors among tuberculosis patients in India. *PLoS One,* 7**,** e41367.

VON REYN, C. F., MTEI, L., ARBEIT, R. D., WADDELL, R., COLE, B., MACKENZIE, T., MATEE, M., BAKARI, M., TVAROHA, S., ADAMS, L. V., HORSBURGH, C. R. & PALLANGYO, K. 2010. Prevention of tuberculosis in Bacille Calmette-Guerin-primed, HIV-infected adults boosted with an inactivated whole-cell mycobacterial vaccine. *Aids,* 24**,** 675-85.

VORDERMEIER, H. M., VENKATAPRASAD, N., HARRIS, D. P. & IVANYI, J. 1996. Increase of tuberculous infection in the organs of B cell-deficient mice. *Clin Exp Immunol,* 106**,** 312-6.

VYNNYCKY, E. & FINE, P. E. 2000. Lifetime risks, incubation period, and serial interval of tuberculosis. *Am J Epidemiol,* 152**,** 247-63.

WALLACE, R. J., JR. 1989. The clinical presentation, diagnosis, and therapy of cutaneous and pulmonary infections due to the rapidly growing mycobacteria, *M. fortuitum* and *M. chelonae*. *Clin Chest Med,* 10**,** 419-29.

WALLEY, A. J., BLAKEMORE, A. I. & FROGUEL, P. 2006. Genetics of obesity and the prediction of risk for health. *Hum Mol Genet,* 15 Spec No 2**,** R124-30.

WALSH, M. C., CAMERLIN, A. J., MILES, R., PINO, P., MARTINEZ, P., MORA-GUZMAN, F., CRESPO-SOLIS, J. G., FISHER-HOCH, S. P., MCCORMICK, J. B. & RESTREPO, B. I. 2011. The sensitivity of interferon-gamma release assays is not compromised in tuberculosis patients with diabetes. *Int J Tuberc Lung Dis,* 15**,** 179-84, i-iii.

WANG, C. S., YANG, C. J., CHEN, H. C., CHUANG, S. H., CHONG, I. W., HWANG, J. J. & HUANG, M. S. 2009. Impact of type 2 diabetes on manifestations and treatment outcome of pulmonary tuberculosis. *Epidemiol Infect,* 137**,** 203-210.

WANG, J., DONG, X., CAO, L., SUN, Y., QIU, Y., ZHANG, Y., CAO, R., COVASA, M. & ZHONG, L. 2016. Association between telomere length and diabetes mellitus: A meta-analysis. *J Int Med Res,* 44**,** 1156-1173.

WANG, J., SANTOSUOSSO, M., NGAI, P., ZGANIACZ, A. & XING, Z. 2004. Activation of CD8 T cells by mycobacterial vaccination protects against pulmonary tuberculosis in the absence of CD4 T cells. *J Immunol,* 173**,** 4590-7.

WANG, J., WAKEHAM, J., HARKNESS, R. & XING, Z. 1999. Macrophages are a significant source of type 1 cytokines during mycobacterial infection. *J Clin Invest,* 103**,** 1023-9.

WANG, L., TURNER, M. O., ELWOOD, R. K., SCHULZER, M. & FITZGERALD, J. M. 2002. A meta-analysis of the effect of Bacille Calmette Guerin vaccination on tuberculin skin test measurements. *Thorax,* 57**,** 804-9.

WANG, T., LAFUSE, W. P. & ZWILLING, B. S. 2000. Regulation of toll-like receptor 2 expression by macrophages following *Mycobacterium avium* infection. *J Immunol,* 165**,** 6308-13.

WEERDENBURG, E. M., PETERS, P. J. & VAN DER WEL, N. N. 2010. How do mycobacteria activate CD8+ T cells? *Trends Microbiol,* 18**,** 1-10.

WEINRICH OLSEN, A., VAN PINXTEREN, L. A., MENG OKKELS, L., BIRK RASMUSSEN, P. & ANDERSEN, P. 2001. Protection of mice with a tuberculosis subunit vaccine based on a fusion protein of antigen 85b and esat-6. *Infect Immun,* 69**,** 2773-8.

WESTERMARK, P., WERNSTEDT, C., O'BRIEN, T. D., HAYDEN, D. W. & JOHNSON, K. H. 1987. Islet amyloid in type 2 human diabetes mellitus and adult diabetic cats contains a novel putative polypeptide hormone. *Am J Pathol,* 127**,** 414-7.

WESTERMARK, P., WERNSTEDT, C., WILANDER, E. & SLETTEN, K. 1986. A novel peptide in the calcitonin gene related peptide family as an amyloid fibril protein in the endocrine pancreas. *Biochem Biophys Res Commun,* 140**,** 827-31.

WEYER, C., BOGARDUS, C., MOTT, D. M. & PRATLEY, R. E. 1999. The natural history of insulin secretory dysfunction and insulin resistance in the pathogenesis of type 2 diabetes mellitus. *J Clin Invest,* 104**,** 787-94.

WHALEN, C. C. 2005. Diagnosis of latent tuberculosis infection: measure for measure. *Jama,* 293**,** 2785-7.

WHITE, A. D., SIBLEY, L., DENNIS, M. J., GOOCH, K., BETTS, G., EDWARDS, N., REYES-SANDOVAL, A., CARROLL, M. W., WILLIAMS, A., MARSH, P. D., MCSHANE, H. & SHARPE, S. A. 2013. Evaluation of the safety and immunogenicity of a candidate tuberculosis vaccine, MVA85A, delivered by aerosol to the lungs of macaques. *Clin Vaccine Immunol,* 20**,** 663-72.

WHO. 2006. World Health Organisaiton, Consultation. Definition and diagnosis of diabetes mellitus and intermediate hyperglycemia, 2006. Available: http://whqlibdoc.who.int/publications/2006/9241594934_eng.pdf.

WHO. 2008. World Health Organisation. Fact sheet: obesity and overweight. Available at: http://www.who.int/mediacentre/factsheets/fs311/en/print.html.

WHO. 2009. Global tuberculosis control: surveillance, planning, financing: World Health Organisation report 2009. Geneva: world Health Organization.

WHO. 2010. New laboratory diagnostic tools for tuberculosis control. Geneva: World Health Organization, 2008. http://whqlibdoc.who. int/publications/2008/9789241597487_eng.pdf.

WHO. 2011a. Rapid implementation of the Xpert MTB/RIF diagnostic test: technical and operational 'how-to': practical considerations. Geneva: World Health Organization, 2011 (http://whqlibdoc.who.int/ publications/2011/9789241501569_eng .pdf). .

WHO. 2011b. Tuberculosis MDR-TB and XDR-TB: 2011 progress report. Geneva: World Health Organization (http://www.who.int/tb/challenges/mdr/factsheet_mdr_progress_march2011.pdf).

WHO. 2013a. Global tuberculosis report, World Health Organization, 2013.

WHO. 2013b. Trade, foreign policy, diplomacy and health of Tuberculosis, World Health Organization, 2013, available at: http://www.who.int/trade/distance_learning/gpgh/gpgh3/en/index7.html.

WHO. 2015. "Tuberculosis". World Health Organization. 2015.

WHO. 2016a. Diabetes Fact sheet. World Health Organisation. October 2016.

WHO. 2016b. Global report on diabetes. World Health Organization, 20 Avenue Appia, 1211 Geneva 27, Switzerland. 1-86.

WHO. 2017. Global Tuberculosis report 2017 © World Health Organization 2017,ISBN 978-92-4-156551-6.

WIELAND, C. W., KNAPP, S., FLORQUIN, S., DE VOS, A. F., TAKEDA, K., AKIRA, S., GOLENBOCK, D. T., VERBON, A. & VAN DER POLL, T. 2004. Non-mannose-capped lipoarabinomannan induces lung inflammation via toll-like receptor 2. *Am J Respir Crit Care Med,* 170**,** 1367-74.

WILDING, J. P., KHANDAN-NIA, N., BENNET, W. M., GILBEY, S. G., BEACHAM, J., GHATEI, M. A. & BLOOM, S. R. 1994. Lack of acute effect of amylin (islet associated polypeptide) on insulin sensitivity during hyperinsulinaemic euglycaemic clamp in humans. *Diabetologia,* 37**,** 166-9.

WILLI, C., BODENMANN, P., GHALI, W. A., FARIS, P. D. & CORNUZ, J. 2007. Active smoking and the risk of type 2 diabetes: a systematic review and meta-analysis. *Jama,* 298**,** 2654-64.

WILLIAMS, N. L., KLOEZE, E., GOVAN, B. L., KORNER, H. & KETHEESAN, N. 2008. *Burkholderia pseudomallei* enhances maturation of bone marrow-derived dendritic cells. *Trans R Soc Trop Med Hyg,* 102 Suppl 1**,** S71-5.

WILLIAMS, N. L., MORRIS, J. L., RUSH, C., GOVAN, B. L. & KETHEESAN, N. 2011. Impact of streptozotocin-induced diabetes on functional responses of dendritic cells and macrophages towards *Burkholderia pseudomallei*. *FEMS Immunol Med Microbiol,* 61**,** 218-27.

WILSON, M. L. 2013. Rapid diagnosis of *Mycobacterium tuberculosis* infection and drug susceptibility testing. *Arch Pathol Lab Med,* 137**,** 812-9.

WINER, D. A., WINER, S., SHEN, L., WADIA, P. P., YANTHA, J., PALTSER, G., TSUI, H., WU, P., DAVIDSON, M. G., ALONSO, M. N., LEONG, H. X., GLASSFORD, A., CAIMOL, M., KENKEL, J. A., TEDDER, T. F., MCLAUGHLIN, T., MIKLOS, D. B., DOSCH, H. M. & ENGLEMAN, E. G. 2011. B cells promote insulin resistance through modulation of T cells and production of pathogenic IgG antibodies. *Nat Med,* 17**,** 610-7.

WINER, S., CHAN, Y., PALTSER, G., TRUONG, D., TSUI, H., BAHRAMI, J., DORFMAN, R., WANG, Y., ZIELENSKI, J., MASTRONARDI, F., MAEZAWA, Y., DRUCKER,

D. J., ENGLEMAN, E., WINER, D. & DOSCH, H. M. 2009. Normalization of obesity-associated insulin resistance through immunotherapy. *Nat Med,* 15**,** 921-9.

WISNIVESKY, J. P., KAPLAN, J., HENSCHKE, C., MCGINN, T. G. & CRYSTAL, R. G. 2000. Evaluation of clinical parameters to predict *Mycobacterium tuberculosis* in inpatients. *Arch Intern Med,* 160**,** 2471-6.

WONG, P. & PAMER, E. G. 2003. CD8 T cell responses to infectious pathogens. *Annu Rev Immunol,* 21**,** 29-70.

WOODWORTH, J. S., WU, Y. & BEHAR, S. M. 2008. *Mycobacterium tuberculosis*-specific CD8+ T cells require perforin to kill target cells and provide protection in vivo. *J Immunol,* 181**,** 8595-603.

WORKNEH, M. H., BJUNE, G. A. & YIMER, S. A. 2017. Prevalence and associated factors of tuberculosis and diabetes mellitus comorbidity: A systematic review. *PLoS One,* 12**,** e0175925.

WRIGHT, E., SCISM-BACON, J. L. & GLASS, L. C. 2006. Oxidative stress in type 2 diabetes: the role of fasting and postprandial glycaemia. *Int J Clin Pract Suppl,* 60**,** 308-314.

WU, Y., LI, H., LOOS, R. J., YU, Z., YE, X., CHEN, L., PAN, A., HU, F. B. & LIN, X. 2008. Common variants in CDKAL1, CDKN2A/B, IGF2BP2, SLC30A8, and HHEX/IDE genes are associated with type 2 diabetes and impaired fasting glucose in a Chinese Han population. *Diabetes,* 57**,** 2834-42.

XIANG, A. H., WANG, C., PETERS, R. K., TRIGO, E., KJOS, S. L. & BUCHANAN, T. A. 2006. Coordinate changes in plasma glucose and pancreatic beta-cell function in Latino women at high risk for type 2 diabetes. *Diabetes,* 55**,** 1074-9.

XU, L., MATROVA, E. & DIETZ, N. E. 2016. *Mycobacterium avium* Infection of Nasal Septum in a Diabetic Adult: A Case Report. *Head Neck Pathol,* 10**,** 552-555.

YADAV, M. & SCHOREY, J. S. 2006. The beta-glucan receptor dectin-1 functions together with TLR2 to mediate macrophage activation by mycobacteria. *Blood,* 108**,** 3168-75.

YAMAMOTO, M., SATO, S., HEMMI, H., HOSHINO, K., KAISHO, T., SANJO, H., TAKEUCHI, O., SUGIYAMA, M., OKABE, M., TAKEDA, K. & AKIRA, S. 2003. Role of adaptor TRIF in the MyD88-independent toll-like receptor signaling pathway. *Science,* 301**,** 640-3.

YAMASHIRO, S., KAWAKAMI, K., UEZU, K., KINJO, T., MIYAGI, K., NAKAMURA, K. & SAITO, A. 2005. Lower expression of Th1-related cytokines and inducible nitric oxide synthase in mice with streptozotocin-induced diabetes mellitus infected with *Mycobacterium tuberculosis*. *Clin Exp Immunol,* 139**,** 57-64.

YAN, J., MENG, X., WANCKET, L. M., LINTNER, K., NELIN, L. D., CHEN, B., FRANCIS, K. P., SMITH, C. V., ROGERS, L. K. & LIU, Y. 2012. Glutathione Reductase Facilitates Host Defense by Sustaining Phagocytic Oxidative Burst and Promoting the Development of Neutrophil Extracellular Traps. *J Immunol (Baltimore, Md. : 1950),* 188**,** 2316-2327.

YANG, S. C., HSUEH, P. R., LAI, H. C., TENG, L. J., HUANG, L. M., CHEN, J. M., WANG, S. K., SHIE, D. C., HO, S. W. & LUH, K. T. 2003. High prevalence of antimicrobial resistance in rapidly growing mycobacteria in Taiwan. *Antimicrob Agents Chemother,* 47**,** 1958-62.

YANG, X. Y., CHEN, Q. F., CUI, X. H., YU, Y. & LI, Y. P. 2010. *Mycobacterium vaccae* vaccine to prevent tuberculosis in high risk people: a meta-analysis. *J Infect,* 60**,** 320-30.

YEAGER, H., JR., LACY, J., SMITH, L. R. & LEMAISTRE, C. A. 1967. Quantitative studies of mycobacterial populations in sputum and saliva. *Am Rev Respir Dis,* 95**,** 998-1004.

YKI-JARVINEN, H. 1992. Glucose toxicity. *Endocr Rev,* 13**,** 415-31.

YOUNG, F., WOTTON, C. J., CRITCHLEY, J. A., UNWIN, N. C. & GOLDACRE, M. J. 2012. Increased risk of tuberculosis disease in people with diabetes mellitus: record-linkage study in a UK population. *J Epidemiol Community Health,* 66**,** 519-23.

YU, K., MITCHELL, C., XING, Y., MAGLIOZZO, R. S., BLOOM, B. R. & CHAN, J. 1999. Toxicity of nitrogen oxides and related oxidants on mycobacteria: *M. tuberculosis* is resistant to peroxynitrite anion. *Tuber Lung Dis,* 79**,** 191-8.

ZENG, C., SHI, X., ZHANG, B., LIU, H., ZHANG, L., DING, W. & ZHAO, Y. 2012. The imbalance of Th17/Th1/Tregs in patients with type 2 diabetes: relationship with metabolic factors and complications. *J Mol Med (Berl),* 90**,** 175-86.

ZHANG, H., POTTER, B. J., CAO, J. M. & ZHANG, C. 2011. Interferon-gamma induced adipose tissue inflammation is linked to endothelial dysfunction in type 2 diabetic mice. *Basic Res Cardiol,* 106**,** 1135-45.

ZHANG, L., ZHANG, H., ZHAO, Y., MAO, F., WU, J., BAI, B., XU, Z., JIANG, Y. & SHI, C. 2012. Effects of *Mycobacterium tuberculosis* ESAT-6/CFP-10 fusion protein on the autophagy function of mouse macrophages. *DNA Cell Biol,* 31**,** 171-9.

ZHANG, M., LV, X. Y., LI, J., XU, Z. G. & CHEN, L. 2008. The characterization of high-fat diet and multiple low-dose streptozotocin induced type 2 diabetes rat model. *Exp Diabetes Res,* 2008**,** 704045.

ZHANG, X., SAADDINE, J. B., CHOU, C. F., COTCH, M. F., CHENG, Y. J., GEISS, L. S., GREGG, E. W., ALBRIGHT, A. L., KLEIN, B. E. & KLEIN, R. 2010. Prevalence of diabetic retinopathy in the United States, 2005-2008. *Jama,* 304**,** 649-56.

ZHANG, Y., BROSER, M., COHEN, H., BODKIN, M., LAW, K., REIBMAN, J. & ROM, W. N. 1995. Enhanced interleukin-8 release and gene expression in macrophages after exposure to *Mycobacterium tuberculosis* and its components. *J Clin Invest,* 95**,** 586-92.

ZHANG, Y., PROENCA, R., MAFFEI, M., BARONE, M., LEOPOLD, L. & FRIEDMAN, J. M. 1994. Positional cloning of the mouse obese gene and its human homologue. *Nature,* 372**,** 425-32.

ZHAO, H. J., WANG, S., CHENG, H., ZHANG, M. Z., TAKAHASHI, T., FOGO, A. B., BREYER, M. D. & HARRIS, R. C. 2006. Endothelial nitric oxide synthase deficiency produces accelerated nephropathy in diabetic mice. *J Am Soc Nephrol,* 17**,** 2664-9.

ZHENG, S., NOONAN, W. T., METREVELI, N. S., COVENTRY, S., KRALIK, P. M., CARLSON, E. C. & EPSTEIN, P. N. 2004. Development of late-stage diabetic nephropathy in OVE26 diabetic mice. *Diabetes,* 53**,** 3248-57.

ZIGNOL, M., VAN GEMERT, W., FALZON, D., SISMANIDIS, C., GLAZIOU, P., FLOYD, K. & RAVIGLIONE, M. 2012. Surveillance of anti-tuberculosis drug resistance in the world: an updated analysis, 2007-2010. *Bull World Health Organ,* 90**,** 111-119d.

ZIMMET, P., COWIE, C., EKOE, J. & SHAW, J. 2004. Classification of Diabetes Mellitus and Other Categories of Glucose Intolerance. Bennet P, (Editor). International textbook of Diabetes Mellitus. Chichester: John Wiley and Sons, 2004:3-15.

ZUMLA, A., RAVIGLIONE, M., HAFNER, R. & VON REYN, C. F. 2013. Tuberculosis. *N Engl J Med,* 368**,** 745-55.

APPENDIX 1

A1.1 General solutions and media

A1.1.1 Single strength culture medium — 50 mL

RPMI 1640 (87%)	43.50 mL
L- glutamine (1%)	0.5 mL
HI-FBS (10%)	5 mL
HEPES (2%)	1 mL
Penicillin/streptomycin	500 µL

A1.1.1.1 L-glutamine stock solution

Aliquot 200 mL (Gibco^{TM} 200 mL bottle, 200 mM), into 5 mL tubes and store at -20°C.

A1.1.1.2 Heat-inactivated foetal bovine serum (HI-FBS)

Defrost Fetal Bovine Serum (Gibco^{TM}, 500 mL bottle, storage -5 to -20^{0}C), then, heat 500 mL of Fetal Bovine Serum (FBS) at 56^{0}C for 25 minutes. Cool to room temperature (RT) and aliquot into 10 mL plastic tubes followed by storage at -20^{0}C until use.

A1.1.1.3 Penicillin and Streptomycin

Gibco^{TM} Pen Strep, 100 mL bottle. This solution contains 10,000 units/mL (i.e 100 U/mL) of Penicillin and 10,000 µg/mL of Streptomycin. Defrost a bottle and aliquot into 5 mL tube, storage -5°C to -20°C. Add 1 mL Gibco^{TM} Pen Strep in 100 mL RPMI/or 5 mL Gibco Pen Strep in 500 mL of RPMI 1640.

A1.1.2 Amikacin sulfate salt (1300 µg/mL)

Amikacin sulfate salt (cat. no A2324-5G, sigma)	13 mg
Distilled water (autoclaved)	10 mL

A1.1.3 Phosphate/ Dulbecco's phosphate-buffered saline/ 1x Cold harvest medium

Sodium chloride (NaCl)	8 g
Sodium dihydrogen orthophosphate (NaH_2PO_4)	0.64 g
Potassium chloride (KCl)	0.2 g
Potassium dihydrogen orthophosphate (KH_2PO_4)	0.16 g

Make up to 950 mL with single distilled water and adjust pH to 7.2 before bringing the final volume to 1000 mL. Autoclave at 121^0C for 15 minutes.

A1.1.4 Trypan blue (0.4%) (w/v) (for 10 mL)

Trypan blue	0.04 g
Distilled water	10 mL

A1.1.5 Ethanol (30%)

Absolute ethanol	30 mL
Distilled water	70 mL

A1.1.6 Ethanol (1%)

Absolute ethanol	1 mL
Distilled water	99 mL

A1.1.7 F68 buffer (0.1%)

F68 buffer stock (10x) (cat. no. P566, Sigma)	1 mL
Distilled water	99 mL

A1.1.8 EDTA (ethylenediaaminetraacetic acid), 0.5 M (pH 8.0)

Disodium EDTA dehydrate	186.1 g
Distilled water	700 mL

Adjust pH to 8.0 with 10 M NaOH. Add water to make 1 litre and autoclave

A1.1.9 10 mM EDTA

EDTA stock 0.5 M	1 mL
1x PBS (autoclaved)	49 mL

A1.1.10 Triton 100x (0.1%)

Triton X-100 (cat. no. X100-100 mL, Sigma)	0.5 mL
Distilled water	500 mL

A1.1.11 Azide buffer

PBS (pH 7.2)	1000 mL
HI-FBS (1%)	10 mL
Sodium Azide (0.1%)	1mL

A1.1.12 Brewer's thioglycollate medium (3%) (w/v)

Brewer's thioglycollate medium	1.5 g
Distilled water	50 mL

A1.1.13 Broncho-alveolar buffer

PBS	500 mL
BSA fraction V (culture graded, Sigma A-2153)	1 g
EDTA (0.25 M)	400 µL

Filter sterilise by 63 µm filter unit

A1.1.14 RBC lysis buffer (1x)

RBC lysis buffer stock (cat no. 004300, eBioscience, 10x)	2 mL
Distilled water	18 mL

A1.1.15 Middlebrook 7H9 liquid medium

Middlebrook 7H9 powder (cat. no. DF0713-17-9, BD Biosciences)	4.7 g
Glycerol (50%, w/v)	10 mL
Tween 80 (20%)	2.5 mL
Distilled water	up to 900 mL

Autoclave it and cool on bench for 30 minutes with stirring

OADC medium (cat. no. 212240, BD Biosciences)	100 mL

A1.1.16 Middlebrook 7H11 solid medium

Middlebrook 7H11 powder (cat. no. DF0838-17-9, BD Biosciences)	21 g
Glycerol (50%, w/v)	10 mL

Autoclave it and cool on bench for 30 minutes with stirring

OADC medium (add before use)	100 mL

A1.1.17 Storage medium for mycobacteria

Middlebrook 7H9 powder	0.47 g
Glycerol (50%, w/v)	90 mL
Tween 80 (20%)	0.25 mL

Autoclave it and cool on bench for 30 minutes

OADC medium (add before use)	10 mL

A1.1.18 Tween 80, 20% (v/v)

Tween 80	20 mL
Distilled water	80 mL

A1.1.19 Carbonate-bicarbonate buffer (100 mL)

Buffer capsule (cat. no. C3041, Sigma)	1
Deionised water	100 mL

A1.1.20 Chloroform: methanol solution (100 mL)

Chloroform	10 mL
Methanol	90 mL

A1.1.21 Neutral buffered formalin (10%)

Formalin (37-40% stock solution)	100 mL
Water	900 mL
NaCl	9 g
Na_2HPO_4 (dibasic/anhydrous)	12 g

A1.1.22 Lithium-heparin stock

Lithium-heparin (1.5 mg/mL or 210 IU/mL)	150 mg
PBS	100 mL

A1.1.23 BD IMag™ buffer (1x working solution)

BD IMag™ buffer (cat. no. 55236, BD Biosciences, 10x)	2 mL
Deionised water	18 mL

A1.2 Staining methods and reagents

A1.2.1 Haematoxylin and Eosin staining

Procedure: Paraffin sections were dewaxed in two changes of xylene (2 minutes each), three changes of graded ethanol (descending concentration; 100 to 70% v/v; 2 minutes, 1 minute and 1 minute) and washed in running tap water (1 minute). The sections were stained with Mayer's haematoxylin (8 minutes) followed by washing in running tap water for 30 seconds, Scott's tap water for 30 seconds and again running tap water for 2 minutes. Slides were then stained with eosin (4 minutes) and washed in running tap water (5 dips). The stained slides were dehydrated through a series of graded ethanol (70 to 100%) and xylene. Slides were mounted in DPX.

A1.2.1.1 Mayer's hamatoxilin

Haematoxylin	2 g
Sodium idodate	4 g
Aluminium sluphate	100 g
Citric acid	2 g
Chlorol hydrate	100 g

Combine ingredients with 2 litres of distilled water

A1.2.1.2 Eosin

Eosin	15 g
Erythrosin	5 g
Calcium chloride	5 g

Combine ingredients with 2 litres of distilled water

A1.2.1.3 Scott's tap water

Sodium carbonate	8.75 g
Magnesium sulphate	50 g

Combine ingredients with 2.5 litres of distilled water

A1.2.2 Modified Herxheimer's staining

Procedure: Frozen sections were stained with Herxheimer's solution (8 minutes) and followed by rinsing with ethanol (70%) and water (2 minutes). Slides were then rinsed in Scott's tap

water substitute for 30 seconds and water. The stained slides were mounded on aqueous mounting media.

A1.2.2.1 Herxheimer's solution

Acetone (saturated with oil Red O and Sudan IV0)	50 mL
Ethanol (70%)	50 mL

A1.2.3 Periodic Acid Schiff's staining

Procedure: Paraffin sections were dewaxed and oxidised in periodic acid (2 minutes) followed by washing in running tap water (5 minutes) and distilled water (twice). Sections were then placed in Schiff's reagent for 10 minutes. Slides were washed again with distilled water (once) and running tap water to stain with Mayer's hematoxylin (30 seconds). After rinsing the sections in water, they were dehydrated through a series of graded ethanol and xylene. The stained slides were mounted in DPX.

A1.2.3.1 Periodic Acid (1%)

Periodic Acid	1 g
Distilled water	100 mL

A1.2.3.2 Schiff's reagent

Basic Fuschin	1 g
Distilled water	200 mL
1 N HCl	20 mL
Sodium metabisulfite	1 g

Dissolve Basic Fuchsin and metabisulfite in HCl and add 200 mL of water. Store in the dark 18-24 hours. Add 2 g of activated charcoal and shake for 1 minute. Remove charcoal by filtration and store the solution in the dark at 0-4°C.

A1.2.4 Ziehl-Neelsen staining

Procedure: Paraffin sections were dewaxed in two changes of xylene (2 minutes each), three changes of graded ethanol (descending concentration; 100 to 70% v/v; 2 minutes, 1 minute and 1 minute) and washed in running tap water (1 minute). The sections were stained in Carbol fuschin. Heat was applied until streaming and left the slide for 5 minutes. The slides were then decolorise using acid alcohol for 10-15 seconds. After washing with tap water, counter

staining was done using 0.5% Methylene blue for 5-10 seconds. The stained slides were dehydrated through a series of graded ethanol (70 to 100%) and xylene. Slides were mounted in DPX.

A1.2.4.1 Carbol fuschin solution

Basic fuschsin	0.3 g
Ethanol (95%, v/v)	10 mL
Phenol (heat-melted crystals)	5 mL
Distilled water	95 mL

A1.2.4.2 Acid Alcohol

Ethanol (95%, v/v)	97 mL
HCl (concentrated)	3 mL

A1.2.4.3 Methylene blue solution (0.5%)

Methylene blue	0.5 g
Distilled water	100 mL

A1.3 Miscellaneous methods and reagents

A1.3.1 Preparation of glucose solution for glucose tolerance test

Method: Glucose solution should be prepared in advance prior (usually before the test day) to the glucose tolerance test (GTT). An appropriate amount of the D-glucose (Ajax Chemicals D-glucose) was measured based on the lean body weight of mice (70 and 90% of the total body mass of mice on energy-dense diet and standard rodent diet; respectively). The required amount of glucose for each mouse is usually delivered through 100 µL of PBS. The total volume of PBS based on total number of animals was calculated. The required amount of D-glucose and PBS was taken into a 70 mL container and mixed until fully dissolved. The fluid was then filtered through a 2 µm syringe filter unit (Millex-GP Syringe Filter Unit). One mL syringes were filled, labelled appropriately and kept in 4^0C until use. For injection, an appropriate sized needle (TERUMO® needle 27G x ½ (#NN+2713R) were used.

D-Glucose Solution

Ajax Chemicals D-glucose ($CH_2OH.CH.(CHOH)_4.O$), 2 g/kg lean body mass

PBS (pH 7.2)	10 mL
TERUMO® syringes (#SS+01T; 1 per cage)	1 cc/mL

TERUMO® needle 27 G x ½ (#NN+2713R; 1 per cage)

Millex-GP Syringe Filter Unit, 0.2 µm (SLGP033RS)

Sarstedt 70 mL container

A1.3.2 Beckman Coulter AU480 methods of analysis

A1.3.2.1 Beckman Coulter AU480 reagents for whole blood and urine analysis

Glucose reagent 1 and 2 (OSR6121)

HbA1c reagent 1 and 2 (OSR6192)

Total haemoglobin reagent (OSR6192)

Haemoglobin denaturant (OSR0004)

Microalbumin reagent 1 and 2 (OSR6167)

Creatinine reagent 1 and 2 (OSR6178)

Control serum 1 and 2 (ODC0003, ODC0004)

Thermo Scientific MAS Diabetes 1 and 2 (DBCL-MP)

Thermo Scientific MAS Omni•CORE™ (OCR-101)

Bio-Rad Liquichek® Urine Chemistry Control 1 and 2

System calibrator (ODC66300)

Urine calibrator (ODC0025)

HbA1c calibrator (ODR3032)

Microalbumin calibrator (ODR3024)

Beckman Coulter 0.5 mL sample cups (#651412)

Cartel Cobas Cups (#2940-04)

Method: Daily maintenance and calibration were done according to the manufacturer's instructions. Samples were analysed if quality control samples were within the acceptable ranges. Test samples were distributed into Beckman Coulter sample cups (#651412) or Cartel Cobas Cups (#2940-04) depending on the volume available and into appropriate racks (blood or urine sample racks) in order from rack 1 to 20.

A1.3.3 Sterilisation of mycobacterial samples

Method: The mycobacterial cultures ($1.5x10^7$ CFU/ 100 µL for *M. tuberculosis* H37Rv and $3.5x10^6$ CFU/100 µL for *M. bovis* BCG) were treated with paraformaldehyde (PFA) solution (3.33%). A 100 µL of the mycobacterial culture was treated with 500 µL of the PFA for 0, 30, 40 and 50 minutes. In the control groups, PBS was used instead of the PFA. Immediately after the end of timepoint, the PFA and PBS treated culture tubes were washed with PBS and

resuspended into the initial volume. Then, 200 µL of the treated bacterial culture from each tube were plated on 7H11 agar plates. The plates were checked for the growth of the bacteria following incubation at 37^0C for 3-4 weeks. The untreated bacterial cultures were also plated to confirm the presence of the mycobacteria in the suspension as positive control (Figure A1.1).

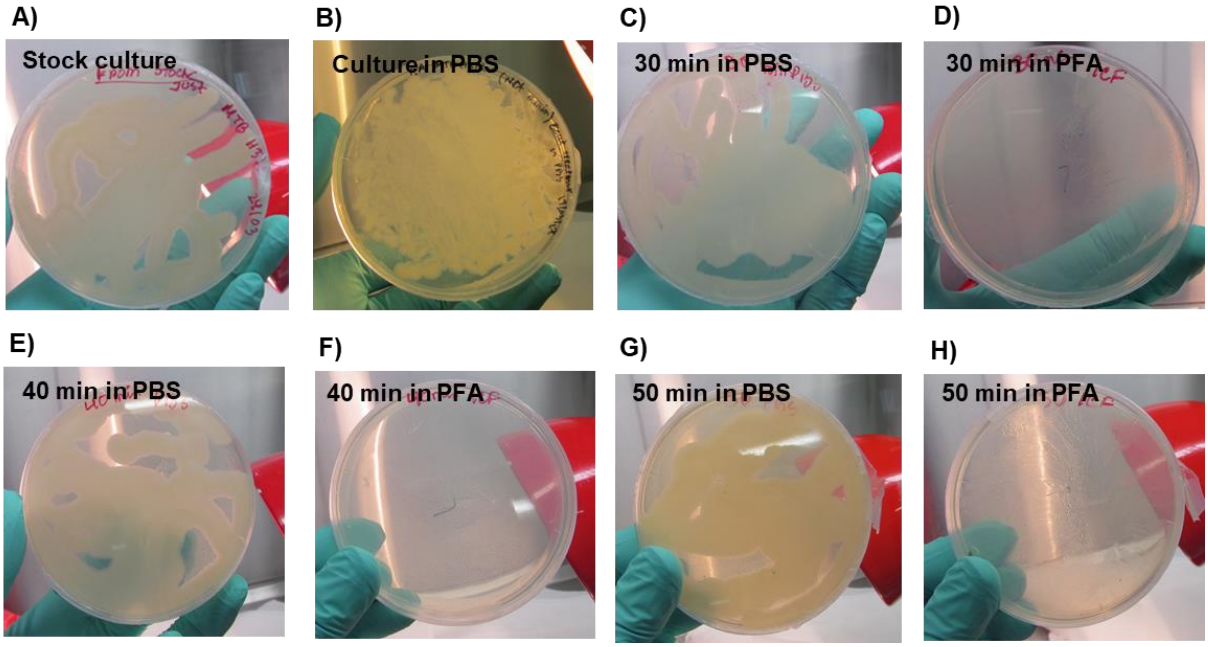

Figure A1.1 Sterility checking of the pure culture of *M. tuberculosis* (H37Rv) after paraformaldehyde treatment

The pure culture of *M. tuberculosis* (H37Rv) was treated with 3.33% paraformaldehyde (PFA) and phosphate buffer saline (PBS). There was no mycobacterial growth in PFA treated culture (clear agar plates), whereas numerous bacterial growth was observed in the PBS treated culture (deep white/cream colour on the agar plates). The photographs illustrate the pure culture without any treatment (A), pure culture in PBS (B), culture treated with PBS *versus* (*vs*) PFA at 30 minutes (C *vs* D), 40 minutes (E *vs* F) and 50 minutes (G *vs* H) post treatment.

APPENDIX 2

Supplementary data from mouse model characterisation study (Chapter 4)

Table A2.1 Feed intake by JCU bred mice (week 1 to 30) on standard rodent diet and energy-dense diet

Week	JCU bred mice, feed intake/mouse/day					
	SRD		EDD			
	No. cages	Mean(g)±SEM	No. cages	Mean(g)±SEM	p-value	Level of significance
1	7	3.90±0.00	8	2.95±0.04	0.1158	ns
2	7	3.90±0.00	8	3.34±0.34	0.9359	ns
3	7	3.90±0.00	8	2.98±0.13	0.1535	ns
4	7	3.52±0.21	8	3.10±0.15	0.9984	ns
5	7	3.85±0.03	8	3.57±0.29	>0.9999	ns
6	7	3.75±0.08	8	3.55±0.41	>0.9999	ns
7	7	3.76±0.08	8	3.07±0.19	0.6630	ns
8	7	3.70±0.06	8	3.07±0.21	0.8261	ns
9	7	3.66±0.08	8	3.98±0.59	>0.9999	ns
10	7	3.49±0.14	8	3.33±0.13	>0.9999	ns
11	7	3.85±0.05	8	4.34±0.76	0.9872	ns
12	7	4.57±0.28	8	3.27±0.22	0.0027	**
13	7	3.90±0.00	8	3.68±0.21	>0.9999	ns
14	7	4.37±0.13	8	3.54±0.13	0.3178	ns
15	7	3.95±0.11	8	4.41±0.74	0.9957	ns
16	7	4.00±0.10	8	3.98±0.36	>0.9999	ns
17	7	4.06±0.09	8	3.67±0.17	0.9998	ns
18	7	4.30±0.08	8	3.24±0.07	0.0397	*
19	7	4.15±0.09	8	3.41±0.20	0.5341	ns
20	7	4.11±0.13	8	3.66±0.09	0.9975	ns
21	7	4.21±0.14	8	3.79±0.25	0.9990	ns
22	7	4.31±0.07	8	3.24±0.16	0.0371	*
23	7	4.22±0.11	8	3.98±0.32	>0.9999	ns
24	7	4.42±0.04	8	3.30±0.11	0.0212	*
25	7	3.97±0.04	8	3.57±0.12	0.9995	ns
26	7	4.14±0.11	8	3.25±0.05	0.1947	ns
27	7	4.38±0.09	8	3.57±0.12	0.3364	ns
28	7	4.28±0.08	8	3.63±0.08	0.8006	ns
29	7	3.91±0.14	8	3.19±0.10	0.6101	ns
30	7	3.91±0.14	8	3.19±0.10	0.6101	ns

Statistical analysis: Data were analysed using the two-way ANOVA with Sidak's multiple comparisons test. The level of significance was indicated as *p≤0.05, **p≤0.01 and ns=non-significant. In the table, SRD; Standard rodent diet, EDD; Energy-dese diet. Each mouse cage contains 5 mice.

Table A2.2 Energy intake by JCU bred mice (week 1 to 30) on standard rodent diet and energy-dense diet

Week	JCU bred mice, energy intake/mouse/day					
	SRD		EDD			
	No. cages	Mean(kcal) ±SEM	No. cages	Mean (kcal)±SEM	p-value	Level of significance
1	7	11.97±0.00	8	14.08±0.19	0.9961	ns
2	7	11.97±0.00	8	15.94±1.00	0.2588	ns
3	7	11.50±0.33	8	14.25±0.63	0.9001	ns
4	7	10.82±0.66	8	14.79±0.72	0.2576	ns
5	7	11.81±0.09	8	17.07±1.37	0.0198	*
6	7	11.52±0.24	8	16.97±1.94	0.0126	*
7	7	11.55±0.25	8	14.65±0.89	0.7398	ns
8	7	11.37±0.18	8	14.69±1.00	0.6121	ns
9	7	11.24±0.25	8	19.01±2.82	<0.0001	****
10	7	10.70±0.44	8	15.89±0.63	0.0229	*
11	7	11.82±0.15	8	20.76±3.65	<0.0001	****
12	7	14.02±0.88	8	15.60±1.06	>0.9999	ns
13	7	11.97±0.00	8	17.58±0.99	0.0086	**
14	7	13.47±0.35	8	16.93±0.63	0.5251	ns
15	7	12.12±0.34	8	21.06±3.52	<0.0001	****
16	7	12.28±0.32	8	19.01±1.74	0.0004	***
17	7	12.46±0.28	8	17.56±0.81	0.0285	*
18	7	13.20±0.23	8	15.46±0.34	0.9896	ns
19	7	12.75±0.29	8	16.30±0.96	0.4670	ns
20	7	12.61±0.39	8	17.51±0.45	0.0432	*
21	7	12.93±0.43	8	18.12±1.18	0.0229	*
22	7	13.24±0.23	8	15.49±0.74	0.9901	ns
23	7	12.97±0.34	8	19.03±1.53	0.0027	**
24	7	13.58±0.12	8	15.77±0.51	0.9935	ns
25	7	12.19±0.12	8	17.06±0.60	0.0470	*
26	7	12.71±0.35	8	15.53±0.25	0.8737	ns
27	7	13.46±0.27	8	17.04±0.55	0.4541	ns
28	7	13.13±0.25	8	17.37±0.37	0.1632	ns
29	7	11.99±0.44	8	15.26±0.46	0.6430	ns
30	7	11.99±0.44	8	15.26±0.46	0.6430	ns

Statistical analysis: Data were analysed using the two-way ANOVA with Sidak's multiple comparisons test. The level of significance was indicated as *p≤0.05, **p≤0.01, ***p≤0.001, ****p≤0.0001 and ns=non-significant. In the table, SRD; Standard rodent diet, EDD; Energy-dese diet. Each mouse cage contains 5 mice.

Table A2.3 Body weight of JCU bred mice (week 1 to 30) on standard rodent diet and energy-dense diet

Week	JCU bred mice, body weight					
	SRD		EDD			
	Number	Mean(g)±SEM	Number	Mean (g)±SEM	p-value	Level of significance
0	35	15.49±0.29	35	15.03±0.43	>0.9999	ns
1	35	18.00±0.22	35	20.14±0.32	0.0398	*
2	35	18.81±0.24	35	22.62±0.28	<0.0001	****
3	35	19.22±0.23	35	24.54±0.31	<0.0001	****
4	35	21.18±0.24	35	25.82±0.32	<0.0001	****
5	35	21.93±0.21	35	27.43±0.36	<0.0001	****
6	35	21.39±0.32	35	28.53±0.40	<0.0001	****
7	35	21.84±0.35	35	29.40±0.45	<0.0001	****
8	35	23.15±0.28	35	29.84±0.56	<0.0001	****
9	34	23.69±0.30	35	31.05±0.53	<0.0001	****
10	34	23.79±0.33	35	31.91±0.64	<0.0001	****
11	34	23.96±0.26	35	32.82±0.64	<0.0001	****
12	34	25.53±0.25	35	33.33±0.65	<0.0001	****
13	34	25.87±0.21	35	34.12±0.67	<0.0001	****
14	34	26.07±0.23	35	34.99±0.68	<0.0001	****
15	34	25.91±0.25	35	36.63±0.74	<0.0001	****
16	34	26.33±0.25	35	37.99±0.77	<0.0001	****
17	34	26.61±0.25	35	38.74±0.77	<0.0001	****
18	34	27.18±0.25	35	39.91±0.81	<0.0001	****
19	34	26.93±0.25	35	41.13±0.81	<0.0001	****
20	34	27.07±0.23	35	42.05±0.76	<0.0001	****
21	34	27.45±0.24	35	42.80±0.72	<0.0001	****
22	34	27.42±0.29	35	42.99±0.72	<0.0001	****
23	34	28.31±0.29	35	44.24±0.68	<0.0001	****
24	34	27.61±0.26	35	44.43±0.67	<0.0001	****
25	34	27.75±0.26	35	44.41±0.65	<0.0001	****
26	34	28.14±0.28	35	43.44±0.67	<0.0001	****
27	34	27.65±0.31	35	44.53±0.70	<0.0001	****
29	34	28.04±0.26	35	45.90±0.70	<0.0001	****
30	34	27.86±0.29	35	46.31±0.69	<0.0001	****

Statistical analysis: Data were analysed using the two-way ANOVA with Sidak's multiple comparisons test. The level of significance was indicated as *p≤0.05, ****p≤0.0001 and ns=non-significant. In the table, SRD; Standard rodent diet, EDD; Energy-dese diet.

Table A2.4 Glucose tolerance test of JCU and ARC bred mice on standard rodent diet and energy-dense diet at 25th and 30th week of diet intervention

JCU bred mice, 25th week,						
Time (minutes)	**Number**	**SRD (mmol/L)**	**Number**	**EDD (mmol/L)**	**p-value**	**Level of significance**
Baseline	35	7.83±0.27	34	9.09±0.34	0.5138	ns
15	35	21.12±0.81	34	20.60±0.63	0.9780	ns
30	35	17.75±0.75	34	20.73±0.82	0.0021	**
60	35	12.44±0.62	34	16.81±0.64	<0.0001	****
120	35	8.34±0.32	34	11.16±0.34	0.0041	**
JCU bred mice, 30th week						
Baseline	35	8.50±0.25	34	8.80±0.25	0.9905	ns
15	35	17.33±0.48	34	19.41±0.58	0.0017	**
30	35	12.95±0.40	34	17.89±0.67	<0.0001	****
60	35	11.04±0.29	34	13.21±0.42	0.0010	***
120	35	8.72±0.22	34	10.10±0.24	0.0821	ns
ARC bred mice, 25th week						
Baseline	40	7.70±0.15	39	9.02±0.17	0.0767	ns
15	40	17.31±0.55	39	20.47±0.45	<0.0001	****
30	40	12.19±0.43	39	17.95±0.55	<0.0001	****
60	40	10.37±0.34	39	14.96±0.46	<0.0001	****
120	40	7.48±0.24	39	10.57±0.22	<0.0001	****
ARC bred mice, 30th week						
Baseline	40	8.67±0.23	39	9.34±0.23	0.7998	ns
15	40	17.99±0.52	39	18.91±0.47	0.5204	ns
30	40	13.65±0.48	39	17.01±0.64	<0.0001	****
60	40	10.83±0.34	39	15.57±0.59	<0.0001	****
120	40	8.46±0.22	39	11.73±0.42	<0.0001	****

Statistical analysis: Data were analysed using the two-way ANOVA with Sidak's multiple comparisons test. Data presented as mean±SEM. The level of significance was indicated as **p≤0.01, ***p≤0.001, ****p≤0.0001 and ns=non-significant. In the table, SRD; Standard rodent diet, EDD; Energy-dese diet.

Table A2.5 Histological features of JCU bred mice on standard rodent diet and energy-dense diet at 30th week of the diet intervention

Replicate	Herxheimer's stained area in liver (%)		Adipocyte size (µm²)		Islet area on pancreatic area (%)		PAS+ stained area in kidney (%)		Glomerular area (µm²)	
	SRD	**EDD**	**SRD**	**EDD**	**SRD**	**EDD**	**SRD**	**EDD**	**SRD**	**EDD**
R1	0	40.6	585.94	1157.15	0.91	0.76	19.12	18.49	986.57	2612.7
R2	0	15.64	547.23	1331.55	0.38	1.38	15.79	27.87	1067.44	1867.84
R3	0.04	42.56	420.64	1027.86	1	1.74	27.89	26.08	1448.69	2252.97
R4	0.02	30.74	615.48	1956.56	0.73	1.97	16.1	31.31	1213.88	2228.16
R5	0.02	16.34	333.75	2415.48	0.55	3.25	15.17	18.28	1474.63	1990.05
R6	0.12	32.11	343.42	1586.15	0.25	1.13	10.51	26.72	1402.71	2088.95
R7	0.02	28.64	966.21	1773.49	0.67	1.27	13.3	19.89	1680.93	2860.31
R8	0.12	26.06	113.85	1862.63	1.23	2.42	23.28	24.02	1291.99	2400.42
R9	0.02	27.2	283.55	2135.93	1.11	0.97	18.77	21.15	1706.08	2701.74
R10	1.9	30.9	817.6	2655.52	0.81	1.33	14.02	27.22	1616.6	2111.81
R11	0.6	34.62	513.83	2104.62	1.28	1.42	14.62	19.24	1157.9	2531.65
R12	0.44	33.52	412.92	2326.75	0.29	2.11		33.12	1887.93	2110.03
R13	0.2	36.92	561.63	1826.38	0.21	0.89		23.69	1131.61	2143.98
R14	0	13.18	327.11	1936.27	0.38	0.59		34.27	1885.41	2638.28
R15	0	21.6	604.39	2138.69	0.49	1.05		27.03		1592.28
R16	0.18	21.6		2227.89	0.42	1.42				
R17	0			3188.6	0.55	2.06				
R18	0.08				0.65	0.96				
R19	0.1				1.16	2.41				
R20	0.08				0.37	0.7				
R21	0.06				0.93	1.01				
R22					0.45					
R23					0.21					
R24					0.54					
R25					0.2					
R26					0.72					
R27					0.21					
Mean ± SEM	**0.19± 0.19**	**28.26± 2.20**	**496.50± 55.54**	**1979.50 ±130.0**	**0.62± 0.06**	**1.47± 0.14**	**17.14± 1.48**	**25.23± 1.34**	**1425.17 ±79.52**	**2275.41 ±89.27**
p-value	**** <0.0001♦		***** <0.0001		**** <0.0001		*** <0.0005		***** <0.0001	

Statistical analysis: Data were checked for normality using Shapiro-Wilk's test. Data passed the test if p≥0.05. The normality distributed data were compared between groups using the unpaired *t*-test with Welch's correction. The non-normally distributed data (♦) were compared between groups using Mann-Whitney U test. Data presented as mean±SEM. The level of significance was indicated as ***p≤0.0001 and ****p≤0.0001. In the table, SRD; Standard rodent diet, EDD; Energy-dese diet.

Table A2.6 Calculation of percentage of diabetic mice based on baseline fasting blood glucose in JCU and ARC bred mice on energy-dense diet at 25th and 30th week of diet intervention

Baseline fasting blood glucose level (mmol/L)							
25th week				30th week			
JCU bred mice, Upper 99% CI of mean >9.86		ARC bred mice, Upper 99% CI of mean >9.57		JCU bred mice, Upper 99% CI of mean >9.35		ARC bred mice, Upper 99% CI of mean >10.11	
SRD	EDD	SRD	EDD	SRD	EDD	SRD	EDD
6.8	**11.7**	11	**9.9**	7.3	**15.5**	12.4	**14.4**
9	9	9.5	**12**	9	6.9	11.7	**12.3**
11.5	**13.9**	9.2	**12.9**	8.8	**13.9**	8.7	**15.8**
9.5	**11.4**	11	8.6	7	**13.5**	12	**12.8**
10.4	5.8	11.9	**12.9**	9.4	7.6	7.9	**12.9**
8.9	8.4	8.2	**12.1**	8.9	**10.5**	8	**10.9**
8.4	**14.5**	9.4	**11.9**	11.3	**14.4**	11.2	**13**
9.1	8.4	6.9	**14.4**	10.8	**12.1**	11.1	9.7
8.9	7.5	10.6	**10.5**	11.3	**10.6**	8.2	**12.4**
13.5	9.2	9.5	7.2	10.3	**11.9**	11.3	**10.8**
9.8	**9.8**	10.4	**12.2**	10.7	7.7	9.9	**12.2**
9.7	**10**	8.9	**10.3**	8.7	**10.8**	10.4	**14.2**
8.3	**13.1**	9.7	**11.6**	8.9	**13.3**	11.4	**13.7**
10.9	**10.2**	11.5	**11.8**	8.5	7.4	8.2	8.2
9	**10.2**	9.7	**12**	8.7	7.5	7.5	**10.5**
9.7	**11.4**	6.6	8.2	9	**13.4**	8.1	9.4
8.2	8.3	8.6	**10.8**	8.7	**10**	11.3	9.3
7.3	8	7.8	7.1	8.9	7.5	10	9.7
8.9	**11**	8.7	8.7	6.9	**12.5**	11.5	9.4
10.6	**13.3**	7.1	7.9	7	**12.2**	11.5	**10.8**
8	**11**	7.7	**12.6**	7.4	**11.2**	6.5	**12.7**
10.7	**9.4**	6.9	**11.9**	5.7	**10.3**	7.7	**14.8**
8.2	**15.1**	7.3	**11.4**	5.4	**14.5**	8.8	**13.2**
7.7	9.7	5.9	**13**	10	**13.9**	8.2	**10.7**
12.3	**10.4**	7.1	**13.4**	6.3	6.8	6.5	**13.4**
6.5	**9.9**	10.3	**14**	8.4	9.3	10.9	**11.3**
5.8	**12.4**	10.2	**13.9**	9.5	**12.1**	7.1	**13.8**
9.5	**13.2**	9.5	**9.8**	8.9	**12.5**	8.8	**13.8**
7.5	**10.6**	6	**14.7**	7.5	**9.8**	9.5	9.6
9.9	**10.4**	11.2	**13.4**	9.3	**12.9**	9.2	**10.9**
8.1	**10.3**	8.7	7	8.5	**13.2**	9.5	**10.6**
7.8	**10.2**	8.1	**13.2**		**13.5**	10.1	**12.6**
10.5	8.4	10.9	8.7		**11.8**	7.5	**10.5**
10	**9.9**	8.2	**10.6**		**9.4**	6.4	**14.7**
8.3		8	**10.1**			8	**13.7**
		9.3	**13.5**			6.4	**14.1**
		8.6	**12.9**			10.1	8.6
		8.9	**13.2**			6.8	8.8
		9.5				11.7	
		8.1				11.2	
% diabetic	**67.64% (23/34)**		**78.94% (30/38)**		**76.47% (26/34)**		**76.31% (29/38)**
Note: Mice on EDD considered T2D if they demonstrated a raised fasting blood glucose at levels higher the upper 99% confidence interval (CI) for the mean of age-matched control group fed on a standard rodent diet.							

SRD; Standard rodent diet, EDD; Energy-dese diet.

Table A2.7 Calculation of percentage of diabetic mice based HbA1c in JCU and ARC bred mice on energy-dense diet at 25th and 30th weeks of diet intervention

HbA1c (%)							
25th week				**30th week**			
JCU bred mice, Upper 99% CI of mean >2.76		**ARC bred mice, Upper 99% CI of mean >2.85**		**JCU bred mice, Upper 99% CI of mean >2.56**		**ARC bred mice, Upper 99% CI of mean >2.72**	
SRD	EDD	SRD	EDD	SRD	EDD	SRD	EDD
1.65	**2.81**	2.69	**3.39**	2.15	**3.09**	2.49	**3.46**
2.34	2.11	2.7	2.81	2.7	2.47	2.53	**2.71**
2.27	2.4	2.44	**3.46**	2.48	2.09	2.6	**3.47**
2.44	**3.14**	3.07	2	1.14	**3.01**	1.37	**3.01**
2.4	**3.33**	2.14	2.79	2.64	**3.09**	2.19	**3.18**
2.81	2.75	3.33	**2.95**	2.58	**2.71**	2.49	**2.87**
2.93	**2.77**	2.55	2.62	2.39	**2.69**	2.77	2.58
3.14	2.68	3.16	**3.08**	2.23	**2.78**	2.44	**2.98**
2.8	**3.03**	3.13	**3.01**	2.97	**2.72**	2.99	**2.93**
2.67	**2.94**	3.53	2.67	2.9	**2.28**	2.91	2.55
2.95	1.67	3.06	**2.88**	2.88	**3.19**	2.67	**3.29**
3.05	2.61	2.61	**3.43**	2.7	2.48	2.66	2.8
2.74	**3.01**	2.98	**3.04**	2.58	**2.82**	2.29	**3.32**
2.82	2.7	3.05	**3.12**	1.84	**2.78**	3.07	**3.08**
3.03	**2.81**	1.9	**2.88**	1.72	**2.6**	2.95	**3.12**
2.77	2.51	2.38	**3.08**	2.74	**2.74**	2.91	**2.88**
2.49	**2.81**	2.5	**3.22**	1.97	2.55	3.29	**2.95**
2.86	**2.85**	3.06	2.73	1.87	2.54	2.59	1.74
3.09	**3.02**	2.72	**3.04**	2.47	3.13	2.4	**2.89**
2.18	**3.62**	2.56	**3.23**	2.27	**2.73**	1.88	2.49
2.16	**3.08**	2.87	**2.96**	2.37	**2.82**	2.87	2.53
1.88	**3.1**	1.79	**3**	1.67	**2.99**	1.56	2.68
2.02	**3.29**	2.63	**3.01**	2.12	**2.76**	2.47	**3.09**
2.85	**3.2**	2.52	**3.15**	2.54	2.38	2.37	2.82
1.55	**2.79**	1.92	2.84	2.67	**2.65**	1.42	**2.86**
2.5	2.17	3.34	2.74	2.23	**2.63**	2.34	**2.93**
3.15	2.75	2.99	**2.99**	2.34	2.51	2.4	**2.99**
2.32	2.73	2.85	2.61	2.4	**2.71**	1.9	1.89
2.68	**2.91**	2.2	**2.92**		**2.96**	2.61	**2.85**
1.8	**3.07**	3	1.92		**2.05**	2.85	**2.79**
2.47	**3.07**	2.88	**2.91**			2.53	2.15
	3.37	2.38	**3.31**			1.5	**3.06**
	2.46	3.09	2.02			2.77	**3.03**
	2.77	1.94	**2.98**			2.19	**2.82**
		2.56	**2.92**			2.61	**3.12**
		2.59	**2.85**			2.91	**2.75**
		2.36	**2.92**			3.45	**2.78**
		2.56	2.7			2.29	**2.75**
		2.28				2.96	
		2.72				2.98	
% diabetic	**64.70% (22/34)**		**68.42% (26/38)**		**73.33% (22/30%)**		**76.31% (29/38)**

Note: Mice on EDD considered T2D if they demonstrated a raised HbA1c at levels higher the upper 99% confidence interval (CI) for the mean of age-matched control group fed on a standard rodent diet.

In the table, SRD; Standard rodent diet, EDD; Energy-dese diet.

Table A2.8 Calculation of percentage of diabetic mice based on area under the curve in JCU and ARC bred mice on energy-dense diet at 25th and 30th weeks of diet intervention

GTT (AUC)							
25th week				**30th week**			
JCU bred mice, Upper 99% CI of mean >1757		**ARC bred mice, Upper 99% CI of mean >1381**		**JCU bred mice, Upper 99% CI of mean >1454**		**ARC bred mice, Upper 99% CI of mean >1481**	
SRD	EDD	SRD	EDD	SRD	EDD	SRD	EDD
1178	**1826**	1445	**1799**	1144	**1453**	1486	**1787**
1429	1334	1516	**1488**	1277	1364	1449	**2226**
1919	1712	1237	**1697**	1101	**1965**	1897	**2771**
1871	**1900**	1652	**1695**	1352	**1742**	1461	**1888**
1556	1724	1745	**1622**	1469	**1594**	1435	**2363**
1784	1627	1103	**1787**	990	**1692**	1447	**1637**
1526	**1728**	1219	**1895**	1440	**2157**	1568	**1870**
2429	1460	1129	**1656**	1451	**1540**	976.5	**1790**
1987	**2315**	1203	**1694**	1447	**1571**	1043	**1895**
1961	**1991**	1196	**1802**	1552	1367	1626	1421
1512	**2047**	1444	**1737**	1460	**1490**	1491	1393
1775	**1868**	1414	**2027**	1732	**1463**	1671	1409
1078	**2151**	1319	**1829**	1536	**1929**	1274	**2006**
1706	1703	1447	**2111**	1384	1365	1467	**1534**
2345	1527	1590	1188	1163	**1646**	1830	**1666**
1829	**1770**	923.3	**1752**	1341	1352	1265	**1620**
1514	1318	744	**2032**	1402	1139	1220	**2086**
1787	**1912**	1055	**2504**	1497	1443	1494	1349
1934	**1998**	870.8	1256	1409	**1905**	1505	1402
1004	**2488**	953.3	**1750**	1552	**1831**	1410	**1746**
1893	**2135**	1058	**1709**	1217	**1850**	1020	**1635**
1713	**2618**	1019	**1738**	1550	1406	1097	1395
1643	**2655**	1152	**1770**	1294	**2183**	1268	**1490**
1840	**2297**	1257	**1827**	1020	**1646**	1222	**2263**
1487	**1943**	894	**2282**	1551	**1859**	955.5	**1721**
591.8	1713	1582	**1517**	1188	**1482**	1499	**2082**
1218	**2252**	1406	**1478**	1081	**1954**	1112	**2171**
1389	**1987**	1465	**1696**	1487	**1691**	1334	**1996**
1507	**2001**	1183	**1861**	1238	**1873**	1265	**1925**
1673	**2676**	1243	**1835**	1469	**1625**	1190	**2105**
1245	**2054**	1316	**1745**	1481	**1668**	1617	**1686**
1256	1722	1433	**1724**	1397	**1983**	1254	**2261**
1236	1642	1589	**2066**	1414	**1674**	1835	**1933**
1359	1695	1327	**1577**	1393	1432	1191	**1856**
1292		1487	**2043**	1595		1433	**1476**
		1449	**1922**			1307	**1499**
		1278	**1581**			1599	1300
		1424	**1578**			1302	1331
		1256	**1718**			1487	
		1272				1329	
% diabetic	**64.70% (22/34)**		**94.43% (37/39)**		**76.64% (26/34)**		**78.94% (30/38)**

Note: Mice on EDD considered T2D if they demonstrated a raised glucose tolerance test-Area under the curve (GTT-AUC) at levels higher the upper 99% confidence interval (CI) for the mean of age-matched control group fed on a standard rodent.

In the table, SRD; Standard rodent diet, EDD; Energy-dese diet.

Table A2.9 Calculation of percentage of diabetic mice based fasting blood glucose (2 hours post-glucose challenge) in JCU and ARC bred mice on energy-dense diet at 25th and 30th weeks of diet intervention

FBG (2 hours post-glucose challenge, mmol/L)							
25th week				30th week			
JCU bred mice, Upper 99% CI of mean >9.22		ARC bred mice, Upper 99% CI of mean >8.13		JCU bred mice, Upper 99% CI of mean >9.32		ARC bred mice, Upper 99% CI of mean >9.05	
SRD	EDD	SRD	EDD	SRD	EDD	SRD	EDD
6.4	**11.7**	8.2	**9.8**	6.7	**10.7**	9.5	**11.3**
7	8.5	9.9	**9.2**	7.9	**9.4**	8.5	**17.1**
8.9	**11**	8.1	**9.3**	7.4	**11.4**	10.1	**18.8**
8.6	**14**	10.3	**10**	9.1	8.9	9.1	**14**
10.2	8.4	8.2	7.6	11	7.4	8.5	**14.2**
10.2	**10.7**	7.4	**11**	7.8	**10.5**	9.2	**10.7**
8.5	**9.9**	7.4	**11.4**	10.1	**11.3**	9.4	**9.4**
13.2	**9.7**	7.2	**9.7**	10.1	9	7.5	**12**
11.6	**11.9**	7.4	**11.3**	9.8	**9.6**	8.3	**12.2**
9.7	**11.2**	6.4	**10.9**	10.3	8.8	8.6	**9.9**
8	**12**	7.3	**12.2**	8.6	**9.8**	8.6	**9.4**
10	**11.2**	7.7	**10**	11.5	9	9.9	8.9
7.4	**12.5**	6.8	**9.7**	9.5	**10.8**	7.7	**11.8**
9.5	8	8.2	**11.9**	7	8.3	8.7	**10.7**
10.6	8.9	8.4	**8.1**	9.3	**11.7**	11	**9.8**
7.1	9.2	5.3	**10.8**	8.5	8.9	7.9	**10.4**
7	7.5	5.3	**12**	7.9	8	8.1	**13.1**
9.7	**11.7**	5.3	**9.7**	9.2	8.7	8.1	8.5
9.5	**11.5**	4.9	**7.4**	7.4	**10.7**	9.5	8
6.5	**14.1**	4.7	**11.7**	8.2	**11.7**	8.7	**12.7**
9.6	**14.2**	5.2	**10.8**	7.7	**10.8**	5.7	8.4
8.8	**13.7**	5.5	**10.4**	9.8	**9.8**	6.9	8.3
7.5	**13.9**	5.9	**11.8**	8.2	**12.8**	5.6	**10**
9.2	**12.5**	6.9	**13.9**	6.5	**10.1**	7	**15.4**
8.9	**9.9**	4.6	**12.9**	10.6	9	4.9	**12.8**
2.8	**12.7**	9.4	**10.1**	7.9	**11.3**	8.9	**15.4**
7.8	**13.7**	9	**10**	5.4	**12.5**	7.3	**15.2**
7.7	**13.5**	8.3	**9.8**	9.3	**9.2**	8.5	**14.3**
7.3	**11.4**	6.8	**11.7**	9	**11.1**	7.4	**13.2**
10	**11.8**	7.6	**10.3**	8.8	**10.2**	8	**13.1**
6.5	**11.3**	9.2	**11.9**	8.9	**9.4**	10.9	**10.4**
6	**10.3**	7.3	**9.7**	8.6	**13.3**	7.8	**13.7**
6.7	8.2	9.2	**12.9**	9	8.8	11.7	**12.8**
7	8.7	7.4	**11.4**	8.7	**10.4**	7.8	**11.9**
6.4		10.1	**11.2**	9.4		8.8	**9.8**
		9.2	**10.5**			9.1	**9.9**
		8.4	**9.8**			9.1	**9.4**
		8	**9.1**			7.4	8.7
		8	**10.4**			9.4	
		8.6				9.3	
% diabetic	**76.47% (26/34)**		**97.43% (38/39)**		**67.64% (23/34)**		**84.21% (32/38)**

Note: Mice on EDD considered T2D if they demonstrated a raised FBG (2 hours post-glucose challenge) levels higher the upper 99% confidence interval (CI) for the mean of age-matched control group fed on a SRD.

In the table, SRD; Standard rodent diet, EDD; Energy-dese diet, FBG; Fasting blood glucose

Table A2.10 Calculation of percentage of diabetes mice based on histological findings at 30 weeks of the energy-dense diet intervention of JCU bred mice

ACR, Upper 99% CI of mean >1.30		Islet area on pancreas (%), Upper 99% CI of mean >0.80		% PAS+ stain on kidney, Upper 99% CI of mean >21.84		Glomerular area (µm^2), Upper 99% CI of mean >1665	
SRD	**EDD**	**SRD**	**EDD**	**SRD**	**EDD**	**SRD**	**EDD**
0.22	**3.48**		0.76	19.12			
0.62	**2.13**	0.91	**1.38**	15.79	18.49	986.57	**2612.7**
1.00	**3.63**	0.38	**1.74**	27.89	**27.87**	1067.44	**1867.84**
1.27	**2.87**	1	**1.97**	16.1	**26.08**	1448.69	**2252.97**
5.12	**1.44**	0.73	**3.25**	15.17	**31.31**	1213.88	**2228.16**
0.8	**2.11**	0.55	**1.13**	10.51	18.28	1474.63	**1990.05**
1.48	**1.97**	0.25	**1.27**	13.3	**26.72**	1402.71	**2088.95**
0.7	0.71	0.67	**2.42**	23.28	19.89	1680.93	**2860.31**
1.12	1.21	1.23	**0.97**	18.77	**24.02**	1291.99	**2400.42**
0.96	1.1	1.11	**1.33**	14.02	**21.15**	1706.08	**2701.74**
0.97	**3.05**	0.81	**1.42**	14.62	**27.22**	1616.6	**2111.81**
0.68	**22.69**	1.28	**2.11**		19.24	1157.9	**2531.65**
0.87	**1.91**	0.29	**0.89**		**33.12**	1887.93	**2110.03**
0.66	**3.43**	0.21	0.59		**23.69**	1131.61	**2143.98**
0.75	0.52	0.38	**1.05**		**34.27**	1885.41	**2638.28**
0.88	**3.79**	0.49	**1.42**		**27.03**		1592.28
1.23	**4.5**	0.42	**2.06**				
1.05	**1.33**	0.55	**0.96**				
1	**3.05**	0.65	**2.41**				
0.64	**5.26**	1.16	0.7				
0.46	**2.99**	0.37	**1.01**				
0.56	**1.32**	0.93					
0.55	**3.03**	0.45					
0.37	**3.7**	0.21					
0.5	**2.61**	0.54					
0.89	**3.19**	0.2					
0.29	**3.69**	0.72					
0.84	**3.49**	0.21					
1.07	**4.1**						
0.21	0.87						
1.03	**4.11**						
0.66							
0.43							
% diabetic	**83.87 % (26/31)**		**85.71% (18/21)**		**73.33% (11/15)**		**93.33% (14/15)**

Note: Mice on EDD considered T2D if they demonstrated a raised parameter (e.g. ACR) levels higher the upper 99% confidence interval (CI) for the mean of age-matched control group fed on a standard rodent diet.

SRD; Standard rodent diet, EDD; Energy-dese diet., ACR; albumin creatinine ratio, PAS; periodic acid Schiff

All supplementary photographs and figure from mouse model characterisation study (Chapter 4)

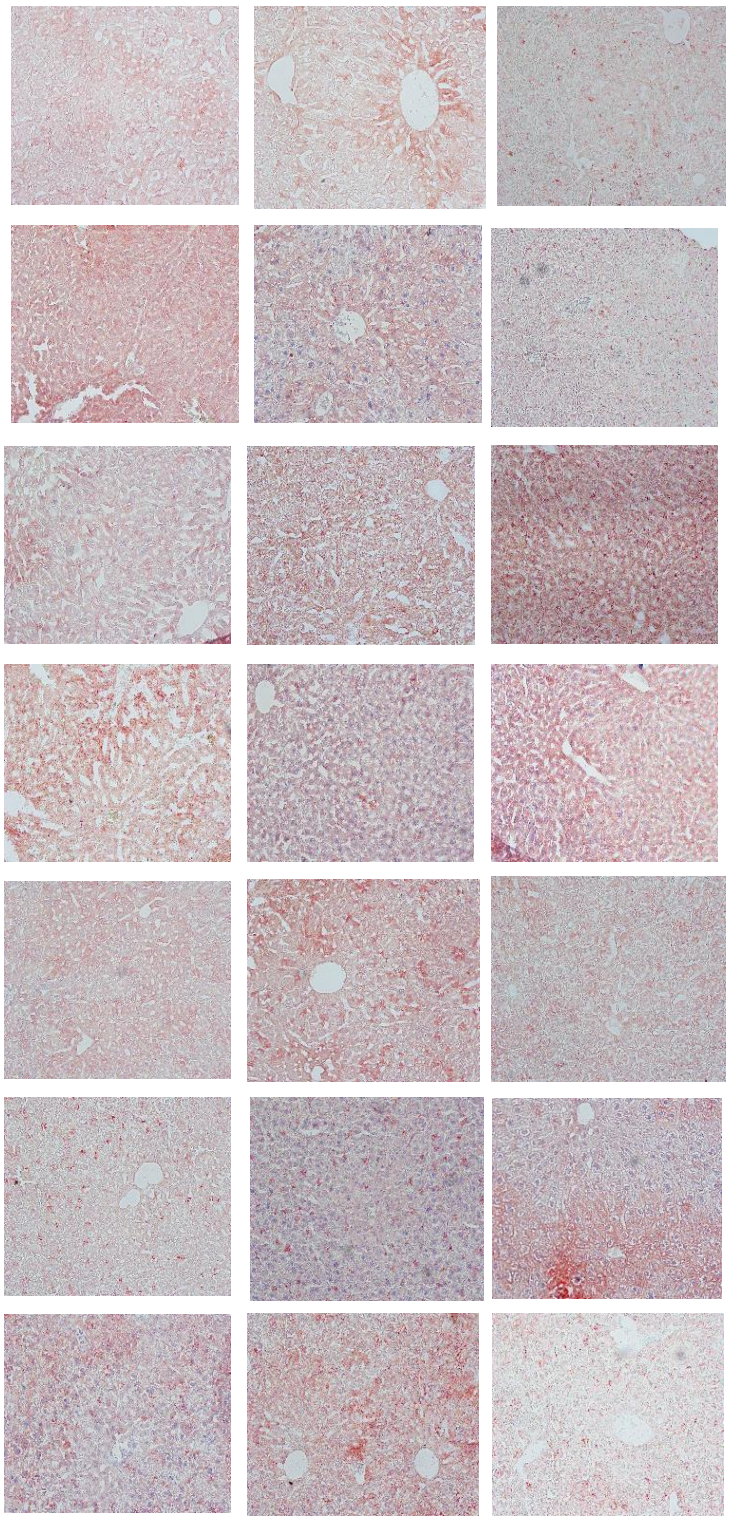

Figure A2.1 The representative photographs (one photo/mouse) of liver sections of JCU bred mice (n=21) on standard rodent diet (SRD) for a period of 30 weeks. All the photographs were taken at 200x magnification after Modified Herxheimer's staining. Photographs represent the deposition of lipid in liver (red colour indicates lipid).

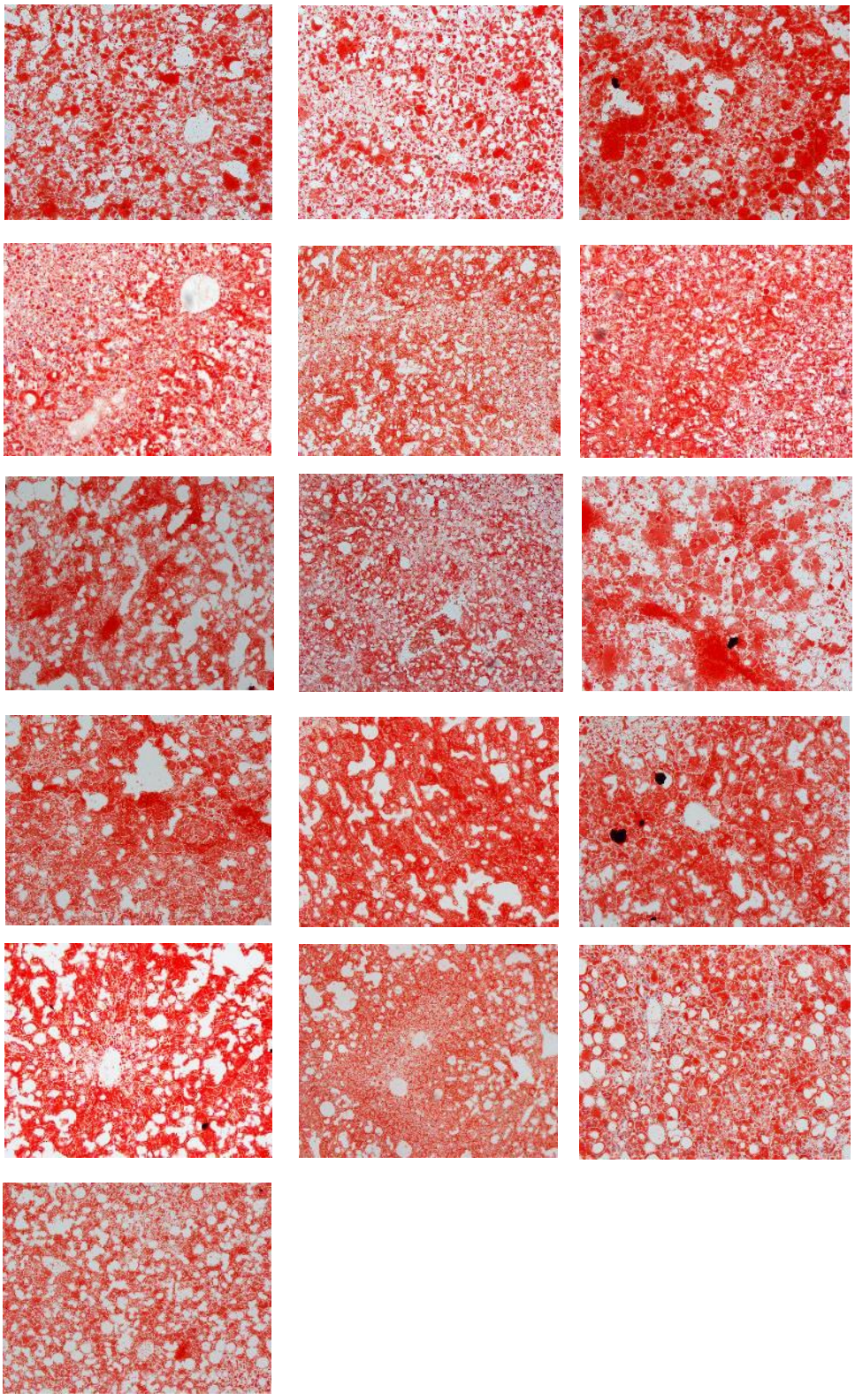

Figure A2.2 The representative photographs (one photo/mouse) of liver sections of JCU bred mice (n=16) on energy-dense diet (EDD) for a period of 30 weeks. All the photographs were taken at 200x magnification after Modified Herxheimer's staining. Photographs represent the deposition of lipid in liver (red colour indicates lipid).

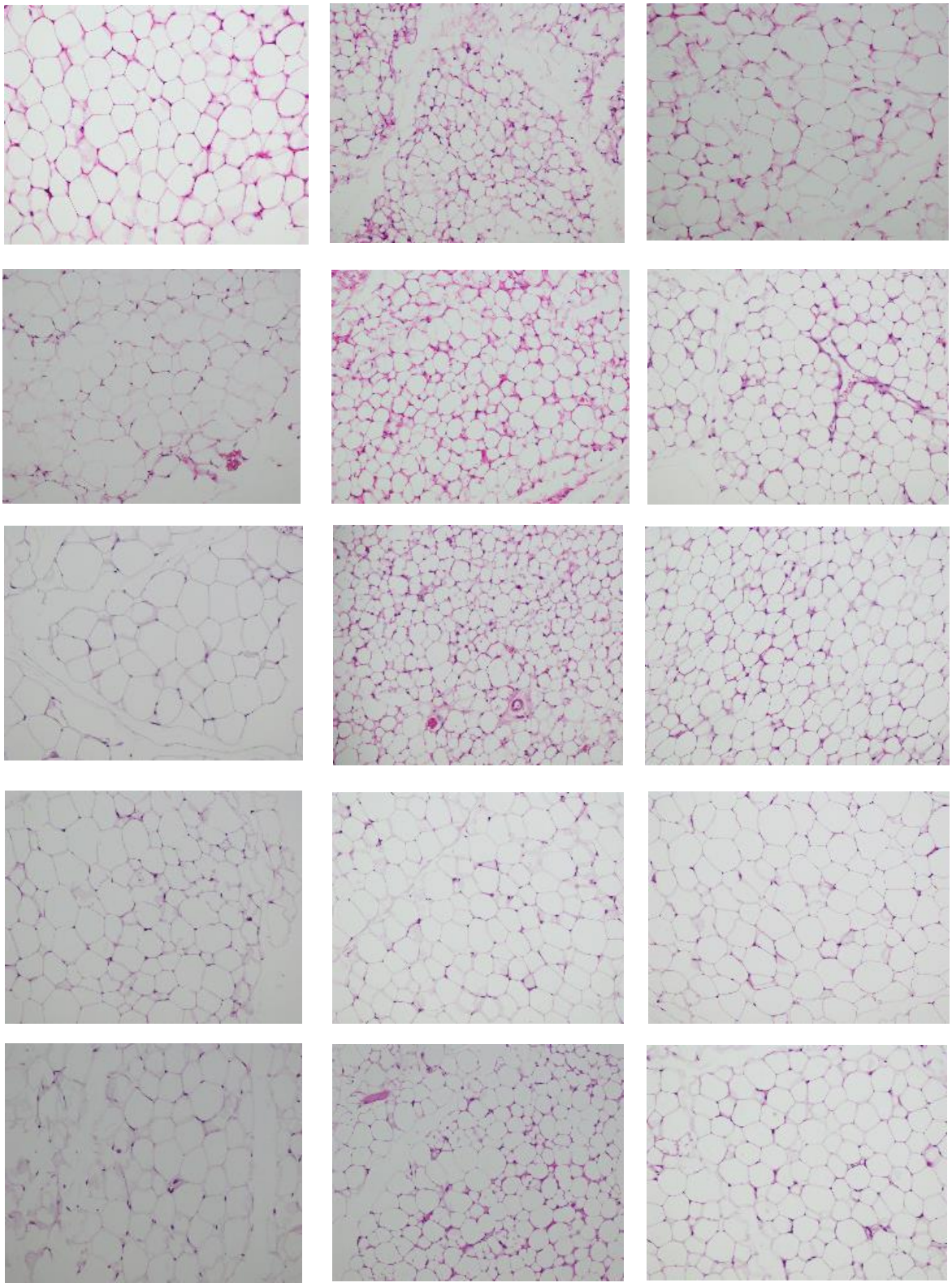

Figure A2.3 The representative photographs (one photo/mouse) of visceral adipose tissue sections of JCU bred mice (n=15) on standard rodent diet (SRD) for a period of 30 weeks. All the photographs were taken at 200x magnification after H&E staining. Photographs represent the size of the adipocyte in visceral adipose tissue after diet intervention period.

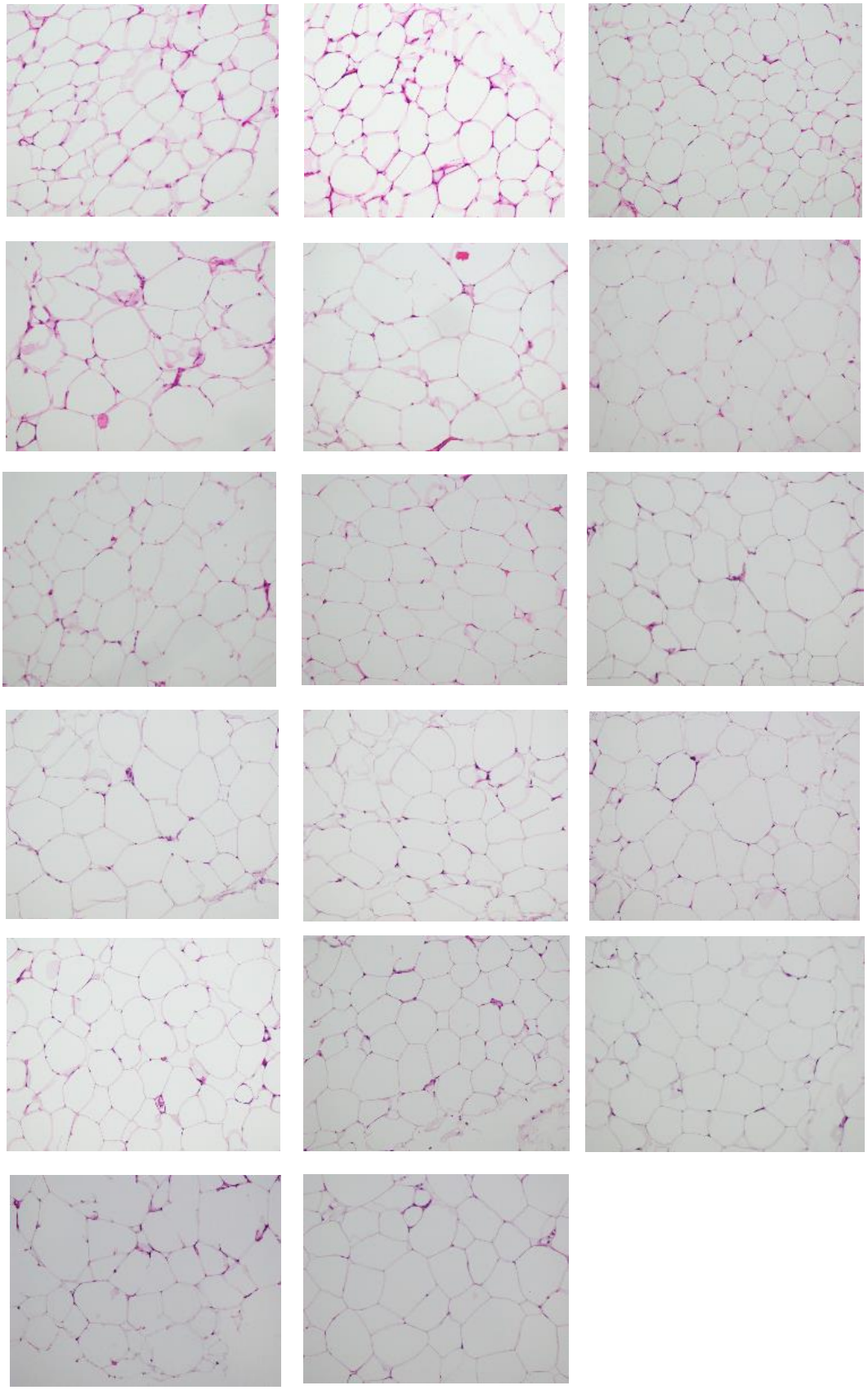

Figure A2.4 The representative photographs (one photo/mouse) of visceral adipose tissue sections of JCU bred mice (n=17) on energy-dense diet (EDD) for a period of 30 weeks. All the photographs were taken at 200x magnification after H&E staining. Photographs represent the size of the adipocyte in visceral adipose tissue after diet intervention period.

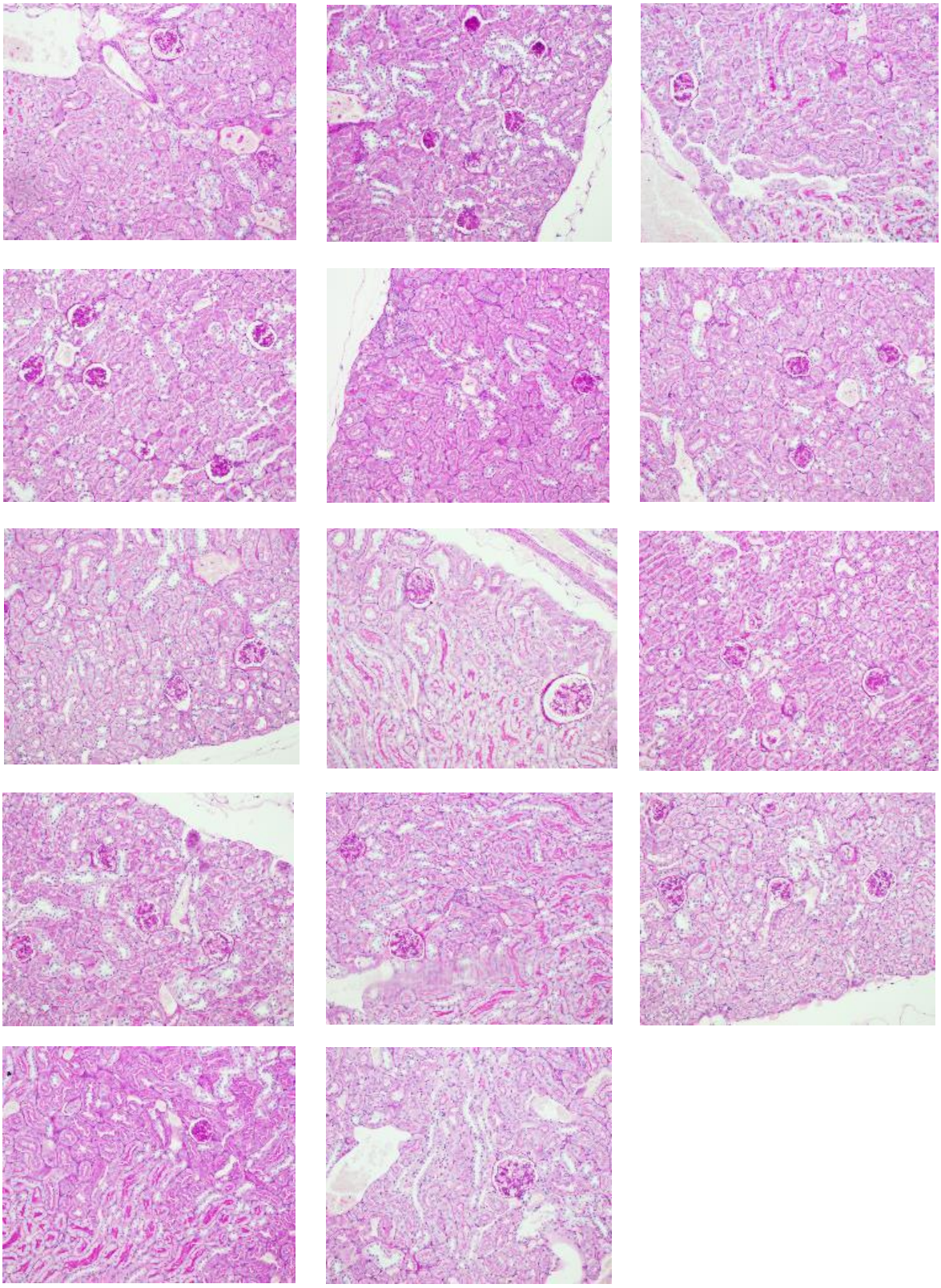

Figure A2.5 The representative photographs (one photo/mouse) of kidney section of JCU bred mice (n=14) on standard rodent diet (SRD) for a period of 30 weeks. All the photographs were taken at 200x magnification after periodic acid Schiff's (PAS) staining. Photographs represent the size of the glomerulus after the diet intervention period.

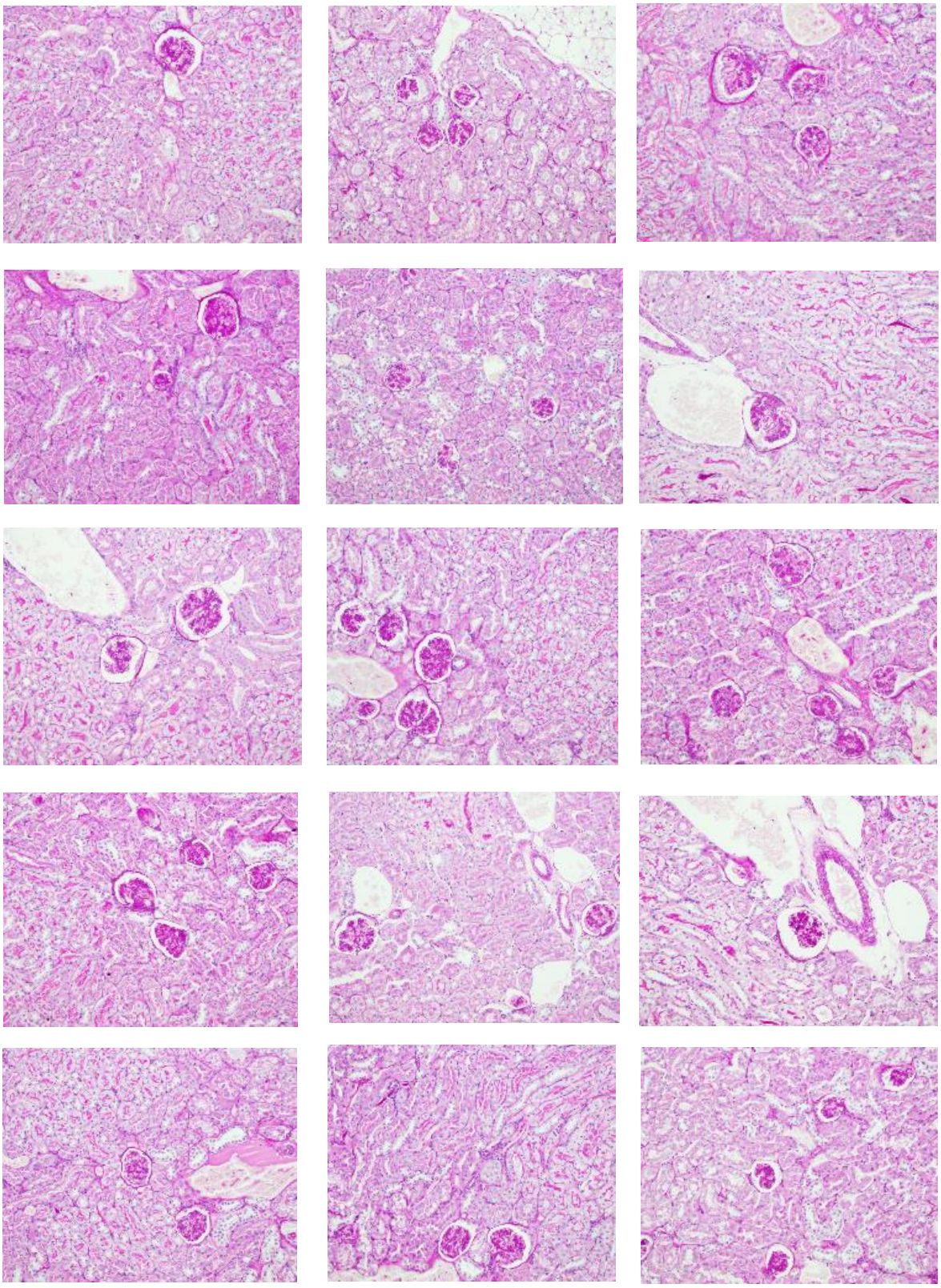

Figure A2.6 The representative photographs (one photo/mouse) of kidney section of JCU bred mice (n=15) on energy-dense diet (EDD) for a period of 30 weeks. All the photographs were taken at 200x magnification after PAS staining. Photographs represent the size of the glomerulus after diet intervention period.

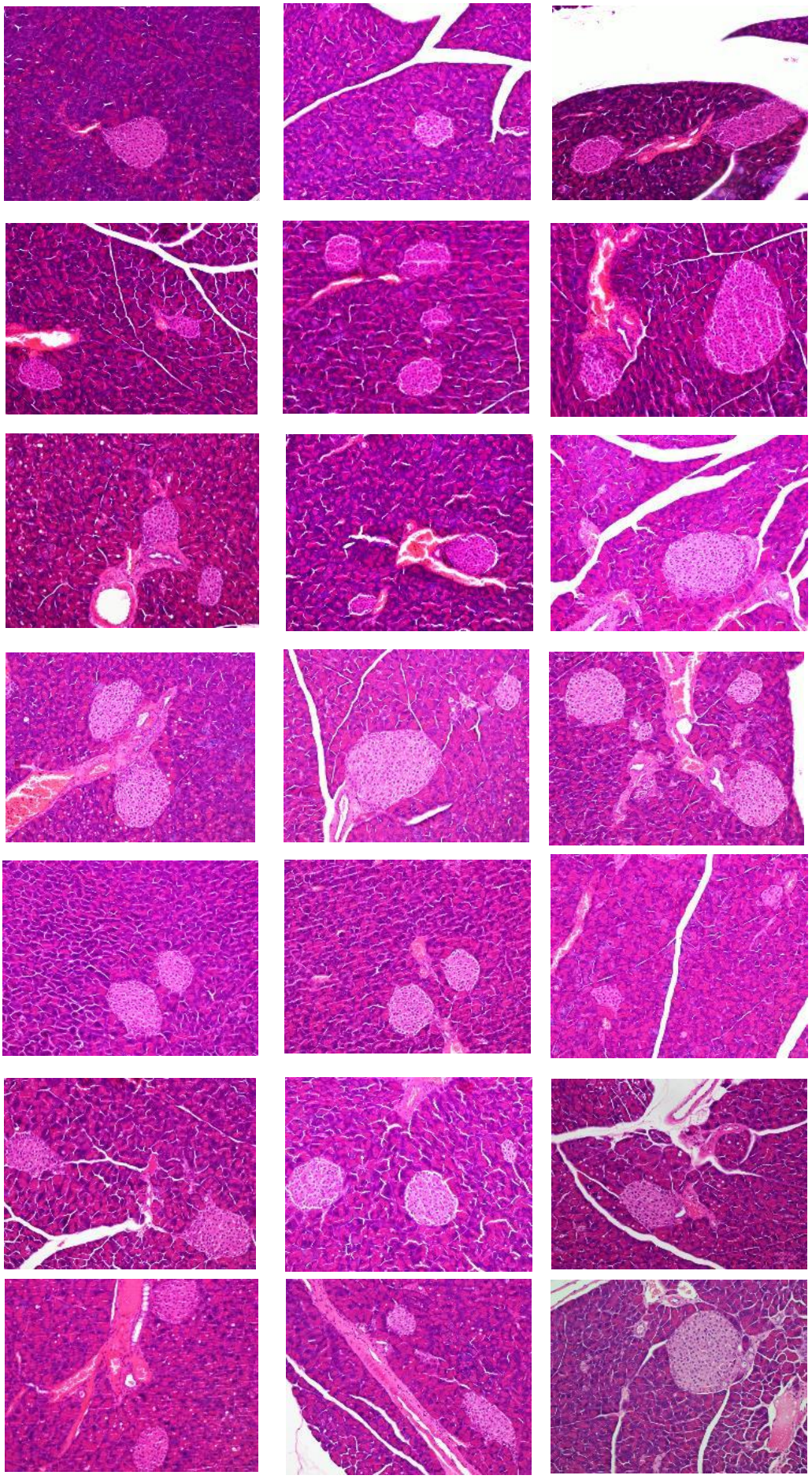

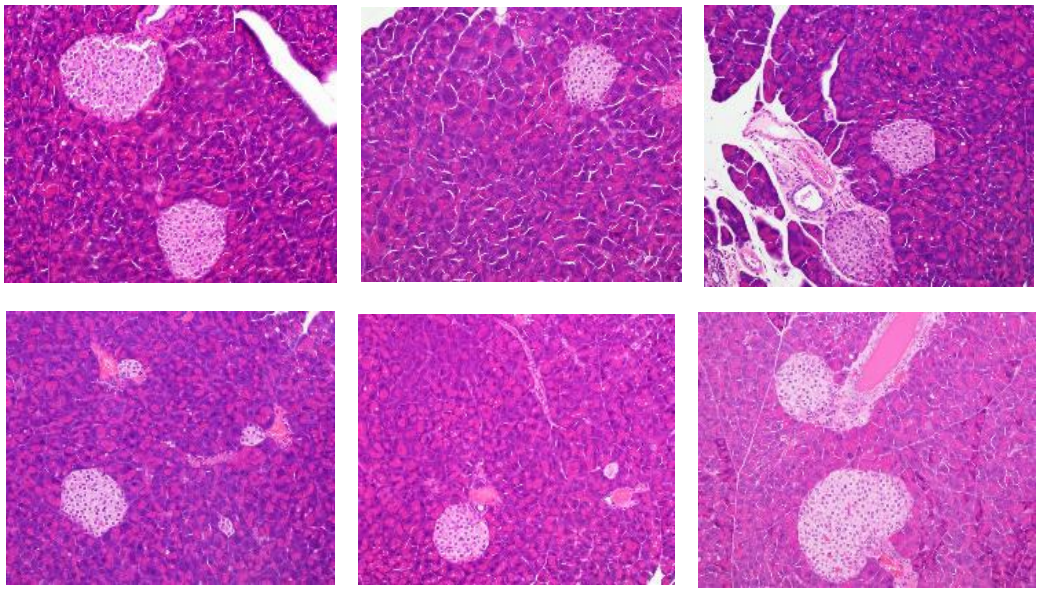

Figure A2.7 The representative photographs (one photo/mouse) of pancreatic sections of JCU bred mice (n=27) on standard rodent diet (SRD) for a period of 30 weeks. All the photographs were taken at 200x magnification after H&E staining. Photographs represent the size of the pancreatic islet after diet intervention.

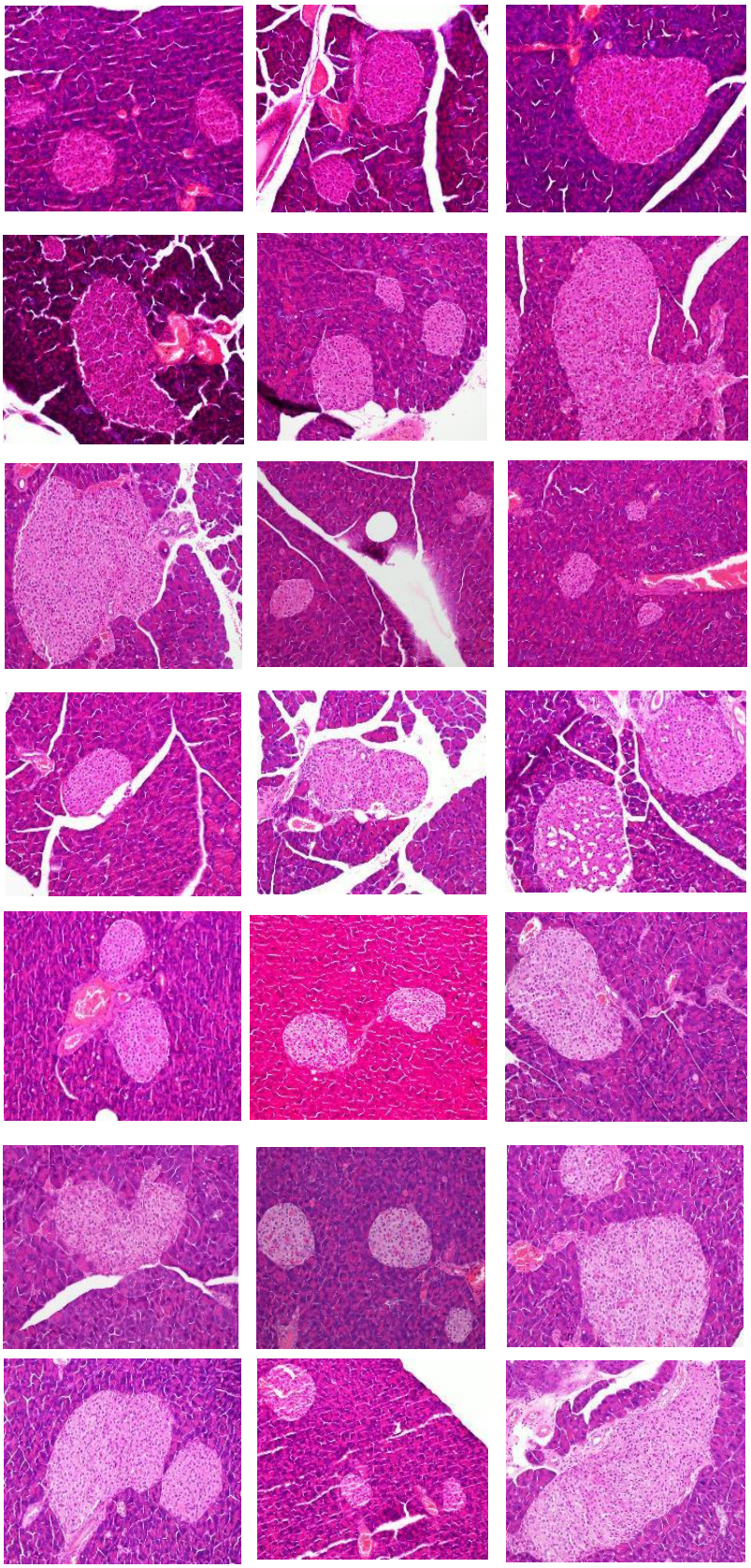

Figure A2.8 The representative photographs (one photo/mouse) of pancreatic sections of JCU bred mice (n=21) on energy-dense diet for a period of 30 weeks. All the photographs were taken at 200x magnification after H&E staining. Photographs represent the size of the pancreatic islet area after diet intervention period.

APPENDIX 3

All supplementary data from Chapter 5 (mycobacterial uptake, killing and cytokine production by macrophages)

Table A3.1 Bead phagocytosis assay using peritoneal exudate macrophages (elicited) and resident peritoneal exudate macrophages (non-elicited) at a multiplicity of infection 1:1 and 1:10

	Control (%, n=3),	Diabetic (%, n=3)	p-value	Level of significance
Peritoneal exudate macrophages (PEM, elicited), MOI 1:1, 4 hours incubation				
FB	8.42±0.08	7.33±0.25	0.0151	*
MACB	4.78±0.31	5.79±0.49	0.1568	ns
CB	4.75±0.12	6.91±0.80	0.0567	ns
Peritoneal exudate macrophages (PEM), MOI 1:10, 4 hours incubation				
FB	10.84±0.38	5.75±0.14	0.0002	***
MACB	11.60±0.46	7.43±1.00	0.0193	*
CB♦	12.45±0.76	8.33±0.44	0.0495	*
Resident peritoneal macrophages (RPM, non-elicited), MOI 1:1, 4 hours incubation				
FB	4.28±0. 20	2.23±0.26	0.0033	**
MACB	2.36±0.12	1.93±0.56	0.4938	ns
CB	3.20±1.15	2.59±0.20	0.6260	ns
Resident peritoneal macrophages (RPM, non-elicited), MOI 1:10, 4 hours incubation				
FB	9.44±0.17	4.66±0.40	0.0004	***
MACB	12.11±0.31	5.33±0.94	0.0024	**
CB♦	11.33±0.65	6.98±0.57	0.0495	*

Statistical analysis: Data were checked for normality using Shapiro-Wilk's test. Data passed the test if $p \geq 0.05$. The normally distributed data were compared between the groups using independent sample *t*-test. The non-normally distributed data (♦) were compared between the groups using Mann-Whitney U test. Data presented as mean (%)±SEM. The level of significance was indicated as *$p \leq 0.05$, **$p \leq 0.01$, ***$p \leq 0.001$ and ns=non-significant. In the table, FB; fresh beads, MACB; mycolic acid coated beads and CB; control beads, MOI; multiplicity of infection.

Table A3.2 Bead phagocytosis by alveolar macrophages and resident peritoneal macrophages from the same group of control and diabetic mice at a multiplicity of infection 1:10

	Control (%, n=4-5)	Diabetic (%, n=4-5)	p-value	Level of significance
Alveolar macrophages (AM), MOI 1:10, 4 hours incubation				
CB	22.96±0.74	19.84±0.79	0.0260	*
MACB	13.49±0.39	9.69±0.82	0.0057	**
TDMCB	12.58±0.89	8.92±0.11	0.0148	*
Resident peritoneal macrophages (RPM, non-elicited), MOI 1:10, 4 hours incubation				
CB	28.96±1.10	23±1.66	0.0285	*
MACB	5.56±0.34	3.84±0.32	0.0107	**
TDMCB	2.86±0.12	1.87±0.11	0.0005	***

Statistical analysis: Data were compared between the groups using independence sample *t*-test as they passed the test of normality (Shapiro-Wilk's test, $p \geq 0.05$). Data presented as mean (%)±SEM. The level of significance was indicated as *$p \leq 0.05$, **$p \leq 0.01$ and ***$p \leq 0.001$ and ns=non-significant. In the table, CB; controls beads, MACB; mycolic acid coated beads and TDMCB; trehalose 6, 6′ dimycolate coated beads; MOI; multiplicity of infection.

Table A3.3 Cytokine production by alveolar leucocytes and resident peritoneal exudate cells from control and diabetic mice during co-culture with mycolic acid coated beads

Alveolar leucocytes (AL): Beads, 4 hours incubation				
Category	**Control (pg/mL, n=3-5)**	**Diabetic (pg/mL, n=3-5)**	**p-value**	**Level of significance**
TNF-α				
Cell (AL)	417.89±97.35	213.68±9.88	0.0063	**
AL:CB	307.19±5.06	223.75±13.36	0.0051	**
AL:MACB	272.27±23.16	186.23±8.54	0.0039	**
AL:TDMCB	318.55±10.05	161.72±13.56	<0.0001	****
IL-6				
Cell (AL)	3.83±0.28	16.7±3.15	<0.0001	****
AL:CB	10.81±0.59	3.03±0.54	<0.0001	****
AL:MACB	9.96±1.39	2.72±0.18	0.0003	***
AL:TDMCB	13.40	1.26	<0.0001	****
Resident peritoneal exudate cells (RPEC): Beads, 4 hours incubation				
	Control (n=3-5)	**Diabetic (n=3-5)**	**p-value**	**Level of significance**
TNF-α				
Cell (RPEC)	4.32±3.00	2.43±2.43	>0.9999	ns
RPEC:CB	6.61±1.06	2.40±2.40	>0.9999	ns
RPEC:MACB	7.74±0.	2.40±1.77	0.8411	ns
RPEC:TDMCB	8.31±0.97	1.10±0.77	0.1972	ns
IL-6♦				
Cell (RPC)	132.46±5.12	65.27±4.73	<0.0001	****
RPEC:CB	125.12±5.22	53.57±4.71	<0.0001	****
RPEC:MACB	129.66±7.50	54.63±3.92	<0.0001	****
RPEC:TDMCB	134.66±4.04	51.60±1.90	<0.0001	****

Statistical analysis: The normally distributed data were compared among the groups using the ordinary one-way ANOVA with Holm Sidak's multiple comparisons test. The non-normally distributed data (♦) were compared among the groups using the Kruskal-Wallis test with Dunn's multiple comparisons test. Data presented as mean (pg/mL)±SEM. The level of significance was indicated as **p≤0.01, ***p≤0.001 and ****p≤0.0001. In the table, CB; controls beads, MACB; mycolic acid coated beads and TDMCB; trehalose 6, 6′ dimycolate coated beads.

Table A3.4 Uptake by resident peritoneal exudate cells (RPEC) and its-associated *Mycobacterium fortuitum* and killing of *M. fortuitum* by RPEC from control and diabetic mice at a multiplicity of infection 1:1 and 1:10

Category	Replicate	Control	Diabetic	p-value	Level of significance
		Mean (%)±SEM			
Peritoneal exudate cells (RPEC): *M. fortuitum*, MOI: 1:1					
4 hours uptake and cell associated bacteria	3	29.32±6.03	25.17±4.05	0.6023	ns
24 hours killing	3	58.08±6.48	38.30±4.15	0.0725	ns
Peritoneal exudate cells (RPEC): *M. fortuitum*, MOI: 1:10					
4 hours uptake and cell associated bacteria	3	21.95±1.36	16.20±2.61	0.1448	ns
24 hours killing	3	43.29±5.88	28.93±2.98	0.1185	ns

Statistical analysis: Data were compared between groups using the Unpaired *t*-test with Welch's correction as data sets passed the test of normality (Shapiro-Wilk's test, $p \geq 0.05$). The level of significance was indicated and ns=non-significant ($p \geq 0.05$). In the table, MOI; multiplicity of infection.

Table A3.5 Percent uptake and killing of *M. fortuitum* by alveolar macrophages and resident peritoneal macrophages from control and diabetic mice

Category	Replicate (C, D)	Control	Diabetic	p-value	Level of significance
		Mean (%)±SEM			
CD11c+ cells as alveolar macrophage (AM): *M. fortuitum*, MOI 1:10					
4 hours uptake	3, 3	6.94±0.25	4.17±0.07	0.0052	**
24 hours killing	3, 2	64.56±0.92	44.24±4.58	0.0099	**
CD11b+ cells as resident peritoneal macrophage (RPM): *M. fortuitum*, MOI 1:10					
4 hours uptake	3, 3	4.46±0.82	2.39±0.09	0.1268	ns
24 hours killing	3, 3	53.91±5.32	31.66±2.36	0.0365	*

Statistical analysis: Data were compared between groups using the Unpaired *t*-test with Welch's correction as data sets passed the test of normality (Shapiro-Wilk's test, $p \geq 0.05$). The level of significance was indicated as *$p \leq 0.05$, **$p \leq 0.01$ and ns=non-significant. In the table, C; control and D; diabetic, MOI; multiplicity of infection.

Table A3.6 Cytokine production by alveolar macrophages from control and diabetic mice infected with *M. fortuitum* for 4 and 24 hours

		AM (cell), 4 hr, n=2-4		AM:*Mft*, 4 hr, n=4-6		AM (cell), 24 hr, n=2		AM:*Mft*, 24 hr, n=3-4	
Cytokine	**Mouse**	**Mean±SEM (pg/mL)**	**p-value**	**Mean±SEM (pg/mL)**	**p-value**	**Mean±SEM (pg/mL)**	**p-value**	**Mean±SEM (pg/mL)**	**p-value**
TNF-α	Control	22.92±1.00	ns 0.4757	219.7±14.83	**** <0.0001	13.85±0.85	ns 0.0995	2309±69.67	**** <0.0001
	Diabetic	7.12±2.44		40.47±1.56		5.61±0.47		169.4±20.36	
MCP-1	Control	2.52±1.51	ns 0.9511	0.00±0.00	0.4251	0.00±0.00	-	96.83±6.62	*** 0.001♦
	Diabetic	2.36±1.64		4.67±2.76		0.00±0.00		10.56±3.71	
IL-6	Control	3.39±0.96	ns 0.6028	15.60±4.76	** 0.0016	1.99±0.44	ns 0.9909	613.4±81.08	**** 0.0001
	Diabetic	0.00±0.00		3.57±0.73		1.10±1.10		31.27±3.17	
IL-12p70	Control	0.00±0.00	-	0.00±0.00	-	0.00±0.00	-	0.00±0.00	-
	Diabetic	0.00±0.00		0.00±0.00		0.00±0.00		0.00±0.00	
IFN-γ	Control	0.00±0.00	-	0.00±0.00	-	0.00±0.00	-	0.00±0.00	-
	Diabetic	0.00±0.00		0.00±0.00		0.00±0.00		0.00±0.00	
IL-10	Control	0.00±0.00	-	0.00±0.00	-	0.00±0.00	-	0.00±0.00	-
	Diabetic	0.00±0.00		0.00±0.00		0.00±0.00		0.00±0.00	

Statistical analysis: The normally distributed data were compared among the groups using the ordinary one-way ANOVA with Holm Sidak's multiple comparisons test. The normally distributed data (♦) were compared between the groups using the Unpaired *t*-test with Welch's correction. The level of significance was indicated as **p≤0.01, ***p≤0.001, ****p≤0.0001 and ns=non-significant. In the table, AM; alveolar macrophages, hr; hour, *Mft*; *Mycobacterium fortuitum*.

Table A3.7 Cytokine production by resident peritoneal macrophages from control and diabetic mice infected with *M. fortuitum* for 4 and 24 hours

		RPM (cell), 4 hr, n=4		RP:*Mft*, 4 hr, n=4-6		RPM (cell), 24 hr, n=4		RPM:*Mft*, 24 hr, n=3	
Cytokine	**Mouse**	**Mean±SEM (pg/mL)**	**p-value**	**Mean±SEM (pg/mL)**	**p-value**	**Mean±SEM (pg/mL)**	**p-value**	**Mean±SEM (pg/mL)**	**p-value**
TNF-α	Control	0.00±0.00	-	124.0±6.56	**** 0.0001♦	9.70±5.50	ns 0.5670	150.2±21.36	* 0.0311
	Diabetic	0.00±0.00		69.93±3.04		1.68±1.14		104.7±9.62	
MCP-1	Control	2.71±2.71	ns >0.9999▪	6.15±2.24	ns >0.9999▪	2.57±1.84	ns 0.8959	257.0±10.1	**** <0.0001
	Diabetic	4.99±3.13		5.74±1.48		3.67±2.18		151.5±10.30	
IL-6	Control	5.95±1.04	ns 0.5474	148.4±6.70	**** <0.0001	13.96±4.75	ns 0.8820	1063±108.1	**** 0.0001
	Diabetic	1.63±0.94		77.45±2.65		4.24±1.86		587.32±43.22	
IL-12p70	Control	0.00±0.00	-	0.00±0.00	-	0.00±0.00	-	0.00±0.00	-
	Diabetic	0.00±0.00		0.00±0.00		0.00±0.00		0.00±0.00	
IFN-γ	Control	0.00±0.00	-	0.00±0.00	--	0.00±0.00	-	0.00±0.00	-
	Diabetic	0.00±0.00		0.00±0.00		0.00±0.00		0.00±0.00	
IL-10	Control	0.00±0.00	-	36.45±1.41	*** 0.0003♦	0.00±0.00	-	7.66±1.72	>0.9999□
	Diabetic	0.00±0.00		26.78±1.01		0.00±0.00		7.30±1.40	

Statistical analysis: The normally distributed data were compared among the groups using the ordinary one-way ANOVA with Holm Sidak's multiple comparison test. The normally distributed data (♦) were compared between the groups using the Unpaired *t*-test with Welch's correction. The non-normally distributed data (▪) were compared among the groups using Kruskal-Wallis test with Dunn's multiple comparisons test. The non-normally distributed data (□) were compared between groups using Mann-Whitney U test. The level of significance was indicated as *p≤0.05, ***p≤0.001, ****p≤0.0001 and ns=non-significant. In the table, RPM; resident peritoneal macrophages, hr; hour, *Mft*; *Mycobacterium fortuitum.*

Table A3.8 Uptake and killing of *M. bovis* (BCG) by alveolar macrophages and resident peritoneal macrophages from control and diabetic mice

Category	Replicate (C, D)	Control	Diabetic	p-value	Level of significance
		Mean (%)±SEM			
CD11c+ cells as alveolar macrophages (AM): *M. bovis*, MOI 1:10					
4 hours uptake	3, 4	4.56±0.31	3.37±0.23	0.0378	*
24 hours killing	3, 4	93.77±0.13	89.97±0.79	0.0156	*
CD11b+ cells as resident peritoneal macrophages (RPM): *M. bovis*, MOI 1:10					
4 hours uptake	5, 5	3.84±0.28	2.54±0.21	0.0070	**
24 hours killing	5, 5	90.93±1.03	87.41±0.75	0.0272	*
48 hours killing	5, 5	95.51±0.70	93.92±0.61	0.1266	ns

Statistical analysis: Data were compared between the groups using the Unpaired *t*-test with Welch's correction as data sets passed the test of normality (Shapiro-Wilk's test, $p \geq 0.05$). The level of significance was indicated as *$p \leq 0.05$, **$p \leq 0.010$ and ns=non-significant. In the table, C; control and D; diabetic, MOI; multiplicity of infection.

Table A3.9 Cytokine production by alveolar macrophage from control and diabetic mice infected with *M. bovis* (BCG) for 4 and 24 hours

		AM (cell), 4 hr, n=2-3		AM: *M. bovis*, 4 hr, n=3		AM (cell), 24 hr, n=2-3		AM: *M. bovis*, 24 hr, n=3-4	
Cytokine	**Mouse**	**Mean±SEM (pg/mL)**	**p-value**	**Mean±SEM (pg/mL)**	**p-value**	**Mean±SEM (pg/mL)**	**p-value**	**Mean±SEM (pg/mL)**	**p-value**
TNF-α	Control	37.08±17.09	ns 0.2275	69.76±0.57	ns 0.1062	7.18±0.69	ns 0.9195	319.79±52.04	** 0.0041
	Diabetic	18.96±3.50		44.41±6.14		2.72±0.34		140.18±10.37	
MCP-1	Control	0.00±0.00	-	0.00±0.00	-	0.00±0.00	-	0.00±0.00	-
	Diabetic	0.00±0.00		0.00±0.00		0.00±0.00		0.00±0.00	
IL-6	Control	0.15±0.15	ns 0.9401	4.00±3.15	** 0.0096	0.00±0.00	-	5.25±0.33	**** <0.0001
	Diabetic	0.41±0.06		17.64±2.29		0.00±0.00		17.13±0.82	
IL-1β	Control	0.00±0.00	-	0.00±0.00	-	0.00±0.00	-	0.00±0.00	ns >0.9999
	Diabetic	0.00±0.00		0.00±0.00		0.00±0.00		0.23±0.17	
IL-12p70	Control	0.00±0.00	-	0.00±0.00	-	0.00±0.00	ns 0.4000□	0.05±0.00	>0.9999□
	Diabetic	0.49±0.20		0.00±0.00		0.05±0.05		0.00±0.00	
IFN-γ	Control	0.00±0.00	-	0.00±0.00	-	0.00±0.00	-	0.00±0.00	-
	Diabetic	0.00±0.00		0.00±0.00		0.00±0.00		0.00±0.00	
IL-10	Control	8.31±0.28	0.4183	10.04±2.48	0.2892	12.70±2.43	ns 0.9989	9.10±1.34	ns 0.7844
	Diabetic	5.30±1.00		13.88±0.63		12.58±2.32		12.98±2.32	

Statistical analysis: The normally distributed data were compared among the groups using the ordinary one-way ANOVA with Holm Sidak's multiple comparisons test. The non-normally distributed data (□) were compared between the groups using the Mann-Whitney U test. The level of significance was indicated as **p≤0.01, ****p≤0.0001 and ns=non-significant. In the table, AM; alveolar macrophages, hr; hour.

Table A3.10 Cytokine production by resident peritoneal macrophages from control and diabetic mice infected with *M. bovis* (BCG) for 4 and 24 hours

		RPM (cell), 4 hr, n=3		RPM: *M. bovis*, 4 hr, n=4		RPM (cell), 24 hr, n=3		RPM: *M. bovis*, 24 hr, n=4	
Cytokine	**Mouse**	**Mean±SEM (pg/mL)**	**p-value**	**Mean±SEM (pg/mL)**	**p-value**	**Mean±SEM (pg/mL)**	**p-value**	**Mean±SEM (pg/mL)**	**p-value**
TNF-α	Control	2.84±0.68	ns 0.8695	129.36±16.54	*** 0.0005	5.92±1.80	ns 0.9859	289.43±63.91	ns 0.9859
	Diabetic	0.21±0.18		47.50±5.45		1.54±1.09		281.26±25.15	
MCP-1	Control	0.00±0.00	-	0.00±0.00	-	0.00±0.00	-	149.90±27.91	** 0.0081♦
	Diabetic	0.00±0.00		0.00±0.00		0.00±0.00		47.00±15.89	
IL-6	Control	38.09±3.39	ns 0.6446	601.26±58.55	**** <0.0001	2.08±0.68	ns 0.9877	467.54±105.94	ns 0.0751
	Diabetic	9.73±1.64		168.77±31.78		0.42±0.35		213.81±51.21	
IL-1β	Control	0.00±0.00	-	0.00±0.00	-	0.00±0.00	-	8.55±2.02	0.0530♦
	Diabetic	0.00±0.00		0.00±0.00		0.00±0.00		2.64±1.00	
IL-12p70	Control	0.00±0.00	0.4000□	0.00±0.00	-	0.19±0.19	0.9685	0.30±0.30	0.9784
	Diabetic	0.08±0.04		0.00±0.00		0.01±0.01		0.24±0.13	
IFN-γ	Control	0.00±0.00	-	0.00±0.00	--	0.00±0.00	-	0.00±0.00	-
	Diabetic	0.00±0.00		0.00±0.00		0.00±0.00		0.00±0.00	
IL-10	Control	30.89±1.28	ns 0.4296	171.63±10.78	**** <0.0001	15.08±3.32	ns 0.9895	57.24±5.00	** 0.0044
	Diabetic	21.19±4.02		95.70±6.96		15.01±1.94		38.10±2.06	

Statistical analysis: The normally distributed data were compared among the groups using the ordinary one-way ANOVA with Holm Sidak's multiple comparisons test. The normally distributed data (♦) were compared between the groups using the Unpaired *t*-test with Welch's correction. The non-normally distributed data (□) were compared between the groups using the Mann-Whitney U test. The level of significance was indicated as **p≤0.01, ***p≤0.001, ****p≤0.0001 and ns=non-significant. In the table, RPM; resident peritoneal macrophages, hr; hour.

Table A3.11 Uptake and killing of *M. tuberculosis* (H37Rv) by alveolar macrophages and resident peritoneal macrophages from control and diabetic mice

Category	Replicate (C, D)	Control	Diabetic	p-value	Level of significance
		Mean (%)±SEM			
CD11c+ cells as alveolar macrophages (AM): *M. tuberculosis*, MOI 1:10					
4 hours uptake	4, 5	5.17±0.41	3.56±0.35	0.0232	*
24 hours killing	4, 5	91.73±0.33	85.41±1.96	0.0308	*
CD11b+ cells as resident peritoneal macrophages (RPM): *M. tuberculosis*, MOI 1:10					
4 hours uptake	2, 4	4.20±0.07	2.56±0.36	0.0892	ns
24 hours killing	2, 4	88.83±0.34	75.61±3.01	0.0212	*

Statistical analysis: Data were compared between groups using the Unpaired *t*-test with Welch's correction as data sets passed the test of normality (Shapiro-Wilk's test, $p \geq 0.05$). The level of significance was indicated as *$p \leq 0.05$ and ns=non-significant. In the table, MOI; multiplicity of infection.

Table A3.12 Cytokine production by alveolar macrophages from control and diabetic mice infected with *M. tuberculosis* (H37Rv) for 4 and 24 hours

		AM (cell), 4 hr, n=1		AM: *Mtb*, 4 hr, n=4-5		AM (cell), 24 hr, n=2		AM: *Mtb*, 24 hr, n=4	
Cytokine	**Mouse**	**Mean±SEM (pg/mL)**	**p-value**	**Mean±SEM (pg/mL)**	**p-value**	**Mean±SEM (pg/mL)**	**p-value**	**Mean±SEM (pg/mL)**	**p-value**
TNF-α	Control	12.16	ns 0.8927	128.79±4.06	**** <0.0001	10.52±3.34	ns 0.9620	1586.14±105.36	**** <0.0001
	Diabetic	13.46		38.56±2.33		4.17±1.45		91.46±6.03	
MCP-1	Control	0.00±0.00	-	0.00±0.00	-	0.00±0.00		85.49±6.84	*** 0.0006♦
	Diabetic	0.00±0.00		0.00±0.00		0.00±0.00		0.00±0.00	
IL-6	Control	0.33	ns >0.9999	11.85±1.05	**** 0.0001	1.00±1.00	ns 0.9946	581.19±52.42	**** <0.0001
	Diabetic	0.33		2.46±0.15		0.55±0.55		19.10±1.22	
IL-1β	Control	0.00±0.00	-	0.00±0.00	-	0.00±0.00	-	3.67±0.74	** 0.0042♦
	Diabetic	0.00±0.00		0.00±0.00		0.00±0.00		179.36±22.20	
IL-12p70	Control	0.00±0.00	-	0.00±0.00	-	0.00±0.00	-	0.00±0.00	-
	Diabetic	0.00±0.00		0.00±0.00		0.00±0.00		0.00±0.00	
IFN-γ	Control	0.00±0.00	-	0.00±0.00	-	0.00±0.00	-	0.00±0.00	-
	Diabetic	0.00±0.00		0.00±0.00		0.00±0.00		0.00±0.00	
IL-10	Control	0.00±0.00	-	0.00±0.00	-	0.00±0.00	-	0.00±0.00	-
	Diabetic	0.00±0.00		0.00±0.00		0.00±0.00		0.00±0.00	

Statistical analysis: The normally distributed data were compared among the groups using the ordinary one-way ANOVA with Holm Sidak's multiple comparisons test. The normally distributed data (♦) were compared between groups using the Unpaired *t*-test with Welch's corrections. The level of significance was indicated as **p≤0.01, ***p≤0.001, ****p≤0.0001 and ns=non-significant. In the table, AM; alveolar macrophages, hr; hour.

Table A3.13 Cytokines production by resident peritoneal macrophages from control and diabetic mice infected with *M. tuberculosis* (H37Rv) for 4 and 24 hours

		RPM (cell), 4 hr, n=1		RP:*Mtb*, 4 hr, n=4		RPM (cell), 24 hr, n=2		RPM:*Mtb*, 24 hr, n=2-4	
Cytokine	**Mouse**	**Mean±SEM (pg/mL)**	**p-value**	**Mean±SEM (pg/mL)**	**p-value**	**Mean±SEM (pg/mL)**	**p-value**	**Mean±SEM (pg/mL)**	**p-value**
TNF-α	Control	0.00±0.00	-	60.22±7.28	* 0.0202♦	3.80±2.12	ns 0.6386	68.49±3.92	*** 0.0002
	Diabetic	0.00±0.00		27.62±0.70		5.62±4.08		35.97±0.83	
MCP-1	Control	0.00±0.00	-	0.00±0.00	-	1.84±1.84	ns 0.9683	248.52±3.05	**** 0.0001
	Diabetic	0.00±0.00		0.00±0.00		1.29±1.29		135.65±9.25	
IL-6	Control	3.68	ns 0.8911	93.66±10.40	** 0.0080	8.02±5.94		780.51±36.60	**** 0.0001
	Diabetic	0.70		39.26±0.79		2.33±1.91		372.54±26.81	
IL-1β	Control	0.00±0.00	-	0.00±0.00	-	0.00±0.00	-	43.69±5.22	ns 0.1333□
	Diabetic	0.00±0.00		0.00±0.00		0.00±0.00		21.14±4.42	
IL-12p70	Control	0.00±0.00	-	0.00±0.00	-	0.00±0.00	-	0.00±0.00	-
	Diabetic	0.00±0.00		0.00±0.00		0.00±0.00		0.00±0.00	
IFN-γ	Control	0.00±0.00	-	0.00±0.00	-	0.00±0.00	-	0.00±0.00	-
	Diabetic	0.00±0.00		0.00±0.00		0.00±0.00		0.00±0.00	
IL-10	Control	0.00±0.00	-	1.70±0.170	ns >0.9999□	0.00±0.00	-	0.00±0.00	-
	Diabetic	0.00±0.00		0.00±0.00		0.00±0.00		0.00±0.00	

Statistical analysis: The normally distributed data were compared among the groups using the ordinary one-way ANOVA with Holm Sidak's multiple comparison test. The normally distributed data (♦) were compared between the groups using the Unpaired *t*-test with Welch's corrections. The non-normally distributed data (□) were compared between the groups using Mann-Whitney U test. The level of significance was indicated as *p≤0.05, **p≤0.01, ***p≤0.001, ****p≤0.0001 and ns=non-significant. In the table, *Mtb*; *Mycobacterium tuberculosis* (H37Rv), RPM; resident peritoneal macrophages, hr; hour.

APPENDIX 4

All supplementary data of *M. fortuitum* infection study (Chapter 6-8)
Dose: 1x10^7 CFU/mouse (low-dose) and 3x10^8 CFU/mouse (high-dose)

Table A4.1 Body weight and area under the curve of mice on standard rodent diet and energy-dense diet

Parameters	Mouse	Number	Mean±SEM	p-value	Level of significance
Body weight (0 week; g) ♦	SRD	33	18.81±0.32	>0.9999	ns
	EDD	33	19.97±0.30		
Body weight (30th week; g) ♦	SRD	33	29.76±0.28	0.0050	**
	EDD	33	48.54±0.86		
	EDD	33	9.12±0.20		
Area under the curve (AUC)	SRD	33	1030.88±21.26	0.0000	****
	EDD	33	1677.39±37.25		

Statistical analysis: Data were checked for normal distribution using Shaprio-Wilk's test. Data passed the test if p≥0.05. The non-normally distributed data (♦) were compared among the groups using the Kruskal-Wallis test with Dunn's multiple comparisons test. The area under the curve was compared between the groups using the Mann-Whitney U test as data set didn't pass the test of normality. The level of significance was indicated as **p≤0.01, ****p≤0.0001 and ns=non-significant. In the table, SRD; standard rodent diet, EDD; energy-dense diet.

Table A4.2: Glucose tolerance test after 30 weeks of standard rodent diet and energy-dense diet intervention

Time (minutes)	SRD (mmol/L, n=33)	EDD (mmol/L, n=33)	p-value	Level of significance
0	6.65±0.13	9.12±0.20	<0.0001	****
15	13.66±0.39	18.80±0.44	<0.0001	****
30	9.65±0.28	16.69±0.54	<0.0001	****
120	5.99±0.12	10.01±0.25	<0.0001	****

Statistical analysis: Data were analysed using the two-way ANOVA with Sidak's multiple comparisons test. Data presented as mean±SEM. The level of significance was indicated as ****p≤0.0001. In the table, SRD; standard rodent diet, EDD; energy-dense diet.

Table A4.3 Percentage of diabetic mice after 30 weeks of energy-dense diet intervention based on fasting blood glucose and area under the curve-glucose tolerance test

Column statistics: Baseline fasting blood glucose (FBG) Area under the curve (AUC)

Col. stats	A	B
	Control baseline FBG	Diabetic baseline FBG
	Y	Y
1 Number of values	33	33
2		
3 Minimum	5.2	6.4
4 Maximum	8.4	11.1
5		
6 Mean	6.655	9.118
7 Std. Deviation	0.7383	1.134
8 Std. Error of Mean	0.1285	0.1974
9		
10 Lower 99% CI of mean	6.303	8.578
11 Upper 99% CI of mean	7.006	9.659

Col. stats	A	B
	Control	Diabetic
	Y	Y
1 Number of values	33	33
2		
3 Minimum	841.5	1319
4 Maximum	1509	2404
5		
6 Mean	1031	1677
7 Std. Deviation	122.1	214
8 Std. Error of Mean	21.26	37.25
9		
10 Lower 99% CI of mean	972.7	1575
11 Upper 99% CI of mean	1089	1779

Mice on EDD	Diabetic	Mice on EDD	Diabetic
Baseline FBG (mmol/L)	**Upper 99% CI of mean (>7mmol/L) (Yes/No)**	**AUC-GTT**	**Upper 99% CI of mean (>1089) (Yes/No)**
8.2	Yes	1628.00	Yes
7.4	Yes	1319.00	Yes
10	Yes	1792.00	Yes
8.1	Yes	1812.00	Yes
10.7	Yes	1761.00	Yes
10.7	Yes	1764.00	Yes
9.8	Yes	2099.00	Yes
7.2	Yes	1621.00	Yes
8.2	Yes	1458.00	Yes
10.5	Yes	2404.00	Yes
10.7	Yes	1488.00	Yes
6.4	NO	1453.00	Yes
8.4	Yes	1557.00	Yes
10	Yes	1699.00	Yes
8.4	Yes	1711.00	Yes
8.7	Yes	1417.00	Yes
9.9	Yes	1679.00	Yes
10.2	Yes	1793.00	Yes
8.3	Yes	1598.00	Yes
9.5	Yes	2052.00	Yes
11.1	Yes	1748.00	Yes
9.6	Yes	1607.00	Yes
9	Yes	1673.00	Yes
9.9	Yes	1866.00	Yes
9.6	Yes	1700.00	Yes
8.7	Yes	1378.00	Yes
10	Yes	1705.00	Yes
8.6	Yes	1472.00	Yes
8.4	Yes	1654.00	Yes
9.1	Yes	1664.00	Yes
8.8	Yes	1564.00	Yes
7.6	Yes	1608.00	Yes
9.2	Yes	1610.00	Yes
% diabetic	**96.97% (32/33)**	**% diabetic**	**100 (33/33)**

Note: Mice were considered type 2 diabetes if they demonstrated a raised baseline FBG and AUG-GTT with evidence of glucose intolerance at levels higher the upper 99% confidence interval (CI) for the mean of age-matched control group fed on a standard rodent diet.

FBG; fasting blood glucose, EDD; energy-dense diet, AUC-GTT; area under the curve-glucose tolerance test

Table A4.4 Daily feed intake by mice following *M. fortuitum* infection

Week	Mouse	Cage no.	Feed intake (g/mouse/day) Mean±SEM	p-value	Level of significance
Low-dose (1x10^7 CFU/mouse)					
0 (baseline)	Control	3	4.50±0.00	0.3235	ns
	Diabetic	3	3.50 ±.00		
1	Control	5	4.14±0.11	0.1593	ns
	Diabetic	5	2.94±0.57		
2	Control	3	4.43±0.04	0.1802	ns
	Diabetic	4	3.01±0.11		
3	Control	3	4.19±0.20	>0.9999	ns
	Diabetic	4	4.31±0.94		
4	Control	3	4.56±0.06	0.9924	ns
	Diabetic	4	4.88±1.31		
High-dose (3x10^8 CFU/mouse)					
0 (baseline)	Control	3	4.50±0.00	0.4227	ns
	Diabetic	3	3.50 ±.00		
1	Control	3	3.44±0.20	0.0792	ns
	Diabetic	2	1.60±0.01		
2	Control	3	3.00±0.52	0.0351	*
	Diabetic	2	0.74±0.01		

Statistical analysis: Data were analysed using the two-way ANOVA with Sidak's multiple comparisons test. The level of significance was indicated as *p≤0.05 and ns=non-significant. Each cage contains 1-5 mice.

Table A4.5 Energy intake by mice following *M. fortuitum* infection

Week	Mouse	Number	Energy intake (kcal/mouse/day) Mean±SEM	p-value	Level of significance
Low-dose (1x10^7 CFU/mouse)					
0 (baseline)	Control	3	13.82±0.00	0.7876	ns
	Diabetic	3	16.73±0.00		
1	Control	5	12.73±0.34	0.7876	ns
	Diabetic	5	14.05±2.71		
2	Control	3	13.59±0.13	0.9909	ns
	Diabetic	4	14.40±0.52		
3	Control	3	12.86±0.61	0.9996	ns
	Diabetic	4	20.60±4.50		
4	Control	3	14.00±0.18	0.0257	^
	Diabetic	4	23.33±6.26		
High-dose (3x10^8 CFU/mouse)					
0 (baseline)	Control	3	13.82±0.00	0.1196	ns
	Diabetic	3	16.73±0.00		
1	Control	3	10.56±0.06	0.3130	ns
	Diabetic	2	7.58+0.00		
2	Control	3	9.21±1.58	0.0285	*
	Diabetic	2	3.51±0.03		

Statistical analysis: Data were analysed using the two-way ANOVA with Sidak's multiple comparisons test. The level of significance was indicated as *p≤0.05 and ns=non-significant. Each cage contains 1-5 mice.

Table A4.6 Body weight of mice following *M. fortuitum* infection

Week	Mouse	Number	Body weight (g) Mean±SEM	p-value	Level of significance
Low-dose ($1x10^7$ CFU/mouse)					
0 (baseline)	Control	33	27.62±0.30	<0.0001	****
	Diabetic	30	46.97±0.53		
1	Control	27	29.61±0.31	<0.0001	****
	Diabetic	24	43.65±0.75		
2	Control	27	29.22±0.32	<0.0001	****
	Diabetic	24	42.09±0.90		
3	Control	17	30.50±0.52	<0.0001	****
	Diabetic	14	39.60±1.66		
4	Control	17	31.13±0.52	<0.0001	****
	Diabetic	14	39.00±1.60		
5	Control	17	30.00±0.45	<0.0001	****
	Diabetic	14	38.63±1.55		
High-dose ($3x10^8$ CFU/mouse)					
0 (baseline)	Control	8	26.78±1.62	<0.0001	****
	Diabetic	3	52.83±2.49		
1	Control	8	24.22±0.91	0.0002	***
	Diabetic	3	42.10±1.89		
2	Control	8	23.61±1.03	0.5953	ns
	Diabetic	3	28.45±7.85		

Statistical analysis: Data were analysed using the two-way ANOVA with Sidak's multiple comparisons test. The level of significance was indicated as ***p≤0.001, ****p≤0.0001 and ns=non-significant.

Table A4.7 Blood glucose level of mice following *M. fortuitum* infection

Week	Mouse	Number	Body glucose (mmol/L) Mean±SEM	p-value	Level of significance
Low-dose ($1x10^7$ CFU/mouse)					
0 (baseline)	Control	33	6.65±0.13	<0.0001	****
	Diabetic	30	9.23±0.20		
1	Control	27	6.10±0.19	<0.0001	****
	Diabetic	24	10.42±0.42		
2	Control	17	8.54±0.19	0.9980	ns
	Diabetic	14	8.36±0.49		
3	Control	17	8.33±0.35	0.0577	ns
	Diabetic	14	7.12±0.32		
4	Control	17	7.70±0.36	0.0000	****
	Diabetic	14	11.07±0.54		
High-dose ($3x10^8$ CFU/mouse)					
0 (baseline)	Control	8, 3	7.60±0.28	0.0685	ns
	Diabetic	8, 3	9.85±1.55		
1	Control	8, 3	5.86±0.50	0.8789	ns
	Diabetic	8, 3	5.22±0.94		
2	Control	8, 3	6.86±0.30	0.1629	ns
	Diabetic	8, 3	5.00±0.51		

Statistical analysis: Data were analysed using the two-way ANOVA with Sidak's multiple comparisons test. The level of significance was indicated as ****p≤0.0001 and ns=non-significant.

Table A4.8 Organ weight of mice following *M. fortuitum* infection

Organs	DPI	Number /group or (C, D)	Control	Diabetic	p-value	Level of significance
			Mean (g)±SEM			
Low-dose ($1x10^7$ CFU/mouse)						
Spleen	1	6	0.09±0.01	0.14±.01	0.0046	**
	14 ♦	10	0.14±0.02	0.19±0.02	0.0405	*
	35	9	0.28±0.04	0.36±0.03	0.1347	ns
Liver	1	6	1.42±0.09	2.52±0.20	0.0004	***
	14	10	1.70±0.11	2.68±0.17	0.0001	****
	35	9	1.90±0.10	2.98±0.19	0.0001	****
Lungs	1	6	0.24±0.01	0.27±0.03	0.4963	ns
	14	10	0.26±0.02	0.26±0.02	0.8129	ns
	35 ♦	9	0.27±0.01	0.29±0.02	0.0921	ns
Kidney (left)	14 ♦	10	0.21±0.01	0.31±0.02	0.0080	**
	35 ♦	10	0.23±0.01	0.35±0.02	0.0003	***
High-dose ($3x10^8$ CFU/mouse)						
Spleen	14	4, 6	0.41±0.03	0.43±0.10	0.8337	ns
Liver	14♦	4, 6	2.19±0.12	2.85±0.49	0.5224	ns
Lungs	14	4, 6	0.33±0.02	0.30±0.05	0.5938	ns
Kidney (left)	14	4, 6	0.23±0.01	0.38±0.04	0.0063	**

Statistical analysis: Data were checked for normality using Shapiro-Wilk's test. Data passed the test if $p \geq 0.05$. The normally distributed data were compared between the groups using the independent sample *t*-test. The non-normally distributed data (♦) were compared between the groups using the Mann-Whitney U test. The level of significance was indicated as *$p \leq 0.05$, **$p \leq 0.01$, ***$p \leq 0.001$, ****$p \leq 0.0001$ and ns=non-significant. In the table, DPI; days post-infection, C; control and D; diabetic.

Table A4.9 Organ bacterial kinetics of mice following *M. fortuitum* infection

Organs	DPI	Number /group or (C, D)	Control	Diabetic	p-value	Level of significance
			Mean (log_{10} CFU) ±SEM			
Low-dose ($1x10^7$ CFU/mouse)						
Spleen	1	3	2.43E+05±5.65E+04	3.24E+05±5.14E+04	0.3468	ns
	14	5	1.64E+05±5.77E+03	1.19E+05±2.26E+04	0.0905	ns
	35	5	3.37E+04±3.67E+03	6.02E+04±1.08E+04	0.0484	*
Liver	1	3	1.10E+06±3.99E+05	1.17E+06±5.14E+05	0.9179	ns
	14♦	4, 5	2.53E+06±4.42E+05	5.06E+06±1.02E+06	0.0500	*
	35	5, 4	9.14E+05±9.22E+04	2.21E+06±2.78E+05	0.0141	*
Lungs	1	3	3.52E+04±6.40E+03	3.95E+04±2.97E+03	0.5359	ns
	14	2, 5	5.00E+03±1.00E+03	2.13E+04±7.43E+03	0.0336	*
	35	5, 4	4.88E+03±1.59E+03	1.80E+04±3.53E+03	0.0081	**
	14	5	3.37E+04±4.18E+03	9.89E+04±3.87E+04	0.0283	*
	35	5, 4	3.88E+04±9.80E+03	2.06E+05±3.48E+04	0.0013	**
Kidneys	14♦	5,5	3.37E+04±4.18E+03	9.89E+04±3.87E+04	0.0283	*
	35	5,4	3.88E+04±9.80E+03	2.06E+05±3.48E+04	0.0013	**
High-dose ($3x10^8$ CFU/mouse)						
Spleen	14	3, 2	1.95E+05±1.68E+05	1.27E+06±1.90E+05	0.0255	*
Liver	14	3, 2	5.34E+05±2.27E+05	9.05E+06±4.25E+06	0.0752	ns
Lungs	14	3, 2	1.21E+05±6.06E+04	1.79E+06±2.25E+05	0.0029	**
Kidneys	14	3, 2	5.31E+05±1.59E+05	2.01E+06±2.30E+05	0.1160	ns

Statistical analysis: The normally distributed data were compared between groups using the independent sample *t*-test. The non-normally distributed data (♦) were compared between the groups using Mann-Whitney U test. The level of significance was indicated as *p≤0.05, **p≤0.01 and ns=non-significant. In the table, DPI; days post-infection, C; control and D; diabetic.

Table A4.10 Liver lesions of *M. fortuitum* infected mice

Parameter	DPI	Control	Diabetic	p-value	Level of significance
		Mean±SEM, n=5/group			
Low-dose (1x10^7 CFU/mouse)					
Inflamed area on liver (%)	14	2.51±0.49	6.97±1.38	0.0163	*
Number of foci on liver/ 200x)		3.47±0.56	7.68±0.74	0.0021	**
Mean area of each inflammatory focus (μm^2)		1071.34±89.57	1295.24±158.1	0.2528	ns
Inflamed area on liver (%)	35	10.75±0.36	16.77±1.61	0.0163	*
Number of inflammatory foci on liver/200x)		7.97±0.20	11.36±0.71	0.0069	**
Mean area of each inflammatory focus (μm^2)		1985.95±72.48	2165.38±123.68	0.2460	ns
Acid-fast bacilli/inflammatory focus	35♦	5.66±0.61	9.91±1.50	0.0079	**
High-dose (3x10^8 CFU/mouse)		**n=3 control and 2 diabetic mice**			
Inflamed area on liver (%)	14	18.69±1.68	35.99±6.22	0.2002	ns
Number of foci on liver/200x		15.33±0.73	32.20±2.80	0.0872	ns
Mean area of each inflammatory focus (μm^2)		1686.99±67.38	1611.07±75.12	0.5162	ns
Acid-fast bacilli/inflammatory focus		87.3±4.60	102.15±16.65	0.4806	ns

Statistical analysis: The normally distributed data were compared between the groups using the independent sample *t*-test. The non-normally distributed data (♦) were compared between the groups using the Mann-Whitney U test. The level of significance was indicated as *p≤0.05, **p≤0.01 and ns=non-significant.

Table A4.11 Lungs lesions of *M. fortuitum* infected mice

Parameter	DPI	Control	Diabetic	p-value	Level of significance
		Mean (%)±SEM, n=5/group			
Low-dose (1x10^7 CFU/mouse)					
Inflamed area in lungs	14	16.16±1.24	22.24±2.83	0.0846	ns
	35	20.53±0.87	24.80±0.79	0.0080	**
High-dose (3x10^8 CFU/mouse)		**n=3 control and 2 diabetic mice**			
Inflamed area in lungs	14	40.23±2.51	52.04±1.31	0.0398	*

Statistical analysis: Data were compared between the groups using the independent sample *t*-test as they passed the test of normality (Shapiro-Wilk's test). The level of significance was indicated as *p≤0.05, **p≤0.01, and ns=non-significant. In the table, DPI; days post-infection

Supplementary figures and photographs from *M. fortuitum* study (Chapter 6-7)

Dose: 1x10^7 (low-dose) and 3x10^8 CFU/mouse (high-dose)

***M. fortuitum* infection (low-dose)**

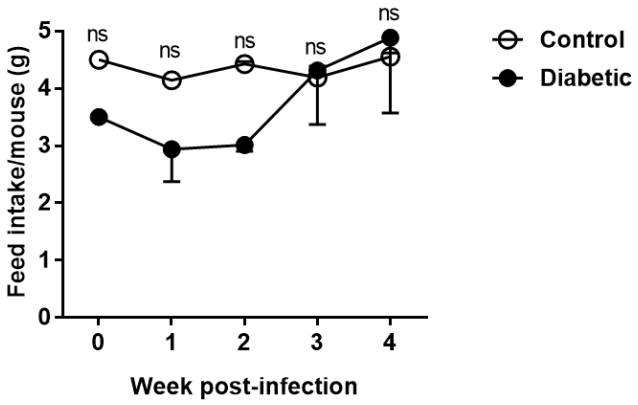

Figure A4.1 Daily feed intake by each mouse following a low-dose of *M. fortuitum* infection

Mice were infected with low-dose of *M. fortuitum* (1x10^7 CFU/mouse). Daily feed intake by each mouse was monitored for a period of 4 weeks. The feed intake by the diabetic mice dropped at first 2 weeks of infection. Then, the feed intake rose gradually in the same group of mice at later few weeks of infection. In contrast, there was a fluctuation of feed intake in the control group throughout the infection. Data presented as mean±SEM. The significant difference between the groups was determined using the two-way ANOVA with Sidak's multiple comparisons test. The level of significance was indicated as ns=non-significant.

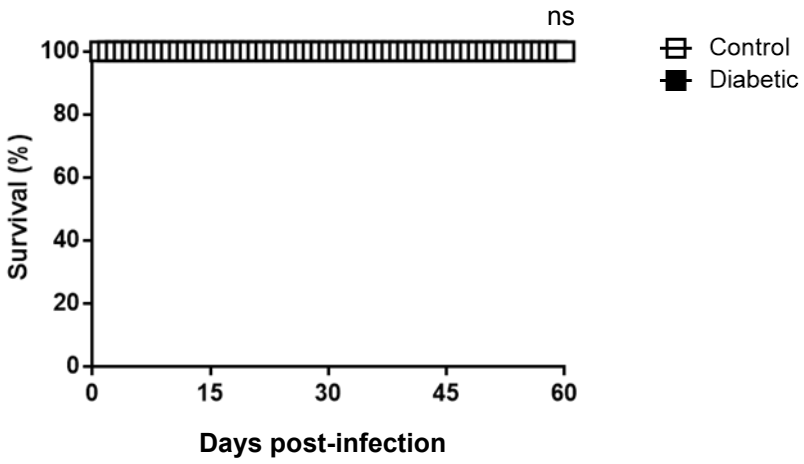

Figure A4.2 Survival of mice following a low-dose of *M. fortuitum* infection

Diabetic and control mice were infected with low-dose of *M. fortuitum* (1x10^7 CFU/mouse) intravenously to determine the kinetics of infection and their survival after 60 days post-infection (dpi). There was no mortality observed in both diabetic and control groups. The Kaplan Meier survival curves with Log-rank (Mantel-Cox) tests were used to compare the susceptibility between the groups. The level of significance was indicated as ns=non-significant.

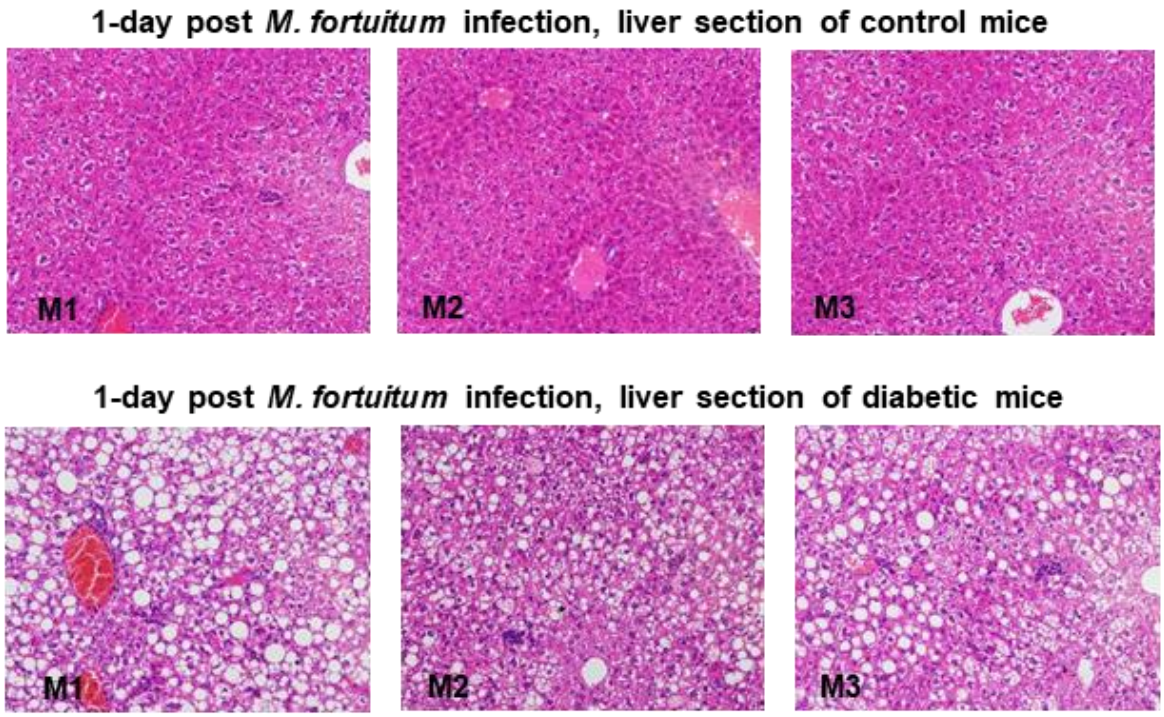

Figure A4.3 The representative photographs (one photo/mouse) of liver sections of control and diabetic mice infected with low-dose of *M. fortuitum*. All the photographs were taken at 200x magnification after the Hematoxylin and Eosin (H&E) staining of the liver sections at 1 day post-infection. In both diabetic and control mice, a diffuse inflammation was observed at this timepoint of infection.

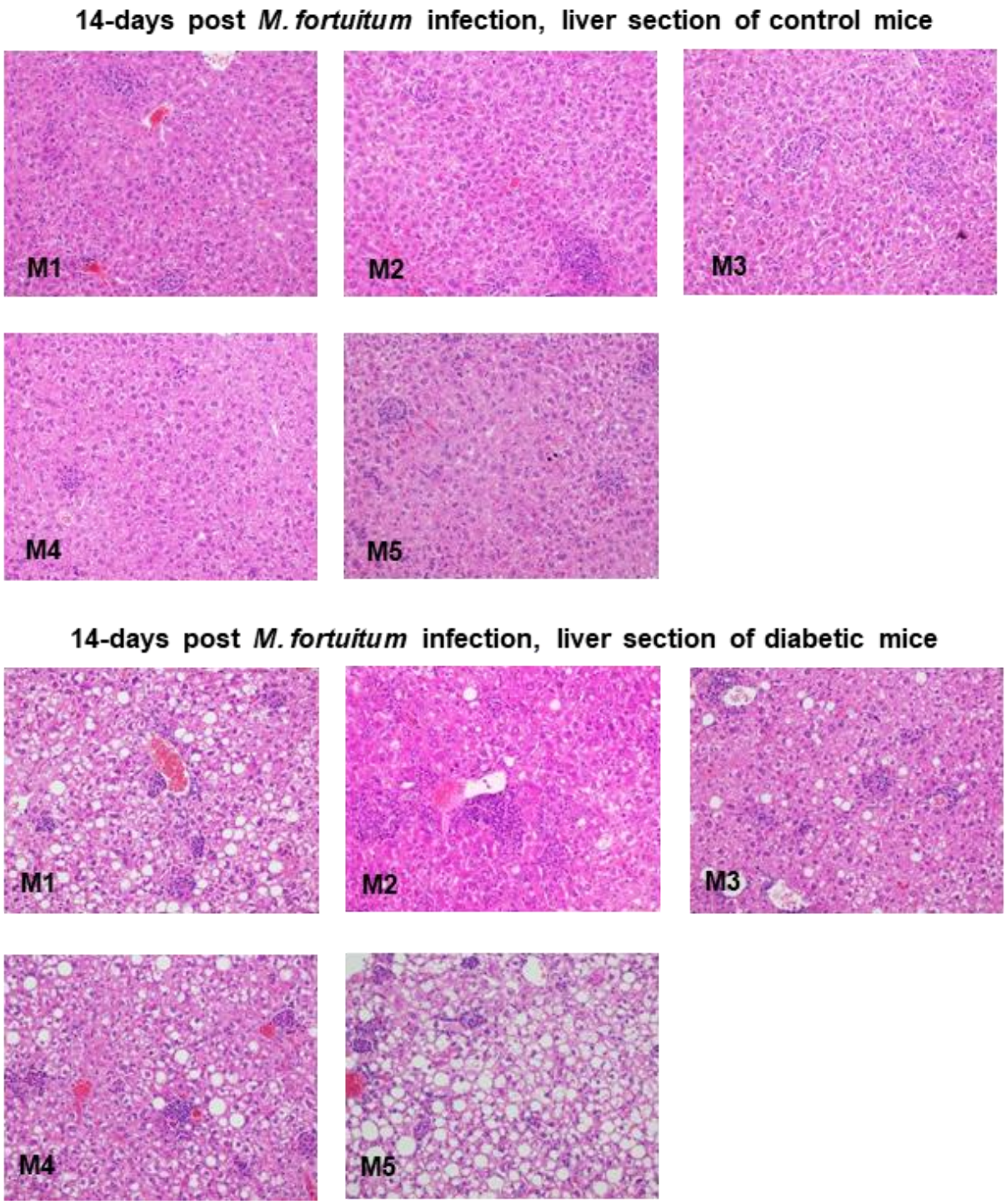

Figure A4.4 The representative photographs (one photo/mouse) of liver sections of control and diabetic mice infected with low-dose of *M. fortuitum*. All the photographs were taken at 200x magnification after the H&E staining to quantify the inflamed area over the liver at 14 days post-infection. In both diabetic and control mice, foci of inflammation/granuloma formation were evident at this timepoint of infection.

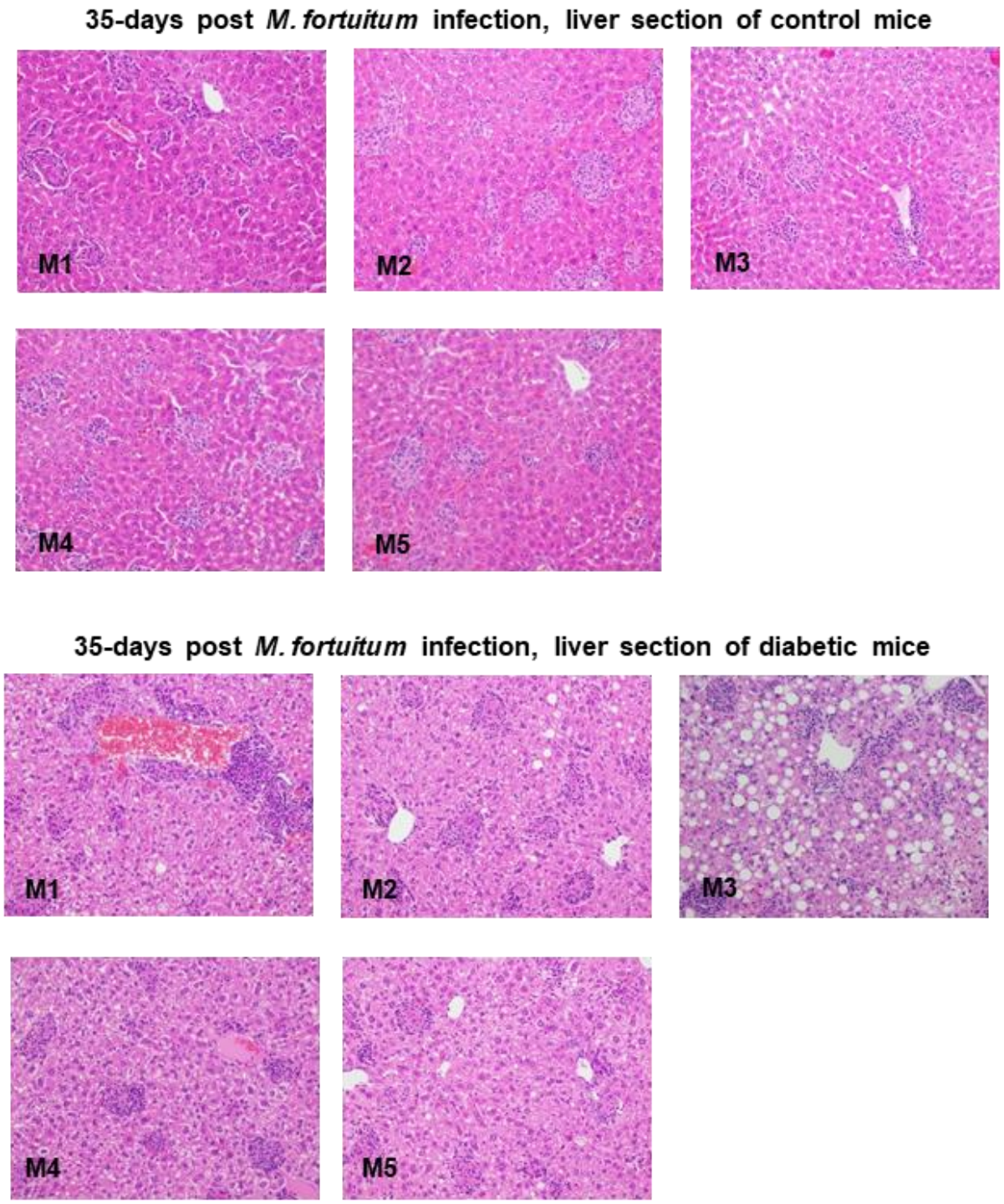

Figure A4.5 The representative photographs (one photo/mouse) of liver sections of control and diabetic mice infected with low-dose of *M. fortuitum*. All the photographs were taken at 200x magnification after H&E staining to quantify the inflamed area in the liver at 35 days post-infection. In both diabetic and control mice, more foci of inflammation/granuloma formation were evident at this timepoint of infection.

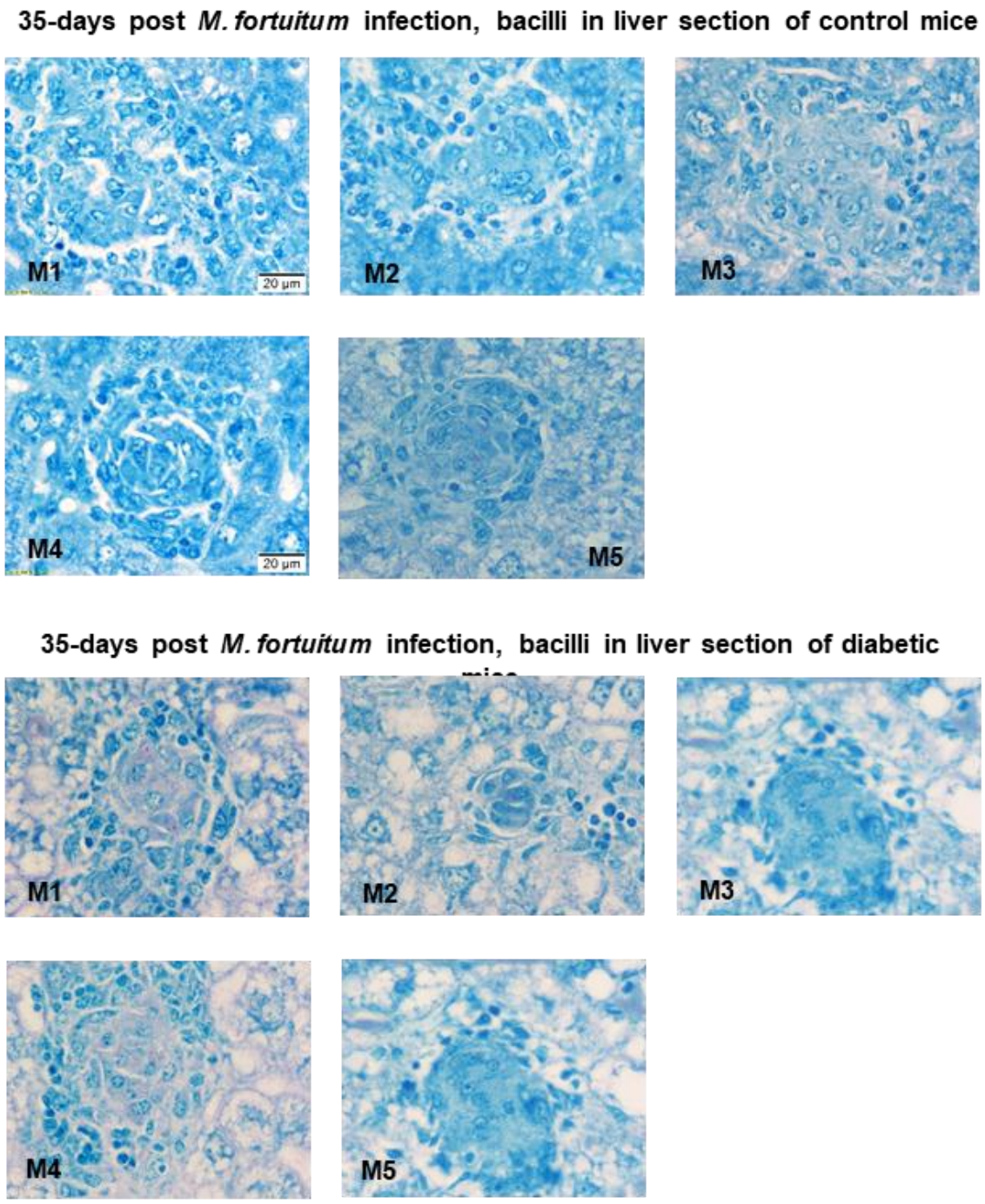

Figure A4.6 The representative photographs (one photo/mouse) of liver sections of control and diabetic mice infected with low-dose of *M. fortuitum*. All the photographs were taken at 1000x magnification after Ziehl-Neelsen staining to quantify the number of acid-fast bacilli (magenta) in each inflammatory focus /granuloma.

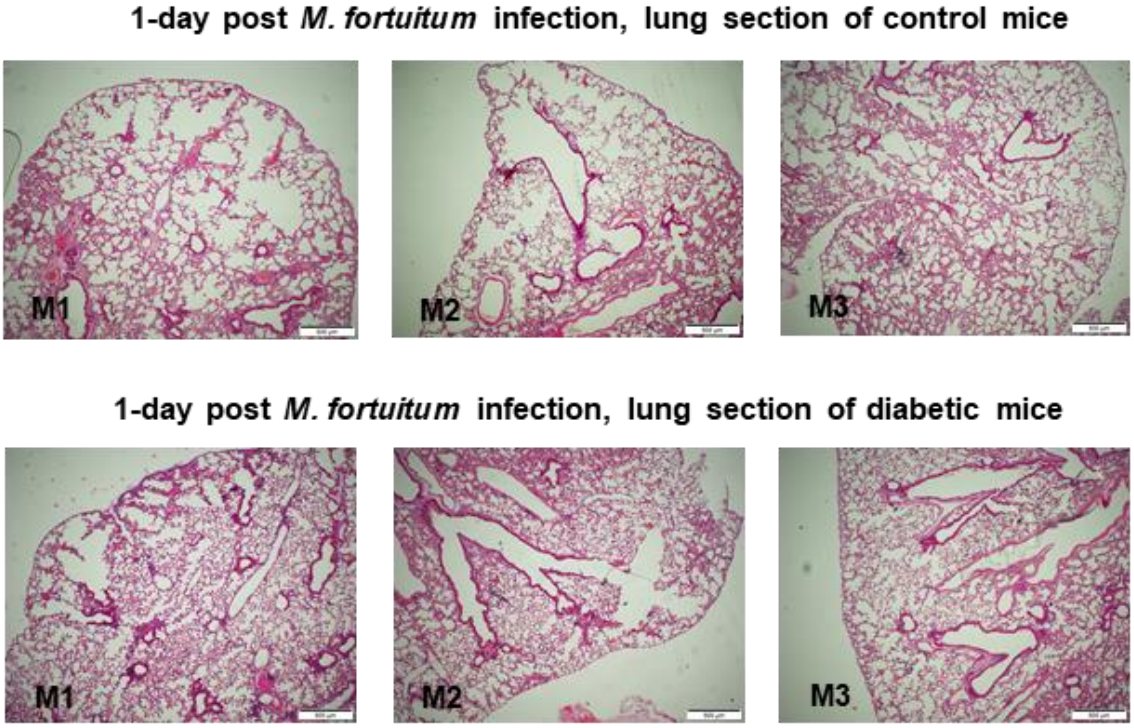

Figure A4.7 The representative photographs (one photo/mouse) of lung sections of control and diabetic mice infected with low-dose of *M. fortuitum*. All the photographs were taken at 40x magnification after H&E staining of lung sections at 1 day post-infection. In both diabetic and control mice, a diffuse inflammation was observed at this timepoint of infection.

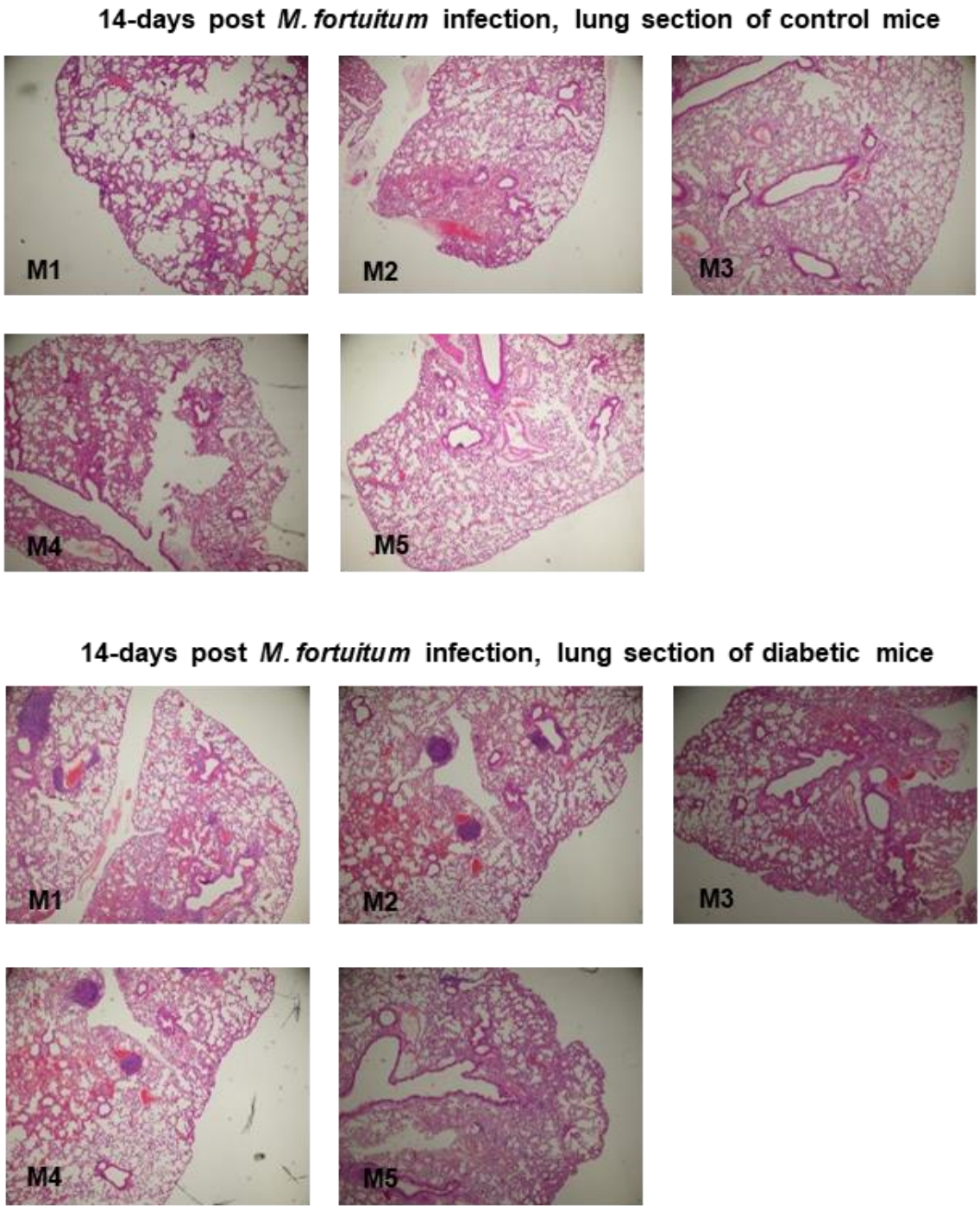

Figure A4.8 The representative photographs (one photo/mouse) of lung sections of control and diabetic mice infected with low-dose of *M. fortuitum*. All the photographs were taken at 40x magnification after H&E staining to quantify the total area of the lungs at 14 days post-infection. The inflamed area over the total area of lungs was measured on the photographs taken at 100x magnification (not shown here).

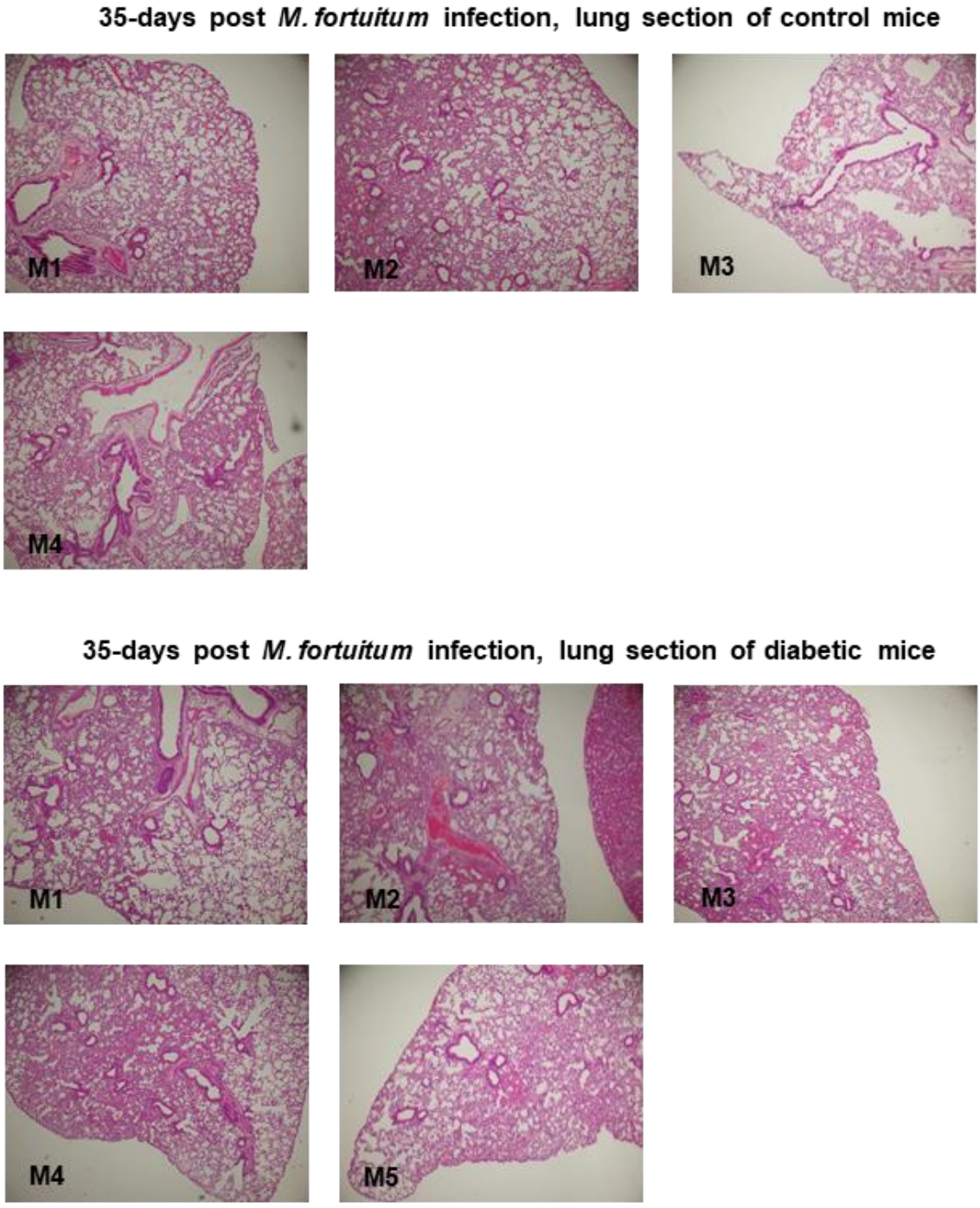

Figure A4.9 The representative photographs (one photo/mouse) of lung sections of control and diabetic mice infected with low-dose of *M. fortuitum*. All the photographs were taken at 40x magnification after H&E staining to quantify the total area of the lungs at 35 days post-infection. The inflamed area over the total area of lungs was measured on the photographs taken at 100x magnification (not shown here).

***M. fortuitum* infection (high-dose)**

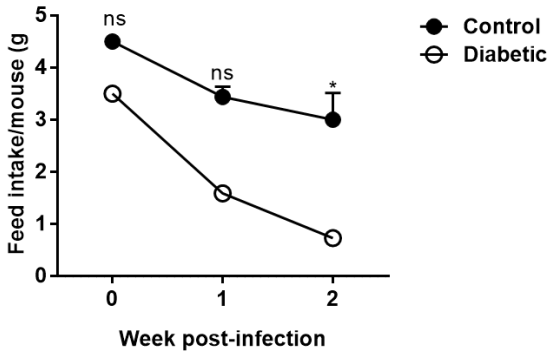

Figure A4.10 Daily feed intake by each mouse following a high-dose of *M. fortuitum* infection

Mice were infected with a high-dose of *M. fortuitum* ($3x10^8$ CFU/mouse). Daily feed intake by each mouse was monitored for a period of 2 weeks (until the death of the mice). There was a dramatic fall in the daily feed intake by each mouse in both control and diabetic group following infection. Data presented as mean±SEM. The significant difference between groups was determined using the two-way ANOVA with Sidak's multiple comparisons test. The level of significance indicated as *p≤0.05 and ns=non-significant.

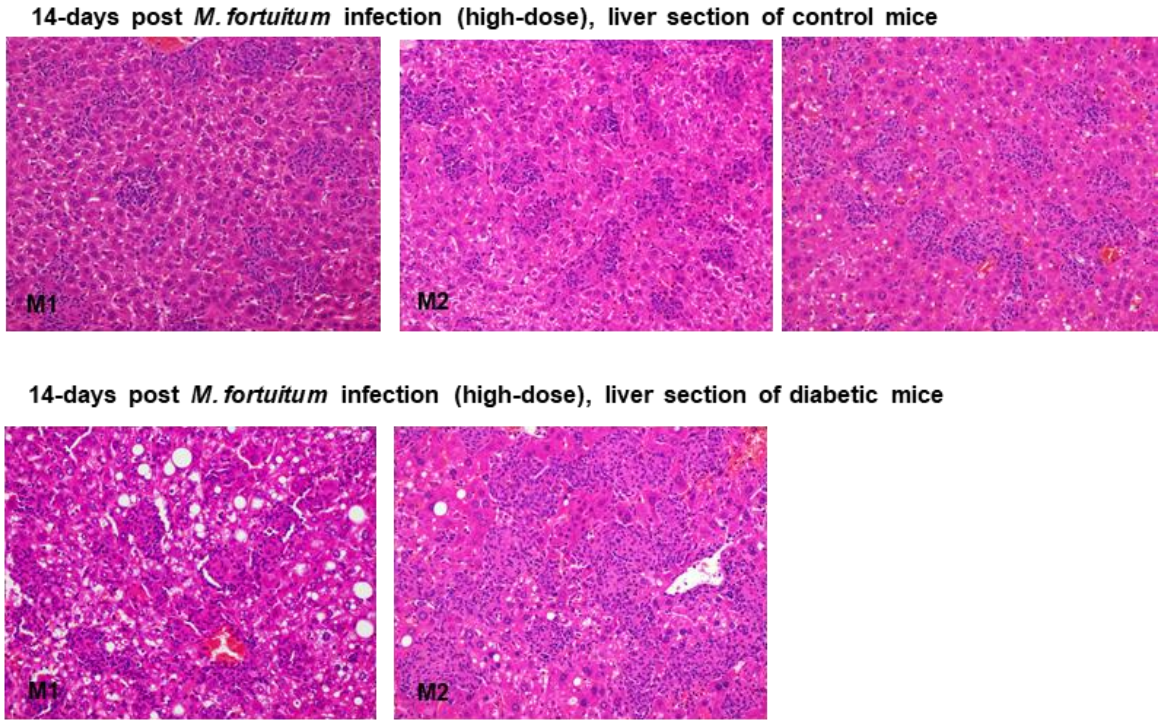

Figure A4.11 The representative photographs (one photo/mouse) of liver sections of control and diabetic mice infected with high-dose of *M. fortuitum*. All the photographs were taken at 200x magnification after H&E staining to quantify the inflamed area over the liver at 14 days post-infection. In both diabetic and control mice, more foci of inflammation/granuloma formation were evident at this timepoint of infection.

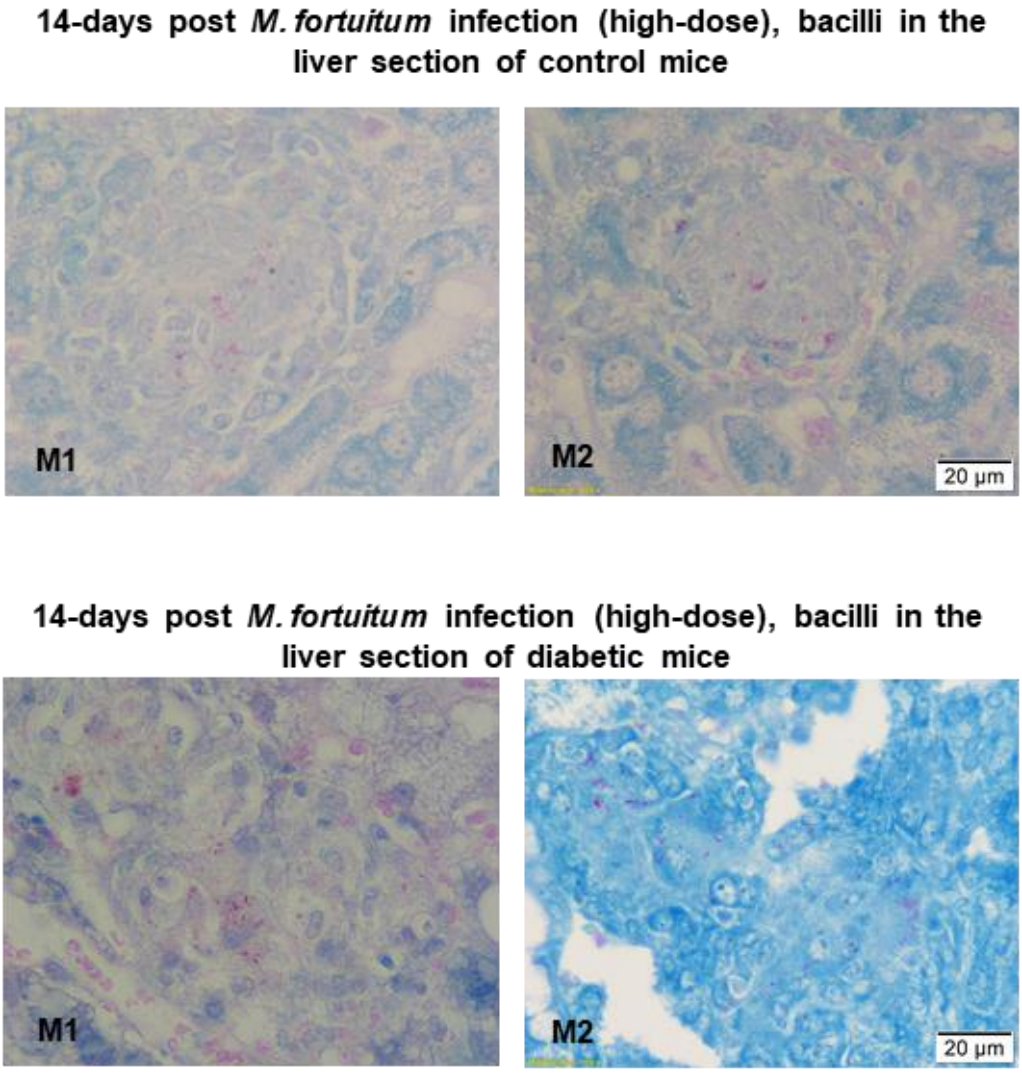

Figure A4.12 The representative photographs (one photo/mouse) of liver sections of control and diabetic mice infected with *M. fortuitum*. All the photographs were taken at 100x magnification after Ziehl-Neelsen staining to quantify the number of acid-fast bacilli (magenta) in each inflammatory focus/granuloma.

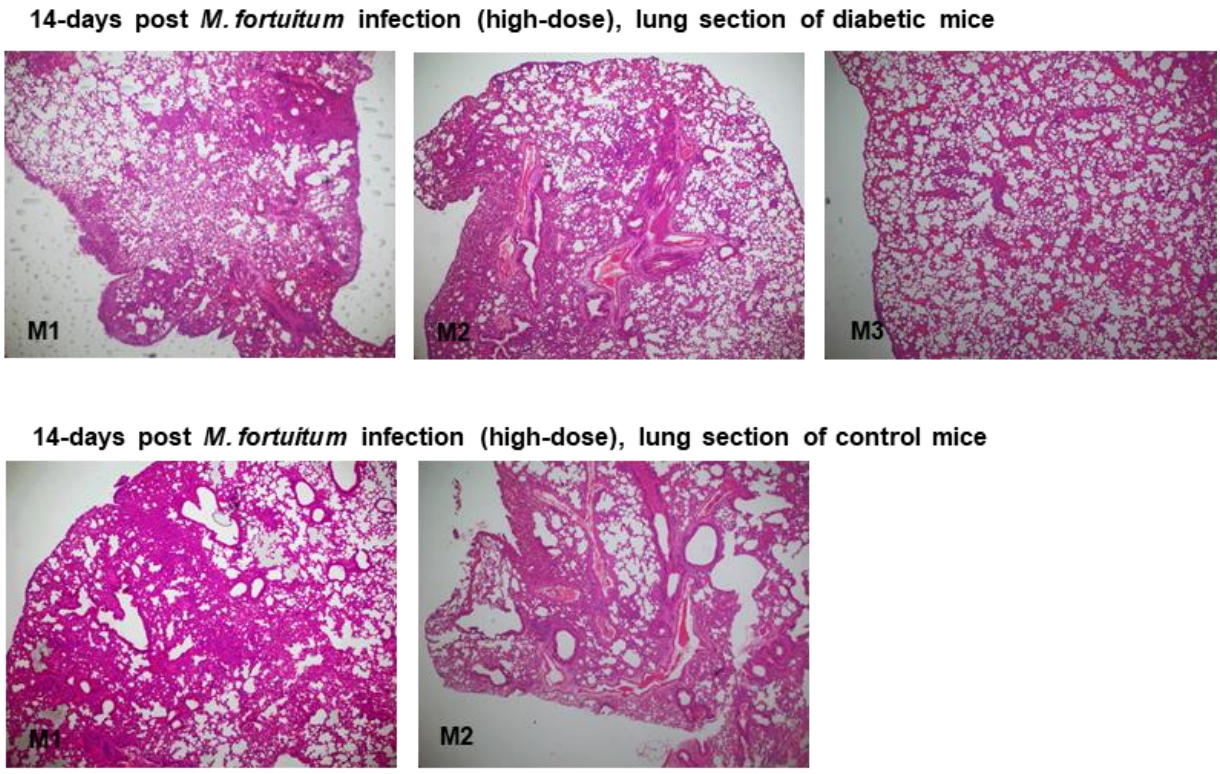

Figure A4.13 The representative photographs (one photo/mouse) of lung sections of control and diabetic mice infected with high-dose *M. fortuitum*. All the photographs were taken at 40x magnification after H&E staining to quantify the total area of the lungs at 14 days post-infection. The Inflamed area over the total area of lungs was measured on the photographs taken at 100x magnification (not shown here).

APPENDIX 5

All supplementary data from *M. bovis* (BCG) infection study (Chapter 6-8)
Dose: 1x10^6 CFU/mouse (low-dose) and 2x10^6/mouse (high-dose)

Table A5.1 Body weight and area under the curve of mice on standard rodent diet and energy-dense diet

Parameters	Mouse	Number	Mean±SEM	p-value	Level of significance
Body weight (0 week; g) ♦	SRD	32	25.18±0.30	0.9849	ns
	EDD	34	25.17±0.30		
Body weight (30th week; g) ♦	SRD	31	27.44±0.26	<0.0001	****
	EDD	33	46.19±0.65		
Area under the curve (AUC)	SRD	31	1199.86±31.11	0.0000	****
	EDD	33	1963.36±47.16		

Statistical analysis: Data were checked for normal distribution using Shaprio-Wilk's test. Data passed the test if p≥0.05. The non-normally distributed data (♦) were compared among the groups using the Kruskal-Wallis test with Dunn's multiple comparisons test. Area under the curve was compared between the groups using the Mann-Whitney U test as data set didn't pass the test of normality. The level of significance was indicated as ****p≤0.0001 and ns=non-significant. In the table, EDD; energy-dense diet, SRD; standard rodent diet.

Table A5.2 Glucose tolerance test after 30 weeks of energy-dense diet and standard rodent diet intervention

Time (minutes)	SRD (mmol/L, n=31)	EDD (mmol/L, n=33)	p-value	Level of significance
0	9.83±0.20	6.07±0.14	<0.0001	****
15	19.58±0.50	15.06±0.42	<0.0001	****
30	20.22±0.63	12.69±0.48	<0.0001	****
120	11.88±0.37	5.83±0.12	<0.0001	****

Statistical analysis: Data were analysed using the two-way ANOVA with Sidak's multiple comparisons test. Data presented as mean±SEM. The level of significance was indicated as ****p≤0.0001 and ns=non-significant. In the table, EDD; energy-dense diet, SRD; standard rodent diet.

Table A5.3 Percentage of diabetic mice after 30 weeks of energy-dense diet intervention based on baseline fasting blood glucose and area under the curve

Column statistics: Baseline fasting blood glucose

Col. stats	A	B
	Control baseline FBG	Diabetic baseline FBG
	Y	Y
1 Number of values	31	33
2		
3 Minimum	4.9	7.3
4 Maximum	8.3	12.3
5		
6 Mean	6.071	9.827
7 Std. Deviation	0.8009	1.169
8 Std. Error of Mean	0.1438	0.2035
9		
10 Lower 99% CI of mean	5.675	9.27
11 Upper 99% CI of mean	6.467	10.38
12		
13 Coefficient of variation	13.19%	11.89%
14		
15 Sum	188.2	324.3

Area under the curve

Col. stats	A	B
	Control AUC	Diabetic AUC
	Y	Y
1 Number of values	31	33
2		
3 Minimum	882	1228
4 Maximum	1547	2489
5		
6 Mean	1200	1963
7 Std. Deviation	173.2	270.9
8 Std. Error of Mean	31.11	47.16
9		
10 Lower 99% CI of mean	1114	1834
11 Upper 99% CI of mean	1285	2093
12		
13 Coefficient of variation	14.44%	13.80%
14		
15 Sum	37196	64791

Mice on EDD	Diabetic	Mice on EDD	Diabetic
Baseline FBG (mmol/L)	**Upper 99% CI of mean (>6.47 mmol/L) (Yes/No)**	**AUC-GTT**	**Upper 99% CI of mean (>1285) (Yes/No)**
10	Yes	2090	Yes
11	Yes	2489	Yes
8.3	Yes	1688	Yes
9.2	Yes	2132	Yes
10.5	Yes	2234	Yes
10.1	Yes	1687	Yes
11	Yes	1984	Yes
8.8	Yes	2337	Yes
10.8	Yes	2282	Yes
10.2	Yes	1988	Yes
11.3	Yes	2027	Yes
8.2	Yes	1661	Yes
9.3	Yes	1646	Yes
10.2	Yes	1853	Yes
7.3	Yes	2000	Yes
10.8	Yes	1822	Yes
10.8	Yes	1889	Yes
9.7	Yes	1883	Yes
9.2	Yes	2297	Yes
9.5	Yes	1379	Yes
9.5	Yes	2318	Yes
10.7	Yes	2159	Yes
12.3	Yes	2263	Yes
10.8	Yes	2032	Yes
9.3	Yes	1979	Yes
11	Yes	2039	Yes
7.7	Yes	1865	Yes
10.6	Yes	1744	Yes
7.9	Yes	1228	NO
8.5	Yes	1973	Yes
9.8	Yes	1912	Yes
9.2	Yes	1950	Yes
10.8	Yes	1961	Yes
% diabetic	**100% (33/33)**	**% diabetic**	**96.97 (32/33)**

Note: Mice were considered type 2 diabetes if they demonstrated a raised baseline FBG and AUG-GTT with evidence of glucose intolerance at levels higher the upper 99% confidence interval (CI) for the mean of age-matched control group fed on a standard rodent diet.

FBG; fasting blood glucose, AUC; area under the curve; AUC-GTT; area under the curve, EDD; energy-dense diet

Table A5.4 Daily feed intake by mice following *M. bovis* (BCG) infection

Week	Mouse	Cage no.	Feed intake (g/mouse/day) Mean±SEM	p-value	Level of significance
Low-dose (1x10^6 CFU/mouse)					
0 (baseline)	Control	3	4.50±0.00	<0.0001	****
	Diabetic	3	3.50±0.00		
1	Control	6	2.94±0.04	0.0703	ns
	Diabetic	4	3.22±0.11		
2	Control	6	2.54±0.10	0.1488	ns
	Diabetic	4	2.81±0.14		
3	Control	4	3.01±0.24	0.6257	ns
	Diabetic	3	2.81±0.31		
4	Control	4	3.88±0.20	0.0075	**
	Diabetic	3	3.13±0.17		
High-dose (2x10^6 CFU/mouse)					
0 (baseline)	Control	3	4.50±0.00	0.2383	ns
	Diabetic	3	3.50±0.00		
1	Control	2	4.73±0.51	<0.0001	****
	Diabetic	2	1.83±0.50		
2	Control	2	5.43±0.25	<0.0001	****
	Diabetic	2	2.48±0.17		
3	Control	2	4.16±0.01	0.0009	***
	Diabetic	2	1.97±0.02		
4	Control	2	4.16±0.02	0.0998	ns
	Diabetic	2	2.96±0.58		
5	Control	2	4.60±0.39	0.9997	ns
	Diabetic	2	4.39±0.44		
6	Control	2	4.10±0.30	0.9995	ns
	Diabetic	2	4.32±0.17		
7	Control	2	4.17±0.27	0.8439	ns
	Diabetic	2	3.60±0.02		

Statistical analysis: Data were analysed using the two-way ANOVA with Sidak's multiple comparisons test. The level of significance was indicated as **p≤0.01, ***p≤0.001, ****p≤0.0001 and ns=non-significant. Each cage contains 1-5 mice.

Table A5.5 Daily energy intake by mice following *M. bovis* (BCG) infection

Week	Mouse	Cage no.	Energy intake (kcal/mouse/day) Mean±SEM	p-value	Level of significance
Low-dose ($1x10^6$ CFU/mouse)					
0 (baseline)	Control	3	13.82±0.00	0.0013	**
	Diabetic	3	16.73±0.00		
1	Control	6	9.02±0.13	<0.0001	****
	Diabetic	4	15.38±0.50		
2	Control	6	7.80±0.30	<0.0001	****
	Diabetic	4	13.42±0.68		
3	Control	4	9.23±0.74	0.0001	***
	Diabetic	3	13.42±1.50		
4	Control	4	11.91±0.62	0.0056	**
	Diabetic	3	14.98±0.81		
High-dose ($2x10^6$ CFU/mouse)					
0 (baseline)	Control	3	13.82±0.00	0.4923	ns
	Diabetic	3	16.73±0.00		
1	Control	2	14.53±1.57	0.0286	*
	Diabetic	2	8.73±2.37		
2	Control	2	16.66±0.77	0.0955	ns
	Diabetic	2	11.86±0.83		
3	Control	2	12.79±0.03	0.4296	ns
	Diabetic	2	9.43±0.12		
4	Control	2	12.78±0.06	0.9896	ns
	Diabetic	2	14.16±2.78		
5	Control	2	14.11±1.20	0.0073	**
	Diabetic	2	21.00±2.10		
6	Control	2	12.58±0.81	0.0017	**
	Diabetic	2	17.20±0.09		
7	Control	2	12.80±0.84	0.1509	ns
	Diabetic	2	17.20±0.09		

Statistical analysis: Data were analysed using the two-way ANOVA with Sidak's multiple comparisons test. The level of significance was indicated as *p≤0.05, **p≤0.01, ***p≤0.001, ****p≤0.0001 and ns=non-significant. Each cage contains 1-5 mice.

Table A5.6 Body weight of mice following *M. bovis* (BCG) infection

Week	Mouse	Number	Body weight Mean(g)±SEM	p-value	Level of significance
Low-dose (1x10^6 CFU/mouse)					
0 (baseline)	Control	32	27.08±0.86	0.0000	****
	Diabetic	29	46.44±0.80		
1	Control	26	27.36±0.32	0.0000	****
	Diabetic	19	45.52±1.14		
2	Control	26	26.34±0.80	0.0000	****
	Diabetic	23	45.22±1.23		
3	Control	16	27.50±0.40	0.0000	****
	Diabetic	13	41.27±2.13		
4	Control	16	27.00±0.37	0.0000	****
	Diabetic	13	40.47±2.28		
5	Control	16	26.75±0.46	0.0000	****
	Diabetic	13	36.92±2.07		
High-dose (2x10^6 CFU/mouse)					
0 (baseline)	Control	12	28.75±0.59	<0.0001	****
	Diabetic	9	50.47±1.40		
1	Control	12	28.40±0.59	<0.0001	****
	Diabetic	9	50.12±1.40		
2	Control	12	28.65±0.48	<0.0001	****
	Diabetic	9	44.08±2.09		
3	Control	11	28.19±0.66	<0.0001	****
	Diabetic	9	36.79±1.95		
4	Control	11	28.24±0.52	<0.0001	****
	Diabetic	7	37.02±1.90		
5	Control	11	28.24±0.55	<0.0001	****
	Diabetic	7	36.77±1.79		
6	Control	11	27.22±0.42	<0.0001	****
	Diabetic	7	35.05±1.56		
7	Control	10	27.41±0.50	<0.0001	****
	Diabetic	7	35.61±1.68		

Statistical analysis: Data were analysed using the two-way ANOVA with Sidak's multiple comparisons test. The level of significance was indicated as ****p≤0.0001.

Table A5.7 Blood glucose level following *M. bovis* (BCG) infection

Week	Mouse	Number	Blood glucose Mean(mmol/L)±SEM	p-value	Level of significance
Low-dose (1x10^6 CFU/mouse)					
0 (baseline)	Control	32	7.35±0.20	0.0012	**
	Diabetic	29	8.54±0.29		
1	Control	26	8.12±0.23	0.9929	ns
	Diabetic	19	8.13±0.29		
2	Control	25	8.11±0.17	0.0809	ns
	Diabetic	22	8.59±0.24		
3	Control	16	7.72±0.20	0.3089	ns
	Diabetic	13	8.22±0.47		
4	Control	16	7.74±0.28	0.2980	ns
	Diabetic	13	8.29±0.47		
5	Control	16	8.39±0.22	0.2632	ns
	Diabetic	13	9.01±0.53		
High-dose (2x10^6 CFU/mouse)					
0 (baseline)	Control	11	7.40±0.22	0.0095	**
	Diabetic	9	9.57±0.77		
1	Control	12	7.02±0.25	0.1233	ns
	Diabetic	9	8.58±0.39		
2	Control	12	6.02±0.26	0.4532	ns
	Diabetic	9	7.18±0.45		
3	Control	11	5.50±0.15	0.0184	*
	Diabetic	8	7.60±0.35		
4	Control	11	6.25±0.31	0.0811	ns
	Diabetic	7	8.07±0.37		
5	Control	11	7.07±0.37	0.1426	ns
	Diabetic	7	8.74±0.66		
6	Control	11	8.23±0.48	0.0757	ns
	Diabetic	7	10.07±1.13		
7	Control	11	7.65±0.37	0.0102	*
	Diabetic	7	9.13±0.50		

Statistical analysis: Data were analysed using the two-way ANOVA with Sidak's multiple comparisons test. The level of significance was indicated as *p≤0.05, **p≤0.01 and ns=non-significant.

Table A5.8 Organ weight of mice following *M. bovis* (BCG) infection

Organs	DPI	Number /group	Control	Diabetic	p-value	Level of significance
			Mean(g)±SEM			
Low-dose (1x10^6 CFU/mouse)						
Spleen	1	8	0.09±0.01	0.15±0.03	0.0476	*
	14	10	0.15±0.02	0.38±0.04	0.0002	***
	35	4	0.20±0.03	0.35±0.02	0.0064	**
Liver	1	8	1.57±0.07	2.9±0.35	0.0069	**
	14	10	1.90±0.07	3.37±0.15	0.0000	****
	35	4	2.44±0.14	3.81±0.10	0.0002	***
Lungs	1	8	0.23±0.02	0.30±0.02	0.0230	*
	14♦	10	0.24±0.02	0.29±0.03	0.1304	ns
	35	4	0.38±0.04	0.45±0.03	0.1884	ns

Statistical analysis: Data were checked for normality using Shapiro-Wilk's test. Data passed the test if p≥0.05. The normally distributed data were compared between the groups using the independent sample *t*-test. The non-normally distributed data (♦) were compared between the groups using the Mann-Whitney U test. The level of significance was indicated as *p≤0.05, **p≤0.01, ***p≤0.001, ****p≤0.0001 and ns=non-significant. In the table, DPI; days post-infection.

Table A5.9 Organ bacterial kinetics of mice following *M. bovis* (BCG) infection

Organs	DPI	Number /group	Control	Diabetic	p-value	Level of significance
			Mean(log_{10} CFU)±SEM			
Low-dose (1x10^6 CFU/mouse)						
Spleen	1	4	1.36E+04±1.81E+03	1.68E+04±4.01E+03	0.4976	ns
	14♦	5	1.10E+05±1.89E+04	2.80E+05±5.68E+04	0.1161	ns
	35	5	1.97E+04±3.04E+03	3.57E+04±5.87E+03	0.0419	*
Liver	1♦	4	1.05E+05±1.64E+04	2.57E+05±1.45E+05	0.5637	ns
	14	5	3.70E+06±5.13E+05	1.26E+07±2.77E+06	0.0306	*
	35	5	1.50E+05±3.78E+04	9.15E+05±2.37E+05	0.0311	*
Lungs	1	4	6.63E+03±9.87E+02	8.75E+03±3.66E+02	0.0901	ns
	14	3	3.60E+04±4.41E+03	8.04E+04±6.43E+03	0.0029	**
	35	5	1.92E+03±2.87E+02	5.54E+03±4.69E+02	0.0002	***

Statistical analysis: The normally distributed data were compared between the groups using the independent sample *t*-test. The non-normally distributed data (♦) were compared between the groups using Mann-Whitney U test. The level of significance was indicated as *p≤0.05, **p≤0.01, ***p≤0.001 and ns=non-significant. In the table, DPI; days post-infection.

Table A5.10 Liver lesions of *M. bovis* (BCG) infected mice

Parameter	DPI	Control	Diabetic	p-value	Level of significance
		Mean±SEM, n=5/group			
Low-dose (1x10^6 CFU/mouse)					
Inflamed area on liver (%)	14	4.49±0.44	8.23±0.82	0.0038	**
Number of inflammatory foci on liver/ 200x)		4.40±0.43	6.68±0.44	0.0059	**
Mean area of each inflammatory focus (μm^2)		3598.80±135.85	4322.06±301.32	0.0601	ns
Inflamed area on liver (%)	35	9.05±0.39	12.19±0.80	0.0075	**
Number of inflammatory foci on liver/ 200x)		6.82±0.46	8.08±0.78	0.2010	ns
Mean area of each inflammatory (μm^2)		4766.06±416.05	5436.45±485.25	0.3249	ns
Acid-fast bacilli/inflammatory focus	14	13.00±1.08	17.56±3.96	0.2985	ns
	35	17.59±2.09	23.25±5.01	0.2940	ns

Statistical analysis: Data were compared between the groups using the independent sample *t*-test as they passed the test of normality (Shapiro-Wilk's test, p≥0.05). The level of significance was indicated as *p≤0.05, **p≤0.01 and ns=non-significant. In the table, DPI; days post-infection.

Table A5.11 Lung lesions in *M. bovis* (BCG) infected mice

Parameter	DPI	Control	Diabetic	p-value	Level of significance
		Mean (%)±SEM, n=5/group			
Low-dose (1x10^6 CFU/mouse)					
Inflamed area in lungs	14	11.28±1.00	18.61±3.06	0.0524	*
	35	22.74±0.74	25.47±0.69	0.0274	*

Statistical analysis: Data were compared between the groups using the independent sample *t*-test as they passed the test of normality (Shapiro-Wilk's test). The level of significance was indicated as *p≤0.05. In the table, DPI; days post-infection.

Table A5.12 Cytokine production in spleen following *M. bovis* (BCG) infection (low-dose)

Spleen		Days-post infection, n=4-5 mice/group					
		1		14		35	
Cytokine	**Mouse**	**Mean±SEM (pg/mL)**	**p-value**	**Mean±SEM (pg/mL)**	**p- value**	**Mean±SEM (pg/mL)**	**p-value**
IL-1β	Control	3.93±0.69	ns 0.0576	75.06±7.69	ns 0.1954	20.12±4.97	* 0.0546
	Diabetic	8.96±2.03		98.09±14.37		41.04±7.86	
TNF-α	Control	39.16±4.95	ns 0.0810	196.40±18.25	ns 0.8415	52.72±1.98	ns 0.1478
	Diabetic	28.21±2.36		203.47±26.50		46.84±3.09	
MCP-1	Control	6.48±3.75	ns 0.1445	172.32±30.31	ns 0.2601	25.59±3.48	** 0.0056
	Diabetic	21.58±8.47		214.64±17.34		54.50±6.86	
IL-6	Control	6.22±0.63	* 0.0350	15.01±2.81	ns 0.1131	7.13±1.96	ns 0.1271
	Diabetic	3.56±0.84		21.22±2.08		3.65±0.60	
IFN-γ	Control	1.88±0.62	ns 0.7150	49.17±16.87	ns 0.5321	11.10±1.57	* 0.0343
	Diabetic	2.28±0.84		35.78±11.67		6.68±0.74	
IL-12p70	Control	0.23±0.13	ns 0.7457♦	0.47±0.43	ns 0.2812	2.25±1.69	ns 0.8877♦
	Diabetic	1.09±1.07		2.33±1.47		1.97±0.91	
IL-2	Control	8.37±0.98	ns 0.3475	9.76±4.06	* 0.0245♦	8.02±2.14	* 0.0380
	Diabetic	6.56±1.49		1.75±0.30		2.21±0.96	
IL-4	Control	0.76±0.76	ns 0.3173	0.00±0.00	-	0.00±0.00	-
	Diabetic	0.00±0.00		0.00±0.00		0.00±0.00	
IL-10	Control	30.21±5.27	ns 0.1745♦	22.22±4.40	ns 0.5097	26.18±6.90	ns 0.6952
	Diabetic	24.46±3.88		18.86±2.08		23.19±2.57	
IL-17A	Control	0.00±0.00	ns 0.3173♦	0.04±0.04	ns 0.3173♦	0.00±0.00	ns 0.1360♦
	Diabetic	0.20±0.20		0.00±0.00		0.21±0.13	

Statistical analysis: The normally distributed data were compared between the groups using the independent sample *t*-test. The non-normally distributed data (♦) were compared between the groups using the Mann-Whitney U test. The level of significance was indicated as *p≤0.05, **p≤0.01 and ns=non-significant.

Table A5.13 Cytokine production in liver following *M. bovis* (BCG) infection (low-dose)

Liver		Days-post infection, n=4-5 mice/group					
		1		14		35	
Cytokine	**Mouse**	**Mean±SEM (pg/mL)**	**p-value**	**Mean±SEM (pg/mL)**	**p-value**	**Mean±SEM (pg/mL)**	**p-value**
IL-1β	Control	3.55±1.22	** 0.0057	61.50±14.74	ns 0.1148	46.43±18.27	ns 0.6132
	Diabetic	11.86±1.51		30.78±9.17		32.67±18.73	
TNF-α	Control	21.78±4.88	ns 0.0999	72.25±7.78	* 0.0163♦	45.47±3.69	*** 0.0008
	Diabetic	33.06±2.50		48.92±3.83		19.51±2.06	
MCP-1	Control	48.23±5.48	* 0.0358	125.16±23.14	ns 0.2813	41.46±8.15	ns 0.3127
	Diabetic	69.21±5.90		162.22±22.22		52.89±6.40	
IL-6	Control	20.10±3.72	ns 0.7768	24.91±6.93	ns 0.6683	23.39±7.87	* 0.0563
	Diabetic	22.63±8.52		31.77±13.76		4.63±1.08	
IFN-γ	Control	2.09±0.54	ns 0.0630	27.53±1.42	* 0.0301	6.70±0.48	*** 0.0008
	Diabetic	3.56±0.29		21.69±1.69		3.23±0.28	
IL-12p70	Control	16.31±3.60	0.2149	9.90±2.12	ns 0.3962	15.48±4.23	ns 0.1889
	Diabetic	33.96±11.12		13.80±4.04		7.45±3.39	
IL-2	Control	15.41±5.28	0.8855	15.36±5.88	ns 0.1638	8.49±3.68	ns 0.2669
	Diabetic	16.28±2.37		28.43±6.17		14.94±3.97	
IL-4	Control	2.28±1.53	* 0.0198	2.29±1.82	* 0.0300	0.75±0.49	ns 0.6107♦
	Diabetic	7.85±0.89		14.96±4.45		0.45±0.26	
IL-10	Control	33.27±4.00	ns 0.2369	18.34±2.22	ns 0.0871	36.19±1.98	ns 0.1409
	Diabetic	39.80±2.53		29.29±4.81		27.27±4.87	
IL-17A	Control	0.15±0.15	ns 0.0907♦	0.27±0.27	ns 0.1389	0.05±0.05	ns 0.1955♦
	Diabetic	1.12±0.44		1.28±0.53		0.45±0.26	

Statistical analysis: The normally distributed data were compared between the groups using the independent sample *t*-test. The non-normally distributed data (♦) were compared between the groups using the Mann-Whitney U test. The level of significance was indicated as *p≤0.05, **p≤0.01, ***p≤0.001 and ns=non-significant.

Table A5.14 Cytokine production in lungs following *M. bovis* (BCG) infection (low-dose)

Lungs		Days-post infection, n=4-5 mice/group					
		1		14		35	
Cytokine	**Mouse**	**Mean±SEM (pg/mL)**	**p-value**	**Mean±SEM (pg/mL)**	**p value**	**Mean±SEM (pg/mL)**	**p value**
IL-1β	Control	6.44±3.40	ns 0.0800	4.81±0.83	ns 0.8222	14.41±7.36	ns 0.3193
	Diabetic	17.69±6.40		4.08±3.05		5.56±3.32	
TNF-α	Control	22.31±6.30	ns 0.0947	38.89±1.39	* 0.0374	66.40±28.49	ns 0.1102♦
	Diabetic	34.44±1.17		29.41±3.54		27.59±7.58	
MCP-1	Control	85.58±17.83	ns 0.2627	120.15±13.34	* 0.0541	39.34±16.94	ns 0.3493
	Diabetic	133.23±35.30		167.11±15.99		65.64±19.61	
IL-6	Control	17.38±7.54	ns 0.1610	5.81±0.85	ns 0.9430	18.88±7.55	ns 0.0907♦
	Diabetic	44.11±15.56		5.92±1.16		3.59±0.76	
IFN-γ	Control	0.05±0.04	ns 0.7231♦	14.85±3.41	* 0.0330	6.17±0.95	** 0.0026
	Diabetic	0.10±0.06		4.84±1.90		1.11±0.38	
IL-12p70	Control	2.54±1.39	ns 0.7600♦	0.47±0.32	ns 0.1900♦	2.86±0.75	* 0.0181
	Diabetic	3.18±1.46		1.76±0.85		0.29±0.29	
IL-2	Control	0.00±0.00	-	0.00±0.00	ns 0.3739	3.76±1.93	ns 0.1306♦
	Diabetic	0.00±0.00		0.70±0.70		1.34±1.34	
IL-10	Control	17.08±2.57	** 0.0070	21.87±2.53	ns 0.9638	28.16±5.17	ns 0.0829
	Diabetic	34.20±4.05		21.49±7.71		11.56±6.09	
IL-4	Control	0.00±0.00	-	0.00±0.00	-	0.00±0.00	-
	Diabetic	0.00±0.00		0.00±0.00		0.00±0.00	
IL-17A	Control	0.00±0.00	-	0.00±0.00	-	0.00±0.00	-
	Diabetic	0.00±0.00		0.00±0.00		0.00±0.00	

Statistical analysis: The normally distributed data were compared between groups using the independent sample *t*-test. The non-normally distributed data (♦) were compared between the groups using the Mann-Whitney U test. The level of significance was indicated as *p≤0.05, **p≤0.01 and ns=non-significant.

All supplementary figures and photographs from *M. bovis* (BCG) infection study (Chapter 6-7)
Dose: 1x10^6 (low-dose) and 2x10^6 (high-dose)

***M. bovis* (BCG) infection (low-dose)**

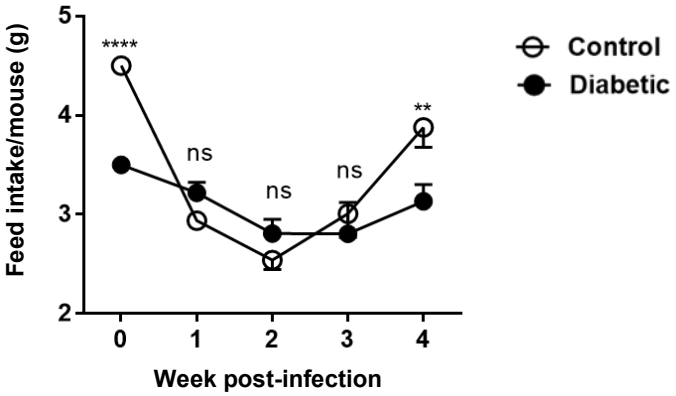

Figure A5.1 Daily feed intake by each mouse following low-dose of *M. bovis* (BCG) infection

Mice were infected with low-dose of *M. bovis* (1x10^6 CFU/mouse). Daily feed intake by each mouse was monitored for a period of 4 weeks. The feed intake by the diabetic mice dropped gradually followed by a slight increased at last 2 weeks of infection. In control group, there was a sharp reduction of the daily feed intake by each mouse at first 2 weeks of infection followed by a rapid raise at last few weeks of infection. Data presented as mean±SEM. The significance difference was determined using the two-way ANOVA with Sidak's multiple comparisons test. The level of significance was indicated as **p≤0.01 and ***** p≤0.0001 and ns=non-significant.

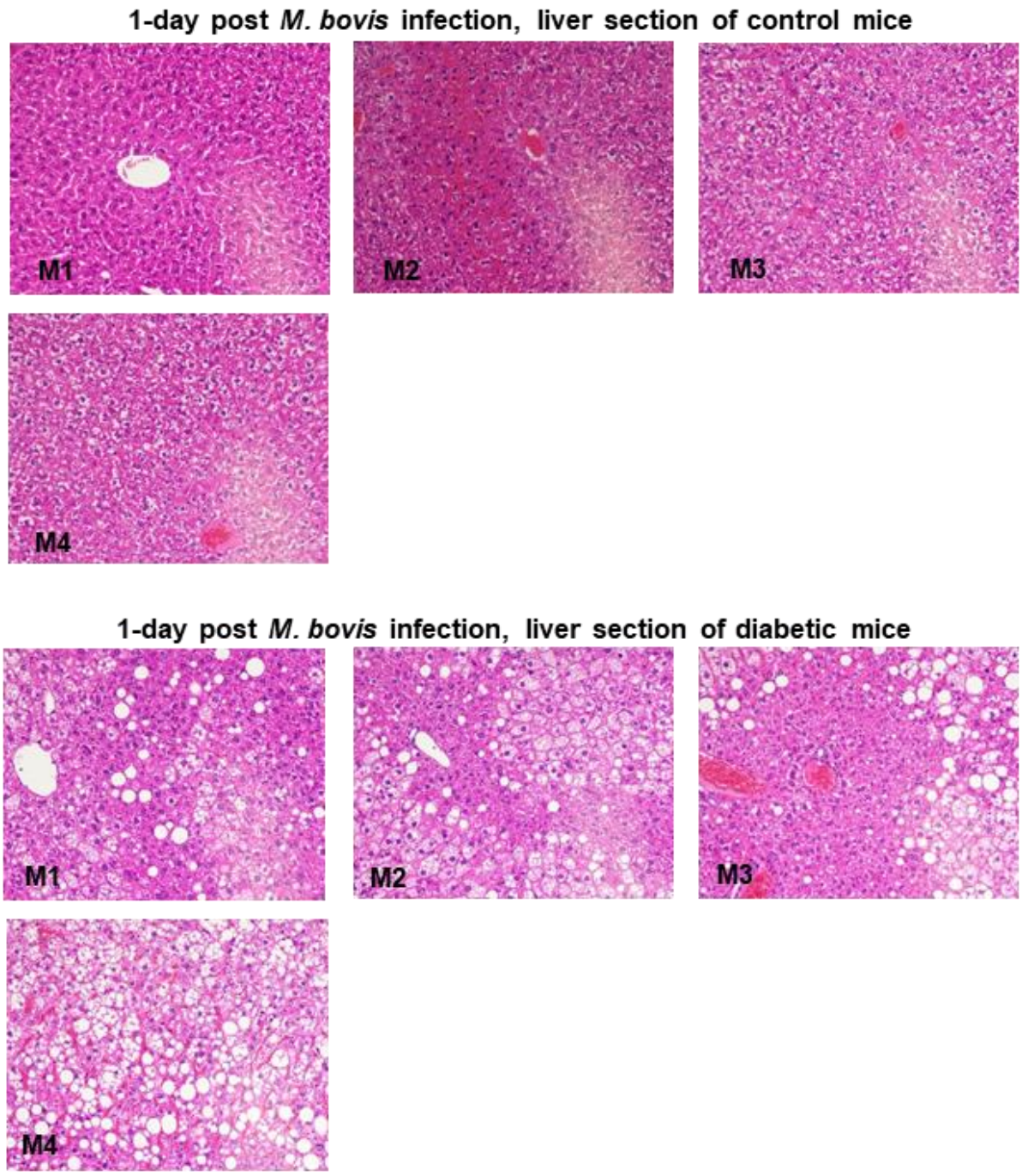

Figure A5.2 The representative photographs (one photo/mouse) of liver sections of control and diabetic mice infected with low-dose of *M. bovis* (BCG). All the photographs were taken at 200x magnification after Hematoxylin and Eosin (H&E) staining of the liver sections at 1 day post-infection. In both diabetic and control mice, a diffuse inflammation was observed at this timepoint of infection.

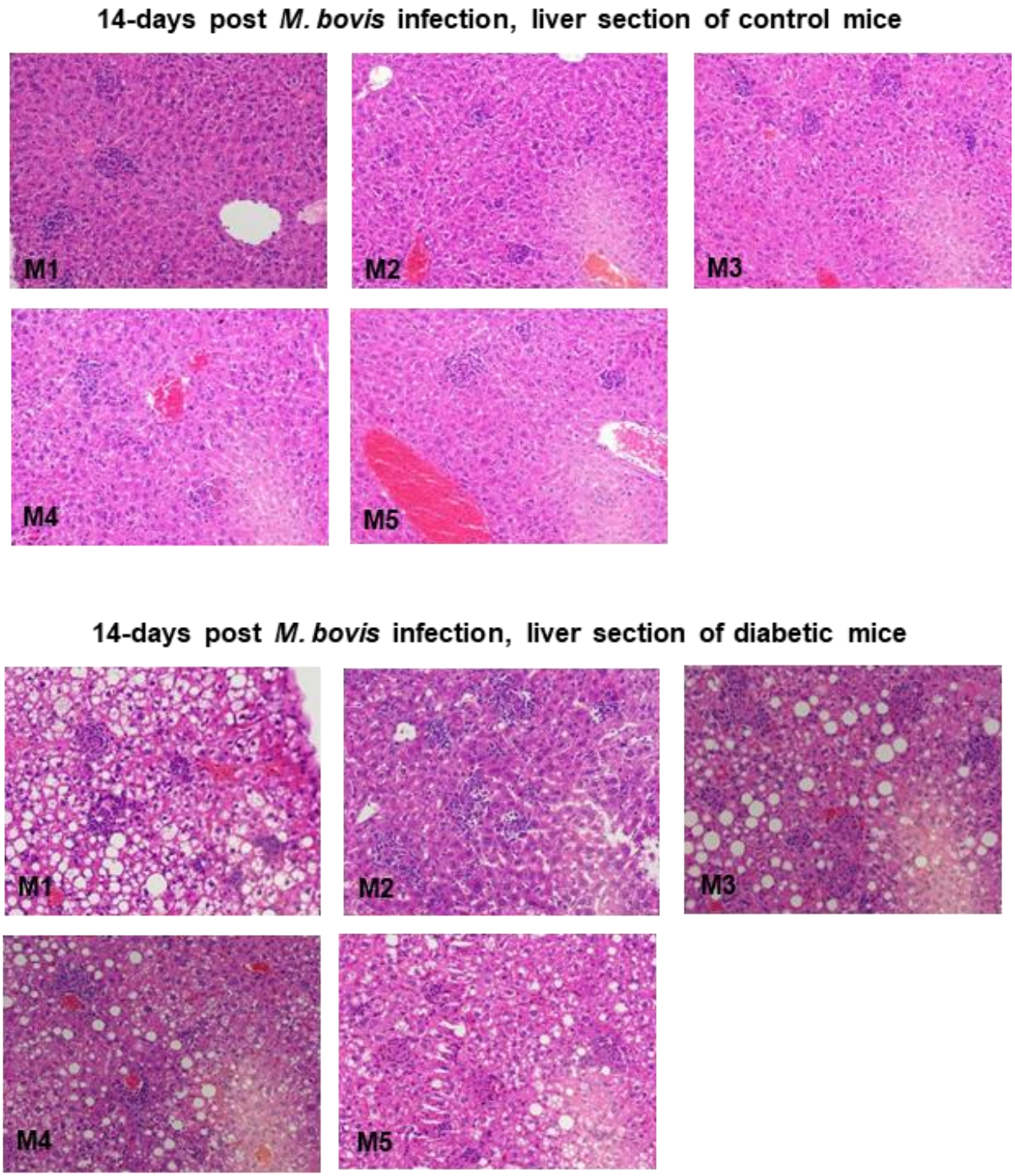

Figure A5.3 The representative photographs (one photo/mouse) of liver sections of control and diabetic mice infected with low-dose of *M. bovis* (BCG). All the photographs were taken at 200x magnification after H&E staining to quantify the inflamed area in liver at 14 days post-infection. In both diabetic and control mice, foci of inflammation/granuloma formation were evident at this timepoint of infection.

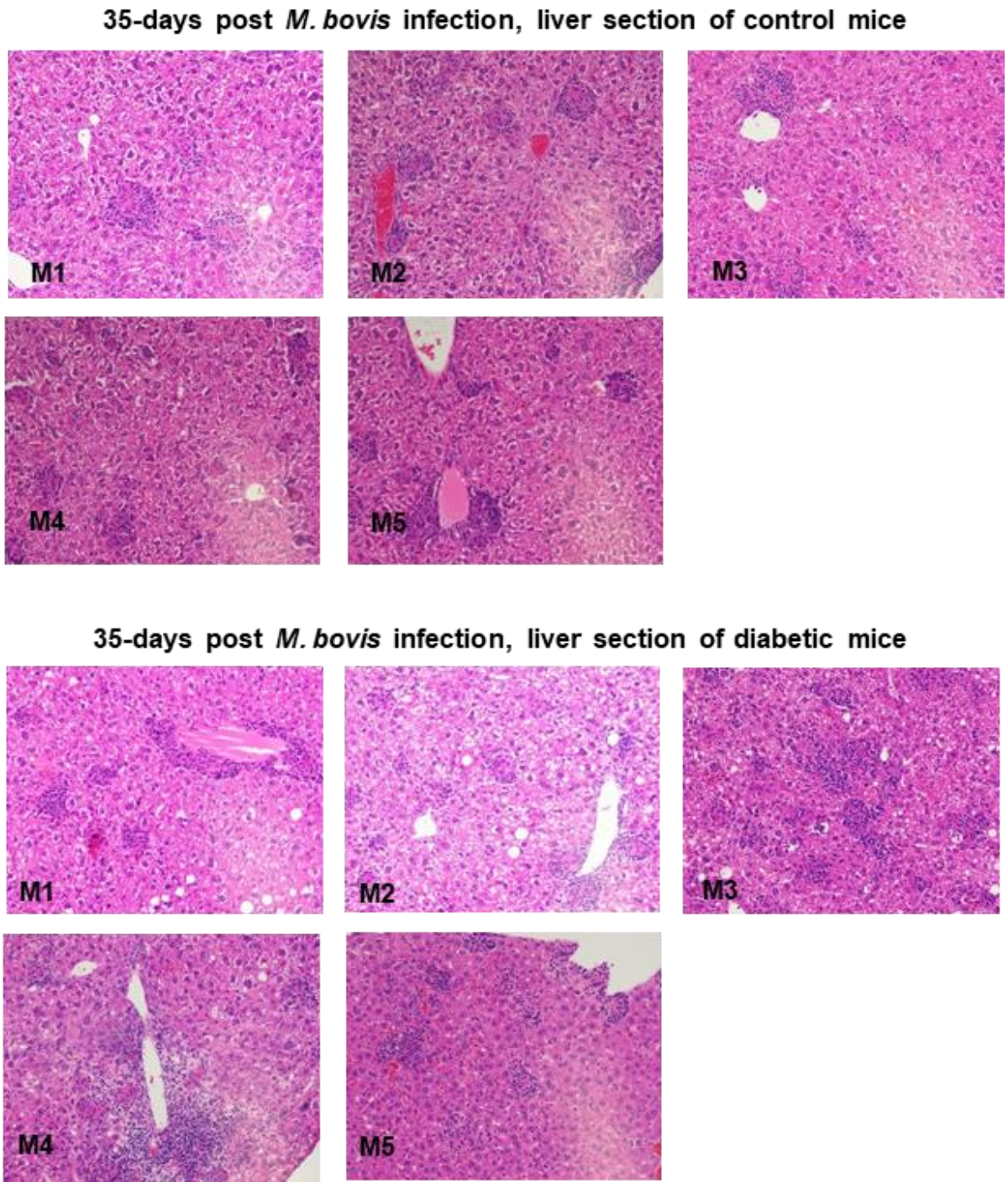

Figure A5.4 The representative photographs (one photo/mouse) of livers section of control and diabetic mice infected with low-dose of *M. bovis* (BCG). All the photographs were taken at 200x magnification after H&E staining to quantify the inflamed area in liver at 35 days post-infection. In both diabetic and control mice, more foci of inflammation/granuloma formation were evident at this timepoint of infection.

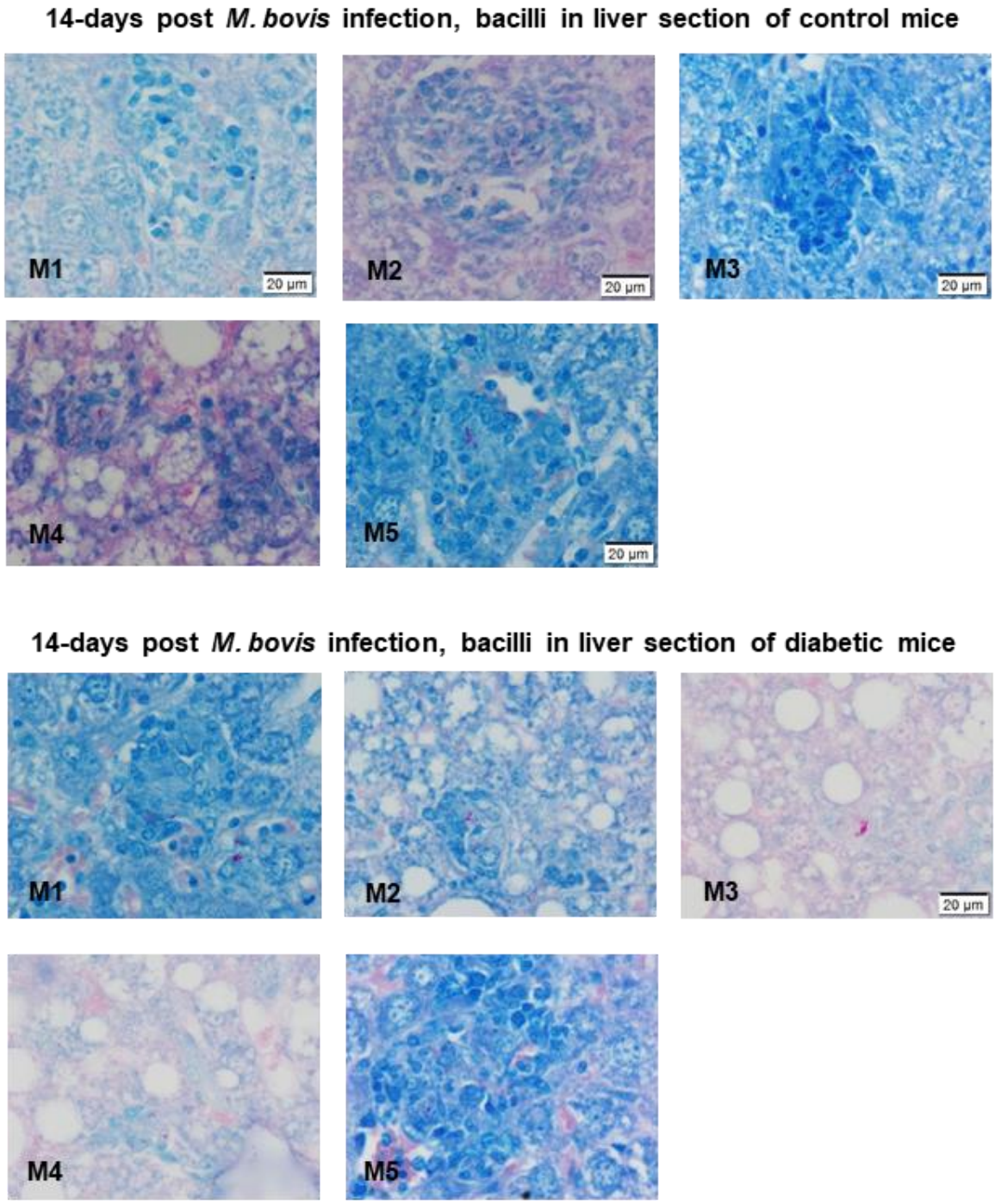

Figure A5.5 The representative photographs (one photo/mouse) of liver sections of control and diabetic mice infected with low-dose of *M. bovis* (BCG). All the photographs were taken at 1000x magnification after Ziehl-Neelsen staining to quantify the number of acid-fast bacilli (magenta) in each inflammatory foci/granuloma at 14 days-post infection.

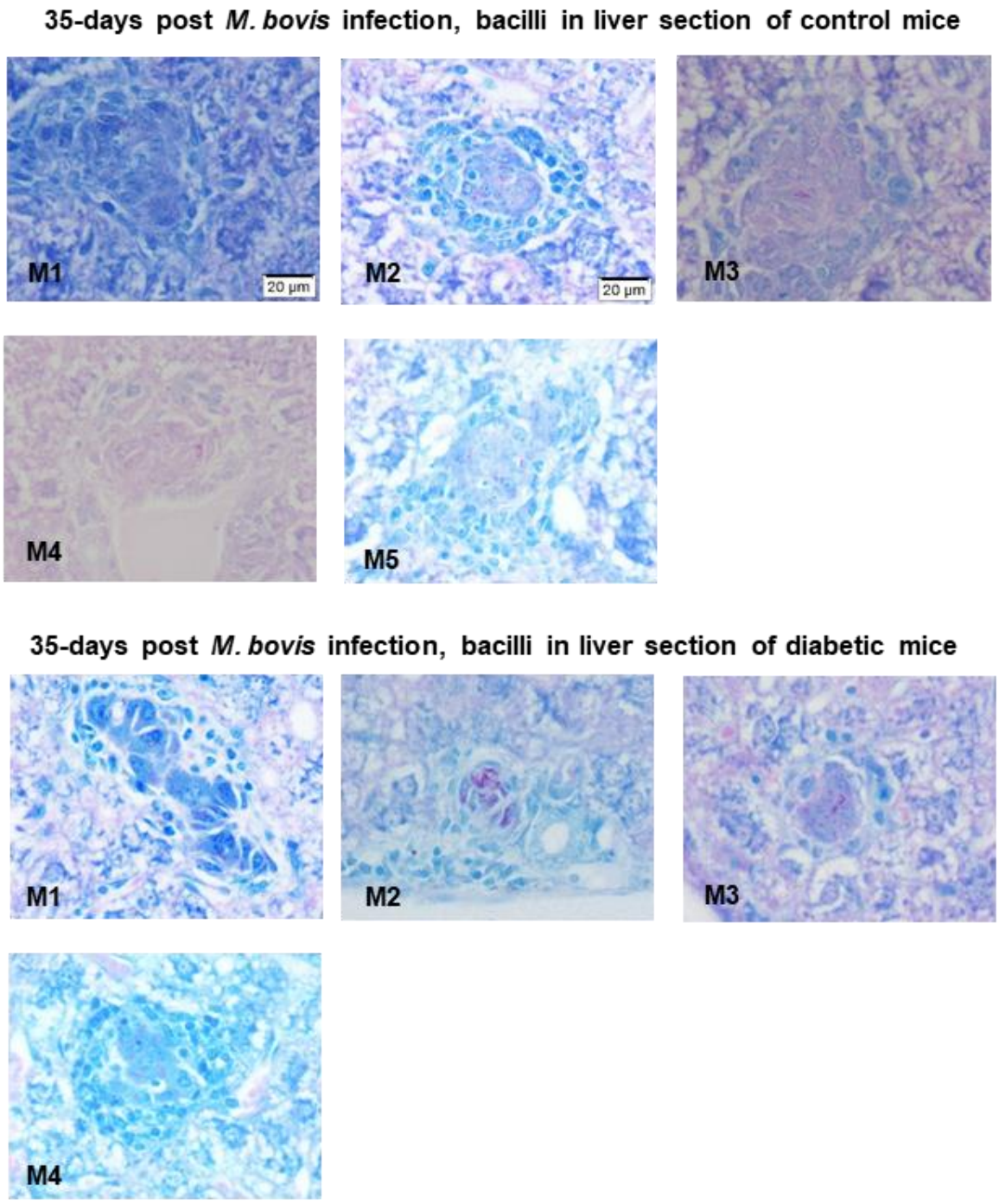

Figure A5.6 The representative photographs (one photo/mouse) of liver sections of control and diabetic mice infected with low-dose of *M. bovis* (BCG). All the photographs were taken at 1000x magnification after Ziehl-Neelsen staining to quantify the number of acid-fast bacilli (magenta) in inflammatory foci/granuloma at 35 days-post infection.

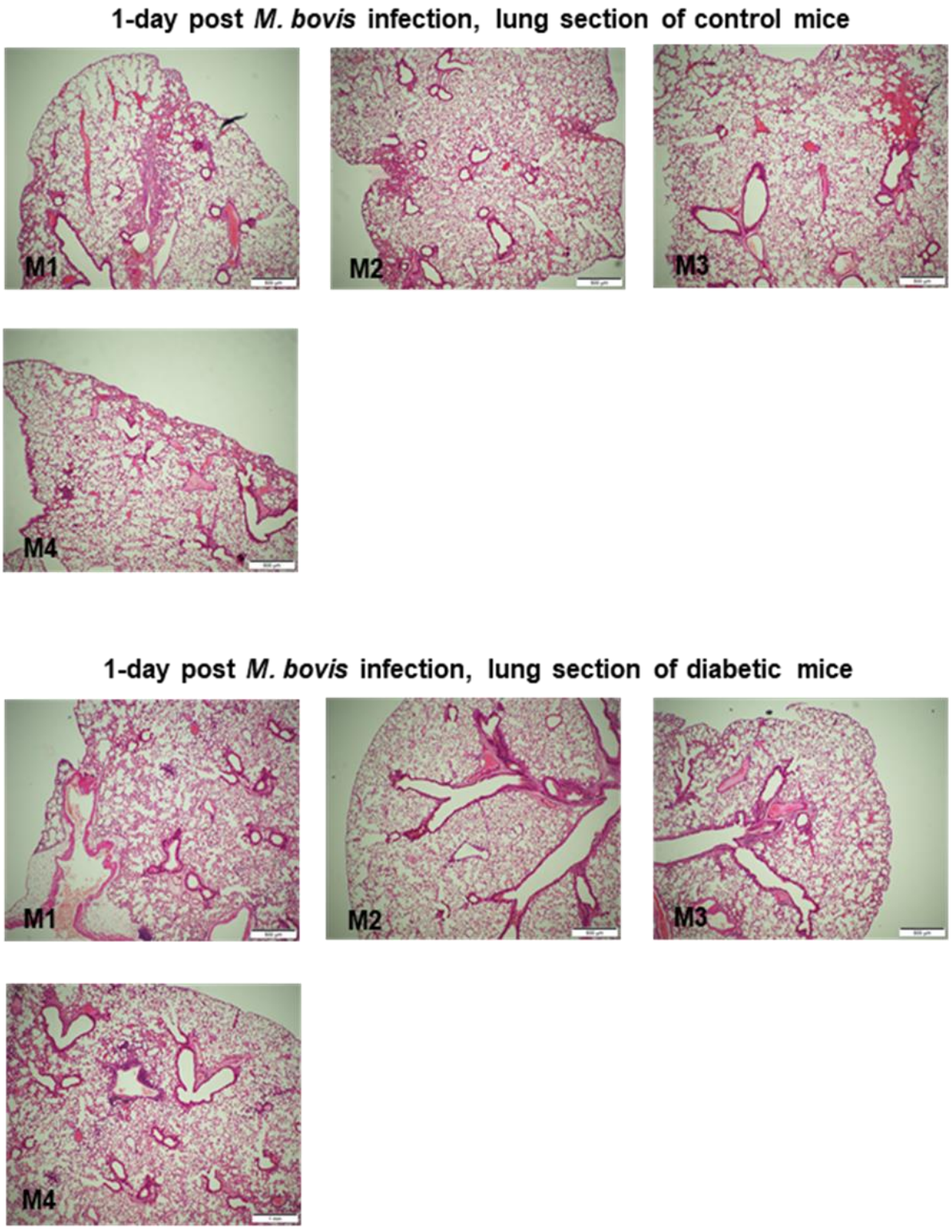

Figure A5.7 The representative photographs (one photo/mouse) of lung sections of control and diabetic mice infected with low-dose of *M. bovis* (BCG). All the photographs were taken at 40x magnification after H&E staining of the lung sections at 1 day post-infection. In both diabetic and control mice, a diffuse inflammation was observed at this timepoint of infection.

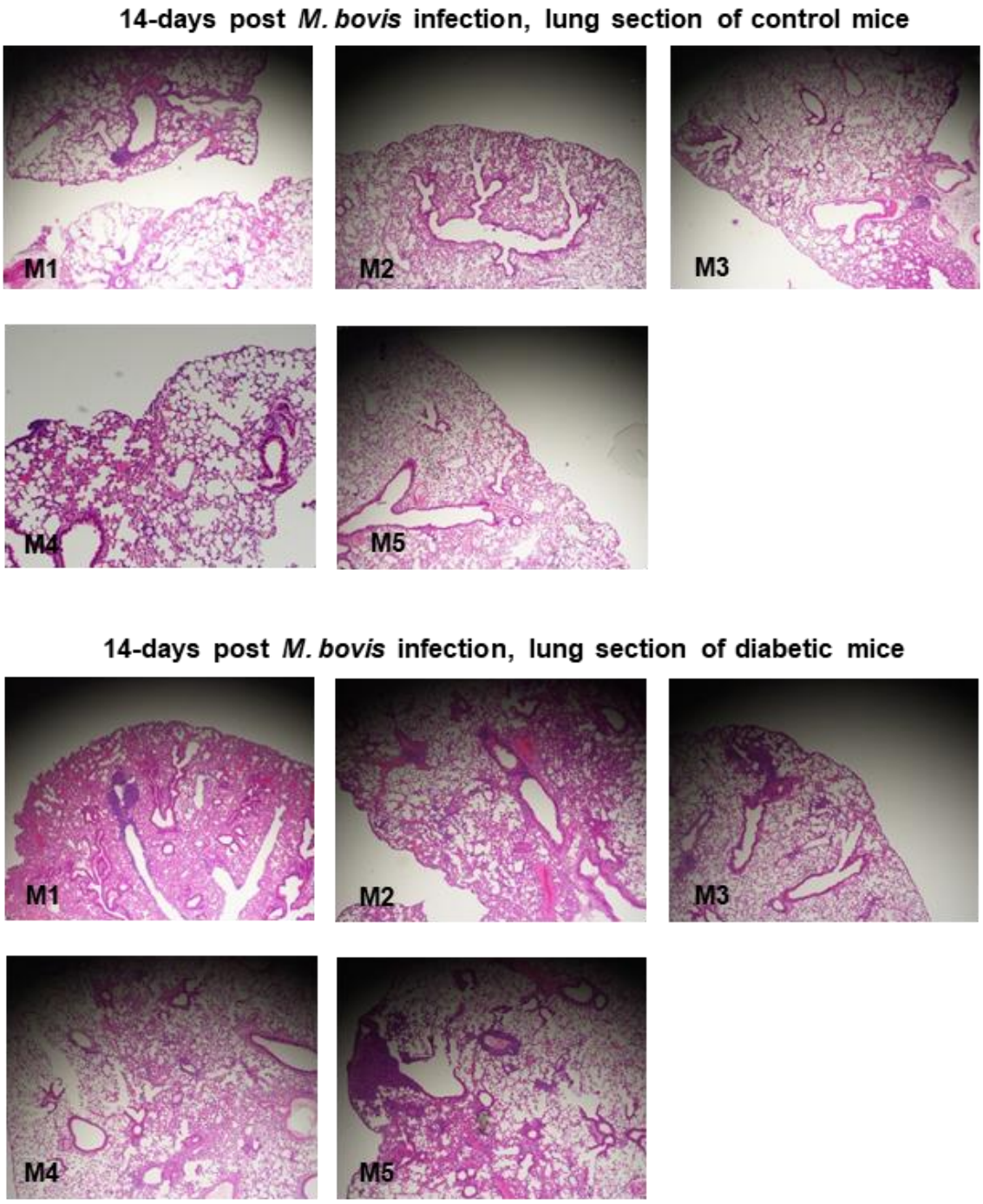

Figure A5.8 The representative photographs (one photo/mouse) of lung sections of control and diabetic mice infected with low-dose of *M. bovis* (BCG). All the photographs were taken at 40x magnification after H&E staining to quantify the total area of the lungs at 14 days post-infection. The Inflamed area over the total area of the lungs was measured on the photographs taken at 100x magnification (not shown here).

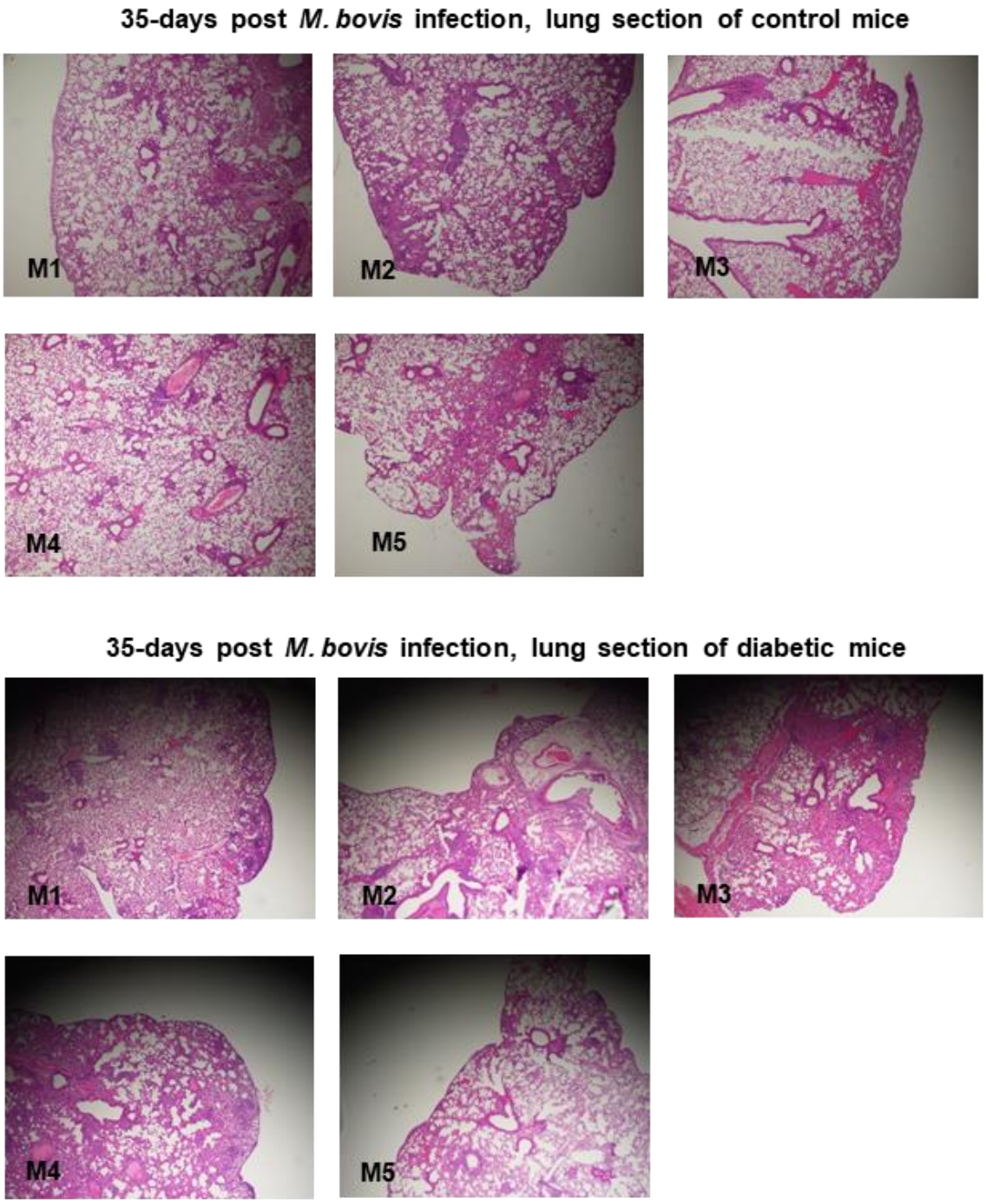

Figure A5.9 The representative photographs (one photo/mouse) of lung sections of control and diabetic mice infected with low-dose of *M. bovis* (BCG). All the photographs were taken at 40x magnification after H&E staining to quantify the total area of the lungs at 35 days post-infection. The Inflamed area over the total area of the lungs was measured on the photographs taken at 100x magnification (not shown here).

***M. bovis* (BCG) infection (high-dose)**

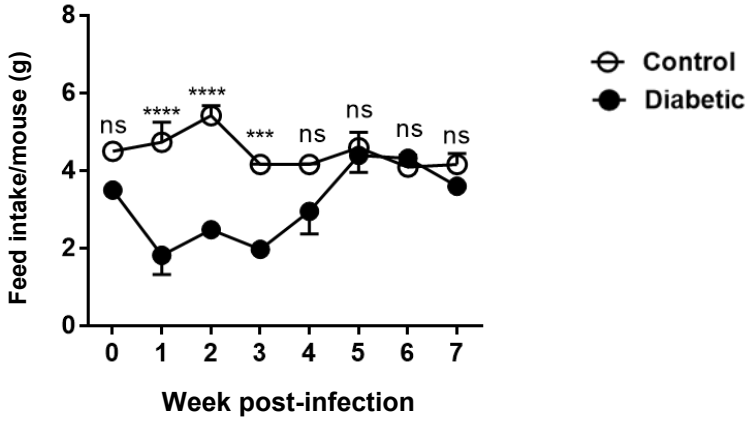

Figure A5.10 Daily feed intake by each mouse following high-dose of *M. bovis* (BCG) infection

Mice were infected with high-dose of *M. bovis* (BCG, $2x10^6$ CFU/mouse). Daily feed intake by each mouse was monitored for a period of 7 weeks. A reduction of the daily feed intake by each diabetic mouse at first 3 weeks of infection was observed although an opposite trend was observed in later weeks. In control group, there was a fluctuation of daily feed intake by each mouse throughout the infection. Data presented as mean±SEM. The significant difference between the groups was determined using the two-way ANOVA with Sidak's multiple comparisons test. The level of significance was indicated as ***$p \leq 0.001$, ****$p \leq 0.0001$ and ns=non-significant.

APPENDIX 6

All supplementary data from *M. tuberculosis* (H37Rv) infection study (Chapter 6-8) Dose: 4x10^6 CFU/mouse (low-dose) and 2x10^7/mouse (high-dose)

Table A6.1 Body weight and area under the curve of mice on standard rodent diet and energy-dense diet

Parameters	Mouse	Number	Mean±SEM	p-value	Level of significance
Body weight (0 week, g) ♦	SRD	39	20.91±0.34	0.4536	ns
	EDD	40	21.44±0.30		
Body weight (30th week, g) ♦	SRD	39	28.39±0.28	0.0000	****
	EDD	40	50.97±0.55		
Area under the curve (AUC)	SRD	39	1379.43±48.72	0.0000	****
	EDD	40	2074.73±51.86		

Statistical analysis: Data were checked for normal distribution using Shaprio Wilk's test. Data passed the test if p≥0.05. The non-normally distributed data (♦) were compared among the groups using the Kruskal-Wallis test with Dunn's multiple comparisons test. The area under the curve was compared between the groups using the independent sample *t*-test as the data sets passed the test of normality. The level of significance was indicated as ****p≤0.0001 and ns=non-significant. In the table, EDD; energy-dense diet, SRD; standard rodent diet.

Table A6.2 Glucose tolerance test after 30 weeks of energy-dense diet and standard rodent diet intervention

Time (minutes)	SRD (mmol/L, n=39)	EDD (mmol/L, n=40)	p-value	Level of significance
0	7.87±1.98	10.16±0.24	0.2057	ns
15	18.96±0.57	24.60±0.57	<0.0001	****
30	14.35±0.66	21.69±0.75	<0.0001	****
120	6.27±0.20	10.89±0.26	0.0005	***

Statistical analysis: Data were analysed using the two-way ANOVA with Sidak's multiple comparisons test. Data were mean±SEM. The level of significance was indicated as ***p≤0.001, ****p≤0.0001 and ns=non-significant. In the table, EDD; energy-dense diet, SRD; standard rodent diet.

Table A6.3 Percentage of diabetic mice after 30 weeks of energy-dense-diet intervention based on fasting blood glucose and area under the curve

Column statistics: Baseline fasting blood glucose

Col. stats	A	B
	Control baseline FBG	Diabetic baseline FBG
	Y	Y
1 Number of values	39	40
2		
3 Minimum	4.4	7.1
4 25% Percentile	5.2	8.85
5 Median	5.8	10.5
6 75% Percentile	6.5	11.28
7 Maximum	8.3	12.9
8		
9 Mean	5.959	10.16
10 Std. Deviation	1.008	1.519
11 Std. Error of Mean	0.1614	0.2402
12		
13 Lower 95% CI of mean	5.632	9.669
14 Upper 95% CI of mean	6.286	10.64
15		
16 Sum	232.4	406.2

Area under the curve

Col. stats	A	B
	Control AUC	Diabetic AUC
	Y	Y
1 Number of values	39	40
2		
3 Minimum	738.8	1553
4 25% Percentile	1197	1830
5 Median	1340	2001
6 75% Percentile	1607	2266
7 Maximum	2159	2801
8		
9 Mean	1379	2074
10 Std. Deviation	304.2	328
11 Std. Error of Mean	48.72	51.86
12		
13 Lower 99% CI of mean	1247	1933
14 Upper 99% CI of mean	1512	2214
15		
16 Sum	53798	82949

Mice on EDD Baseline FBG (mmol/L)	Diabetic Upper 99% CI of mean (>6.27 mmol/L) (Yes/No)	Mice on EDD AUC-GTT	Diabetic Upper 99% CI of mean (>1512) (Yes/No)
9	YES	1757	YES
9.8	YES	2082	YES
7.9	YES	1931	YES
7.1	YES	1726	YES
7.9	YES	1553	YES
10.9	YES	1980	YES
10.8	YES	2157	YES
8.2	YES	1897	YES
11.7	YES	2258	YES
10.1	YES	1812	YES
10.6	YES	1968	YES
11.4	YES	2211	YES
11.7	YES	1712	YES
10.7	YES	2516	YES
10.4	YES	1812	YES
11.8	YES	2268	YES
9.7	YES	2196	YES
9.8	YES	1974	YES
7.4	YES	1849	YES
11.3	YES	2557	YES
8.3	YES	1889	YES
9.6	YES	2037	YES
8.8	YES	1582	YES
11.2	YES	1823	YES
7.8	YES	1616	YES
10.9	YES	2801	YES
10.3	YES	2021	YES
12.9	YES	2602	YES
10.4	YES	2082	YES
11.4	YES	1969	YES
12.3	YES	2028	YES
12.3	YES	2684	YES
10.8	YES	2163	YES
10.7	YES	2306	YES
10.6	YES	2594	YES
8.1	YES	1714	YES

10.2	YES	2323	YES
10.6	YES	2723	YES
12.5	YES	1904	YES
8.3	YES	1872	YES
% diabetic	**100% (40/40)**	**% diabetic**	**100 (40/40)**
Note: Mice were considered type 2 diabetes if they demonstrated a raised baseline FBG and AUG-GTT with evidence of glucose intolerance at levels higher the upper 99% confidence interval (CI) for the mean of age-matched control group fed on a standard rodent diet.			

FBG; fasting blood glucose, AUC; area under the curve; AUC-GTT; area under the curve, EDD; energy-dense diet

Table A6.4 Daily feed intake by mice following *M. tuberculosis* (H37Rv) infection

Week	Mouse	Cage no.	Feed intake (g/mouse/day) Mean±SEM	p-value	Level of significance
Low-dose ($4x10^6$ CFU/mouse)					
0 (baseline)	Control	5	4.50±0.00	0.3270	ns
	Diabetic	5	3.50±0.00		
1	Control	6	5.06±0.20	0.0011	**
	Diabetic	4	2.73±0.68		
2	Control	6	4.93±0.26	0.0002	***
	Diabetic	4	1.99±0.15		
3	Control	4	5.84±0.90	<0.0001	****
	Diabetic	3	2.27±0.35		
4	Control	4	6.14±0.89	0.0008	***
	Diabetic	3	3.36±0.70		
High-dose ($2x10^7$ CFU/mouse)					
0 (baseline)	Control	2	4.50±0.00	0.0209	*
	Diabetic	2	3.50±0.00		
1	Control	2	5.53±0.04	<0.0001	****
	Diabetic	2	2.62±0.16		
2	Control	2	4.15±0.06	<0.0001	****
	Diabetic	2	0.69±0.23		
3	Control	2	4.24±0.34	<0.0001	****
	Diabetic	2	1.80±0.07		
4	Control	2	5.19±0.14	<0.0001	****
	Diabetic	2	2.88±0.84		
5	Control	2	6.02±0.04	<0.0001	****
	Diabetic	2	3.07±0.26		
6	Control	2	5.18±0.17	<0.0001	****
	Diabetic	2	2.06±0.26		
7	Control	2	5.60±0.17	<0.0001	****
	Diabetic	2	2.57±0.01		

Statistical analysis: Data were analysed using the two-way ANOVA with Sidak's multiple comparisons test. The level of significance was indicated as *p≤0.05, **p≤0.01, ***p≤0.001, ****p≤0.0001 and ns=non-significant. Each cage contains 1-5 mice.

Table A6.5 Daily energy intake by mice following *M. tuberculosis* (H37Rv) infection

Week	Mouse	Cage no.	Energy intake (kcal/mouse/day) Mean±SEM	p-value	Level of significance
Low-dose ($4x10^6$ CFU/mouse)					
0 (baseline)	Control	5	13.82±0.00	0.5556	ns
	Diabetic	5	16.73±0.00		
1	Control	6	15.52±0.62	0.7107	ns
	Diabetic	4	13.06±0.39		
2	Control	6	15.13±0.80	0.0663	ns
	Diabetic	4	9.52±0.73		
3	Control	4	17.91±2.77	0.0222	*
	Diabetic	3	10.85±1.68		
4	Control	4	18.16±2.75	0.7212	ns
	Diabetic	3	16.05±3.33		
High-dose ($2x10^7$ CFU/mouse)					
0 (baseline)	Control	2	13.82±0.00	0.2660	ns
	Diabetic	2	16.73±0.00		
1	Control	2	16.97±0.14	0.0925	ns
	Diabetic	2	12.53±0.78		
2	Control	2	12.73±0.19	0.0001	***
	Diabetic	2	3.32±1.08		
3	Control	2	13.01±1.05	0.0987	ns
	Diabetic	2	8.61±0.34		
4	Control	2	15.94±0.42	0.8081	ns
	Diabetic	2	13.76±4.00		
5	Control	2	18.47±0.13	0.2084	ns
	Diabetic	2	14.69±1.22		
6	Control	2	15.90±0.52	0.0102	**
	Diabetic	2	9.84±1.24		
7	Control	2	17.19±0.51	0.0508	*
	Diabetic	2	12.29±0.07		

Statistical analysis: Data were analysed using the two-way ANOVA with Sidak's multiple comparisons test. The level of significance was indicated as *p≤0.05, **p≤0.01and ns=non-significant. Each cage contains 1-5 mice.

Table A6.6 Body weight of mice following *M. tuberculosis* (H37Rv) infection

Week	Mouse	Number	Body weight Mean(g)±SEM	p-value	Level of significance
Low-dose ($4x10^6$ CFU/mouse)					
0 (baseline)	Control	23	28.29±0.35	<0.0001	****
	Diabetic	23	50.41±0.83		
1	Control	16	28.90±0.42	<0.0001	****
	Diabetic	18	47.48±0.96		
2	Control	16	29.23±0.41	<0.0001	****
	Diabetic	18	43.11±0.95		
3	Control	11	28.48±0.57	<0.0001	****
	Diabetic	13	40.21±1.26		
4	Control	11	28.29±0.56	<0.0001	****
	Diabetic	13	39.80±1.44		
High-dose ($2x10^7$ CFU/mouse)					
0 (baseline)	Control	9	26.08±0.49	<0.0001	****
	Diabetic	10	48.91±0.93		
1	Control	9	26.24±0.45	<0.0001	****
	Diabetic	9	42.08±0.89		
2	Control	9	24.48±0.96	<0.0001	****
	Diabetic	9	32.68±0.80		
3	Control	7	24.01±1.50	0.9385	ns
	Diabetic	7	25.81±1.66		
4	Control	6	24.67±1.08	>0.9999	ns
	Diabetic	5	25.07±2.55		
5	Control	6	24.60±1.29	0.9747	ns
	Diabetic	4	26.47±2.29		
6	Control	6	24.17±0.97	0.9898	ns
	Diabetic	4	25.11±2.34		
7	Control	6	23.03±0.92	>0.09999	ns
	Diabetic	4	23.20±2.73		

Statistical analysis: Data were analysed using the two-way ANOVA with Sidak's multiple comparisons test. The level of significance was indicated ****p≤0.0001 and ns=non-significant.

Table A 6.7 Blood glucose level of mice following *M. tuberculosis* (H37Rv) infection

Week	Mouse	Number	Blood glucose (mmol/L) Mean±SEM	p-value	Level of significance
Low-dose ($4x10^6$ CFU/mouse)					
0 (baseline)	Control	23	5.68±0.17	0.0000	****
	Diabetic	23	9.78±0.30		
1	Control	16	8.80±0.19	0.3425	ns
	Diabetic	18	8.11±0.43		
2	Control	16	8.02±0.17	0.9636	ns
	Diabetic	18	7.74±0.28		
3	Control	11	8.95±0.22	0.1458	ns
	Diabetic	13	7.94±0.28		
4	Control	11	8.90±0.28	0.7843	ns
	Diabetic	13	8.38±0.29		
High-dose ($2x10^7$ CFU/mouse)					
0 (baseline)	Control	10	6.82±0.24	<0.0001	****
	Diabetic	10	12.80±0.62		
1	Control	9	6.96±0.22	0.9964	ns
	Diabetic	9	6.47±0.17		
2	Control	6	5.52±0.30	0.9925	ns
	Diabetic	7	6.07±0.62		
3	Control	6	5.32±0.74	>0.9999	ns
	Diabetic	5	5.63±0.47		
4	Control	6	7.40±0.52	0.6503	ns
	Diabetic	4	5.94±0.90		
5	Control	6	7.23±0.53	0.6863	ns
	Diabetic	4	5.73±0.73		
6	Control	6	8.18±0.49	0.6488	ns
	Diabetic	4	6.63±1.35		
7	Control	6	7.13±0.53	0.9374	ns
	Diabetic	4	6.08±1.30		

Statistical analysis: Data were analysed using the two-way ANOVA with Sidak's multiple comparisons test. The level of significance was indicated as ****p≤0.0001 and ns=non-significant.

Table A6.8 Organ weight of mice following *M. tuberculosis* (H37Rv) infection

Organs	DPI	Number /group	Control	Diabetic	p-value	Level of significance
			Mean±SEM			
Low-dose (4x10^6 CFU/mouse)						
Spleen	1♦	5	0.11±0.01	0.29±0.13	0.0147	*
	14	5	0.55±0.02	0.77±0.06	0.0151	*
	30	5	0.26±0.03	0.55±0.07	0.0087	**
Liver	1	5	1.33±0.10	2.36±0.14	0.0003	***
	14	5	2.74±0.13	3.31±0.19	0.0405	*
	30	5	1.80±0.06	3.36±0.25	0.0003	***
Lungs	1♦	5	0.23±0.02	0.26±0.02	0.1150	ns
	14	5	0.31±0.01	0.81±0.50	0.3723	ns
	30	5	0.31±0.01	0.35±0.04	0.4265	ns

Statistical analysis: Data were checked for normality using Shapiro-Wilk's test. Data passed the test if p≥0.05. The normally distributed data were compared between the groups using the independent sample *t*-test. The non-normally distributed data (♦) were compared between the groups using the Mann-Whitney U test. The level of significance was indicated as *p≤0.05, **p≤0.01, ***p≤0.001 and ns=non-significant. In the table, DPI; days post-infection.

Table A6.9 Organ bacterial kinetics of mice following *M. tuberculosis* (H37Rv) infection

Organs	DPI	Number /group	Control	Diabetic	p-value	Level of significance
			Mean (log_{10} CFU)±SEM			
Low-dose (4x10^6 CFU/mouse)						
Spleen	1	5	2.29E+05±2.86E+04	2.21E+05±4.88E+04	0.8856	ns
	14	5	3.89E+06±7.77E+05	1.26E+07±2.16E+06	0.0053	**
	30♦	5	1.89E+06±2.55E+05	9.37E+06±3.11E+06	0.0431	*
Liver	1	5	1.10E+06±8.08E+04	1.11E+06±7.14E+04	0.9598	ns
	14	5	4.02E+06±4.00E+05	7.21E+06±1.09E+06	0.0254	*
	30	5	2.30E+06±1.17E+05	6.03E+06±6.71E+05	0.0045	**
Lungs	1	5	3.19E+04±3.31E+03	2.54E+04±2.65E+03	0.1628	ns
	14♦	5	3.69E+05±7.08E+04	1.29E+06±3.51E+05	0.0331	*
	30	5	9.93E+05±2.58E+05	1.95E+06±5.59E+05	0.1576	ns

Statistical analysis: The normally distributed data were compared between the groups using the independent sample *t*-test. The non-normally distributed data (♦) were compared between groups using the Mann-Whitney U test. The level of significance was indicated as *p≤0.05, **p≤0.01 and ns=non-significant.

Table A6.10 Liver lesions of *M. tuberculosis* (H37Rv) infected mice

Parameter	DPI	Control	Diabetic	p-value	Level of significance
		Mean±SEM, n=5/group			
Low-dose (1x10^6 CFU/mouse)					
Inflamed area on liver (%)	14	10.76±0.50	14.83±1.49	0.0325	*
Number of inflammatory foci on liver/ 200x)		7.68±0.61	7.31±1.32	0.8083	ns
Mean area of each inflammatory focus (μm^2) ♦		4991.50±260.66	8658.03±2552.10	0.0283	*
Inflamed area on liver (%)	30	12.87±0.60	16.96±1.54	0.0388	*
Number of inflammatory foci on liver/ 200x)		7.22±0.17	7.96±0.77	0.3763	ns
Mean area of each focus (μm^2) ♦		6594.02±104.22	6594.02±104.22	0.1172	ns
Acid-fast bacilli/inflammatory focus (n=4-5 mouse/group at 14 dpi♦)	14	21.74±3.27	28.08±6.74	1.000	ns
	30	32.78±1.77	45.07±5.08	0.0714	ns

Statistical analysis: The normally distributed data were compared between the groups using the independent sample *t*-test. The non-normally distributed data (♦) were analysed using Mann-Whitney U test. The level of significance was indicated as *p≤0.05 and ns=non-significant.

Table A6.11 Lungs lesions in *M. tuberculosis* (H37Rv) infected mice

Parameter	DPI	Control	Diabetic	p-value	Level of significance
		Mean (%)±SEM, n=5/group			
Low-dose (4x10^6 CFU/mouse)					
Inflamed area in lungs	14	15.34±0.72	22.06±1.91	0.0109	**
	30	23.80±1.67	31.39±2.40	0.0317	*

Statistical analysis: Data were compared between the groups using the independent sample *t*-test as they passed the test of normality (Shapiro-Wilk's test, p≥0.05). The level of significance was indicated as *p≤0.05, **p≤0.01and ns=non-significant.

Table A6.12 Cytokine production in spleen following *M. tuberculosis* (H37Rv) infection (low-dose)

Spleen		Days post-infection, n=4-5 mouse/group					
		1		14		30	
Cytokine	**Mouse**	**Mean±SEM (pg/mL)**	**p-value**	**Mean±SEM (pg/mL)**	**p-value**	**Mean±SEM (pg/mL)**	**p-value**
IL-1β	Control	10.30±1.84	ns 0.4098	325.18±38.21	* 0.0283♦	106.59±18.46	ns 0.1745♦
	Diabetic	13.65±3.37		1075.05±323.77		212.24±51.40	
TNF-α	Control	42.79±6.41	ns 0.0894	174.77±22.60	* 0.0265	72.78±4.54	* 0.0363
	Diabetic	28.96±3.18		262.46±23.08		110.96±12.67	
MCP-1	Control	73.42±12.15	* 0.0163♦	98.15±7.10	* 0.0256	45.05±2.16	* 0.0758♦
	Diabetic	30.72±1.28		125.45±7.01		61.37±7.77	
IL-6	Control	4.73±0.70	ns 0.7220	10.04±1.05	* 0.0476	6.53±0.23	ns 0.2248
	Diabetic	4.37±0.70		13.72±1.17		7.65±0.77	
IFN-γ	Control	64.04±14.38	** 0.0090♦	107.68±6.53	* 0.0359	44.82±5.59	ns 0.1197
	Diabetic	15.42±3.00		87.99±4.30		32.81±4.04	
IL-12p70	Control	0.00±0.00	ns 0.3466	0.00±0.00	ns 0.1547	0.17±0.17	ns 0.3466
	Diabetic	0.12±0.12		0.59±0.37		0.00±0.00	
IL-2	Control	5.42±2.32	ns 0.9748	12.03±2.22	* 0.0149	11.54±1.80	** 0.0042
	Diabetic	5.52±2.28		5.38±0.63		4.00±0.62	
IL-10	Control	24.09±4.39	ns 0.9049	17.48±1.21	ns 0.0622	29.76±1.27	ns 0.1032
	Diabetic	23.43±3.05		21.78±1.57		24.56±5.16	
IL-4	Control	0.00±0.00	-	0.08±0.08	ns 0.3882	0.00±0.00	-
	Diabetic	0.00±0.00		0.97±0.97		0.00±0.00	
IL-17A	Control	0.04±0.04	ns 0.4777	0.27±0.14	ns 0.1021	0.56±0.34	ns 0.1418
	Diabetic	0.14±0.13		0.00±0.00		0.00±0.00	

Statistical analysis: The normally distributed data were compared between the groups using the independent sample *t*-test. The non-normally distributed data (♦) were compared between the groups using the Mann-Whitney U test. The level of significance was indicated as *p≤0.05, **p≤0.01 and ns=non-significant.

Table A6.13 Cytokine production in liver following *M. tuberculosis* (H37Rv) infection (low-dose)

Liver		Days post-infection, n=4-5 mouse/group					
		1		14		30	
Cytokine	**Mouse**	**Mean±SEM (pg/mL)**	**p-value**	**Mean±SEM (pg/mL)**	**p-value**	**Mean±SEM (pg/mL)**	**p-value**
IL-1β	Control	21.04±3.59	ns 0.1754	203.08±39.03	ns 0.6881	71.76±14.54	ns 0.2606
	Diabetic	13.12±3.94		177.30±48.06		50.64±9.63	
TNF-α	Control	81.11±20.69	* 0.0472♦	115.26±10.81	* 0.0120	68.17±6.58	*** 0.0006
	Diabetic	39.90±6.04		77.02±4.79		29.93±2.28	
MCP-1	Control	341.84±93.28	* 0.0213♦	89.74±9.49	ns 0.0902	92.51±20.87	ns 0.4647♦
	Diabetic	72.94±13.10		122.40±14.05		68.24±5.65	
IL-6	Control	29.78±11.87	ns 0.3472♦	8.16±1.37	ns 0.6015♦	13.13±4.44	ns 0.0758♦
	Diabetic	13.34±3.37		15.62±7.80		6.04±0.84	
IFN-γ	Control	97.59±23.83	* 0.0174♦	75.81±6.06	ns 0.2595	21.86±1.70	* 0.0256
	Diabetic	24.99±4.67		62.55±9.09		16.22±0.83	
IL-12p70	Control	53.81±22.75	ns 0.1172♦	4.03±1.68	ns 0.9107	17.62±4.37	* 0.0160♦
	Diabetic	19.79±6.15		3.80±1.16		6.56±1.29	
IL-2	Control	18.87±6.32	ns 0.8433	2.20±0.85	* 0.0170♦	17.45±3.04	* 0.0134
	Diabetic	16.93±7.09		0.17±0.17		5.41±2.30	
IL-10	Control	45.85±7.73	ns 0.8130	24.32±3.44	ns 0.3108	47.74±5.70	* 0.0134
	Diabetic	48.30±6.40		29.04±2.70		34.72±4.20	
IL-4	Control	3.80±2.03	ns 0.6752♦	0.00±0.00	ns 0.3466	1.82±0.81	ns 0.1564
	Diabetic	7.29±4.50		0.21±0.21		0.39±0.24	
IL-17A	Control	2.03±1.27	ns 0.9113♦	0.00±0.00	-	4.99±2.85	ns 0.1955♦
	Diabetic	0.97±0.77		0.00±0.00		0.38±0.38	

Statistical analysis: The normally distributed data were compared between the groups using the independent sample *t*-test. The non-normally distributed data (♦) were compared between the groups using the Mann-Whitney U test. The level of significance was indicated as *p≤0.05, ***p≤0.001 and ns=non-significant.

Table A6.14 Cytokine production in lungs following *M. tuberculosis* (H37Rv) infection (low-dose)

Lungs		Days post-infection, n=4-5 mouse/group					
		1		14		30	
Cytokine	**Mouse**	**Mean±SEM (pg/mL)**	**p-value**	**Mean±SEM (pg/mL)**	**p-value**	**Mean±SEM (pg/mL)**	**p-value**
IL-1β	Control	0.00±0.00	ns 0.1484	20.08±10.76	ns 0.4094	16.66±4.94	ns 0.9814
	Diabetic	0.60±0.38		31.90±8.27		16.42±8.87	
TNF-α	Control	12.56±0.73	ns 0.0772	62.55±6.48	ns 0.2506♦	54.54±9.88	ns 0.5226
	Diabetic	7.78±2.03		59.05±18.07		45.67±8.86	
MCP-1	Control	98.59±8.54	*** 0.0007	98.49±8.08	ns 0.3573	28.19±2.41	** 0.0095
	Diabetic	34.67±3.92		77.97±19.40		45.85±4.62	
IL-6	Control	4.39±0.45	ns 0.1713	23.07±2.10	ns 0.7269	6.85±2.05	ns 0.2506♦
	Diabetic	3.14±0.70		20.44±6.79		4.25±0.36	
IFN-γ	Control	7.00±2.68	* 0.0157♦	128.70±26.82	* 0.0163♦	17.89±2.27	* 0.0293
	Diabetic	0.70±0.55		40.14±4.00		9.93±1.94	
IL-12p70	Control	0.12±0.12	ns 0.3466	0.00±0.00	-	0.16±0.11	ns 0.2014
	Diabetic	0.00±0.00		0.00±0.00		0.00±0.00	
IL-10	Control	20.22±2.43	ns 0.4211	14.19±1.39	ns 0.0445	27.16±4.70	ns 0.0927♦
	Diabetic	16.80±3.22		22.62±2.97		19.36±2.55	
IL-2	Control	0.00±0.00	ns 0.3466	0.09±0.09	ns 0.3466	0.24±0.24	ns 0.4386♦
	Diabetic	1.34±1.34		0.00±0.00		1.93±1.64	
IL-4	Control	0.00±0.00	-	0.00±0.00	-	0.00±0.00	-
	Diabetic	0.00±0.00		0.00±0.00		0.00±0.00	
IL-17A	Control	0.00±0.00	-	0.00±0.00	-	0.00±0.00	-
	Diabetic	0.00±0.00		0.00±0.00		0.00±0.00	

Statistical analysis: The normally distributed data were compared between the groups using the independent sample *t*-test. The non-normally distributed data (♦) were compared between the groups using the Mann-Whitney U test. The level of significance was indicated as *p≤0.05, **p≤0.01, ***p≤0.001 and ns=non-significant.

All supplementary figures and photographs from *M. tuberculosis* (H37Rv) study (Chapter 6-7)

Dose: 4x10^6 CFU/mouse (low-dose) and 2x10^7 CFU/mouse (high-dose)

***M. tuberculosis* (H37Rv) infection (low-dose)**

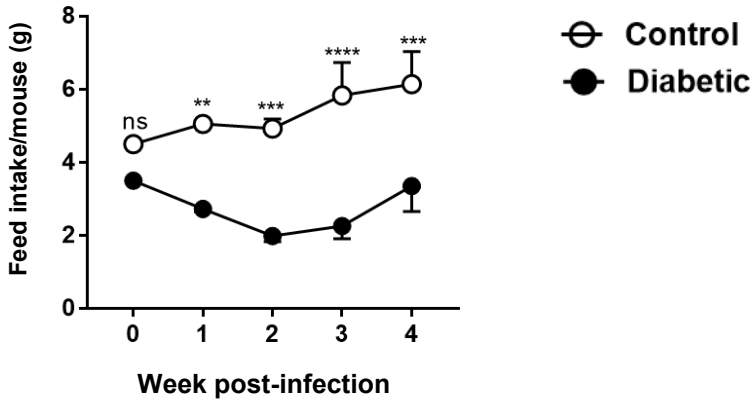

Figure A6.1 Daily feed intake by each mouse following low-dose of *M. tuberculosis* (H37Rv) infection

Mice were infected with low-dose of *M. tuberculosis* (H37Rv, 4x10^6 CFU/mouse). The daily feed intake by each mouse were monitored for a period of 4 weeks. The daily feed intake by the diabetic mice reduced gradually followed by a slight increase at last 2 weeks of infection. In control group, there was a gradual rise of the feed intake by each mouse until the end of the infection. Data presented as mean±SEM. The significant difference between groups was determined using the two-way ANOVA with Sidak's multiple comparisons test. The level of significance was indicated as **p≤0.01, ***p≤0.01 and ***0p≤0.0001 and ns=non-significant.

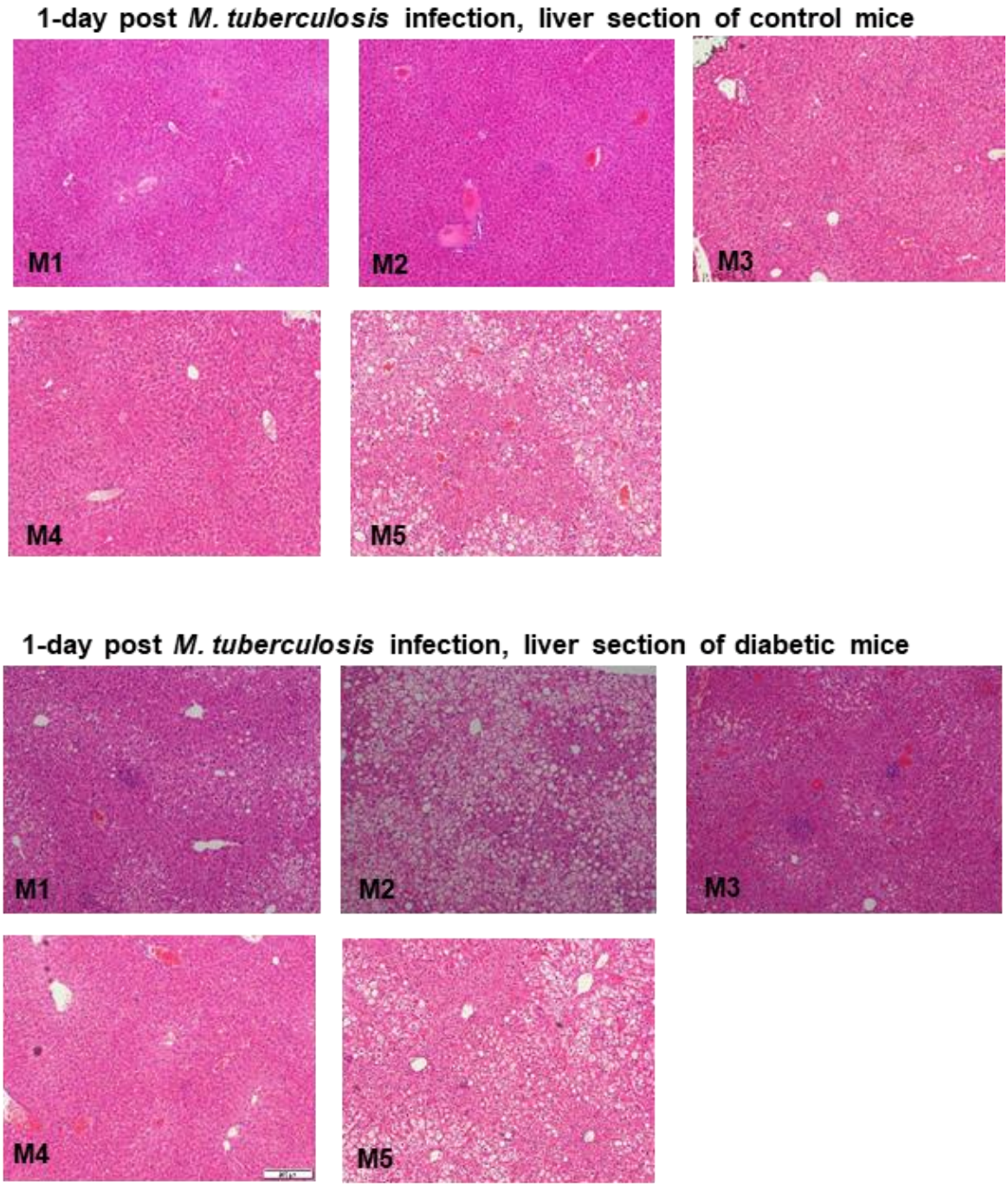

Figure A6.2 The representative photographs (one photo/mouse) of liver sections of control and diabetic mice infected with low-dose of *M. tuberculosis* (H37Rv). All the photographs were taken at 100x magnification after the H&E staining of liver sections at 1-day post-infection. In both diabetic and control mice, a diffuse inflammation was observed at this timepoint of infection.

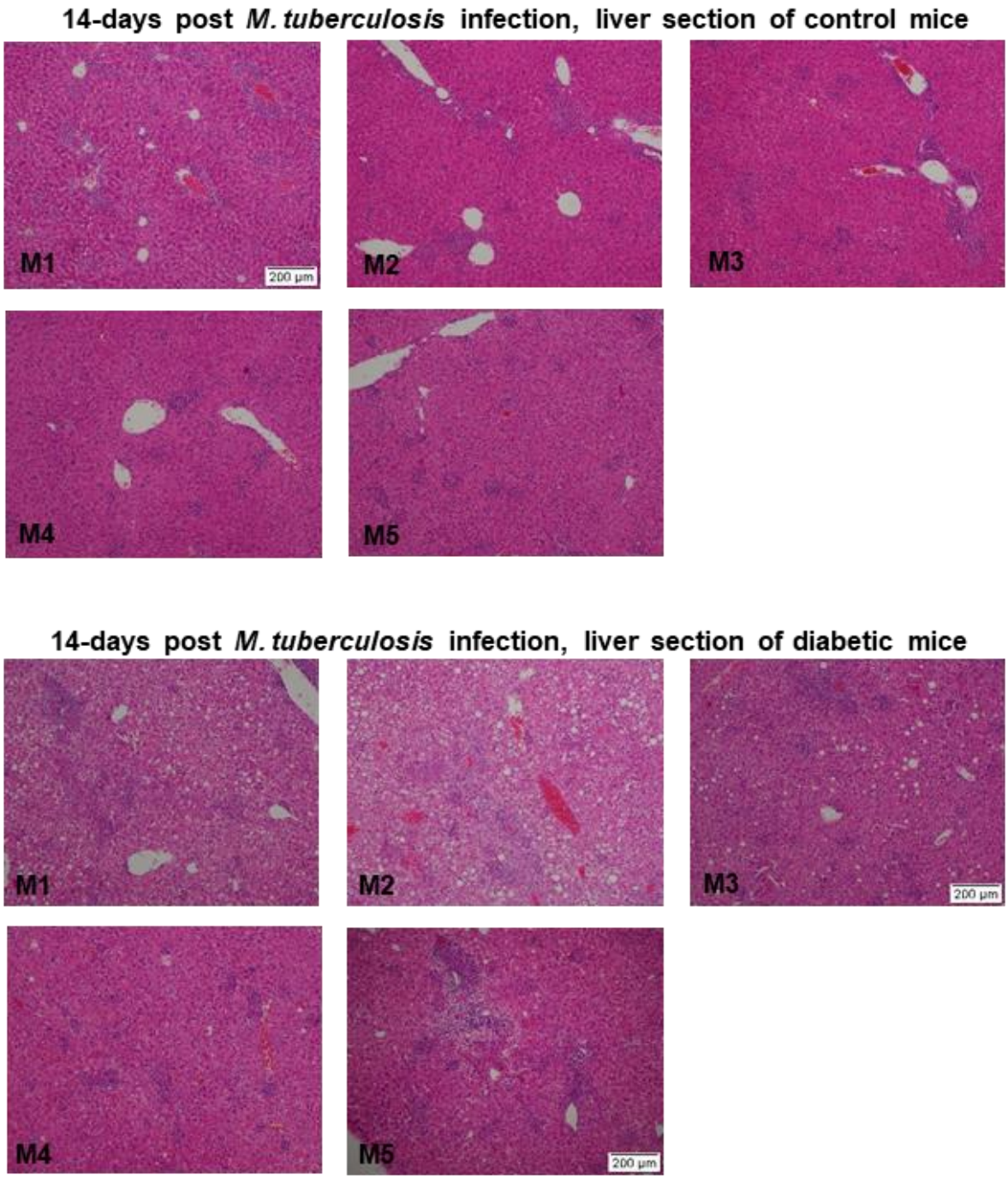

Figure A6.3 The representative photographs (one photo/mouse) of liver sections of control and diabetic mice infected with low-dose of *M. tuberculosis* (H37Rv). All the photographs were taken at 100x magnification after H&E staining to quantify the inflamed area in liver at 14 day post-infection. In both diabetic and control mice, foci of inflammation/granuloma formation were evident at this timepoint of infection.

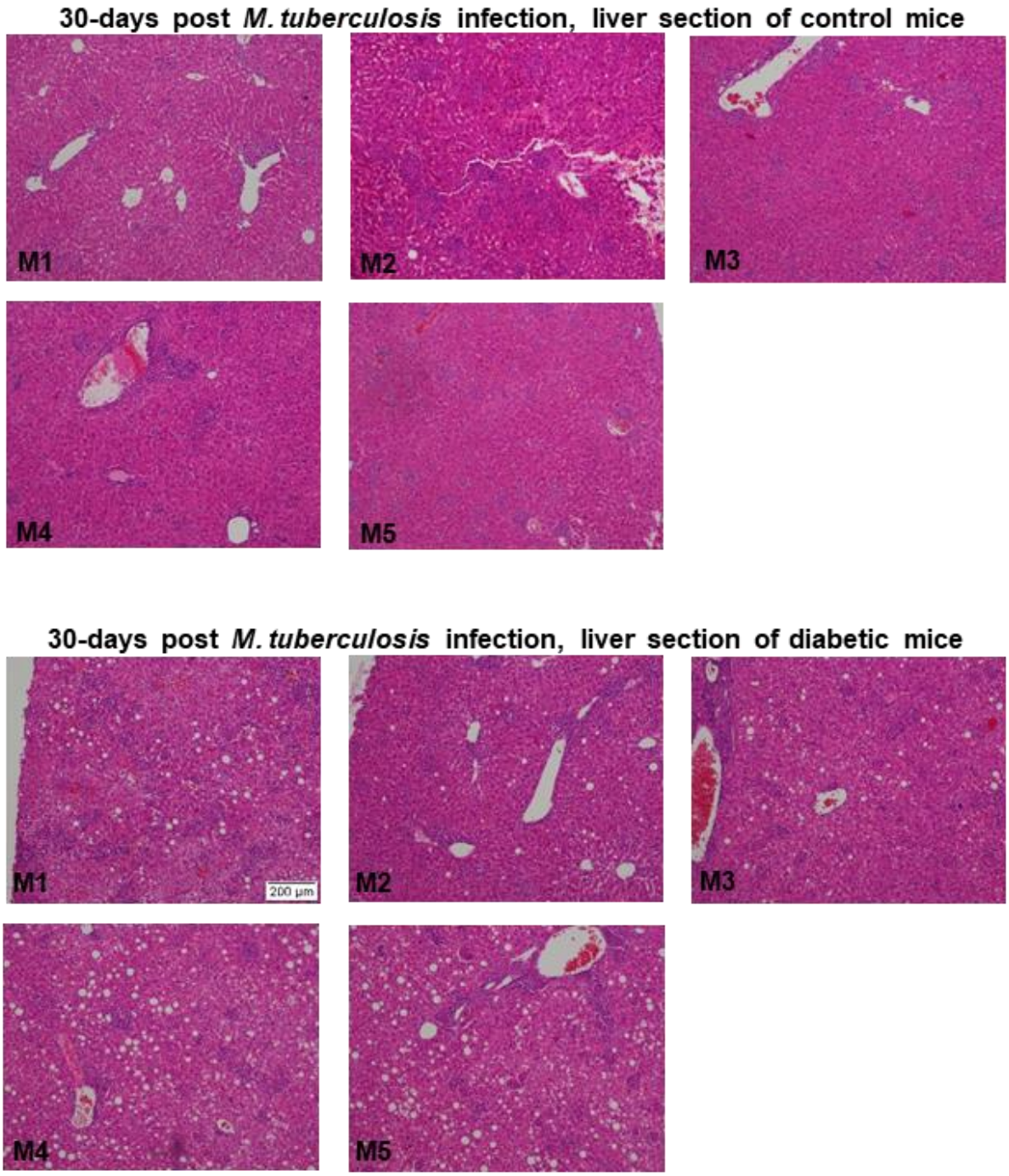

Figure A6.4 The representative photographs (one photo/mouse) of liver sections of control and diabetic mice infected with low-dose of *M. tuberculosis* (H37Rv). All the photographs were taken at 100x magnification after H&E staining to quantify the inflamed area in liver at 30 days post-infection. In both diabetic and control mice, more foci of inflammation/granuloma formation were evident at this timepoint of infection.

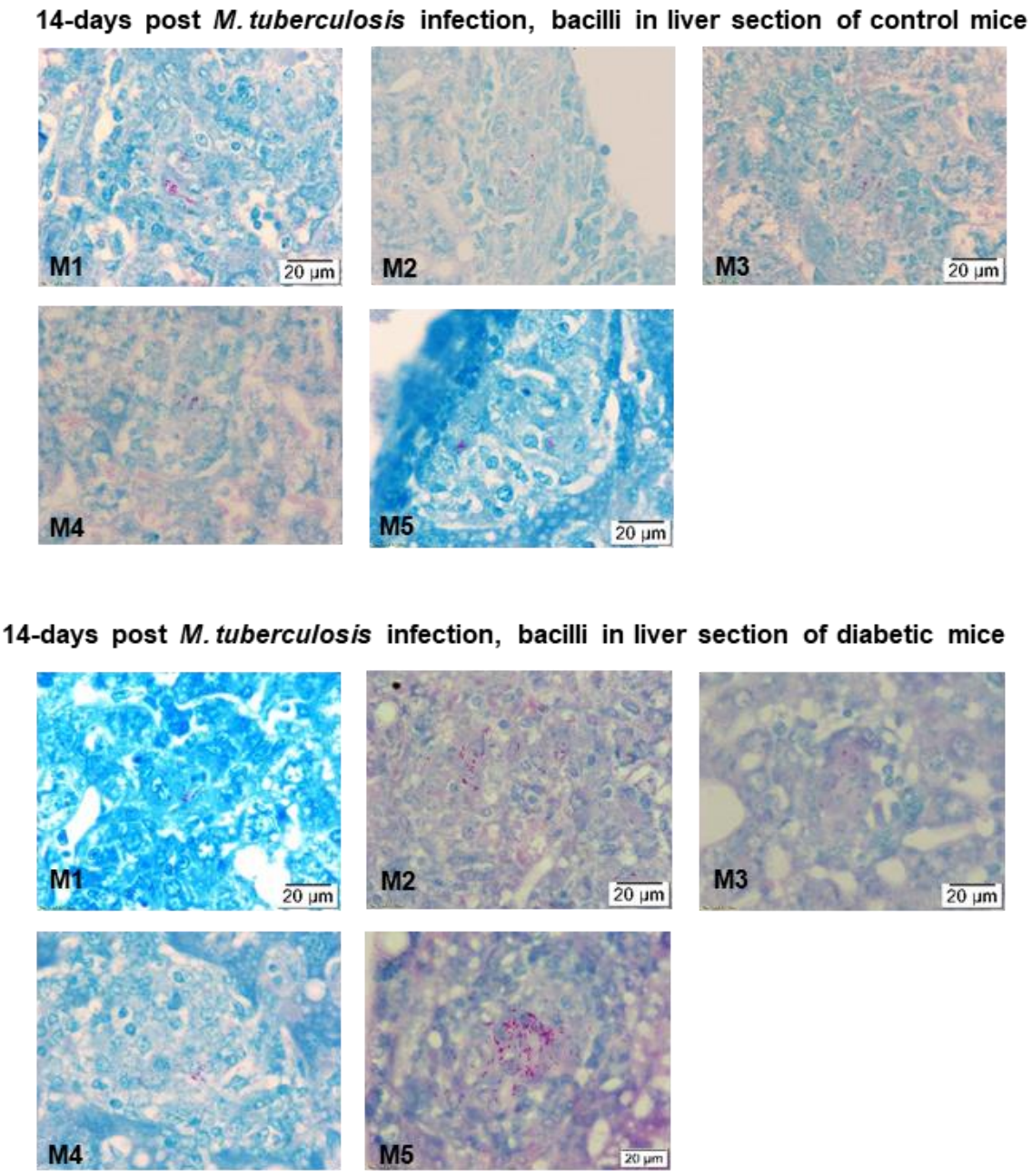

Figure A6.5 The representative photographs (one photo/mouse) of liver sections of control and diabetic mice infected with low-dose of *M. tuberculosis* (H37Rv). All the photographs were taken at 1000x magnification after Ziehl-Neelsen staining to quantify the number of acid-fast bacilli (magenta) in each of inflammatory focus/granuloma at 14 days post infection.

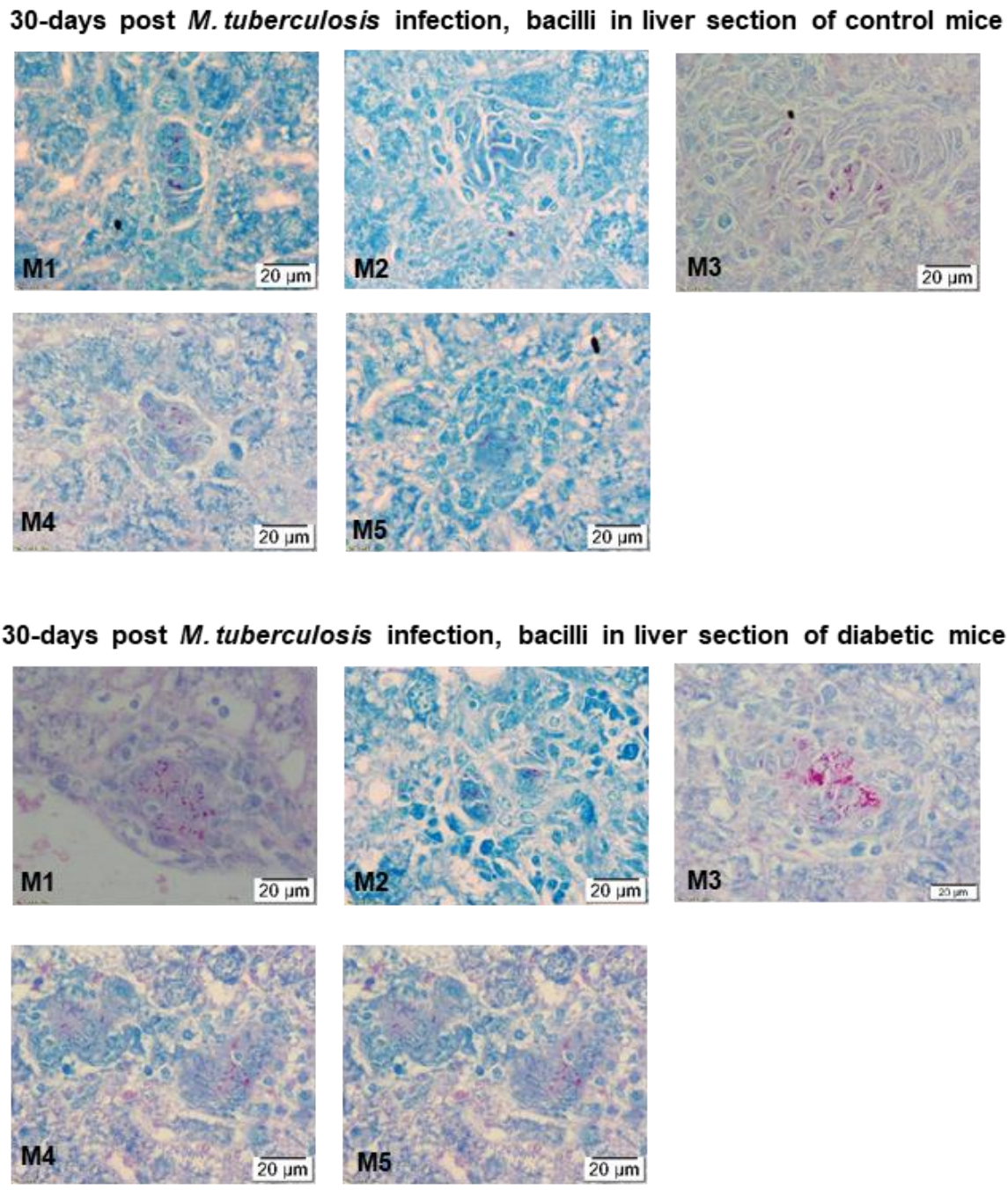

Figure A6.6 The representative photographs (one photo/mouse) of liver sections of control and diabetic mice infected with low-dose of *M. tuberculosis* (H37Rv). All the photographs were taken at 1000x magnification after the Ziehl-Neelsen staining to quantify the number of acid-fast bacilli (magenta) in each of inflammatory focus/granuloma at 30 days post infection.

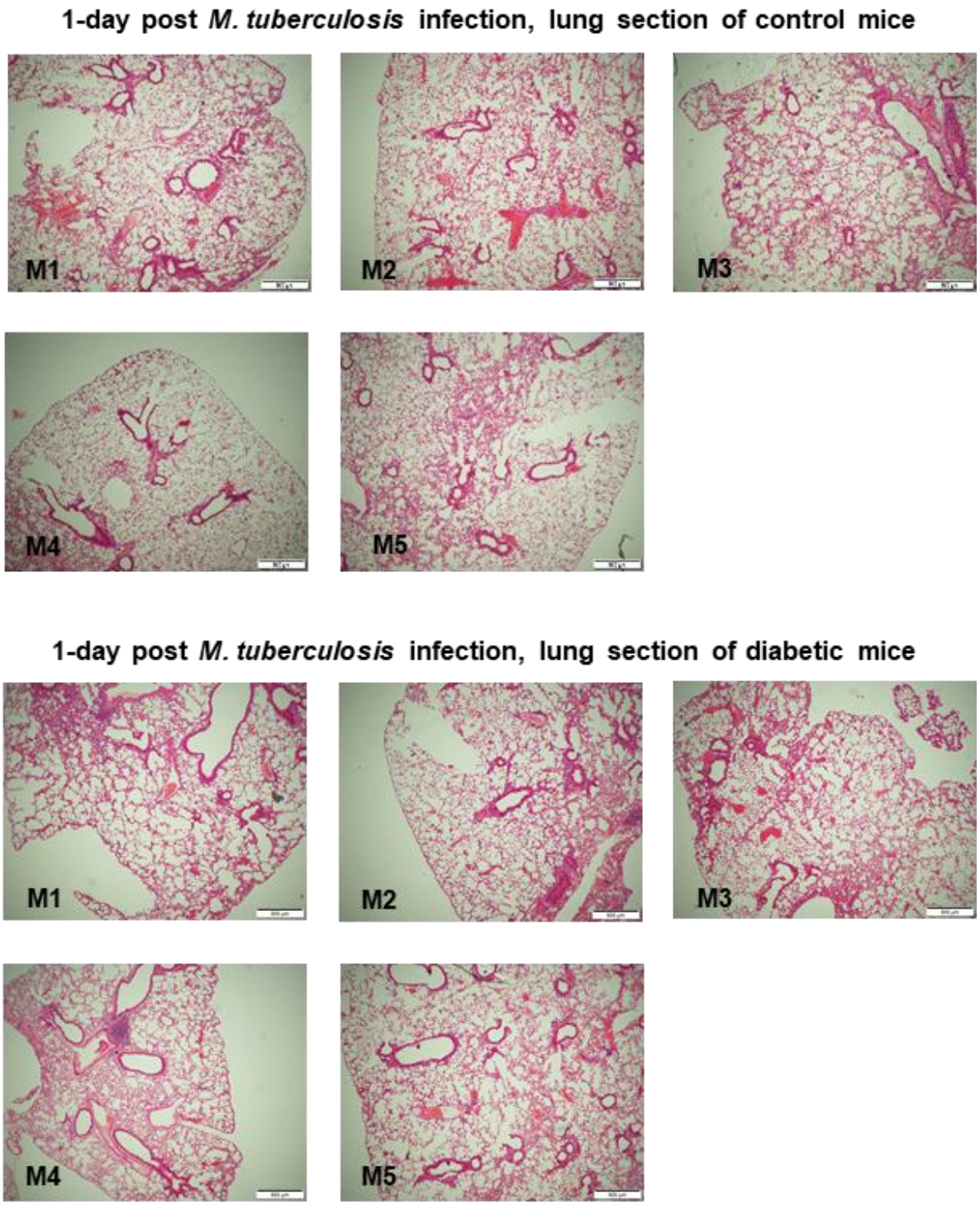

Figure A6.7 The representative photographs (one photo/mouse) of lung sections of control and diabetic mice infected with low-dose of *M. tuberculosis* (H37Rv). All the photographs were taken at 40x magnification after H&E staining of the lung sections at 1 day post-infection. In both diabetic and control mice, a diffuse inflammation was observed at this timepoint of infection.

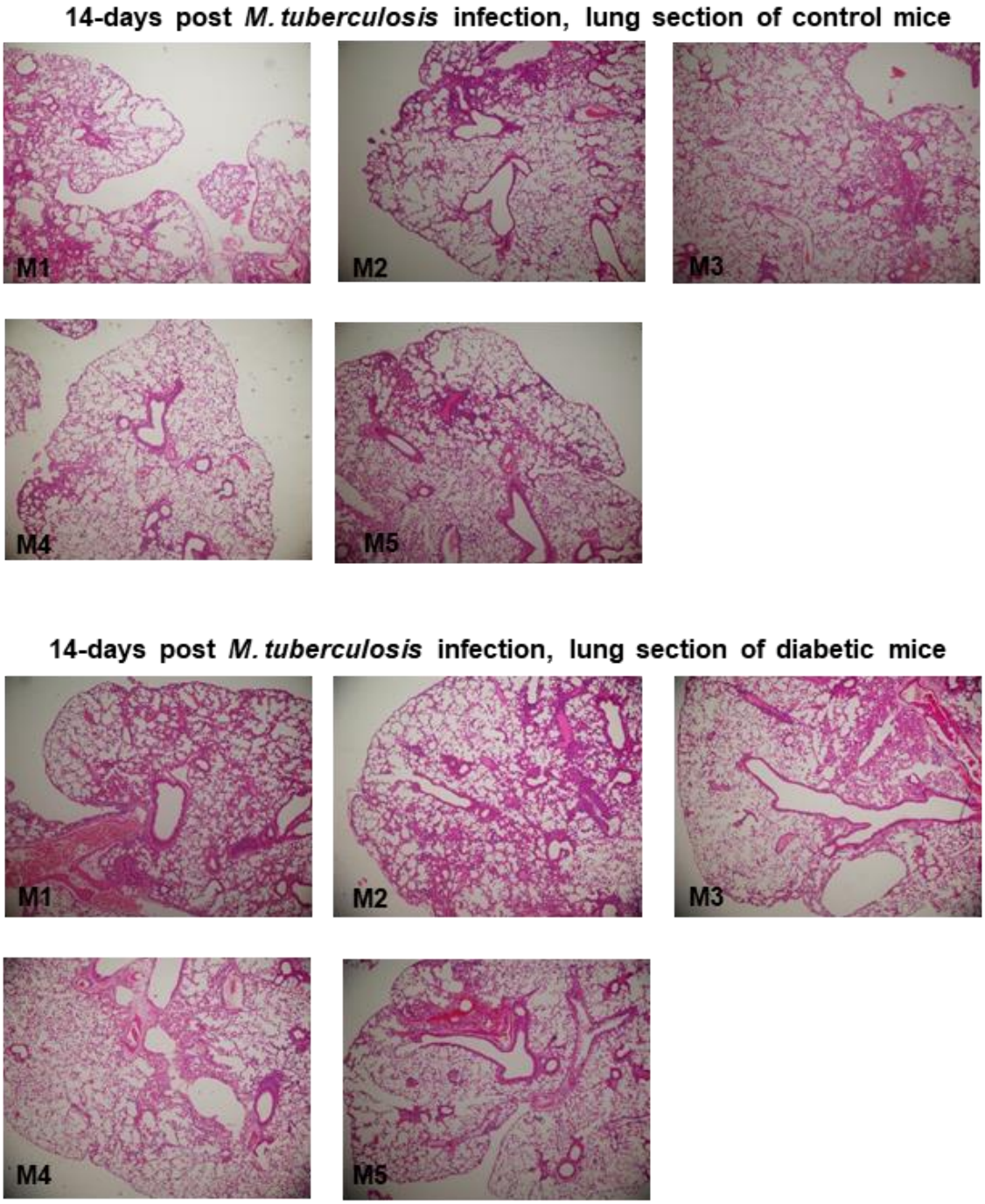

Figure A6.8 The representative photographs (one photo/mouse) of lung sections of control and diabetic mice infected with low-dose of *M. tuberculosis* (H37Rv). All the photographs were taken at 40x magnification after H&E staining to quantify the total area of the lung at 14 days post-infection. The Inflamed area over the total area of lungs was measured on the photographs taken at 100x magnification (not shown here).

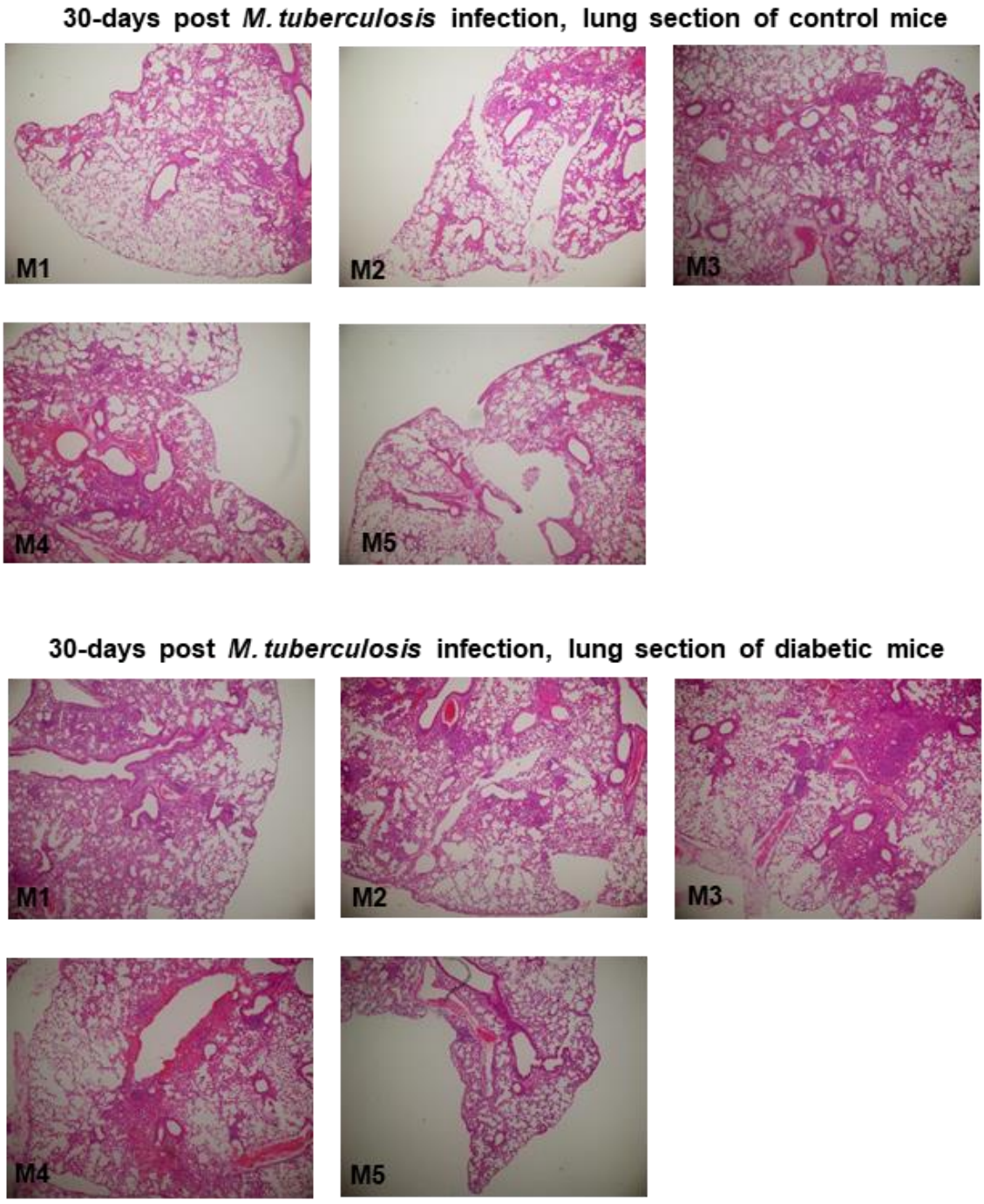

Figure A6.9 The representative photographs (one photo/mouse) of lung sections of control and diabetic mice infected with low-dose of *M. tuberculosis* (H37Rv). All the photographs were taken at 40x magnification after H&E staining to quantify the total area of lungs at 30 days post-infection. The Inflamed area over the total area of the lung was measured on the photographs taken at 100x magnification (not shown here).

***M. tuberculosis* (H37Rv) infection (high-dose)**

Liver lesions of *M. tuberculosis* (H37Rv) infected mice

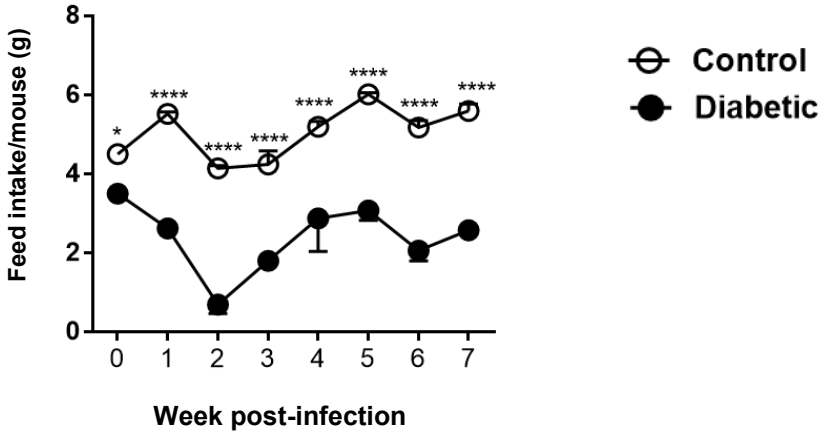

Figure A6.10 Daily feed intake by each mouse following high-dose of *M. tuberculosis* (H37Rv) infection

Mice were infected with high-dose of *M. tuberculosis* (H37Rv, $2x10^7$ CFU/mouse). Daily feed intake by each mouse was monitored for a period of 7 weeks. A dramatic fall of the daily feed was observed in diabetic mice until the second week of infection. Whereas a progressive reduction of feed was observed in control mice at the same timepoint of infection compared to their pre-infection period (0 week). After the second week of infection, feed intake rose gradually in both control and diabetic mice although some fluctuation was noticed at last 3 weeks of infection. Data presented as mean±SEM. The significant difference between the groups was determined using the two-way ANOVA with Sidak's multiple comparisons test. The level of significance was indicated as *$p \leq 0.05$ and ****$p \leq 0.0001$.

APPENDIX 7

Publication resulting from this thesis

ALIM, M. A., SIKDER, S., BRIDSON, T. L., RUSH, C. M., GOVAN, B. L. & KETHEESAN, N. 2017. Anti-mycobacterial function of macrophages is impaired in a diet induced model of type 2 diabetes. *Tuberculosis (Edinb),* 102**,** 47-54.

Tuberculosis 102 (2017) 47–54

Contents lists available at ScienceDirect

Tuberculosis

journal homepage: http://intl.elsevierhealth.com/journals/tube

Anti-mycobacterial function of macrophages is impaired in a diet induced model of type 2 diabetes

Md Abdul Alim, Suchandan Sikder, Tahnee L. Bridson, Catherine M. Rush, Brenda L. Govan, Natkunam Ketheesan*

Infectious Diseases and Immunopathogenesis Research Group, College of Public Health, Medical and Veterinary Sciences, Australian Institute of Tropical Health and Medicine, James Cook University, Townsville, Queensland, 4811, Australia

ARTICLE INFO

Article history:
Received 29 September 2016
Received in revised form
13 November 2016
Accepted 5 December 2016

Keywords:
Murine model
Macrophage
Tuberculosis
Type 2 diabetes
Phagocytosis

ABSTRACT

Type 2 diabetes (T2D) is one of the major risk factors for tuberculosis (TB). In this study, a diet induced murine model of T2D (DIMT2D) was developed and characterized in the context of metabolic, biochemical and histopathological features following diet intervention. Mycobacterial susceptibility was investigated using *Mycobacterium fortuitum* as a surrogate. Phagocytic capability of alveolar macrophages and resident peritoneal macrophages were determined by *in vitro* assays using mycolic acid coated beads and *M. fortuitum*. Results demonstrated that bacillary loads were significantly higher in liver, spleen, and lungs of diabetic mice compared to controls. Higher inflammatory lesions and impaired cytokine kinetics (TNF-α, MCP-1, IL-12, IFN-γ) were also observed in diabetic mice. Macrophages isolated from diabetic mice had lower uptake of mycolic acid coated beads, reduced bacterial internalization and killing and altered cytokine responses (TNF-α, IL-6, MCP-1). This model will be useful to further investigate different facets of host-pathogen interactions in TB-T2D.

1. Introduction

The incidence of type 2 diabetes (T2D) has increased substantially over the last 50 years with 415 million people living with the disease worldwide [1]. Epidemiological studies have shown that T2D is one of the major risk factors associated with susceptibility to both tuberculosis and nontuberculous mycobacterial (NTM) infections [2–6]. Appropriate animal models are essential to explore the underlying mechanism of mycobacterial infections and T2D comorbidity. Most animal models available are based on genetic modification or chemical alteration of pancreatic β cells. These models fail to incorporate nutritional and polygenic determinants involved in the aetiopathology of T2D in humans [7,8]. Although no single animal model will necessarily encompass all the characteristics of T2D in patients, a more appropriate model is required. Diet induced diabetic murine models have been developed using a high fat diet (60% energy from fat), which markedly exceeds the typical dietary fat intake providing 34% of energy [8,9]. In a recent study, pronounced hyperglycaemic state in C57BL/6 mice was observed after 10 weeks of high fat, high glycaemic index diet intervention [8]. Based on these findings, a more robust model using an energy dense diet has been developed [7].

The diet induced murine model of T2D (DIMT2D) was used in this study to investigate mycobacterial infection and T2D comorbidity. Since, macrophages are the initial phagocytic cells that interact with pathogens and are particularly important in anti-mycobacterial defence [10], *in vitro* phagocytic capability of alveolar and resident peritoneal macrophages isolated from both diabetic and control mice were compared. In this study, *M. fortuitum* and mycolic acid including trehalose 6, 6′dimycolate (cell wall extract of *Mycobacterium tuberculosis*) coated beads were used as surrogates for the more virulent *M. tuberculosis* to characterize host-pathogen interactions in T2D.

2. Materials and methods

2.1. Induction of diet induced murine model of T2D

Male C57BL/6 mice were obtained from the Small Animal and Breeding Unit of James Cook University. Mice at 6 weeks of age

* Corresponding author. Building 087-105 James Cook University, Townsville, Queensland, 4811, Australia.
E-mail addresses: mdabdul.alim@my.jcu.edu.au (M.A. Alim), suchandan.sikder@my.jcu.edu.au (S. Sikder), tahnee.bridson@my.jcu.edu.au (T.L. Bridson), catherine.rush@jcu.edu.au (C.M. Rush), brenda.govan@jcu.edu.au (B.L. Govan), n.ketheesan@jcu.edu.au (N. Ketheesan).

http://dx.doi.org/10.1016/j.tube.2016.12.002
1472-9792/

were divided into two dietary groups. One group of mice received *ad libitum* access to an energy dense diet, while the control group received a standard rodent diet [7].

In initial studies, following 30 weeks of diet intervention, mice were euthanized and metabolic (glucose tolerance), biochemical (blood glucose, albumin, creatinine, $HbA1_c$, urine glucose and creatinine) and histological studies were performed. Haematoxylin and eosin (H&E) staining was used to compare pancreatic and visceral adipose tissue sections. Kidney sections were stained with the Periodic Acid Schiff stain, while cryosections of liver were stained with Oil Red O stain. CellSense® image analysis software (Olympus) was used for quantitative analysis of the tissue sections according to previously published methods [7].

2.2. Bacterial culture and infection

M. fortuitum was grown in 7H9 medium containing 0.05% Tween 80 and supplemented with 10% OADC (Oleic Albumin Dextrose Catalase) to mid-log phase and stored at −80 °C until use. The aliquots of frozen bacterial culture were thawed and vortexed vigorously for several minutes. The bacterial clumps were further broken down by passing the suspension through 29 gauge needle for several times. Diet induced diabetic and control mice were injected intravenously via the tail vein, at a dose of 1×10^7 CFU/mouse in a final volume of 200 μL of saline [11].

2.3. Organ bacterial load and histopathology

Three to five mice from each group were euthanized on 1, 14, 35 days post-infection (pi). Livers were homogenised in 3 mL of phosphate buffer saline (PBS) and spleens and lungs were macerated with 1 mL of PBS. Organ homogenates were centrifuged and supernatant were collected for cytokine assays. Homogenates were further treated with Triton-X (0.1%) for 10 min to lyse the cells. A serial 10-fold dilution was prepared to enumerate the viable bacterial colonies.

Formalin fixed liver samples were stained with H&E and Ziehl-Neelsen staining. Pathological lesions in liver sections were quantified according to previously published methods [12]. CellSense® image analysis software (Olympus) was used for quantitative analysis.

2.4. Mycolic acid coated bead phagocytosis

Fluoresbrite® 2 μm YG microspheres (Polysciences, USA) beads were coated with a commercially available cell wall extract of *M. tuberculosis* (Sigma, Cat. no. M4537 and T3034) as previously described [13,14].

Resident peritoneal cells (RPC) and broncho-alveolar lavage (BAL) cells were harvested from mice and cultured in RPMI-culture media supplemented with 10% fetal bovine serum [15,16]. The re-suspended RPC and BAL cells were plated in 24 well cell culture plates at 1×10^5 cells/well in 500 μL of cell culture media. Mycolic acid coated beads as trehalose 6, 6′-dimycolate coated beads (TDMCB) and whole mycolic acid coated beads (MACB) were then added to the respective wells (5 replicates) at a MOI 1:10. Following 4 h of incubation, RPC (F4/80 and CD11b) and BAL cell (CD11c) were stained with macrophage surface markers and viability dye (7AAD) and data acquired by BD FACS Calibur™ flow cytometer. Data analysis was performed using BD CellQuest® software.

2.5. Internalization and killing assay

For internalization and killing assays, CD11b + cells from RPC and CD11c + cells from BAL cells were isolated using BD IMag™ anti-mouse CD11b particles, (BD bioscience) and EasySep Mouse CD11c positive selection kit® (Stemcell), respectively. The magnetically sorted cell suspensions (>90% purity) were re-suspended in RPMI-cultured media at a concentration of 1×10^5 cells/well in 48 well cell culture plates. To assess the phagocytic and mycobactericidal capacity of macrophages, internalization for 4 h and survival for 24 h were measured according to previously described protocols [11]. Briefly, *M. fortuitum* was added to triplicate wells at a MOI 1:10. After 4 h of co-culture, supernatants were collected for cytokine assays. The wells were washed and treated with Amikacin (200 μg/mL) for a further 2 h to kill extracellular bacteria. To determine uptake, a 48 well cell culture plate was washed with PBS and lysed with Triton-X (0.1%) for 10 min. Another plate was washed and cultured with fresh cell culture media for a further 24 h. Following collection of supernatants, plates were washed, cells lysed with Triton-X and samples plated on 7H11 agar for determining viable bacteria. For enumeration of bacterial colonies, a serial 10-fold dilution was carried out using the lysates.

2.6. Measurement of cytokines

Supernatants of liver homogenates at 1, 14, 35 days pi and *M. fortuitum* infected cell culture supernatants (4 and 24 h) were used to determined cytokine levels using a BD Cytometric Bead Array Mouse Inflammation Kit® (Cat. no. 552364, TNF-α, IL-6, MCP-1, IL-10, IL-12 and IFN-γ). Flow cytometry data was analyzed by BD FCAP Array™ software version 3.0.

2.7. Statistical analysis

Statistical analysis was performed using SPSS Statistics 22.0 and GraphPad Prism 6.0 software. Data was compared using unpaired Student's *t*–test and Two-way ANOVA with Kruskal-Wallis nonparametric tests. Data was expressed as mean ± SEM and significance was set at $P < 0.05$.

3. Results

3.1. Characteristics of the diet induced murine model of T2D

Following 30 weeks of diet of intervention, an overall increase in body mass of 56.51% for diabetic and 35.0% for control mice was observed. Significantly impaired glucose tolerance (Fig. 1A & B) and higher HbA_{1c} levels (Fig. 1C) were observed in the diabetic mice. Histopathological analysis of tissue samples from diabetic mice confirmed the presence of features indicative of T2D. Adipocyte hypertrophy in visceral adipose tissue (Fig. 1E & J) and marked ectopic lipid accumulation in liver (Fig. 1F & L) was observed in diabetic mice. Pancreatic islet cell pathology in diabetic mice (Fig. 1G, M & N) reflected the compensatory islet hyperplasia. Renal impairment was observed through significantly higher albumin creatinine ratio (ACR) (Fig. 1D) and lower clearing of urine creatinine (control, 4.51 ± 0.21 *vs* diabetic, 3.15 ± 0.17 mmol/L, $P < 0.0001$) in diabetic mice compared to controls. Compared to control, mesangial thickening of the glomeruli (Fig. 1H & P, asterisk), thickening of the basement membrane of the Bowmans's capsule (Fig. 1P, arrow) and glomerular hypertrophy (control, 1425 ± 79.52 *vs* diabetic, 2275 ± 89.27 μm^2, $P < 0.0001$) in the kidneys of diabetic mice were also observed.

3.2. Impaired phagocytosis and inflammatory response in diet induced murine model of T2D

Following infection, diabetic mice were unable to control

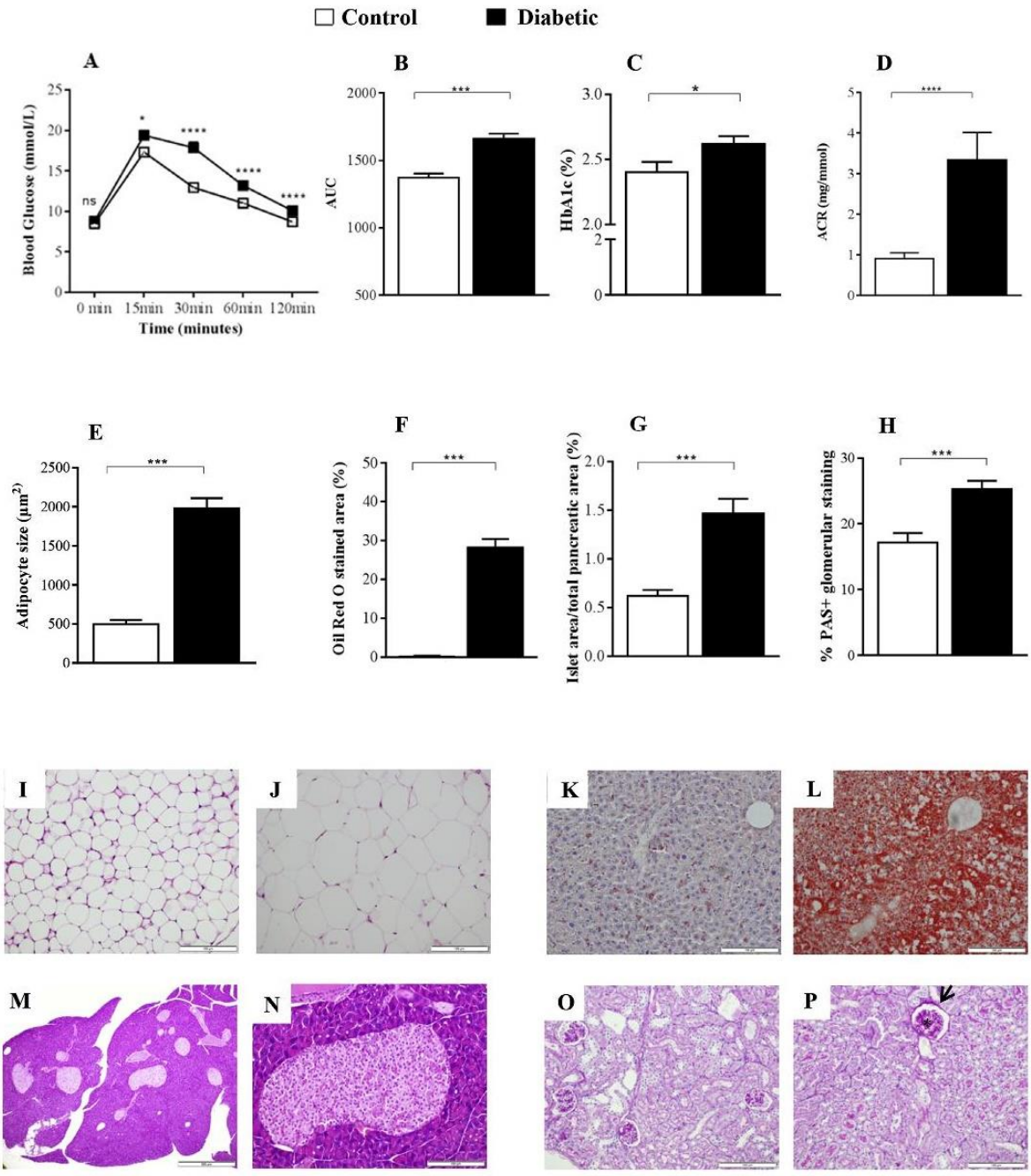

Fig. 1. Metabolic, biochemical and histopathological features of the diet induced diabetic mice. Each dietary group (diabetic and non-diabetic controls) included 35 mice. Diabetic mice demonstrated significantly higher glucose intolerance (A–B), glycosylated haemoglobin (HbA_{1c}; C), albumin creatinine ratio (ACR; D), adipocyte hypertrophy (E), hepatic steatosis (F), pancreatic islet hyperplasia (G) and PAS (Periodic Acid Schiff) positive glomerular staining (H) compared to non-diabetic controls. Histological changes were also observed in diabetic mice compared to control mice: Visceral adipose tissue in controls (I) and diabetic (J) mice demonstrated hypertrophy in the diabetic mice. Oil Red O staining of liver section from control (K) and diabetic (L) mice demonstrated significant increase in staining in diabetic animals. There was pancreatic hyperplasia (M & N) in diabetic mice. Compared to controls (O), mesangial thickening (*) within glomeruli and thickening of the Bowman's capsule (→) in kidney sections were observed in diabetic mice (P). Magnification: I-P 20× (scale bar: 100 μm); M 10× (scale bar: 500 μm). Data presented as mean ± SEM, significance $^{*}P < 0.05$, $^{***}P < 0.001$, $^{****}P < 0.0001$.

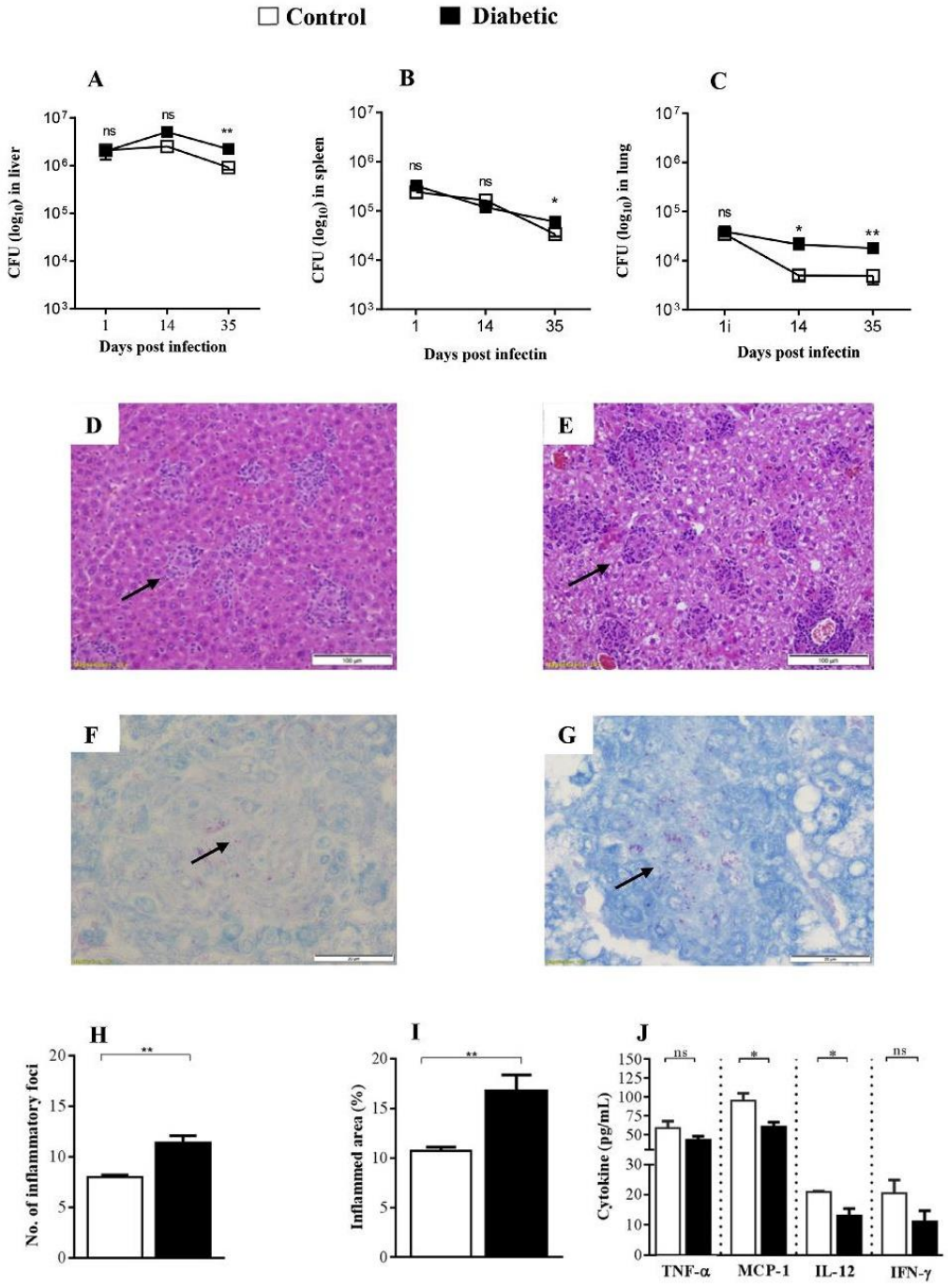

2. Diet induced diabetic mice are susceptible to mycobacterial infection. Diet induced diabetic and control mice were infected intravenously with *M. fortuitum* (1×10^7 CFU/se) for a period of 35 days. Mice were culled at 1, 14 and 35 days post-infection (pi) and organ bacterial load, histopathological lesions and cytokine responses were determined. days pi, organ bacterial load as colony forming unit (CFU) were significantly higher in liver (A), spleen (B) and lung (C) in diabetic mice compared to controls. Microphoaphs showed granulomatous type response as inflammatory foci (arrows) in the liver section of control (D) and diabetic mice (E). Ziehl–Neelsen staining of the hepatic tissue ons confirmed the presence of *M. fortuitum* (arrows) in control (F) and diabetic mice (G). Quantification of the liver lesions revealed that the number of inflammatory foci in etic mice was significantly higher compared to controls (H). Similarly, relative percentage of inflamed areas in hepatic tissue sections was significantly higher in diabetic mice pared to controls (I). Differential cytokine responses were also observed in the liver following infection (J). There was a significant reduction in monocyte chemoattractant ein-1 (MCP-1) and interleukin-12 (IL-12) in diabetic mice compared to control. A similar trend was also observed in tumor necrosis factor-α (TNF-α) and interferon-γ (IFN-γ) in iver of diabetic mice. Magnification: D-E 20× (scale bar: 100 μm); F-G 100× (scale bar: 20 μm), Data presented as mean ± SEM, significance $^{*}P<0.05$, $^{**}P<0.01$, *ns = non-ficant.*

bacterial replication efficiently compared to controls (Fig. 2A–C). A progressive reduction of bacterial burden was observed in spleen and lungs over 1, 14 and 35 days pi whereas the highest bacillary load was found in 14 days pi in the liver of both diabetic and control mice. At 35 days pi, bacterial load in liver was two times higher in diabetic mice compared to controls (Fig. 2A). These values were 1.8 and 3.7 times higher in spleen and lungs of diabetic mice, respectively (Fig. 2B & C).

Histology of the liver demonstrated a noticeable inflammatory response in both diabetic (Fig. 2E) and control mice (Fig. 2D). At 14 days pi, the number of inflammatory foci (control, 3.47 ± 0.56 *vs* diabetic, 7.68 ± 0.73, $P < 0.01$) and percent area of inflammation in the liver (control, 2.51 ± 0.0.49 *vs* diabetic, 6.97 ± 0.1.38%, $P < 0.05$) was higher in diabetic mice compared to controls. At 35 days pi, a similar trend in liver lesions was observed in the diabetic mice compared to controls (Fig. 2H & I). Ziehl-Neelsen staining of the liver sections demonstrated higher bacterial burden in the diabetic mice (Fig. 2G) compared to controls (Fig. 2F).

Following *M. fortuitum* infection, TNF-α secretion was comparable in the liver of both groups but declined in diabetic mice by 35 days pi (Fig. 2J). Although MCP-1 production was highest at 14 days pi in both groups (control, 143.76 ± 28.76 *vs* diabetic103.97 ± 16.62 pg/mL), it was significantly decreased in diabetic mice by 35 days pi (Fig. 2J). Interleukin-12 secretion was lower in diabetic mice at 1 and 14 days pi and significantly lowered by 35 days pi (Fig. 2J). A similar trend in IFN- γ secretion was also observed at all time points but did not reach significance. A reduced level of IL-12 and IFN-γ secretion in spleen and lungs of diabetic mice was also observed, although they did not reach significance.

3.3. Alveolar and resident peritoneal macrophage function is impaired in diet induced murine model of T2D

The phagocytic capability of alveolar macrophages (AM) and resident peritoneal macrophages (RPM) was assessed following 4 h incubation with mycolic acid coated beads (TDMCB and MACB). The uptake of TDMCB and MACB by AM and RPM from diabetic mice was significantly lower compared to controls (Fig. 3A & G). Further, internalization of *M. fortuitum* by AM from diabetic mice was more than 40% lower than controls after 4 h of co-culture (Fig. 3B). Killing of *M. fortuitum* in AM from diabetic mice after 24 h of co-culture was significantly lower compared to controls (Fig. 3C). Similar trends in uptake (Fig. 3H) and killing of *M. fortuitum* (Fig. 3I) were observed in RPM from diabetic mice compared to controls. Overall, AM were more efficient in phagocytosis and killing compared to RPM.

Alveolar macrophages from diabetic mice produced lower amounts of TNF-α at both 4 h (control, 219.7 ± 14.83 *vs* diabetic, 40.47 ± 1.56 pg/mL, $P < 0.001$) and 24 h of co-culture with the bacteria compared to controls (Fig. 3D). Similarly, TNF-α secretion was significantly reduced in RPM from diabetic mice at 4 h (control, 124.0 ± 6.56 *vs* diabetic, 69.93 ± 3.30 pg/mL, $P < 0.001$) and 24 h time points (Fig. 3J). Further, RPM were more efficient in secreting IL-6 at 4 h (control, 148.4 ± 6.70 *vs* diabetic, 77.45 ± 2.65 pg/mL, $P < 0.001$) and 24 h post infection (Fig. 3K) compared to AM (Fig. 3E). Macrophages of diabetic mice co-cultured with bacterium had significantly lower amount of MCP-1 compared to controls (Fig. 3F & L). A significantly higher quantity of IL-10 was also produced by RPM of control mice compared to diabetic mice at 4 h but this level was not sustained over time. Interferon-γ and IL-12 secretion by AM and RPM was minimal in the *in vitro* culture.

4. Discussion

Globally, T2D has become a "pandemic", with over 70% of patients living in TB endemic areas [2,4,5]. To understand the increased mycobacterial susceptibility in patients with T2D [2–4], a suitable animal model of T2D is desirable. The diet induced murine model of T2D (DIMT2D) we developed, closely resembles the overt signs of clinical T2D observed in humans, including induction of hyperglycaemia, hyperlipidaemia, glucose intolerance, insulin resistance, elevated HbA_{1c} level and pathological changes to hepatic, pancreatic, renal and adipose tissue.

The immune response to *M. tuberculosis* and bacteria belonging to NTM have both similarities and disparities. The most recognised virulence factor of mycobacteria is the glycopeptidiolipids and lipoglycans on the hydrophobic cell wall. The roles these cell wall components of *M. tuberculosis* and NTM in immunomodulation during host pathogen interaction have been discussed in detail in the literature [17–19].

In host-mycobacterial interactions, macrophages play the pivotal role in phagocytosis of the bacilli, secretion of chemical mediators, antigen presentation and subsequent activation of the adaptive immune responses [10]. Following infection with *M. fortuitum*, we observed disseminated infection in spleen, liver and lungs (Fig. 3A–C). The kinetics of *M. fortuitum* infection in different organs of diabetic and control mice were similar to the trends described in previously published reports [11,20]. However, bacterial kinetics were different from those reported by Orme and Collins [21] for *M. kansaii* and *M. avium*. Furthermore, the number and size of granulomas (data not shown) was increased in 35 days pi compared to 14 days pi in both diabetic and control mice. This difference could be due to the surface lipid component of the cell wall and subsequent host recognition and responses [22]. Previous studies reported that T helper 1 cell response particularly CD4 cell and its secretory products IFN- γ were crucial in the activation of macrophages followed by granuloma formation, to effeciently protect *M. fortuitum* infection [11,20]. Saiki et al. [23] first described altered phagocytic function of macrophages as a cause for increased TB susceptibility in streptozotocin (STZ) induced diabetic mice. As observed in this study, bacterial burden in the liver, spleen and lungs of diabetic mice were higher than in non-diabetic mice. Yamashiro et al. [24] observed a similar trend in bacterial burden at 14 and 35 days pi in *M. tuberculosis* infected diabetic mice. Higher *M. tuberculosis* burden in lungs was also observed in STZ induced diabetic mice [25]. One reason for higher organ bacterial loads in diabetic mice could be due to impaired phagocytosis and diminished expression or secretion of cytokine by the macrophages [26]. Bacterial burden is almost 1-log higher in diabetic mice during the first weeks after infection possibly due to delayed myeloid cell recruitment to the lungs and activation of the adaptive immune defense.

In our *in vivo* study, we observed a less efficient TNF-α and MCP-1, IL-12 and IFN-γ production in the liver of diabetic mice, which are essential for defense against mycobacterial infections [27]. TNF-α and MCP-1 are critical for recruitment of myeloid cells to control bacterial burden, granuloma formation and in activating T helper 1 cells by the secretion of IL-12. Interferon-γ is another key cytokine for further activation of the macrophages for effective control of the bacilli [26]. Similar to *M. tuberculosis* infection, TNF-α and IFN-γ were found to be crucial for both protection and granuloma formation in *M. avium* and *M. fortuitum* infection in mice [11,20,28]. Fatal inflammatory responses along with severe necrosis was observed in TNF-α deficient mice infected with *M. avium* [29]. A recent report showed that use of anti-TNF factor and other anti-rheumatic medications increase the risk of TB and NTM infections [30] suggesting that there are significant similarities in the host response and immune parameters across different mycobacteria. Furthermore, a reduction of IL-12 and IFN-γ secretion, considered to be important mediators of anti-mycobacterial activity in liver,

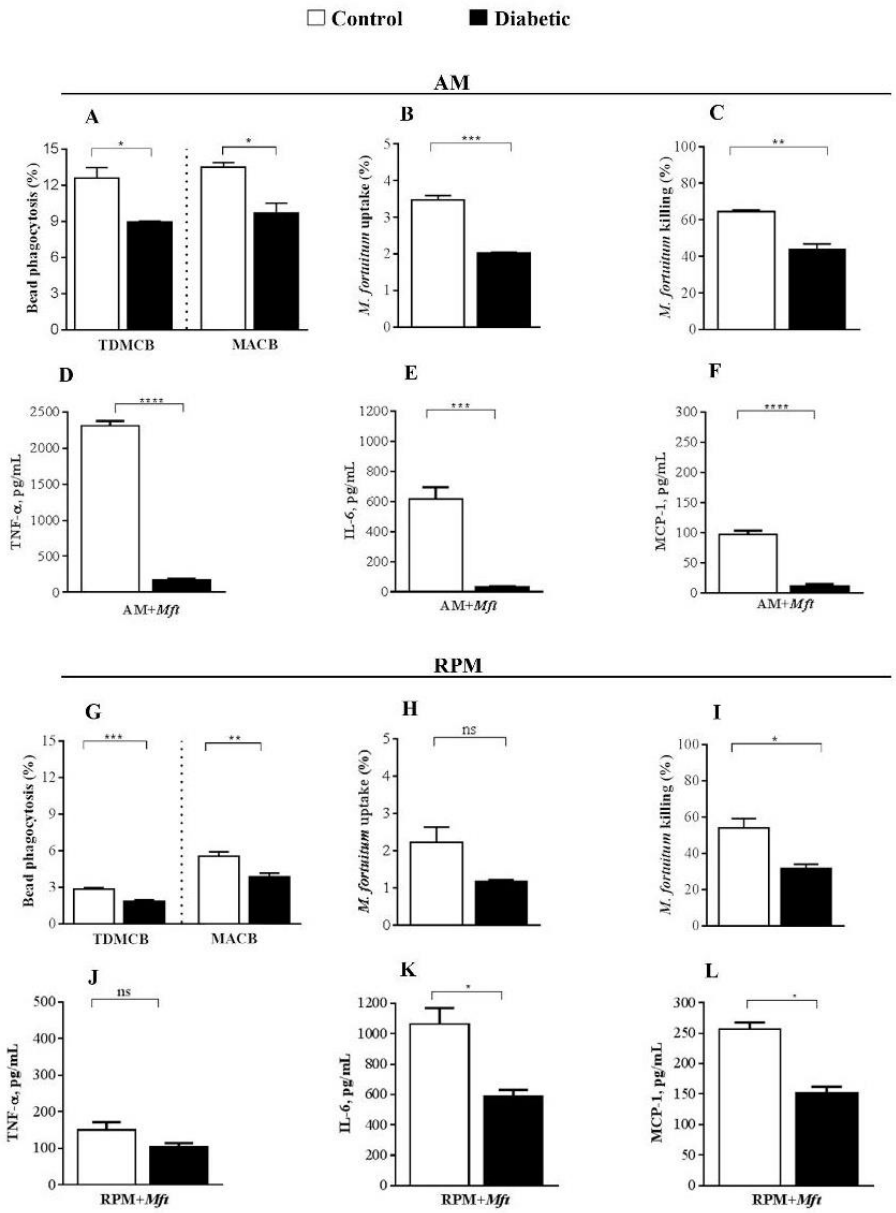

Fig. 3. Phagocytosis and bactericidal capacity of alveolar and peritoneal macrophages are suppressed in diabetic mice. Phagocytosis of trehalose 6, 6′-dimycolate coated beads (TDMCB) and whole mycolic acid coated beads (MACB) was significantly lower in alveolar macrophages (AM) from diabetic mice compared to control mice (A). Macrophages were also co-cultured with *M. fortuitum* at a MOI 1:10 for a period of 4 and 24 h. *M. fortuitum* uptake after 4 h (B) and killing of the internalized bacteria after 24 h (C) was reduced significantly in AM from diabetic mice compared to control mice. After 24 h of co-culturing with the bacterium, there was a significant reduction in production of tumor necrosis factor-α (TNF-α) (D), interleukin-6 (IL-6) (E) and monocyte chemoattractant protein-1 (MCP-1) (F) in AM from diabetic mice compared to controls. Similar to AM, beads uptake by resident peritoneal macrophages (RPM) from diabetic mice was significantly lower compared to RPM from control mice (G). There was a reduction in *M. fortuitum* uptake by RPM from diabetic mice co-cultured with the bacterium at 4 h (H) and a significant reduction in killing of the bacterium after 24 h of co-culture (I). A similar trend was also observed in TNF-α (J), IL-6 (K) and MCP-1 production (L) by RPM of diabetic mice co-culturing with the bacterium for a period of 24 h. These experiments were repeated thrice with similar results. Results of a representative experiment are given above. Data presented as mean ± SEM, significance $^{*}P < 0.05$, $^{**}P < 0.01$, $^{***}P < 0.001$, $^{****}P < 0.0001$, *ns = non-significant*.

spleen and lungs has been previously observed in STZ induced diabetic mice [24,25]. We also observed lower secretion of IL-12 and IFN-γ in spleen and lungs of diabetic mice, which may have contributed to the higher bacterial burden in those organs [24,25].

We investigated the phagocytic capability, killing and cytokine response in AM and RPM *in vitro*. The phagocytic capacity of mycolic acid coated beads and *M. fortuitum* was significantly reduced in both AM and RPM from diabetic mice. In previous

studies on STZ induced diabetic mice, a decreased bead uptake was observed in RPM [23,31]. This was also supported in our study, where RPM of diabetic mice were less capable of internalizing the mycolic acid coated beads and bacteria compared to controls. Recent findings indicate that impaired phagocytosis of mycolic acid coated beads in diabetic macrophages might be due to the lower expression of macrophage receptor with collagenous structure (MARCO), TLR2 and CD14 on the surface of macrophages [27,32]. Advanced glycation end products (AGE) accumulation in diabetes has also been shown to alter the expression of macrophage surface receptors [32,33]. In the current study, higher survival of the internalized bacteria was observed in both AM and RPM from diabetic mice (as opposed to *M. tuberculosis* infection). Higher survival of *M. fortuitum* in macrophages might be due to restricted secretion of antimycobacterial compounds, differences in bacterial cell wall components in delaying acidification of phagosome, phagosome-lysosome fusion and cytokine production [28,34,35]. The higher survival of *M. fortuitum* in both AM and RPM from diabetic mice compared to controls corresponds to the higher organ bacterial load and greater inflammatory changes in tissues of the diabetic animals in our *in vivo* study.

Furthermore, as demonstrated *in vitro*, lower TNF-α production by macrophages in diabetic mice may lead to impaired TNF-α mediated protection. Similar observations have been reported using AM from a type 1 diabetic rat model [36]. Lower production of TNF-α by macrophages from diabetic mice also correlated with reduced killing of *M. fortuitum* and higher organ bacterial load (Fig. 2A–C). TNF-α can also enhance the secretion of antimycobacterial compounds such as reactive oxygen species and inducible nitrous oxide synthase, which enables the killing of internalized bacteria [37]. Compared to AM, bacterial killing was lower in RPM, which also correlated with higher IL-10 production by them. Increased IL-10 production by RPM at early time points post-infection has been shown to downregulate TNF-α production, hence leading to increased survival of the bacilli [38]. Congruent to this study, Sun and colleagues [39] also reported reduced secretion of TNF-α from RPM in STZ induced diabetic mice.

The overall production of IL-6 was greater in RPM compared to AM. However, IL-6 production was significantly lower in RPM and AM from diabetic mice compared to controls. It has been found that RPM co-cultured with less pathogenic mycobacteria such as *M. smegmatis*, heat killed and avirulent *M. tuberculosis* produce high level of IL-6 [40]. Our study using *M. fortuitum* also yielded higher IL-6 in RPM compared to AM. Higher IL-6 secretion in infection with the less-pathogenic mycobacteria could be attributed to the differences in the lipoarabinomannan cell wall structure of the bacteria [40]. Lower IL-6 productions by macrophages from diabetic mice observed in our study may have contributed to increased bacterial survival. Martinez and colleagues [41] observed higher *M. tuberculosis* growth in macrophages of IL-6 knockout mice, suggesting that IL-6 has a protective role in mycobacterial infection. Similarly in our study, despite lower IL-6 production by AM, high TNF-α production by these cells may have compensated to reduce bacterial growth and survival. Similar to other pro-inflammatory cytokines, MCP-1 enables the recruitment of immune cells [42]. We found that macrophages from diabetic mice were less effective in secreting MCP-1. Prior research also support our observation where STZ induced diabetic mice demonstrated delayed recruitment of myeloid cells [26].

In conclusion, phagocytic dysfunction of macrophages is one of the key factors responsible for increased mycobacterial susceptibility in T2D patients, as ultimately, this leads to higher bacterial burden, delayed antigen presentation followed by late T cell mediated immunity. In this study, we observed impaired phagocytic activity, reduced killing efficacy of *M. fortuitum* and altered cytokine production in macrophages of DIMT2D animals. This model will be useful for future mycobacterial infections and T2D comorbidity research to investigate the immunological mechanisms contributing to this increasing comorbidity.

Funding

This research was supported by James Cook University internal grants awarded to Natkunam Ketheesan, Brenda L Govan and Catherine M Rush.

Competing interests

No conflicts of interest relevant to this manuscript were reported.

Ethical approval

All animal experiments were conducted following the National Health and Medical Research Council (NHMRC) guidelines under approved institutional ethics (A2016).

Acknowledgements

The authors wish to thank Dr Jodie L Morris for her assistance with the experiments. The authors acknowledge the assistance of Dr Andreas Kupz of James Cook University and Dr Nuria Martinez of the University of Massachusetts Medical School for the critical review of this manuscript. Md Abdul Alim is a recipient of an Endeavour PhD Scholarship from the Australian Government, Department of Education and Training.

References

[1] Anonymous. Global report on diabetes. 20 Avenue Appia, 1211 Geneva 27, Switzerland: World Health Organization; 2016. p. 1–86.
[2] Martinez N, Kornfeld H. Diabetes and immunity to tuberculosis. Eur J Immunol 2014;44(3):617–26.
[3] Bridson TL, Govan BL, Norton RE, Schofield L, Ketheesan N. The double burden: a new-age pandemic meets an ancient infection. Trans R Soc Trop Med Hyg 2014;108(11):676–8.
[4] Hodgson K, Morris J, Bridson T, Govan B, Rush C, Ketheesan N. Immunological mechanisms contributing to the double burden of diabetes and intracellular bacterial infections. Immunology 2015;144(2):171–85.
[5] Bridson T, Govan B, Ketheesan N, Norton R. Overrepresentation of diabetes in soft tissue nontuberculous mycobacterial infections. Am J Trop Med Hyg 2016;95(3):528–30.
[6] Ioachimescu OC, Tomford JW. Nontuberculous mycobacterial disorders. In: Carey W, editor. Disease management project. Cleveland, OH, USA: Cleveland Clinic—Centre for Continuing Education; 2016. Available online: http://www.clevelandclinicmeded.com/medicalpubs/diseasemanagement/infectious disease/nontuberculous-mycobacterial-disorders/ (Accessed on 31 October 2016), 2016.
[7] Morris JL, Bridson TL, Alim MA, Rush CM, Rudd DM, Govan BL, et al. Development of a diet-induced murine model of diabetes featuring cardinal metabolic and pathophysiological abnormalities of type 2 diabetes. Biol Open 2016;5(8):1149–62.
[8] Hodgson K, Govan B, Ketheesan N, Morris J. Dietary composition of carbohydrates contributes to the development of experimental type 2 diabetes. Endocrine 2013;43(2):447–51.
[9] Surwit RS, Kuhn CM, Cochrane C, McCubbin JA, Feinglos MN. Diet-induced type II diabetes in C57BL/6J mice. Diabetes 1988;37(9):1163–7.
[10] Cooper AM. Cell-mediated immune responses in tuberculosis. Annu Rev Immunol 2009;27:393–422.
[11] Parti RP, Srivastava S, Gachhui R, Srivastava KK, Srivastava R. Murine infection model for Mycobacterium fortuitum. Microbes Infect 2005;7(3):349–55.
[12] Flynn JL, Scanga CA, Tanaka KE, Chan J. Effects of aminoguanidine on latent murine tuberculosis. J Immunol 1998;160(4):1796–803.
[13] Retzinger GS, Meredith SC, Takayama K, Hunter RL, Kezdy FJ. The role of surface in the biological activities of trehalose 6,6'-dimycolate. Surface properties and development of a model system. J Biol Chem 1981;256(15):8208–16.
[14] Indrigo J, Hunter Jr RL, Actor JK. Cord factor trehalose 6,6'-dimycolate (TDM) mediates trafficking events during mycobacterial infection of murine

macrophages. Microbiology 2003;149(Pt 8):2049–59.
[15] Collins AM, Rylance J, Wootton DG, Wright AD, Wright AK, Fullerton DG, et al. Bronchoalveolar lavage (BAL) for research; obtaining adequate sample yield. J Vis Exp 2014;85.
[16] Hodgson KA, Morris JL, Feterl ML, Govan BL, Ketheesan N. Altered macrophage function is associated with severe Burkholderia pseudomallei infection in a murine model of type 2 diabetes. Microbes Infect 2011;13(14–15):1177–84.
[17] Honda JR, Knight V, Chan ED. Pathogenesis and risk factors for nontuberculous mycobacterial lung disease. Clin Chest Med 2015;36(1):1–11.
[18] Orme IM, Ordway DJ. Host response to nontuberculous mycobacterial infections of current clinical importance. Infect Immun 2014;82(9):3516–22.
[19] Ahmad S. Pathogenesis, immunology, and diagnosis of latent Mycobacterium tuberculosis infection. Clin Dev Immunol 2011;2011:814943.
[20] Silva TR, Petersen AL, Santos Tde A, Almeida TF, Freitas LA, Veras PS. Control of Mycobacterium fortuitum and Mycobacterium intracellulare infections with respect to distinct granuloma formations in livers of BALB/c mice. Mem Inst Oswaldo Cruz 2010;105(5):642–8.
[21] Orme IM, Collins FM. Resistance of various strains of mycobacteria to killing by activated macrophages in vivo. J Immunol 1983;131(3):1452–4.
[22] Maeda N, Nigou J, Herrmann JL, Jackson M, Amara A, Lagrange PH, et al. The cell surface receptor DC-SIGN discriminates between Mycobacterium species through selective recognition of the mannose caps on lipoarabinomannan. J Biol Chem 2003;278(8):5513–6.
[23] Saiki O, Negoro S, Tsuyuguchi I, Yamamura Y. Depressed immunological defence mechanisms in mice with experimentally induced diabetes. Infect Immun 1980;28(1):127–31.
[24] Yamashiro S, Kawakami K, Uezu K, Kinjo T, Miyagi K, Nakamura K, et al. Lower expression of Th1-related cytokines and inducible nitric oxide synthase in mice with streptozotocin-induced diabetes mellitus infected with Mycobacterium tuberculosis. Clin Exp Immunol 2005;139(1):57–64.
[25] Martens GW, Arikan MC, Lee J, Ren F, Greiner D, Kornfeld H. Tuberculosis susceptibility of diabetic mice. Am J Respir Cell Mol Biol 2007;37(5):518–24.
[26] Vallerskog T, Martens GW, Kornfeld H. Diabetic mice display a delayed adaptive immune response to Mycobacterium tuberculosis. J Immunol 2010;184(11):6275–82.
[27] Bowdish DM, Sakamoto K, Kim MJ, Kroos M, Mukhopadhyay S, Leifer CA, et al. MARCO, TLR2, and CD14 are required for macrophage cytokine responses to mycobacterial trehalose dimycolate and Mycobacterium tuberculosis. PLoS Pathog 2009;5(6):e1000474.
[28] Appelberg R, Castro AG, Pedrosa J, Silva RA, Orme IM, Minóprio P. Role of gamma interferon and tumor necrosis factor alpha during T-cell-independent and -dependent phases of Mycobacterium avium infection. Infect Immun 1994;62(9):3962–71.
[29] Ehlers S, Benini J, Kutsch S, Endres R, Rietschel ET, Pfeffer K. Fatal granuloma necrosis without exacerbated mycobacterial growth in tumor necrosis factor receptor p55 gene-deficient mice intravenously infected with Mycobacterium avium. Infect Immun 1999;67(7):3571–9.
[30] Brode SK, Jamieson FB, Ng R, Campitelli MA, Kwong JC, Paterson JM, et al. Increased risk of mycobacterial infections associated with anti-rheumatic medications. Thorax 2015;70(7):677–82.
[31] Ma H, Liu G, Ding W, Wu Y, Cai L, Zhao Y. Diabetes-induced alteration of F4/80+ macrophages: a study in mice with streptozotocin-induced diabetes for a long term. J Mol Med Berl 2008;86(4):391–400.
[32] Martinez N, Ketheesan N, West K, Vallerskog T, Kornfeld H. Impaired recognition of mycobacterium tuberculosis by alveolar macrophages from diabetic mice. J Infect Dis 2016;214(11):1629–37.
[33] Lachmandas E, Vrieling F, Wilson LG, Joosten SA, Netea MG, Ottenhoff TH, et al. The effect of hyperglycaemia on in vitro cytokine production and macrophage infection with Mycobacterium tuberculosis. PLoS One 2015;10(2):e0117941.
[34] Cebula BR, et al. Mycobacterium avium serovars 2 and 8 infections elicit unique activation of the host macrophage immune responses. Eur J Clin Microbiol Infect Dis 2012;31(12):3407–12.
[35] Da Silva TR, De Freitas JR, Silva QC, Figueira CP, Roxo E, Leao SC, et al. Virulent Mycobacterium fortuitum restricts NO production by a gamma interferon-activated J774 cell line and phagosome-lysosome fusion. Infect Immun 2002;70(10):5628–34.
[36] Sugawara I, Mizuno S. Higher susceptibility of type 1 diabetic rats to Mycobacterium tuberculosis infection. Tohoku J Exp Med 2008;216(4):363–70.
[37] Scanga CA, Mohan VP, Tanaka K, Alland D, Flynn JL, Chan J. The inducible nitric oxide synthase locus confers protection against aerogenic challenge of both clinical and laboratory strains of Mycobacterium tuberculosis in mice. Infect Immun 2001;69(12):7711–7.
[38] Fulton SA, Cross JV, Toossi ZT, Boom WH. Regulation of interleukin-12 by interleukin-10, transforming growth factor-beta, tumor necrosis factor-alpha, and interferon-gamma in human monocytes infected with Mycobacterium tuberculosis H37Ra. J Infect Dis 1998;178(4):1105–14.
[39] Sun C, Sun L, Ma H, Peng J, Zhen Y, Duan K, et al. The phenotype and functional alterations of macrophages in mice with hyperglycemia for long term. J Cell Physiol 2012;227(4):1670–9.
[40] Singh PP, Goyal A. Interleukin-6: a potent biomarker of mycobacterial infection. SpringerPlus 2013;2(1):1–8.
[41] Martinez AN, Mehra S, Kaushal D. Role of interleukin 6 in innate immunity to Mycobacterium tuberculosis infection. J Infect Dis 2013;207(8):1253–61.
[42] Kipnis A, Basaraba RJ, Orme IM, Cooper AM. Role of chemokine ligand 2 in the protective response to early murine pulmonary tuberculosis. Immunology 2003;109(4):547–51.